PROCEEDINGS OF IMMM 2019 – INTERNATIONAL MOLECULAR MYCORRHIZA MEETING

EDITED BY: Paola Bonfante, Luisa Lanfranco, Alessandra Salvioli, Stefano Ghignone, Veronica Volpe, Valentina Fiorilli, Silvia Perotto, Raffaella Balestrini and Andrea Genre

PUBLISHED IN: Frontiers in Plant Science and Frontiers in Microbiology

frontiers Research Topics

frontiers

ISSN 1664-8714
ISBN 978-2-88966-501-3
DOI 10.3389/978-2-88966-501-3

About Frontiers

Frontiers is more than just an open-access publisher of scholarly articles: it is a pioneering approach to the world of academia, radically improving the way scholarly research is managed. The grand vision of Frontiers is a world where all people have an equal opportunity to seek, share and generate knowledge. Frontiers provides immediate and permanent online open access to all its publications, but this alone is not enough to realize our grand goals.

Frontiers Journal Series

The Frontiers Journal Series is a multi-tier and interdisciplinary set of open-access, online journals, promising a paradigm shift from the current review, selection and dissemination processes in academic publishing. All Frontiers journals are driven by researchers for researchers; therefore, they constitute a service to the scholarly community. At the same time, the Frontiers Journal Series operates on a revolutionary invention, the tiered publishing system, initially addressing specific communities of scholars, and gradually climbing up to broader public understanding, thus serving the interests of the lay society, too.

Dedication to Quality

Each Frontiers article is a landmark of the highest quality, thanks to genuinely collaborative interactions between authors and review editors, who include some of the world's best academicians. Research must be certified by peers before entering a stream of knowledge that may eventually reach the public - and shape society; therefore, Frontiers only applies the most rigorous and unbiased reviews.
Frontiers revolutionizes research publishing by freely delivering the most outstanding research, evaluated with no bias from both the academic and social point of view. By applying the most advanced information technologies, Frontiers is catapulting scholarly publishing into a new generation.

What are Frontiers Research Topics?

Frontiers Research Topics are very popular trademarks of the Frontiers Journals Series: they are collections of at least ten articles, all centered on a particular subject. With their unique mix of varied contributions from Original Research to Review Articles, Frontiers Research Topics unify the most influential researchers, the latest key findings and historical advances in a hot research area! Find out more on how to host your own Frontiers Research Topic or contribute to one as an author by contacting the Frontiers Editorial Office: frontiersin.org/about/contact

PROCEEDINGS OF IMMM 2019 – INTERNATIONAL MOLECULAR MYCORRHIZA MEETING

Topic Editors:
Paola Bonfante, University of Turin, Italy
Luisa Lanfranco, University of Turin, Italy
Alessandra Salvioli, University of Turin, Italy
Stefano Ghignone, National Research Council (CNR), Italy
Veronica Volpe, University of Turin, Italy
Valentina Fiorilli, University of Turin, Italy
Silvia Perotto, University of Turin, Italy
Raffaella Balestrini, National Research Council (CNR), Italy
Andrea Genre, University of Turin, Italy

Citation: Bonfante, P., Lanfranco, L., Salvioli, A., Ghignone, S., Volpe, V., Fiorilli, V., Perotto, S., Balestrini, R., Genre, A., eds. (2021). Proceedings of iMMM 2019 – International Molecular Mycorrhiza Meeting. Lausanne: Frontiers Media SA. doi: 10.3389/978-2-88966-501-3

Table of Contents

05 ***Editorial: Proceedings of iMMM 2019 – International Molecular Mycorrhiza Meeting***
Paola Bonfante, Luisa Lanfranco, Alessandra Salvioli di Fossalunga, Stefano Ghignone, Veronica Volpe, Valentina Fiorilli, Silvia Perotto, Raffaella Balestrini and Andrea Genre

07 ***The* Rhizophagus irregularis *Genome Encodes Two CTR Copper Transporters That Mediate Cu Import Into the Cytosol and a CTR-Like Protein Likely Involved in Copper Tolerance***
Tamara Gómez-Gallego, Karim Benabdellah, Miguel A. Merlos, Ana M. Jiménez-Jiménez, Carine Alcon, Pierre Berthomieu and Nuria Ferrol

23 ***Transcriptomic Responses to Water Deficit and Nematode Infection in Mycorrhizal Tomato Roots***
Raffaella Balestrini, Laura C. Rosso, Pasqua Veronico, Maria Teresa Melillo, Francesca De Luca, Elena Fanelli, Mariantonietta Colagiero, Alessandra Salvioli di Fossalunga, Aurelio Ciancio and Isabella Pentimone

40 ***Interactions Between Phosphorus, Zinc, and Iron Homeostasis in Nonmycorrhizal and Mycorrhizal Plants***
Xianan Xie, Wentao Hu, Xiaoning Fan, Hui Chen and Ming Tang

55 ***Ramf: An Open-Source R Package for Statistical Analysis and Display of Quantitative Root Colonization by Arbuscular Mycorrhiza Fungi***
Marco Chiapello, Debatosh Das and Caroline Gutjahr

66 **In vitro *Propagation of Arbuscular Mycorrhizal Fungi May Drive Fungal Evolution***
Vasilis Kokkoris and Miranda Hart

75 ***Contrasting Nitrogen Fertilisation Rates Alter Mycorrhizal Contribution to Barley Nutrition in a Field Trial***
Tom Thirkell, Duncan Cameron and Angela Hodge

84 ***Imbalanced Regulation of Fungal Nutrient Transports According to Phosphate Availability in a Symbiocosm Formed by Poplar, Sorghum, and* Rhizophagus irregularis**
Silvia Calabrese, Loic Cusant, Alexis Sarazin, Annette Niehl, Alexander Erban, Daphnée Brulé, Ghislaine Recorbet, Daniel Wipf, Christophe Roux, Joachim Kopka, Thomas Boller and Pierre-Emmanuel Courty

104 ***TPLATE Recruitment Reveals Endocytic Dynamics at Sites of Symbiotic Interface Assembly in Arbuscular Mycorrhizal Interactions***
Giulia Russo, Gennaro Carotenuto, Valentina Fiorilli, Veronica Volpe, Antonella Faccio, Paola Bonfante, Mireille Chabaud, Marco Chiapello, Daniel Van Damme and Andrea Genre

113 ***Digging Deeper: In Search of the Mechanisms of Carbon and Nitrogen Exchange in Ectomycorrhizal Symbioses***
Emiko K. Stuart and Krista L. Plett

124 **MLO *Differentially Regulates Barley Root Colonization by Beneficial Endophytic and Mycorrhizal Fungi***
Magdalena Hilbert, Mara Novero, Hanna Rovenich, Stéphane Mari, Carolin Grimm, Paola Bonfante and Alga Zuccaro

135 ***A Flexible, Low-Cost Hydroponic Co-Cultivation System for Studying Arbuscular Mycorrhiza Symbiosis***
Debatosh Das, Salar Torabi, Philipp Chapman and Caroline Gutjahr

147 ***SNARE Complexity in Arbuscular Mycorrhizal Symbiosis***
Rik Huisman, Jan Hontelez, Ton Bisseling and Erik Limpens

161 ***More Filtering on SNP Calling Does Not Remove Evidence of Inter-Nucleus Recombination in Dikaryotic Arbuscular Mycorrhizal Fungi***
Eric C. H. Chen, Stephanie Mathieu, Anne Hoffrichter, Jeanne Ropars, Steven Dreissig, Jörg Fuchs, Andreas Brachmann and Nicolas Corradi

frontiers in Plant Science

EDITORIAL
published: 18 December 2020
doi: 10.3389/fpls.2020.627988

Editorial: Proceedings of iMMM 2019 – International Molecular Mycorrhiza Meeting

*Paola Bonfante[1], Luisa Lanfranco[1], Alessandra Salvioli di Fossalunga[1], Stefano Ghignone[2], Veronica Volpe[1], Valentina Fiorilli[1], Silvia Perotto[1,2], Raffaella Balestrini[2] and Andrea Genre[1]**

[1] Department of Life Science and Systems Biology, University of Turin, Turin, Italy, [2] Institute for Sustainable Plant Protection, Italian National Research Council, Turin, Italy

Keywords: plant symbiosis, mycorrhiza, endomycorrhiza, ectomycorrhiza, endophytes

Editorial on the Research Topic

Proceedings of iMMM 2019 – International Molecular Mycorrhiza Meeting

This Research Topic was launched on the occasion of the 4th International Molecular Mycorrhiza Meeting (IMMM 2019), held in Torino, Italy, on 7–8th February 2019 (**Figure 1**) and has collected 13 selected contributions from the IMMM 2019 meeting attendants.

The articles include original research, methods, reviews, and perspective papers covering most of the main topics presented at the meeting. These embrace molecular, cellular and nutritional aspects of mycorrhizas, the beneficial plant associations with soil fungi, as well as methodological approaches. Mycorrhizal fungi are considered key components of natural and agricultural ecosystems because they colonize the roots of most land plants developing different types of symbiotic interactions that greatly contribute to plant growth and health. A broad interest is focused on mycorrhizal symbioses, in particular arbuscular mycorrhiza (AM), for their potential contribution to agricultural practices that reduce the use of chemical fertilizers and pesticides and support sustainable crop production to feed a growing human population in a scenario of global climate change. It is therefore not surprising that the majority of contributions to both the meeting and the Research Topic concerned the AM symbiosis. In addition to agricultural applications, the great interest for AM symbiosis also derives from its ecological success (being found in over 72% of land plant species), its long evolutionary history (since plants and AM fungi started to live together at least 400 million years ago), and the refined coordination between major developmental and physiological processes of both partners (Genre et al., 2020).

In line with the meeting's major focus, many studies illustrate molecular aspects of mycorrhizal interactions. On the fungal side, Chen et al. propose new evidence in support of nuclear recombination in dikaryotic AM fungal isolates, reinforcing the hypothesis of the occurrence of parasexual or sexual reproduction processes and adding to the lively debate on this topic in the scientific community (Reinhardt et al., 2020). The paper by Miranda Hart's group offers food for thought, focusing on the unexplored effects of environmental constraints on AM fungal genomes. The article (Kokkoris and Hart) discusses whether the use of transformed root cultures—which is very common for *in vitro* mass production of AM fungi—may generate domesticated AM fungal strains, genetically and functionally different from their wild relatives. By deep mining the *Rhizophagus irregularis* genome, Gómez-Gallego et al. identified two fungal genes encoding Cu transporters of the copper transport (CTR) family and two alternative spliced variants of a third gene possibly involved in Cu perception and tolerance.

A second group of contributions investigates plant molecular responses to AM symbiosis in combination with biotic and abiotic stress. Balestrini et al. report

OPEN ACCESS

Edited by:
Dirk Albert Balmer, Syngenta, Switzerland

Reviewed by:
Katarzyna Turnau, Jagiellonian University, Poland

***Correspondence:**
Andrea Genre
andrea.genre@unito.it

Specialty section:
This article was submitted to Plant Pathogen Interactions, a section of the journal Frontiers in Plant Science

Received: *10 November 2020*
Accepted: *30 November 2020*
Published: *18 December 2020*

Citation:
Bonfante P, Lanfranco L, Salvioli di Fossalunga A, Ghignone S, Volpe V, Fiorilli V, Perotto S, Balestrini R and Genre A (2020) Editorial: Proceedings of iMMM 2019 – International Molecular Mycorrhiza Meeting. Front. Plant Sci. 11:627988. doi: 10.3389/fpls.2020.627988

FIGURE 1 | Logo of the iMMM 2019 conference.

changes in the transcriptome of mycorrhizal tomato roots in response to drought and root-knot nematode infection (two major causes of tomato yield losses) and highlight how plant and fungal gene regulation acts synergistically to face adverse environmental condition. Novel results on the role of AM fungi in plant nutrition are provided by Calabrese et al. Their analysis of the extra- and intra-radical mycelium transportome in *R. irregularis* highlights the role of the common mycorrhizal network in connecting perennial/C3 and annual/C4 hosts and in distributing mineral and organic nutrients between partners.

The role of AM fungi in plant nitrogen nutrition has been demonstrated in several *in vitro* studies, but Thirkell et al. now extend the investigation to field conditions, demonstrating a nitrogen acquisition from soil cores that are not reached by the root system, and providing valuable information for agricultural management practices.

The beneficial role of AM symbiosis in plant nutrition is also discussed in the review by Xie et al., who propose that a better understanding of the cross-talk between phosphate, zinc, and iron homeostasis and signaling in mycorrhizal crops can lead to new strategies for nutrient management. A related topic is discussed by Stuart and Plett in the field of ectomycorrhizas (ECM). Their study illustrates the impact of environmental conditions on nitrogen acquisition and transport by ECM fungi, stressing the importance of extending molecular studies of ECM to provide more solid bases to understand their complex ecology and multiple interactions.

Concerning the cellular aspects of plant-fungal interactions, two contributions investigate plant membrane dynamics in AM development through cell and molecular biology approaches. Russo et al. show the involvement of endocytosis-based processes in perifungal membrane remodeling during the development of the symbiotic interface compartment in legume and non-legume hosts, while Huisman et al. provide a deep insight in the characterization of *M. truncatula* SNARE proteins that have a specific role in symbiosis-associated exocytic mechanisms.

Another acknowledged advantage of AM plants is their improved resistance to pathogens, through the basal activation of mild defense mechanisms. However, investigations on how pathogen resistance may also modulate plant responsiveness to mycorrhization are limited. Hilbert et al. analyze root colonization by the beneficial endophyte *Serendipita indica* and by the AM fungus *Funneliformis mosseae* in a pathogen-resistant barley mutant. Their results demonstrate that while root colonization by the beneficial endophyte is reduced, AM development is promoted in the barley mutant, confirming the uniqueness of the plant-fungus relationship in AM interactions.

Lastly, two studies propose new experimental methods to investigate AM interactions. Das et al. describe a hydroponic set-up to obtain AM colonized roots under strictly controlled conditions suitable for testing specific nutrient concentrations or candidate signaling molecules, while Chiapello et al. propose "Ramf," an open-source R package for the elaboration of quantitative data of AM colonization to rapidly obtain statistical summaries and publication-ready plots.

Less than 2 years after the acceptance of the first manuscript, the IMMM 2019 Research Topic has gained more than 40,000 views and 6,000 downloads. This success mirrors the growing audience of IMMM meetings and the increasing interest in mycorrhizal interactions both for their applicative potential and their uniqueness as biological models for elucidating inter-kingdom relationships.

The 5th IMMM conference was planned to take place in Shanghai, China in July 2020. Unfortunately, the SARS-CoV-2 outbreak has imposed a rescheduling of the meeting, but we are looking very much forward to welcoming an even larger audience and more outstanding research at the next edition. For more information and updates, please visit the IMMM 2019 website at http://www.societabotanicaitaliana.it/immm2019/.

AUTHOR CONTRIBUTIONS

All authors listed have made a substantial, direct and intellectual contribution to the work, and approved it for publication.

REFERENCES

Genre, A., Lanfranco, L., Perotto, S., and Bonfante, P. (2020). Unique and common traits in mycorrhizal symbioses. *Nat. Rev. Microbiol.* 18, 649–660. doi: 10.1038/s41579-020-0402-3

Reinhardt, D., Roux, C., Corradi, N., and Di Pietro, A. (2020). Lineage-specific genes and cryptic sex: parallels and differences between arbuscular mycorrhizal fungi and fungal pathogens. *Trends Plant Sci.* in press. doi: 10.1016/j.tplants.2020.09.006

Conflict of Interest: The authors declare that the research was conducted in the absence of any commercial or financial relationships that could be construed as a potential conflict of interest.

frontiers in Plant Science

ORIGINAL RESEARCH
published: 16 May 2019
doi: 10.3389/fpls.2019.00604

The *Rhizophagus irregularis* Genome Encodes Two CTR Copper Transporters That Mediate Cu Import Into the Cytosol and a CTR-Like Protein Likely Involved in Copper Tolerance

*Tamara Gómez-Gallego[1], Karim Benabdellah[2], Miguel A. Merlos[1†], Ana M. Jiménez-Jiménez[1†], Carine Alcon[3], Pierre Berthomieu[3] and Nuria Ferrol[1]**

[1] *Departamento de Microbiología del Suelo y Sistemas Simbióticos, Estación Experimental del Zaidín, Consejo Superior de Investigaciones Científicas, Granada, Spain,* [2] *Genomic Medicine Department, GENYO, Centre for Genomics and Oncological Research, Pfizer-University of Granada-Andalusian Regional Government, Granada, Spain,* [3] *Biochimie et Physiologie Moléculaire des Plantes, Institut National de la Recherche Agronomique, Centre National de la Recherche Scientifique, Université de Montpellier, Montpellier SupAgro, Montpellier, France*

Arbuscular mycorrhizal fungi increase fitness of their host plants under Cu deficient and toxic conditions. In this study, we have characterized two Cu transporters of the CTR family (RiCTR1 and RiCTR2) and a CTR-like protein (RiCTR3A) of *Rhizophagus irregularis*. Functional analyses in yeast revealed that *RiCTR1* encodes a plasma membrane Cu transporter, *RiCTR2* a vacuolar Cu transporter and *RiCTR3A* a plasma membrane protein involved in Cu tolerance. *RiCTR1* was more highly expressed in the extraradical mycelia (ERM) and *RiCTR2* in the intraradical mycelia (IRM). In the ERM, *RiCTR1* expression was up-regulated by Cu deficiency and down-regulated by Cu toxicity. *RiCTR2* expression increased only in the ERM grown under severe Cu-deficient conditions. These data suggest that RiCTR1 is involved in Cu uptake by the ERM and RiCTR2 in mobilization of vacuolar Cu stores. Cu deficiency decreased mycorrhizal colonization and arbuscule frequency, but increased *RiCTR1* and *RiCTR2* expression in the IRM, which suggest that the IRM has a high Cu demand. The two alternatively spliced products of *RiCTR3, RiCTR3A* and *RiCTR3B*, were more highly expressed in the ERM. Up-regulation of *RiCTR3A* by Cu toxicity and the yeast complementation assays suggest that RiCTR3A might function as a Cu receptor involved in Cu tolerance.

Keywords: arbuscular mycorrhizal fungi, copper homeostasis, copper transporters, CTR family, *Rhizophagus irregularis*, symbiosis

OPEN ACCESS

Edited by:
Alessandra Salvioli, University of Turin, Italy

Reviewed by:
Philipp Franken, University of Applied Sciences Erfurt, Germany
Ilaria Colzi, University of Florence, Italy

****Correspondence:***
Nuria Ferrol
nuria.ferrol@eez.csic.es

†Present address:
Miguel A. Merlos, Department of Chemistry and Biochemistry, Mendel University in Brno, Brno, Czechia
Ana M. Jiménez-Jiménez, Central European Institute of Technology, Brno University of Technology, Brno, Czechia

Specialty section:
This article was submitted to Plant Microbe Interactions, a section of the journal Frontiers in Plant Science

Received: *26 February 2019*
Accepted: *24 April 2019*
Published: *16 May 2019*

Citation:
Gómez-Gallego T, Benabdellah K, Merlos MA, Jiménez-Jiménez AM, Alcon C, Berthomieu P and Ferrol N (2019) The Rhizophagus irregularis Genome Encodes Two CTR Copper Transporters That Mediate Cu Import Into the Cytosol and a CTR-Like Protein Likely Involved in Copper Tolerance. Front. Plant Sci. 10:604. doi: 10.3389/fpls.2019.00604

INTRODUCTION

The transition metal copper (Cu) is a micronutrient acting as a redox active cofactor of key enzymes involved in a wide array of biochemical processes essential for life, such as respiration, superoxide scavenging and iron mobilization (Linder, 1991; Festa and Thiele, 2011). However, when in excess, it becomes toxic due to its ability to displace other metal ions in structural or catalytic protein

motifs (Macomber and Imlay, 2009) and through the generation of hydroxyl radicals by Fenton-like reactions (Halliwell and Gutteridge, 1984). Due to the dual nature of Cu, organisms have developed sophisticated homeostatic networks to tightly regulate its intracellular levels, in which membrane transporters mediating Cu uptake and efflux and specific chaperones that handle and deliver Cu to its specific target enzymes play a key role (Puig and Thiele, 2002; Kim et al., 2008; Smith et al., 2017).

In eukaryotes, the major entrance of Cu into the cells occurs through members of the Cu transporter (CTR) family, small integral membrane proteins of variable length (from 150 to 500 amino acid residues) that have three transmembrane (TM) domains and the characteristic signature MetXXXMet-X_{12}-GlyXXXGly embedded within TM2 and TM3 (Dumay et al., 2006; De Feo et al., 2007). CTRs are present in the membranes as a homo-oligomer or hetero-oligomer complex, being the cooperation between the different subunits crucial for Cu transport (Puig et al., 2002; Beaudoin et al., 2011). The MetXXXMet motif is located in TM2 and together with a cluster of Met residues in the N terminal domain is involved in Cu sensing and uptake (Puig et al., 2002; Guo et al., 2004), while TM3 harbors the GlyXXXGly motif that is critical for protein folding and oligomerization (Aller et al., 2004). The carboxy terminal domain usually contains Cys and/or His motifs that bind and transfer Cu to cytosolic chaperones for its final targeted distribution (Dancis et al., 1994b; Xiao et al., 2004; Puig, 2014). Additionally, under Cu toxicity this domain allows protein inactivation through conformational structural changes (Wu et al., 2009). This family of transporters has been widely studied in *Saccharomyces cerevisiae*, which encodes three members (Ctr1, Ctr2, and Ctr3). Ctr1 and Ctr3 are functionally redundant plasma membrane transporters that mediate Cu acquisition from the environment (Dancis et al., 1994a; Peña et al., 2000), while Ctr2 is located in the vacuolar membrane and pumps vacuolar Cu stores to the cytosol (Portnoy et al., 2001; Rees et al., 2004). *Ctr1* and *Ctr3* expression is highly induced under Cu deficiency in order to facilitate high-affinity Cu acquisition and Ctr2 mobilizes Cu vacuolar stores when Cu levels are extremely low. Apart from other yeasts (Bellemare et al., 2002; Marvin et al., 2003; Beaudoin et al., 2011), CTRs have been characterized in the basidiomycetes *Pleurotus ostreatus* (Penas et al., 2005), *Coprinopsis cinerea* (Nakagawa et al., 2010) and *Amanita strobiliformis* (Beneš et al., 2016), as well as in the filamentous ascomycetes *Podospora anserina* (Borghouts et al., 2002), *Colletotrichum gloeosporioides* (Barhoom et al., 2008) and *Neurospora crassa* (Korripally et al., 2010). Fungal Ctr proteins have been shown to be involved in different processes. For example, the vacuolar Cu transporter Ctr2 of the plant pathogen *C. gloeosporioides* is essential for optimal spore germination and pathogenesis (Barhoom et al., 2008) and the high-affinity Cu transporter TCU-1 of *N. crassa* is essential for saprophytic conidical germination and vegetative growth under Cu limiting conditions (Korripally et al., 2010). However, very little is known about the mechanisms of Cu uptake in arbuscular mycorrhizal (AM) fungi, the most ancient and widespread fungal plant symbionts.

Arbuscular mycorrhizal fungi are soil-borne microorganisms of the subphylum Glomeromycotina within the Mucoromycota (Spatafora et al., 2016) that establish a mutualistic symbiosis with the majority of land plants. In this mutualistic relationship the fungal partner receives carbon compounds from the plant in exchange of low mobility mineral nutrients in soil, mainly phosphorus and some micronutrients, such as Zn and Cu (Smith and Read, 2008; Lanfranco et al., 2018). Besides improving plant mineral nutrition, AM fungi increase plant ability to overcome biotic and abiotic stress conditions, such as salinity, drought and metal toxicity (Ruiz-Lozano, 2003; Pozo et al., 2013; Ferrol et al., 2016). It is noteworthy the ability of AM fungi to increase plant fitness under deficient and excess Cu availability (Lehmann and Rillig, 2015; Ferrol et al., 2016). As revealed by isotopic labeling experiments, improvements in Cu nutrition by AM fungi are due to the capability of the extraradical mycelia (ERM) to absorb the micronutrient beyond the depletion zone that develops around the roots (Li et al., 1991; Lee and George, 2005). On the other hand, increased plant performance in Cu-polluted soils is mainly due to the ability of the fungus to act as a barrier for Cu entry into the plant tissues (Ferrol et al., 2016; Merlos et al., 2016). Despite the central role Cu transporters play in all organisms to cope with a range of Cu availability, from scarcity to excess, the mechanisms of Cu import in AM fungi have not been characterized yet. In a previous genome-wide analysis of metal transporters in the AM fungus *Rhizophagus irregularis*, we identified three genes putatively encoding Cu transporters of the CTR family that mediate Cu transport into the cytosol (Tamayo et al., 2014). With the aim to get further insights into the mechanisms of Cu homeostasis in AM fungi, in this work we carried out the first characterization of the *R. irregularis* CTR transporters.

MATERIALS AND METHODS

Biological Materials and Growth Conditions

The AM fungal isolate used in this study was *Rhizophagus irregularis* (Blaszk., Wubet, Renker & Buscot) C. Walker & A. Schüßler DAOM 197198. The fungal inoculum used for the root organ cultures and for the seedlings was obtained in monoxenic cultures. AM monoxenic cultures were established according to St-Arnaud et al. (1996), with some modifications. Briefly, Ri T-DNA transformed carrot (*Daucus carota* L. clone DC2) roots were cultured with *R. irregularis* in solid M medium (Chabot et al., 1992) in two-compartment Petri dishes. Cultures were started in one compartment by placing the fungal inoculum (ERM, spores and mycorrhizal roots fragments) and some pieces of carrot roots. Plates were incubated in the dark at 24°C for 6–8 weeks until the other compartment of the Petri dish was profusely colonized by the fungus and roots (root compartment). The older compartment was removed and filled with liquid M medium without sucrose (M-C medium) and the fungal mycelium was allowed to colonize this compartment (hyphal compartment) during the two subsequent weeks (Control plates).

For the Cu deficiency treatments, monoxenic cultures were established in media without Cu and started with roots and inoculum previously grown either in M media, which contains 0.5 μM $CuSO_4$, (moderate Cu deficiency treatment) or in M

media without Cu (severe Cu deficiency treatment), and grown in the same conditions than the control plates but in media lacking Cu. ERM and mycorrhizal roots grown, respectively, in the hyphal and root compartment of each plate were collected, rapidly dried on filter paper, immediately frozen in liquid N and stored at −80°C until used. An aliquot of the roots from each treatment was separated to estimate mycorrhizal colonization.

For the Cu toxicity and H_2O_2 treatments, the M-C medium of the hyphal compartment was removed and replaced with fresh liquid M-C medium (Control, 0.5 μM $CuSO_4$) or with M-C medium supplemented with 250 μM $CuSO_4$, 500 μM $CuSO_4$ or 1 mM H_2O_2 and incubated at 24°C. The time of medium exchange was referred as time 0. Mycelia were collected 1, 2, and 7 days after Cu addition and 1 h after H_2O_2 supplementation.

For gene expression comparison between ERM and IRM, several non-mycorrhizal carrot roots pieces were placed on the top of a densely fungal colonized compartment and grown for 15 days at 24°C. Roots were carefully collected with tweezers under a bionocular microscope trying to remove the attached extraradical hyphae, frozen in liquid N and stored at −80°C until used. An aliquot of root fragments was separated to estimate mycorrhizal colonization.

Rhizophagus irregularis ERM was also collected from mycorrhizal plants grown in the *in vivo* whole plant bidimensional experimental system described by Pepe et al. (2017) with some modifications (**Supplementary Figure S1**). Briefly, chicory (*Cichorium intybus* L.) seeds were surface-sterilized and germinated for 10–15 days in sterilized sand. Seedlings were transplanted into 50 mL pots filled with sterilized sand and inoculated with spores, ERM and colonized roots obtained from monoxenic cultures. Pots were placed in sun-transparent bags (Sigma-Aldrich, B7026) and maintained during 1 month in a growth chamber at 24°C/21°C day/night and 16 h light photoperiod. The root system of each plant was cleaned, wrapped in a nylon net (41 μM mesh, Millipore NY4100010) and placed between two 13 cm membranes of mixed cellulose esters (0.45 μm pore diameter size, MF-Millipore HAWP14250) in 14 cm diameter Petri dishes having a hole on the edge to allow plant shoot growth and containing sterilized sand. Petri plates containing plants were sealed with parafilm, wrapped with aluminum foil, placed into sun-transparent bags and maintained in a growth chamber. Plants were watered weekly with a 0.5X modified Hoagland nutrient solution containing 125 μM KH_2PO_4 and 0.16 μM $CuSO_4$ (control treatment) or without Cu (Cu deficiency treatment). Each treatment consisted of five replicates. Petri dishes were opened 2 weeks after preparing the root sandwiches and ERM spreading from the nylon net onto the membranes was collected with tweezers, frozen in liquid N and stored at −80°C until used. Roots wrapped in the nylon net were also frozen and stored at −80°C. An aliquot of the roots was separated to estimate mycorrhizal colonization.

The *Saccharomyces cerevisiae* strains used in this study were MPY17 (*ctr1*Δ*ctr3*Δ), a double-mutant lacking the plasma membrane transporters Ctr1 and Ctr3 (Peña et al., 1998) and MPY17 *ctr2*Δ (*ctr1*Δ*ctr2*Δ*ctr3*Δ), a triple mutant lacking also the vacuolar transporter ScCtr2 (Rees et al., 2004) and WYT (*yap1*Δ) a strain lacking the transcription factor yap1 (Kuge and Jones, 1994). Detailed characteristics of yeast strains are listed in **Supplementary Table S1**. Yeast cells were maintained on YPD or minimal synthetic dextrose (SD) medium, supplemented with appropriate amino acids.

Mycorrhizal Colonization

Histochemical quantification of mycorrhizal colonization was performed according to Trouvelot et al. (1986) using the Mycocalc program[1] in root samples previously cleared with 10% KOH and stained with 0.05% trypan blue (Phillips and Hayman, 1970). The abundance of the AM fungus was also assessed by determining the expression level of the *R. irregularis* elongation factor 1α (*RiEF1α*; GenBank Accession No. DQ282611), using as internal control the elongation factor 1α of the corresponding host plant (*Daucus carota* L. *DcEF1α*, GenBank Accession No. XM_017391845; *Cichorium intybus* L. *CiEF1α*, GenBank Accession No. KP752079).

Nucleic Acids Extraction and cDNA Synthesis

Rhizophagus irregularis genomic DNA was isolated from ERM developed in the hyphal compartment of control plates using the DNeasy Plant Mini Kit (Qiagen), according to the manufacturer's instructions.

Total RNA extraction from fungal ERM and mycorrhizal carrot roots developed in monoxenic cultures was performed using the Plant RNeasy Kit (Qiagen) following manufacturer's instructions. Total RNA from mycorrhizal chicory roots was isolated using the phenol/SDS method followed by LiCl precipitation (Kay et al., 1987). RNAs were DNase treated with the RNA-free DNase set (Qiagen) according to manufacturer's instructions and quantified using the NanoDrop 1000 Spectrophotometer (Thermo Scientific). cDNAs were synthetized from 1 μg of total DNase-treated RNAs in a 20 μL reaction containing 200 U of SuperScript III Reverse Transcriptase (Invitrogen) and 2.5 μM oligo $(dT)_{20}$ primer (Invitrogen), following the manufacturer's instructions.

RiCTRs Identification and Sequences Analyses

Candidate gene sequences putatively encoding RiCTRs were previously identified by Tamayo et al. (2014). Additional Blastp searches were performed in the filtered model datasets of the *R. irregularis* isolates DAOM197198 v2.0 and A1, A4, A5, B3, and C2 v1.0 (Chen et al., 2018) recently deposited at the JGI website[2], using as a query the previously identified RiCTR candidates. These sequences were also used to identify CTR homologs via Blastp in the sequence datasets of other Glomeromycotina species deposited on the JGI (*Gigaspora rosea* v1.0, *Rhizophagus cerebriforme* DAOM 227022 v1.0 and *Rhizophagus diaphanus* v1.0 (Morin et al., 2019) and NCBI [*Diversispora epigaea* (Sun et al., 2019) and *Rhizophagus clarus* (Kobayashi et al., 2018)] websites.

[1] https://www2.dijon.inra.fr/mychintec/Mycocalc-prg/download.html
[2] https://genome.jgi.doe.gov/portal/

Sequence analyses were performed using the DNAstar Lasergene software package (DNAstar), BLAST tool of NCBI[3] and Clustal Omega for sequence alignments[4]. Gene promoter sequences were screened for the presence of regulatory *cis* elements employing the tools included in the Promoter Database of *Saccharomyces cerevisiae* SCPD[5]. Specific Cu responsive elements (CuREs) and AP-1 sites were further screened through DNA pattern matching analyses in the fungal RSAT server[6]. Identity and Similarity percentages between proteins were calculated using Ident and Sim tool from Sequence Manipulation Suite[7]. Conserved domains of proteins were identified using the Conserved Domain Database at NCBI[8], predictions of putative TM domains via the TMHMM Server v.2.0[9], the SOSUI engine v. 1.11[10] and the TOPCONS web server[11], Structural models of the RiCTRs were generated using MyDomains tool of Prosite[12]. Phylogenetic analyses were performed via the Neighbor-Joining method implemented in the Molecular Evolutionary Genetics Analysis software v. 6. (MEGA), with 1,000 bootstrap replicates, using Poisson model and pairwise deletion of gaps options for distance computation.

Gene Isolation

The cDNA sequences of the 5′ and 3′ends of *RiCTR1-3* were confirmed and completed, when necessary, by RACE using the SMARTer® RACE 5′/3′ kit (Clontech) according to the manufacturer's protocol. The primers used for RACE reactions are listed in **Supplementary Table S2**. Genomic clones and full length cDNAs were obtained by PCR amplification of *R. irregularis* genomic DNA and cDNA, respectively, from ERM grown under control conditions in monoxenic cultures, using a set of primers flanking the complete open reading frames (**Supplementary Table S2**). PCR products were cloned into the pGEM-T Easy vector (Promega), following manufacturer's instructions. Plasmids were amplified by transformation of chemically *Escherichia coli* DH5α competent cells according to standard procedures and purified using the GenElute^{TM} Plasmid Miniprep Kit (Sigma-Aldrich). All plasmids were checked by sequencing (ABI PRISM 3130*xl* Genetic Analyzer, Applied Biosystems, Carlsbad, CA, United States).

Functional Complementation Analyses in Yeast

RiCTR open reading frames were sub-cloned between *Sma*I and *Xho*I sites (*RiCTR1*) or *Pst*I and *Sal*I sites (*RiCTR2* and *RiCTR3*) of the yeast expression vector pDR196. For this purpose, the respective full-length cDNA sequences were flanked with the sequences recognized by the corresponding restriction enzymes by PCR using the primers described in **Supplementary Table S2**. PCR products were cloned into the pGEM-T Easy vector (Promega), following manufacturer's instructions. The full-length cDNAs were then isolated from the pGEM-T Easy vector by digestion with the corresponding restriction enzymes and ligated into the digested pDR196 vector. All constructs were verified by sequencing. The *S. cerevisiae* strains *ctr1*Δ*ctr3*Δ, *ctr1*Δ*ctr2*Δ*ctr3*Δ and *yap-1*Δ were transformed with the corresponding pDR196-*RiCTR* constructs or with the empty vector using a lithium acetate-based method (Gietz and Schiestl, 2007). Transformants were selected in SD medium by autotrophy to uracil. For drop tests, transformants were grown to exponential phase in SD medium without uracil. Cells were harvested by centrifugation, washed twice and adjusted to a final OD_{600} of 1. Then, 5 μL of serial 1:10 dilutions were spotted on the corresponding selective medium. The transformed *ctr1*Δ*ctr3*Δ and *ctr1*Δ*ctr2*Δ*ctr3*Δ strains were spotted onto a non-fermentable carbon source ethanol-glycerol medium (YPEG: 1% yeast extract, 2% bacto-peptone, 2% ethanol, 3% glycerol, 1.5% bacto-agar) supplemented with 0, 10, or 20μM $CuSO_4$. The transformed *yap-1*Δ cells were spotted onto SD without uracil supplemented either with 1.5 mM $CuSO_4$ or 0.5 mM H_2O_2.

Protein Localization

Subcellular localization of RiCTR1-3 was assessed with N or C terminal fusions of these genes to the enhanced green fluorescent protein (eGFP) in the *S. cerevisiae* triple mutant *ctr1*Δ*ctr2*Δ*ctr3*Δ or in *yap-1*Δ. The coding sequences of *RiCTR1*, *RiCTR2* and *RiCTR3A* were cloned with or without their stop codon into pENTR/D-TOPO (Invitrogen) via TOPO reactions and then into the destination vectors pFGWDR196 or pGWFDR196 by using the Gateway LR Clonase recombination system (Invitrogen) for eGFP-tagging at the amino- or carboxy-terminus, respectively. Primers pairs used are listed in **Supplementary Table S2**. The corresponding yeast mutants were transformed with the resulting pFGWDR/pGWFDR196-*RiCTR* constructs or with the empty vector (negative control). Functionality of the GFP-tagged versions of RiCTRT1, RiCTR2, and RiCTR3A was tested in complementation assays, as previously described. For the protein localization assays, yeast cells were grown to exponential phase in liquid SD without uracil and visualized using a Leica TCS SP8 laser scanning microscope with a 63× oil N.A. 1.4 immersion objective. Emission fluorescence of GFP was excited at 488 nm and the emitted signal was collected between 500 and 540 nm. To reduce overexpression artifacts, yeast cells were treated just before visualization with the protein synthesis inhibitor cycloheximide (100 μM) for 45 min. Images were processed using ImageJ software.

Gene Expression Analyses

Gene expressions were analyzed by real-time quantitative RT-PCR using an iQ^{TM} 5 Multicolor Real-Time PCR Detection System (Bio-Rad). Each 20 μl reaction contained 1 μl of a 1:10 dilution of the cDNA, 200 nM each primer and 10 μl iQ^{TM} SYBR Green Supermix (Bio-Rad). The primer sets used are

[3]https://blast.ncbi.nlm.nih.gov/Blast.cgi
[4]https://www.ebi.ac.uk/Tools/msa/clustalo/
[5]http://rulai.cshl.edu/SCPD/
[6]http://rsat-tagc.univ-mrs.fr/rsat/
[7]http://www.bioinformatics.org/sms2/ident_sim.html
[8]https://www.ncbi.nlm.nih.gov/Structure/cdd/wrpsb.cgi
[9]http://www.cbs.dtu.dk/services/TMHMM/
[10]http://harrier.nagahama-i-bio.ac.jp/sosui/sosui_submit.html
[11]http://topcons.cbr.su.se/
[12]https://prosite.expasy.org/mydomains/

listed in **Supplementary Table S2**. The program consisted in an initial incubation at 95°C for 3 min, followed by 38 cycles of 95°C for 30 s, 58°C for 30 s and 72°C for 30 s, where the fluorescence signal was measured. The specificity of the PCR amplification procedure was checked with a heat-dissociation protocol (from 58 to 95°C) after the final PCR cycle. Since RNA extracted from mycorrhizal roots contains plant and fungal RNAs, specificity of the primers pairs was also analyzed by PCR amplification of carrot and chicory genomic DNA and cDNA from non-mycorrhizal carrot and chicory roots. Specificity of the *RiCTR3A* and *RiCTR3B* primer pairs was analyzed by PCR amplification of the *RiCTR3A* and *RiCTR3B* plasmid DNAs. RT-PCR determinations were performed in three independent biological samples with the threshold cycle (Ct) determined in duplicate in at least two independent PCR experiments. The relative abundance of the transcripts was calculated by using $2^{-\Delta\Delta CT}$ method (Livak and Schmittgen, 2001) and normalized according to the expression of the *R. irregularis* elongation factor 1α (*RiEF1α*; GenBank Accession No. DQ282611).

Statistical Analyses

IBM SPSS Statistic software v.23 was used for the statistical analysis of the means and standard error determinations. Data were subjected to the Student's *t*-test when two means were compared or by one-way ANOVA followed by a Fisher's LSD to find out differences among groups of means ($P < 0.05$). All the analyses are based on at least three biological replicates per each treatment ($n \geq 3$).

RESULTS

Features of the *R. irregularis* CTR Proteins

The *R. irregularis CTR1*, *CTR2*, and *CTR3* full-length cDNA sequences were obtained by RACE using gene-specific primers based on the sequences described by Tamayo et al. (2014) [GenBank Accession No. /JGI IDs: PKC06371/1491164 (*RiCTR1*), EXX67481/1726366 (*RiCTR2*) and PKC14368/495436 (*RiCTR3*)]. Interestingly, two types of *CTR3* transcripts were identified in the *R. irregularis* ERM, *RiCTR3A* of 531 bp and *RiCTR3B* of 606 bp. Comparisons of the full-length cDNAs with the genomic sequences revealed the presence of three introns in *RiCTR1* and two in *RiCTR2* and *RiCTR3*, all of them flanked by the canonical splicing sequences GT and AG at the 5′ and 3′ ends, respectively (**Figure 1A**). Alignment of the *RiCTR3A* and *RiCTR3B* transcripts with the *RiCTR3* gene sequence indicates that both transcripts are alternatively spliced products of the same gene, as the *RiCTR3A* and *RiCTR3B* sequences are contained within the genomic sequence. *RiCTR3B*, the longest

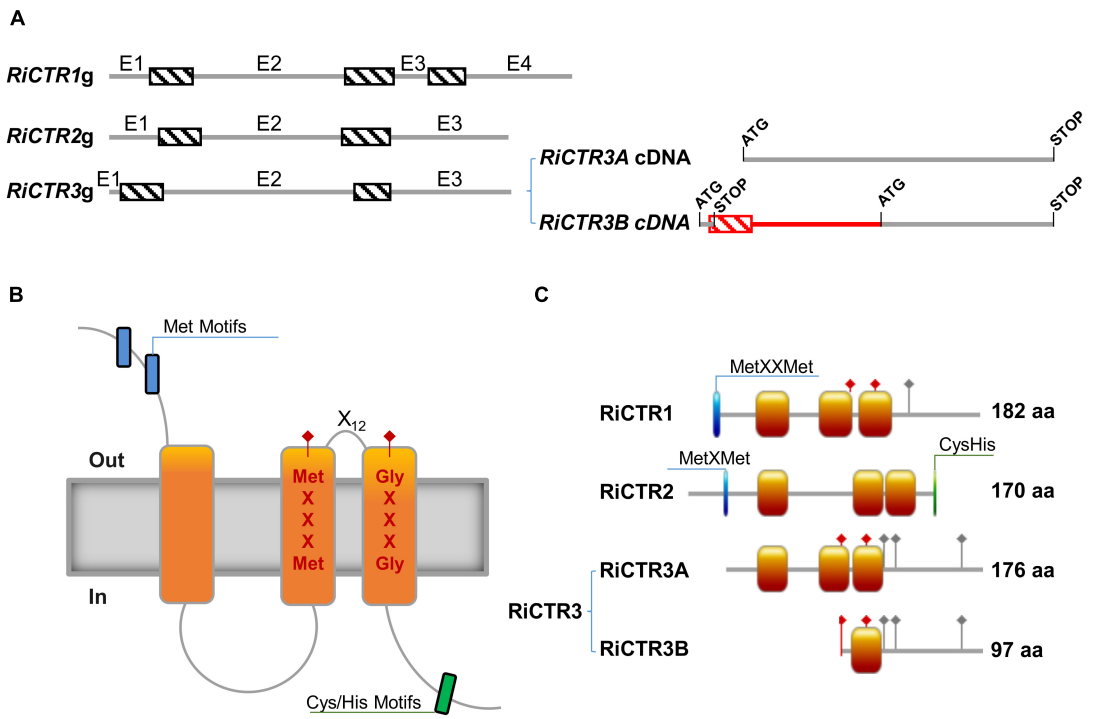

FIGURE 1 | Structure of the *R. irregularis* CTR proteins. **(A)** Exon/intron organization of the *R. irregularis* CTR genes. Exons (E) and introns are represented by gray lines and dashed boxes, respectively. The two transcript variants of *RiCTR3* are illustrated at the right. The coding regions of the two spliced variants of *RiCTR3* are shown in gray and the non-coding in red. The start and stop codons are indicated. **(B)** Typical topological model of a CTR transporter. **(C)** Schematic representation of the structure of the *R. irregularis* CTR transporters. Orange boxes illustrate transmembrane domains, blue boxes Met motifs and green boxes Cys and His motifs. Red diamonds show the positions of the MetXXXMet and the GlyXXXGly motives of the CTRs master signature and gray diamonds the positions of the C-terminal His/Cys residues. Amino acid lengths are also indicated.

RiCTR3 variant, contains the first intron after the *RiCTR3A* start codon generating a premature termination codon-containing mRNA. However, an additional start codon located within the second exon becomes available to produce a protein that contains the last 97 amino acids of RiCTR3A.

RiCTR1, *RiCTR2*, and *RiCTR3A* encode proteins of 182, 170, and 176 amino acids, respectively, that have three TM domains with the MetXXXMet-X_{12}-GlyXXXGly signature embedded within TM2 and TM3, an intracellular loop connecting TM1 and TM2, the N terminus toward the extracellular space and the C terminus facing the cytosol (**Figures 1B,C**). RiCTR1 and RiCTR2 present a Met motif, MetXXMet in RiCTR1 and MetXMet in RiCTR2, in the N terminal extracytosolic region 29 and 23 amino acids before TM1, respectively. This methionine motif, which is essential for CTR function (Puig et al., 2002), is absent in RiCTR3A. RiCTR2 harbors a Cys/His motif in the carboxy-terminal region facing the cytoplasm, while RiCTR1 has a single His residue and RiCTR3A a Cys and two His residues (**Figure 1C** and **Supplementary Figure S2**). Despite the similar structure and sequence amino acid length of RiCTR1, RiCTR2, and RiCTR3A, similarity between their deduced amino acid sequences is lower than 53%, displaying RiCTR1 and RiCTR3A the highest similarity (**Supplementary Table S3**). *RiCTR3B* encodes a protein of 97 amino acids that harbors the MetXXXMet-X_{12}-GlyXXXGly signature of CTR proteins, but has a single TM domain, the MetXXXMet is mislocalized in the N terminal domain and the GlyXXXGly motif is embedded in its only TM domain.

A phylogenetic analysis of fungal CTR transporters revealed that RiCTR1 and RiCTR3 clustered with the *S. cerevisiae* plasma membrane Ctr1/Ctr3-like Cu transporters and RiCTR2 with the *S. cerevisiae* vacuolar Ctr2-like transporters. Within each

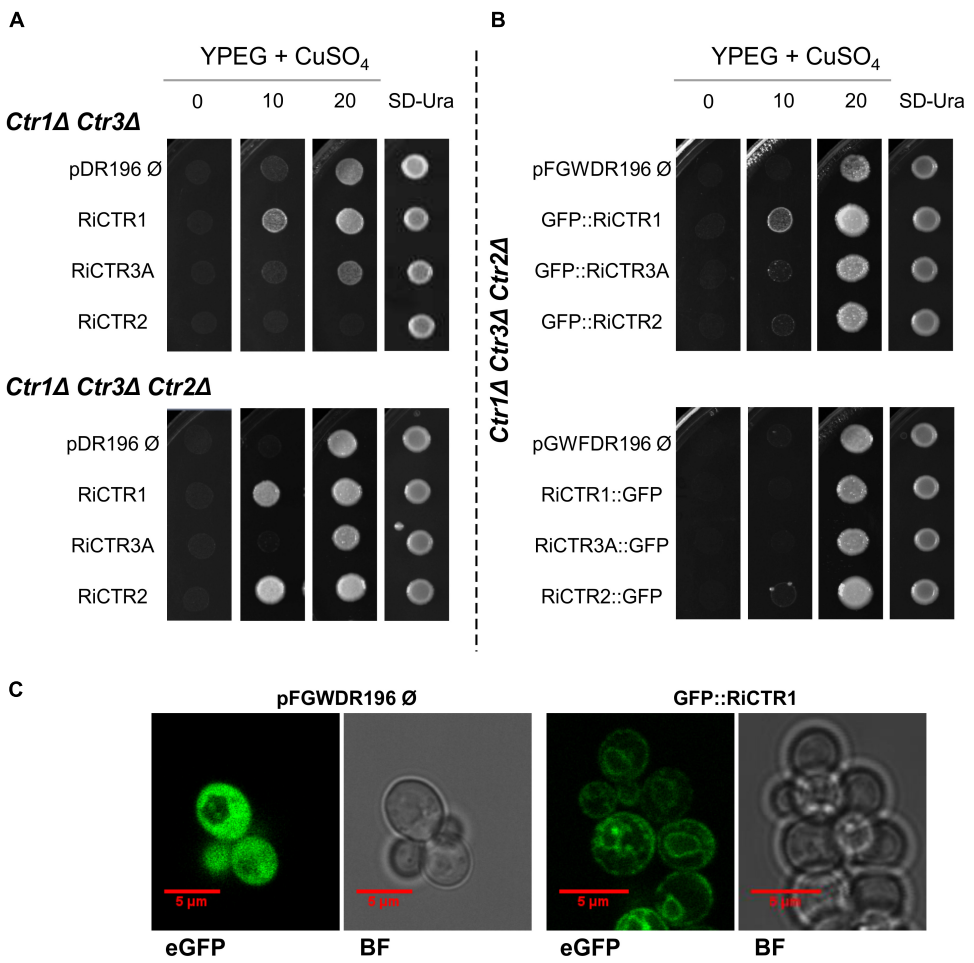

FIGURE 2 | Analysis of the Cu transport activity and subcellular localization of the *R. irregularis* CTRs in yeast. **(A)** *ctr1*Δ*ctr3*Δ and *ctr1*Δ*ctr2*Δ*ctr3*Δ yeast cells transformed with the empty vector or expressing *RiCTR1*, *RiCTR2*, *RiCTR3A or RiCTR3B* were plated on YPEG media supplemented with Cu (0, 10, or 20 μM $CuSO_4$) or on SD medium without uracil. *ctr1*Δ*ctr3*Δ and *ctr1*Δ*ctr2*Δ*ctr3*Δ plated cells were incubated at 30°C for 4 and 7 days, respectively. RiCTR3A and RiCTR3B had the same effect (see **Supplementary Figure S5**), only the result with RiCTR3A is illustrated. **(B)** *ctr1*Δ*ctr2*Δ*ctr3*Δ yeast cells expressing *GFP* (empty vector), N-terminal (upper panel) or C-terminal (lower panel) *GFP*-tagged versions of *RiCTR1*, *RiCTR2* and *RiCTR3A* were plated on YPEG media supplemented with Cu (0, 10, or 20 μM $CuSO_4$) or on SD medium without uracil. Plates were incubated at 30°C for 7 days. **(C)** *ctr1*Δ*ctr2*Δ*ctr3*Δ cells expressing *GFP* (the empty vector pFGWDR196) and *GFP::RiCTR1* were visualized with a confocal microscope. eGFP, enhanced GFP fluorescence; BF, bright field.

clade, all Glomeromycotina sequences were grouped together (**Supplementary Figure S3**).

In silico searches for putative regulatory elements in their promoter sequences resulted in the identification of several core elements identical to the Cu response *cis*-element (CuRE) GTAC present in the promoters of Cu-responsive genes (Jamison McDaniels et al., 1999; Kropat et al., 2005) and the consensus sequence of the AP-1 *cis*-acting element (TTATTAA/TTAGTAA) recognized as a conserved motif in the oxidative stress-responsive genes (Toone and Jones, 1999) (**Supplementary Figure S4**). Interestingly, the 5′-flanking region of *RiCTR3* is especially rich in AP-1 motifs and contains the preferred DNA binding site (TTACTAA) of the transcription factor YAP1 (Toone and Jones, 1999), which is essential for the oxidative stress response in *S. cerevisiae* (Kuge and Jones, 1994).

RiCTR1 and *RiCTR2* Encode Functional Cu Transporters

Since AM fungi cannot be genetically manipulated, functionality of the RiCTRs was assessed in yeast by testing their ability to revert the inability of the double (*ctr1*Δ*ctr3*Δ) and triple (*ctr1*Δ*ctr2*Δ*ctr3*Δ) *S. cerevisiae* CTR mutants, which lack the plasma membrane Ctr1 and Ctr3 Cu transporters and the plasma membrane Ctr1/Ctr3 and the vacuolar Ctr2 transporters, to grow on a non-fermentable carbon source at low Cu concentrations. This growth defect is due to the inability of the cytochrome c oxidase to obtain its Cu cofactor, resulting in a defective mitochondrial respiratory chain (Dancis et al., 1994a; Glerum et al., 1996; Rees et al., 2004). To perform the yeast complementation assays, the full-length cDNA coding sequences of *RiCTR1*, *RiCTR2*, *RiCTR3A*, or *RiCTR3B* were expressed under the control of the yeast PMA1 promoter in both yeast CTR mutants and plated on ethanol-glycerol (YPEG) medium supplemented with different Cu concentrations. The empty vector-expressing cells were unable to grow on YPEG medium containing <20 μM Cu (**Figure 2A**). Expression of *RiCTR1* restored the inability of the *ctr1*Δ*ctr3*Δ and *ctr1*Δ*ctr2*Δ*ctr3*Δ yeast strains to grow on YPEG medium supplemented with 10 μM Cu, indicating that RiCTR1 is a functional homolog of the yeast plasma membrane Cu transporters Ctr1/Ctr3. RiCTR2 complemented the inability of the *ctr1*Δ*ctr2*Δ*ctr3*Δ mutant strain to grow on YPEG medium supplemented with 10 μM Cu but not of the double mutant lacking the two plasma membrane transporters, which suggests that RiCTR2 is a functional homolog of the *S. cerevisiae* vacuolar transporter Ctr2. However, none of the *RiCTR3* variants rescued the phenotype of either the double or the triple CTR mutants (**Figure 2A** and **Supplementary Figure S5**), which was expected since their encoded proteins did not contain the required features for CTR function.

Subcellular localization of RiCTR1 and RiCTR2 was assessed in the heterologous system by expressing N- and C-terminal GFP-tagged versions of these proteins in the *ctr1*Δ*ctr2*Δ*ctr3*Δ strain and visualizing the fusion proteins with a confocal fluorescence microscope. *S. cerevisiae* cells transformed with the empty vector and expressing GFP under the control of the PMA1 promoter were used as a negative control; and functionality of the RiCTR1-2 fusion proteins was assessed before their visualization (**Figure 2B**). The control cells expressing the soluble GFP showed a general cytosolic fluorescence (**Figure 2C**). The RiCTR1-GFP, RiCTR2-GFP and GFP-RiCTR2 fusion proteins were unable to revert the mutant phenotype of the *ctr1*Δ*ctr2*Δ*ctr3*Δ strain and were expressed within the perinuclear endoplasmic reticulum region (data not shown), indicating that the fusion proteins failed to exit the endoplasmic reticulum. As expected from the complementation assays, the *GFP-RiCTR1*-expressing cells showed a clear fluorescent signal at the cell periphery indicative of a plasma membrane localization. GFP-RiCTR1 was also localized within the perinuclear endoplasmic reticulum membrane, a phenomenon commonly found in yeast membrane protein overexpression assays (**Figure 2C**).

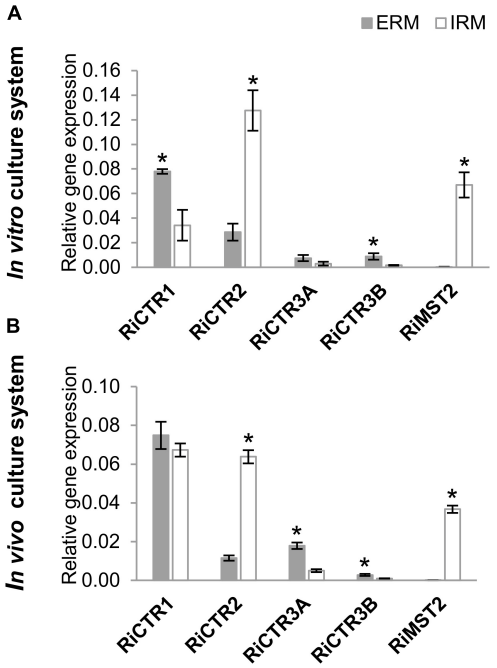

FIGURE 3 | *RiCTR*s expression levels in the *R. irregularis* ERM and IRM. **(A)** *R. irregularis* ERM and mycorrhizal carrot roots (IRM) were grown in compartmented monoxenic cultures (*in vitro* culture system). **(B)** *R. irregularis* ERM and mycorrhizal chicory roots (IRM) were grown in the whole plant bidimensional experimental system (*in vivo* culture system). Relative gene expression levels were calculated by the $2^{-\Delta CT}$ method using *RiEF1*α as a normalizer. Bars represent standard error. Asterisks show statistically significant differences ($P < 0.05$; $n = 4$) between ERM and IRM.

RiCTR Genes Are Differentially Expressed in the IRM and ERM

To gain information about the expression of *RiCTR1-3* during symbiosis and about their relative abundance in the intraradical mycelia (IRM) and ERM, their expression levels were determined by real time quantitative RT-PCR (RT-qPCR) in ERM grown in liquid monoxenic cultures and in the *in vivo* sandwich system, and in the IRM developed in carrot roots grown *in vitro* for 2 weeks on a densely colonized hyphal compartment and devoid

of ERM and in mycorrhizal chicory roots collected from the *in vivo* sandwich system. Mycorrhizal colonization levels of the carrot and chicory roots were 10 and 78%, respectively. As a reference for fungal activity, we measured transcript levels of the *R. irregularis* high-affinity monosaccharide transporter *RiMST2,* which is highly expressed in the IRM during AM symbiosis (Helber et al., 2011). In both experimental systems, *RiCTR1* was the isoform more highly expressed in the ERM and the expression levels of *RiCTR2* were higher in the IRM than in the ERM. Expression levels of the two spliced-variants of *RiCTR3* were very low in both fungal structures and more highly expressed in the ERM (**Figure 3**).

Cu Deficiency Inhibits AM Colonization and Regulates *RiCTR* Expression in the IRM

To further understand the role of RiCTR1-3 in the intraradical phase of the fungus, their expression levels were analyzed in mycorrhizal carrot roots grown *in vitro* in monoxenic cultures and in mycorrhizal chicory roots grown *in vivo* in the sandwich system under Cu-optimal and -deficient conditions. Interestingly, irrespective of the culture method, development of the roots under Cu-deficient conditions decreased mycorrhizal intensity and arbuscule frequency (**Figure 4**). These results were confirmed by determining the transcript levels of the *R. irregularis* elongation factor *RiEF1α* by qRT-PCR (**Figure 4**).

Cu deficiency increased *RiCTR1* expression in the IRM developed in the carrot root organ cultures and in the chicory roots grown in the sandwich system (**Figure 5A**). However, *RiCTR2* expression was only up-regulated in the IRM of the carrot roots grown under the severe Cu deficiency treatment and of the chicory roots fed with a nutrient solution without Cu (**Figure 5B**). None of the *RiCTR3* splicing variants were detected in the mycorrhizal roots grown under Cu-limiting conditions, probably because their low expression levels in the IRM and the decrease in mycorrhizal colonization.

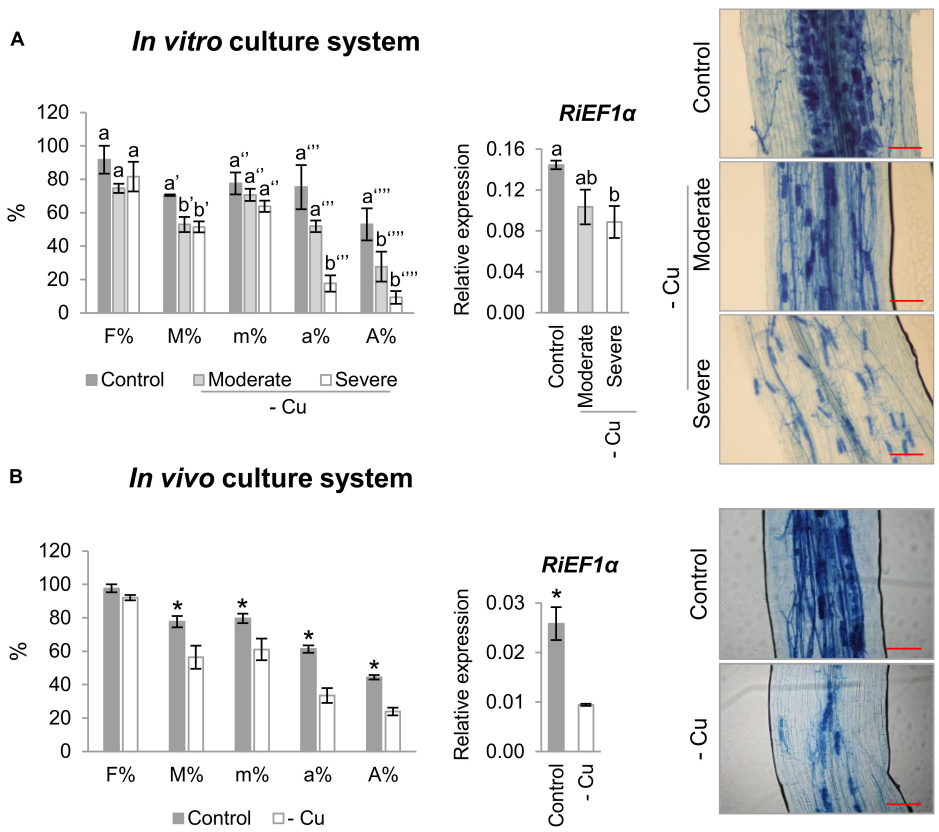

FIGURE 4 | Effect of Cu deficiency on mycorrhizal colonization. **(A)** Mycorrhizal colonization of carrot roots grown in monoxenic cultures in M media (control, 0.5 μM Cu) or in M media lacking Cu in plates started either with roots and inoculum previously grown in M media containing 0.5 μM $CuSO_4$ (moderate Cu deficiency) or without Cu (severe Cu deficiency). **(B)** Mycorrhizal colonization of chicory roots grown in the whole plant bidimensional experimental system fertilized with half-strength Hoagland solution (control, 0.16 μM Cu) or with a modified nutrient solution without Cu. Colonization rates were determined by using the Trouvelot method after histochemical staining and by determining the expression level of the *R. irregularis* elongation factor 1α (*RiEF1α*). The relative expression of Ri*EF1α* was calculated using the $2^{-\Delta CT}$ method with *EF1α* of the corresponding host plant as internal control. Bars represent standard error. Different letters indicate significant differences ($P < 0.05$; $n = 4$) between treatments and asterisks statistically significant differences ($P < 0.05$; $n = 4$) in comparison with the control. F%, frequency of mycorrhiza in the root system; M%, intensity of the mycorrhizal colonization in the root system; m%, intensity of the mycorrhizal colonization in the root fragments; a%, arbuscule abundance in mycorrhizal parts of root fragments; A%, arbuscule abundance in the root system. Scale bar of the left panels: 100 μm.

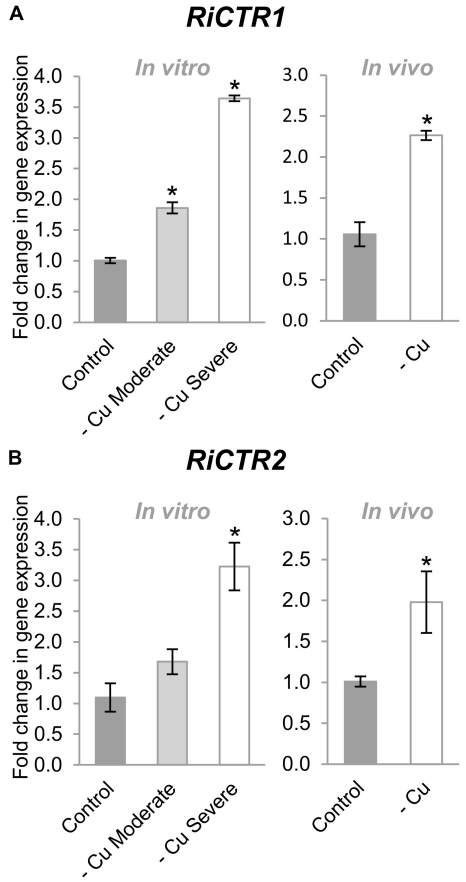

FIGURE 5 | Effect of Cu deficiency on *RiCTR1* and *RiCTR2* IRM expression. **(A)** *RiCTR1* and **(B)** *RiCTR2* expression in mycorrhizal carrot roots developed in monoxenic cultures in M media (control, 0.5 μM Cu) or in M media lacking Cu in plates started either with roots and inoculum previously grown in M media containing 0.5 μM $CuSO_4$ (moderate Cu deficiency) or without Cu (severe Cu deficiency) (left panel) and in mycorrhizal chicory roots grown in the whole plant bidimensional experimental system and fertilized with half-strength Hoagland solution (control, 0.16 μM Cu) or with a modified nutrient solution without Cu (right panel). Relative gene expression levels were calculated by the $2^{-\Delta\Delta CT}$ method using *RiEF1α* as a normalizer. Bars represent standard error. Asterisks show statistically significant differences ($P < 0.05$; $n = 4$) in comparison to the corresponding control value.

RiCTRs Expression in the ERM Is Regulated by Cu Availability

To get further insights into the role of the *R. irregularis* CTR family members on fungal Cu homeostasis, their gene expression patterns were assessed in ERM grown monoxenically under Cu deficient and toxic conditions. Given that development of the ERM was seriously inhibited when the hyphal compartment of the split Petri dishes was supplied with high Cu levels (data not shown), the Cu toxicity treatments were applied by exposing the ERM grown in M media to 250 μM $CuSO_4$ for 1, 2, and 7 days or to 500 μM $CuSO_4$ for 1 and 2 days.

RiCTR1 expression was up-regulated by Cu deficiency and down-regulated by Cu toxicity. A twofold induction was observed in the ERM grown both under moderate and severe Cu limiting conditions (**Figure 6A**). In contrast, *RiCTR2* transcript levels were significantly increased (twofold) only in the ERM grown under the severe Cu-limiting treatment. *RiCTR2* expression was not affected by any of the toxic Cu conditions considered in our study (**Figure 6B**).

The expression levels of *RiCTR3A* and *RiCTR3B* were similar in the control untreated ERM. Interestingly, *RiCTR3A* expression was highly up-regulated in ERM subjected to the Cu toxicity treatments and down-regulated in the ERM grown under Cu limiting conditions. *RiCTR3A* induction by Cu toxicity seemed to be transient, reaching a maximum expression level (>20-fold induction) in the ERM exposed to 500 μM $CuSO_4$ for 1 day (**Figure 6C**). This expression pattern was unexpected for a gene encoding a protein that transports Cu into the cytosol and suggests a role for RiCTR3A in Cu tolerance. *RiCTR3B* expression was just slightly up-regulated in the ERM grown for 7 d at 250 μM Cu and for 1 d at 500 μM Cu (**Figure 6D**). Differential regulation of the two *RiCTR3* splicing variants by Cu leads to higher transcript levels of *RiCTR3A* than of *RiCTR3B* under Cu toxic levels and to higher transcript levels of *RiCTR3B* under the severe Cu deficient treatment (**Supplementary Figure S6**).

RiCTRs Expression Is Regulated by Oxidative Stress

Taking into account that several oxidative-stress response elements were identified in the promoter sequences of the *R. irregularis CTR* genes and that toxic Cu levels induce an oxidative stress to the ERM (Benabdellah et al., 2009), in an attempt to further understand the role of the *R. irregularis* CTRs, their gene expression patterns were analyzed in the ERM exposed to H_2O_2. As a marker of the oxidative stress treatment, the expression of the *R. irregularis* Cu, Zn superoxide dismutase gene *RiSOD1* (González-Guerrero et al., 2010) was determined. Exposure of the ERM to 1 mM H_2O_2 for 1 h up-regulated *RiCTR1, RiCTR2, RiCTR3B* and *RiSOD1* expression (**Figures 7A,B,D,E**). However, *RiCTR3A* expression was not significantly affected by H_2O_2, which indicates that its activation by Cu was independent of the Cu-induced oxidative stress (**Figure 7C**). Differential regulation of the two *RiCTR3* splicing variants by H_2O_2 leads to higher *RiCTR3B* transcript levels in the H_2O_2-treated ERM (**Supplementary Figure S7**).

RiCTR3A Enhances Metal Tolerance of the *yap1*Δ Yeast Strain

As a step forward to understand RiCTR3A and RiCTR3B function and taking into account that their transcript levels were regulated by Cu toxicity or H_2O_2, we assessed their capability to rescue metal and H_2O_2 sensitivity of the *yap1*Δ *S. cerevisiae* strain lacking the transcriptional regulator Yap1 that mediates cell's response to oxidants and metals. Neither the empty vector-transformed cells nor the *RiCTR3B*-expressing cells were able to grow on SD media supplemented with Cu or H_2O_2 (**Figure 8A**). However, RiCTR3A rescued the growth defect of the mutant yeast in media supplemented with 1.5 mM $CuSO_4$ but not the inability of the *yap1*Δ cells to grow in the presence of 0.5 mM H_2O_2 (**Figure 8A**). These data indicate that

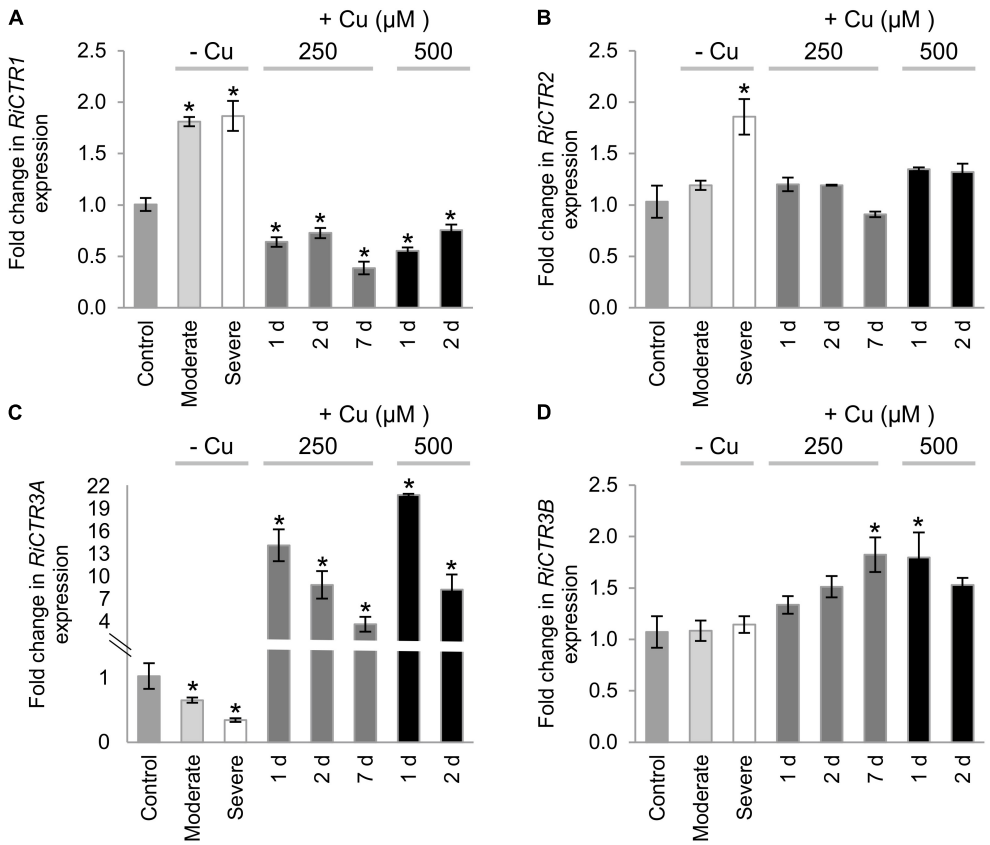

FIGURE 6 | Regulation of *RiCTRs* expression by Cu availability. *R. irregularis* ERM was grown in monoxenic cultures in M media containing 0.5 μM $CuSO_4$ (control) or in M media lacking Cu in plates started with roots and inoculum previously grown either in M media containing 0.5 μM $CuSO_4$ (moderate Cu deficiency) or in M media without Cu (severe Cu deficiency). For the Cu toxicity treatments, the ERM grown in optimal M media was exposed for 1, 2, and 7 days to 250 μM $CuSO_4$ or for 1 and 2 days to 500 μM $CuSO_4$. **(A)** *RiCTR1*, **(B)** *RiCTR2*, **(C)** *RiCTR3A* and **(D)** *RiCTR3B* gene expression. Relative expression levels were calculated by the $2^{-\Delta\Delta CT}$ method using *RiEF1*α as a normalizer. Bars represent standard error. Asterisks show statistically significant differences ($P < 0.05$; $n = 3$) in comparison to the corresponding control value.

RiCTR3A plays, at least in the heterologous system, a role in Cu tolerance. To determine RiCTR3A subcellular location in *yap1*Δ, N- and C-terminal GFP-tagged versions of RiCTR3A were expressed in the mutant yeast cells. However, only GFP-RiCTR3A remained functional (**Figure 8B**). This fusion protein was localized to the yeast plasma membrane. Additionally, as usually occurs when transport proteins are overexpressed in yeast, a perinuclear fluorescence pattern indicative of endoplasmic reticulum localization was observed (**Figure 8C**).

DISCUSSION

The ability of AM fungi to acquire Cu from the soil and to transfer it to their host plants has been shown in several physiological studies. Whereas much progress has been made in understanding the mechanisms of phosphorus and nitrogen transport in the AM symbiosis, very little is known about the mechanisms of Cu acquisition by AM fungi. Here, we characterize for the first time the Cu transporters of the CTR family in an AM fungus. Our data strongly suggest that *R. irregularis* acquires Cu (I) from the soil through the activity of RiCTR1, a plasma membrane Cu transporter that is highly expressed in the ERM, and that RiCTR2 and RiCTR3A play a role in Cu homeostasis in *R. irregularis*.

A previous genome-wide analysis of Cu transporters in *R. irregularis* revealed the presence of three candidate gene sequences, *RiCTR1*, *RiCTR2*, and *RiCTR3*, encoding transporters belonging to the CTR family (Tamayo et al., 2014). Interestingly, our RACE approach identified two *RiCTR3* transcripts, which result from an alternative splicing event through the retention of the first intron in its coding sequence, the most common alternative splicing type described in fungi (Grutzmann et al., 2014; Gonzalez-Hilarion et al., 2016). Alternative splicing is a common mechanism used to produce multiple proteins from a single gene, thereby increasing the proteome size of an organism (Black, 2003; Benabdellah et al., 2007; Kornblihtt et al., 2013; Mockenhaupt and Makeyev, 2015). In addition, it can influence gene expression through its impact on different stages of mRNA metabolism including transcription, polyadenylation, nuclear mRNA export, translation efficiency and the rate of mRNA decay (Le Hir et al., 2003; Jacob and Smith, 2017). Although functionality of alternative splicing is poorly understood in fungi,

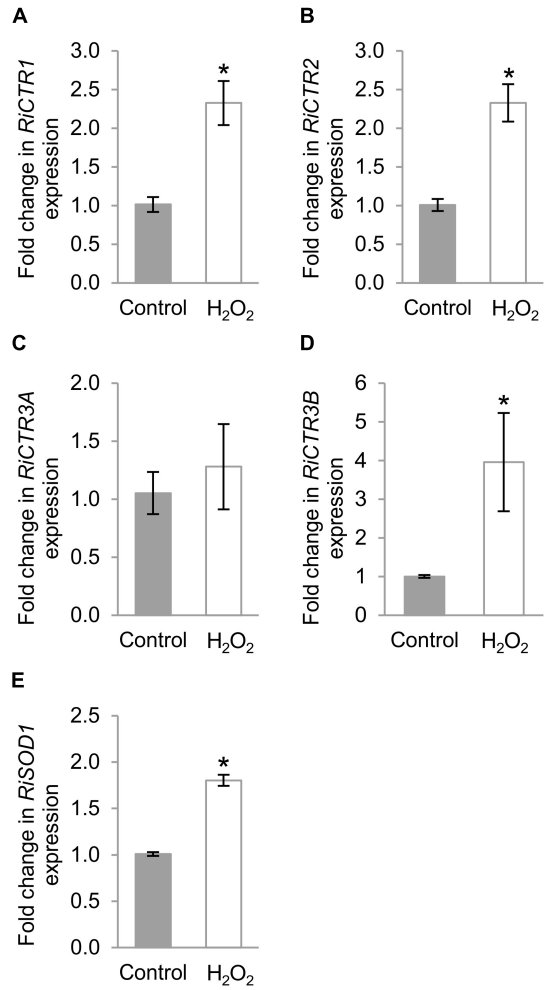

FIGURE 7 | Regulation of *RiCTRs* expression by oxidative stress. *R. irregularis* ERM grown in monoxenic cultures in M-C medium was exposed or not (Control) for 1 h to 1 mM H_2O_2. **(A)** *RiCTR1*, **(B)** *RiCTR2*, **(C)** *RiCTR3A* **(D)** *RiCTR3B,* and **(E)** *RiSOD1* gene expression. Relative expression levels were calculated by the $2^{-\Delta\Delta CT}$ method using *RiEF1*α as a normalizer. Bars represent standard error. Asterisks show statistically significant differences ($P < 0.05$; $n = 3$) in comparison to the control value.

it seems that usually leads to non-functional isoforms, providing an additional mechanism to regulate the overall expression of a gene (Goebels et al., 2013; Grutzmann et al., 2014; Gonzalez-Hilarion et al., 2016; Jin et al., 2017; Sieber et al., 2018). However, the extent and biological significance of this process in AM fungi is currently unknown.

CTR proteins contain three TM regions, with a characteristic MetXXXMet motif located in the second TM domain that is absolutely necessary for Cu transport, and an amino-terminal region rich in Met motifs (De Feo et al., 2007). Although most of these methionine motifs are dispensable for Cu transport, a Met/Cys-X-Met motif near the first TM domain is essential for function (Puig et al., 2002). Our *in silico* analyses revealed that out of the four identified RiCTR open reading frames, only RiCTR1 and RiCTR2 present all the structural features of CTR proteins. In fact, these two proteins were the only *R. irregularis* CTRs displaying Cu transport activity in the heterologous system. The finding that RiCTR1 reverts the mutant phenotype of the *ctr1*Δ*ctr3*Δ strain lacking the high affinity plasma membrane Cu transporters Ctr1 and Ctr3 indicates that RiCTR1 encodes a plasma membrane Cu transporter that transports Cu (I). Localization of RiCTR1 in the yeast plasma membrane and *RCTR1* expression patterns in the ERM in response to external Cu, that is up-regulation by Cu deficiency and down-regulation by Cu toxicity, supports this hypothesis. Although RiCTR2 subcellular localization could not be demonstrated in the heterologous system, it seems to be the functional ortholog of the *S. cerevisiae* vacuolar Cu transporter Ctr2, as it complemented the growth defect of the triple CTR mutant yeast *ctr1*Δ*ctr2*Δ*ctr3*Δ lacking both the vacuolar and plasma membrane transporters but not of the double mutant lacking only the plasma membrane transporters. These data strongly suggest a role for RiCTR2 in mobilization of vacuolar Cu stores, which is supported by up-regulation of *RiCTR2* expression when the ERM was grown under the severe Cu deficient conditions. Therefore, as it has been shown for the *S. cerevisiae* plasma membrane transporters Ctr1 and Ctr3 (Dancis et al., 1994a; Peña et al., 2000) and the vacuolar transporter Ctr2 (Rees et al., 2004), RiCTR1 is required to facilitate Cu acquisition under Cu deficient conditions and RiCTR2 to mobilize Cu vacuolar stores when Cu levels are extremely low.

Interestingly, *RiCTR1* and *RiCTR2* transcript levels raised in the ERM in response to H_2O_2. A potential explanation could be that under these conditions RiCTR1 and RiCTR2 are needed to increase Cu availability for Cu/Zn-superoxide dismutase, one of the cofactors needed for its reactive oxygen species scavenging activity. In fact, yeast cells lacking CTR transporters show oxidative stress sensitive phenotypes linked with an insufficient delivery of Cu, either from the external environment or from the vacuolar reserves, to the Cu/Zn superoxide dismutase (Dancis et al., 1994a; Knight et al., 1996). These data suggest, therefore, a role for Cu in oxidative stress protection in *R. irregularis*.

As reported for the *R. irregularis* genes *RiPT* (Fiorilli et al., 2013) *RiAMT1-3* (Pérez-Tienda et al., 2011; Calabrese et al., 2016) and *RiFTR1* (Tamayo et al., 2018) encoding, respectively, plasma membrane phosphate, ammonium and iron transporters, *RiCTR1* and *RiCTR2* mRNAs were detected in the IRM. Expression of *RiCTR1* in the IRM suggests, as it has been proposed for the other fungal transporters, that there might exist a competition between the plant and the fungus for the Cu present in the apoplast of the symbiotic interface (Balestrini et al., 2007; Kiers et al., 2011). It is tempting to hypothesize that during its *in planta* phase, the fungus needs to take up Cu from the interfacial apoplast to meet its Cu demands for growth and activity. This hypothesis is supported by the observed increase of the *RiCTR1* transcript levels in the IRM when the symbiosis was developed under Cu-limiting conditions. Under these conditions, Cu released by the fungus into the apoplast of the arbuscular interface should be perceived not only by the plant but also by the fungus. Further experiments are needed to understand how Cu homeostasis is regulated at the symbiotic

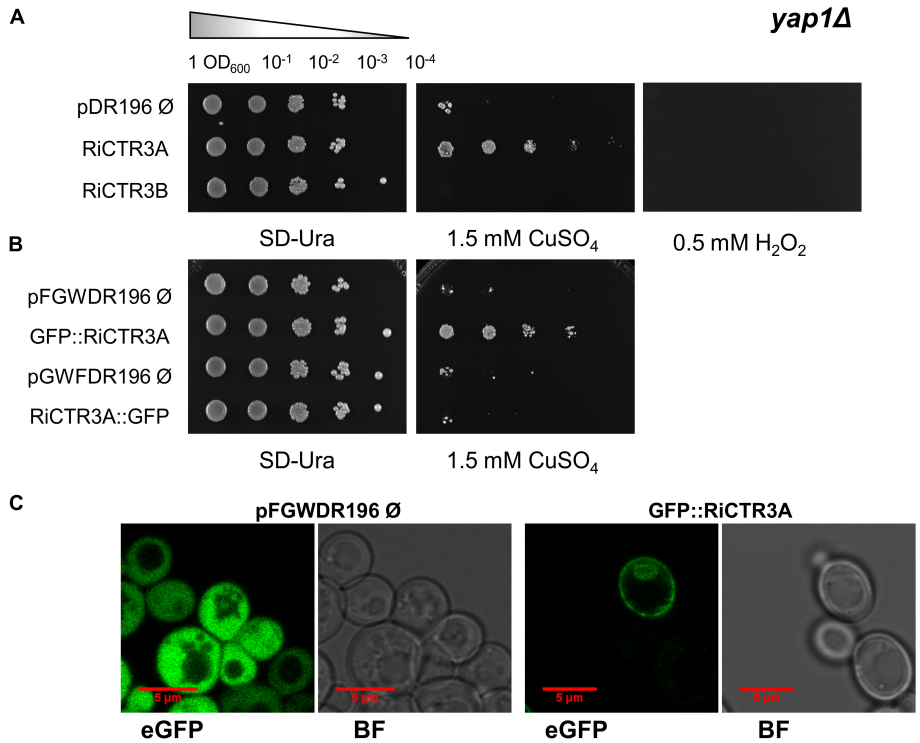

FIGURE 8 | Functional analysis of RiCTR3A and RiCTR3B in the Δ-*yap1 S. cerevisiae* mutant. **(A)** Δ-*yap1* cells transformed with the empty vector or expressing *RiCTR3A* or *RiCTR3B* were plated on SD media supplemented or not with 1.5 mM $CuSO_4$ or with 0.5 mM H_2O_2. **(B)** Δ-*yap1* cells transformed with the corresponding empty vector expressing *GFP* or N-terminal or C-terminal GFP-tagged versions of *RiCTR3A* were plated on SD media supplemented or not with 1.5 mM $CuSO_4$. Plates were incubated 4 days at 30°C. **(C)** Δ-*yap1* cells expressing *GFP* (the empty vector pFGWDR196) and *GFP::RiCTR3A* were visualized with a confocal microscope. eGFP, enhanced GFP fluorescence; BF, bright field.

interface, a process that will require fine-tuning between the plant and the fungus and that will depend on the Cu status of both symbionts. The high expression levels of *RiCTR2* in the IRM together with its up-regulation when the symbiosis was developed under Cu-deficient conditions suggest that the fungus needs to mobilize its vacuolar Cu reserves to support its growth and metabolism. Overall, these data indicate that the fungus has a high Cu demand for growth and activity within the roots, which is supported by the observation that root colonization and arbuscule development are inhibited when the symbiosis was developed under Cu-deficient conditions. The requirement of Cu for AM fungal colonization it is not surprising given that this transition metal is an essential micronutrient that acts as cofactor of key enzymes involved in a wide array of biochemical processes essential for growth (Pena et al., 1999; Festa and Thiele, 2011).

Unlike RiCTR1 and RiCTR2, none of the *RiCTR3* gene products seem to have a role in Cu transport. RiCTR3A presents the typical topology of CTR proteins but lacks the conserved Met/Cys-X-Met motif near the first TM domain that is strictly required for Cu transport; and RiCTR3B has a single TM domain. As expected, neither RiCTR3A nor RiCTR3B restored the respiratory defect of the CTR mutant yeasts. Furthermore, their gene expression patterns in response to external Cu presented the opposite trend of a protein that mediates Cu transport into the cytosol, as both were transiently up-regulated when the ERM was exposed to high Cu levels. The strong up-regulation of *RiCTR3A* expression in the Cu-treated ERM together with the capability of its gene product to revert metal sensitivity of the Δ*yap-1* yeast cells suggest that RiCTR3A is involved in metal tolerance in the ERM. Given that RiCTR3A was unable to complement oxidative stress sensitivity of the Δ*yap-1* mutant and that a functional GFP-RiCTR3A fusion protein was localized to the Δ*yap-1* plasma membrane, it is temping to hypothesize that RiCTR3A might function as a Cu sensor that activates downstream signal transduction pathways involved in Cu tolerance. Nutrient sensing in fungi is mediated by different classes of plasma membrane proteins that activate downstream signaling pathways, such as non-transporting receptors, transceptors and G-proteins-coupled receptors (Van Dijck et al., 2017). Non-transporting receptors are structural homologs to nutrient transporters that have lost their transport capacity while gaining a receptor function (Conrad et al., 2014). It is believed that these transporter-like proteins are used as sensors for the nutrient they likely once transported previously in evolution. This is the case of the *S. cerevisiae* glucose receptors Snf3 and Rgt2, structural homologs glucose transporters that sense availability of external glucose but cannot transport glucose (Ozcan et al., 1998), and of the nitrogen receptor SSy1, a member of the amino acid permease family that does not transport

amino acids but senses them at the plasma membrane (Klasson et al., 1999). Despite failure of RiCTR3A to complement the mutant phenotype of the yeast CTR mutants could be an artifact of the heterologous system, the absence in its N-terminal end of the Met/Cys-X-Met motif that is strictly required for CTR function supports the hypothesis that RiCTR3A does not have Cu transport activity. Although micronutrient receptors have been not reported yet, the yeast iron transporter Ftr1 and the zinc transporter Ztr1 have recently been identified as the first micronutrient transceptors, since they present both transport and receptor functions (Schothorst et al., 2017). RiCTR3A might be the first described micronutrient receptor. However, further studies are required to confirm this hypothesis.

Unfortunately, we could not assign a role to *RiCTR3B*, the intron-retaining transcript of *RiCTR3*. Alternative splicing variants of CTR genes have been previously described in other fungi, such as *C. gloeosporioides* (Barhoom et al., 2008) and *N. crassa* (Korripally et al., 2010). However, in contrast with what happens with the protein encoded by *RiCTR3B*, the predicted proteins of the two spliced variants of the *C. gloeosporioides CTR2* gene and of the *N. crassa* TCU-2 present all the characteristic features of CTR proteins and their gene products are fully functional in the yeast Ctr triple mutant. Since intron retention in *RiCTR3B* produces a frame shift that generates a premature termination codon, it is possible that the alternative *RiCTR3* protein RiCTR3B is not produced. If that were the case, as it has been described for other fungi (Gonzalez-Hilarion et al., 2016), intron retention might be a post-transcriptional mechanism to regulate *RiCTR3* gene expression. A systemic genome-wide comparative analysis of alternative splicing in 23 fungal species has revealed that most of the alternative splicing-affected genes encode proteins that mediate the stress response (Grutzmann et al., 2014). Interestingly, RiCTR3A seems to be involved in the ERM response to Cu toxicity. The finding that both *RiCTR3* splicing variants were differentially expressed during Cu and oxidative stress agrees with previous observations in several human pathogenic fungi that the expression of a certain isoform is not exclusive to a certain condition and that the ratio between expressed isoforms changes (Sieber et al., 2018). These authors suggested that alternative splicing is important in fungi for adaptation and stress tolerance via the generation of suitable splice variants. The higher expression levels of the *RiCTR3A,* the transcript lacking the first intron, under Cu toxicity suggests that alternative splicing may be a mechanism to control the activation of the RiCTR3A protein during Cu stress. The finding that *RiCTR3B* expression increased in the H_2O_2-exposed ERM suggests that it might play a role in oxidative stress tolerance. However, further studies are needed to determine whether *RiCTR3B* encodes a functional protein and the significance of the alternative splicing of *RiCTR3*.

CONCLUSION

Here, we show for the first time that the AM fungus *R. irregularis* expresses two genes encoding Cu transporters of the CTR family, *RiCTR1* and *RiCTR2,* and two alternative spliced variants of a third gene, *RiCTR3*. *RiCTR3A*, the shortest spliced variant of *RiCTR3*, encodes a protein that is likely involved in Cu tolerance while *RiCTR3B* might contribute to oxidative stress protection. Our data also show for the first time the requirement of Cu for AM fungal colonization.

DATA AVAILABILITY

The raw data supporting the conclusions of this manuscript will be made available by the authors, without undue reservation, to any qualified researcher.

AUTHOR CONTRIBUTIONS

TG-G performed the majority of the experimental work. KB, MM, and AJ-J contributed to RiCTR2 characterization. CA and PB contributed to the protein localization assays. NF defined the research theme, supervised all the experiments, and coordinated the research project. TG and NF contributed to data interpretations and wrote the manuscript. All authors have revised and approved the manuscript.

FUNDING

This research was supported by the Spanish Ministry of Science, Innovation and Universities (MINECO) through projects AGL2012-35611, AGL2015-67098-R, and RTI2018-098756-B-I00, and by the Consejería de Salud (CS) of the Junta de Andalucía through the research grant PI-0014-2016. TG-G was supported by a Ph.D. contract (FPI) from the MINECO and KB by a Nicolás Monardes (0088/2018) contract. CSIC Library covered part of the open access publication fees.

ACKNOWLEDGMENTS

We are grateful to Ascensión Valderas for excellent technical assistance.

SUPPLEMENTARY MATERIAL

The Supplementary Material for this article can be found online at: https://www.frontiersin.org/articles/10.3389/fpls.2019.00604/full#supplementary-material

REFERENCES

Aller, S. G., Eng, E. T., De Feo, C. J., and Unger, V. M. (2004). Eukaryotic CTR copper uptake transporters require two faces of the third transmembrane domain for helix packing, oligomerization, and function. *J. Biol. Chem.* 279, 53435–53441. doi: 10.1074/jbc.M409421200

Balestrini, R., Gómez-Ariza, J., Lanfranco, L., and Bonfante, P. (2007). Laser microdissection reveals that transcripts for five plant and one fungal phosphate transporter genes are contemporaneously present in arbusculated cells. *Mol. Plant Microb. Interact.* 20, 1055–1062. doi: 10.1094/mpmi-20-9-1055

Barhoom, S., Kupiec, M., Zhao, X., Xu, J.-R., and Sharon, A. (2008). Functional characterization of CgCTR2, a putative vacuole copper transporter that is involved in germination and pathogenicity in *Colletotrichum gloeosporioides*. *Eukaryot. Cell* 7, 1098–1108. doi: 10.1128/ec.00109-07

Beaudoin, J., Thiele, D. J., Labbé, S., and Puig, S. (2011). Dissection of the relative contribution of the *Schizosaccharomyces pombe* Ctr4 and Ctr5 proteins to the copper transport and cell surface delivery functions. *Microbiology* 157, 1021–1031. doi: 10.1099/mic.0.046854-0

Bellemare, D. R., Shaner, L., Morano, K. A., Beaudoin, J., Langlois, R., and Labbe, S. (2002). Ctr6, a vacuolar membrane copper transporter in *Schizosaccharomyces pombe*. *J. Biol. Chem.* 277, 46676–46686. doi: 10.1074/jbc.M206444200

Benabdellah, K., Gonzalez-Rey, E., and Gonzalez, A. (2007). Alternative trans-splicing of the *Trypanosoma cruzi* LYT1 gene transcript results in compartmental and functional switch for the encoded protein. *Mol. Microbiol.* 65, 1559–1567. doi: 10.1111/j.1365-2958.2007.05892.x

Benabdellah, K., Merlos, M. A., Azcón-Aguilar, C., and Ferrol, N. (2009). GintGRX1, the first characterized glomeromycotan glutaredoxin, is a multifunctional enzyme that responds to oxidative stress. *Fungal Genet. Biol.* 46, 94–103. doi: 10.1016/j.fgb.2008.09.013

Beneš, V., Hložková, K., Matěnová, M., Borovička, J., and Kotrba, P. (2016). Accumulation of Ag and Cu in *Amanita strobiliformis* and characterization of its Cu and Ag uptake transporter genes AsCTR2 and AsCTR3. *BioMetals* 29, 249–264. doi: 10.1007/s10534-016-9912-x

Black, D. L. (2003). Mechanisms of alternative pre-messenger RNA splicing. *Annu. Rev. Biochem.* 72, 291–336. doi: 10.1146/annurev.biochem.72.121801.161720

Borghouts, C., Scheckhuber, C. Q., Stephan, O., and Osiewacz, H. D. (2002). Copper homeostasis and aging in the fungal model system *Podospora anserina*: differential expression of PaCtr3 encoding a copper transporter. *Int. J. Biochem. Cell Biol.* 34, 1355–1371. doi: 10.1016/S1357-2725(02)00078-X

Calabrese, S., Pérez-Tienda, J., Ellerbeck, M., Arnould, C., Chatagnier, O., Boller, T., et al. (2016). GintAMT3 – a low-affinity ammonium transporter of the arbuscular mycorrhizal *Rhizophagus irregularis*. *Front. Plant Sci.* 7:679. doi: 10.3389/fpls.2016.00679

Chabot, S., Bécard, G., and Piché, Y. (1992). Life cycle of *Glomus intraradix* in root organ culture. *Mycologia* 84, 315–321. doi: 10.2307/3760183

Chen, E. C. H., Morin, E., Beaudet, D., Noel, J., Yildirir, G., Ndikumana, S., et al. (2018). High intraspecific genome diversity in the model arbuscular mycorrhizal symbiont *Rhizophagus irregularis*. *New Phytol.* 220, 1161–1171. doi: 10.1111/nph.14989

Conrad, M., Schothorst, J., Kankipati, H. N., Van Zeebroeck, G., Rubio-Texeira, M., and Thevelein, J. M. (2014). Nutrient sensing and signaling in the yeast *Saccharomyces cerevisiae*. *FEMS Microbiol. Rev.* 38, 254–299. doi: 10.1111/1574-6976.12065

Dancis, A., Haile, D., Yuan, D. S., and Klausner, R. D. (1994a). The *Saccharomyces cerevisiae* copper transport protein (Ctr1p). Biochemical characterization, regulation by copper, and physiologic role in copper uptake. *J. Biol. Chem.* 269, 25660–25667.

Dancis, A., Yuan, D. S., Haile, D., Askwith, C., Eide, D., Moehle, C., et al. (1994b). Molecular characterization of a copper transport protein in S. cerevisiae: an unexpected role for copper in iron transport. *Cell* 76, 393–402. doi: 10.1016/0092-8674(94)90345-X

De Feo, C. J., Aller, S. G., and Unger, V. M. (2007). A structural perspective on copper uptake in eukaryotes. *BioMetals* 20, 705–716. doi: 10.1007/s10534-006-9054-7

Dumay, Q. C., Debut, A. J., Mansour, N. M., and Saier, M. H. Jr. (2006). The copper transporter (Ctr) family of Cu+ uptake systems. *J. Mol. Microbiol. Biotechnol.* 11, 10–19. doi: 10.1159/000092815

Ferrol, N., Tamayo, E., and Vargas, P. (2016). The heavy metal paradox in arbuscular mycorrhizas: from mechanisms to biotechnological applications. *J. Exp. Bot.* 67, 6253–6265. doi: 10.1093/jxb/erw403

Festa, R. A., and Thiele, D. J. (2011). Copper: an essential metal in biology. *Curr. Biol.* 21, R877–R883. doi: 10.1016/j.cub.2011.09.040

Fiorilli, V., Lanfranco, L., and Bonfante, P. (2013). The expression of GintPT, the phosphate transporter of *Rhizophagus irregularis*, depends on the symbiotic status and phosphate availability. *Planta* 237, 1267–1277. doi: 10.1007/s00425-013-1842-z

Gietz, R. D., and Schiestl, R. H. (2007). High-efficiency yeast transformation using the LiAc/SS carrier DNA/PEG method. *Nat. Protoc.* 2, 31–34. doi: 10.1038/nprot.2007.13

Glerum, D. M., Shtanko, A., and Tzagoloff, A. (1996). Characterization of COX17, a yeast gene involved in copper metabolism and assembly of cytochrome oxidase. *J. Biol. Chem.* 271, 14504–14509. doi: 10.1074/jbc.271.24.14504

Goebels, C., Thonn, A., Gonzalez-Hilarion, S., Rolland, O., Moyrand, F., Beilharz, T. H., et al. (2013). Introns regulate gene expression in *Cryptococcus neoformans* in a Pab2p dependent pathway. *PLoS Genet.* 9:e1003686. doi: 10.1371/journal.pgen.1003686

González-Guerrero, M., Oger, E., Benabdellah, K., Azcon-Aguilar, C., Lanfranco, L., and Ferrol, N. (2010). Characterization of a CuZn superoxide dismutase gene in the arbuscular mycorrhizal fungus *Glomus intraradices*. *Curr. Genet.* 56, 265–274. doi: 10.1007/s00294-010-0298-y

Gonzalez-Hilarion, S., Paulet, D., Lee, K. T., Hon, C. C., Lechat, P., Mogensen, E., et al. (2016). Intron retention-dependent gene regulation in *Cryptococcus neoformans*. *Sci. Rep.* 6:32252. doi: 10.1038/srep32252

Grutzmann, K., Szafranski, K., Pohl, M., Voigt, K., Petzold, A., and Schuster, S. (2014). Fungal alternative splicing is associated with multicellular complexity and virulence: a genome-wide multi-species study. *DNA Res.* 21, 27–39. doi: 10.1093/dnares/dst038

Guo, Y., Smith, K., Lee, J., Thiele, D. J., and Petris, M. J. (2004). Identification of methionine-rich clusters that regulate copper-stimulated endocytosis of the human Ctr1 copper transporter. *J. Biol. Chem.* 279, 17428–17433. doi: 10.1074/jbc.M401493200

Halliwell, B., and Gutteridge, J. M. (1984). Oxygen toxicity, oxygen radicals, transition metals and disease. *Biochem. J.* 219, 1–14.

Helber, N., Wippel, K., Sauer, N., Schaarschmidt, S., Hause, B., and Requena, N. (2011). A versatile monosaccharide transporter that operates in the arbuscular mycorrhizal fungus *Glomus* sp is crucial for the symbiotic relationship with plants. *Plant Cell* 23, 3812–3823. doi: 10.1105/tpc.111.089813

Jacob, A. G., and Smith, C. W. J. (2017). Intron retention as a component of regulated gene expression programs. *Hum. Genet.* 136, 1043–1057. doi: 10.1007/s00439-017-1791-x

Jamison McDaniels, C. P., Jensen, L. T., Srinivasan, C., Winge, D. R., and Tullius, T. D. (1999). The yeast transcription factor Mac1 binds to DNA in a modular fashion. *J. Biol. Chem.* 274, 26962–26967. doi: 10.1074/jbc.274.38.26962

Jin, L., Li, G., Yu, D., Huang, W., Cheng, C., Liao, S., et al. (2017). Transcriptome analysis reveals the complexity of alternative splicing regulation in the fungus *Verticillium dahliae*. *BMC Genomics* 18:130. doi: 10.1186/s12864-017-3507-y

Kay, R., Chan, A., Daly, M., and McPherson, J. (1987). Duplication of CaMV 35S promoter sequences creates a strong enhancer for plant genes. *Science* 236, 1299–1302. doi: 10.1126/science.236.4806.1299

Kiers, E. T., Duhamel, M., Beesetty, Y., Mensah, J. A., Franken, O., Verbruggen, E., et al. (2011). Reciprocal rewards stabilize cooperation in the mycorrhizal symbiosis. *Science* 333, 880–882. doi: 10.1126/science.1208473

Kim, B.-E., Nevitt, T., and Thiele, D. J. (2008). Mechanisms for copper acquisition, distribution and regulation. *Nat. Chem. Biol.* 4, 176–185. doi: 10.1038/nchembio.72

Klasson, H., Fink, G. R., and Ljungdahl, P. O. (1999). Ssy1p and Ptr3p are plasma membrane components of a yeast system that senses extracellular amino acids. *Mol. Cell Biol.* 19, 5405–5416. doi: 10.1128/MCB.19.8.5405

Knight, S. A., Labbé, S., Kwon, L. F., Kosman, D. J., and Thiele, D. J. (1996). A widespread transposable element masks expression of a yeast copper transport gene. *Genes Dev.* 10, 1917–1929. doi: 10.1101/gad.10.15.1917

Kobayashi, Y., Maeda, T., Yamaguchi, K., Kameoka, H., Tanaka, S., Ezawa, T., et al. (2018). The genome of *Rhizophagus clarus* HR1 reveals a common genetic basis for auxotrophy among arbuscular mycorrhizal fungi. *BMC Genomics* 19:465. doi: 10.1186/s12864-018-4853-0

Kornblihtt, A. R., Schor, I. E., Allo, M., Dujardin, G., Petrillo, E., and Munoz, M. J. (2013). Alternative splicing: a pivotal step between eukaryotic transcription and translation. *Nat. Rev. Mol. Cell Biol.* 14, 153–165. doi: 10.1038/nrm3525

Korripally, P., Tiwari, A., Haritha, A., Kiranmayi, P., and Bhanoori, M. (2010). Characterization of Ctr family genes and the elucidation of their role in the life cycle of *Neurospora crassa*. *Fungal Genet. Biol.* 47, 237–245. doi: 10.1016/j.fgb.2009.12.006

Kropat, J., Tottey, S., Birkenbihl, R. P., Depege, N., Huijser, P., and Merchant, S. (2005). A regulator of nutritional copper signaling in *Chlamydomonas* is an SBP domain protein that recognizes the GTAC core of copper response element. *Proc. Natl. Acad. Sci. U.S.A.* 102, 18730–18735. doi: 10.1073/pnas.0507693102

Kuge, S., and Jones, N. (1994). YAP1 dependent activation of TRX2 is essential for the response of *Saccharomyces cerevisiae* to oxidative stress by hydroperoxides. *EMBO J.* 13, 655–664.

Lanfranco, L., Fiorilli, V., and Gutjahr, C. (2018). Partner communication and role of nutrients in the arbuscular mycorrhizal symbiosis. *New Phytol.* 220, 1031–1046. doi: 10.1111/nph.15230

Le Hir, H., Nott, A., and Moore, M. J. (2003). How introns influence and enhance eukaryotic gene expression. *Trends Biochem. Sci.* 28, 215–220. doi: 10.1016/s0968-0004(03)00052-5

Lee, Y.-J., and George, E. (2005). Contribution of mycorrhizal hyphae to the uptake of metal cations by cucumber plants at two levels of phosphorus supply. *Plant Soil* 278, 361–370. doi: 10.1007/s11104-005-0373-1

Lehmann, A., and Rillig, M. C. (2015). Arbuscular mycorrhizal contribution to copper, manganese and iron nutrient concentrations in crops – a meta-analysis. *Soil Biol. Biochem.* 81, 147–158. doi: 10.1016/j.soilbio.2014.11.013

Li, X.-L., Marschner, H., and George, E. (1991). Acquisition of phosphorus and copper by VA-mycorrhizal hyphae and root-to-shoot transport in white clover. *Plant Soil* 136, 49–57. doi: 10.1007/bf02465219

Linder, M. C. (1991). *The Biochemistry of Copper*. New York, NY: Plenum Press.

Livak, K. J., and Schmittgen, T. D. (2001). Analysis of relative gene expression data using real-time quantitative PCR and the 2(-Delta Delta C(T)) method. *Methods* 25, 402–408. doi: 10.1006/meth.2001.1262

Macomber, L., and Imlay, J. A. (2009). The iron-sulfur clusters of dehydratases are primary intracellular targets of copper toxicity. *Proc. Natl. Acad. Sci. U.S.A.* 106, 8344–8349. doi: 10.1073/pnas.0812808106

Marvin, M. E., Williams, P. H., and Cashmore, A. M. (2003). The *Candida albicans* CTR1 gene encodes a functional copper transporter. *Microbiology* 149, 1461–1474. doi: 10.1099/mic.0.26172-0

Merlos, M. A., Zitka, O., Vojtech, A., Azcón-Aguilar, C., and Ferrol, N. (2016). The arbuscular mycorrhizal fungus *Rhizophagus irregularis* differentially regulates the copper response of two maize cultivars differing in copper tolerance. *Plant Sci.* 253, 68–76. doi: 10.1016/j.plantsci.2016.09.010

Mockenhaupt, S., and Makeyev, E. V. (2015). Non-coding functions of alternative pre-mRNA splicing in development. *Semin. Cell Dev. Biol.* 4, 32–39. doi: 10.1016/j.semcdb.2015.10.018

Morin, E., Miyauchi, S., San Clemente, H., Chen, E. C., Pelin, A., de la Providencia, I., et al. (2019). Comparative genomics of *Rhizophagus irregularis*, *R. cerebriforme*, *R. diaphanus* and *Gigaspora rosea* highlights specific genetic features in Glomeromycotina. *New Phytol.* 222, 1584–1598. doi: 10.1111/nph.15687

Nakagawa, Y., Kikuchi, S., Sakamoto, Y., and Yano, A. (2010). Identification and characterization of CcCTR1, a copper uptake transporter-like gene, in *Coprinopsis cinerea*. *Microbiol. Res.* 165, 276–287. doi: 10.1016/j.micres.2009.05.004

Ozcan, S., Dover, J., and Johnston, M. (1998). Glucose sensing and signaling by two glucose receptors in the yeast *Saccharomyces cerevisiae*. *EMBO J.* 17, 2566–2573. doi: 10.1093/emboj/17.9.2566

Pena, M. M., Lee, J., and Thiele, D. J. (1999). A delicate balance: homeostatic control of copper uptake and distribution. *J. Nutr.* 129, 1251–1260. doi: 10.1093/jn/129.7.1251

Peña, M. M. O., Koch, K. A., and Thiele, D. J. (1998). Dynamic regulation of copper uptake and detoxification genes in *Saccharomyces cerevisiae*. *Mol. Cell. Biol.* 18, 2514–2523.

Peña, M. M. O., Puig, S., and Thiele, D. J. (2000). Characterization of the *Saccharomyces cerevisiae* high affinity copper transporter Ctr3. *J. Biol. Chem.* 275, 33244–33251. doi: 10.1074/jbc.M005392200

Penas, M. M., Azparren, G., Dominguez, A., Sommer, H., Ramirez, L., and Pisabarro, A. G. (2005). Identification and functional characterisation of ctr1, a *Pleurotus ostreatus* gene coding for a copper transporter. *Mol. Genet. Genomics* 274, 402–409. doi: 10.1007/s00438-005-0033-4

Pepe, A., Sbrana, C., Ferrol, N., and Giovannetti, M. (2017). An *in vivo* whole-plant experimental system for the analysis of gene expression in extraradical mycorrhizal mycelium. *Mycorrhiza* 27, 659–668. doi: 10.1007/s00572-017-0779-7

Pérez-Tienda, J., Testillano, P. S., Balestrini, R., Fiorilli, V., Azcón-Aguilar, C., and Ferrol, N. (2011). GintAMT2, a new member of the ammonium transporter family in the arbuscular mycorrhizal fungus *Glomus intraradices*. *Fungal Genet. Biol.* 48, 1044–1055. doi: 10.1016/j.fgb.2011.08.003

Phillips, J. M., and Hayman, D. S. (1970). Improved procedures for clearing roots and staining parasitic and vesicular-arbuscular mycorrhizal fungi for rapid assessment of infection. *Trans. Br. Mycol. Soc.* 55, 158–161. doi: 10.1016/S0007-1536(70)80110-3

Portnoy, M. E., Schmidt, P. J., Rogers, R. S., and Culotta, V. C. (2001). Metal transporters that contribute copper to metallochaperones in *Saccharomyces cerevisiae*. *Mol. Genet. Genomics* 265, 873–882. doi: 10.1007/s004380100482

Pozo, M. J., Jung, S. C., Martínez-Medina, A., López-Ráez, J. A., Azcón-Aguilar, C., and Barea, J.-M. (2013). "Root allies: arbuscular mycorrhizal fungi help plants to cope with biotic stresses," in *Symbiotic Endophytes*, ed. R. Aroca (Berlin: Springer), 289–307.

Puig, S. (2014). Function and regulation of the plant COPT family of high-affinity copper transport proteins. *Adv. Bot.* 2014:476917. doi: 10.1155/2014/476917

Puig, S., Lee, J., Lau, M., and Thiele, D. J. (2002). Biochemical and genetic analyses of yeast and human high affinity copper transporters suggest a conserved mechanism for copper uptake. *J. Biol. Chem.* 277, 26021–26030. doi: 10.1074/jbc.M202547200

Puig, S., and Thiele, D. J. (2002). Molecular mechanisms of copper uptake and distribution. *Curr. Opin. Chem. Biol.* 6, 171–180. doi: 10.1016/S1367-5931(02)00298-3

Rees, E. M., Lee, J., and Thiele, D. J. (2004). Mobilization of intracellular copper stores by the Ctr2 vacuolar copper transporter. *J. Biol. Chem.* 279, 54221–54229. doi: 10.1074/jbc.M411669200

Ruiz-Lozano, J. M. (2003). Arbuscular mycorrhizal symbiosis and alleviation of osmotic stress. New perspectives for molecular studies. *Mycorrhiza* 13, 309–317. doi: 10.1007/s00572-003-0237-6

Schothorst, J., Zeebroeck, G. V., and Thevelein, J. M. (2017). Identification of Ftr1 and Zrt1 as iron and zinc micronutrient transceptors for activation of the PKA pathway in *Saccharomyces cerevisiae*. *Microb. Cell* 4, 74–89. doi: 10.15698/mic2017.03.561

Sieber, P., Voigt, K., Kämmer, P., Brunke, S., Schuster, S., and Linde, J. (2018). Comparative study on alternative splicing in human fungal pathogens suggests its involvement during host invasion. *Front. Microbiol.* 9:2313. doi: 10.3389/fmicb.2018.02313

Smith, A. D., Logeman, B. L., and Thiele, D. J. (2017). Copper acquisition and utilization in fungi. *Annu. Rev. Microbiol.* 71, 597–623. doi: 10.1146/annurev-micro-030117-020444

Smith, S. E., and Read, D. J. (2008). *Mycorrhizal Symbiosis*, 3rd Edn. London: Academic Press.

Spatafora, J. W., Chang, Y., Benny, G. L., Lazarus, K., Smith, M. E., Berbee, M. L., et al. (2016). A phylum-level phylogenetic classification of zygomycete fungi based on genome-scale data. *Mycologia* 108, 1028–1046. doi: 10.3852/16-042

St-Arnaud, M., Hamel, C., Vimard, B., Caron, M., and Fortin, J. A. (1996). Enhanced hyphal growth and spore production of the arbuscular mycorrhizal fungus *Glomus intraradices* in an *in vitro* system in the absence of host roots. *Mycol. Res.* 100, 328–332. doi: 10.1016/S0953-7562(96)80164-X

Sun, X., Chen, W., Ivanov, S., MacLean, A. M., Wight, H., Ramaraj, T., et al. (2019). Genome and evolution of the arbuscular mycorrhizal fungus *Diversispora epigaea* (formerly *Glomus versiforme*) and its bacterial endosymbionts. *New Phytol.* 221, 1556–1573. doi: 10.1111/nph.15472

Tamayo, E., Gómez-Gallego, T., Azcón-Aguilar, C., and Ferrol, N. (2014). Genome-wide analysis of copper, iron and zinc transporters in the arbuscular

mycorrhizal fungus *Rhizophagus irregularis*. *Front. Plant Sci.* 5:547. doi: 10.3389/fpls.2014.00547

Tamayo, E., Knight, S. A. B., Valderas, A., Dancis, A., and Ferrol, N. (2018). The arbuscular mycorrhizal fungus *Rhizophagus irregularis* uses a reductive iron assimilation pathway for high-affinity iron uptake. *Environ. Microbiol.* 20, 1857–1872. doi: 10.1111/1462-2920.14121

Toone, W. M., and Jones, N. (1999). AP-1 transcription factors in yeast. *Curr. Opin. Genet. Dev.* 9, 55–61. doi: 10.1016/S0959-437X(99)80008-2

Trouvelot, A., Kough, J., and Gianinazzi-Pearson, V. (1986). "Evaluation of VA infection levels in root systems. Research for estimation methods having a functional significance," in *Physiological and Genetical Aspects of Mycorrhizae*, eds V. Gianinazzi-Pearsonand and S. Gianinazzi (Paris: INRA), 217–221.

Van Dijck, P., Brown, N. A., Goldman, G. H., Rutherford, J., Xue, C., and Van Zeebroeck, G. (2017). Nutrient sensing at the plasma membrane of fungal cells. *Microbiol. Spectr.* 5, 419–439. doi: 10.1128/microbiolspec.FUNK-0031-2016

Wu, X., Sinani, D., Kim, H., and Lee, J. (2009). Copper transport activity of yeast Ctr1 is down-regulated via its C terminus in response to excess copper. *J. Biol. Chem.* 284, 4112–4122. doi: 10.1074/jbc.M807909200

Xiao, Z., Loughlin, F., George, G. N., Howlett, G. J., and Wedd, A. G. (2004). C-terminal domain of the membrane copper transporter Ctr1 from *Saccharomyces cerevisiae* binds four Cu(I) ions as a cuprous-thiolate polynuclear cluster: sub-femtomolar Cu(I) affinity of three proteins involved in copper trafficking. *J. Am. Chem. Soc.* 126, 3081–3090. doi: 10.1021/ja039 0350

Conflict of Interest Statement: The authors declare that the research was conducted in the absence of any commercial or financial relationships that could be construed as a potential conflict of interest.

frontiers in Microbiology

ORIGINAL RESEARCH
published: 13 August 2019
doi: 10.3389/fmicb.2019.01807

Transcriptomic Responses to Water Deficit and Nematode Infection in Mycorrhizal Tomato Roots

Raffaella Balestrini[1]†, Laura C. Rosso[1], Pasqua Veronico[1], Maria Teresa Melillo[1], Francesca De Luca[1], Elena Fanelli[1], Mariantonietta Colagiero[1], Alessandra Salvioli di Fossalunga[2], Aurelio Ciancio[1] and Isabella Pentimone[1]†*

[1] Consiglio Nazionale delle Ricerche, Istituto per la Protezione Sostenibile delle Piante, Turin, Italy, [2] Dipartimento di Scienze della Vita e Biologia dei Sistemi, Università di Torino, Turin, Italy

Climate changes include the intensification of drought in many parts of the world, increasing its frequency, severity and duration. However, under natural conditions, environmental stresses do not occur alone, and, in addition, more stressed plants may become more susceptible to attacks by pests and pathogens. Studies on the impact of the arbuscular mycorrhizal (AM) symbiosis on tomato response to water deficit showed that several drought-responsive genes are differentially regulated in AM-colonized tomato plants (roots and leaves) during water deficit. To date, global changes in mycorrhizal tomato root transcripts under water stress conditions have not been yet investigated. Here, changes in root transcriptome in the presence of an AM fungus, with or without water stress (WS) application, have been evaluated in a commercial tomato cultivar already investigated for the water stress response during AM symbiosis. Since root-knot nematodes (RKNs, *Meloidogyne incognita*) are obligate endoparasites and cause severe yield losses in tomato, the impact of the AM fungal colonization on RKN infection at 7 days post-inoculation was also evaluated. Results offer new information about the response to AM symbiosis, highlighting a functional redundancy for several tomato gene families, as well as on the tomato and fungal genes involved in WS response during symbiosis, underlying the role of the AM fungus. Changes in the expression of tomato genes related to nematode infection during AM symbiosis highlight a role of AM colonization in triggering defense responses against RKN in tomato. Overall, new datasets on the tomato response to an abiotic and biotic stress during AM symbiosis have been obtained, providing useful data for further researches.

Keywords: abiotic stress, AM symbiosis, RKN, transcriptomics, stress response

OPEN ACCESS

Edited by:
Carolina Escobar, University of Castilla–La Mancha, Spain

Reviewed by:
Tina Kyndt, Ghent University, Belgium
Juan Manuel Ruiz-Lozano, Spanish National Research Council (CSIC), Spain

***Correspondence:**
Raffaella Balestrini
raffaella.balestrini@ipsp.cnr.it

† These authors have contributed equally to this work

Specialty section:
This article was submitted to Plant Microbe Interactions, a section of the journal Frontiers in Microbiology

Received: *24 May 2019*
Accepted: *22 July 2019*
Published: *13 August 2019*

Citation:
Balestrini R, Rosso LC, Veronico P, Melillo MT, De Luca F, Fanelli E, Colagiero M, Salvioli di Fossalunga A, Ciancio A and Pentimone I (2019) Transcriptomic Responses to Water Deficit and Nematode Infection in Mycorrhizal Tomato Roots. Front. Microbiol. 10:1807. doi: 10.3389/fmicb.2019.01807

INTRODUCTION

Drought is a devastating environmental condition that dramatically affects plant growth and crop production. Its adverse impact on global food security is mostly severe in semi-arid and arid regions from many parts of the world (Boyer, 1982). Additionally, climate changes are intensifying the frequency, duration and severity of drought in many agro-environments. In response to drought, domesticated plants rely on a number of physiological and structural adaptations to counteract water deficit or at least to escape most severe effects, as a result of selection for

local cropping environments. The understanding of these adaptive mechanisms may be useful to sustain crop production, as well as for developing future breeding strategies. In addition to leaves, also roots, which are the first organ to detect a water deficit, are subjected to several modifications under drought, increasing water uptake and regulating water traffic between plant and soil (Gamboa-Tuz et al., 2018).

Water limiting conditions lead to changes in the expression of drought responsive genes in different plant tissues (Shinozaki and Yamaguchi-Shinozaki, 2007). Advances in technology, i.e., the development of -omics approaches, flanked by a parallel progress for *in silico* analyses, allowed the elucidation of the molecular mechanisms involved in the response to water deficit, in model and non-model plants. These include several economically important crops such as maize, rice, poplar, tomato, wheat or tropical fruits such as papaya (Kakumanu et al., 2012; Oono et al., 2014; Barghini et al., 2015; Gamboa-Tuz et al., 2018; Iovieno et al., 2018).

Tomato (*Solanum lycopersicum* L.) is one of the major horticultural crops cultivated worldwide and is a key component of the diet of many billion people. It has been reported that modern cultivars are sensitive to water deficit, which leads to a reduction in seed development and germination, impairing vegetative growth and reproduction (Iovieno et al., 2018). These authors exposed tomato plants to two cycles of prolonged drought stress and a single recovery by re-watering. Transcriptome datasets were generated for multiple time points during the stress and recovery cycles. Results allowed the identification and comprehension of the coordinated responses taking place under drought stress and subsequent recovery in leaves, highlighting the transcriptomic changes that control such physiological modifications (Iovieno et al., 2018).

Apart of abiotic stressors, plants interact in their environment with a complex soil and epiphytic microbiome, including both beneficial and noxious microorganisms. The mutualistic symbiosis established by arbuscular mycorrhizal (AM) fungi with the roots of most crops, have an important role in sustaining yields, as they act as bio-fertilizers and bio-protectors against both abiotic and biotic stresses (Balestrini et al., 2018). The latter include several soil pathogens and pests including plant parasitic nematodes (Schouteden et al., 2015). Root-knot nematodes (RKN; *Meloidogyne* species) are among the most devastating plant-parasitic nematodes (Jones et al., 2013). Having a wide host range, they cause large economic losses in cultivated plants that are expected to increase as a result of climate change leading water depletion and crop systems intensification. The increasing concern about the environmental impact of traditional nematicides have stimulated research for alternative control practices, including the use of biological control organisms. AM fungi have been reported to be effective against different pathogens and pests (Selosse et al., 2014; Martinez-Medina et al., 2016) and could represent a new environmental-friendly strategy to control nematode infection (Elsen et al., 2008; Vos et al., 2012; Schouteden et al., 2015; Sharma and Sharma, 2017).

Tomato has already been used as a crop model to study AM-colonized plants (Balestrini et al., 2018) as well as nematode–plant interactions (Portillo et al., 2013; Iberkleid et al., 2015; Shukla et al., 2018). Large-scale gene expression analyses have been carried out in mycorrhizal tomato plants using microarrays to identify genes differentially expressed (DE) in roots and shoots of AM-colonized plants (Fiorilli et al., 2009), as well as during the early interaction stages (Dermatsev et al., 2010). A deep sequencing of root transcriptome, using a wild-type tomato and a mutant incapable of supporting a functional AM symbiosis, showed the expression of several genes associated to AM symbiosis (Ruzicka et al., 2013). Comparison between transcriptomic profiles of tomato and *Lotus* AM-colonized roots has also been performed, suggesting that a certain proportion of AM-responsive genes are conserved across plant species (Sugimura and Saito, 2017). The authors also highlighted the fact that species-dependent AM-responsive genes might be related to specific root features, characterizing each host plant.

Several studies have been carried out on the impact of the AM symbiosis on the tomato response to water deficit (Dell'Amico et al., 2002; Subramanian et al., 2006; Aroca et al., 2008; Wang et al., 2014; Chitarra et al., 2016; Ruiz-Lozano et al., 2016; Rivero et al., 2018; Volpe et al., 2018). Targeted approaches already showed that several drought-responsive genes are differentially regulated in AM-colonized tomato plants (roots and leaves) during water deficit (Chitarra et al., 2016; Ruiz-Lozano et al., 2016). However, global changes in transcripts of mycorrhizal tomato roots, as affected by a water stress condition, have not yet been investigated, as this interaction was thus far studied only in AM-colonized bean roots (Recchia et al., 2018). We hence studied changes in the whole root transcriptome of *S. lycopersicum cv* San Marzano nano, which was previously tested to evaluate the impact of the AM symbiosis on the tomato water stress responses (Chitarra et al., 2016; Volpe et al., 2018). These previous works showed that the AM symbiosis positively affects the tomato tolerance to water deficit and how the adaptive plant response is dependent on the AM fungal species involved. Additionally, Volpe et al. (2018) have evaluated the impact of the colonization on tomato plants subjected to combined stresses (moderate water stress and aphid infestation) in controlled conditions. A positive effect on the tomato indirect defense toward aphids in terms of enhanced attractiveness toward their natural enemies was observed, as also supported by the characterization of volatile organic compound (VOC) released. In the present study, new information on the role of AM symbiosis to enhance crop tolerance to abiotic and biotic stresses in a global climatic change scenario has been obtained. In detail, changes induced in the transcriptome profile in roots colonized with the AM fungus *Rhizophagus intraradices* (i) in the presence of a moderate-water stress (abiotic stress), and (ii) following parasitism by the root-knot nematode *Meloidogyne incognita* (biotic stress) have been evaluated.

MATERIALS AND METHODS

Plant Material and Growth Conditions

The *S. lycopersicum* 'San Marzano nano' genotype, important for its consumption in Italy, was used. Tomato seeds were surface sterilized in sodium hypochlorite for 20 min, washed

five times in sterile water, and germinated on wet paper. Seedlings were then moved to pots containing a mixture of quartz sand (50%), sterile pumice (20%), and an inoculum (30%) of *R. intraradices* (FR 121), containing AM fungal propagules (spores, mycelium and mycorrhizal root pieces) in a carrier of mixed inert mineral, purchased from MycAgro Lab (Dijon, France). For non-inoculated plants, the sterile inoculum carrier was used alone, instead of the specific inoculum. The plants were maintained in a growth chamber under controlled conditions at 25°C, with a light intensity of 150 μmol/m^2/s and a 16 h:8 h light/dark cycle.

Water Stress Treatment

Plants were abundantly irrigated with filtered tap water (twice a week) and Long Ashton solution containing 300 μM of inorganic phosphate (once a week) for 35 days prior the imposition of a moderate water stress treatment. Considered treatments were: (i) AM fungal colonization [non-colonized (C), *R. intraradices*-colonized (AM)] and (ii) water stress [none (unstressed or NS), moderate (WS) as described in Volpe et al. (2018)]. Nine replicates for each group (C, AM, WS, AM_WS) have been used, arranged in a randomized block design. Before starting the treatments, pots were weighed. Control plants were regularly watered throughout the entire experimental period whereas plants to be stressed were not watered until the pots reached a loss of about 210–220 g of the initial weight, a loss previously described to be needed to reach a moderate WS condition (Volpe et al., 2018). From this moment the plants received the amount of water or nutritive solution required to get them back to their last weight, in order to maintain a moderate stress level. At the end of the experiment (i.e., after 9 weeks), roots were sampled and 60 randomly chosen 1-cm-long root segments per 2 plants were stained with 0.1% cotton blue in lactic acid, to evaluate the presence of the AM fungus, before the RNA extraction. Due to the low quantity of root materials, mainly in the WS treatments, AM fungal colonization has been only qualitatively evaluated.

Nematode Infection Assay

Control and AM-colonized 8-week-old plants were inoculated with 1200 freshly hatched juveniles of *Meloidogyne incognita* per plant. Juveniles were collected from egg masses of infested tomato roots, which were allowed to hatch in water in a growth chamber at 25°C. At 7 days post-nematode inoculation (dpi) roots were harvested. Root galls from infected colonized (RKN_AM) and uncolonized (RKN) tomato plants were hand-picked and pooled in two biological replicates for each treatment. Samples were immediately frozen in liquid nitrogen and stored at −80°C until RNA-Seq experiments.

Histological Observations

Galls at 7 dpi from AM-colonized and non-colonized tomato roots were hand-dissected under a stereomicroscope. At least five to ten galls were excised from each plant and fixed in a mixture of 1.5% glutaraldehyde and 3% paraformaldehyde (Sigma-Aldrich), dehydrated in ethanol and embedded in acrylic resin LR White (Sigma, St. Louis, MO, United States) according to Melillo et al. (2014). Embedded galls were cut in serial cross-semithin sections (2.5 μm) through all their length, then stained briefly with 1% toluidine blue in 1% borax solution and mounted in Depex. Microscopic observations were performed using bright-field optics on a Leica DM 4500 B light microscope equipped with a Leica DFC 450C camera.

RNA Extraction and Sequencing

Six different treatments (C, WS, AM, RKN, AM_WS, RKN_AM) were set up to study the response in tomato roots. Total RNAs were extracted from root samples (two independent replicates for each treatment) using a RNeasy Plant Mini Kit (Qiagen, La Jolla, CA, United States) with addition of an on-column DNase I digestion, following the manufacturer's protocol. RNA quantity and quality were determined with a Nanodrop 2000 spectrophotometer (Thermo Fisher Scientific Inc., Wilmington, DE, United States) and sent to IGA Technology Services (Udine, Italy)[1]. cDNA libraries were prepared from 4 μg total RNA using TruSeq RNA Sample Preparation Kit v2 (Illumina, Inc., San Diego, CA, United States) and validated according to Illumina's low-throughput protocol. After normalization, cDNA libraries were pooled for multiplexing before loading onto a flow cell (8–9 samples per lane). The hybridization and cluster generation were performed on a cBot System using TruSeq SR Cluster Kit v3. Sequencing was performed on an Illumina HiScanSQ platform using TruSeq SBS kit v3 (Illumina, Inc.) to obtain Single Reads, 50 nt in length. Due to the scarcity of the collected material in WS treatment, and according to ENCODE standard for RNAseq experiments[2], requiring at least two biological replicates, data analysis has then been performed only on C, AM, AM_WS, RKN and RKN_AM. Raw data have been deposited to NCBI and the accession number for this project is PRJNA545411.

RNA-Seq Data Analysis and Differential Gene Expression Quantification

The quality of the raw sequence reads was checked using FastQC[3]. Raw sequences were processed to eliminate adapters, indexes, as well as genomic sequences added during the sequencing process, using the "RNA-seq analysis" functions included in the CLC Genomics Workbench software v.8.5 (QIAGEN, Aarhus, Denmark)[4]. Filtered reads from each sample were then separately aligned to the reference genome of *S. lycopersicum* (SL2.40.26, Sol Genomics Network)[5], using CLC (similarity parameter: 0.8; identity parameter: 0.8, mismatch/insertion/deletion penalties: 2/3/3) and employed to quantify the abundance of tomato gene transcripts, measured as the Reads Per Kilobase per Million mapped reads (RPKM) (Mortazavi et al., 2008). A gene was considered to be expressed and included in the downstream analysis if at least five reads were mapped to it and its RPKM value was >0.

[1] www.igatechnology.com

[2] https://www.encodeproject.org/about/experiment-guidelines/

[3] https://www.bioinformatics.babraham.ac.uk/projects/fastqc

[4] http://www.clcbio.com

[5] ftp://ftp.solgenomics.net

A multiple correlation test (Pearson's correlation) on RPKM values for all pairwise combinations was performed for preliminary batch comparisons of replicates. To identify differentially expressed gene (DEG), statistical analysis was carried out for each treatment group against a reference group (equivalent developmental stages of un-colonized un-stressed roots). RNA-Seq library set differential expression analysis was performed applying "Empirical analysis of Digital Gene Expression (DEG) in R" (EDGE) that implements, in the EdgeR Bioconductor package (Robinson et al., 2010), the 'Exact Test' for two-group comparisons (Robinson and Smyth, 2008), able to account for over-dispersion caused by biological variability. Raw counts for each gene were normalized in relation to different sequence depths between duplicate bioassay samples.

Genes in libraries were considered DE when compared with the controls, by applying the Benjamini–Hochberg algorithm for Fold Change (FC) estimation. DEGs displaying at least a *P*-value (p) ≤ 0.05, in almost one condition, were submitted to further analysis. The terms up-regulation and down-regulation indicate, respectively, transcript levels that were significantly higher or lower than those observed in non-inoculated controls.

Functional Analysis of Tomato DEG

Enrichment analysis of each DEG gene ontology (GO) term was performed by AgriGO device[6] (Du et al., 2010) to identify GO category related to single or multiple interactions. GO Enrichment analysis detect functional categories of biological processes, molecular functions and cellular components over-represented, with statistical significance (Fisher's Exact Test: p-value ≤ 0.05; Hochberg Multi-test adjustment method: FDR ≤ 0.05), in a gene sub set using annotations for that gene set as compared with the remaining genes of the reference organism (*S. lycopersicum* cDNA library, version 2.4[7].

Identification of AM Fungal Transcripts in Tomato Roots

To discover AM fungal genes expressed in roots, fungal reads were separated from those of tomato by mapping the complete RNA-Seq data set of AM-colonized roots onto the draft genome sequence of tomato version SL.2.46. Unmapped reads, potentially fungus-derived, were isolated and mapped, with CLC utility and parameter previously described, to the *Rhizophagus irregularis* DAOM 181602 v1.0 (formerly *Glomus intraradices*, GLOIN) genome, retrieved from JGI genome portal[8] (Tisserant et al., 2013). The RPKM were determined and used to estimate the GLOIN transcripts abundance. To assess differential gene expression between AM_WS and AM samples, proportions-based *Z*-test statistical analysis (Kal et al., 1999) was applied, assigning the samples different weights depending on library size (total counts). A GO functional enrichment analysis was conducted using Fisher's exact test with a weight algorithm in AgriGo. The GO annotations of *R. irregularis* genes were obtained from the Mycocosm JGI genome portal (Tisserant et al., 2013)[8].

[6]http://bioinfo.cau.edu.cn/agriGO

[7]ftp://ftp.solgenomics.net/tomato_genome/annotation/ITAG2.4_release/ITAG2.4_cdna.fasta

[8]https://genome.jgi.doe.gov

RESULTS

To gain a comprehensive understanding of the mechanisms activated in mycorrhizal tomato roots under abiotic and biotic stress conditions, plants were subjected to a moderate water stress and to a 7-days long RKN infection. Transcriptome root profiles were obtained from C, AM, AM_WS treatments, while the biotic stress impact was studied using the infection structure (gall) from non-mycorrhizal (RKN) and mycorrhizal (RKN_AM) plants.

Sequencing Data and Transcriptome Mapping

Transcriptome sequencing generated a total of $187{,}7 \cdot 10^6$ reads of 50 bp in length, for all samples. Good-quality reads (99%) were retained, which were mapped onto the reference genome with CLC. In total, 76–97% of good-quality reads were mapped onto the *S. lycopersicum* genome (SL2.40.26 assembly) across all samples (**Table 1**). Expressed tomato genes arose from 16347 (AM_WS2_7) up to 22959 (RKN1_7) out of 34647 predicted genes in the reference genome (**Table 1**), using a cutoff value of RPKM > 0 to declare a gene as expressed. A high Pearson's correlation coefficient (r) was observed between RPKM values of each sample replicates sequenced set (average $r = 0.92$) (**Table 2**).

Whole Transcriptome Profiles and Differentially Expressed Genes

The genes DE respect to control (p-value < 0.05) arose from 10 (RKN) up to 12 % (AM) of total SL2.40.26 predicted protein coding genes (**Table 3**). A higher percentage of up-regulated genes was observed only in the AM condition (**Figure 1**). For further analyses, 7316 differentially expressed genes (DEGs), when compared with un-colonized/un-stressed control, and with a p-value < 0.05 in at least one treatment (AM, AM_WS, RKN, and RKN_AM) were considered (**Supplementary Tables S1, S2**).

To have an overview of the regulation of the main metabolic processes and signaling pathways involved in the different stress conditions, a GO enrichment analysis was carried out for DEGs in AM_WS and RKN_AM. Data showed that transcripts involved in processes such as "response to oxidative stress," "functions of peroxidase activity" and "heme binding" were involved in both situations. Specific GO terms enriched during abiotic stress (AM_WS) were related to the molecular function "transcription regulator activity," while in biotic stress (RKN_AM) to the metabolic process "protein ubiquitination and protein amino acid phosphorylation" and cellular process "microtubule-based movement," that were particularly over represented (**Table 4**, **Supplementary Tables S3, S4**, and **Supplementary Figures S1**, **S2**).

In the 7316 DEGs subset, a number of common and exclusive genes were observed among the treatments (**Figure 2**). Focusing on the 924 transcripts in common among AM, AM_WS, RKN, and RKN_AM treatments, 188 e 689 of them were up- and down-regulated, respectively, whereas the remaining 47

TABLE 1 | Statistics of good-quality reads mapped onto the tomato reference genomes.

SAMPLE	Cleaned reads*10^6	Aligned reads on SL2.40 (%)	SL expressed transcripts (≥5 aligned reads)
C1_7	4.66	97.89	18417
C2_7	14.65	97.53	20065
RKN1_7	54.62	97.11	22959
RKN2_7	14.3	96.48	20917
AM1_7	15.49	78.56	20443
AM2_7	8.63	76.95	20064
RKN_AM1_7	15.55	93.98	21648
RKN_AM2_7	43.43	96.37	22957
AM_WS1_7	14.68	90.64	21460
AM_WS2_7	1.75	86.79	16347

TABLE 2 | Correlation (Pearson's correlation coefficient) between RPKM values of biological replicate of each sample pairwise combinations of sample set.

SAMPLE		r
C	1 *vs.* 2	0.87
RKN	1 *vs.* 2	0.90
AM	1 *vs.* 2	0.95
RKN_AM	1 *vs.* 2	0.96
AM_WS	1 *vs.* 2	0.93

TABLE 3 | Differentially expressed tomato genes comparing to uninoculated unstressed plants (C) ($P < 0.05$).

Condition	% DEG*	Up regulated	Down regulated
RKN	10	1659	1884
AM	12	2242	1938
RKN_AM	11	1855	2084
AM_WS	11	1905	2034

**Calculated using DEG out of 34647 predicted genes in the reference tomato genome.*

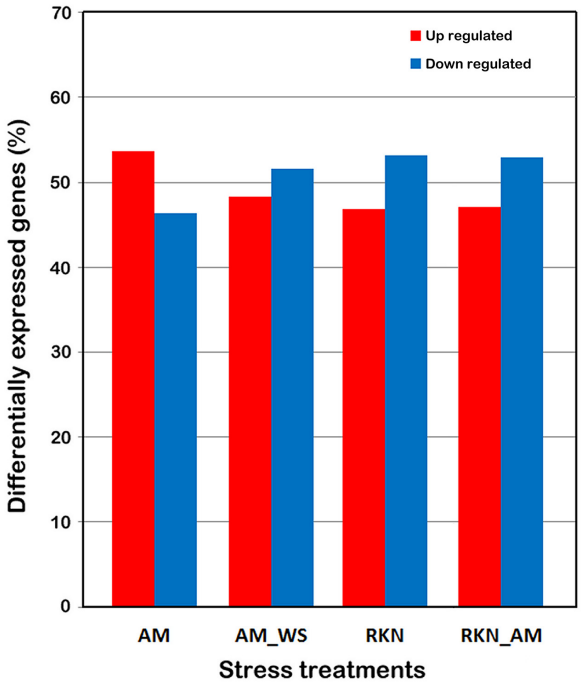

FIGURE 1 | Differentially expressed tomato genes. DEGs were identified by comparing the expression profiles from treated roots (AM, AM_WS, RKN, RKN_AM) with the equivalent developmental stages of control roots (C) ($P \leq 0.05$). Each column represents a treatment.

transcripts showed an opposite expression trend, in at least one condition (**Supplementary Table S5**). GO enrichment analysis conducted for this subset showed up regulated transcripts belonging to processes involved in "biotic stimulus," "oxidative stress response" and functions like "heme binding," "transition metal ion binding" and "peroxidase activity." Processes such as "post-translational protein modification" and "regulation of transcription" were down-regulated, while transcripts ascribed to the "heme binding" function showed different expression trends (**Supplementary Table S6**). Looking at the AM fungal presence, 196 genes were DE in all the AM-colonized plants, independently from the applied stress condition (**Figure 2**).

Among the twenty most up-regulated genes found in each condition (**Supplementary Table S7**), all genes of AM_WS sample were also retrieved in the top 20 DEGs of unstressed AM-colonized plants (AM), although a lower fold change was often recorded in AM_WS plants, probably reflecting a low level of colonization in stressed plants with respect to the AM ones. One transcript (Solyc01g067860.2.1) was up regulated in all stress conditions. Considering the biotic stresses (RKN and RKN_AM), 12 transcripts were in common. The most up-regulated genes in the infection structures (galls) were mainly related to biotic stress response, independently from the AM fungal presence.

Specific Responses to the AM Fungus in Drought Stressed *Versus* Unstressed Roots

To deeper explore this novel dataset and to further understand the tomato response to WS during AM interaction, as well as the impact of the imposed stress on the symbiosis, the expression profiles of genes described in the literature as specifically involved during AM symbiosis in different plant species have been considered (Fiorilli et al., 2009; Guether et al., 2009; Hogekamp et al., 2011; Hogekamp and Küster, 2013; Fiorilli et al., 2015, 2018; Handa et al., 2015; Balestrini et al., 2017; Li et al., 2018; Recchia et al., 2018; Vangelisti et al., 2018). Particularly, AM symbiosis is known for the improved nutrient exchange established between the two symbionts, involving fine-tuned plant and fungal transporter genes (Casieri et al., 2013; Berruti et al., 2016). A consistent group of plant transporters were identified as DE between unstressed colonized plants (AM) and the control (C) ones (**Supplementary Table S8**) also confirming that a functional symbiosis was established. Several transporters were significantly up-regulated in AM-colonized plants subjected to a moderate water stress (**Supplementary Table S8** and **Table 5**). Two of them code for two inorganic phosphate transporters (Solyc09g090080.1.1 and Solyc06g051860.1.1), which show

TABLE 4 | GO Enrichment analysis (P-value ≤ 0.05) for differentially expressed genes during abiotic and biotic stress.

Gene ontology	Categories	AM_WS	RKN_AM
GO:0006979	P_response to oxidative stress	x	x
GO:0006950	P_response to stress	x	x
GO:0042221	P_response to chemical stimulus	x	x
GO:0050896	P_response to stimulus	x	x
GO:0016684	F_oxidoreductase activity, acting on	x	x
GO:0004601	F_peroxidase activity	x	x
GO:0020037	F_heme binding	x	x
GO:0005506	F_iron ion binding	x	x
GO:0046906	F_tetrapyrrole binding	x	x
GO:0016209	F_antioxidant activity	x	x
GO:0003824	F_catalytic activity	x	x
GO:0003700	F_transcription factor activity	x	
GO:0046914	F-transition metal ion binding	x	
GO:0005576	C_extracellular region	x	
GO:0004497	F_monooxygenase activity	x	
GO:0030528	F_transcription regulator activity	x	
GO:0046872	F_metal ion binding	x	
GO:0043167	F_ion binding	x	
GO:0055114	P_oxidation reduction	x	
GO:0016491	F_oxidoreductase activity	x	
GO:0043169	F_cation binding	x	
GO:0005524	F_ATP binding		x
GO:0032559	F_adenyl ribonucleotide binding		x
GO:0006464	P_protein modification process		x
GO:0006468	P_protein amino acid phosphorylation		x
GO:0006796	P_phosphate metabolic process		x
GO:0032555	F_purine ribonucleotide binding		x
GO:0016310	P_phosphorylation		x
GO:0004672	F_protein kinase activity		x
GO:0016772	F_transferase activity, transferring p-containing groups		x
GO:0043687	P_post-translational protein modification		x
GO:0007018	P_microtubule-based movement		x
GO:0016773	F_phosphotransferase activity, alcohol group as acceptor		x
GO:0005507	F_copper ion binding		x
GO:0016798	F_hydrolase activity, acting on glycosyl bonds		x
GO:0032553	F_ribonucleotide binding		x
GO:0016301	F_kinase activity		x
GO:0006793	P_phosphorus metabolic process		x
GO:0032446	P_protein modification by small protein conjugation		x
GO:0016567	P_protein ubiquitination		x
GO:0070647	P_protein modification by small protein conjugation or removal		x
GO:0043412	P_macromolecule modification		x

Over-represented functional categories of biological processes (P), molecular functions (F) and cellular components (C).

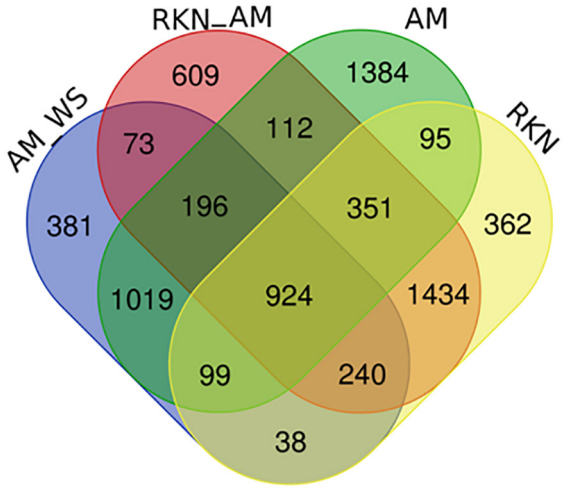

FIGURE 2 | Venn diagram of DEGs ($P \leq 0.05$) comparing un-inoculated un-stressed tomato (C) *vs.* AM, AM_WS, RKN, RKN_AM.

TABLE 5 | Transporter genes significantly regulated by the AM fungus in non-stressed (NS) and stressed (WS) growth conditions.

Transporter category	# of genes		Fold change mean	
	C *vs.* AM	C *vs.* AM_WS	C *vs.* AM	C *vs.* AM_WS
ABC transporter G	8	7	238.26	56.78
Amino acid permease	8	7	1.71	0.76
Cationic amino acid transporter	3	1	117.39	94.67
Peptide transporters	13	8	141.77	73.43
Aquaporins	15	11	10.80	4.62
Putative SWEET transporter	1	0	21.37	0.00
Phosphate transporters	4	3	85.76	30.31
Potassium transporters	7	4	22.88	10.42
Ammonium transporters	6	5	426.36	121.11
Nitrate transporters	6	4	−2.93	−12.66
Sulfate transporters	3	0	2.05	0.00
Zinc transporters	5	3	8.41	1.80
Copper transporters	1	7	75.80	20.07
Glucose transporters	8	7	−14.51	−9.74
Lipid A export permease	8	5	31.18	10.40

homology with the mycorrhizal inducible *LePT3* and *LePT4* (Balestrini et al., 2007). The other mycorrhiza-inducible *LePT5* (Solyc06g051850.1.1) was still up-regulated in AM_WS, although not in a significant way ($P > 0.05$), in agreement with the fact that this one was the AM-inducible PT gene significantly affected only by the "stress" factor (Volpe et al., 2018). Many other genes coding proteins involved in molecule transport were significantly up-regulated in the presence of the AM fungus upon water stress, such as three ammonium transporters (AMT; i.e., Solyc08g067080.1.1, Solyc03g033300.1.1, Solyc09g065740.1.1) and four potassium (K^+) transporters (Solyc03g097860.1.1, Solyc06g051860.1.1 Solyc07g014680.2.1, Solyc05g005740.2.1). Tomato genes coding for three ABC transporter family G (Solyc11g007300.1.1, Solyc01g097430.2.1, Solyc09g098410.1.1), with the last two homologs of the AM symbiosis-induced ABCG

transporter *LjSTR2* and *LjSTR*, were among the ten most up-regulated genes in AM_WS, in addition to the three AMT genes, two genes coding for peptide transporters (Solyc01g102360.1.1, Solyc05g009500.2.1) and one gene encoding an high affinity cationic amino acid transporter (CAT; Solyc12g096380.1.1). Sulfate transporters were also regulated and two of them were significantly induced by AM symbiosis (Solyc12g056920.1.1, Solyc10g047170.1.1). In AM_WS they were up- and down-regulated respectively, although not significantly different. Among the down-regulated genes in AM symbiotic roots, both in unstressed and stressed plants, there was a PT gene (Solyc09g066410.1.1) that shows homology with an inorganic phosphate transporter 1-4 (XP_004247235.1) expressed in tomato fruit from mycorrhizal plants (Zouari et al., 2014).

Almost all the genes reported by Sugimura and Saito (2017) as symbiosis marker genes both in tomato and *Lotus* were also found strongly up-regulated in AM-colonized roots (**Supplementary Table S9**), both in unstressed and AM_WS stressed plants. Additionally, other members within gene families already known to be involved in AM symbiosis (e.g., blue copper proteins, germin-like proteins, glutathione-*S*-transferase, ripening-related proteins, cell wall-related genes etc.) were strongly up-regulated in the presence of the AM fungus (**Supplementary Table S10**). Generally, expression levels were almost always lower in AM_WS than in AM roots, probably due to an opposite impact of the water stress on their regulation. Among the genes strongly up-regulated in AM_WS (i.e., with fold changes >50), there were those encoding three putative glutathione-*S*-transferases (Solyc02g081240.1.1, Solyc10g007620.1.1, Solyc10g084960.1.1) in addition to a putative germin-like (Solyc11g068570.1.1), three blue copper (Solyc12g056500.1.1, Solyc10g081520.1.1, Solyc08g079780.1.1), two major allergen (Solyc03g117460.1.1, Solyc03g117450.1.1), four ripening-related (Solyc01g094440.1.1, Solyc05g048780.1.1, Solyc01g094450.1.1, Solyc01g094430.1.1), two putative dirigent-like proteins (Solyc07g052170.1.1, Solyc04g010270.1.1) with three putative cysteine proteinases (Solyc12g056000.1.1, Solyc08g065710.1.1, Solyc08g065690.1.1), and two subtilisin-like proteases (Solyc08g080010.1.1, Solyc02g072370.1.1) (**Supplementary Tables S9, S10**).

Hormonal related transcript levels have been also already reported to change in the presence of the AM fungus (Gutjahr, 2014; Bedini et al., 2018; McGuiness et al., 2019). The AM marker gene *CCD7* (Solyc01g090660.2.1) coding for a carotenoid cleavage dioxygenase 7 with a role in strigolactone (SL) biosynthesis, was found to be still regulated in AM-colonized WS roots (AM_WS) in addition to *CCD8* gene (**Supplementary Tables S5, S6**). Gibberellin-related genes have been also found to be affected by AM symbiosis in *Medicago truncatula*. In agreement with the data in Ortu et al. (2012), tomato DELLA GAI protein (Solyc11g011260.1.1; Nir et al., 2017) resulted to be up-regulated in the AM treatment, while Gibberellin receptor GID1L2 (Solyc09g075670.1.1) was down-regulated. Gibberellin 20-oxidase-like proteins were up-regulated in AM-colonized roots (Solyc12g013780.1.1 and Solyc01g093980.2.1), while a putative Gibberellin 20-oxidase-1 (Solyc03g006880.2.1) was induced only in the AM treatment. Among the Gibberellin 2-oxidases, one gene (Solyc02g070430.2.1) resulted to be down-regulated in both AM-colonized roots, while Solyc07g061730.2.1 was significantly repressed only in AM_WS and Solyc07g061720.2.1 was up-regulated in AM roots (**Supplementary Table S10**). Interestingly, genes coding for enzymes with a key regulatory role in the biosynthesis of phenylpropanoid products, which can have diverse functions and are particularly important in plant defense (Mandal et al., 2010), were upregulated in AM plants. In detail, genes coding for two phenylalanine ammonia lyases (PAL; Solyc03g042560.1.1, Solyc09g007900.2.1) and a 4-coumarate-CoA ligase (4CL; Solyc11g007970.1) were significantly up-regulated in AM-colonized plants, suggesting an effect of the AM fungus for enhanced defense ahead of stress occurrence.

In agreement with data already reported (Liu F. et al., 2015), several non-specific lipid transfer proteins were also detected as significantly regulated during AM symbiosis also under WS condition (**Supplementary Table S10**). A core of differentially regulated genes was related to genes involved in cell wall metabolism and modification, in agreement with previous works (Balestrini and Bonfante, 2014). Among the genes putatively involved in arbuscule development and fungal accommodation, four genes coding for cellulose synthases were significantly up-regulated (Solyc00g030000.1.1, Solyc00g154480.1.1, Solyc07g051820.2.1, Solyc08g076320.2.1), independently from the stress level, in addition to an endo-β-1,4-glucanase (Solyc04g064900.1.1). Several genes encoding expansin proteins were also differentially up- or down regulated in both AM and AM_WS roots, confirming a role for these proteins during the AM colonization.

Transcription factors (TFs) have been reported to be highly involved in the response to drought as well as in AM symbiosis establishment. In our dataset, AM colonization, independently from the growth conditions, elicited the expression of several TF genes belonging to different groups, while other members inside these families were down-regulated (**Supplementary Table S9**). Looking at the genes expressed in AM and AM_WS, two ethylene responsive transcription factor 2a (Solyc04g071770.2.1, Solyc12g056590.1.1) resulted to be down-regulated, while an opposite trend was observed for the *LeERF5* (Solyc03g093560.1.1), up-regulated in AM-colonized roots, independently from the imposed stress. Due to the role in the adventitious roots and in the regulation of auxin responsive genes, the up-regulation in both AM and AM_WS roots of auxin responsive factor (ARF) genes (Solyc07g043610.2.1, Solyc03g118290.2.1) is worth noting since they are considered to be related to the modification of the root apparatus occurring during symbiosis (Vangelisti et al., 2018).

The expression of WS-responsive genes has been considered, to verify the efficacy of the WS stress imposition on tomato transcriptome in the presence of the AM fungus. The relevance of ABA in the response of plants to a water deficit event has already been highlighted by the differential regulation of target genes, directly associated with the ABA biosynthesis and signaling (Kuromori et al., 2018). The co-regulation with negative regulators has already been reported, suggesting the presence of a mechanism to fine-tune plants stress responses

(Garcia et al., 2008). The presence of the fungus, independently from the growth condition (NS and WS), induced in roots the expression of a gene (Solyc07g056570.1.1, i.e., LeNCED1) coding a 9-*cis*-epoxycaratenoid dioxygenase involved in the ABA biosynthetic process, with a fold change value higher in AM than in AM_WS plants. A gene coding for a NAC transcription factor JA2 (Solyc12g013620), reported to be induced by ABA and WS in tomato leaves, and promoting stomatal closure through the induction of the expression of ABA biosynthetic gene NCED1, was down-regulated in AM-colonized roots, both in stressed and unstressed condition, suggesting a specific role in leaves. Solyc03g116390.2.1, coding for a late embryogenesis abundant (LEA) protein already shown to be inducible by drought stress (Gong et al., 2010) was significantly up-regulated in AM_WS, additionally to other two LEA genes (Solyc12g098900.1.1, Solyc10g078770.1.1) and the ABA-responsive gene coding for dehydrin TAS14 (Solyc02g084850.2.1; Sacco et al., 2013), confirming the efficacy of the imposed water stress. Additionally, Solyc06g019170.2.1, the ABA responsive gene Delta l-pyrroline-5-carboxylate synthetase SlP5CS1, involved in proline production, was significantly up-regulated only in AM_WS (**Supplementary Tables S1, S2**).

As expected, the several tomato aquaporin (AQP) genes showed different regulations among the considered conditions. Several AQP genes (**Table 6**) were significantly up- or down-regulate in AM roots, and many were significantly regulated also in AM_WS ones. The significant up-regulation observed for the AQP Solyc09g007770.2.1 (*SlPIP2;1*) in AM_WS roots is worth of noting, suggesting a specific role in WS response for this transcript.

TABLE 6 | List of AQPs regulated in the several conditions (AM, unstressed AM-colonized roots; AM_WS, water stressed AM-colonized roots; RKN, nematode infection; RKN_AM, nematode infection in AM-colonized plants).

Transcript ID	Gene name	AM	AM_WS	RKN	RKN_AM
Solyc12g057050.1.1	*SlNIP3;2*	**121.30**	**36.08**	1.09	3.39
Solyc03g005980.2.1	*SlNIP1;1*	**12.26**	**4.90**	1.41	1.31
Solyc10g084120.1.1	*SlPIP2;5*	**9.32**	**4.76**	−1.01	1.63
Solyc06g011350.2.1	*SlPIP2;4*	**8.97**	**7.34**	−1.05	−1.17
Solyc06g060760.2.1	*SlTIP2;3*	**4.43**	1.90	**−4.59**	**−3.23**
Solyc08g081190.2.1	*SlPIP1;5*	**4.20**	**2.61**	1.59	1.79
Solyc12g056220.1.1	*SlPIP1;3*	**4.12**	2.00	1.46	1.63
Solyc12g019690.1.1	*SlSIP1;1*	**3.64**	**2.46**	1.35	1.39
Solyc11g069430.1.1	*SlPIP2;6*	**3.38**	**2.43**	1.73	1.82
Solyc10g083880.1.1	*SlTIP1;3*	**3.17**	**2.57**	**−2.98**	−1.38
Solyc03g013340.2.1	*SlNIP2;1*	**2.81**	−1.49	−1.52	1.15
Solyc06g074820.2.1	*SlTIP1;1*	2.62	**2.84**	1.14	1.50
Solyc06g075650.2.1	*SlTIP1;2*	1.94	1.82	**−3.00**	**−2.17**
Solyc08g008050.2.1	*SlPIP1;1*	1.79	1.26	**−5.83**	−2.68
Solyc09g007770.2.1	*SlPIP2;1*	1.33	**8.68**	−1.44	1.84
Solyc02g071920.2.1	*SlNIP1;2*	1.16	−1.71	**−3.82**	**−2.37**
Solyc01g094690.2.1	*SlPIP1;2*	1.01	1.80	**6.67**	**5.93**
Solyc06g073590.2.1	*SlNIP3;1*	−2.02	**−5.81**	**−11.36**	**−8.89**
Solyc10g078490.1.1	*SlSIP1;2*	**−2.21**	**−2.25**	−1.73	−1.48
Solyc08g066840.2.1	*SlTIP4;1*	**−2.38**	−1.65	−1.22	−1.21
Solyc12g044330.1.1	*SlTIP2;1*	**−5.43**	**−4.87**	−2.95	−2.06
Solyc03g096290.2.1	*SlPIP1;7*	**−5.59**	**−5.23**	1.68	1.29

Values in bold are significantly regulated (P < 0.05).

TABLE 7 | Summary statistics for Illumina sequencing and mapping against reference *R. irregularis* DAOM198197 genome assembly (Gloin1).

	AM	AM_WS	RKN_AM
Total raw reads	24,243,262	16,586,731	59,231,940
Reads mapped against *R. irregularis* reference sequence	2,884,324	885,917	193,410
Mapped reads /total raw reads (%)	11.9	5.34	0.33

AM Fungal Gene Regulation Upon Water Stress

Gene expression analysis of *R. irregularis* colonizing tomato roots was performed by mapping short reads against the *R. irregularis* genome. The proportion of *R. irregularis*-derived reads was less than 12% in AM roots and of 5% in AM_WS (**Table 7**), consistent with the results of previous studies (Tisserant et al., 2013; Handa et al., 2015; Sugimura and Saito, 2017). We identified 19057 and 16364 *R. irregularis* expressed genes (RPKM > 0), respectively, in AM and AM_WS roots, with 78.8% of overlapping, corresponding to 52% of the *R. irregularis* putative protein-coding genes expressed in both conditions. The expression levels of *R. irregularis* genes were significantly correlated between AM and AM_WS samples (Pearson correlation = 0.85). 77% of the *R. irregularis* genes found in tomato roots (RPKM > 0) coincided with those expressed by the fungus in *Lotus japonicus* roots, according to Handa et al. (2015). A total of 1224 *R. irregularis* genes, 4% of the entire transcriptome, were DE between AM and AM_WS treatments (FC ≥ 2; *p*-value ≤ 0,01), of which 779 were up-regulated and 445 down- regulated in roots subjected to moderate water stress (**Supplementary Table S11**). A GO enrichment analysis of the subset of genes highly expressed upon water stress revealed an overrepresentation of GO terms related to molecular function "monooxigenase activity" and "heme binding" (**Supplementary Table S12**). The most remarkable difference was the higher expression of 18 cytochrome P450 (CYPs), belonging to "heme binding" molecular function, 2 to 12-fold overexpressed in stressed roots (**Supplementary Table S11**). By contrast, only 5 CYP genes turned out to be down-regulated, with a mean fold change of −2.7 (**Supplementary Table S11**). Concerning the 20 most up- and down regulated genes, it is worth noting that the majority of them lacks a KOG annotation (16 out of 20 genes both for the up- and the down-regulated). However, the most up-regulated sequence (FC 74.5) contains a CsbD domain, that is present in a bacterial gene induced upon abiotic stresses such as nutrient-limitation (Prágai and Harwood, 2002). Another highly up-regulated gene (FC 65.23) contains a "conidiation protein 6" domain.

TABLE 8 | Most relevant fungal DEGs.

Fold change (mean value)		n°	Feature ID
Cytochrome P450			
Up	4.04	18	jgi| Gloin1| 43670|;jgi| Gloin1| 322668|; jgi| Gloin1| 54382|; jgi| Gloin1| 36234|; jgi| Gloin1| 82149|; jgi| Gloin1| 35874|; jgi| Gloin1| 59731|; jgi| Gloin1| 57850|; jgi| Gloin1| 54172|; jgi| Gloin1| 348593|; jgi| Gloin1| 330761|; jgi| Gloin1| 70184|; jgi| Gloin1| 347608|; jgi| Gloin1| 74648|; jgi| Gloin1| 54229|; jgi| Gloin1| 337700|; jgi| Gloin1| 348383|; jgi| Gloin1| 1959|
Down	−2.75	5	jgi| Gloin1| 130232|; jgi| Gloin1| 21462|; jgi| Gloin1| 300912|; jgi| Gloin1| 51235|; jgi| Gloin1| 62820|
Defense-related genes			
Up	4.99	6	jgi| Gloin1| 350397|; jgi| Gloin1| 250811|; jgi| Gloin1| 20587|; jgi| Gloin1| 78868|; jgi| Gloin1| 23533|; jgi| Gloin1| 7020|
Down	−2.43	2	jgi| Gloin1| 18774|; jgi| Gloin1| 342859|
Stress-related genes			
Up	4.36	2	jgi| Gloin1| 342251|; jgi| Gloin1| 336918|
Down	−2.82	1	jgi| Gloin1| 342324|
Vesicular trafficking			
Up	2.97	9	jgi| Gloin1| 5531|; jgi| Gloin1| 347798|; jgi| Gloin1| 336277|; jgi| Gloin1| 28807|; jgi| Gloin1| 341557|; jgi| Gloin1| 348182|; jgi| Gloin1| 265701|; jgi| Gloin1| 289764|; jgi| Gloin1| 342517|
Down	−2.96	4	jgi| Gloin1| 174850|; jgi| Gloin1| 23226|; jgi| Gloin1| 30939|; jgi| Gloin1| 5044|
Chaperones and protein turnover			
Up	5.84	40	jgi| Gloin1| 113616|; jgi| Gloin1| 336528|; jgi| Gloin1| 46676|; jgi| Gloin1| 71363|; jgi| Gloin1| 16998|; jgi| Gloin1| 22115|; jgi| Gloin1| 340280|; jgi| Gloin1| 323494|; jgi| Gloin1| 46515|; jgi| Gloin1| 6786|; jgi| Gloin1| 345683|; jgi| Gloin1| 302299|; jgi| Gloin1| 5369|; jgi| Gloin1| 79494|; jgi| Gloin1| 16101|; jgi| Gloin1| 58870|; jgi| Gloin1| 52235|; jgi| Gloin1| 44858|; jgi| Gloin1| 57249|; jgi| Gloin1| 327|; jgi| Gloin1| 27674|; jgi| Gloin1| 66066|; jgi| Gloin1| 21968|; jgi| Gloin1| 349345|; jgi| Gloin1| 34571|; jgi| Gloin1| 299589|; jgi| Gloin1| 328597|; jgi| Gloin1| 53501|; jgi| Gloin1| 163681|; jgi| Gloin1| 345252|; jgi| Gloin1| 55552|; jgi| Gloin1| 66159|; jgi| Gloin1| 339540|; jgi| Gloin1| 24173|; jgi| Gloin1| 340241|; jgi| Gloin1| 345467|; jgi| Gloin1| 345863|; jgi| Gloin1| 343006|; jgi| Gloin1| 84344|; jgi| Gloin1| 311043|; jgi| Gloin1| 289764|
Down	−3.26	15	jgi| Gloin1| 106703|; jgi| Gloin1| 177771|; jgi| Gloin1| 188968|; jgi| Gloin1| 219634|; jgi| Gloin1| 330117|; jgi| Gloin1| 336698|; jgi| Gloin1| 338665|; jgi| Gloin1| 339110|; jgi| Gloin1| 345483|; jgi| Gloin1| 345595|; jgi| Gloin1| 348922|; jgi| Gloin1| 6665|; jgi| Gloin1| 69178|; jgi| Gloin1| 78516|; jgi| Gloin1| 79920|
Secondary metabolite-related			
Up	3.84	29	jgi| Gloin1| 43670|; jgi| Gloin1| 322668|; jgi| Gloin1| 54382|; jgi| Gloin1| 334957|; jgi| Gloin1| 36234|; jgi| Gloin1| 22144|; jgi| Gloin1| 82149|; jgi| Gloin1| 17041|; jgi| Gloin1| 35874|; jgi| Gloin1| 74321|; jgi| Gloin1| 338850|; jgi| Gloin1| 20810|; jgi| Gloin1| 59731|; jgi| Gloin1| 57850|; jgi| Gloin1| 54172|; jgi| Gloin1| 60375|; jgi| Gloin1| 348593|; jgi| Gloin1| 330761|; jgi| Gloin1| 70184|; jgi| Gloin1| 343651|; jgi| Gloin1| 347608|; jgi| Gloin1| 54229|; jgi| Gloin1| 337700|; jgi| Gloin1| 348383|; jgi| Gloin1| 1959|; jgi| Gloin1| 83047|; jgi| Gloin1| 67532|; jgi| Gloin1| 2086|; jgi| Gloin1| 5484|
Down	−3.43	9	jgi| Gloin1| 130232|; jgi| Gloin1| 17438|; jgi| Gloin1| 21462|; jgi| Gloin1| 22126|; jgi| Gloin1| 300912|; jgi| Gloin1| 349273|; jgi| Gloin1| 51235|; jgi| Gloin1| 62820|; jgi| Gloin1| 71955|
BTP/POZ and Kelch domain-containing			
Up	10.70	8	jgi| Gloin1| 19708|; jgi| Gloin1| 15897|; jgi| Gloin1| 28179|; jgi| Gloin1| 335861|; jgi| Gloin1| 20150|; jgi| Gloin1| 6286|; jgi| Gloin1| 347430|; jgi| Gloin1| 33301|
Down	−4.26	3	jgi| Gloin1| 22970|; jgi| Gloin1| 336766|; jgi| Gloin1| 337622|
Transporters and ion channels			
Up	3.71	17	jgi| Gloin1| 12610|; jgi| Gloin1| 13617|; jgi| Gloin1| 22239|; jgi| Gloin1| 163857|; jgi| Gloin1| 23158|; jgi| Gloin1| 347430|; jgi| Gloin1| 75317|; jgi| Gloin1| 234547|; jgi| Gloin1| 345912|; jgi| Gloin1| 22144|; jgi| Gloin1| 17041|; jgi| Gloin1| 49664|; jgi| Gloin1| 338850|; jgi| Gloin1| 17710|; jgi| Gloin1| 336277|; jgi| Gloin1| 338361|; jgi| Gloin1| 144344|; jgi| Gloin1| 289764|
Down	−4.10	5	jgi| Gloin1| 15318|; jgi| Gloin1| 2573|; jgi| Gloin1| 343898|; jgi| Gloin1| 193343|; jgi| Gloin1| 298419|; jgi| Gloin1| 346110|

Several genes encoding proteins containing BTB/POZ and Kelch domains, involved in signaling transduction and regulation at the protein level, were also highly regulated in our dataset (mean up and down FC: 10.7 and −4.3, respectively). Genes encoding for proteins involved in protein turnover (ubiquitin pathway and chaperones) were DE, with 40 transcripts found as up-regulated. Remarkably, three sequences ascribed to glutathione S-transferase were up-regulated in the AM_WS treatment, none of them being down-regulated. As for *R. irregularis* genes down regulated in stressed tomato roots, they were fewer compared with the up-regulated ones, and no overrepresented GO terms was recorded (**Table 8**).

Specific Responses to Nematode Infection in Galls From Mycorrhizal and Non-mycorrhizal Roots

During the compatible interaction, RKN trigger complex morphological and physiological changes in parenchymatic cells of the vascular cylinder to establish multinucleate feedings cells, called giant cells (GC), which serve as nutrient sinks for feeding. Nematode feeding sites, surrounded by cortical and epidermal cells, appear in the host root as the typical root-knot or gall.

Microscopic observations were carried out on serial cross sections of AM-colonized and non-colonized galls at 7 dpi.

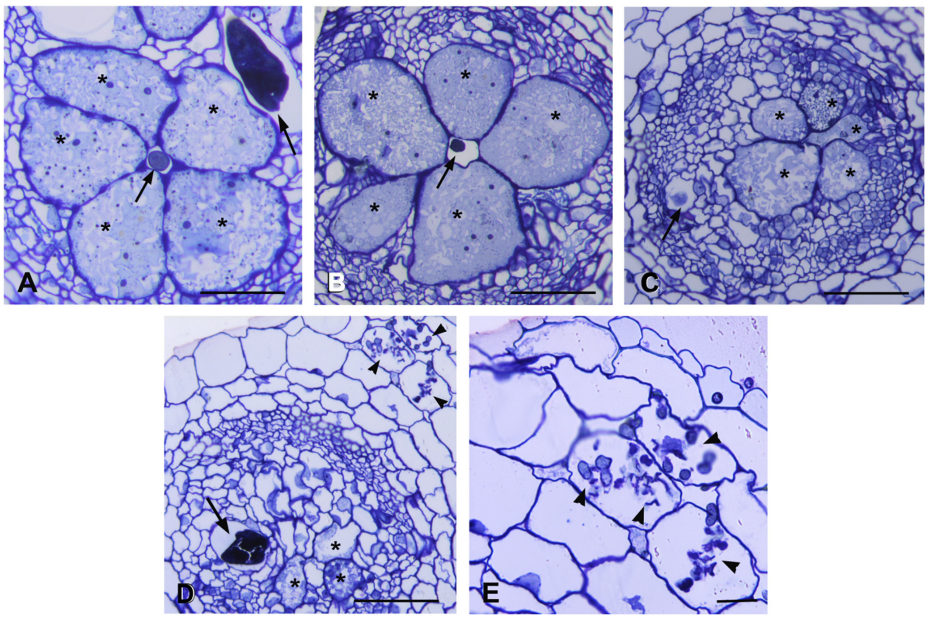

FIGURE 3 | Histological analysis of feeding sites induced by *Meloidogyne incognita* in non-colonized and in *Rhizophagus intraradices*-colonized tomato roots at 7 days post inoculation. Cross sections (2.5 μm) were stained with toluidine blue and observed at light microscope. **(A)** Non-colonized gall contained well developed and metabolically active giant cells surrounding the nematode. **(B)** Giant cells in a AM-colonized gall with an appearance similar to those in non-colonized gall. **(C,D)** Feeding sites in AM-colonized roots presented giant cells with degraded cytoplasm and clear symptoms of early senescence. Note the presence of numerous hyphae in cortical cells **(D,E)**. Asterisk, giant cell; arrow, nematode; arrowhead, hyphae. Scale bars: 100 μm in **(A–D)** and 50 μm in **(E)**.

Morphological changes were analyzed to monitor possible alterations in the development of the nematode feeding sites. Non-colonized galls showed large multinucleate GCs occupying the most part of vascular cylinder. The GCs presented small vacuoles and a dense granular cytoplasm containing numerous organelles, acting as a food sink for the growing nematode (**Figure 3A**). Several sections of AM-colonized galls revealed different features of the feeding sites (**Figures 3B–D**). Some of them showed GCs comparable with those of non-colonized galls (**Figure 3B**). Where AM fungal hyphae were observed near to the nematode feeding site (**Figures 3D,E**), GCs showed scarce cytoplasm with fewer organelles and clear symptoms of early senescence (**Figures 3C,D**). AM presence supported expression data of AM symbiosis marker genes and reads belonging to the fungus itself in this infection structure. In order to understand the tomato response during AM_RKN interaction, namely the impact of the symbiosis on the parasitism, data analysis was focused on a subset of genes already reported as specifically involved during susceptible RKN-tomato interaction (Iberkleid et al., 2015; Shukla et al., 2018).

AM-symbiosis differentially modulated the expression level of a set of genes involved in the parasitism response (**Supplementary Table S12**). DEGs ($P > 0.05$) showing an increased transcription level included those related to cell wall (8%), root development (25%), transport (33%), secondary metabolism (13%), hormone (15%), oxidative stress (21%), and stress response (4%). Down-regulated transcripts were mostly related to cell wall (23%), secondary metabolism (13%), hormone (17%), oxidative stress (10%), and stress response (4%) (**Supplementary Table S12**). The effect on the plant gene expression was evaluated calculating the ratio between AM_RKN/RKN and RKN/AM_RKN fold changes. Genes with ratio > |1.5| (for both up- or down-regulated) were considered in subsequent analyses (**Table 9**). The expression of all members from categories "root development" (Solyc04g078470.2.1, Solyc01g107710.2.1, Solyc05g009320.2.1) and "transport" (Solyc02g071070.2.1, Solyc04g079510.1.1, and Solyc09g074230.2.1) was induced by the fungus in galls (**Supplementary Table S12**), and among them the root cap protein 3 (Solyc01g107710.2.1) showed the highest ratio (11.95). Members of other categories (cell wall, hormone, secondary metabolite, oxidative stress response, and stress response-related genes) showed instead an uneven behavior (**Table 9**). The fungus colonization reduced the expression (negative ratio) of several genes involved in cell-wall metabolism, i.e., those acting on pectin fraction (Solyc03g083730.1.1 and Solyc04g076660.2.1, Solyc09g098270.2.1), two genes coding for an endo-1,4-b-xylanase (Solyc04g077190.2.1) and an endo-1,4-mannosidase (Solyc10g074920.1.1). By contrast, it positively affected the expression of three genes for putative expansins (Solyc07g054170.2.1, Solyc01g090810.2.1, Solyc05g007830.2.1). Among hormone category, genes coding for ethylene-responsive transcription factors (Solyc07g042230.1.1, Solyc08g007820.1.1, Solyc08g007830.1.1, Solyc11g042560.1.1 and Solyc10g050970.1.1) were negatively affected, except Solyc04g012050.2.1. Interestingly, the *CCD7* gene (Solyc01g090660.2.1), which is considered also an AM-symbiosis marker, was induced also in colonized galls. Among the

TABLE 9 | Effect of AM colonization on gene expression in galls, compared to untreated control (fold changes).

	Transcript ID	Annotation	RKN	RKN_AM	RKN_AM/RKN	RKN/RKN_AM
Cell wall	Solyc01g090810.2.1	Expansin protein	42.91	203.61	**4.74**	
	Solyc05g007830.2.1	Expansin 2	16.32	33.62	**2.06**	
	Solyc07g054170.2.1	Expansin B1	14.97	31.29	**2.09**	
	Solyc03g083730.1.1	Pectinesterase	−4.10	−6.95	**−1.70**	
	Solyc04g076660.2.1	Rhamnogalacturonate lyase	4.37	2.69		**1.63**
	Solyc04g077190.2.1	Endo-1 4-beta-xylanase	12.86	5.56		**2.31**
	Solyc09g098270.2.1	Polygalacturonase	31.62	19.02		**1.66**
	Solyc08g007090.1.1	Expansin-like protein	8.37	3.56		**2.35**
	Solyc10g074920.1.1	Mannan endo-1 4-beta-mannosidase	13.07	5.67		**2.31**
Root Development	Solyc04g078470.2.1	Cyclin D3-1	6.26	12.73	**2.03**	
	Solyc01g107710.2.1	Root cap protein 3	−76.43	−6.40		**−11.95**
	Solyc05g009320.2.1	LOB domain protein 42	−14.19	−6.14		**−2.31**
Transport	Solyc02g071070.2.1	Cation/H	−8.65	−4.15		**−2.08**
	Solyc04g079510.1.1	Peptide transporter	−27.47	−9.44		**−2.91**
	Solyc09g074230.2.1	Glucose transporter 8	−7.25	−2.69		**−2.69**
	Solyc11g008200.1.1	Nodulin-like protein	−5.79	−3.71		**−1.56**
Secondary metabolism	Solyc12g042460.1.1	4-coumarate CoA ligase	−18.22	−10.96		**−1.66**
	Solyc10g076660.1.1	Anthocyanidin synthase	−14.15	−8.39		**−1.69**
	Solyc10g076670.1.1	Anthocyanidin synthase	−12.11	−7.95		**−1.52**
	Solyc10g076680.1.1	1-aminocyclopropane-1-carboxylate oxidase	−10.54	−5.24		**−2.01**
	Solyc06g073580.2.1	1-aminocyclopropane-1-carboxylate oxidase 1	80.32	46.66		**1.72**
	Solyc01g009370.1.1	Cytochrome P450	27.77	17.79		**1.56**
	Solyc05g051010.2.1	Dihydroflavonol 4-reductase family	98.83	54.11		**1.83**
	Solyc05g051020.2.1	Dihydroflavonol 4-reductase family	24.33	14.51		**1.68**
Hormone	Solyc03g096050.2.1	1-aminocyclopropane-1-carboxylate oxidase 1	−8.49	−5.19		**−1.63**
	Solyc04g012050.2.1	Ethylene responsive transcription factor 2a	−8.97	−5.94		**−1.51**
	Solyc05g006220.2.1	IAA-amino acid hydrolase	−10.87	−5.07		**−2.14**
	Solyc02g077430.2.1	Lipase-like	−3.95	−2.53		**−1.56**
	Solyc08g006860.2.1	Patatin	−8.97	−5.47		**−1.64**
	Solyc09g075870.1.1	Lipoxygenase	−4.47	−2.94		**−1.52**
	Solyc01g090660.2.1	Carotenoid cleavage dioxygenase 7	−18.87	−5.30		**−3.56**
	Solyc07g042230.1.1	Ethylene-responsive transcription factor 7	−3.73	−6.95	**−1.86**	
	Solyc07g049530.2.1	1-aminocyclopropane-1-carboxylate oxidase	−3.03	−5.52	**−1.82**	
	Solyc08g007820.1.1	Ethylene-responsive transcription factor 10	−6.07	−11.81	**−1.95**	
	Solyc08g007830.1.1	Ethylene-responsive transcription factor 10	−14.92	−24.04	**−1.61**	
	Solyc10g050970.1.1	Ethylene responsive transcription factor 2b	−9.49	−17.23	**−1.82**	
	Solyc11g042560.1.1	Ethylene-responsive transcription factor 4	17.78	10.49		**1.70**
	Solyc01g109140.2.1	Cytochrome P450	−2.24	−4.17	**−1.86**	
	Solyc04g007790.2.1	Major latex-like protein	154.36	81.88		**1.89**
Oxidative stress	Solyc02g064970.2.1	Peroxidase	−9.34	−3.51		**−2.66**
	Solyc03g116120.1.1	Glutathione *S*-transferase 12	−24.40	−8.02		**−3.04**
	Solyc05g006740.2.1	Glutathione *S*-transferase	−17.48	−3.41		**−5.13**
	Solyc05g006750.2.1	Glutathione *S*-transferase 1	−7.57	−3.30		**−2.30**
	Solyc05g006860.2.1	Thioredoxin H	−17.81	−11.33		**−1.57**
	Solyc05g046000.2.1	Peroxidase 27	−19.32	−3.59		**−5.37**
	Solyc02g083480.2.1	Peroxidase	10.13	3.99		**2.54**
	Solyc12g094620.1.1	Catalase	9.52	5.82		**1.63**
	Solyc06g082420.2.1	Peroxidase 3	−15.99	−40.81	**−2.55**	
Stress response	Solyc03g091010.1.1	Cortical cell-delineating protein	−47.01	−10.25		**−4.59**
	Solyc03g091020.1.1	Cortical cell-delineating protein	−11.41	−5.92		**−1.93**
	Solyc08g079200.1.1	Cortical cell-delineating protein	−5.94	−3.31		**−1.79**
	Solyc08g079230.1.1	Cortical cell-delineating protein	25.45	13.23		**1.92**
	Solyc08g078900.1.1	Cortical cell-delineating protein	6.52	4.23		**1.54**
	Solyc12g014620.1.1	Cortical cell-delineating protein	333.57	178.73		**1.87**
	Solyc06g053950.1.1	Heat stress transcription factor A-2c	−4.14	−7.43	**−1.80**	
	Solyc10g086680.1.1	Class I heat shock protein. HSP20-like chaperone	−4.63	−8.45	**−1.83**	

Ratios were calculated by using RKN_AM and RKN data. Only ratios > |1.5| are reported.

genes involved in stress response some members of the cortical cell-delineating protein family (Solyc08g079230.1.1, Solyc08g078900.1.1 and Solyc12g014620.1.1) (**Supplementary Table S12**) appeared down-regulated in AM-colonized galls whereas others (Solyc03g091020.1.1, Solyc08g079200.1.1) were positively affected by the symbiosis.

DISCUSSION

Several studies addressed the effect of water stress on growth, yield, secondary metabolite production and gene expression in tomato (Nuruddin et al., 2003; Sánchez-Rodríguez et al., 2011; Giannakoula and Ilias, 2013; Sacco et al., 2013; Iovieno et al., 2018). Previous works also studied some specific aspects of the relationship between tomato and AM fungi under drought stress (Dell'Amico et al., 2002; Subramanian et al., 2006; Aroca et al., 2008; Wang et al., 2014; Chitarra et al., 2016; Ruiz-Lozano et al., 2016; Volpe et al., 2018). An untargeted metabolomic analysis of tomato roots colonized by three AM fungi of different genera, verifying their impact on tolerance to drought or salt stress during symbiosis, showed DEGs from several processes, by looking at genome-wide transcriptional changes (Rivero et al., 2018). Massive transcriptional changes are known to occur during AM symbiosis both in dicots and monocots, and a core of marker genes, considered the functional signature of AM symbiosis, have been identified (Guether et al., 2009; Sugimura and Saito, 2017; Fiorilli et al., 2018).

Previous experiments, using the same biological system and water stress level herein studied, showed that *R. intraradices* colonization did not lead to a significant difference in plant performance traits. Tomato plants inoculated with *R. intraradices* showed enhanced internodes/height ratios under water deficit, suggesting a positive AM influence in water stress regimes, likely due to a more compact plant architecture less subject to water dispersion (Volpe et al., 2018). However, in agroecosystems, in addition to water limitation, crops often face other concurrent abiotic and biotic stresses, e.g., insect pests and pathogens (Bai et al., 2018). In the same study, *R. intraradices* appeared effective in sustaining the plant response to a combined abiotic (moderate WS) and biotic stress (aphid attack), the latter in terms of attractiveness toward aphid natural enemies (Volpe et al., 2018). The impact of AM symbiosis on the transcriptomic profile of nematode infection structure (i.e., the gall), firstly confirms the regulation in AM-colonized plants of diverse metabolic pathways, such as primary and secondary metabolisms, ion transport, transcriptional regulation, including several AM symbiosis markers.

Our dataset emphasizes the putative role of specific gene families during symbiosis establishment and functioning. For example, five out of the six genes coding for putative ripening-related proteins (RRP) were strongly significantly up-regulated both in AM-colonized unstressed and water stressed plants (with FC from 4000 to 395 in AM and from 1000 to 38 in AM_WS). Although their function during symbiosis have not been demonstrated, RRP are known to be regulated in several plant/AM combinations (Fiorilli et al., 2015, 2018; Handa et al., 2015). Genes belonging to this family have been found to be strongly induced in rice large lateral roots colonized by the AM fungus (Fiorilli et al., 2015), including *OsAM8*, previously identified as a mycorrhiza-responsive gene (Güimil et al., 2005). Additionally, RRP have been reported among the cysteine-rich peptides highly induced genes in AM *Lotus* roots (Handa et al., 2015). The expression of several *Medicago* RRP was activated, with respect to wild type plants, in a mutant (*pt4*) that leads to early arbuscule degeneration (Floss et al., 2017), opening new questions on the role during symbiosis.

Other gene families showed almost all members as significantly regulated in AM-colonized roots (e.g. blue copper-binding proteins, which are considered markers for AM symbiosis and include phytocyanins that play an important role in plant development and stress resistance), suggesting a functional redundancy as already demonstrated for phosphate transport. However, the location of their regulation remains still unknown (i.e., arbuscule-containing cells *vs.* non-colonized ones). Looking at nutritional aspects, it is worth noting the huge number of up-regulated transporter genes, that indirectly confirm the symbiosis functionality. Interestingly, most of them were significantly up-regulated in AM_WS roots, suggesting that the symbiosis was still functional after imposition of the water stress. The lower gene expression levels in comparison to those in AM roots is in agreement with a decrease in the colonization rate previously reported during water deficit (Chitarra et al., 2016) and also confirmed in this work by a lower percentage of AM fungal reads in AM_WS roots with respect to unstressed plants (AM). However, although symbiosis seems to be affected by water limitation, the impact on root transcriptome is evident also in AM_WS roots. This result reflects the fact that a functional symbiosis seems to be still present during the progression of the water stress, at least for the plant/fungus combination considered in this study.

The 20 most up-regulated genes in AM_WS, compared with those involved in regulation of stress, indicate that AM-colonized roots may differently "sense" the water stress with respect to the uncolonized ones. The most up-regulated genes were in fact still those involved in the symbiosis, at least upon a moderate stress.

Regulation of stress marker genes (i.e., LEA, dehydrin, ABA-responsive genes, P5CS), as observed in AM_WS roots, confirmed the effect of the imposed stress.

The physiological plant response to water deficit is also regulated by the aquaporin proteins (AQPs), controlling water movement through the plant in different physiological conditions. Their regulation is considered as an adaptative mechanism to stress conditions (Kapilan et al., 2018). Molecular analyses already demonstrated a complex transcriptional and post-transcriptional regulation. Data from several studies indicate that AM symbiosis has an impact on host AQPs, altering both plant-water relationships and plant physiology, to better cope with stressful conditions such as drought. However, as reported for other functional aspects related to AM symbiosis, the regulation of AQPs seems to be dependent on the plant and fungal species involved in the symbiosis (Ruiz-Lozano and Aroca, 2017). Data from AM-colonized maize roots, exposed to several growing and water-stressed conditions, showed that the fungus

may regulate a large number of AQP genes in the host plants, in several sub-families. Regulation, however, was also dependent on water status and the duration and severity of the imposed stress (Ruiz-Lozano and Aroca, 2017; Balestrini et al., 2018). This can explain the different result with respect to the data already reported by Chitarra et al. (2016) in the same plant/AM fungus combination, but upon a severe water stress level.

If relevant data are nowadays available on the plant protective effect of AM fungi under water stress, the impact of drought on the fungus itself has not been extensively investigated. Our dataset revealed that cytochrome P450 (CYPs) genes were mainly up-regulated in *R. intraradices*, in presence of water stress. Fungi possess many diverse CYPs, mainly involved in sterol biosynthesis, developmental processes and production of secondary metabolites such as those involved in virulence (Shin et al., 2018). The *R. irregularis* genome, used for the mapping of fungal genes, contains about 200 CYP-encoding genes, indicating an expansion of such a gene family in AMFs that likely deals with the peculiar AM lifestyle (Tisserant et al., 2013; Handa et al., 2015). As cytochrome P450 is involved in the synthesis of sterols for membrane biogenesis during arbuscule formation (Handa et al., 2015), it could be inferred that their over expression reflects a change in fungal development under water deficit. Other most highly up-regulated fungal genes include a "conidiation protein 6" domain (*con-6*). In *Neurospora crassa con-6* encodes a small protein expressed during the formation of conidia (White and Yanofsky, 1993). Fungal conidiation can be induced by nutrient deprivation or mycelium desiccation, a process worth to verify for *R. irregularis* propagules upon drought. The sequences most DE in our database included several that were poorly characterized. This situation may reflect the lack of a functional annotation for a consistent part of the AMF genomes so far sequenced, but might also underlie unprecedented, unknown mechanisms exploited to cope with water stress. Several sequences encoding for stress response-related proteins were regulated, suggesting an impact of the water deficit on the AM fungal metabolism, but their mechanism of action could not be hypothesized, based on current annotation data. Fungal genes containing domains involved in signaling transduction, regulation at the protein level and protein turnover were significantly influenced by the WS treatment, being mainly up-regulated. Such gene families underwent a significant expansion in the *R. irregularis* genome, likely due to the biotrophic lifestyle of the fungus (Zuccaro et al., 2014). Our current data strengthen this idea, suggesting that BTB/POZ and Kelch domain-containing proteins might play a central role in the fungal sensing of environmental stimuli, including the perception of and the response to abiotic stresses.

Three glutathione *S*-transferases (GSTs) were overexpressed in *R. intraradices* upon water stress. GSTs are acknowledged players in the cell protection from oxidative damage, and in tomato one GST is involved in osmotic and salt stress tolerance (Xu et al., 2015). Taken together, these data suggest that the up regulation of GST-encoding genes might represent a conserved hallmark of water stress response, from plants to fungi. Additionally, this confirms previously results on the fact that specific categories of genes involved in stress response can be activated in both the symbiotic partners, such as for AQP (Chitarra et al., 2016) and mitogen-activated protein kinase (MAPK) genes (Liu Z. et al., 2015), in tomato and soybean, respectively.

Plant responses to different stresses are highly complex and dynamic and involve changes at the transcriptome, cellular, and physiological level that are related to the specific environmental stress factors encountered. Only a few data are still available on the molecular basis of AM symbiosis-induced resistance against nematodes (Hao et al., 2012; Vos et al., 2012). Data from our study allowed the identification of a core of tomato DEGs related to parasitism response, essential for a successful RKN-tomato association, that was differently modulated in galls from mycorrhizal colonized roots.

RKN induced GCs, that are characterized by cytoskeleton rearrangements, a fragmented vacuolar system, and an increased cytoplasm density with many organelles, may be 100 times as large as normal root parenchyma cells. Thus, an extensive, coordinated remodeling of the cell wall must occur to allow cell expansion (Williamson and Hussey, 1996; Gheysen and Mitchum, 2011). Our data showed different responses in genes associated to cell wall modification in AM-colonized galls.

Several transcripts coding for proteins involved in cell wall biosynthesis and modification were significantly down-regulated in AM-colonized *vs.* non-colonized galls, suggesting that AM colonization might induce changes in nematode feeding sites by counteracting cell expansion. Conversely, three expansin genes up-regulated during susceptible interaction were highly over expressed in colonized galls. Plant expansins are cell wall loosening proteins involved in the extension of the cell wall (Sampedro and Cosgrove, 2005) and may have a role in the establishment of RKN in tomato (Gal et al., 2006). They have been also reported to be involved in the AM fungal symbiosis development, at different stages of the interaction (Balestrini et al., 2005; Dermatsev et al., 2010). Therefore, we can hypothesize that the highest expression of these genes in *R. intraradices* colonized galls could be explained by the combined action of RKN infection and AM fungal colonization.

The presence of the AM fungus affected other pathways involved in oxygen species (ROS) homeostasis, and cell cycle/root development and response to stress (**Table 7**), which can have a role during the establishment of compatible plant-nematode interaction. Nematodes modulate the production of plant ROS that otherwise would be detrimental for their development. Plant peroxidases (POXs) have an important role in ROS homeostasis as they oxidize phenolics, lignin precursors, auxins and secondary metabolites using hydrogen peroxide (Almagro et al., 2009). In addition to the generation/scavenging of ROS, peroxidase activities have been also associated to loosening/stiffening of the cell wall (Shigeto and Tsutsumi, 2016). Due to the large set of peroxidase isoforms, it is difficult to determine their role in the different biological processes and especially in plant defense response. In the compatible tomato-*M. incognita* interaction genes coding for peroxidases are up- or down-regulated at the same infection time, suggesting that each individual enzyme has its own unique physiological and developmental role (Melillo et al.,

2014). Likewise, in galls from AM-colonized roots some genes coding for POXs were differently regulated with respect to galls from non-colonized plants. Peroxidase genes were also regulated in AM-colonized soybean roots, in presence of infection by *Fusarium virguliforme* (Marquez et al., 2018). The decreased down-regulation of several genes coding for glutathione-*S*-transferase (GST) in galls from AM-colonized plants compared to non-colonized ones suggests a putative protective role of GST against nematode damage, as previously reported during the *R. intraradices*-induced biocontrol of the ectoparasitic nematode *Xiphinema index* in grapevine (Hao et al., 2012).

Members of heat shock protein families (Hsp100, Hsp90, Hsp40, and Hsp20) were down-regulated in RKN and RKN-AM galls, suggesting that plant machinery related to Hsp families is silenced and other pathways may be activated. Interestingly, members of the plant non-specific lipid transfer proteins (LTP), classified as pathogenesis-related proteins, were modulated in the same way in RKN and RKN-AM galls, suggesting different functions in several physiological and stress pathways (Edqvist et al., 2018). Recently, it has been reported that some LTP can induce secondary messengers involved in the induction of different signaling proteins (MAPK family, heat shock factors, etc.) (Li et al., 2014). Another class of LPT is that of the cortical cell delineating proteins, which accumulate in normal root tips and are responsible in the responses of the roots to physical impedance (Huang et al., 1998). Our results showed that they were differentially regulated in RKN and RKN_AM galls and, in particular, the significant increase of the expression of three genes in RKN_AM galls could suggest a protective role of AM in root defense. Other genes associated with stress responses are those encoding major latex protein family (MLP), active in a wide range of developmental processes and in response to biotic and abiotic stresses (Sun et al., 2010; Yang et al., 2015). In our study the Solyc04g007790.2.1 was strongly up-regulated in RKN galls, while in RKN_AM galls the level of this MLP was reduced but still up-regulated, suggesting a role of this protein in the defense response to *M. incognita*, and that AM could activate other defense pathways.

Galls also showed a different modulation of genes involved in root development and cell cycle, in presence of AM. Expression of cell cycle genes in the plant host appears tightly regulated, implying a strict control of the cell cycle machinery and its molecular components during the plant–nematode interaction (Vieira and de Almeida Engler, 2015, 2017). Our results suggested that in galls from AM-colonized roots a different modulation of gene related to the cell cycle, root tip and lateral root development takes place, indicating a transcriptional reprogramming of the root development, also affected by the fungus. By antagonizing the host plant immune response, RKN manipulate defense pathways in the root galls to promote their own development. Our data agree with previous studies stating that genes involved in JA and ET biosynthesis and signaling are suppressed during fully established RKN compatible interaction (Barcala et al., 2010; Nahar et al., 2011). Several genes involved in JA and ET biosynthesis were in fact less down-regulated by AM, suggesting a complex interaction mediated by the fungus.

Additionally, the carotenoid-derived phytohormones strigolactones (SLs) can enhance symbiosis between plants and AM fungi by inducing hyphal branching (Akiyama et al., 2005) and are also important in tomato defense against RKNs (Xu et al., 2019). It was in fact observed that the silencing of *CCD7*, coding for an enzyme involved in SLs biosynthesis, increased plant susceptibility to RKNs (Xu et al., 2019). Our data showed that *CCD7* was strongly down-regulated in non-colonized galls, while it appeared to be induced in galls from AM-colonized roots, in agreement with their known role in AM-symbiosis, associated to early senescence of AM-colonized galls. In presence of the RKN, a suppression of plant defense responses during parasitism has been also observed, involving an alteration of secondary metabolism. Conversely, in galls from AM-colonized roots, transcription of 4-coumarate CoA ligase and anthocyanidin synthase, i.e., two enzymes involved in the flavonoid pathway leading to anthocyanins and condensed tannins, was activated. Flavonoids act during plant-nematode interactions as defense compounds or signals affecting nematode fitness at different life stages (Chin et al., 2018). They may also be involved in nematode feeding site development by maintaining local auxin accumulation. Therefore, the induction of these two enzymes as well as the reduction of the expression of genes belonging to dihydroflavonol-4-reductase family, up-regulated also in other plant–pathogen interactions (Liu et al., 2010), suggest that AM colonization help plants to respond to nematode challenges.

CONCLUSION

Our transcriptome dataset offers new information about the symbiotic-responsive genes both from tomato and the AM fungus, representing a solid basis for future investigations. Moreover, data provided new information on the water stress perception by AM-colonized roots as well as on the response to a biotic stress. Several marker genes (for both AM-colonization and stress factors) have been identified, confirming the robustness of the obtained dataset. Lastly, results on the regulation of AM fungal genes upon a moderate water stress condition have been obtained, suggesting a synergy between plant and fungus in this condition. Sequencing data and morphological observations also indicate that the mechanisms involved in the tomato responses to nematode colonization may also be mediated by the AM symbiosis.

AUTHOR CONTRIBUTIONS

RB, LR, AC, and IP conceived and designed the experiments, and oversaw the manuscript preparation. LR, PV, and MC performed the RNA extraction. PV and MM performed the histopathology and morphological observations. IP performed the bioinformatics analyses. RB, LR, PV, EF, FDL, ASdF, and

IP performed the data analysis. RB, LR, PV, and AC wrote the manuscript. All authors read and approved the final manuscript.

FUNDING

This study was partially funded by the AQUA project (Progetto Premiale, Consiglio Nazionale delle Ricerche) and by the Eureka!Eurostars Programme, project E-7364 "Poch-art."

SUPPLEMENTARY MATERIAL

The Supplementary Material for this article can be found online at: https://www.frontiersin.org/articles/10.3389/fmicb.2019.01807/full#supplementary-material

FIGURE S1 | Specific GO terms enriched during abiotic stress (AM_WS).

FIGURE S2 | Specific GO terms enriched during biotic stress (RKN_AM).

REFERENCES

Akiyama, K., Matsuzaki, K., and Hayashi, H. (2005). Plant sesquiterpenes induce hyphal branching in arbuscular mycorrhizal fungi. *Nature* 435, 824–827. doi: 10.1038/nature03608

Almagro, L., Gómez Ros, L. V., Belchi-Navarro, S., Bru, R., Ros Barceló, A., and Pedreno, M. A. (2009). Class III peroxidases in plant defence reactions. *J. Exp. Bot.* 60, 377–390. doi: 10.1093/jxb/ern277

Aroca, R., Del Mar Alguacil, M., Vernieri, P., and Ruiz-Lozano, J. M. (2008). Plant responses to drought stress and exogenous ABA application are modulated differently by mycorrhization in tomato and an ABA-deficient mutant (*sitiens*). *Microb. Ecol.* 56, 704–719. doi: 10.1007/s00248-008-9390-y

Bai, Y., Sunarti, S., Kissoudis, C., Visser, R. G. F., and van der Linden, C. G. (2018). The role of tomato WRKY genes in plant responses to combined abiotic and biotic stresses. *Front. Plant Sci.* 9:801. doi: 10.3389/fpls.2018.00801

Balestrini, R., and Bonfante, P. (2014). Cell wall remodeling in mycorrhizal symbiosis: a way towards biotrophism. *Front. Plant Sci.* 5:237. doi: 10.3389/fpls.2014.00237

Balestrini, R., Chitarra, W., Antoniou, C., Ruocco, M., and Fotopoulos, V. (2018). Improvement of plant performance under water deficit with the employment of biological and chemical priming agents. themed issue: assessment and monitoring of crop water use and productivity under present and future climate. *J. Agric. Sci.* 156, 680–688. doi: 10.1017/s0021859618000126

Balestrini, R., Cosgrove, D. J., and Bonfante, P. (2005). Differential location of α-expansin proteins during the accommodation of root cells to an arbuscular mycorrhizal fungus. *Planta* 220, 889–899. doi: 10.1007/s00425-004-1431-2

Balestrini, R., Gómez-Ariza, J., Lanfranco, L., and Bonfante, P. (2007). Laser microdissection reveals that transcripts for five plant and one fungal phosphate transporter genes are contemporaneously present in arbusculated cells. *Mol. Plant Microbe Interact.* 20, 1055–1062. doi: 10.1094/mpmi-20-9-1055

Balestrini, R., Salvioli, A., Dal Molin, A., Novero, M., Gabelli, G., Paparelli, E., et al. (2017). Impact of an arbuscular mycorrhizal fungus versus a mixed microbial inoculum on the transcriptome reprogramming of grapevine roots. *Mycorrhiza* 27, 417–430. doi: 10.1007/s00572-016-0754-8

Barcala, M., Garcia, A., Cabrera, J., Casson, S., Lindsey, K., Favery, B., et al. (2010). Early transcriptomic events in microdissected *Arabidopsis* nematode-induced giant cells. *Plant J.* 61, 698–712. doi: 10.1111/j.1365-313X.2009.04098.x

Barghini, E., Cossu, R. M., Cavallini, A., and Giordani, T. (2015). Transcriptome analysis of response to drought in poplar interspecific hybrids. *Genome Data* 3, 143–145. doi: 10.1016/j.gdata.2015.01.004

Bedini, A., Mercy, L., Schneider, C., Franken, P., and Lucic-Mercy, E. (2018). Unraveling the initial plant hormone signaling, metabolic mechanisms and plant defense triggering the endomycorrhizal symbiosis behavior. *Front. Plant Sci.* 9:1800. doi: 10.3389/fpls.2018.01800

Berruti, A., Lumini, E., Balestrini, R., and Bianciotto, V. (2016). Arbuscular mycorrhizal fungi as natural biofertilizers: let's benefit from Past Successes. *Front. Microbiol.* 6:1559. doi: 10.3389/fmicb.2015.01559

Boyer, J. S. (1982). Plant productivity and environment. *Science* 218, 443–448. doi: 10.1126/science.218.4571.443

Casieri, L., Ait Lahmidi, N., Doidy, J., Veneault-Fourrey, C., Migeon, A., Bonneau, L., et al. (2013). Biotrophic transportome in mut, ualistic plant-fungal interactions. *Mycorrhiza* 23, 597–625. doi: 10.1007/s00572-013-0496-9

Chin, S., Behm, C. A., and Mathesius, U. (2018). Functions of flavonoids in plant-nematode interactions. *Plants* 7:85. doi: 10.3390/plants7040085

Chitarra, W., Pagliarani, C., Maserti, B., Lumini, E., Siciliano, I., Cascone, P., et al. (2016). Insights on the impact of arbuscular mycorrhizal symbiosis on tomato tolerance to water stress. *Plant Physiol.* 171, 1009–1023. doi: 10.1104/pp.16.00307

Dell'Amico, J., Torrecillas, A., Rodríguez, P., Morte, A., and Sánchez-Blanco, M. J. (2002). Responses of tomato plants associated with the arbuscular mycorrhizal fungus *Glomus clarum* during drought and recovery. *J. Agric. Sci.* 138, 387–393. doi: 10.1017/s0021859602002101

Dermatsev, V., Weingarten Baror, C., Resnick, N., Gadkar, V., Wininger, S., Kolotilin, I., et al. (2010). Microarray analysis and functional tests suggest the involvement of expansins in the early stages of symbiosis of the arbuscular mycorrhizal fungus *Glomus intraradices* on tomato (*Solanum lycopersicum*). *Mol. Plant Path.* 11, 121–135. doi: 10.1111/j.1364-3703.2009.00581.x

Du, Z., Zhou, X., Ling, Y., Zhang, Z., and Su, Z. (2010). agriGO: a GO analysis toolkit for the agricultural community. *Nucleic Acids Res.* 38, W64–W70. doi: 10.1093/nar/gkq310

Edqvist, J., Blomqvist, C., Nieuwland, J., and Salminen, T. A. (2018). Plant lipid transfer proteins: are we finally closing in on the roles of these enigmatic proteins? *J.Lipid Res.* 59, 1374–1382. doi: 10.1194/jlr.R083139

Elsen, A., Gervacio, D., Swennen, R., and De Waele, D. (2008). AMF-induced biocontrol against plant parasitic nematodes in *Musa* sp.: a systemic effect. *Mycorrhiza* 18, 251–256. doi: 10.1007/s00572-008-0173-6

Fiorilli, V., Catoni, M., Miozzi, L., Novero, M., Accotto, G. P., and Lanfranco, L. (2009). Global and cell-type gene expression profiles in tomato plants colonized by an arbuscular mycorrhizal fungus. *New Phytol.* 184, 975–987. doi: 10.1111/j.1469-8137.2009.03031.x

Fiorilli, V., Vallino, M., Biselli, C., Faccio, A., Bagnaresi, P., and Bonfante, P. (2015). Host and non-host roots in rice: cellular and molecular approaches reveal differential responses to arbuscular mycorrhizal fungi. *Front. Plant Sci.* 6:636. doi: 10.3389/fpls.2015.00636

Fiorilli, V., Vannini, C., Ortolani, F., Garcia-Seco, D., Chiapello, M., Novero, M., et al. (2018). Omics approaches revealed how arbuscular mycorrhizal symbiosis enhances yield and resistance to leaf pathogen in wheat. *Sci. Rep.* 8:9625. doi: 10.1038/s41598-018-27622-8

Floss, D. S., Gomez, S. K., Park, H.-J., MacLean, A. M., Müller, L. M., Bhattarai, K.-K., et al. (2017). A Transcriptional program for arbuscule degeneration during AM symbiosis is regulated by MYB1. *Curr. Biol.* 27, 1206–1212. doi: 10.1016/j.cub.2017.03.003

Gal, T. Z., Aussenberg, E. R., Burdman, S., Kapulnik, Y., and Koltai, H. (2006). Expression of a plant expansin is involved in the establishment of root knot nematode parasitism in tomato. *Planta* 224, 155–162. doi: 10.1007/s00425-005-0204-x

Gamboa-Tuz, S. D., Pereira-Santana, A., Zamora-Briseño, J. A., Castano, E., Espadas-Gil, F., Ayala-Sumuano, J. T., et al. (2018). Transcriptomics and co-expression networks reveal tissue-specific responses and regulatory hubs under mild and severe drought in papaya (*Carica papaya* L.). *Sci. Rep.* 8:14539. doi: 10.1038/s41598-018-32904-2

Garcia, M. E., Lynch, T., Peeters, J., Snowden, C., and Finkelstein, R. (2008). A small plant-specific protein family of ABI five binding proteins (AFPs) regulates stress response in germinating *Arabidopsis* seeds and seedlings. *Plant Mol. Biol.* 67, 643–658. doi: 10.1007/s11103-008-9344-2

Gheysen, G., and Mitchum, M. G. (2011). How nematodes manipulate plant development pathways for infection. *Curr. Opin. Plant Biol.* 14, 415–421. doi: 10.1016/j.pbi.2011.03.012

Giannakoula, A. E., and Ilias, I. F. (2013). The effect of water stress and salinity on growth and physiology of tomato. *Arch. Biol. Sci. Belgrade* 65, 611–620. doi: 10.2298/abs1302611g

Gong, P., Zhang, J., Li, H., Yang, C., Zhang, C., Zhang, X., et al. (2010). Transcriptional profiles of drought-responsive genes in modulating transcription signal transduction, and biochemical pathways in tomato. *J. Exp. Bot.* 61, 3563–3575. doi: 10.1093/jxb/erq167

Guether, M., Balestrini, R., Hannah, M. A., Udvardi, M. K., and Bonfante, P. (2009). Genome-wide reprogramming of regulatory networks, transport, cell wall and membrane biogenesis during arbuscular mycorrhizal symbiosis in *Lotus japonicus*. *New Phytol.* 182, 200–212. doi: 10.1111/j.1469-8137.2008.02725.x

Güimil, S., Chang, H. S., Zhu, T., Sesma, A., Osbourn, A., Roux, C., et al. (2005). Comparative transcriptomics of rice reveals an ancient pattern of response to microbial colonization. *Proc. Nat. Acad. Sci. U. S. A.* 102, 8066–8070. doi: 10.1073/pnas.0502999102

Gutjahr, C. (2014). Phytohormone signaling in arbuscular mycorrhiza development. *Curr. Op. Plant Biol.* 20, 26–34. doi: 10.1016/j.pbi.2014.04.003

Handa, Y., Nishide, H., Takeda, N., Suzuki, Y., Kawaguchi, M., and Saito, K. (2015). RNA-seq transcriptional profiling of an arbuscular mycorrhiza provides insights into regulated and coordinated gene expression in *Lotus japonicus* and *Rhizophagus irregularis*. *Plant Cell Physiol.* 8, 1490–1511. doi: 10.1093/pcp/pcv071

Hao, Z., Fayolle, L., van Tuinen, D., Chatagnier, O., Xiaolin, L., Gianinazzi, S., et al. (2012). Local and systemic mycorrhiza-induced protection against the ectoparasitic nematode *Xiphinema index* involves priming of defence gene responses in grapevine. *J. Exp. Bot.* 63, 3657–3672. doi: 10.1093/jxb/ers046

Hogekamp, C., Arndt, D., Pereira, P. A., Becker, J. D., Hohnjec, N., and Küster, H. (2011). Laser microdissection unravels cell-type-specific transcription in arbuscular mycorrhizal roots, including CAAT-box transcription factor gene expression correlating with fungal contact and spread. *Plant Physiol.* 157, 2023–2043. doi: 10.1104/pp.111.186635

Hogekamp, C., and Küster, H. (2013). A roadmap of cell-type specific gene expression during sequential stages of the arbuscular mycorrhiza symbiosis. *BMC Genomics* 14:306. doi: 10.1186/1471-2164-14-306

Huang, Y. F., Jordan, W. R., Wing, R. A., and Morgan, P. W (1998). Gene expression induced by physical impedance in maize roots. *Plant Mol. Biol.* 37:921.

Iberkleid, I., Sela, N., and Brown Miyara, S. (2015). *Meloidogyne javanica* fatty acid- and retinol-binding protein (Mj-FAR-1) regulates expression of lipid-, cell wall-, stress- and phenylpropanoid-related genes during nematode infection of tomato. *BMC Genomics* 16:272. doi: 10.1186/s12864-015-1426-3

Iovieno, P., Punzo, P., Guida, G., Mistretta, C., Van Oosten, M. J., Nurcato, R., et al. (2018). Transcriptomic changes drive physiological responses to progressive drought stress and rehydration in tomato. *Front. Plant Sci.* 7:371. doi: 10.3389/fpls.2016.00371

Jones, J. T., Haegeman, A., Danchin, E. G., Gaur, H. S., Helder, J., Jones, M. G., et al. (2013). Top 10 plant-parasitic nematodes in molecular plant pathology. *Mol. Plant Pathol.* 14, 946–961. doi: 10.1111/mpp.12057

Kakumanu, A., Ambavaram, M. M. R., Klumas, C., Krishnan, A., Batlang, U., Myers, E., et al. (2012). Effects of drought on gene expression in maize reproductive and leaf meristem tissue revealed by RNA-seq. *Plant Physiol.* 160, 846–867. doi: 10.1104/pp.112.200444

Kal, A. J., van Zonneveld, A. J., Benes, V., van den Berg, M., Koerkamp, M. G., Albermann, K., et al. (1999). Dynamics of gene expression revealed by comparison of serial analysis of gene expression transcript profiles from yeast grown on two different carbon sources. *Mol. Biol. Cell* 10, 1859–1872. doi: 10.1091/mbc.10.6.1859

Kapilan, R., Vaziri, M., and Zwiazek, J. J. (2018). Regulation of aquaporins in plants under stress. *Biol. Res.* 51:4. doi: 10.1186/s40659-018-0152-0

Kuromori, T., Seo, M., and Shinozaki, K. (2018). ABA transport and plant water stress responses. *Trends Plant Sci.* 23, 513–522. doi: 10.1016/j.tplants.2018.04.001

Li, J., Gao, G. Z., Xu, K., Chen, B. Y., Yan, G. X., Li, F., et al. (2014). Genome-wide survey and expression analysis of the putative non-specific lipid transfer proteins in *Brassica rapa* L. *PLoS One* 9:e84556. doi: 10.1371/journal.pone.0084556

Li, M., Wang, R., Tian, H., and Gao, Y. (2018). Transcriptome responses in wheat roots to colonization by the arbuscular mycorrhizal fungus *Rhizophagus irregularis*. *Mycorrhiza* 28, 747–759. doi: 10.1007/s00572-018-0868-2

Liu, F., Zhang, X., Lu, C., Zeng, X., Li, Y., Fu, D., et al. (2015). Non-specific lipid transfer proteins in plants: presenting new advances and an integrated functional analysis. *J. Exp. Bot.* 66, 5663–5681. doi: 10.1093/jxb/erv313

Liu, Z., Li, Y., Ma, L., Wei, H., Zhang, J., He, X., et al. (2015). Coordinated regulation of arbuscular mycorrhizal fungi and soybean MAPK pathway genes improved mycorrhizal soybean drought tolerance. *Mol. Plant Microbe Interact.* 28, 408–419. doi: 10.1094/MPMI-09-14-0251-R

Liu, H., Du, Y., Chu, H., Shih, C. H., Wong, Y. W., Wang, M., et al. (2010). Molecular dissection of the pathogen-inducible 3-deoxyanthocyanidin biosynthesis pathway in sorghum. *Plant Cell Physiol.* 51, 1173–1185. doi: 10.1093/pcp/pcq080

Mandal, S. M., Chakraborty, D., and Dey, S. (2010). Phenolic acids act as signaling molecules in plant-microbe symbioses. *Plant Signal. Behav.* 5, 359–368. doi: 10.4161/psb.5.4.10871

Marquez, N., Giachero, L., Adrien, G., Debat, H., Declerck, S., and Ducasse, D. A. (2018). Transcriptome analysis of mycorrhizal and non-mycorrhizal soybean plantlets upon infection with *Fusarium virguliforme*, one causal agent of sudden death syndrome. *Plant Pathol.* 68, 470–480. doi: 10.1111/ppa.12964

Martinez-Medina, A., Flors, V., Heil, M., Mauch-Mani, B., Pieterse, C. M. J., Pozo, M. J., et al. (2016). Recognizing plant defense priming. *Trends Plant Sci.* 21, 818–822. doi: 10.1016/j.tplants.2016.07.009

McGuiness, P. N., Reid, J. B., and Foo, E. (2019). The role of gibberellins and brassinosteroids in nodulation and arbuscular mycorrhizal associations. *Front. Plant Sci.* 10:269. doi: 10.3389/fpls.2019.00269

Melillo, M. T., Leonetti, P., and Veronico, P. (2014). Benzothiadiazole effect in the compatible tomato-*Meloidogyne incognita* interaction: changes in giant cell development and priming of two root anionic peroxidases. *Planta* 240, 841–854. doi: 10.1007/s00425-014-2138-7

Mortazavi, A., Williams, B. A., McCue, K., Schaeffer, L., and Wold, B. (2008). Mapping and quantifying mammalian transcriptomes by RNA-Seq. *Nat. Methods* 5, 621–628. doi: 10.1038/nmeth.1226

Nahar, K., Kyndt, T., De Vleesschauwer, D., Hofte, M., and Gheysen, G. (2011). The jasmonate pathway is a key player in systemically induced defence against root-knot nematodes in rice. *Plant Physiol.* 157, 305–316. doi: 10.1104/pp.111.177576

Nir, I., Shohat, H., Panizel, I., Olszewski, N., Aharoni, A., and Weiss, D. (2017). The tomato DELLA protein PROCERA acts in guard cells to promote stomatal closure. *Plant Cell* 29, 3186–3197. doi: 10.1105/tpc.17.00542

Nuruddin, M. M., Madramootoo, C. A., and Dodds, G. T. (2003). Effects of water stress at different growth stages on greenhouse tomato yield and quality. *HortScience* 38, 1389–1393. doi: 10.21273/hortsci.38.7.1389

Oono, Y., Yazawa, T., Kawahara, Y., Kanamori, H., Kobayashi, F., Sasaki, H., et al. (2014). Genome-wide transcriptome analysis reveals that cadmium stress signaling controls the expression of genes in drought stress signal pathways in rice. *PLoS One* 9:e96946. doi: 10.1371/journal.pone.0096946

Ortu, G., Balestrini, R., Pereira, P. A., Becker, J. D., Küster, H., and Bonfante, P. (2012). Plant genes related to gibberellin biosynthesis and signaling are differentially regulated during the early stages of AM fungal interactions. *Mol. Plant* 5, 951–954. doi: 10.1093/mp/sss027

Portillo, M., Cabrera, J., Lindsey, K., Topping, J., Andrés, M. F., Emiliozzi, M., et al. (2013). Distinct and conserved transcriptomic changes during nematode-induced giant cell development in tomato compared with *Arabidopsis*: a functional role for gene repression. *New Phytol.* 197, 1276–1290. doi: 10.1111/nph.12121

Prágai, Z., and Harwood, C. R. (2002). Regulatory interactions between the Pho and σB-dependent general stress regulons of *Bacillus subtilis*. *Microbiology* 148, 1593–1602. doi: 10.1099/00221287-148-5-1593

Recchia, G. H., Konzen, E. R., Cassieri, F., Caldas, D. G. G., and Tsai, S. M. (2018). Arbuscular mycorrhizal symbiosis leads to differential regulation of drought-responsive genes in tissue-specific root cells of common bean. *Front. Microbiol.* 9:1339. doi: 10.3389/fmicb.2018.01339

Rivero, J., Álvarez, D., Flors, V., Azcón-Aguilar, C., and Pozo, M. J. (2018). Root metabolic plasticity underlies functional diversity in mycorrhiza-enhanced stress tolerance in tomato. *New Phytol.* 220, 1322–1336. doi: 10.1111/nph.15295

Robinson, M. D., McCarthy, D. J., and Smyth, G. K. (2010). edgeR: a bioconductor package for differential expression analysis of digital gene expression data. *Bioinformatics* 26, 139–140. doi: 10.1093/bioinformatics/btp616

Robinson, M. D., and Smyth, G. K. (2008). Small-sample estimation of negative binomial dispersion, with applications to SAGE data. *Biostatistics* 9, 321–332. doi: 10.1093/biostatistics/kxm030

Ruiz-Lozano, J. M., and Aroca, R. (2017). "Plant aquaporins and mycorrhizae: their regulation and involvement in plant physiology and performance," in *Plant Aquaporins. Signaling and Communication in Plants*, eds F. Chaumont and S. Tyerman (Cham: Springer).

Ruiz-Lozano, J. M., Aroca, R., Zamarreño, A. M., Molina, S., Andreo-Jiménez, B., Porcel, R., et al. (2016). Arbuscular mycorrhizal symbiosis induces strigolactone biosynthesis under drought and improves drought tolerance in lettuce and tomato. *Plant Cell Environ.* 39, 441–452. doi: 10.1111/pce.12631

Ruzicka, D., Chamala, S., Barrios-Masias, F. H., Martin, F., Smith, S., Jackson, L. E., et al. (2013). Inside arbuscular mycorrhizal roots - molecular probes to understand the symbiosis. *Plant Genome* 6, 1–13.

Sacco, A., Greco, B., Di Matteo, A., De Stefano, R., and Barone, A. (2013). Evaluation of tomato genetic resources for response to water deficit. *Am. J. Plant Sci.* 4, 131–145. doi: 10.4236/ajps.2013.412a3016

Sampedro, J., and Cosgrove, D. J. (2005). The expansin superfamily. *Genome Biol.* 6:242.

Sánchez-Rodríguez, E., Moreno, D. A., Ferreres, F., del Mar Rubio-Wilhelmi, M., and Ruiz, J. M. (2011). Differential responses of five cherry tomato varieties to water stress: changes on phenolic metabolites and related enzymes. *Phytochemistry* 72, 723–729. doi: 10.1016/j.phytochem.2011.02.011

Schouteden, N., Waele, D. D., Panis, B., and Vos, C. M. (2015). Arbuscular mycorrhizal fungi for the biocontrol of plant-parasitic nematodes: a review of the mechanisms involved. *Front. Microbiol.* 6:1280. doi: 10.3389/fmicb.2015.01280

Selosse, M.-A., Bessis, A., and Pozo, M. J. (2014). Microbial priming of plant and animal immunity: symbionts as developmental signals. *Trends Microbiol.* 22, 607–613. doi: 10.1016/j.tim.2014.07.003

Sharma, I. P., and Sharma, A. K. (2017). Co-inoculation of tomato with an arbuscular mycorrhizal fungus improves plant immunity and reduces root-knot nematode infection. *Rhizosphere* 4, 25–28. doi: 10.1016/j.rhisph.2017.05.008

Shigeto, J., and Tsutsumi, Y. (2016). Diverse functions and reactions of class III peroxidases. *New Phytol.* 209, 1395–1402. doi: 10.1111/nph.13738

Shin, J., Kim, J.-E., Lee, Y.-W., and Son, H. (2018). Fungal cytochrome P450s and the P450 complement (CYPome) of *Fusarium graminearum*. *Toxins* 10:112. doi: 10.3390/toxins10030112

Shinozaki, K., and Yamaguchi-Shinozaki, K. (2007). Gene networks involved in drought stress response and tolerance. *J. Exp. Bot.* 58, 221–227. doi: 10.1093/jxb/erl164

Shukla, N., Yadav, R., Kaur, P., Rasmussen, S., Goel, S., Agarwal, M., et al. (2018). Transcriptome analysis of root-knot nematode (*Meloidogyne incognita*)-infected tomato (*Solanum lycopersicum*) roots reveals complex gene expression profiles and metabolic networks of both host and nematode during susceptible and resistance responses. *Mol. Plant Pathol.* 19, 615–633. doi: 10.1111/mpp.12547

Subramanian, K. S., Santhanakrishnan, P., and Balasubramanian, P. (2006). Responses of field grown tomato plants to arbuscular mycorrhizal fungal colonization under varying intensities of drought stress. *Sci. Hortic.* 107, 245–253. doi: 10.1016/j.scienta.2005.07.006

Sugimura, Y., and Saito, K. (2017). Comparative transcriptome analysis between *Solanum lycopersicum* L. *and Lotus japonicus L. during arbuscular mycorrhizal development*. *Soil Sci. Plant Nutr.* 63, 127–136. doi: 10.1080/00380768.2017.1280378

Sun, H., Kim, M., Pulla, R. K., Kim, Y., and Yang, D. (2010). Isolation and expression analysis of a novel major latex-like protein (MLP151) gene from panax ginseng. *Mol. Boil Rep.* 37, 2215–2222. doi: 10.1007/s11033-009-9707-z

Tisserant, E., Malbreil, M., Kuo, A., Kohler, A., Symeonidi, A., Balestrini, R., et al. (2013). Genome of an arbuscular mycorrhizal fungus provides insight into the oldest plant symbiosis. *Proc. Natl. Ac. Sci. U. S. A.* 110, 20117–20122. doi: 10.1073/pnas.1313452110

Vangelisti, A., Natali, L., Bernardi, R., Sbrana, C., Turrini, A., Hassani-Pak, K., et al. (2018). Transcriptome changes induced by arbuscular mycorrhizal fungi in sunflower (*Helianthus annuus* L.) roots. *Sci. Rep.* 8:4. doi: 10.1038/s41598-017-18445-0

Vieira, P., and de Almeida Engler, J. (2015). The plant cell inhibitor KRP6 is involved in multinucleation and cytokinesis disruption in giant-feeding cells induced by root-knot nematodes. *Plant Signal. Behav.* 10:e1010924. doi: 10.1080/15592324.2015.1010924

Vieira, P., and de Almeida Engler, J. (2017). Plant cyclin-dependent kinase inhibitors of the KRP family: potent inhibitors of root-knot nematode feeding sites in plant roots. *Front. Plant Sci.* 8:1514. doi: 10.3389/fpls.2017.01514

Volpe, V., Chitarra, W., Cascone, P., Volpe, M. G., Bartolini, P., Moneti, G., et al. (2018). The association with two different arbuscular mycorrhizal fungi differently affects water stress tolerance in tomato. *Front. Plant Sci.* 9:1480. doi: 10.3389/fpls.2018.01480

Vos, C., Tesfahun, A. N., Panis, B., De Waele, D., and Elsen, A. (2012). Arbuscular mycorrhizal fungi induce systemic resistance in tomato against the sedentary nematode *Meloidogyne incognita* and the migratory nematode *Pratylenchus penetrans*. *Appl. Soil Ecol.* 61, 1–6. doi: 10.1016/j.apsoil.2012.04.007

Wang, B., Yao, Z., Zhao, S., Guo, K., Sun, J., and Zhang, H. (2014). Arbuscular mycorrhizal fungal application to improve growth and tolerance of processing tomato (*Lycopersicon esculentum* Miller) under drought stress. *J. Food Agric. Environ.* 12, 452–457.

White, B. T., and Yanofsky, C. (1993). Structural characterization and expression analysis of the *Neurospora* conidiation egne con-6. *Develop. Biol.* 160, 254–264. doi: 10.1006/dbio.1993.1303

Williamson, V. M., and Hussey, R. S. (1996). Nematode pathogenesis and resistance in plants. *Plant Cell* 8, 1735–1745. doi: 10.1105/tpc.8.10.1735

Xu, J., Xing, X.-J., Tian, Y.-S., Peng, R.-H., Xue, Y., Zhao, W., et al. (2015). Transgenic *Arabidopsis* plants expressing tomato glutathione S-transferase showed enhanced resistance to salt and drought stress. *PLoS One* 10:e0136960. doi: 10.1371/journal.pone.0136960

Xu, X., Fang, P., Zhang, H., Chi, C., Song, L., Xia, X., et al. (2019). Strigolactones positively regulate defense against root-knot nematodes in tomato. *J. Exp. Bot.* 70, 1325–1337. doi: 10.1093/jxb/ery439

Yang, C., Liang, S., Wang, H., Han, L., Wang, F., Cheng, H., et al. (2015). Cotton Major Latex Protein 28 functions as a positive regulator of the ethylene responsive factor 6 in defense against *Verticillium dalhliae*. *Mol. Plant* 8, 399–411. doi: 10.1016/j.molp.2014.11.023

Zouari, I., Salvioli, A., Chialva, M., Novero, M., Miozzi, L., Tenore, G. C., et al. (2014). From root to fruit: RNA-Seq analysis shows that arbuscular mycorrhizal symbiosis may affect tomato fruit metabolism. *BMC Genomics* 15:221. doi: 10.1186/1471-2164-15-221

Zuccaro, A., Lahrmann, U., and Langen, G. (2014). Broad compatibility in fungal root symbioses. *Curr. Op. Plant Biol.* 20, 135–145. doi: 10.1016/j.pbi.2014.05.013

Conflict of Interest Statement: The authors declare that the research was conducted in the absence of any commercial or financial relationships that could be construed as a potential conflict of interest.

frontiers in Plant Science

REVIEW
published: 26 September 2019
doi: 10.3389/fpls.2019.01172

Interactions Between Phosphorus, Zinc, and Iron Homeostasis in Nonmycorrhizal and Mycorrhizal Plants

Xianan Xie[1], Wentao Hu[1], Xiaoning Fan[2], Hui Chen[1] and Ming Tang[1]**

[1] State Key Laboratory of Conservation and Utilization of Subtropical Agro-Bioresources (South China Agricultural University), Guangdong Key Laboratory for Innovative Development and Utilization of Forest Plant Germplasm, College of Forestry and Landscape Architecture, South China Agricultural University, Guangzhou, China, [2] Department of Plant Pathology, Guangdong Province Key Laboratory of Microbial Signals and Disease Control, College of Agriculture, South China Agricultural University, Guangzhou, China

Phosphorus (P), zinc (Zn), and iron (Fe) are three essential elements for plant survival, and severe deficiencies in these nutrients lead to growth retardation and crop yield reduction. This review synthesizes recent progress on how plants coordinate the acquisition and signaling of Pi, Zn, and Fe from surrounding environments and which genes are involved in these Pi–Zn–Fe interactions with the aim of better understanding of the cross-talk between these macronutrient and micronutrient homeostasis in plants. In addition, identification of genes important for interactions between Pi, Zn, and/or Fe transport and signaling is a useful target for breeders for improvement in plant nutrient acquisition. Furthermore, to understand these processes in arbuscular mycorrhizal plants, the preliminary examination of interactions between Pi, Zn, and Fe homeostasis in some relevant crop species has been performed at the physiological level and is summarized in this article. In conclusion, the development of integrative study of cross-talks between Pi, Zn, and Fe signaling pathway in mycorrhizal plants will be essential for sustainable agriculture all around the world.

Keywords: phosphorus, zinc, iron, Pi–Zn–Fe interactions, arbuscular mycorrhizal plants

OPEN ACCESS

Edited by:
Valentina Fiorilli, University of Turin, Italy

Reviewed by:
Nuria Ferrol, Experimental Station of Zaidín (EEZ), Spain
Cristiana Sbrana, Istituto di Biologia e Biotecnologia Agraria (IBBA), Italy

****Correspondences:***
Xianan Xie
xiexianan8834203@126.com
Ming Tang
tangmingyl@163.com

Specialty section:
This article was submitted to Plant Microbe Interactions, a section of the journal Frontiers in Plant Science

Received: *17 March 2019*
Accepted: *27 August 2019*
Published: *26 September 2019*

Citation:
Xie X, Hu W, Fan X, Chen H and Tang M (2019) Interactions Between Phosphorus, Zinc, and Iron Homeostasis in Nonmycorrhizal and Mycorrhizal Plants. Front. Plant Sci. 10:1172. doi: 10.3389/fpls.2019.01172

INTRODUCTION

Inorganic phosphate (Pi), zinc (Zn), and iron (Fe) are three essential macronutrient and micronutrients for the survival and development of all living organisms including mycorrhizal plants and edible crops (Westheimer, 1987; Briat et al., 1995; Marschner, 1995; Salgueiro et al., 2000). These three mineral elements are relatively inaccessible to plants and crops because of their low solubility and relative immobilization in the agricultural soils (Lopez et al., 2000; Hirsch et al., 2006). Crops are therefore subjected to Pi, Zn, and Fe deficiencies, which can adversely impact multiple metabolic processes in cells. Nevertheless, plants have evolved a number of strategies to cope with low Pi, Zn, and Fe availabilities, including development of a mycorrhizal symbiosis (Karandashov and Bucher, 2005; Smith and Read, 2008), conversion of metabolism, remodeling of root morphology, secretion of root exudates, and induction of the high-affinity transport systems.

In recent decades, the effects of Pi, Zn, and Fe deficiencies on crop yield and quality have become a global concern due to the issues of food availability and malnutrition (Abelson, 1999; Neset and Cordell, 2012; Shahzad et al., 2014). To guarantee the sustainable food source for the growing

population, worldwide agriculture has become dependent on the massive use of Pi, Zn, and Fe fertilizers for improving crop yield and quality. Nevertheless, this strategy has adverse long-term economic and ecological impacts. Development of sustainable agricultural practices will require crops with improved Pi, Zn, and Fe nutrition in order to reduce the application of these fertilizers. The novel plant genotypes with high-efficiency nutrient use are genetically desired in an appropriate way to fit the lower input into the environment. Despite the importance of these issues, the biological interactions between P, Zn, and Fe elements still remain incompletely studied, and our understanding is limited of how various signaling pathways are induced in response to nutrient availability and how these changes are integrated with relation to other nutrients (Briat et al., 2015). On the other hand, some key genes involved in the acquisition and distribution of macronutrient and micronutrients in nonmycorrhizal and mycorrhizal plants have been identified (Javot et al., 2007a; Gojon et al., 2009; Pilon et al., 2009; Giovannetti et al., 2014; Watts-Williams and Cavagnaro, 2018), and their expression in response to nutrient status has started to be elucidated (Schachtman and Shin, 2007; Giehl et al., 2009; Liu et al., 2009; Hindt and Guerinot, 2012).

Approximately 72% of terrestrial vascular plant species are capable of establishing symbiotic mutualistic associations with obligate biotrophic soil-borne arbuscular mycorrhizal fungi (AMF) from the phylum Glomeromycota (Remy et al., 1994; Schüßler et al., 2001; Bonfante, 2018). The endosymbiotic associations between plants and AMF, namely, arbuscular mycorrhizas (AM), are widespread in terrestrial ecosystems (Parniske, 2008). In AM symbiosis, the fungal symbiont provides mineral nutrients to the plant and in return obtains sugars and lipids (Smith and Read, 2008; Jiang et al., 2017), and thus, this symbiosis has significant contribution to plant productivity and ecosystem function (van der Heijden et al., 1998).

AM symbiosis not only is capable of significantly improving the acquisition of macronutrients such as Pi, N, and S to host plant (Ames et al., 1983; Smith et al., 2003; Smith and Read, 2008; Allen and Shachar, 2009; Leigh et al., 2009; Sieh et al., 2013) but also facilitates the uptake and translocation of micronutrients such as Zn and Fe in the soil–AMF–plant continuum (Caris et al., 1998; Liu et al., 2000; Chen et al., 2003; Farzaneh et al., 2011; González et al., 2016). The acquisition of Pi, N, and S in AM symbiosis through a specific symbiotic uptake pathway has been extensively described (Rausch et al., 2001; Harrison et al., 2002; Javot et al., 2007b; Chen et al., 2007; Guether et al., 2009; Yang et al., 2012; Giovannetti et al., 2014; Volpe et al., 2016). However, very few studies have been undertaken to uncover the molecular mechanisms underlying the uptake and homeostasis of Zn and Fe from AM fungus *Rhizophagus irregularis* to the plant (González et al., 2005; Tamayo et al., 2014; Tamayo et al., 2018), and the impact of this symbiosis on Zn and Fe homeostasis in plant is far from being understood (Chorianopoulou et al., 2015; Watts-Williams et al., 2015). A very recent study has revealed the involvement of AM-modified *ZmNAS1*, *ZmNAS3*, and *ZmYS1* genes in the regulation of Fe homeostasis in mycorrhizal maize through sulfate deficiency signaling (Chorianopoulou et al., 2015), suggesting the existence of a cross-talk between S and Fe homeostasis in mycorrhizal symbiosis. Nevertheless, the molecular basis of the double or tripartite interactions between Pi, Zn, and Fe homeostasis in AM symbiosis is still lacking in mycorrhizal plants. Therefore, it is of biological significance to decipher the mechanisms of coordinating the Pi, Zn, and Fe deficiency signaling in AM symbiosis and consequently profit mycorrhizal plant growth and fitness during multiple Pi–Zn–Fe deficiency stresses.

In such context, the aim of this review is to summarize current knowledge on cross-talk between Pi and Zn, Pi and Fe, Zn and Fe, and tripartite Pi–Zn–Fe homeostasis in both nonmycorrhizal and mycorrhizal plants. Additionally, Pi (or Fe) nutrition is also affected by the interaction between Zn and Fe (or Pi) in plants, such as *Arabidopsis* and rice. The MYB transcription factor (TF) PHR1 acting as a potential integrator of Pi, Zn, and Fe nutrient signals to regulate mineral nutrition in plants is discussed. Moreover, a novel role of the OsPHO1;1 in Fe transport through integrating Pi and Zn deficiency signaling is proposed, and these complicated nutritional interactions are presented, with a focus on the emerging roles of nutrient transporters in mycorrhizal plants.

Membrane Transporters and Their Roles in Mineral Uptake and Homeostasis in Plants

In plants, Pi, Zn, and Fe are acquired at the root periphery in the form of free ions (Guerinot, 2000; Curie et al., 2001; Vert et al., 2002; Nussaume et al., 2011; Milner et al., 2013), and the uptake and translocation of these minerals in plants involve multiple and complex transport systems.

The Pi is taken up at the root system *via* the high-affinity $Pi:H^+$ symporters belonging to members of the PHT1 family (Schachtman et al., 1998; Bucher, 2007; Nussaume et al., 2011). The *Arabidopsis*, rice, soybean, and tomato genomes harbor 9, 13, 14, and 8 members of the PHT1 family, respectively (Paszkowski et al., 2002; Poirier and Bucher, 2002; Fan et al., 2013; Chen et al., 2014). Some of these *Pht1* genes are predominantly expressed in roots, and the encoded proteins function as high-affinity Pi uptake transporters (Muchhal et al., 1996; Shin et al., 2004; Remy et al., 2012; Sun et al., 2012). Nevertheless, the transcripts of *Pht1* genes are also detected in shoots (including vegetative and reproductive tissues), implicating their role beyond Pi uptake at the root surface (Mudge et al., 2002; Nagarajan et al., 2011; Chen et al., 2014). In *Arabidopsis*, five out of nine *Pht1* members have been functionally characterized by genetic approaches. Earlier work reported that both AtPT1 and AtPT4 transporters contributed to Pi uptake in *Arabidopsis thaliana* under both low and high Pi levels (Shin et al., 2004). However, the double mutant *pht1;1Δpht1;4Δ* showed a more pronounced reduction in Pi acquisition relative to wild-type from both low and high Pi environments, suggesting redundant functions of these two Pi transporters (Shin et al., 2004). Nevertheless, Nagarajan et al. (2011) showed that the AtPT5 could mobilize Pi between the source and sink organs for Pi homeostasis in *A. thaliana*. Recently, it was demonstrated that AtPT8 and AtPT9 transporters act in a redundant manner during Pi uptake in *Arabidopsis* seedlings during Pi starvation (Remy et al., 2012). These results indicated the compensatory effects of root Pi uptake and shoot Pi accumulation between the four *Arabidopsis* Pi transporters AtPT1, AtPT4, AtPT8, and AtPT9 during Pi deficiency. In rice (*Oryza sativa*), a total of 13 members of the PHT1 family have been identified (Goff

et al., 2002), and 10 out of 13 genes had been well characterized in *O. sativa* by reverse genetics. The constitutively expressed OsPT1 mediates Pi translocation in shoots and also induces root hair growth in rice during Pi-repletion (Sun et al., 2012). Ai et al. (2009) demonstrated that *OsPT2* was transcriptionally induced in roots under Pi deficiency and functioned in Pi translocation in rice, while OsPT3 mediated Pi uptake, translocation, and remobilization in rice under extremely low Pi regimes (Chang et al., 2019). OsPT4 not only facilitated Pi mobilization but also played a pivotal role in embryo development (Zhang F et al., 2015), whereas OsPT6 displayed a broad role in Pi acquisition and translocation throughout the plant (Ai et al., 2009). It was observed that the high-affinity Pi transporter gene *OsPT8* was involved in Pi homeostasis in rice (Jia et al., 2011). However, Wang et al. (2014b) found that OsPT9 and OsPT10 redundantly functioned in Pi uptake under both low and high Pi conditions. OsPT11 and OsPT13 were exclusively induced in arbusculated cells and non-redundantly regulated the arbuscular mycorrhizal symbiosis in rice (Paszkowski et al., 2002; Yang et al., 2012). The current understanding of the Pi transport activities of Pht1 transporters and their complex regulation in plants has been well documented and intensively summarized in multiple reviews in recent years (Poirier and Bucher, 2002; Bayle et al., 2011; Lin et al., 2013; Chen et al., 2015; Poirier and Jung, 2015; Gu et al., 2016).

For Zn^{2+} acquisition in roots, transmembrane transporters belonging to the ZIP (ZRT and IRT-like protein) family are considered to be the primary Zn^{2+} uptake transporters, which have been identified in both dicotyledons and monocotyledons (Eng et al., 1998; Maser et al., 2001; López et al., 2004; Palmer and Guerinot, 2009; Lee et al., 2010; Tiong et al., 2014). Some ZIP family transporters preferentially localize to the plasma membrane of root epidermal cells and deletion, or overexpression of these genes results in plants that accumulate less or more Zn^{2+} than do wild-type plants, respectively. This is indicative of their roles in Zn^{2+} acquisition at root–soil interface (Lee et al., 2010; Milner et al., 2012). In *Arabidopsis*, the plasma membrane-localized AtIRT1, belonging to the ZIP gene family, is involved in Zn^{2+} uptake at root epidermal cells (Henriques et al., 2002; Vert et al., 2002; Barberon et al., 2011). The well-characterized ZIP gene *IRT3* is transcriptionally induced in response to Zn^{2+} deficiency and confers increased shoot Zn^{2+} accumulation when overexpressed in *Arabidopsis* (van de Mortel et al., 2006; Sinclair and Krämer, 2012). Moreover, AtIRT3 is localized to the plasma membrane where it transports Zn^{2+} across the plasma membrane into the cell (Lin et al., 2009). In rice, the node-localized transporter, OsZIP3, is responsible for unloading Zn^{2+} from the xylem as well as Zn^{2+} distribution to the developing tissues (Sasaki et al., 2015), whereas the OsZIP4 located in the phloem cells acts as a Zn^{2+} transporter that may be responsible for Zn^{2+} translocation within plant (Ishimaru et al., 2005). Other *Arabidopsis* and rice ZIP family members involved in Zn^{2+} uptake and homeostasis are barely known, and therefore, further works need to determine their precise roles in plants.

Iron (Fe) from the soils enters the root cells through two distinct strategies (**Figure 1**), according to non-Graminacea plants (strategy I) and Graminacea plants (strategy II). In strategy I plants, the ferric iron (Fe^{3+}) is reduced in the ferrous iron (Fe^{2+}) prior to uptake into the root epidermal cells (Morrissey and Guerinot, 2009; Conte and Walker, 2011). For example, in *Arabidopsis*, under Fe deficiency, the FIT and bHLH TFs, bHLH38 and bHLH39, are activated in roots and bind to the promoters of the iron-responsive genes. Subsequently, the induction of ferric reductase oxidase 2 (FRO2) and IRT1 activity is co-regulated in response to iron deficiency through the reduction-based strategy I for iron uptake (**Figure 1A**), while iron in rhizosphere is firstly solubilized by the activated H^+-ATPase AHA2 and is then reduced from ferric (Fe^{3+}) to ferrous (Fe^{2+}) iron by the reductase FRO2 (Ivanov et al., 2012). Fe^{2+} is then imported into the root cell by the metal transporter IRT1 (Vert et al., 2002).

In strategy II plants, the ferric iron (Fe^{3+}) is first chelated by interaction with mugineic acids (MAs) (**Figure 1B**), and then these Fe^{3+}–MA complexes are taken up into root cells by plasma membrane-localized transporter proteins (Curie et al., 2001). For example, in maize, under iron deficiency, MAs are synthesized in root cells by nicotianamine synthase (NAS), NA aminotransferase (NAAT), and deoxymugineic acid synthase (DMAS); and MAs are secreted into rhizosphere by transporter of MA family phytosiderophores1 (TOM1) (Li et al., 2018). Then, Fe^{3+}–MAs are transported into root cells by the transmembrane transporter yellow stripe 1-like (YSL) (Curie et al., 2001).

After their uptake at the root surface, these minerals can be transported to the vacuoles. Alternatively, Pi, Zn^{2+}, and iron can undergo symplastic journey towards the root xylem for movement upward to the aerial tissues. For Pi, phosphate exporters PHO1 and PHO1;H1 have been identified as important components in the long-distance transfer of Pi from roots to shoots (Poirier et al., 1991; Hamburger et al., 2002; Stefanovic et al., 2011; Kisko et al., 2015).

For Zn^{2+}, two plasma membrane transporters AtHMA2 and AtHMA4 belonging to P_{1B}-ATPase subfamily played key roles in Zn loading into the xylem and root-to-shoot translocation of Zn^{2+} in *Arabidopsis* (Hussain et al., 2004; Verret et al., 2004; Hanikenne et al., 2008; Wong et al., 2009). NA had been proposed to form stable complexes with Zn and to play an important role in Zn^{2+} movement in the xylem and phloem (Stephan and Scholz, 1993). NAS genes were induced under Zn^{2+} deficiency (Wintz et al., 2003) and were functionally involved in the intercellular movement and long-distance transport of Zn^{2+} in *A. thaliana* (Takahashi et al., 2003). Overexpression of *AhNAS2* gene in roots contributed to Zn^{2+} hyperaccumulation of *Arabidopsis halleri* (Deinlein et al., 2012). Interestingly, the constitutive expression of NAS genes from other plant species caused an increase in Zn^{2+} translocation and accumulation in polished rice grains (Masuda et al., 2009; Lee et al., 2011), illustrating the significant importance of the NAS proteins in the Zn^{2+} translocation in plants. The major facilitator superfamily (MFS) transporter (Pao et al., 1998), zinc-induced facilitator 1 (ZIF1), was shown to contribute to Zn^{2+} tolerance in *Arabidopsis* (Haydon and Cobbett, 2007), and tonoplast-localized ZIF1 proteins have been implicated in vacuolar Zn^{2+} sequestration (Arrivault et al., 2006; Kawachi et al., 2009). Under Zn^{2+} deficiency, the vacuole-stored Zn^{2+} was remobilized (Lanquar et al., 2004) to the cytosol. Natural resistance-associated macrophage protein (NRAMP) family members played roles in heavy metal transport in plants (Belouchi et al., 1995; Thomine et al., 2000). *Arabidopsis* NRAMP4

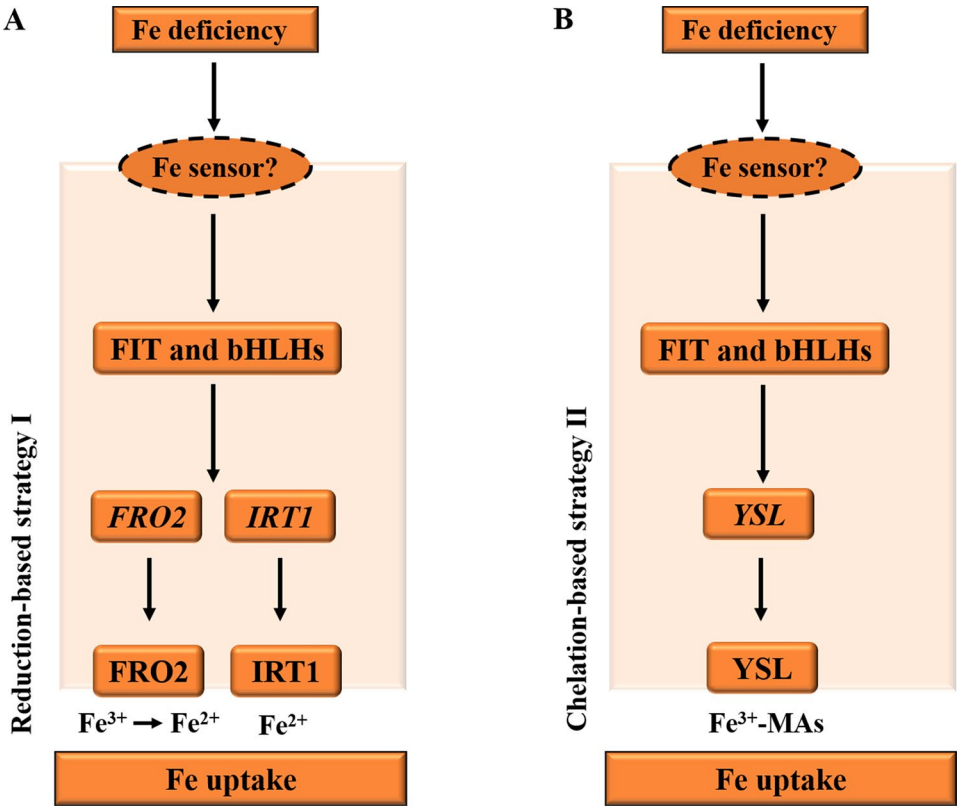

FIGURE 1 | Diagrams illustrating the iron deficiency response in *Arabidopsis* and *Graminacea* plants. **(A)** Under Fe deficiency, in *Arabidopsis* roots, the FIT and bHLH transcription factors, such as bHLH38 and bHLH39 in *Arabidopsis*, are activated by an unknown PM iron sensor in order to bind to the promoters of the iron-responsive genes. Subsequently, the induction of FRO2 and IRT1 activity is co-regulated in response to iron deficiency through the reduction-based strategy I for iron uptake. Iron is firstly reduced from ferric (Fe^{3+}) to ferrous (Fe^{2+}) iron by the reductase FRO2. Fe^{2+} is then imported into the root cell by the metal transporter IRT1. **(B)** Under Fe deficiency, the FIT and bHLH transcription factors are activated to induce the strategy II Fe uptake system in *Graminacea* plant roots. Fe^{3+}–MAs are transported into the root cell by the YSL. PM, plasma membrane; YSL, yellow stripe like; IRT1, iron-regulated transporter 1. The arrows refer to the positive interactions, while the question marks indicate the unknown iron sensor.

localized to the vacuolar membrane and associated with Zn^{2+} remobilization (Lanquar et al., 2004). Whether other members of the NRAMP family could contribute to Zn^{2+} remobilization in plants remains unknown.

For Fe, many transporters and soluble proteins responsible for Fe long-distance transfer and distribution have been characterized in recent years (Morrissey and Guerinot, 2009; Kobayashi and Nishizawa, 2012). In *Arabidopsis*, the AtFRD3 protein, which is a member of the multidrug and toxic compound extrusion (MATE) family, functions during efflux of citrate into xylem and is responsible for Fe long-distance transport from root xylem to shoots (Green and Rogers, 2004; Durrett et al., 2007; Magalhaes et al., 2007), whereas the rice OsFRDL1, the ortholog of FRD3, maintains the Fe^{3+} levels in the xylem sap (Yokosho et al., 2009). YSL transporters play a significant role in the transportation and distribution of Fe through the phloem (Curie et al., 2009) and are also involved in loading Fe from old leaves to flowers and developing seeds (Kobayashi and Nishizawa, 2012). Moreover, in rice, OsYSL2 and OsYSL15 may coordinate the long-distance Fe transport from root to shoot to seed (Koike et al., 2004; Inoue et al., 2009). In addition to YSLs, the iron transport protein ITP, which is an Fe-binding dehydrin in the phloem sap, helps promote Fe^{3+} mobility within the phloem of *Ricinus communis* (Kruger et al., 2002). Plant NAS genes are also required for long-distance Fe transport. For instance, in *Arabidopsis*, AtNAS2 and AtNAS4 may be involved in Fe translocation from roots to shoots (Klatte et al., 2009). Interestingly, the rice *OsIRT1* are highly expressed in the companion cells of phloem under Fe deficiency (Ishimaru et al., 2006), and it is possible that the corresponding encoding protein OsIRT1 could transport Fe^{2+} into the phloem prior to being chelated by NA. More recently, the involvement of OsPHO1;1 in the Fe loading into the root xylem has been reported, where it may affect overaccumulation of Fe in roots of the *Ospho1;1* mutant under Pi and Zn deficiency (Saenchai et al., 2016).

Nutrition Sensing and Signaling in Plants

Considerable advances have been made in studying the molecular mechanisms underlying Pi, Zn, and Fe sensing and signaling in plants in recent decades (Abel et al., 2002; Chiou and Lin, 2011; Assunção et al., 2013; Kobayashi and Nishizawa, 2014; Zhang et al., 2014). Nevertheless, the cross-talks between these signaling pathways integrating the tripartite interaction among Pi, Zn, and

Fe homeostasis remains poorly understood (Briat et al., 2015; Saenchai et al., 2016). How Pi homeostasis is regulated in plants has already been documented in numerous studies, and plant Pi sensing seems to be conserved in flowering plants, with several signaling networks having been proposed (Rouached et al., 2010; Wang et al., 2014a). The defined mechanism is the systemic Pi signaling cascade, which contains the MYB TF PHR1, the miRNA399, and the ubiquitin E2 conjugase PHO2 components (Bari et al., 2006; Pant et al., 2008). Generally, the well-characterized PHR1–PHO2–miRNA399 signaling pathway controls the expression of most Pi starvation-induced (*PSI*) genes in plants (**Figure 2**). In response to low Pi, *miRNA399* is transcriptionally induced by PHR1 activity (**Figure 2A**) and then mediates shoot-to-root Pi signaling *via* the phloem, where it targets the mRNA of *PHO2* (Lin et al., 2008; Pant et al., 2008). The inhibition of *PHO2* leads to an increase in the PHR1-dependent expression of root Pi transporters that include the members of PHT1 and PHO1, and hence an increase in Pi acquisition in roots and Pi translocation to shoots (Bari et al., 2006; Lin et al., 2008). Under high Pi conditions, *miRNA399* is down-regulated due to the inhibition of PHR1 activity (**Figure 2B**), and the PHO2–miR399 pathway in roots is dysfunctional through target mimicry between miR399 and PHR1-dependent IPS1 (Franco et al., 2007). Target genes of PHR1 are also reduced at transcriptional level, and PHO2 protein is activated to facilitate the degradation of Pi transporters.

Recently, the SPX domain-containing proteins have been proposed to function as the intracellular Pi sensors for sensing cellular Pi levels and controlling Pi homeostasis in both monocotyledonous and dicotyledonous plants. In *Arabidopsis*, the PHR1-dependent *AtSPX1* gene is transcriptionally induced under Pi deficiency (**Figure 2A**), while the AtSPX1 protein can interact with the AtPHR1 at the protein level under Pi sufficiency, inhibiting AtPHR1 binding to P1BS *cis*-element (GNATATNC) (Puga et al., 2014). Similarly, in rice, OsSPX1 and OsSPX2 inhibit Pi deficiency response through interaction with OsPHR2 in a Pi-dependent manner (Wang et al., 2014a), involvement of SPX proteins in the Pi sensing, and signaling mechanisms in plants (**Figure 2B**). Very recently, it has demonstrated that both the diphosphoinositol pentakisphosphate kinases (PPIP5K) VIH1 and VIH2 function redundantly to synthesize the inositol pyrophosphate ($InsP_8$) (see **Figure 2B**), and $InsP_8$ can directly bind to the intracellular Pi sensor SPX1 to control Pi homeostasis in *Arabidopsis* during Pi repletion (Dong et al., 2019). This study revealed that $InsP_8$ acts as an intracellular phosphate signal in plants. The next major challenge in this field is to unmask the extracellular Pi sensor sensing.

In plants, how Zn-deficient signal is sensed, relayed, and integrated into a signal response remains elusive. Nevertheless, a first working model of Zn deficiency signaling has been proposed by Assunção et al. (2013). Two bZIP TFs, bZIP19/23, have been identified in Zn homeostasis *via* the regulation of target genes,

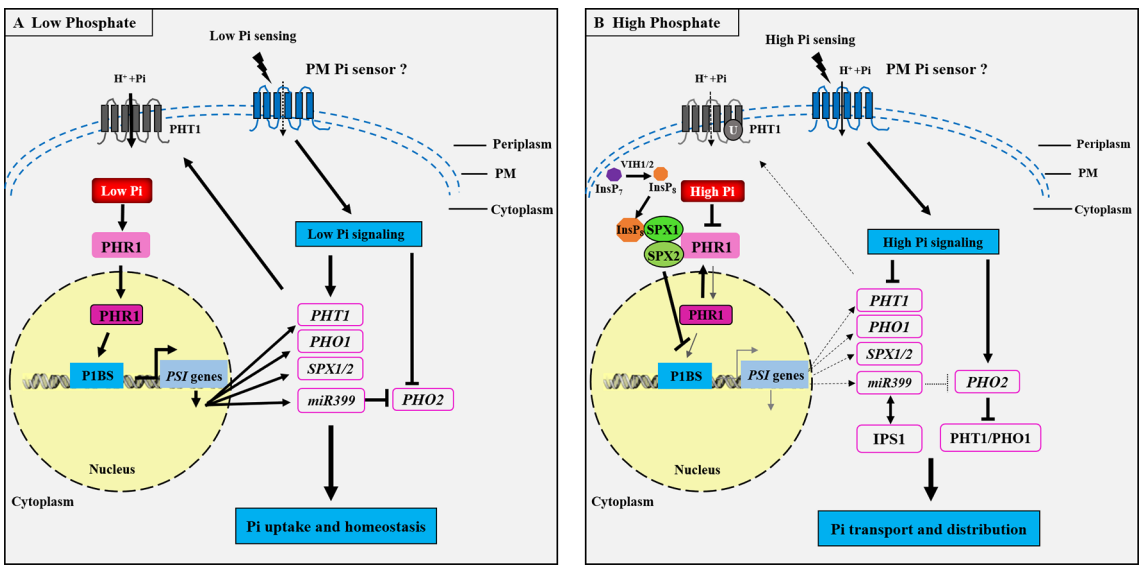

FIGURE 2 | Schematic representation of the phosphate (Pi) signaling pathway essential for plant adaptation to low Pi concentration. Under Pi deficiency **(A)**, a set of phosphate starvation-induced (*PSI*) genes are transcriptionally activated through binding of the transcription factor PHOSPHATE STARVATION RESPONSE 1 (PHR1) to the cis-element (P1BS) present in the promoter region of the *PSI* genes, and subsequently *PHT1* and *PHO1* mRNAs are induced to be necessary for Pi uptake and translocation in roots. The *SPX1/2* and *miR399* genes are also activated by PHR1 during Pi starvation. miR399 inhibits the ubiquitin E2 conjugase PHO2 in order to maintain the PHT1 protein activity at the PM. It could be proposed that the Pi signaling is activated for sensing external low Pi through an unknown PM Pi sensor, which induces the low Pi responsive genes *PHT1*, *PHO1*, *SPX1/2*, and *miR399*, whereas the *PHO2* is repressed, thus activating the Pi regulatory pathway to modulate Pi uptake and homeostasis. Under high Pi concentration **(B)**, the Pi signaling pathway is repressed, the diphosphoinositol pentakisphosphate kinases VIH1 and VIH2 function redundantly to synthesize $InsP_8$, and $InsP_8$ can directly bind to the SPX domain of SPX1 and is essential for the interaction between SPX1/2 and PHR1. This interaction leads to the inhibition of PHR1 binding to the *cis*-element P1BS present in the promoter region of the *PSI* genes. Thus, the *PSI* genes, including *PHT1*, *PHO1*, *SPX1/2*, and *miR399*, are transcriptionally repressed, while the *PHO2* is activated to be responsible of the ubiquitination of PHT1 and PHO1 proteins to promote Pi transporters degradation. *IPS1* encodes a non-coding RNA and enables post-transcriptional regulation under high Pi through RNA mimicry. IPS1-miR399 matching thus results in the inhibition of the miR399 activity to target PHO2. It is also predicted that there may exist an unknown PM Pi sensor responsible for high Pi sensing. PM, plasma membrane. The arrows and flat-ended lines refer to the positive and negative interactions, respectively. The dotted arrows represent the repression processes.

including the members of ZIP family (Guerinot, 2000; Assunção et al., 2010a) for root Zn transport and *NAS2/4* for NA synthesis (Assunção et al., 2010b), since the shoots appear to the first organ to sense the Zn deficiency and then transmit the signal to the roots where these ZIP transporters are activated (Assunção et al., 2013). This observation has led to the proposal of the existence of unknown long-distance Zn deficiency signaling molecules. Additionally, a ZDRE element (RTGTCGACAY) is present in the promoter regions of both the *ZIP* and *NAS* genes in response to Zn deficiency (Assunção et al., 2010; Assunção et al., 2010b).

How the Fe status of plant is sensed and how this signal is transmitted to the transcriptional networks for Fe acquisition and response are currently areas of great interest in the field of Fe homeostasis in plants (Briat et al., 2015). A major goal is to find a master Fe sensor controlling Fe homeostasis in plants (Hindt and Guerinot, 2012). Some degree of progress towards these aims has been achieved by exploiting members of the basic helix-loop-helix (bHLH) TF family (Hindt and Guerinot, 2012; Ivanov et al., 2012; Kobayashi and Nishizawa, 2012; Moran et al., 2014). Also, hemerythrin motif-containing RING and zinc-finger proteins HRZ1/2 and its ortholog E3 ligase BTS that have been recently characterized in both the monocotyledonous and dicotyledonous plants, respectively (Kobayashi and Nishizawa, 2014). The tomato FIT is referred as to FER (Ling et al., 2002; Brumbarova and Bauer, 2005), and FER mutant *fit-1* repressed about 50% of Fe deficiency-induced genes in roots (Colangelo and Guerinot, 2004). A second PYE bHLH protein is exclusively induced in roots under Fe deficiency. The *pye-1* mutant line is sensitive to low Fe. In *pye-1* mutant, three Fe transport-related genes, *NAS4*, *FRO3*, and *ZIF1*, are strongly induced under Fe deficiency and are identified as the targets of PYE (Long et al., 2010). In addition, *Arabidopsis* bHLH104 and ILR3 play crucial roles in the regulation of Fe deficiency responses through targeting other bHLH genes and PYE expression (Zhang et al., 2015). The overexpression lines of rice iron-related TF 2 (OsIRO2), ortholog of *Arabidopsis* bHLH38/39, showed both enhanced Fe uptake and transportation to seeds (Ogo et al., 2007; Ogo et al., 2011). Furthermore, a PYE homologous protein OsIRO3 is induced under Fe deficiency, whereas it is a negative regulator of Fe deficiency responses due to the hypersensitivity to Fe deficiency and the inhibition of genes up-regulated by Fe deficiency (Zheng et al., 2010). Recently, rice bHLH133 was identified to play an important role in the regulation of Fe translocation from roots to shoots (Wang et al., 2013). On the other hand, BTS and its orthologs HRZ1/2 could negatively regulate Fe acquisition, accumulation of Fe, and tolerance to Fe deficiency in rice *HRZ1/2* mutants (Kobayashi et al., 2013).

Interactions Between P, Zn, and Fe Homeostasis in Plants

Cross-talks between macronutrient and micronutrients in plants have long been recognized, and these interactions are understood to some extent. Hence, we here emphasize the interactions between Pi, Zn, and iron (Fe) homeostasis at the physiological and molecular levels. The interaction between two nutrients homeostasis has been observed in crop species.

The interaction between Pi and Zn homeostasis in plants is relatively well understood. Pi deficiency results in overaccumulation of Zn in shoots, and inversely, Zn deficiency leads to overaccumulation of Pi in the aerial part of plants (Reed, 1946; Cakmak and Marschner, 1986; Huang et al., 2000; Bouain et al., 2014a; Khan et al., 2014; Ova et al., 2015). In addition to the well-known antagonistic effect of Pi and Zn nutrition in plants, there is some evidence of similar physiological interactions between Pi and Fe nutrition (Zheng et al., 2009), and between Zn and Fe nutrition (Haydon et al., 2012) as well. Pi acquisition in both roots and shoots is promoted under Fe deficiency, and conversely, Pi deficiency significantly increases Fe availability within the plants (Misson et al., 2005; Hirsch et al., 2006; Ward et al., 2008; Zheng et al., 2009; Briat et al., 2015). Fe deficiency leads to an accumulation of Zn, while an excess Zn causes physiological Fe deficiency (Haydon et al., 2012; Shanmugam et al., 2012; Briat et al., 2015).

In plants, the intricate cross-talks between the homeostasis of macronutrients and micronutrients have recently become clear (Briat et al., 2015), and evidence of a complex tripartite interaction between Pi, Fe, and Zn nutrients for maintenance of Pi homeostasis in *Arabidopsis* has been described (Rai et al., 2015). In addition, Saenchai et al. (2016) have also provided evidence that iron transport in rice is regulated by integration of Pi and Zn deficiencies, highlighting the presence of tripartite cross-talk between Pi, Zn, and Fe homeostasis for better plant survival and fitness (**Figure 3**).

Molecular Evidence for Pi, Zn, and Fe Interactions in Plants

Although the cross-talks between Pi, Zn, and Fe homeostasis have been reported in many plant species (Briat et al., 2015), the molecular basis and biological significance of these nutritional interactions remain thus far largely unknown. It can be first achieved through transcriptomic and genetic analyses of Pi-, Zn-, or Fe-deficient plants (Hammond et al., 2003; Wu et al., 2003; Misson et al., 2005; van de Mortel et al., 2006; Zheng et al., 2009; Bustos et al., 2010; Thibaud et al., 2010; Rouached et al., 2011b; Pineau et al., 2012; Khan et al., 2014; Moran et al., 2014; Rai et al., 2015; Saenchai et al., 2016).

Zn deficiency activates the transcription of numerous Pi-related genes (van de Mortel et al., 2006), while Pi deficiency up-regulates the expression of genes involved in Zn and Fe homeostasis (Misson et al., 2005; Bustos et al., 2010). More recently, several reports have proposed that PHR1, PHO1 and PHO1;H3 are coordinatively involved in the homeostasis between Pi and Zn in *Arabidopsis* (Bouain et al., 2014b; Khan et al., 2014; Kisko et al., 2015), reinforcing the interaction between Pi and Zn signaling at the molecular level (**Figure 3**).

In the absence of Pi, plants induce the expression of genes in response to sufficient Fe, whereas Pi-starvation plants reduce the transcripts of genes in response to Fe deficiency (Misson et al., 2005; Müller et al., 2007; Thibaud et al., 2010). Reciprocally, Fe deficiency alters the transcription of Pi-related genes (Zheng et al., 2009; Moran et al., 2014). Genome-wide analysis further reveals 547 and 579 overlapping genes regulated by both Pi and Fe deficiency in rice and *Arabidopsis* roots, respectively (Zheng

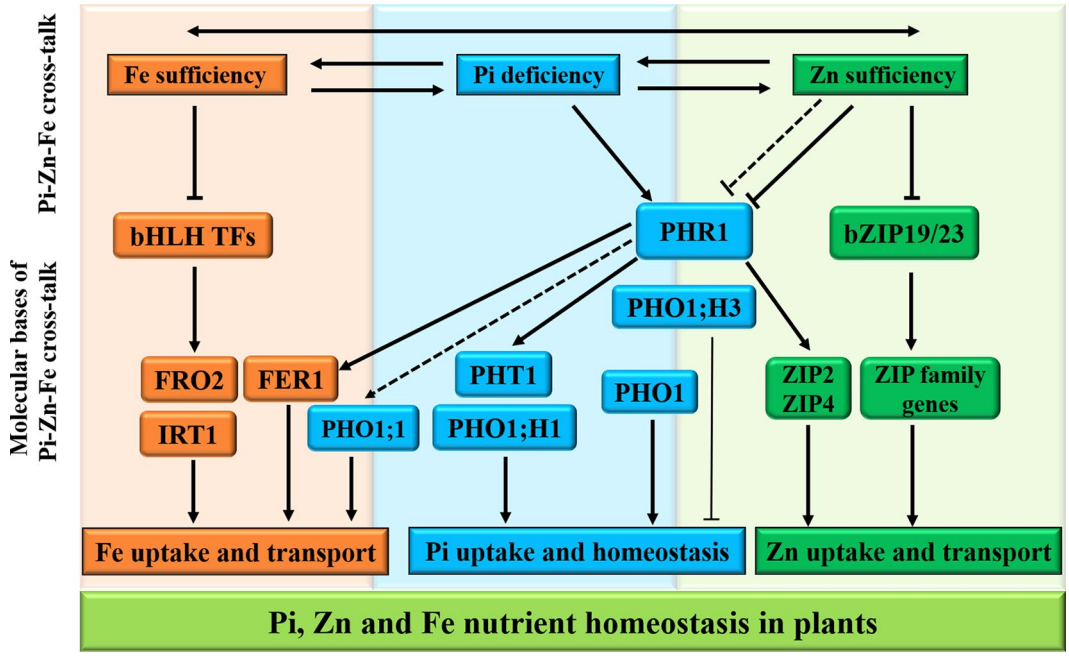

FIGURE 3 | Schematic representation of Pi, Zn, and Fe homeostasis interactions in plants. The cross-talks between phosphate (Pi), zinc (Zn), and iron (Fe) nutrients are shown at the physiological level by two-way arrows. For the molecular bases of the Pi–Zn–Fe cross-talks, the PHR1 acts as a potential integrator of Pi, Zn, and Fe nutrient signals in plants. Firstly, the PHR1 was defined as a key regulator of the expression of Pi transporters PHT1 and PHO1; H1 through the PHR1–miR399–PHO2 pathway (see **Figure 2**). Secondly, *ZIP2* and *ZIP4* genes, belonging to plant ZIP gene family, are transcriptionally induced *via* the activated PHR1 transcription factor binding to the P1BS (GNATATNC) sequences found in the promoter regions of their genes. Under Zn sufficiency, the bZIP19/23 transcription factors are inactivated, and bZIP19/23-mediated Zn regulatory pathways repress the plant ZIP gene family transporters in order to regulate Zn homeostasis. On the other hand, *PHO1;H3*, which is transcriptionally down-regulated by high Zn supply, and the PHR1 and PHO1 proteins contribute to the Pi–Zn nutrient homeostasis cross-talk. In addition, the transcriptional activation of some genes involved in maintaining Fe homeostasis is also shown to be PHR1-dependent manner, including the *FER1* gene encoding the Fe storage protein ferritin, and the *PHO1;1* gene encoding Pi transporter. The arrows and flat-ended lines indicate the positive and negative interactions, respectively.

et al., 2009; Li and Lan, 2015). In these cases, the expression of *FER1* gene encoding Fe storage protein ferritin is in response to Pi starvation mediating by PHR1 (**Figure 3**) and Fe excess (Petit et al., 2001; Bournier et al., 2013), and *NAS3* and *YSL8* genes responsible for Fe homeostasis are also induced upon Pi starvation in plants (Bustos et al., 2010). However, the *IRT1/2*, *FRO3/6*, and *NAS1* genes are repressed in response to Fe deficiency in Pi-deficient plants. Recently, it has reported that the *Arabidopsis phr1* × *phl1* double mutant influenced Fe distribution and Fe-related gene expression (Bournier et al., 2013; Briat et al., 2015), suggesting that PHR1 and PHL1 may integrate Fe and Pi nutrient signals. The high-affinity copper transport protein COPT2 acts as a key player in the interaction between Pi and Fe deficiency signaling in *Arabidopsis* (Perea et al., 2013). COPT2 may play a dual role under Fe deficiency. It participates in copper uptake and distribution in Fe-limited roots to minimize iron loss. On the other hand, loss of COPT2 function exacerbates Pi starvation responses in *Arabidopsis* plants. These findings open new approaches to mitigate iron deficiency in crop species.

For Zn and Fe cross-talk, transcriptomic analysis indicates that many Zn uptake- and homeostasis-related genes are up-regulated in Fe-deficient soybean root and leaf (Moran et al., 2014), including those encoding six members of the ZIP gene family, IRT1, the NAS2, and NRAMP3. Similarly, the Fe deficiency responsive *AtIRT1* gene (**Figure 3**) identified could be a key player in the coordination between Zn- and Fe-deficient signaling in *Arabidopsis* (Connolly et al., 2002; Vert et al., 2002; Briat et al., 2015). Furthermore, the vacuolar membrane protein encoding genes *MTP3*, *HMA3*, and *ZIF* essential for Zn tolerance are up-regulated in response to Fe deficiency or Zn excess (Becher et al., 2003; Arrivault et al., 2006; van de Mortel et al., 2006; Haydon and Cobbett, 2007; Haydon et al., 2012). A recent study has confirmed that the MATE transporter gene *FRD3* is involved in cross-talk between Zn and Fe homeostasis for the tolerance to Zn excess in *Arabidopsis* (Pineau et al., 2012), highlighting the complexity of cross-talk between these signaling pathways to regulate Fe deficiency and Zn excess.

Several recent reports have started to discuss the complex tripartite cross-talks among Pi, Zn, and Fe (Briat et al., 2015; Rai et al., 2015). Pi nutrition is affected by the interaction between Zn and Fe in plants. The MYB TF PHR1 apparently acts as a common regulator of Pi, Zn, and Fe homeostasis (**Figure 3**) and functions as a general integrator of multiple nutrition signals (Briat et al., 2015). Firstly, PHR1 was defined as a key regulator for the expression of Pi transporters PHT1 and PHO1;H1 through PHR1–miR399–PHO2 pathway. Secondly, PHR1 seems to be a regulator of the ZIP transporters ZIP2 and ZIP4 for Zn mobilization. In addition, the transcriptional activation of some genes involved in maintaining Fe homeostasis is also shown to be PHR1-dependent manner, including the *FER1* gene encoding the Fe storage protein ferritin, and the *PHO1;1* gene encoding Pi transporter. Saenchai et al. (2016) have

reported the OsPHO1;1 is involved in the coordination between Fe transport and Pi–Zn deficiency signaling in rice. Nevertheless, fundamental aspects regulating the cross-talk between Pi, Zn, and Fe deficiency signaling and the regulation of nutritional homeostasis in plants remain to be discovered.

Pi and Zn Interactions in Mycorrhizal Plants

In the last several decades, the cross-talk between Pi and Zn nutrient homeostasis has been well recognized at the physiological level in many mycorrhizal plants (Reed, 1946; Cakmak and Marschner, 1986; Huang et al., 2000; Watts-Williams et al., 2014; Watts-Williams et al., 2017; Nafady and Elgharably, 2018). High Pi treatment substantially decreased Zn concentration in wheat shoots and grain when these plants were grown in native soils (Ova et al., 2015), and these data also revealed that the negative effect of increasing Pi application on root Zn accumulation and shoot Zn distribution in wheat is dependent on mycorrhization. Furthermore, Zhang et al. (2016) proposed that Pi treatment decreased the Zn concentration in wheat, and they also found that Zn concentration in roots and shoots of maize decreased with increasing Pi supply, and root Zn accumulation exhibits the Pi-induced Zn deficiency during mycorrhization (Zhang et al., 2017), because Pi treatment inhibits colonization resulting in impaired mycorrhizal uptake pathway and then affects the Zn uptake and tissue Zn status of host plants (Loneragan and Webb, 1993; Marschner, 2012; Watts-Williams et al., 2013). The negative relationship between Pi application and the grain Zn status was also confirmed in field studies (Ryan et al., 2008; Zhang et al., 2012). Conversely, under AM conditions, Pi content in shoots of *Medicago truncatula* was greatly reduced when excess Zn was applied in soil (Watts-Williams et al., 2017). Interestingly, an experiment with lettuce plants grown under excessive Zn levels showed that Zn content in mycorrhizal lettuce was greatly reduced when the nutrient solution contained low Pi concentration (Konieczny and Kowalska, 2017). This is indicative of the "protective effect" of arbuscular mycorrhiza, where host plants acquire much less Zn from the Zn excess soils (Chen et al., 2003; Watts-Williams et al., 2013; Christie et al., 2004). Altogether, the interaction between Pi–Zn nutrients during AM symbiosis can be concluded as follows: Crops grown with sufficient Pi decrease Zn in the roots and/or shoots of crops, and inversely, excess Zn reduces Pi in the shoots. However, the underlying molecular mechanisms of the Pi–Zn interaction in mycorrhizal symbiosis are still unclear, and only a few reports discuss the molecular basis of these interactions (Cakmak and Marschner, 1986; Zhu et al., 2001; Watts-Williams et al., 2013; Watts-Williams et al., 2017). Future studies are required to elucidate the molecular basis of the interactions between Pi and Zn nutrient homeostasis during AM symbiosis.

Pi and Fe Interactions During AM Symbiosis

The antagonistic physiological and molecular interactions between Pi and Fe nutrition have been established in model systems such as *Arabidopsis* and rice (Hirsch et al., 2006; Ward et al., 2008; Zheng et al., 2009; Jain et al., 2013; Rai et al., 2015), but very little information is available on their interactions in mycorrhizal plants.

A couple of studies performed in some edible crop species uncovered the existence of a negative relationship between Pi and Fe uptake in mycorrhizal plants (Azcón et al., 2003; Ferrol et al., 2016; Hoseinzade et al., 2016; Nafady and Elgharably, 2018). Under low Pi supply, the acquisition of Fe increases in mycorrhizal plants (Watts-Williams and Cavagnaro, 2014; Ferrol et al., 2016), and conversely, host plants decrease the Fe accumulation under high Pi conditions during AM symbiosis. Interestingly, Fe content of the straw was greatly increased with low Pi supply during AM symbiosis (Hoseinzade et al., 2016), indicating that mycorrhized rice has reduced Fe nutrient transported to shoots at high Pi status. Very recently, Nafady and Elgharably (2018) reported a similar negative effect of Fe content when maize was treatment with Pi fertilizers. These studies have demonstrated the negative effects of high Pi application in soil on Fe accumulation in mycorrhizal plants (Azcón et al., 2003). Further, the studies have showed the effect of high Pi application on the uptake and transport of Fe nutrition in both rice and maize during AM symbiosis, which could result in the appearance of iron deficiency symptoms under low Fe conditions. However, the effect of Fe treatments on Pi nutrition has not been investigated so far during mycorrhization. The molecular bases of the cross-talk between Pi and Fe in mycorrhizal plants need to be further explored.

Zn and Fe Interactions in Mycorrhizal Plants

Zinc interacts with some micronutrients such as Fe and copper (Cu) in plants (Poshtmasari et al., 2008; Jain et al., 2013). The cross-talk between the effects of Zn rates on Fe accumulation and translocation has been partially studied in several mycorrhizal plants. Zinc treatment resulted in Fe accumulation in soybean roots under arbuscular mycorrhizal conditions but inhibited Fe translocation from roots to shoots (Ibiang et al., 2017), indicating the cross-talk in Zn and Fe status within the whole soybean during AM symbiosis. However, excess Zn increased root to fruit Fe translocation during AM symbiosis in tomato plants (Ibiang et al., 2018), whereas excess Zn could also lead to a decrease in Fe concentration in mycorrhizal roots. These studies performed under AM conditions have revealed that the physiological antagonistic interaction between Zn and Fe nutrients occurred in roots or shoots depending on the host-plant species. Zn status may therefore affect Fe uptake and transport mechanisms in mycorrhizal plants. These studies have indicated the effect of Zn treatment on the accumulation and homeostasis of Fe nutrition in mycorrhizal plants. However, the effect of Fe availability on Zn nutrition in mycorrhizal plants has not been studied yet, and little information is available on this issue. From the nutritional aspect, there exists a competition between Zn and Fe elements; host plants require coordinate Zn–Fe homeostasis to avoid ion imbalances. Under excess Zn, mycorrhizal plants will decrease the overaccumulation of Fe in shoots prone to Fe starvation. Few studies have identified the potential molecular components

involved, and no key genes have been characterized so far acting in the phenomenon. Therefore, the molecular bases of the Zn–Fe interactions in mycorrhizal plants remain largely unknown, and the evidence for the molecular basis of the Zn–Fe co-regulation that mediates the adaptation of a mycorrhizal plant to Zn and Fe availability should be provided in future studies. In particular, the potential genes are involved in the cross-talk between the Zn and Fe homeostasis during AM symbiosis. For instance, the expression of the zinc- and iron-regulated transporter-like proteins (ZRT, IRT-like proteins, referred as to ZIP family) encoding genes in roots and shoots is induced at the transcriptional level by Zn and/or Fe availability (Pedas et al., 2009; Li et al., 2013; Fu et al., 2017), indicating that these ZIP genes may control the uptake and homeostasis of Zn and Fe in mycorrhizal plant species (Grotz et al., 1998; Hall and Williams, 2003).

Cross-Talk Between Pi–Zn–Fe Nutrient Homeostasis in Mycorrhizal Plants

The above studies provide new insights on genes involved in the potential regulation of nutrient homeostasis in conditions when an individual element is limiting. However, recent research indicated that plant survival is affected by a complex cross-talk between Pi, Zn, and Fe homeostasis (Briat et al., 2015). Interestingly, Saenchai et al. (2016) reported that *OsPHO1;1* was transcriptionally up-regulated in response to Pi–Zn–Fe combined stresses and involved in Fe transport and integrative Pi–Zn deficiency signaling in rice, providing a genetic basis for tripartite Pi–Zn–Fe signaling cross-talks in plants. However, how the members of the plant PHO1-type Pi transporter family function as key linkers in the cross-talks between Pi–Zn–Fe signaling during AM symbiosis has not been elucidated. Although the cross-talks between these nutrients have been touched upon in some model plant studies (Misson et al., 2005; Zheng et al., 2009; Saenchai et al., 2016), the molecular mechanisms of the tripartite interactions during AM symbiosis are still lacking.

CONCLUSION

Over the last seven decades, large numbers of studies have focused on how to interpret the potential mechanisms for phosphorus uptake and signaling at molecular and cellular levels in *Arabidopsis* or rice. The combination of molecular and cellular biology, multiple "omics" approaches, and reverse genetics has resulted in the characterization of many important genes that control Pi accumulation and homeostasis in *Arabidopsis* and rice in response to Pi limitation. However, Pi is well known to interact with some micronutrients such as Zn and Fe in plants (Bouain et al., 2014a; Briat et al., 2015). Future research will need to undertake an integrative study to uncover the defined mechanisms by which plants coordinate the Pi, Zn, and Fe deficiency signaling in order to enhance their fitness during multiple Pi, Zn, and Fe deficiency stresses. In such a context, the principal aim of this review is to broaden the current understanding of the cross-talk between the Pi and Zn, Pi and Fe, Zn and Fe, and Pi–Zn–Fe homeostasis in nonmycorrhizal and mycorrhizal plants. In addition, the identification of important genes regulating the interactions between Pi, Zn, and/or Fe transport and signaling in plants, particularly in crop species, will help breeders develop new strategies for nutrient management, and taking into account the interactions between plants and their AM fungal symbionts. In conclusion, the development of the integrative study of cross-talk between Pi, Zn, and Fe signaling pathway will be of great interest and essential for sustainable agricultural development all around the world.

AUTHOR CONTRIBUTIONS

MT and XX conceived and designed this study. XX, WH, and XF wrote the manuscript. HC proposed related theories and assisted with the interpretation of some references. All authors have read, edited, and approved the current version of the manuscript.

FUNDING

This work was supported by grants from the National Natural Science Foundation of China (grant no. 31800092), the Natural Science Foundation of Guangdong Province in China (grant no. 2018A030313141), the Key Projects of Guangzhou Science and Technology Plan (grant no. 201904020022), and the High-level Talent Start Funding Project of South China Agricultural University (grant no. 218066).

ACKNOWLEDGEMENTS

We are grateful for the critical revision on the draft manuscript by the three reviewers. The authors are also grateful for the critical proofreading on the draft manuscript by Prof. Erik Nielsen (*The Plant Cell*, Guest editor) and also thank the Associated Researchers Junwei Liu and Jianyong An (Huazhong Agricultural University, Wuhan, China) and Dr. Nianwu Tang (Kunming Institute of Botany, Chinese Academy of Sciences) for the professional reading and valuable discussion on this manuscript.

REFERENCES

Abelson, P. H. (1999). A potential phosphate crisis. *Science* 283, 2015. doi: 10.1126/science

Abel, S., Ticconi, C. A., and Delatorre, C. A. (2002). Phosphate sensing in higher plants. *Physiol. Plant.* 115, 1–8. doi: 10.1034/j.1399-3054.2002.1150101.x

Ai, P. H., Sun, S. B., Zhao, J. N., Fan, X. R., Xin, W. J., Guo, Q., et al. (2009). Two rice phosphate transporters, OsPht1;2 and OsPht1;6, have different functions and kinetic properties in uptake and translocation. *Plant J.* 57, 798–809. doi: 10.1111/j.1365-313X.2008.03726.x

Allen, J. W., and Shachar, H. Y. (2009). Sulfur transfer through an arbuscular mycorrhiza. *Plant Physiol.* 149, 549–560. doi: 10.1104/pp.108.129866

Ames, R. N., Reid, C. P. P., Porter, L. K., and Cambardella, C. (1983). Hyphal uptake and transport of nitrogen from two 15N-labelled sources by *Glomus mosseae*, a vesicular-arbuscular mycorrhizal fungus. *New Phytol.* 95, 381–396. doi: 10.1111/j.1469-8137.1983.tb03506.x

Arrivault, S., Senger, T., and Krämer, U. (2006). The *Arabidopsis* metal tolerance protein AtMTP3 maintains metal homeostasis by mediating Zn exclusion from the shoot under Fe deficiency and Zn oversupply. *Plant J.* 46, 861–879. doi: 10.1111/j.1365-313X.2006.02746.x

Assuncão, A. G., Herrero, E., Lin, Y. F., Huettel, B., Talukdar, S., Smacznia, C., et al. (2010a). *Arabidopsis thaliana* transcription factors bZIP19 and bZIP23 regulate the adaptation to zinc deficiency. *Proc. Natl. Acad. Sci. U. S. A.* 107, 10296–10301. doi: 10.1073/pnas.1004788107

Assuncão, A. G., Persson, D. P., Husted, S., Schjorring, J. K., Alexander, R. D., and Aarts, M. G. (2013). Model of how plants sense zinc deficiency. *Metallomics.* 5, 1110–1116. doi: 10.1039/c3mt00070b

Assuncão, A. G., Schat, H., and Aarts, M. G. (2010b). Regulation of the adaptation to zinc deficiency in plants. *Plant Signal. Behav.* 5, 1553–1555. doi: 10.4161/psb.5.12.13469

Azcón, R., Ambrosano, E., and Charest, C. (2003). Nutrient acquisition in mycorrhizal lettuce plants under different phosphorus and nitrogen concentration. *Plant Sci.* 165, 1137–1145. doi: 10.1016/S0168-9452(03)00322-4

Barberon, M., Zelazny, E., Robert, S., Conejero, G., Curie, C., Friml, J., et al. (2011). Monoubiquitin-dependent endocytosis of the iron-regulated transporter 1 (IRT1) transporter controls iron uptake in plants. *Proc. Natl. Acad. Sci. U. S. A.* 108, E450–E458 doi: 10.1073/pnas.1100659108

Bari, R., Datt, P., Stitt, M., and Scheible, W. R. (2006). PHO2, microRNA399, and PHR1 define a phosphate-signaling pathway in plants. *Plant Physiol.* 141, 988–999. doi: 10.1104/pp.106.079707

Bayle, V., Arrighi, J. F., Creff, A., Nespoulous, C., Vialaret, J., Rossignol, M., et al. (2011). *Arabidopsis thaliana* high-affinity phosphate transporters exhibit multiple levels of posttranslational regulation. *Plant Cell.* 23, 1523–1535. doi: 10.1105/tpc.110.081067

Becher, M., Talke, I. N., Krall, L., and Krämer, U. (2003). Cross-species microarray transcript profiling reveals high constitutive expression of metal homeostasis genes in shoots of the zinc hyperaccumulator *Arabidopsis halleri. Plant J.* 37, 251–268. doi: 10.1046/j.1365-313X.2003.01959.x

Belouchi, A., Cellier, M., Kwan, T., Saini, H. S., Leroux, G., and Gros, P. (1995). The macrophage-specific membrane protein Nramp controlling natural resistance to infections in mice has homologues expressed in the root system of plants. *Plant Mol. Biol.* 29, 1181–1196. doi: 10.1007/BF00020461

Bereczky, Z., Wang, H. Y., Schubert, V., Ganal, M., and Bauer, P. (2003). Differential regulation of NRAMP and IRT metal transporter genes in wild type and iron uptake mutants of tomato. *J. Biol. Chem.* 278, 24697–24704. doi: 10.1074/jbc.M301365200

Bonfante, P. (2018). The future has roots in the past: the ideas and scientists that shaped mycorrhizal research. *New Phytol.* 220, 982–995. doi: 10.1111/nph.15397

Bournier, M., Tissot, N., Mari, S., Boucherez, J., Lacombe, E., Briat, J. F., et al. (2013). *Arabidopsis* ferritin 1 (*AtFer1*) gene regulation by the phosphate starvation response1 (AtPHR1) transcription factor reveals a direct molecular link between iron and phosphate homeostasis. *J. Biol. Chem.* 288, 22670–22680. doi: 10.1074/jbc.M113.482281

Bouain, N., Kisko, M., Rouached, A., Dauzat, M., Lacombe, B., Belgaroui, N., et al. (2014a). Phosphate/zinc interaction analysis in two lettuce varieties reveals contrasting effects on biomass, photosynthesis, and dynamics of Pi transport. *BioMed. Res. Int.* 2014, 548254. doi: 10.1155/2014/548254

Bouain, N., Shahzad, Z., Rouached, A., Khan, G. A., Berthomieu, P., Abdelly, C., et al. (2014b). Phosphate and zinc transport and signalling in plants: toward a better understanding of their homeostasis interaction. *J. Exp. Bot.* 65, 5725–5741. doi: 10.1093/jxb/eru314

Briat, J. F., Fobis, L. I., Grignon, N., Lobreaux, S., Pascal, N., Savino, G., et al. (1995). Cellular and molecular aspects of iron metabolism in plants. *Biol. Cell.* 84, 69–81. doi: 10.1016/0248-4900(96)81320-7

Briat, J., Rouached, H., Tissot, N., Gaymard, F., and Dubos, C. (2015). Integration of P, S, Fe and Zn nutrition signals in *Arabidopsis thaliana*: potential involvement of PHOSPHATE STARVATION RESPONSE 1 (PHR1). *Front. Plant Sci.* 6, 290. doi: 10.3389/fpls.2015.00290

Brumbarova, T., and Bauer, P. (2005). Iron-mediated control of the basic helix-loop-helix protein FER, a regulator of iron uptake in tomato. *Plant Physiol.* 137, 1018–1026. doi: 10.1104/pp.104.054270

Bucher, M. (2007). Functional biology of plant phosphate uptake at root and mycorrhiza interfaces. *New Phytol.* 173, 11–26. doi: 10.1111/j.1469-8137.2006.01935.x

Bustos, R., Castrillo, G., Linhares, F., Puga, M. I., Rubio, V., Perez, P. J., et al. (2010). A central regulatory system largely controls transcriptional activation and repression responses to phosphate starvation in *Arabidopsis. PloS Genet.* 6, e1001102. doi: 10.1371/journal.pgen.1001102

Cakmak, I., and Marschner, H. (1986). Mechanism of phosphorus induced zinc deficiency in cotton. I. Zinc deficiency-enhanced uptake rate of phosphorus. *Physiol. Plant.* 68, 483–490. doi: 10.1111/j.1399-3054.1986.tb03386.x

Caris, C., Hördt, W., Hawkins, H. J., Römheld, V., and George, E. (1998). Studies of iron transport by arbuscular mycorrhizal hyphae from soil to peanut and sorghum plants. *Mycorrhiza.* 8, 35–39. doi: 10.1007/s005720050208

Chang, M. X., Gu, M., Xia, Y. W., Dai, X. L., Dai, C. R., Zhang, J., et al. (2019). OsPHT1;3 mediates uptake, translocation, and remobilization of phosphate under extremely low phosphate regimes. *Plant Physiol.* 179, 656–670. doi: 10.1104/pp.18.01097

Chen, A., Chen, X., Wang, H., Liao, D., Gu, M., Qu, H., et al. (2014). Genome-wide investigation and expression analysis suggest diverse roles and genetic redundancy of Pht1 family genes in response to Pi deficiency in tomato. *BMC Plant Biol.* 14, 61. doi: 10.1186/1471-2229-14-61

Chen, A., Hu, J., Sun, S., and Xu, G. (2007). Conservation and divergence of both phosphate- and mycorrhiza-regulated physiological responses and expression patterns of phosphate transporters in solanaceous species. *New Phytol.* 173, 817–831. doi: 10.1111/j.1469-8137.2006.01962.x

Chen, B. D., Li, X. L., Tao, H. Q., Christie., P., and Wong, M. H. (2003). The role of arbuscular mycorrhiza in zinc uptake by red clover growing in a calcareous soil spiked with various quantities of zinc. *Chemosphere* 50, 839–846. doi: 10.1016/S0045-6535(02)00228-X

Chen, J. Y., Wang, Y. F., Wang, F., Yang, J., Gao, M. X., Li, C. Y., et al. (2015). The rice CK2 kinase regulates trafficking of phosphate transporters in response to phosphate levels. *Plant Cell.* 27, 711–723. doi: 10.1105/tpc.114.135335

Chiou, T. J., and Lin, S. I. (2011). Signaling network in sensing phosphate availability in plants. *Annu. Rev. Plant Biol.* 62, 185–206. doi: 10.1146/annurev-arplant-042110-103849

Chorianopoulou, S. N., Saridis, Y. I., Dimou, M., Katinakis, P., and Bouranis, D. L. (2015). Arbuscular mycorrhizal symbiosis alters the expression patterns of three key iron homeostasis genes, ZmNAS1, ZmNAS3, and ZmYS1, in S deprived maize plants. *Front. Plant Sci.* 6, 257. doi: 10.3389/fpls.2015.00257

Christie, P., Li, X. L., and Chen, B. D. (2004). Arbuscular mycorrhiza can depress translocation of zinc to shoots of host plants in soils moderately polluted with zinc. *Plant Soil.* 261, 209–217. doi: 10.1023/B:PLSO.0000035542.79345.1b

Colangelo, E. P., and Guerinot, M. L. (2004). The essential basic helix-loop-helix protein FIT1 is required for the iron deficiency response. *Plant Cell.* 16, 3400–3412. doi: 10.1105/tpc.104.024315

Connolly, E. L., Fett, J. P., and Guerinot, M. L. (2002). Expression of the IRT1 metal transporter is controlled by metals at the levels of transcript and protein accumulation. *Plant Cell.* 14, 1347–1357. doi: 10.1105/tpc.001263

Conte, S. S., and Walker, E. L. (2011). Transporters contributing to iron trafficking in plants. *Mol. Plant* 4, 464–476. doi: 10.1093/mp/ssr015

Curie, C., Cassin, G., Couch, D., Divol, F., Higuchi, K., Le Jean, M., et al. (2009). Metal movement within the plant: contribution of nicotianamine and yellow stripe 1-like transporters. *Ann. Bot.* 103, 1–11. doi: 10.1093/aob/mcn207

Curie, C., Panaviene, Z., Loulergue, C., Dellaporta, S. L., Briat, J. F., and Walker, E. L. (2001). Maize yellow stripe1 encodes a membrane protein directly involved in Fe (III) uptake. *Nature* 409, 346–349. doi: 10.1038/35053080

Deinlein, U., Weber, M., Schmidt, H., Rensch, S., Trampczynska, A., Hansen, T. H., et al. (2012). Elevated nicotianamine levels in *Arabidopsis halleri* roots play a key role in Zn hyperaccumulation. *Plant Cell.* 24, 708–723. doi: 10.1105/tpc.111.095000

Dong, J., Ma, G., Sui, L., Wei, M., Satheesh, V., Zhang, R., et al. (2019). Inositol pyrophosphate InsP8 acts as an intracellular phosphate signal in *Arabidopsis. Mol. Plant.* S1674–2052(19)30263–1. doi: 10.1016/j.molp.2019.08.002

Durrett, T. P., Gassmann, W., and Rogers, E. E. (2007). The FRD3-mediated efflux of citrate into the root vasculature is necessary for efficient iron translocation. *Plant Physiol.* 144, 197–205. doi: 10.1104/pp.107.097162

Eng, B. H., Guerinot, M. L., Eide, D., and Saier, M. H. J. (1998). Sequence analyses and phylogenetic characterization of the ZIP family of metal ion transport proteins. *J. Membr. Biol.* 166, 1–7. doi: 10.1007/s002329900442

Fan, C., Wang, X., Hu, R., Wang, Y., Xiao, C., Jiang, Y., et al. (2013). The pattern of phosphate transporter 1 genes evolutionary divergence in *Glycine max* L. *BMC Plant Biol.* 13, 48. doi: 10.1186/1471-2229-13-48

Farzaneh, M., Vierheilig, H., and Loessl, A. (2011). Arbuscular mycorrhiza enhances nutrient uptake in chickpea. *Plant Soil Environ.* 57, 465–470. doi: 10.17221/133/2011-PSE

Ferrol, N., Tamayo, E., and Vargas, P. (2016). The heavy metal paradox in arbuscular mycorrhizas: from mechanisms to biotechnological applications. *J. Exp. Bot.* 22, 6253–6265. doi: 10.1093/jxb/erw403

Franco, Z. J. M., Valli, A., Todesco, M., Mateos, I., Puga, M. I., Rubio, S. I., et al. (2007). Target mimicry provides a new mechanism for regulation of microRNA activity. *Nat. Genet.* 39, 1033–1037. doi: 10.1038/ng2079

Fu, X., Zhou, X., Xing, F., Ling, L., Chun, C., Cao, L., et al. (2017). Genome-wide identification, cloning and functional analysis of the zinc/iron-regulated transporter-like protein (ZIP) gene family in trifoliate orange (*Poncirus trifoliata* L. Raf.). *Front. Plant Sci.* 8, 588. doi: 10.3389/fpls.2017.00588

Giehl, R. F., Meda, A. R., and Von, W. N. (2009). Moving up, down, and everywhere: signaling of micronutrients in plants. *Curr. Opin. Plant Biol.* 12, 320–327. doi: 10.1016/j.pbi.2009.04.006

Giovannetti, M., Tolosano, M., Volpe, V., Kopriva, S., and Bonfante, P. (2014). Identification and functional characterization of a sulfate transporter induced by both sulfur starvation and mycorrhiza formation in *Lotus japonicus*. *New Phytol.* 204, 609–619. doi: 10.1111/nph.12949

Green, L. S., and Rogers, E. E. (2004). FRD3 controls iron localization in *Arabidopsis*. *Plant Physiol.* 136, 2523–2531. doi: 10.1104/pp.104.045633

Goff, S. A., Ricke, D., Lan, T. H., Presting, G., Wang, R., Dunn, M., et al. (2002). A draft sequence of the rice genome (*Oryza sativa* L. ssp. japonica). *Science* 296, 92–100. doi: 10.1126/science.1068275

Gojon, A., Nacry, P., and Davidian, J. C. (2009). Root uptake regulation: a central process for NPS homeostasis in plants. *Curr. Opin. Plant Biol.* 12, 328–338. doi: 10.1016/j.pbi.2009.04.015

González, G. M., Azcón, A. C., Mooney, M., Valderas, A., MacDiarmid, C. W., Eide, D. J., et al. (2005). Characterization of a *Glomus intraradices* gene encoding a putative Zn transporter of the cation diffusion facilitator family. *Fungal Genet. Biol.* 42, 130–140. doi: 10.1016/j.fgb.2004.10.007

González, G. M., Escudero, V., Saez, A., and Tejada, J. M. (2016). Transition metal transport in plants and associated endosymbionts: arbuscular mycorrhizal fungi and rhizobia. *Front. Plant Sci.* 7, 1088. doi: 10.3389/fpls.2016.01088

Grotz, N., Fox, T., Connolly, E., Park, W., Guerinot, M. L., and Eide, D. (1998). Identification of a family of zinc transporter genes from *Arabidopsis* that respond to zinc deficiency. *Proc. Natl. Acad. Sci. U. S. A.* 95, 7220–7224. doi: 10.1073/pnas.95.12.7220

Guerinot, M. L. (2000). The ZIP family of metal transporters. *Biochim. Biophys. Acta* 1465, 190–198. doi: 10.1016/S0005-2736(00)00138-3

Guether, M., Neuhauser, B., Balestrini, R., Dynowsk, M., Ludewig, U., and Bonfante, P. (2009). A mycorrhizal-specific ammonium transporter from *Lotus japonicus* acquires nitrogen released by arbuscular mycorrhizal fungi. *Plant Physiol.* 150, 73–83. doi: 10.1104/pp.109.136390

Gu, M., Chen, A., Sun, S., and Xu, G. (2016). Complex regulation of plant phosphate transporters and the gap between molecular mechanisms and practical application: what is missing? *Mol. Plant* 9, 396–416. doi: 10.1016/j.molp.2015.12.012

Hall, J. L., and Williams, L. E. (2003). Transition metal transporters in plants. *J. Exp. Bot.* 54, 2601–2613. doi: 10.1093/jxb/erg303

Hamburger, D., Rezzonico, E., MacDonald, C. P. J., Somerville, C., and Poirier, Y. (2002). Identification and characterization of the *Arabidopsis* PHO1 gene involved in phosphate loading to the xylem. *Plant Cell.* 14, 889–902. doi: 10.1105/tpc.000745

Hammond, J. P., Bennett, M. J., Bowen, H. C., Broadley, M. R., Eastwood, D. C., May, S. T., et al. (2003). Changes in gene expression in *Arabidopsis* shoots during phosphate starvation and the potential for developing smart plants. *Plant Physiol.* 132, 578–596. doi: 10.1104/pp.103.020941

Hanikenne, M., Talke, I. N., Haydon, M. J., Lanz, C., Nolte, A., Motte, P., et al. (2008). Evolution of metal hyperaccumulation required cis-regulatory changes and triplication of HMA4. *Nature* 453, 391–395. doi: 10.1038/nature06877

Harrison, M. J., Dewbre, G. R., and Liu, J. (2002). A phosphate transporter from *Medicago truncatula* involved in the acquisition of phosphate released by arbuscular mycorrhizal fungi. *Plant Cell.* 14, 2413–2429. doi: 10.1105/tpc.004861

Haydon, M. J., and Cobbett, C. S. (2007). A novel major facilitator superfamily protein at the tonoplast influences zinc tolerance and accumulation in *Arabidopsis*. *Plant Physiol.* 143, 1705–1719. doi: 10.1104/pp.106.092015

Haydon, M. J., Kawachi, M., Wirtz, M., Hillmer, S., Hell, R., and Kramer, U. (2012). Vacuolar nicotianamine has critical and distinct roles under iron deficiency and for zinc sequestration in *Arabidopsis*. *Plant Cell* 24, 724–737. doi: 10.1105/tpc.111.095042

Henriques, R., Jasik, J., Klein, M., Martinoia, E., Feller, U., Schell, J., et al. (2002). Knock-out of *Arabidopsis* metal transporter gene *IRT1* results in iron deficiency accompanied by cell differentiation defects. *Plant Mol. Biol.* 50, 587–597. doi: 10.1023/A:1019942200164

Hindt, M. N., and Guerinot, M. L. (2012). Getting a sense for signals: regulation of the plant iron deficiency response. *Biochim. Biophys. Acta* 1823, 1521–1530. doi: 10.1016/j.bbamcr.2012.03.010

Hirsch, J., Marin, E., Floriani, M., Chiarenza, S., Richaud, P., Nussaume, L., et al. (2006). Phosphate deficiency promotes modification of iron distribution in *Arabidopsis plants*. *Biochimie.* 88, 1767–1771. doi: 10.1016/j.biochi.2006.05.007

Hoseinzade, H., Ardakani, M. R., Shahdi, A., Rahmani, H. A., Noormohammadi, G., and Miransari, M. (2016). Rice (*Oryza sativa* L.) nutrient management using mycorrhizal fungi and endophytic *Herbaspirillum seropedicae*. *J. Integr. Agric.* 6, 1385–1394. doi: 10.1016/S2095-3119(15)61241-2

Huang, C., Barker, S. J., Langridge, P., Smith, F. W., and Graham, R. D. (2000). Zinc deficiency up-regulates expression of high-affinity phosphate transporter genes in both phosphate-sufficient and -deficient barley roots. *Plant Physiol.* 124, 415–422. doi: 10.1104/pp.124.1.415

Hussain, D., Haydon, M. J., Wang, Y., Wong, E., Sherson, S. M., Young, J., et al. (2004). P-type ATPase heavy metal transporters with roles in essential zinc homeostasis in *Arabidopsis*. *Plant Cell.* 16, 1327–1339. doi: 10.1105/tpc.020487

Ibiang, Y. B., Mitsumoto, H., and Sakamoto, K. (2017). Bradyrhizobia and arbuscular mycorrhizal fungi modulate manganese, iron, phosphorus, and polyphenols in soybean (*Glycine max* (L.) Merr.) under excess zinc. *Environ. Exp. Bot.* 137, 1–13. doi: 10.1016/j.envexpbot.2017.01.011

Ibiang, Y. B., Innami, H., and Sakamoto, K. (2018). Effect of excess zinc and arbuscular mycorrhizal fungus on bioproduction and trace element nutrition of tomato (*Solanum lycopersicum* L. cv. Micro-Tom). *Soil Sci. Plant Nutr.* 3, 342–351. doi: 10.1080/00380768.2018.1425103

Inoue, H., Kobayashi, T., Nozoye, T., Takahashi, M., Kakei, Y., Suzuki, K., et al. (2009). Rice OsYSL15 is an iron-regulated iron(III)-deoxymugineic acid transporter expressed in the roots and is essential for iron uptake in early growth of the seedlings. *J. Biol. Chem.* 284, 3470–3479. doi: 10.1074/jbc.M806042200

Ishimaru, Y., Suzuki, M., Kobayashi, T., Takahashi, M., Nakanishi, H., Mori, S., et al. (2005). OsZIP4, a novel zinc-regulated zinc transporter in rice. *J. Exp. Bot.* 56, 3207–3214. doi: 10.1093/jxb/eri317

Ishimaru, Y., Suzuki, M., Tsukamoto, T., Suzuki, K., Nakazono, M., Kobayashi, T., et al. (2006). Rice plants take up iron as an Fe3+-phytosiderophore and as Fe2+. *Plant J.* 45, 335–346. doi: 10.1111/j.1365-313X.2005.02624.x

Ivanov, R., Brumbarova, T., and Bauer, P. (2012). Fitting into the harsh reality: regulation of iron-deficiency responses in dicotyledonous plants. *Mol. Plant* 5, 27–42. doi: 10.1093/mp/ssr065

Jain, A., Sinilal, B., Dhandapani, G., Meagher, R. B., and Sahi, S. V. (2013). Effects of deficiency and excess of zinc on morphophysiological traits and spatiotemporal regulation of zinc-responsive genes reveal incidence of cross talk between micro- and macronutrients. *Environ. Sci. Technol.* 47, 5327–5335. doi: 10.1021/es400113y

Javot, H., Penmetsa, R. V., Terzaghi, N., Cook, D. R., and Harrison, M. J. (2007a). A *Medicago truncatula* phosphate transporter indispensable for the arbuscular mycorrhizal symbiosis. *Proc. Natl. Acad. Sci. U. S. A.* 104, 1720–1725. doi: 10.1073/pnas.0608136104

Javot, H., Pumplin, N., and Harrison, M. J. (2007b). Phosphate in the arbuscular mycorrhizal symbiosis: transport properties and regulatory roles. *Plant Cell Environ.* 30, 310–322. doi: 10.1111/j.1365-3040.2006.01617.x

Jia, H., Ren, H., Gu, M., Zhao, J., Sun, S., Zhang, X., et al. (2011). The phosphate transporter gene *OsPht1;8* is involved in phosphate homeostasis in rice. *Plant Physiol.* 156, 1164–1175. doi: 10.1104/pp.111.175240

Jiang, Y., Wang, W., Xie, Q., Liu, N., Liu, L., Wang, D., et al. (2017). Plants transfer lipids to sustain colonization by mutualistic mycorrhizal and parasitic fungi. *Science* 356, 1172–1175. doi: 10.1126/science.aam9970

Karandashov, V., and Bucher, M. (2005). Symbiotic phosphate transport in arbuscular mycorrhizas. *Trends Plant Sci.* 10, 22–29. doi: 10.1016/j.tplants.2004.12.003

Kawachi, M., Kobae, Y., Mori, H., Tomioka, R., Lee, Y., and Maeshima, M. (2009). A mutant strain *Arabidopsis thaliana* that lacks vacuolar membrane zinc transporter MTP1 revealed the latent tolerance to excessive zinc. *Plant Cell Physiol.* 50, 1156–1170. doi: 10.1093/pcp/pcp067

Khan, G. A., Bouraine, S., Wege, S., Li, Y., De, C. M., Berthomieu, P., et al. (2014). Coordination between zinc and phosphate homeostasis involves the transcription factor PHR1, the phosphate exporter PHO1, and its homologue PHO1;H3 in *Arabidopsis*. *J. Exp. Bot.* 65, 871–884. doi: 10.1093/jxb/ert444

Kisko, M., Bouain, N., Rouached, A., Choudhary, S. P., and Rouached, H. (2015). Molecular mechanisms of phosphate and zinc signaling crosstalk in plants: phosphate and zinc loading into root xylem in *Arabidopsis*. *Environ. Exp. Bot.* 114, 57–64. doi: 10.1016/j.envexpbot.2014.05.013

Klatte, M., Schuler, M., Wirtz, M., Fink-Straube, C., Hell, R., and Bauer, P. (2009). The analysis of *Arabidopsis* nicotianamine synthase mutants reveals functions for nicotianamine in seed iron loading and iron deficiency responses. *Plant Physiol.* 150, 257–271. doi: 10.1104/pp.109.136374

Kobayashi, T., and Nishizawa, N. K. (2012). Iron uptake, translocation, and regulation in higher plants. *Annu. Rev. Plant Biol.* 63, 131–152. doi: 10.1146/annurev-arplant-042811-105522

Kobayashi, T., and Nishizawa, N. K. (2014). Iron sensors and signals in response to iron deficiency. *Plant Sci.* 224, 36–43. doi: 10.1016/j.plantsci.2014.04.002

Kobayashi, T., Nagasaka, S., Senoura, T., Itai, R. N., Nakanishi, H., and Nishizawa, N. K. (2013). Iron-binding haemerythrin RING ubiquitin ligases regulate plant iron responses and accumulation. *Nat. Commun.* 4, 2792. doi: 10.1038/ncomms3792

Koike, S., Inoue, H., Mizuno, D., Takahashi, M., Nakanishi, H., Mori, S., et al. (2004). OsYSL2 is a rice metal-nicotianamine transporter that is regulated by iron and expressed in the phloem. *Plant J.* 39, 415–424. doi: 10.1111/j.1365-313X.2004.02146.x

Konieczny, A., and Kowalska, I. (2017). Effect of arbuscular mycorrhizal fungi on the content of zinc in lettuce grown at two phosphorus levels and an elevated zinc level in a nutrient solution. *J. Elementol.* 2, 761–772. doi: 10.5601/jelem.2016.21.4.1335

Kruger, C., Berkowitz, O., Stephan, U. W., and Hell, R. (2002). A metal-binding member of the late embryogenesis abundant protein family transports iron in the phloem of *Ricinus communis* L. *J. Biol. Chem.* 277, 25062–25069. doi: 10.1074/jbc.M201896200

Lanquar, V., Lelièvre, F., Barbier-Brygoo, H., and Thomine, S. (2004). Regulation and function of AtNRAMP4 metal transporter protein. *Soil Sci. Plant Nutr.* 50, 477–484. doi: 10.1080/00380768.2004.10408587

Lee, S., Kim, S. A., Lee, J., Guerinot, M. L., and An, G. (2010). Zinc deficiency-inducible OsZIP8 encodes a plasma membrane-localized zinc transporter in rice. *Mol. Cells.* 29, 551–558. doi: 10.1007/s10059-010-0069-0

Lee, S., Persson, D. P., Hansen, T. H., Husted, S., Schjoerring, J. K., and Kim, Y. S., et al. (2011). Bio-available zinc in rice seeds is increased by activation tagging of nicotianamine synthase. *Plant Biotechnol. J.* 9, 865–873. doi: 10.1111/j.1467-7652.2011.00606.x

Leigh, J., Hodge, A., and Fitter, A. H. (2009). Arbuscular mycorrhizal fungi can transfer substantial amounts of nitrogen to their host plant from organic material. *New Phytol.* 181, 199–207. doi: 10.1111/j.1469-8137.2008.02630.x

Lin, S. I., Chiang, S. F., Lin, W. Y., Chen, J. W., Tseng, C. Y., Wu, P. C., et al. (2008). Regulatory network of microRNA399 and PHO2 by systemic signaling. *Plant Physiol.* 147, 732–746. doi: 10.1104/pp.108.116269

Lin, Y. F., Liang, H. M., Yang, S. Y., Boch, A., Clemens, S., Chen, C. C., et al. (2009). *Arabidopsis* IRT3 is a zinc-regulated and plasma membrane localized zinc/iron transporter. *New Phytol.* 182, 392–404. doi: 10.1111/j.1469-8137.2009.02766.x

Li, S., Zhou, X., Chen, J., and Chen, R. (2018). Is there a strategy I iron uptake mechanism in maize? *Plant Signal. Behav.* 3, 13 (4), e1161877. doi: 10.1080/15592324.2016.1161877

Li, S., Zhou, X., Huang, Y., Zhu, L., Zhang, S., Zhao, Y., et al. (2013). Identification and characterization of the zinc-regulated transporters, iron-regulated transporter-like protein (ZIP) gene family in maize. *BMC Plant Biol.* 13, 114. doi: 10.1186/1471-2229-13-114

Li, W., and Lan, P. (2015). Genome-wide analysis of overlapping genes regulated by iron deficiency and phosphate starvation reveals new interactions in *Arabidopsis* roots. *BMC. Res. Notes.* 12, 555. doi: 10.1186/s13104-015-1524-y

Lin, W. Y., Huang, T. K., and Chiou, T. J. (2013). NITROGEN LIMITATION ADAPTATION, a target of microRNA827, mediates degradation of plasma membrane-localized phosphate transporters to maintain phosphate homeostasis in *Arabidopsis*. *Plant Cell.* 25, 4061–4074. doi: 10.1105/tpc.113.116012

Ling, H. Q., Bauer, P., Bereczky, Z., Keller, B., and Ganal, M. (2002). The tomato fer gene encoding a bHLH protein controls iron-uptake responses in roots. *Proc. Natl. Acad. Sci. U. S. A.* 99, 13938–13943. doi: 10.1073/pnas.212448699

Liu, A., Hamel, C., Hamilton, R. I., Ma, B. L., and Smith, B. L. (2000). Acquisition of Cu, Zn, Mn and Fe by mycorrhizal maize (*Zea mays* L.) grown in soil at different P and micronutrient levels. *Mycorrhiza.* 9, 331–336. doi: 10.1007/s005720050277

Liu, T. Y., Chang, C. Y., and Chiou, T. J. (2009). The long-distance signaling of mineral macronutrients. *Curr. Opin. Plant Biol.* 12, 312–319. doi: 10.1016/j.pbi.2009.04.004

Loneragan, J. F., and Webb, M. J. (1993). "Interactions between zinc and other nutrients affecting the growth of plants," in *Zinc in soils and plants.* Ed. A. D. Robson (Dordrecht: Springer Netherlands), 119–134. doi: 10.1007/978-94-011-0878-2_9

Long, T. A., Tsukagoshi, H., Busch, W., Lahner, B., Salt, D. E., and Benfey, P. N. (2010). The bHLH transcription factor POPEYE regulates response to iron deficiency in *Arabidopsis* roots. *Plant Cell.* 22, 2219–2236. doi: 10.1105/tpc.110.074096

Lopez, B. J., De, L. V. O., Guevara, G. A., and Herrera, L. (2000). Enhanced phosphorus uptake in transgenic tobacco plants that overproduce citrate. *Nat. Biotechnol.* 18, 450–453. doi: 10.1038/74531

López, M. A., Ellis, D. R., and Grusak, M. A. (2004). Identification and characterization of several new members of the ZIP family of metal ion transporters in *Medicago truncatula*. *Plant Mol. Biol.* 54, 583–596. doi: 10.1023/B:PLAN.0000038271.96019.aa

Magalhaes, J. V., Liu, J., Guimarães, C. T., Lana, U. G., Alves, V. M., Wang, Y. H., et al. (2007). A gene in the multidrug and toxic compound extrusion (MATE) family confers aluminum tolerance in sorghum. *Nat Genet.* 39, 1156–1161. doi: 10.1038/ng2074

Marschner, H. (1995). *Mineral nutrition of higher plants.* London: Academic Press.

Marschner, P. (2012). *Marschner's mineral nutrition of higher plants*. 3rd. USA: Boston: Academic Press, Elsevier.

Mäser, P., Thomine, S., Schroeder, J. I., Ward, J. M., Hirschi, K., Sze, H., et al. (2001). Phylogenetic relationships within cation transporter families of *Arabidopsis*. *Plant Physiol.* 126, 1646–1667. doi: 10.1104/pp.126.4.1646

Masuda, H., Usuda, K., Kobayashi, T., Ishimaru, Y., Kakei, Y., Takahashi, M., et al. (2009). Overexpression of the barley nicotianamine synthase gene HvNAS1 increases iron and zinc concentrations in rice grains. *Rice* 2, 155–166. doi: 10.1007/s12284-009-9031-1

Milner, M. J., Seamon, J., Craft, E., and Kochian, L. (2013). Transport properties of members of the ZIP family in plants and their role in Zn and Mn homeostasis. *J. Exp. Bot.* 64, 369–603. doi: 10.1093/jxb/ers315

Milner, M. J., Craft, E., Yamaji, N., Koyama, E., Ma, J. F., and Kochian, L. V. (2012). Characterization of the high affinity Zn transporter from *Noccaea caerulescens*, NcZNT1, and dissection of its promoter for its role in Zn uptake and hyperaccumulation. *New Phytol.* 195, 113–123. doi: 10.1111/j.1469-8137.2012.04144.x

Misson, J., Raghothama, K. G., Jain, A., Jouhet, J., Block, M. A., Bligny, R., et al. (2005). A genome-wide transcriptional analysis using *Arabidopsis thaliana* Affymetrix gene chips determined plant responses to phosphate deprivation. *Proc. Natl. Acad. Sci. U. S. A.* 102, 11934–11939. doi: 10.1073/pnas.0505266102

Moran, L. A., Peiffer, G. A., Yin, T., Whitham, S. A., Cook, D., Shoemaker, R. C., et al. (2014). Identification of candidate genes involved in early iron deficiency chlorosis signaling in soybean (*Glycine max*) roots and leaves. *BMC Genomics* 15, 702. doi: 10.1186/1471-2164-15-702

Morrissey, J., and Guerinot, M. L. (2009). Iron uptake and transport in plants: the good, the bad, and the ionome. *Chem. Rev.* 109, 4553–4567. doi: 10.1002/chin.201005266

Muchhal, U. S., Pardo, J. M., and Raghothama., K. G. (1996). Phosphate transporters from the higher plant *Arabidopsis thaliana*. *Proc. Natl. Acad. Sci. U. S. A.* 93, 10519–10523. doi: 10.1073/pnas.93.19.10519

Mudge, S. R., Rae, A. L., Diatloff, E., and Smith, F. W. (2002). Expression analysis suggests novel roles for members of the Pht1 family of phosphate transporters in *Arabidopsis*. *Plant J.* 31, 341–353. doi: 10.1046/j.1365-313X.2002.01356.x

Müller, R., Morant, M., Jarmer, H., Nilsson, L., and Hamborg, N. T. H. (2007). Genome-wide analysis of the *Arabidopsis* leaf transcriptome reveals interaction of phosphate and sugar metabolism. *Plant Physiol.* 143, 156–171. doi: 10.1104/pp.106.090167

Nafady, N. A., and Elgharably, A. (2018). Mycorrhizal symbiosis and phosphorus fertilization effects on *Zea mays* growth and heavy metals uptake. *Int. J. Phytorem.* 20, 869–875. doi: 10.1080/15226514.2018.1438358

Nagarajan, V. K., Jain, A., Poling, M. D., Lewis, A. J., Raghothama, K. G., and Smith, A. P. (2011). *Arabidopsis* Pht1;5 mobilizes phosphate between source and sink organs and influences the interaction between phosphate homeostasis and ethylene signaling. *Plant Physiol.* 156, 1149–1163. doi: 10.1104/pp.111.174805

Neset, T. S., and Cordell, D. (2012). Global phosphorus scarcity: identifying synergies for a sustainable future. *J. Sci. Food Agric.* 92, 2–6. doi: 10.1002/jsfa.4650

Nussaume, L., Kanno, S., Javot H, M. E., Pochon, N., Ayadi, A., Nakanishi, T. M., et al. (2011). Phosphate import in plants: focus on the PHT1 transporters. *Front. Plant Sci.* 2, 83. doi: 10.3389/fpls.2011.00083

Ogo, Y., Itai, R. N., Kobayashi, T., Aung, M. S., Nakanishi, H., and Nishizawa, N. K. (2011). OsIRO2 is responsible for iron utilization in rice and improves growth and yield in calcareous soil. *Plant Mol. Biol.* 75, 593–605. doi: 10.1007/s11103-011-9752-6

Ogo, Y., Itai, R. N., Nakanishi, H., Kobayashi, T., Takahashi, M., Mori, S., et al. (2007). The rice bHLH protein OsIRO2 is an essential regulator of the genes involved in Fe uptake under Fe-deficient conditions. *Plant J.* 51, 366–377. doi: 10.1111/j.1365-313X.2007.03149.x

Ova, E. A., Kutman, U. B., Ozturk, L., and Cakmak, I. (2015). High phosphorus supplies reduced zinc concentration of wheat in native soil but not in autoclaved soil or nutrient solution. *Plant Soil* 393, 147–162. doi: 10.1007/s11104-015-2483-8

Palmer, C. M., and Guerinot, M. L. (2009). Facing the challenges of Cu, Fe and Zn homeostasis in plants. *Nat. Chem. Biol.* 5, 333–340. doi: 10.1038/nchembio.166

Pant, B. D., Buhtz, A., Kehr, J., and Scheible, W. R. (2008). MicroRNA399 is a long-distance signal for the regulation of plant phosphate homeostasis. *Plant J.* 53, 731–738. doi: 10.1111/j.1365-313X.2007.03363.x

Pao, S. S., Paulsen, I. T., and Saier, M. H. J. (1998). Major facilitator superfamily. *Microbiol. Mol. Biol. Rev.* 62, 1–34. doi: 10.9783/9781512806809-002

Parniske, M. (2008). Arbuscular mycorrhiza: the mother of plant root endosymbioses. *Nat Rev. Microbiol.* 6, 763–775. doi: 10.1038/nrmicro1987

Paszkowski, U., Kroken, S., Roux, C., and Briggs, S. P. (2002). Rice phosphate transporters include an evolutionarily divergent gene specifically activated in arbuscular mycorrhizal symbiosis. *Proc. Natl. Acad. Sci. U. S. A.* 99, 13324–13329. doi: 10.1073/pnas.202474599

Pedas, P., Schjoerring, J. K., and Husted, S. (2009). Identification and characterization of zinc-starvation-induced ZIP transporters from barley roots. *Plant Physiol. Biochem.* 47, 377–383. doi: 10.1016/j.plaphy.2009.01.006

Perea, G. A., Garcia, M. A., Andrés, N., Vera, S. F., Pérez, A. M. A., Puig, S., et al. (2013). *Arabidopsis* copper transport protein COPT2 participates in the cross talk between iron deficiency responses and low-phosphate signaling. *Plant Physiol.* 162, 180–194. doi: 10.1104/pp.112.212407

Petit, J. M., Briat, J. F., and Lobréaux, S. (2001). Structure and differential expression of the four members of the *Arabidopsis thaliana* ferritin gene family. *Biochem. J.* 359, 575–582. doi: 10.1042/bj3590575

Pilon, M., Cohu, C. M., Ravet, K., Abdel, G. S. E., and Gaymard, F. (2009). Essential transition metal homeostasis in plants. *Curr. Opin. Plant Biol.* 12, 347–357. doi: 10.1016/j.pbi.2009.04.011

Pineau, C., Loubet, S., Lefoulon, C., Chalies, C., Fizames, C., Lacombe, B., et al. (2012). Natural variation at the FRD3 MATE transporter locus reveals cross-talk between Fe homeostasis and Zn tolerance in *Arabidopsis thaliana*. *PLoS Genet.* 8, e1003120. doi: 10.1371/journal.pgen.1003120

Poirier, Y., and Bucher, M. (2002). Phosphate transport and homeostasis in *Arabidopsis*. *Arabidopsis Book*. 1, e0024. doi: 10.1199/tab.0024

Poirier, Y., and Jung, J. Y. (2015). Phosphate transporters. *Annu. Plant Rev.* 48, 125–159. doi: 10.1002/9781118958841.ch5

Poirier, Y., Thoma, S., Somerville, C., and Schiefelbein, J. (1991). Mutant of *Arabidopsis* deficient in xylem loading of phosphate. *Plant Physiol.* 97, 1087–1093. doi: 10.1104/pp.97.3.1087

Poshtmasari, H. K., Bahmanyar, M. A., Pirdashti, H., Shad, M. A. (2008). Effects of Zn rates and application forms on protein and some micronutrients accumulation in common bean (Phaseolus vulgaris L.). *Pak J Biol Sci.* 11, 1042–1046.

Puga, M. I., Mateos, I., Charukesi, R., Wang, Z. Y., Franco, Z. J. M., De, L. L., et al. (2014). SPX1 is a phosphate-dependent inhibitor of PHOSPHATE STARVATION RESPONSE 1 in *Arabidopsis*. *Proc. Natl. Acad. Sci. U. S. A.* 111, 14947–14952. doi: 10.1073/pnas.1404654111

Rai, V., Sanagala, R., Sinilal, B., Yadav, S., Sarkar, A. K., Dantu, P. K., et al. (2015). Iron availability affects phosphate deficiency-mediated responses, and evidence of cross-talk with auxin and zinc in *Arabidopsis*. *Plant Cell Physiol.* 56, 1107–1123. doi: 10.1093/pcp/pcv035

Rausch, C., Daram, P., Brunner, S., Jansa, J., Laloi, M., Leggewie, G., et al. (2001). A phosphate transporter expressed in arbuscule-containing cells in potato. *Nature* 414, 462–470. doi: 10.1038/35106601

Reed, H. (1946). Effects of zinc deficiency on phosphate metabolism of the tomato plant. *Am. J. Bot.* 33, 778–784. doi: 10.1002/j.1537-2197.1946.tb12940.x

Remy, E., Cabrito, T. R., Batista, R. A., Teixeira, M. C., Sa, C. I., and Duque, P. (2012). The Pht1;9 and Pht1;8 transporters mediate inorganic phosphate acquisition by the *Arabidopsis thaliana* root during phosphorus starvation. *New Phytol.* 195, 356–371. doi: 10.1111/j.1469-8137.2012.04167.x

Remy, W., Taylor, T. N., Hass, H., and Kerp, H. (1994). Four hundred million-year-old vesicular arbuscular mycorrhizae. *Proc. Natl. Acad. Sci. U. S. A.* 91, 11841–11843. doi: 10.1073/pnas.91.25.11841

Rouached, H., Arpat, A. B., and Poirier, Y. (2010). Regulation of phosphate starvation responses in plants: signaling players and cross-talks. *Mol. Plant* 3, 288–299. doi: 10.1093/mp/ssp120

Rouached, H., Stefanovic, A., Secco, D., Bulak Arpat, A., Gout, E., Bligny, R., et al. (2011b). Uncoupling phosphate deficiency from its major effects on growth and transcriptome *via* PHO1 expression in *Arabidopsis*. *Plant J.* 65, 557–570. doi: 10.1111/j.1365-313X.2010.04442.x

Ryan, M. H., Mcinerney, J. K., Record, I. R., Angus, J. F. (2008). Zinc bioavailability in wheat grain in relation to phosphorus fertiliser, crop sequence and mycorrhizal fungi. *J. Sci. Food Agric.* 88, 1208–1216. doi: 10.1002/jsfa.3200

Salgueiro, M., Zubillaga, M., Lysionek, A., Sarabia, M. I., Caro, R., De, P. T., et al. (2000). Zinc as an essential micronutrient: a review. *Nutr. Res.* 20, 737–755. doi: 10.1016/S0271-5317(00)00163-9

Saenchai, C., Bouain, N., Kisko, M., Prom, C., Doumas, P., and Rouached, H. (2016). The involvement of OsPHO1;1 in the regulation of iron transport through integration of phosphate and zinc deficiency signaling. *Front. Plant Sci.* 7, 396. doi: 10.3389/fpls.2016.00396

Sasaki, A., Yamaji, N., Mitani-Ueno, N., Kashino, M., and Ma, J. F. (2015). A node-localized transporter OsZIP3 is responsible for the preferential distribution of Zn to developing tissues in rice. *Plant J.* 84, 374–384. doi: 10.1111/tpj.13005

Schachtman, D. P., Reid, R. J., and Ayling, S. M. (1998). Phosphorus uptake by plants: from soil to cell. *Plant Physiol.* 116, 447–453. doi: 10.1104/pp.116.2.447

Schachtman, D. P., and Shin, R. (2007). Nutrient sensing and signaling: NPKS. *Annu. Rev. Plant Biol.* 58, 47–69. doi: 10.1146/annurev.arplant.58.032806.103750

Schüßler, A., Schwarzott, D., and Walker, C. (2001). A new fungal phylum, the Glomeromycota: phylogeny and evolution. *Mycol. Res.* 105, 1413–1421. doi: 10.1017/S0953756201005196

Shahzad, Z., Rouached, H., and Rakha, A. (2014). Combating mineral malnutrition through iron and zinc biofortification of cereals. *Compr. Rev. Food Sci. F.* 13, 329–346. doi: 10.1111/1541-4337.12063

Shanmugam, V., Tsednee, M., and Yeh, K. C. (2012). ZINC TOLERANCE INDUCED BY IRON 1 reveals the importance of glutathione in the cross-homeostasis between zinc and iron in *Arabidopsis thaliana*. *Plant J.* 69, 1006–1017. doi: 10.1111/j.1365-313X.2011.04850.x

Shin, H., Shin, H. S., Dewbre, G. R., and Harrison, M. J. (2004). Phosphate transport in *Arabidopsis*: Pht1;1 and Pht1;4 play a major role in phosphate acquisition from both low- and high-phosphate environments. *Plant J.* 39, 629–642. doi: 10.1111/j.1365-313X.2004.02161.x

Sieh, D., Watanabe, M., Devers, E. A., Brueckner, F., Hoefgen, R., and Krajinski, F. (2013). The arbuscular mycorrhizal symbiosis influences sulfur starvation responses of *Medicago truncatula*. *New Phytol.* 197, 606–616. doi: 10.1111/nph.12034

Sinclair, S. A., and Krämer, U. (2012). The zinc homeostasis network of land plants. *Biochim. Biophys. Acta* 1823, 1553–1567. doi: 10.1016/j.bbamcr.2012.05.016

Smith, S. E., and Read, D. J. (2008). *Mycorrhizal Symbiosis*. San Diego: Academic Press, Inc.

Smith, S. E., Smith, F. A., and Jakobsen, I. (2003). Mycorrhizal fungi can dominate phosphate supply to plants irrespective of growth responses. *Plant Physiol.* 133, 16–20. doi: 10.1104/pp.103.024380

Stefanovic, A., Arpat, A. B., Bligny, R., Gout, E., Vidoudez, C., Bensimon, M., et al. (2011). Overexpression of PHO1 in *Arabidopsis* leaves reveals its role in mediating phosphate efflux. *Plant J.* 66, 689–699. doi: 10.1111/j.1365-313X.2011.04532.x

Stephan, U. W., and Scholz, G. (1993). Nicotianamine: mediator of transport of iron and heavy metals in the phloem? *Physiol. Plant.* 88, 522–529. doi: 10.1111/j.1399-3054.1993.tb01367.x

Sun, S., Gu, M., Cao, Y., Huang, X., Zhang, X., Ai, P., et al. (2012). A constitutive expressed phosphate transporter, OsPht1;1, modulates phosphate uptake and translocation in phosphate-replete rice. *Plant Physiol.* 159, 1571–1581. doi: 10.1104/pp.112.196345

Takahashi, M., Terada, Y., Nakai, I., Yoshimura, E., Mori, S., and Nishizawa, N. K. (2003). Role of nicotianamine in the intracellular delivery of metals and plant reproductive development. *Plant Cell.* 15, 1263–1280. doi: 10.1105/tpc.010256

Tamayo, E., Gómez-Gallego., T., Azcón-Aguilar., C., and Ferrol, N. (2014). Genome-wide analysis of copper, iron and zinc transporters in the arbuscular mycorrhizal fungus *Rhizophagus irregularis. Front. Plant Sci.* 5, 547. doi: 10.3389/fpls.2014.00547

Tamayo, E., Knight, S. A. B., Valderas, A., Dancis, A., and Ferrol, N. (2018). The arbuscular mycorrhizal fungus *Rhizophagus irregularis* uses a reductive iron assimilation pathway for high-affinity iron uptake. *Environ Microbiol.* 20, 1857–1872. doi: 10.1111/1462-2920.14121

Thibaud, M. C., Arrighi, J. F., Bayle, V., Chiarenza, S., Creff, A., Bustos, R., et al. (2010). Dissection of local and systemic transcriptional responses to phosphate starvation in *Arabidopsis. Plant J.* 64, 775–789. doi: 10.1111/j.1365-313X.2010.04375.x

Thomine, S., Wang, R., Ward, J. M., Crawford, N. M., and Schroeder, J. I. (2000). Cadmium and iron transport by members of a plant metal transporter family in *Arabidopsis* with homology to Nramp genes. *Proc. Natl. Acad. Sci. U. S. A.* 97, 4991–4996. doi: 10.1073/pnas.97.9.4991

Tiong, J., McDonald, G. K., Genc, Y., Pedas, P., Hayes, J. E., Toubia, J., et al. (2014). HvZIP7 mediates zinc accumulation in barley (*Hordeum vulgare*) at moderately high zinc supply. *New Phytol.* 201, 131–143. doi: 10.1111/nph.12468

van de Mortel, J. E., Almar, V. L., Schat, H., Kwekkeboom, J., Coughlan, S., Moerland, P. D., et al. (2006). Large expression differences in genes for iron and zinc homeostasis, stress response, and lignin biosynthesis distinguish roots of *Arabidopsis thaliana* and the related metal hyperaccumulator *Thlaspi caerulescens. Plant Physiol.* 142, 1127–1147. doi: 10.1104/pp.106.082073

van der Heijden, M. G. A., Klironomos, J. N., Ursic, M., Moutoglis, P., Streitwolf, R., Boller, T., et al. (1998). Mycorrhizal fungal diversity determines plant biodiversity, ecosystem variability and productivity. *Nature* 396, 69–72. doi: 10.1038/23932

Verret, F., Gravot, A., Auroy, P., Leonhardt, N., David, P., Nussaume, L., et al. (2004). Overexpression of *AtHMA4* enhances root-to-shoot translocation of zinc and cadmium and plant metal tolerance. *FEBS Lett.* 576, 306–312. doi: 10.1016/j.febslet.2004.09.023

Vert, G., Grotz, N., Dedaldechamp, F., Gaymard, F., Guerinot, M. L., Briat, J. F., et al. (2002). IRT1, an *Arabidopsis transporter* essential for iron uptake from the soil and for plant growth. *Plant Cell.* 14, 1223–1233. doi: 10.1105/tpc.001388

Volpe, V., Giovannetti, M., Sun, X. G., Fiorilli, V., and Bonfante, P. (2016). The phosphate transporters LjPT4 and MtPT4 mediate early root responses to phosphate status in nonmycorrhizal roots. *Plant Cell Environ.* 39, 660–671. doi: 10.1111/pce.12659

Wang, L., Ying, Y., Narsai, R., Ye, L., Zheng, L., Tian, J., et al. (2013). Identification of OsbHLH133 as a regulator of iron distribution between roots and shoots in *Oryza sativa. Plant Cell Environ.* 36, 224–236. doi: 10.1111/j.1365-3040.2012.02569.x

Wang, Z., Ruan, W., Shi, J., Zhang, L., Xiang, D., Yang, C., et al. (2014a). Rice SPX1 and SPX2 inhibit phosphate starvation responses through interacting with PHR2 in a phosphate-dependent manner. *Proc. Natl. Acad. Sci. U. S. A.* 111, 14953–14958. doi: 10.1073/pnas.1404680111

Wang, X., Wang, Y., Piñeros, M. A., Wang, Z., Wang, W., Li, C., et al. (2014b). Phosphate transporters OsPHT1;9 and OsPHT1;10 are involved in phosphate uptake in rice. *Plant Cell Environ.* 37, 1159–1170. doi: 10.1111/pce.12224

Ward, J. T., Lahner, B., Yakubova, E., Salt, D. E., and Raghothama, K. G. (2008). The effect of iron on the primary root elongation of *Arabidopsis* during phosphate deficiency. *Plant Physiol.* 147, 1181–1191. doi: 10.1104/pp.108.118562

Watts-Williams, S. J., and Cavagnaro, T. R. (2018). Arbuscular mycorrhizal fungi increase grain zinc concentration and modify the expression of root ZIP transporter genes in a modern barley (*Hordeum vulgare*) cultivar. *Plant Sci.* 247, 163–170. doi: 10.1016/j.plantsci.2018.05.015

Watts-Williams, S. J., and Cavagnaro, T. R. (2014). Nutrient interactions and arbuscular mycorrhizas: a meta-analysis of a mycorrhiza-defective mutant and wild-type tomato genotype pair. *Plant Soil* 2, 79–92. doi: 10.1007/s11104-014-2140-7

Watts-Williams, S. J., Smith, F. A., McLaughlin, M. J., Patti, A. F., and Cavagnaro, T. R. (2015). How important is the mycorrhizal pathway for plant Zn uptake? *Plant Soil.* 390, 157–166. doi: 10.1007/s11104-014-2374-4

Watts-Williams, S. J., Tyerman, S. D., and Cavagnaro, T. R. (2017). The dual benefit of arbuscular mycorrhizal fungi under soil zinc deficiency and toxicity: linking plant physiology and gene expression. *Plant Soil* 420, 375–388. doi: 10.1007/s11104-017-3409-4

Watts-Williams, S. J., Patti, A., and Cavagnaro, T. R. (2013). Arbuscular mycorrhizas are beneficial under both deficient and toxic soil zinc conditions. *Plant Soil* 371, 299–312. doi: 10.1007/s11104-013-1670-8

Westheimer, F. H. (1987). Why nature chose phosphates. *Science* 235, 1173–1178. doi: 10.1126/science.2434996

Wintz, H., Fox, T., Wu, Y., Feng, V., Chen, W., Chang, H., et al. (2003). Expression profiles of *Arabidopsis thaliana* in mineral deficiencies reveal novel transporters involved in metal homeostasis. *J. Biol. Chem.* 278, 47644–47653. doi: 10.1074/jbc.M309338200

Wong, C. K., Jarvis, R. S., Sherson, S. M., and Cobbett, C. S. (2009). Functional analysis of the heavy metal binding domains of the Zn/Cd-transporting ATPase, HMA2, in *Arabidopsis thaliana. New Phytol.* 181, 79–88. doi: 10.1111/j.1469-8137.2008.02637.x

Wu, P., Ma, L., Hou, X., Wang, M., Wu, Y., Liu, F., et al. (2003). Phosphate starvation triggers distinct alterations of genome expression in *Arabidopsis* roots and leaves. *Plant Physiol.* 132, 1260–1271. doi: 10.1104/pp.103.021022

Xue, Y. F., Xia, H. Y., Christie, P., Zhang, Z., Li, L., and Tang, C. X. (2016). Crop acquisition of phosphorus, iron and zinc from soil in cereal/legume intercropping systems: a critical review. *Ann. Bot.* 3, 363–377. doi: 10.1093/aob/mcv182

Yang, S. Y., Grønlund, M., Jakobsen, I., Grotemeyer, M. S., Rentsch, D., Miyao, A., et al. (2012). Nonredundant regulation of rice arbuscular mycorrhizal symbiosis by two members of the phosphate transporter1 gene family. *Plant Cell.* 24, 4236–4251. doi: 10.1105/tpc.112.104901

Yokosho, K., Yamaji, N., Ueno, D., Mitani, N., and Ma, J. F. (2009). OsFRDL1 is a citrate transporter required for efficient translocation of iron in rice. *Plant Physiol.* 149, 297–305. doi: 10.1104/pp.108.128132

Zhang, F., Sun, Y., Pei, W., Jain, A., Sun, R., Cao, Y., et al. (2015). Involvement of OsPht1;4 in phosphate acquisition and mobilization facilitates embryo development in rice. *Plant J.* 82, 556–569. doi: 10.1111/tpj.12804

Zhang, J., Liu, B., Li, M., Feng, D., Jin, H., Wang, P., et al. (2015). The bHLH transcription factor bhlh104 interacts with IAA-LEUCINE RESISTANT3 and modulates iron homeostasis in *Arabidopsis. Plant Cell.* 27, 787–805. doi: 10.1105/tpc.114.132704

Zhang, W., Chen, X. X., Liu, Y. M., Liu, D. Y., Chen, X. P., and Zou, C. Q. (2017). Zinc uptake by roots and accumulation in maize plants as affected by phosphorus application and arbuscular mycorrhizal colonization. *Plant Soil* 413, 59–71. doi: 10.1007/s11104-017-3213-1

Zhang, W., Liu, D. Y., Liu, Y. M., Cui, Z. L., Chen, X. P., and Zou, C. Q. (2016). Zinc uptake and accumulation in winter wheat relative to changes in root morphology and mycorrhizal colonization following varying phosphorus application on calcareous soil. *Field Crop Res.* 197, 74–82. doi: 10.1016/j.fcr.2016.08.010

Zhang, Y. Q., Deng, Y., Chen, R. Y., Cui, Z. L., Chen, X. P., Yost, R., Zhang, F.S., et al. (2012). The reduction in zinc concentration of wheat grain upon increased phosphorus-fertilization and its mitigation by foliar zinc application. *Plant Soil.* 361, 143–152. doi: 10.1007/s11104-012-1238-z

Zhang, Z., Liao, H., and Lucas, W. J. (2014). Molecular mechanisms underlying phosphate sensing, signaling, and adaption in plants. *J. Integr. Plant Biol.* 56, 192–220. doi: 10.1111/jipb.12163

Zheng, L., Huang, F., Narsai, R., Wu, J., Giraud, E., He, F., et al. (2009). Physiological and transcriptome analysis of iron and phosphorus interaction in rice seedlings. *Plant Physiol.* 151, 262–274. doi: 10.1104/pp.109.141051

Zheng, L., Ying, Y., Wang, L., Wang, F., Whelan, J., and Shou, H. (2010). Identification of a novel iron regulated basic helix-loop-helix protein involved in Fe homeostasis in *Oryza sativa*. *BMC Plant Biol.* 10, 166. doi: 10.1186/1471-2229-10-166

Zhu, Y. G., Smith, S. E., and Smith, F. A. (2001). Plant growth and cation composition of two cultivars of spring wheat (Triticum aestivum L.) differing in P uptake efficiency. *J. Exp. Bot.* 52, 1277–1282. doi: 10.1093/jxb/52.359.1277

Conflict of Interest: The authors declare that the research was conducted in the absence of any commercial or financial relationships that could be construed as a potential conflict of interest.

frontiers in Plant Science

METHODS
published: 27 September 2019
doi: 10.3389/fpls.2019.01184

Ramf: An Open-Source R Package for Statistical Analysis and Display of Quantitative Root Colonization by Arbuscular Mycorrhiza Fungi

Marco Chiapello[1]*, *Debatosh Das*[2,3] *and Caroline Gutjahr*[2,3]*

[1] Institute for Sustainable Plant Protection, CNR, Torino, Italy, [2] Faculty of Biology, Genetics, LMU Munich, Martinsried, Germany, [3] Plant Genetics, TUM School of Life Sciences Weihenstephan, Technical University of Munich (TUM), Freising, Germany

Data analysis and graphical representation form an essential part of scientific research dissemination. The life-science community is moving towards a more transparent presentation of single data points or data distributions and away from mean values displayed as bar charts. To facilitate transparent data display to the mycorrhiza community, we present "Ramf" an open-source R package for statistical analysis and preparation of a variety of publication-ready plots, custom-made for analyzing and displaying quantitative root colonization by arbuscular mycorrhiza fungi or any kind of data to be displayed in the same format. Ramf replaces the scripting needed for data analysis and can be readily used by researchers not acquainted with R. In addition, the package is open to improvements by the community. Ramf is available at https://github.com/mchiapello/Ramf.

Keywords: R, data display, arbuscular mycorrhiza (AM), root colonization, statistics

OPEN ACCESS

Edited by:
Andrea Chini,
Centro Nacional de Biotecnología (CNB), Spain

Reviewed by:
Philipp Franken,
University of Applied Sciences Erfurt, Germany
Gregor Langen,
University of Cologne, Germany

***Correspondence:**
Marco Chiapello
marco.chiapello@ipsp.cnr.it
Caroline Gutjahr
caroline.gutjahr@tum.de

Specialty section:
This article was submitted to Plant Microbe Interactions, a section of the journal Frontiers in Plant Science

Received: *02 June 2019*
Accepted: *29 August 2019*
Published: *27 September 2019*

Citation:
Chiapello M, Das D and Gutjahr C (2019) Ramf: An Open-Source R Package for Statistical Analysis and Display of Quantitative Root Colonization by Arbuscular Mycorrhiza Fungi. Front. Plant Sci. 10:1184. doi: 10.3389/fpls.2019.01184

INTRODUCTION

Arbuscular mycorrhiza (AM) is an ancient mutualistic association between arbuscular mycorrhiza fungi (AMF) of the phylum *Glomeromycotina* and approximately 80% of land plant species (Parniske, 2008; Spatafora et al., 2016). The development and function of this symbiosis is investigated by an active research community because of its fascinating biology and because the fungus confers increased mineral nutrition and stress resistance to plants (Smith and Smith, 2011; Gutjahr and Parniske, 2013; Chen et al., 2018). During root colonization, the fungus first attaches to the root surface *via* a hyphopodium, it then enters the root forming intraradical hyphae and subsequently highly branched arbuscules, which are crucial for nutrient exchange between the symbionts, and vesicles, thought to serve as fungal carbon store, in the root cortex (Gutjahr and Parniske, 2013; Choi et al., 2018). An estimation of quantitative total colonization of the root system, and the frequency of hyphopodia, intraradical hyphae, arbuscules, and vesicles is integral to phenotyping arbuscular mycorrhiza development in wild type and mutant plants, and to correlating fungal root colonization with symbiotic function (Montero et al., 2019). In addition, and especially for plant mutants with defects in inducing or supporting hyphopodia formation, also the extraradical hyphae, which have germinated from spores and linger on the root surface, are quantified (Gutjahr et al., 2015; Roth et al., 2018).

Two methods are primarily used by AM researchers to score these fungal structures and to thereby estimate the root colonization level. For the gridline intersect method, root intersections are scored for presence or absence of fungal structures, and % root length colonization is calculated based on the proportion of intersection counts containing fungal structures to total intersection

counts (Giovannetti and Mosse, 1980; McGonigle et al., 1990). The method, based on Trouvelot et al. (1986), scores the frequency and intensity of colonization based on the observation of a number of root pieces with defined size (e.g., 1 cm). The frequency of colonization is calculated as the number of colonized root pieces to the total number of visualized root pieces. The intensity of colonization is recorded by classifying observed root pieces from 1 to 5 by density and coverage of colonization, as well as density and coverage with individual fungal structures, with 1 representing very low colonization, and 5 representing full colonization of the root piece. The scores are then used to calculate a percentage for intensity of colonization as well as individual fungal structures.

Data describing quantitative AM colonization of roots need to be statistically analyzed and visualized with clear graphical display. With the advent of numerous data analysis platforms, statistical analysis and graphical representation have been made easy. However, most of the easy-to-use packages, such as Graphpad Prism, SigmaPlot, SPSS, SAS, BioVinci, XLStat, Matlab, and many others, have complex user interfaces, are costly, platform-specific, and require frequent renewal of the subscription. On the other hand, open-source softwares, such as R and Python, require some scripting knowledge to operate the various packages for analysis and plotting of the data. Even with pre-assembled packages, most data sets require tweaking of the scripts based on the data structure to obtain uniformly drawn plots across different data inputs. To facilitate analysis and display of quantitative AM fungal root colonization data, we present an R package, named Ramf (R for Arbuscular Mycorrhiza Fungi), which requires only specifically formatted input data (based on the counting method). The user simply needs to install the package in R and follow the scripts according to the instructions in the Ramf manual. Excellent usability (minimal scripting, easy, and consistent data output) and robust high-quality output (multiple plot types) are two great advantages of Ramf for the elaboration of AM colonization data to obtain statistical summary and publication-ready plots in a short time.

MATERIALS AND METHODS

Plant Growth, Fungal Inoculation, and Quantification of Root Length Colonization

For the phosphate dose-response experiment *Lotus japonicus* ecotype Gifu seedlings were germinated on 1% water-agar for 3 days in the dark. Then they were moved to a long day photoperiod (16h L/8h D). At the age of 2 weeks the *Lotus japonicus* seedlings were inoculated with 500 spores per plant of *Rhizophagus irregularis* DAOM197198 and subsequently grown in three different growth substrates: sand, sand + Terragreen (Attapulgite clay; OilDry, UK) and sand + calcined clay at three different phosphate concentrations: 2.5 μM (Low phosphate), 250 μM (Medium phosphate), and 2500 μM (High phosphate). Fifteen milliliters of half-Hoagland media containing the indicated concentration of phosphate was provided three times a week to each pot. Plant roots were harvested at 6 weeks post-inoculation (wpi), stained with acid ink (Vierheilig et al., 1998), and scored for fungal structures using the gridline intersection method (McGonigle et al., 1990).

The data of the strigolactone experiment have been previously published in Kountche et al. (2018) and are used here for illustrating the functionalities of Ramf regarding the Trouvelot quantification method (Trouvelot et al., 1986). The method for data acquisition is described in Kountche et al. (2018).

Ramf Manual

Data Preparation, Inspection, and Management in Ramf

Data collected from microscopic visualization is ready for analysis, independent of the scoring system. Data should be prepared in a specific format prior to input into Ramf package. For both scoring systems, data sets contain samples and replicates in the first two columns. The first column contains the sample names, and all replicates of a treatment or genotype should be provided with the correct same sample name since Ramf will treat all samples with misspelled names as different treatments/genotypes. These sample names will also feature in the tables and plots and should therefore be immediately designed to be presentable and easy to understand by the reader. The first treatment/genotype (represented by a set of replicates) is always treated as control. This will be important when Ramf adds the statistical analysis to the plot. The replicate column contains the indication of the replicates (alphabetical letters or numerical values are preferred). If two samples have the same sample name and same replicate name, Ramf will treat the replicates as "technical" replicates, whereas if the sample name is the same, but the replicate name is different, they will be treated as biological replicates. Ramf can handle different numbers of technical and biological replicates.

For the gridline intersect method there are five more columns: total, hyphopodia, intraradical hyphae (IntrHyphae), arbuscules, vesicles. At this stage, the user cannot specify other or additional column names, but Ramf can handle missing columns. Furthermore, Ramf is open to improvements and additional columns can be added in the future. The user can report only the columns needed but should always report information for the two first columns, whereas none of the other ones is strictly required (for example, samples, replicates, arbuscules, vesicles).

For the Trouvelot method, besides the first two columns reporting sample name and replicate, there is a third column called 'scoring', which contains the colonization score (e.g., 1A3, 5A3, 1A2, …).

After table preparation, the data can be read into R using the function: "readData()" (**Figure 1**). The first operation done by the function is the quality check of the input data set: (i) the data set should have correct dimensions, (ii) column names should be labeled as mentioned above, (iii) data should not contain NAs, (iv) for the Trouvelot method Ramf checks whether all scores are valid. If all these conditions are met, the data are read into R, otherwise a warning is thrown in R console, which can then be addressed by inputing the data correctly.

As shown in **Figure 1**, once read as a dataframe in R, a data summary can be obtained using the function "am_summary()". This function summarizes the data in a tabular format and also

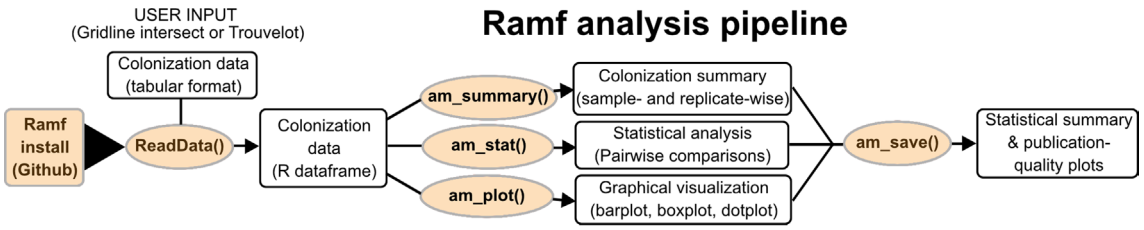

FIGURE 1 | Ramf workflow. Ramf functions are shown in orange boxes and the purpose of the functions in white boxes.

computes the scoring values (F, M, a, A) for the Trouvelot scoring system. The function reports two tables: the first one combines the data for technical replicates of each biological replicate of each sample and summarizes the data for biological replicates of each sample, whereas the second one presents the sample-wise inferential statistics for the data. The columns of the summary tables report the mean and the standard error for each variable (AM fungal structure in the gridline or score in the Trouvelot scoring system).

Statistical Analysis Methods

Subsequently, the function "am_stat()" performs the statistical analysis on the input data set. The function uses the Kruskal–Wallis test (Kruskal and Wallis, 1952), a non-parametric statistical method based on median comparison between two sample groups. This method is meant to test whether samples belong to the same distribution. Ramf package uses this statistical test because it does not assume a normal distribution, as normal distribution is usually not met in data reporting quantitative root colonization by AM fungi. The *post hoc* test is using the criterion of Fisher's least significant difference.

All *p* values resulting from the comparisons are variable dependent, which means that Ramf tests total colonization, arbuscules, and other fungal structures separately.

Additional functions for statistical comparison are: "am_anova_grid()" or "am_anova_trouvelot()," for one-way ANOVA; and am_2anova_grid() and am_2anova_trouvelot() for two-way ANOVA. The functions for one way ANOVA are non-parametric and use the Kruskal–Wallis test, as per am_stat(). The 2-way ANOVA is parametric and provides two plots to check for ANOVA assumptions. The first is a residual versus fitted plot to check whether there is equal variance (homoscedasticity). The second is a Q-Q plot to check whether the data are normally distributed.

Plot Methods and Plot Statistics

To visualize the data, Ramf package provides three plot types: (i) Dotplot, to be used with few data points ("am_dotplot()"), (ii) Barplot, to be used with a larger number of data points ("am_barplot()"), and (iii) Boxplot to be used with a large number of data points ("am_boxplot()"). In Ramf, with one simple R function, you can create ready-to-publish plots. Plots are completely customizable and users can define colors, titles, legends, plot theme, and statistics. The latter is particularly important because statistics can be displayed on the plot in two different ways: 1) asterisks, which compare the control to the treated samples or wild type to mutant genotypes etc with a default or user-defined *p* value cut-off or 2) letters, which group the treatments/genotypes that belong to the same distribution.

Export Data

The last fundamental step is the data export in a ready-to-publish format. Ramf provides a unique function to save all statistical and graphical outputs: "am_save()". The user can save the summary tables, the statistical analysis and the plot, defining dimensions, resolution, and format. The choice for saving the output as a table or plot is made automatically by the function. The default format for saving the tabular data is comma separated value (csv), in order to preserve the highest compatibility in all the operating system (OS), the plot can be saved in several formats and resolutions.

RESULTS AND DISCUSSION

Ramf Workflow

The first operation is to install R and RStudio on your computer. R can be installed from the CRAN website (The Comprehensive R Archive Network, https://cran.r-project.org/) and RStudio, an IDE (integrated development environment) for R, which can be downloaded for free at the following link: https://www.rstudio.com/. The user should download and install R and RStudio compatible with his/her operating system. After launching RStudio, the first step is to install devtools package followed by Ramf package using the following commands:

```
> install.packages("devtools")
> devtools::install_github("mchiapello/Ramf")
```

The next step is to load Ramf package into the R environment:

```
> library("Ramf")
```

Ramf workflow requires four steps: (i) data input, (ii) summary or score analysis, (iii) statistical analysis, and (iv) graphical visualization (**Figure 1**). For each step, a specific function has been designed. Each function aims to perform a specific operation, with less options as possible in order to increase user-friendliness. R functions are designed as follows: functionName, open parenthesis, options for the function, and close parenthesis. For example, the first function in the package, called "readData," takes two options: the first one is the path to the data file and the second one is the scoring method.

```
> readData("data/gridData.csv", type = "grid")
```

Here, a general advice is to always use the same directory folder for the input data file and the script utilizing the data or in other words move the input data file to the current working directory, in order to be as tidy as possible and create a shareable project.

In the upcoming sections, a detailed explanation of all the functions and options will be provided utilizing two case studies for analysing root colonization data.

Case Studies

The aim of this section is to demonstrate the use of Ramf package starting from package installation through data analysis to data export. The complete script will be available as **Supplementary Material**. There are two case studies: one using the gridline scoring system and the second one using the Trouvelot scoring system.

Case Study 1: Sand Is an Optimal Substrate for High Phosphate-Mediated Inhibition of *Lotus japonicus* Root Colonization by *Rhizophagus irregularis*

AM development can be inhibited by high phosphate fertilization (Breuillin et al., 2010; Balzergue et al., 2010). Plant species differ in their physiological optima and, therefore, in the phosphate concentration required for effective AM inhibition as well as the growth substrate permitting optimal inhibition. In this experiment, we searched for an optimal combination of phosphate concentration and growth substrate, which reliably inhibits root colonization by AM fungi in *Lotus japonicus*. We used three phosphate concentrations and three different substrates: sand alone, sand + terragreen, and sand + calcined clay. Statistical comparison using Ramf am_anova_grid() and am_2anova_grid() functions suggested strongest inhibition of root colonization by 2500 µM phosphate (high phosphate) vs. 2.5 µM phosphate (low phosphate) in sand compared to the other two substrates as suggested by the lowest *p* value obtained for sand in the statistical comparison between the total colonization in the two phosphate conditions (**Figure S1**; total colonization data in **Tables S1**, **S2**, **S3** and **S4**; R code in **Code S1**). **Table S4** used for a 2-way ANOVA analysis was prepared by combining **Tables S1**, **S2** and **S3** and including an extra column "trt" providing information on the substrate being used in the combined data set. Diagnostic plots to check ANOVA assumptions for equal variance (homoscedasticity) and normality (Q-Q plot) are provided in **Figures S2** and **S3**.

Corresponding with root colonization, only plants grown in sand displayed observable growth differences in the three different phosphate levels: Low phosphate (2.5 µM), Medium phosphate (250 µM) and High phosphate (2500 µM) (**Figure S4**), whereas ´there were no differences for the other two growth substrates (data not shown), suggesting that terragreen and calcined clay prevented complete plant-availability of the phosphate. We therefore continue here with the colonization data obtained in sand. Quantification of root length colonization (**Table 1**) and statistical analysis show a dose-dependent inhibition of colonization by phosphate in roots of *Lotus japonicus* grown in sand.

The first step is to load the data, formatted as **Table 1** (**Table S5**), into R:

```
> gr <- readData("gridData.csv", type = "grid")
```

The readData() function needs two types of information: the path to the input data file and the scoring method. This step assigns the data to a dataframe "gr". Name variables can be tedious to work with and often they are called 'x' or 'xx' or 'xx2', but we recommend to name your variables in a meaningful way such as "gridline" or "trouvelot".

TABLE 1 | Input data file for gridline intersect quantification method. The data (in %) are from *Lotus japonicus* roots grown in sand at 2.5 µM (low), 250 µM (medium) and 2500 µM (high) phosphate at 6 wpi with *Rhizophagus irregularis*.

Samples	Replicates	Total	Hyphopodia	IntrHyphae	Arbuscule	Vesicle
Low phosphate	A	88	4	88	78	40
Low phosphate	B	95	4	95	76	35
Low phosphate	C	87	6	87	70	31
Low phosphate	D	74	5	74	62	27
Low phosphate	E	95	3	95	79	25
Low phosphate	F	93	4	93	85	41
Low phosphate	G	80	4	80	59	20
Medium phosphate	A	79	4	79	61	27
Medium phosphate	B	72	3	72	59	20
Medium phosphate	C	52	2	52	40	21
Medium phosphate	D	80	4	80	63	29
Medium phosphate	E	53	2	53	41	15
Medium phosphate	F	63	4	63	49	25
Medium phosphate	G	62	4	62	48	24
High phosphate	A	21	2	21	21	8
High phosphate	B	7	1	7	5	2
High phosphate	C	5	1	5	5	2
High phosphate	D	18	2	18	18	6
High phosphate	E	7	1	7	5	1
High phosphate	F	17	2	17	11	2
High phosphate	G	2	0	2	2	1

The second step is to summarize or compute the colonization scores, by using the summary function:

```
> grs <- am_summary(gr)
```

This function does not take any additional arguments other than the dataframe "gr", on which to perform the summary. **Figure 2** reports the output of the "am_summary()" function.

In the third step the statistical analysis is performed, using the "am_stat()" function:

```
> grst <- am_stat(gr)
```

If the analysis does not need a multiple-correction test, the function works with no argument,

```
> grst <- am_stat(gr, method = "fdr")
```

whereas if the correction test is needed, the user can specify the correction method by choosing between: Holm, Hommel, Hochberg, Bonferroni, Benjamini-Hochberg, Benjamini-Yekutieli, or fdr adjustment of *p* values.

The outputs of the "am_stat()" function, with and without the correction method, are shown in **Figure 3**.

The fourth step is data plotting. We recommend using dotplots or otherwise boxplots for graphically representing AM quantification data. Since the data set contains few replicate samples, dotplot is the best choice in this case. The package provides two different possible data displays.

```
> am_dotplot(gr)
> am_dotplot2(gr)
```

Figure 4 shows the default dotplots obtained using our Ramf package; from now on we will use the display shown in **Figure 4A**.

The plot can be customized in different ways as the plotting system is based on the "ggplot2" package. Users need to install and load ggplot2 package before adding extra features to the plots, using the following command:

```
> install.packages("ggplot2")
> library(ggplot2)
```

For example, below we have shown few modifications to the default plot:

a) The color scheme (**Figure 5A**)

```
> am_dotplot(gr, cbPalette = c('#ca0020',
'#f4a582', '#92c5de'))
```

a) Add horizontal grid to better discriminate the samples (**Figure 5B**)

```
> grs <- am_summary(gr)
> grs
$`Summary per Replicate`
# A tibble: 21 x 7
   Samples          Replicates Total Hyphopodia IntrHyphae Arbuscules Vesicles
   <chr>            <chr>      <dbl>      <dbl>      <dbl>      <dbl>    <dbl>
 1 Low phosphate    A             88          4         88         78       40
 2 Low phosphate    B             95          4         95         76       35
 3 Low phosphate    C             87          6         87         70       31
 4 Low phosphate    D             74          5         74         62       27
 5 Low phosphate    E             95          3         95         79       25
 6 Low phosphate    F             93          4         93         85       41
 7 Low phosphate    G             80          4         80         59       20
 8 Medium phosphate A             79          4         79         61       27
 9 Medium phosphate B             72          3         72         59       20
10 Medium phosphate C             52          2         52         40       21
# … with 11 more rows

$`Summary per Sample`
# A tibble: 3 x 11
  Samples          Total_mean Hyphopodia_mean IntrHyphae_mean Arbuscules_mean Vesicles_mean Total_se Hyphopodia_se IntrHyphae_se Arbuscules_se Vesicles_se
  <chr>                 <dbl>           <dbl>           <dbl>           <dbl>         <dbl>    <dbl>         <dbl>         <dbl>         <dbl>       <dbl>
1 Low phosphate          87.4            4.29            87.4            72.7          31.3     3.01         0.360          3.01          3.58        2.97
2 Medium phosphate       65.9            3.29            65.9            51.6          23       4.34         0.360          4.34          3.58        1.79
3 High phosphate         11              1.29            11               9.57          3.14    2.82         0.286          2.82          2.78        1.03
```

FIGURE 2 | Output of am_summary() function. The output includes two tables: the first one called "Summary per Replicate" summarizes the data if technical replicates are present. The second one called "Summary per Sample" summarizes the data by treatment. The first column reports the sample names, whereas the columns between two and six report the means for each variable. The last five columns show the standard errors.

```
A > am_stat(gr)
             group1           group2 Total.pval Hyphopodia.pval IntrHyphae.pval Arbuscule.pval Vesicle.pval
1    Low phosphate Medium phosphate      2e-04          0.0489          2e-04         5e-04       0.0230
2    Low phosphate   High phosphate      0e+00          0.0000          0e+00         0e+00       0.0000
3 Medium phosphate   High phosphate      0e+00          0.0004          0e+00         1e-04       0.0001
B > am_stat(gr, method = "fdr")
             group1           group2 Total.pval Hyphopodia.pval IntrHyphae.pval Arbuscule.pval Vesicle.pval
1    Low phosphate Medium phosphate      2e-04          0.0489          2e-04         5e-04       0.0230
2    Low phosphate   High phosphate      0e+00          0.0000          0e+00         0e+00       0.0000
3 Medium phosphate   High phosphate      1e-04          0.0006          1e-04         1e-04       0.0002
```

FIGURE 3 | Output of am_stat() function. Default output of am_stat() function **(A)**. Output after Kruskall-Wallis test with "False Discovery Rate" correction **(B)**. The first two columns contain the sample names to be compared, whereas the following columns contain the *p* values for each variable of the data set.

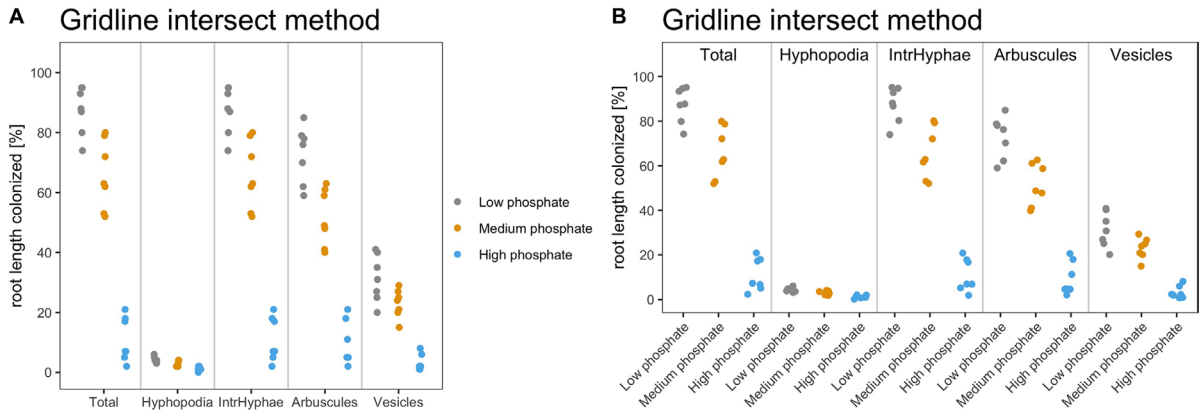

FIGURE 4 | Default output of dotplot() and dotplot2() function. The figure shows the default output of the dotplot() and dotplot2() function. **(A)** The plot is divided into sectors, one per variable, and the variable name is reported at the bottom of each sector. The y-axis shows the percentage of root colonization. Each dot is a biological replicate. **(B)** The variable name is reported on the top of each sector, whereas at the bottom of the x-axis, the treatment (sample name) is reported. Each dot is a biological replicate. Plot titles can be modified according to individual needs.

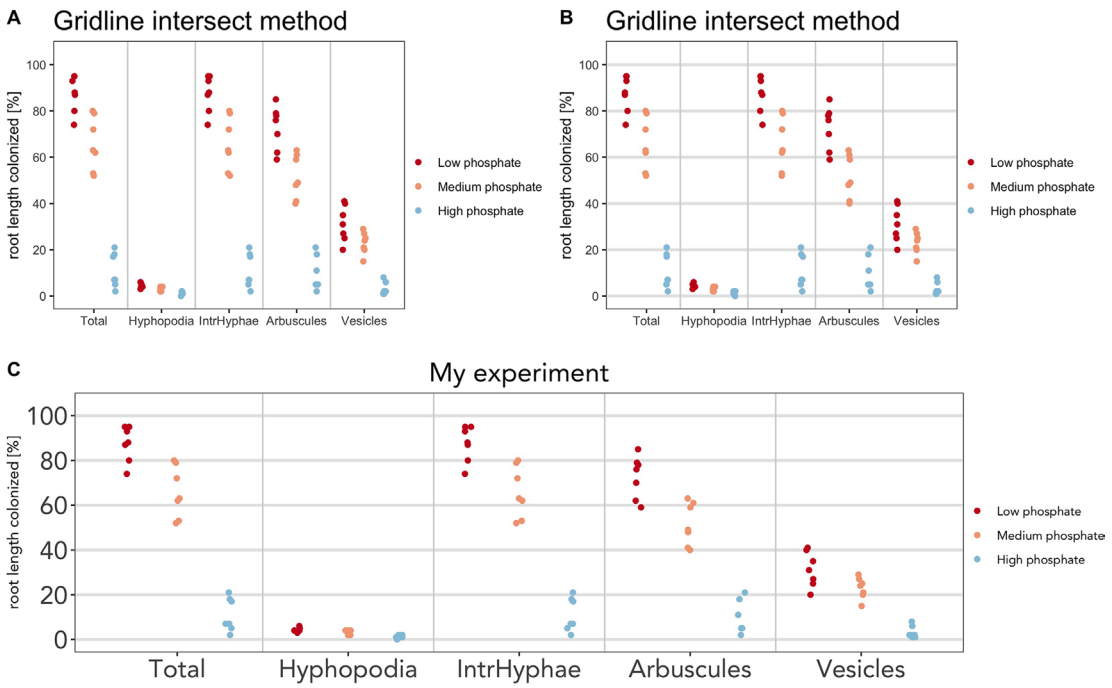

FIGURE 5 | Plot customization. The plot can be customized by the user. **(A)** Plot with different color scheme compared to the default. **(B)** Horizontal lines have been added. **(C)** Font and size of title and x-axis labels have been changed.

```
 > am_dotplot(gr, cbPalette = c('#ca0020',
'#f4a582', '#92c5de'))+ theme(panel.grid.major.y =
element_line(size = 1, colour = "grey90"))
```

a) Add a title, modify its default position, font of the letters, and the dimension on the text (**Figure 5C**)

```
> am_dotplot(gr, main = "My experiment", cbPalette
= c('#ca0020', '#f4a582', '#92c5de'))+
theme(panel.grid.major.y = element_line(size = 1,
colour = "grey90"), plot.title =
element_text(hjust = .5), text = element_
text(family = "Avenir"), axis.text = element_
text(size = 18))
```

Depending on the operating system (OS), some fonts may not be available, and hence, alternative fonts, such as Sans, can be used in the above code.

Furthermore, the result of statistical analysis can be added to the plot. It is possible to include the statistical results on the plot with the desired correction method (default is "none") and

with a *p* value threshold of 0.05. As mentioned above, users can utilize either asterisks or letters to show the statistical differences between the samples.

1) Asterisks: Asterisks above the dots, bars or boxes show, which sample is significantly different from the control for the respective variable (fungal structure or score type). The control is always the first element of the list.

```
> am_dotplot(gr, annot = "asterisks")
```

To include the statistical correction for the *p* values, the user can select, which correction methods to use.

```
> am_dotplot(gr, annot = "asterisks", method =
"BH")
```

Finally, it is possible to combine correction method and *p* value threshold (**Figure 6A**).

```
> am_dotplot(gr, annot = "asterisks", method =
"BH", alpha = 0.01)
```

The asterisks allow to graphically display the statistical difference between the control sample and other samples, with a *p* value cutoff of 0.01 rather than the default value of 0.05. Therefore, *p* values lying between 0.05 and 0.01 will not be displayed with asterisks.

2) As an alternative, to highlight the statistical difference between all the samples, Ramf can add "letters" to the plot. Letters group the samples according to their statistical similarity (**Figure 6B**).

```
> am_dotplot(gr, annot = "letters", method = "BH",
alpha = 0.01)
```

Finally, it is possible to combine all the previous adaptations to produce the final plot (**Figure 7**).

```
> am_dotplot(gr, annot = "letters", method = "BH",
alpha = 0.01, main = "Grid experiment", cbPalette
= c('#ca0020', '#f4a582', '#92c5de'))+
theme(panel.grid.major.y = element_line(size = 1,
colour = "grey90"), plot.title = element_
text(hjust = .5), text = element_text(family =
"Avenir"), axis.text = element_text(size = 16))
```

The fifth step is to save the statistical tables and the plot. Ramf provides a single function to export everything.

1) To save the summary data:

```
> am_save(grs, "Exp001") or > am_save(am_
summary(gr), "Exp001")
```

The two commands produce the same output: two files named "Exp001_per_Replicate.csv" and "Exp001_per_Sample.csv".

2) To save the statistical analysis:

```
> am_save(grst, "Exp001") or > am_save(am_
stat(gr), "Exp001")
```

Also, in this case, the two commands produce the same output: a csv file named "Exp001_stat.csv".

3) To save the plot the "am_save" function can take more options in order to specifically customize the output. It is possible to set the width, the height, the dimension units, and the resolution (dpi) of the plot. Different formats and different resolutions allow the user to produce low-resolution figures for the first manuscript submission and high-resolution figures for the final submission, just by changing a number in the code. Below we have provided a few examples of the export format and resolutions:

```
> p1 <- am_dotplot(gr, main = "Grid experiment",
cbPalette = c('#ca0020', '#f4a582', '#92c5de'),
annot = "letters", method = "BH")+ theme(panel.
grid.major.y = element_line(size = 1, colour =
"grey90"), plot.title = element_text(hjust = .5),
axis.text = element_text(size = 14))
> am_save(p1, "Exp001.pdf", width = 21, height =
21, units = "cm", dpi = 300)
> am_save(p1, "Exp001.jpeg", width = 10, height =
10, units = "in", dpi = 72)
```

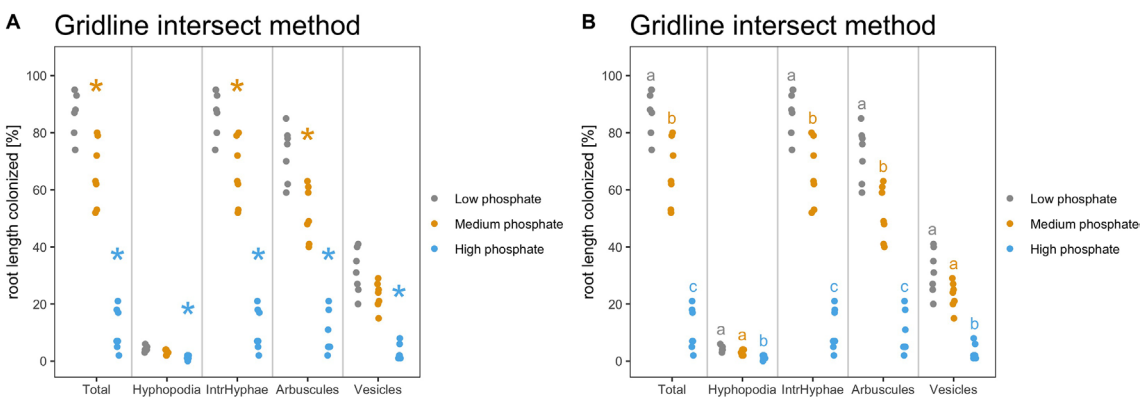

FIGURE 6 | Indication of statistically significant differences on the plot. Strip chart containing indications of statistically significant differences. **(A)** The asterisks compare the treated samples against the control. Plot with Kruskall Wallis test followed by "Bonferroni Hochberg" correction and *p* value threshold set to 0.01. **(B)** Same statistical test as in **(A)** but different letters indicate different statistical groups. **(A, B)** All statistical comparisons have been performed per variable and not across variables to account for the biological meaning of the comparison. For example, the asterisks and letters present in the section "Total" have only a meaning for "Total" and cannot be compared with the asterisks from the other sections.

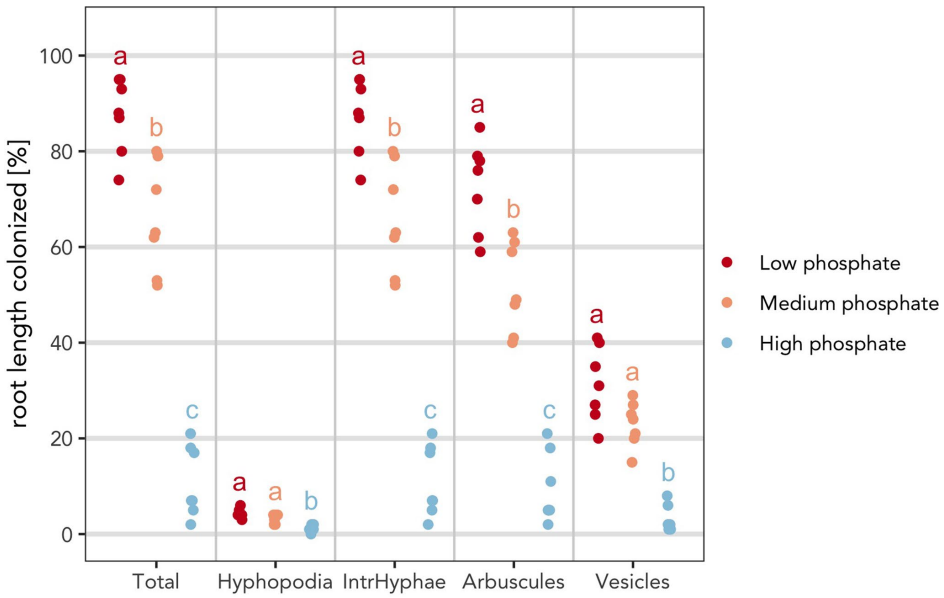

FIGURE 7 | "Complete" plot. The plot combines the statistical analysis and all the features that can be included by the user. Different letters indicate different statistical groups.

```
> am_save(p1, "Exp001.eps", width = 210, height =
210, units = "mm", dpi = 320)
> am_save(p1, "Exp001.svg", width = 21, height =
21, units = "cm", dpi = 300)
```

The complete script is attached as **Code S2.**

Case Study 2: Effect of the Strigolactone Analogs Methyl Phenlactonoate 1 and 3 on Root Colonization by Arbuscular Mycorrhiza Fungi

Strigolactones (SLs) stimulate the activity of AM fungi and also act as key regulators of plant architecture (Waters et al., 2017). Kountche et al. (2018) investigated the effect of the SL analogs methyl phenlactonoate 1 and 3 (MP1, MP3), in comparison to the widely used SL-analog *rac*-GR24 on rice root colonization by the AM fungus *Funneliformis mossae* and quantified colonization according to Trouvelot et al. (1986). To train Ramf for the Trouvelot scoring method we used part of their data in this case-study. **Table 2** shows a subset of these data. In contrast to the data obtained by gridline intersect scoring (case study 1), this data set also contains technical replicates (**Table S6**).

For this case study, we report all commands used to produce the final summary data (**Code S3**). Final plots are shown as dotplot and boxplot (**Figure 8**).

TABLE 2 | Subset of the input data file for arbuscule abundance data for SL-analogs experiment.

Samples	Replicates	Scoring
Control	1	3A3
Control	1	5A3
Control	1	3A3
Control	2	4A3
Control	2	2A3
Control	2	2A3
GR24 10-7M	1	3A3
GR24 10-7M	1	3A3
GR24 10-7M	1	3A3
GR24 10-7M	2	5A3
GR24 10-7M	2	5A3
GR24 10-7M	3	5A3
MP3 10-8M	1	4A3
MP3 10-8M	1	5A3
MP3 10-8M	1	4A3
MP3 10-8M	2	3A2
MP3 10-8M	2	5A3
MP3 10-8M	2	5A3
MP1 10-7M	1	3A2
MP1 10-7M	1	5A2
MP1 10-7M	1	1A2
MP1 10-7M	2	3A2
MP1 10-7M	2	2A3
MP1 10-7M	2	2A3

```
# Load libraries
library(Ramf)
library(ggplot2)
# Read data in
tr <- readData("trouvelotData.csv", type =
"trouvelot")
# Summar
trs <- am_summary(tr)
# Statistics
trst <- am_stat(tr, method = "fdr")
# Plots
p1 <- am_dotplot(tr, main = "Trouvelot
experiment", annot = "letters")+ theme(plot.title
= element_text(hjust = .5), axis.text = element_
text(size = 14))
p2 <- am_boxplot(tr, main = "Trouvelot
experiment", annot = "letters")+ theme(plot.title
```

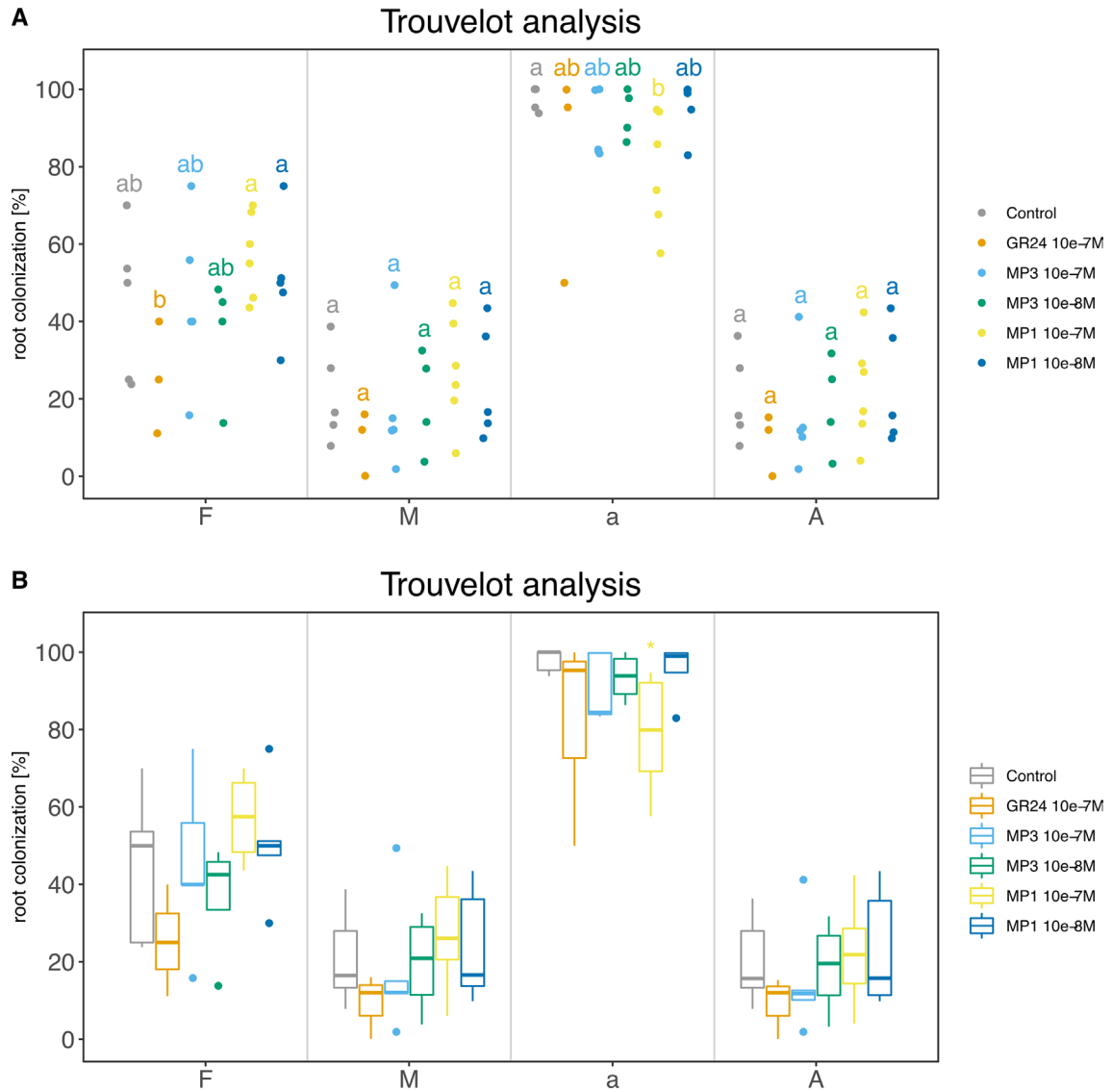

FIGURE 8 | Trouvelot analysis method. The two plots display the same data in two different flavors: **(A)** strip chart with letters to indicate statistical groups and **(B)** box-whisker plot with asterisks to indicate statistical difference compared to the control. Bold black line, median; box, interquartile range; whiskers highest and lowest data point within 1.5 interquartile range; dots, outliers outside the 1.5 times the interquartile range. **(A, B)** Compounds used: GR24; MP (Methyl phenlactonoate) 1 and 3. Kruskall-Wallis test with no correction method and $p < 0.05$ was used to assess statistical differences between samples.

```
= element_text(hjust = .5), axis.text = element_
text(size = 14)) + geom_jitter(width = 0.1, colour
= "black", alpha = 0.3)
# Save
## Summary
am_save(trs, "Exp001")
## Statistics
am_save(trst, "Exp001")
## Plot
am_save(p1, "Exp001.jpeg", width = 29, height =
21, units = "cm", dpi = 300)
am_save(p2, "Exp002.jpeg", width = 29, height =
21, units = "cm", dpi = 300)
```

The complete script is attached as **Code S3**.

Conclusion and Outlook

To our knowledge, no single R package specifically targets AM quantification data like Ramf, so it is not possible to compare our package with any other software. We can only compare the package performance to manual operation. Setting up the script and plot customization will take some time at first use, but once the script is ready, it is a matter of seconds to run the script from the beginning to the end for all future data sets (except when customizing the exported plots for each specific data set). A custom script (**Code S4**) has been run 100 times on gridline data and the duration of the execution has been recorded. The average time to run the script top to bottom is 1.047771 s and the standard deviation 0.08366599 s on 100 executions.

As quite some time is needed to master R, Ramf has been designed to facilitate its use for AM quantification data, with few, well documented functions. The user should be able to perform ready-to-publish statistical analyses and graphics with few lines of code at no cost.

We hope the community will drive the future development of Ramf and aim to integrate the Ramf package to develop a graphical user interface (GUI) with Shiny ("InteRamf") in order to remove the need to learn to use R. With InteRamf, users will be able to produce and quickly save graphical plots and statistical summaries. Before implementation of InteRamf we request the community to try our Ramf package and suggest further improvements on the Ramf github page.

DATA AVAILABILITY STATEMENT

All datasets generated for this study are included in the manuscript/**Supplementary Files**.

AUTHOR CONTRIBUTIONS

MC conceived and developed the Ramf package. DD produced the experimental data set for gridline intersect method, verified the Ramf pipeline with this data set and suggested package function improvements. CG suggested improvements to the data display and output. MC and DD prepared figures; MC, DD, and CG wrote the manuscript.

FUNDING

DD was supported by a grant of Valent BioSciences LLC to CG; CG was supported by the Emmy Noether program (GU1423/1-1) of the Deutsche Forschungsgemeinschaft (DFG) during most of the study. The funding agencies had no role or influence on the design or execution of the work.

ACKNOWLEDGMENTS

The authors thank Mara Novero for kindly providing a published data set generated by quantification of root colonization according to Trouvelot et al. (1986).

SUPPLEMENTARY MATERIAL

The Supplementary Material for this article can be found online at: https://www.frontiersin.org/articles/10.3389/fpls.2019.01184/full#supplementary-material

FIGURE S1 | Substrate selection. Statistical output of **(A)** am_2anova_grid() and **(B)** am_anova_grid() functions to select the optimal substrate for high P mediated AM colonization.

FIGURE S2 | Homoscedasticity plot. Diagnostic plot for checking ANOVA assumption of equal variance.

FIGURE S3 | Q-Q plot. Diagnostic plot for checking ANOVA assumption of normality.

FIGURE S4 | Plant growth in sand at different phosphate regimes. *Lotus japonicus* plants grown in sand at 6 wpi at the indicated phosphate concentrations.

TABLE S1 | Gridline_Sand. Data for total colonization of *Lotus japonicus* roots when grown in sand.

TABLE S2 | Gridline_Sand-Terragreen. Data for total colonization of *Lotus japonicus* roots when grown in a sand terragreen mix (in the ratio 1:1).

TABLE S3 | Gridline_Sand-Calcined clay. Data for total colonization of *Lotus japonicus* roots when grown in a sand:calcined clay mix (in the ratio 3:1).

TABLE S4 | Gridline_substrate. Data for total colonization of *Lotus japonicus* roots when grown in sand, sand-Terragreen and sand-calcined clay. This data set combines Table S1, Table S2 and Table S3.

TABLE S5 | gridData. Root colonization data used for the gridline intersect data set used in the substrate selection experiment (case study 1).

TABLE S6 | trouvelotData. Root colonization data used for the Trouvelot data set used in the strigolactone experiment (case study 2).

CODE S1 | Substrate selection.R R script used for assessing statistical differences between total root colonization in three growth substrates (case study 1).

CODE S2 | gridData.R R script used for the implementation of Ramf package for the gridline intersect data set of the substrate selection experiment (case study 1).

CODE S3 | trouvelotData.R R script used for the implementation of Ramf package for the Trouvelot data set in the strigolactone experiment (case study 2).

CODE S4 | RscriptForBenchmark.R R script used in benchmarking Ramf use.

REFERENCES

Balzergue, C., Puech-Pagès, V., Bécard, G., and Rochange, S. F. (2010). The regulation of arbuscular mycorrhizal symbiosis by phosphate in pea involves early and systemic signalling events. *J. Exp. Bot.* 62 (3), 1049–1060. doi: 10.1093/jxb/erq335

Breuillin, F., Schramm, J., Hajirezaei, M., Ahkami, A., Favre, P., Druege, U., et al. (2010). Phosphate systemically inhibits development of arbuscular mycorrhiza in Petunia hybrida and represses genes involved in mycorrhizal functioning. *Plant J.* 64 (6), 1002–1017. doi: 10.1111/j.1365-313X.2010.04385.x

Chen, M., Arato, M., Borghi, L., Nouri, E., and Reinhardt, D. (2018). Beneficial services of arbuscular mycorrhizal fungi—from ecology to application. *Front. Plant Sci.* 9, 1270. doi: 10.3389/fpls.2018.01270

Choi, J., Summers, W., and Paszkowski, U. (2018). Mechanisms underlying establishment of arbuscular mycorrhizal symbioses. *Ann. Rev. Phytopathol.* 56, 135–160. doi: 10.1146/annurev-phyto-080516-035521

Giovannetti, M., and Mosse, B. (1980). An evaluation of techniques for measuring vesicular arbuscular mycorrhizal infection in roots. *New Phytol.* 84 (3), 489–500. doi: 10.1111/j.1469-8137.1980.tb04556.x

Gutjahr, C., Gobbato, E., Choi, J., Riemann, M., Johnston, M. G., Summers, W., et al. (2015). Rice perception of symbiotic arbuscular mycorrhizal fungi requires the karrikin receptor complex. *Science* 350 (6267), 1521–1524. doi: 10.1126/science.aac9715

Gutjahr, C., and Parniske, M. (2013). Cell and developmental biology of arbuscular mycorrhiza symbiosis. *Ann. Rev. Cell Dev. Biol.* 29, 593–617. doi: 10.1146/annurev-cellbio-101512-122413

Kountche, B. A., Novero, M., Jamil, M., Asami, T., Bonfante, P., and Al-Babili, S. (2018). Effect of the strigolactone analogs methyl phenlactonoates on spore germination and root colonization of arbuscular mycorrhizal fungi. *Heliyon* 4 (11), e00936. doi: 10.1016/j.heliyon.2018.e00936

Kruskal, W. H., and Wallis, W. A. (1952). Use of ranks in one-criterion variance analysis. *J. Am. Stat. Assoc.* 47 (260), 583–621. doi: 10.1080/01621459.1952.10483441

McGonigle, T. P., Miller, M. H., Evans, D. G., Fairchild, G. L., and Swan, J. A. (1990). A new method which gives an objective measure of colonization of roots by vesicular—arbuscular mycorrhizal fungi. *New Phytol.* 115, 495–501. doi: 10.1111/j.1469-8137.1990.tb00476.x

Montero, H., Choi, J., and Paszkowski, U. (2019). Arbuscular mycorrhizal phenotyping: the dos and dont's. *New Phytol.* 221 (3), 1182–1186. doi: 10.1111/nph.15489

Parniske, M. (2008). Arbuscular mycorrhiza: the mother of plant root endosymbioses. *Nat. Rev. Microbiol.* 6 (10), 763. doi: 10.1038/nrmicro1987

Roth, R., Chiapello, M., Montero, H., Gehrig, P., Grossmann, J., O'Holleran, K., et al. (2018). A rice serine/threonine receptor-like kinase regulates arbuscular mycorrhizal symbiosis at the peri-arbuscular membrane. *Nat. Commun.* 9 (1), 4677. doi: 10.1038/s41467-018-06865-z

Smith, S. E., and Smith, F. A. (2011). Roles of arbuscular mycorrhizas in plant nutrition and growth: new paradigms from cellular to ecosystem scales. *Ann. Rev. Plant Biol.* 62, 227–250. doi: 10.1146/annurev-arplant-042110-103846

Spatafora, J. W., Chang, Y., Benny, G. L., Lazarus, K., Smith, M. E., Berbee, M. L., et al. (2016). A phylum-level phylogenetic classification of zygomycete fungi based on genome-scale data. *Mycologia* 108 (5), 1028–1046. doi: 10.3852/16-042

Trouvelot, A., Kough, J. L., and Gianinazzi-Pearson, V. (1986). Mesure du taux de mycorhization VA d'un système radiculaire. Recherche de méthodes d'estimation ayant une signification fonctionnelle. *Physiol. Genet. Aspects Mycorrhizae*, 217–221.

Vierheilig, H., Coughlan, A. P., Wyss, U. R. S., and Piché, Y. (1998). Ink and vinegar, a simple staining technique for arbuscular-mycorrhizal fungi. *Appl. Environ. Microbiol.* 64 (12), 5004–5007.

Waters, M. T., Gutjahr, C., Bennett, T., and Nelson, D. C. (2017). Strigolactone signaling and evolution. *Ann. Rev. Plant Biol.* 68, 291–322. doi: 10.1146/annurev-arplant-042916-040925

Conflict of Interest: The authors declare that the research was conducted in the absence of any commercial or financial relationships that could be construed as a potential conflict of interest.

frontiers in Microbiology

PERSPECTIVE
published: 22 October 2019
doi: 10.3389/fmicb.2019.02420

In vitro Propagation of Arbuscular Mycorrhizal Fungi May Drive Fungal Evolution

Vasilis Kokkoris† and Miranda Hart*

Department of Biology, University of British Columbia, Kelowna, BC, Canada

Transformed root cultures (TRC) are used to mass produce arbuscular mycorrhizal (AM) fungal propagules *in vitro*. These propagules are then used in research, agriculture, and ecological restoration. There are many examples from other microbial systems that long-term *in vitro* propagation leads to domesticated strains that differ genetically and functionally. Here, we discuss potential consequences of in TRC propagation on AM fungal traits, and how this may affect their functionality. We examine weather domestication of AM fungi has already happened and finally, we explore whether it is possible to overcome TRC-induced domestication.

Keywords: arbuscular mycorrhizal fungi, fungal domestication, fungal evolution, *in vitro* propagation, transformed root cultures

OPEN ACCESS

Edited by:
Stefano Ghignone, Italian National Research Council (IPSP-CNR), Italy

Reviewed by:
Marcela Claudia Pagano, Federal University of Minas Gerais, Brazil
Cristiana Sbrana, Istituto di Biologia e Biotecnologia Agraria (IBBA), Italy

****Correspondence:***
Vasilis Kokkoris
bill.kokkoris@ubc.ca;
kokkoris@ubc.ca;
vasilis.kokkoris@canada.ca

†ORCID:
Vasilis Kokkoris
orcid.org/0000-0002-1667-0493

Specialty section:
This article was submitted to Plant Microbe Interactions, a section of the journal Frontiers in Microbiology

Received: *13 July 2019*
Accepted: *07 October 2019*
Published: *22 October 2019*

Citation:
Kokkoris V and Hart M (2019) In vitro Propagation of Arbuscular Mycorrhizal Fungi May Drive Fungal Evolution. Front. Microbiol. 10:2420. doi: 10.3389/fmicb.2019.02420

INTRODUCTION

Domestication of plants and animals has been a hallmark of the Anthropocene (Zeder, 2006), resulting in altered morphology, decreased genetic diversity, altered behavior, and altered function in the domesticant. Such far reaching changes are necessary to maintain the domesticated state but can present a risk to food security (Chen et al., 2015; Whitehead et al., 2017; Egan et al., 2018), and in some cases, to the status of the domesticated species (Pearce, 2003; Ploetz, 2003). For example, domestication of wild bananas led to a sterile and genetically homogeneous cultivar that now faces extinction (Pearce, 2003; Ploetz, 2003). Similarly, decreases in genetic diversity as a result of domestication has been well documented in many crops, including common bean (Bitocchi et al., 2013), rice (Ram et al., 2007), wheat (Reif et al., 2005), soybean (Hyten et al., 2006), and pear (Nishio et al., 2016). This decrease in genetic diversity is often associated with losses of functional traits such as herbivore resistance (Chaudhary and Bhupendra, 2013), reduced immune function (e.g., Honey bees, López-Uribe et al., 2017) or even behavioral changes such as loss of immigration ability in monarch butterflies (Tenger-Trolander et al., 2019).

The effect of domestication on ecological competence is not novel in mycology (Jinks, 1952; Roper et al., 2011); plant pathogens lose pathogenicity when kept in culture for extended periods (Naiki and Cook, 1983), and domestication of *Saccharomyces cerevisiae* created yeasts without the ability to reproduce sexually or survive outside of laboratory conditions (Gallone et al., 2016). *Aspergillus oryzae* diverged from a pathogen to become a commercially important fermenter and subsequently lost genes related to pathogenicity (Machida et al., 2005). Such losses may result from bottleneck effects and environmental selection, especially if the system used in cultivation does not represent the conditions under which they originally evolved (see review by Douglas and Klaenhammer, 2010).

Arbuscular mycorrhizal (AM) fungi are obligate biotrophs that participate in an ancient symbiosis with plants (Smith and Read, 2008; Brundrett and Brundrett, 2009). Through this symbiosis, AM fungi provide plants increased access to soil resources in return for carbon in

SIDEBAR#1 | Transformed root cultures.

TRC involves infection of a "hairy root" culture with an AM fungal spore. A hairy root culture is the product of gene transfer from the root-inducing (Ri) plasmid of the parasite *Agrobacterium rhizogenes* into the genome of a host plant (Willmitzer et al., 1982). The Ri plasmid contains genes that increase rates of both cell division through increased cytokinins production and cell elongation through auxin production. The transformed root also produces opines used as a food source by the colonizing bacteria. After eliminating the bacterium with antibiotics, the resulting plant is a proliferation of "hairy roots" that grow faster and produce higher quantities of secondary metabolites than normal roots (Capone et al., 1989). The roots are kept in dark and there is no photosynthetic tissue or shoot present. This method, in addition to the industrial benefits, including reduced contamination, minimal space and maintenance requirements, and standardization, has enabled long-term laboratory cultures, effectively domesticating certain isolates.

the form of sugar and lipids (Luginbuehl et al., 2017). Besides the nutritional benefit to the plants, AM fungi can also increase plant tolerance to environmental stress [e.g., water (Ruiz-Lozano and Aroca, 2010), salinity (Porcel et al., 2012), and heavy metals (Díaz et al., 1996)]. AM fungi are known to stimulate plant photosynthetic activity (Boldt et al., 2011) and enhance plants' disease resistance (Pozo and Azcón-Aguilar, 2007; Jung et al., 2012). Because of these benefits, considerable effort has focused on finding ways to propagate and study these fungi for potential applications including agriculture, landscaping, and landscape restoration (Sawers et al., 2008; Berruti et al., 2016). One of the most successful methods of propagating clean material employs the use of transformed root cultures (TRC) (see **sidebar#1** for information on TRC) (Mosse and Hepper, 1975; Bécard and Fortin, 1988; Stockinger et al., 2009; Rosikiewicz et al., 2017). While this method is efficient for producing uncontaminated propagules, it represents a highly artificial environment and could potentially lead to domesticated AM fungal strains (**Figure 1**).

Currently, commercial AM fungal inocula are used both in horticulture and field applications (Berruti et al., 2016). Many of the fungal propagules used in commercial products originate from TRC. The effect of TRC on the evolution of "domesticated" AM fungi is not clear (Plenchette et al., 1996). Here, we argue that commercial production of AM fungi *via* TRC represents strong selection pressure on fungi and represents a form of domestication, through changes to nutrient limitations, microbial consortia, and reduced host variation. Such selection pressure may lead to reduced genetic diversity and mutualistic quality.

LUXURIOUS NUTRIENT CONDITIONS

Although AM fungi form functional mycorrhizas in TRC, the unique nutritional strategy of hairy roots may affect the quality of the symbiosis. In association with a normal plant, AM fungi grow in tandem with roots which fluctuate daily and seasonally (Lippu, 1998). In the case of transformed roots, the flow of carbon is consistent and continuous (Fortin et al., 2002), thereby promoting unrestricted fungal growth. In contrast, natural plants, which allocate most carbon to above ground shoots, impose carbon limits to root fungal symbionts. Root fungal symbionts of hairy roots are thus not carbon-limited. Unsurprisingly, such growing conditions promote spore production which demands significant carbon reserves (up to 60,000 per plate for *R. irregulare* DAOM197198) (Rosikiewicz et al., 2017).

In addition to luxury carbon, hairy roots experience no nutrient limitation in TRC (Bécard and Fortin, 1988). Such luxury nutrient conditions do not promote fungal provisioning of nutrients to hosts. There is considerable evidence that luxury soil nutrient status reduces both AM fungal abundance

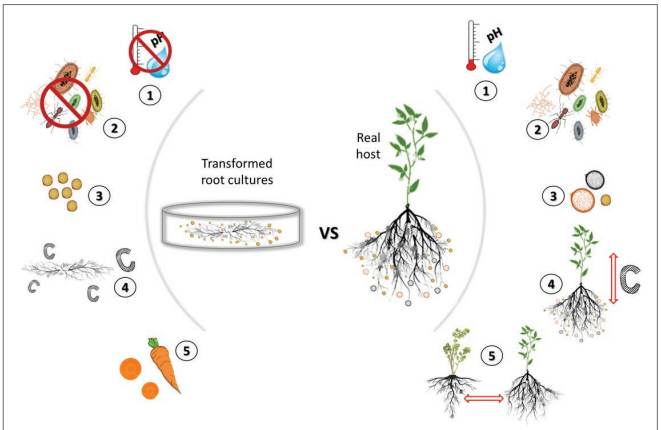

FIGURE 1 | Comparison of the artificial growing environment of transformed root cultures (TRC) to a natural environment. While TRC can produce uncontaminated and abundant AM fungal propagules, they consists a highly artificial and eutrophic environment that lacks environmental stimuli. **(1) Lack of abiotic stimuli**: Petri dishes are kept sealed to retain moisture and are propagated in the dark at a stable temperature that benefits the AM fungal productivity (propagule production). In a natural environment, there is continuous fluctuation of temperature, and moisture as well as high spatial variation in pH but also in multiple other abiotic factors. Such abiotic factors can affect the AM fungal growth as well as the mycorrhizal response (MR) (Wang et al., 1993; Heinemeyer and Fitter, 2004) and have seen to alter the gene expression of fungi (Meyer et al., 2017). **(2, 3) Lack of biotic stimuli**: the main benefit of TRC is the ability to grow AM fungi under sterile conditions that allows for uncontaminated propagation of the desired species/isolate. Each TRC contains only a single isolate of AM fungi. AM fungi have antagonistic and synergetic relations with other soil microbes (Mar Vázquez et al., 2000) as well as with other AM fungi (Wilson, 1984; Engelmoer et al., 2014). The TRC environment lacks biotic interactions that when present can lead to the production of multiple chemical compounds (Naiki and Cook, 1983; Gallone et al., 2016) that confer stress resistance or can enhance the metabolic activity of the engaged microbes (Ola et al., 2013). **(4) Unrestricted carbon flow**: TRC lack a shoot and therefore carbon flow to the AM fungus is consistent and continuous (Fortin et al., 2002) in contrast to a real plant where carbon flow fluctuates daily and seasonally between shoot and root (Lippu, 1998). **(5) Lack of host diversity**: in nature, AM fungi can interact simultaneously with multiple host. Host identity can alter significantly the gene expression of AM fungi (Mateus et al., 2019) and alter the progression of the symbiosis (Angelard et al., 2010). The dramatic reduction of host diversity and continuous re-cultivation using a sole host [most commonly carrot (*Daucus carota*)] may affect the function and genetic diversity of the cultured AM fungi.

Abbreviations: AM, Arbuscular mycorrhizas/arbuscular mycorrhizal; BLOs, Bacterial like organisms; ECM, Ectomycorrhizas/ectomycorrhizal; MRE, Mollicutes/mycoplasma-related endobacteria; MR, Mycorrhizal response; N, Nitrogen; P, Phosphorus; Ri, Root inducing; TRC, Transformed root cultures.

intraradically and mycorrhizal response (MR) in hosts (Menge et al., 1978; Thomson et al., 1986; Breuillin et al., 2010; Bonneau et al., 2013), which may lead to less beneficial associations. For example, increased N levels (*via* nitrogen fertilization) can select for rhizobia (Weese et al., 2015), and AM fungi (Johnson, 1993) that provide reduced benefit to the host plants. It is therefore possible that a highly eutrophic environment, such as TRC, may promote selection for less mutualistic AM fungi.

TALK BETWEEN MICROBIAL NEIGHBORS

The monoxenic environment of TRC lacks much of the hyphosphere/rhizosphere microbial consortia that play an important role in the AM symbiosis. Co-existing microbes engaged in antagonistic or synergetic interactions produce bioactive compounds which can be used in defense, to confer stress tolerance or boost metabolic activities for the producers (Ola et al., 2013). Such compounds are not produced when bacteria (Koskiniemi et al., 2012) and fungi (Naiki and Cook, 1983; Gallone et al., 2016) are maintained under axenic conditions due to lack of appropriate environmental stimuli from neighboring microbes (Marmann et al., 2014). The pathways for these signaling compounds can be lost permanently *via* selective gene deletion over generations of continuous propagation *in vitro*.

Similar to other microbes, AM fungi have antagonistic and synergetic relations with other AM fungi (Wilson, 1984; Engelmoer et al., 2014) and other soil microbes (Mar Vázquez et al., 2000). For example, it was recently demonstrated that AM fungi have the ability to indirectly increase the nitrogen (N) uptake by plants *via* association with soil microbes (Hestrin et al., 2019). Therefore, growing in an environment that inhibits these interactions could reduce the effectiveness of such strains in natural conditions.

In addition to the selection pressure resulting from lack of microbial cross talk, reduction or even elimination of fungal endobacteria and bacteria that reside on the hyphal or spore surface in TRC, can affect fungal function (Dearth et al., 2018) and mutualism performance (Vannini et al., 2016). Establishing AM fungi in TRC requires surface sterilization and antibiotics in order to eliminate surface bacteria (Bécard and Fortin, 1988). However, AM fungi naturally comprise a community of bacteria that reside in, and on, hyphae and spores. Abundant rhizobia and pseudomonads have been found attached on spore and hyphal surface (Bianciotto et al., 1996b; Roesti et al., 2005; Agnolucci et al., 2015), but also bacterium-like organisms (BLOs) (Bianciotto et al., 1996a; Naumann et al., 2010) and Mollicutes/mycoplasma-related endobacteria (MRE) (Desiro et al., 2014; Torres-Cortes et al., 2015; Naito et al., 2017) were detected within the cytoplasm. Some of these bacteria possess chitinolytic abilities (Roesti et al., 2005; Agnolucci et al., 2015) and their abilities to degrade spore walls can play a crucial role in spore germination (Mayo et al., 1986). Of course, the presence of such bacteria can also benefit the colonized plants *via* a cascade of gene activation and chemical signals (Artursson et al., 2006). Long-term *in vitro* culturing could negatively affect the interaction between AM fungi and their own beneficial mutualists (Lumini et al., 2007).

PLANT IDENTITY

There is increasing evidence that plant genotype can significantly affect the symbiosis (Chialva et al., 2018; Mateus et al., 2019). In the case of TRC propagation, fungi are exposed to dramatically reduced host diversity [most commonly carrot (*Daucus carota*) or tomato (*Solanum lycopersicum*)]. While gene activation in the early stages of colonization are preserved among hosts (Delaux et al., 2014), the progression of the symbiosis can be significantly altered depending on host identity both regarding the plant (Angelard et al., 2010) and fungal response (Cavagnaro et al., 2001; Koch et al., 2017). Mateus et al. (2019) observed large differences in the expression between fungal isolates growing on multiple cassava cultivars, but the differences were influenced largely by the genotype of the cultivar host. The reduction in host genetic diversity to a single genotype in TRC may lead to genetic drift and unused gene deletion for the AM fungus (Muller's ratchet in host restricted lineages, see Moran et al., 2008). Recently, Sugiura et al. (2019) identified myristate, a fatty acid, as a usable carbon source from *Rhizoglomus irregulare* during the asymbiotic growth that can promote hyphal growth to the production of daughter spores in a host-free culture. While such information advances our knowledge in AM fungal metabolism, such a mechanism could also lead to host-free AM fungal propagation systems, with unknown effects on the efficacy of the symbiosis. Culturing symbionts in host-free environments has been shown to reduce symbiotic quality (Marx and Daniel, 1976; Speakman, 1982).

IS THERE EVIDENCE OF DOMESTICATION ON ARBUSCULAR MYCORRHIZAL FUNGI?

Given all the opportunities for deleterious selection on AM fungi growing in TRC, is there any evidence that domestication has happened? Evidence for domestication would require reduced genetic variation as well as morphological and functional changes.

Reduced Genetic Variation

There is evidence that controlled conditions such as TRC can lead to loss of genetic diversity among some AM fungal isolates For example, Wyss and Bonfante (1993) showed genotypic changes among isolates of a single species (*Funneliformis mosseae* BEG12) when maintained under long-term lab conditions. In addition, there is evidence of sequence loss in spores of an isolate of a *Glomus coronatum* when maintained in cultures compared to field originated spores (Clapp et al., 2001) and reduced allelic variation in spores of *Claroideoglomus etunicatum* compared to the parent isolate following single spore inoculations (Boon et al., 2013).

Morphological and Functional Alterations

Regardless the mechanism leading to genotype changes, there is evidence that *in vitro* cultivation affects AM fungal functional traits. *In vitro* cultivation has led to increased germination rates (Kokkoris et al., 2019b) and reduced in propagule size (Pawlowska

et al., 1999; Calvet et al., 2013). Plenchette et al. (1996) found that *in vitro* produced spores of *Glomus versiforme* were significantly less infective, even only after three successive generation *in vitro*. Calvet et al. (2013) observed that *in vitro* colonization of AM fungi reduced host nutritional benefit. Similarly, Kokkoris and Hart (2019) showed that *in vitro* propagation resulted in a trade-off between spore production and phosphorus (P) benefit. Copious spore production over nutritional benefit is a trade-off that seems to be preserved even when this isolate is grown in pots with a variety of different hosts (Kokkoris et al., 2019a).

Loss of Endobacterial Symbionts

In vitro cultivation may affect the endocellular bacteria associated with fungal spores. *Candidatus* Glomeribacter gigasporarum is a bacterium that resides in spores of *Gigaspora margarita*. *In vitro*, this bacterium experiences populational dilution and eventually disappears leading to "pure" spores over successive generation *in vitro* (Lumini et al., 2007). Although the bacterium is not required for *G. margarita* to complete its life cycle, its absence alters spore's morphology and negatively affects germination and growth (Lumini et al., 2007) and can significantly alter the fungal activity (including protein expression, and quality and quantity of lipidic profile) (Salvioli et al., 2010, 2016).

Incompatibility Between Isolates?

One potential consequence of TRC cultivation may affect hyphal fusion among compatible fungi. For example, *in vivo* cultivation for 20 years led to vegetative incompatibility for *F. mosseae* (Sbrana et al., 2018). If long-term culturing in TRC inhibits the ability of anastomosis, then domesticated isolates might be unable to interact with other isolates in nature. Incompatibility could even lead to a permanent homokaryotic stage, preventing genetic information exchange between compatible isolates and thus adaptation to novel conditions (see **sidebar#2** for the importance of anastomosis on AM fungi). It could also pose a survivorship disadvantage for such an isolate if used for field inoculations due to the isolation from the natural hyphal network (Sbrana et al., 2011). Loss of anastomosis might be the reason why *in vitro* produced strains often fail to establish and persist in natural environments post inoculation (Corkidi et al., 2004; Farmer et al., 2007; Tarbell and Koske, 2007).

CAN WE OVERCOME TRANSFORMED ROOT CULTURES-INDUCED DOMESTICATION?

If TRC propagation of AM fungi produces inferior mutualists, it is reasonable to wonder whether specific practices in TRC production could prevent such unwanted changes. Such practices, like co-cultivation, medium modifications and re-association with natural hosts, already exist and applied in other microbial systems.

CO-CULTIVATION WITH MICROBES

Axenic, and in case of AM fungi, monoxenic growing conditions can reduce the chemical diversity of the produced compounds due to lack of environmental stimuli. Co-cultivation of microbes can activate silent gene clusters of the microbial partners (Brakhage et al., 2008), protecting fungi against genetic drift and gene deletion. For example co-culture of bacteria and fungi (*Fusarium tricinctum Bacillus subtilis*) showed a 78-fold increase in fungal metabolite production compared to the pure culture of the fungus (Ola et al., 2013). Similarly, a fungal co-culture (*Coprinopsis cinerea* and *Gongronella* sp.) produced 900 times increased oxidation activity compared to pure cultures (Pan et al., 2014). Growing AM fungi with two *Paenibacillus validus* bacterial isolates increased fungal growth even in absence

SIDEBAR#2 | The role of anastomosis in arbuscular mycorrhizal fungi.

Heterokaryosis, first coined by Burgeff (1914), is common in the fungal kingdom. It occurs when compatible hyphae fuse (anastomosis), but do not undergo karyogamy. Heterokaryosis is observed in earlier-diverging lineages of fungi such as Phycomyces (Mucoromycota), where most sexual spores contain three to four nuclei, which can be genetically similar or different (Mehta and Cerdá-Olmedo, 2001). The classical understanding of heterokaryosis emphasizes the dikaryon as a precursor to karyogamy, or the eventual fusing of two nuclei to form a monokaryotic, diploid cell, which then undergoes meiosis leading to the production of haploid, sexual spores. However, there are many examples of fungi for which the heterokaryon plays a role beyond sexual recombination [Jinks, 1952 (*Penicillium*); James et al., 2008 (*Heterobasidion*); Roper et al., 2011; Samils et al., 2014 (*Neurospora*)] Diverse nucleotypes in spores may prevent the loss of genetic variation and functional diversity in the case of population reduction (i.e., prevent genetic drift through bottleneck effects) or ensure maintenance of genetic information when new populations are established from few propagules (prevent genetic drift through founder effects).

Similar to other heterothallic fungal groups (Asco- and Basidiomycotan), nucleotype diversity may be maintained through anastomosis in wild populations of closely related AMF (Giovannetti et al., 1999, 2001, 2003; Croll et al., 2008). For AM fungi, anastomosis has been observed among hyphae of the same isolates during the asymbiotic and symbiotic stage even when growing in different systems but also been observed between closely related isolates (Giovannetti et al., 2001; Croll et al., 2009; Purin and Morton, 2011; De la Providencia et al., 2013; de Novais et al., 2013; Barreto De Novais et al., 2017). During anastomosis, plasmogamy can occur, and mitochondria (De la Providencia et al., 2013) and nuclei (Croll et al., 2008) can be shared between partners. Although anastomosis is recognized primarily as a healing mechanism post disturbance (de la Providencia et al., 2005) especially for *Gigaspora* sp., also plays an important ecological role, since newly germinating spores can connect to the pre-established network prior interacting with a host, gaining an important survivorship benefit (Sbrana et al., 2011).

While debate about their status as homo- versus heterokaryons has circulated for nearly two decades (Kuhn et al., 2001; Hijri and Sanders, 2004; Pawlowska and Taylor, 2004; Croll et al., 2008; Tisserant et al., 2013; Lin et al., 2014; Boon et al., 2015), recent evidence shows that AM fungi can be haploid and homokaryotic (meaning that they contain thousands of genetically similar nuclei with haploid number of chromosomes) or haploid and dikaryotic (meaning that they contain two genetically distinct type of nuclei with in equal proportions, with a haploid number of chromosomes) (Ropars et al., 2016; Chen et al., 2018a). Corradi and Brachmann (2017) proposed that compatible AM fungi have the ability to mix their nuclei continually in the field, through anastomosis, effectively creating genetically novel isolates *via* karyogamy and meiosis. Although it is still not yet clear under which conditions the dikaryons proceed to karyogamy and meiosis aka to sexual reproduction (Chen et al., 2018b), hyphal fusion between compatible isolates seem to represent a vital step for plasmogamy and exchange of genetic information.

of a host (Hildebrandt et al., 2002). Co-cultivation of AM fungi with diverse microorganisms may be a way to maintain genetic variation and function by activating AM fungal genes that would otherwise be silent, due to reduced environmental stimuli, and prone to deletion if maintained long term in TRC.

CULTURING CONDITIONS

The most commonly used TRC medium is the M medium proposed by Bécard and Fortin (1988). While no major modifications have been made on M medium, addition of simulative chemical molecules could compensate for lack of microbial associates and trigger gene activation for secondary metabolite production. For example, the addition of fatty acids (signal from *P. validus*, see previous section) can induce colonization ability and stimulate the spore production of AM fungi (Kameoka et al., 2019). In addition, chemical effectors responsible for promoting hyphal branching, mycorrhization, and the efficiency of the symbiosis have been identified (e.g., strigolactones) (Akiyama et al., 2005; Besserer et al., 2006), which may lead to increased gene activation and help maintaining the genetic and functional variation in TRC.

Additional changes in the medium or in the growing conditions may stimulate recombination in AM fungi and encourage the production of novel genotypes. For example, in *Coprinus congregatus*, a Basidiomycete, the quantity of arginine in the medium controls the expression of the mating type genes and ultimately the growth of the fungus as a homo or dikaryon (Ross et al., 1991). We need to identify environmental controls of AM fungal mating behavior to optimize growing conditions that will choose for efficient symbionts and not just copious spore producers.

RE-ASSOCIATION WITH COMPATIBLE HOSTS

Ectomycorrhizal (ECM) fungi can lose their symbiotic ability and eventually fail to colonize plant roots if maintained *in vitro* long term (Marx and Daniel, 1976). Growing strains *via* host passage (association with a compatible host) every 4 years alleviates this bottleneck (Marx, 1981). The re-isolated strain from the colonized roots shows increased colonization ability but also increased symbiotic quality compared to solely *in vitro* retained strains (Thomson et al., 1993). Similarly for pathogenic fungi, pathogenicity can be lost with long-term *in vitro* cultivation and "passaging" the strains trough a compatible host and re-isolating and can revitalize their infective abilities (Speakman, 1982). Furthermore, the "asexual" yeast *Candida albicans* was stimulated to mate when injected into a mammalian host (Hull et al., 1999) showing the significant role an appropriate host can have even for sexual reproduction. While the presence of a root system is a prerequisite for AM fungal cultures, the important differences between TRC and real plant system may alter the AM fungal function. Passage through real host or even community of hosts could retain the functionality of the domesticated strains.

CONCLUSIONS

There is clear evidence that continuous *in vitro* propagation alters AM fungal morphology, genetics, and functioning, meaning that domestication of such strains is in progress or has occurred. While mass production of AM fungal propagules is needed for a sustainable inoculant industry, *in vitro* propagation may bring unwanted changes to the cultured isolates. If domestication reduces the isolate's ability to anastomose, these fungi would have a fitness disadvantage in the field. Alternatively, if the unnatural environment of TRC creates strains that are less beneficial in natural conditions, but these isolates are still able to anastomose with native fungi, such isolates may impact negatively on the gene pool of natural populations. It is important to further examine the effects of domestication on AM fungi and predict how changes could greatly affect the environment following inoculation with such strains.

DATA AVAILABILITY STATEMENT

No datasets were generated or analyzed for this study.

AUTHOR CONTRIBUTIONS

MH and VK conceptualized the work and shared the writing and revision of the MS. MH and VK approved the publication of the MS in its current form. MH and VK agreed to be accountable for all aspects of the work including accuracy or integrity of any part of the work.

FUNDING

MH was funded by the NSERC Discovery Grant.

REFERENCES

Agnolucci, M., Battini, F., Cristani, C., and Giovannetti, M. (2015). Diverse bacterial communities are recruited on spores of different arbuscular mycorrhizal fungal isolates. *Biol. Fertil. Soils* 51, 379–389. doi: 10.1007/s00374-014-0989-5

Akiyama, K., Matsuzaki, K., and Hayashi, H. (2005). Plant sesquiterpenes induce hyphal branching in arbuscular mycorrhizal fungi. *Nature* 435, 824–827. doi: 10.1038/nature03608

Angelard, C., Colard, A., Niculita-Hirzel, H., Croll, D., and Sanders, I. R. (2010). Segregation in a mycorrhizal fungus alters Rice growth and symbiosis-specific gene transcription. *Curr. Biol.* 20, 1216–1221. doi: 10.1016/j.cub.2010.05.031

Artursson, V., Finlay, R. D., and Jansson, J. K. (2006). Interactions between arbuscular mycorrhizal fungi and bacteria and their potential for stimulating plant growth. *Environ. Microbiol.* 8, 1–10. doi: 10.1111/j.1462-2920.2005.00942.x

Barreto De Novais, C., Pepe, A., Siqueira, J. O., Giovannetti, M., Sbrana, C., and Brazil, M. (2017). Scientia agricola compatibility and incompatibility

in hyphal anastomosis of arbuscular mycorrhizal. *Sci. Agric.* 74, 411–416. doi: 10.1590/1678-992x-2016-0243

Bécard, G., and Fortin, J. A. (1988). Early events of vesicular–arbuscular mycorrhiza formation on Ri T-DNA transformed roots. *New Phytol.* 108, 211–218. doi: 10.1111/j.1469-8137.1988.tb03698.x

Berruti, A., Lumini, E., Balestrini, R., and Bianciotto, V. (2016). Arbuscular mycorrhizal fungi as natural biofertilizers: let's benefit from past successes. *Front. Microbiol.* 6:1559. doi: 10.3389/fmicb.2015.01559

Besserer, A., Puech-Pagè, V., Kiefer, P., Gomez-Roldan, V., Jauneau, A., Bastien Roy, S., et al. (2006). Strigolactones stimulate arbuscular mycorrhizal fungi by activating mitochondria. *PLoS Biol.* 4:e226. doi: 10.1371/journal.pbio.0040226

Bianciotto, V., Bandi, C., Minerdi, D., Sironi, M., Tichy, H. V., and Bonfante, P. (1996a). An obligately endosymbiotic mycorrhizal fungus itself harbors obligately intracellular bacteria. *Appl. Environ. Microbiol.* 62, 3005–3010. Available at: http://www.ncbi.nlm.nih.gov/pubmed/8702293 [Accessed July 11, 2019]

Bianciotto, V., Minerdi, D., Perotto, S., and Bonfante, P. (1996b). Cellular interactions between arbuscular mycorrhizal fungi and rhizosphere bacteria. *Protoplasma* 193, 123–131. doi: 10.1007/BF01276640

Bitocchi, E., Bellucci, E., Giardini, A., Rau, D., Rodriguez, M., Biagetti, E., et al. (2013). Molecular analysis of the parallel domestication of the common bean (*Phaseolus vulgaris*) in Mesoamerica and the Andes. *New Phytol.* 197, 300–313. doi: 10.1111/j.1469-8137.2012.04377.x

Boldt, K., Pörs, Y., Haupt, B., Bitterlich, M., Kühn, C., Grimm, B., et al. (2011). Photochemical processes, carbon assimilation and RNA accumulation of sucrose transporter genes in tomato arbuscular mycorrhiza. *J. Plant Physiol.* 168, 1256–1263. doi: 10.1016/j.jplph.2011.01.026

Bonneau, L., Huguet, S., Wipf, D., Pauly, N., and Truong, H.-N. (2013). Combined phosphate and nitrogen limitation generates a nutrient stress transcriptome favorable for arbuscular mycorrhizal symbiosis in *Medicago truncatula*. *New Phytol.* 199, 188–202. doi: 10.1111/nph.12234

Boon, E., Halary, S., Bapteste, E., and Hijri, M. (2015). Studying genome heterogeneity within the arbuscular mycorrhizal fungal cytoplasm. *Genome Biol. Evol.* 7, 505–521. doi: 10.1093/gbe/evv002

Boon, E., Zimmerman, E., St-Arnaud, M., Hijri, M., Harris, S., Hijri Zimmerman, M. E., et al. (2013). Allelic differences within and among sister spores of the arbuscular mycorrhizal fungus *Glomus etunicatum* suggest segregation at sporulation. *PLoS One* 8:e83301. doi: 10.1371/journal.pone.0083301

Brakhage, A. A., Schuemann, J., Bergmann, S., Scherlach, K., Schroeckh, V., and Hertweck, C. (2008). "Activation of fungal silent gene clusters: A new avenue to drug discovery" in *Natural Compounds as Drugs.* eds. F. Petersen, and R. Amstutz (Basel: Birkhäuser Basel), 1–12. doi: 10.1007/978-3-7643-8595-8_1

Breuillin, F., Schramm, J., Hajirezaei, M., Ahkami, A., Favre, P., Druege, U., et al. (2010). Phosphate systemically inhibits development of arbuscular mycorrhiza in Petunia hybrida and represses genes involved in mycorrhizal functioning. *Plant J.* 64, 1002–1017. doi: 10.1111/j.1365-313X.2010.04385.x

Brundrett, M. C., and Brundrett, M. C. (2009). Mycorrhizal associations and other means of nutrition of vascular plants: understanding the global diversity of host plants by resolving conflicting information and developing reliable means of diagnosis. *Plant Soil* 320, 37–77. doi: 10.1007/s11104-008-9877-9

Burgeff, H. (1914). Untersuchungen über Variabilität, Sexualität und Erblichkeit bei Phycomyces nitens Kunze. *Flora oder Allg. Bot. Zeitung* 107, 259–P4. doi: 10.1016/S0367-1615(17)32823-9

Calvet, C., Camprubi, A., Pérez-Hernández, A., and Lovato, P. E. (2013). *Plant growth stimulation and root colonization potential of in vivo versus in vitro arbuscular mycorrhizal inocula*: American Society for Horticultural Science. Available at: http://hortsci.ashspublications.org/content/48/7/897.short [Accessed January 20, 2019].

Capone, I., Spanò, L., Cardarelli, M., Bellincampi, D., Petit, A., and Costantino, P. (1989). Induction and growth properties of carrot roots with different complements of *Agrobacterium rhizogenes* T-DNA. *Plant Mol. Biol.* 13, 43–52. doi: 10.1007/BF00027334

Cavagnaro, T. R., Gao, L. L., Smith, F. A., and Smith, S. E. (2001). Morphology of arbuscular mycorrhizas is influenced by fungal identity. *New Phytol.* 151, 469–475. doi: 10.1046/j.0028-646x.2001.00191.x

Chaudhary, B., and Bhupendra, (2013). Plant domestication and resistance to herbivory. *Int. J. Plant Genomics* 2013:572784. doi: 10.1155/2013/572784

Chen, E. C., Mathieu, S., Hoffrichter, A., Sedzielewska-Toro, K., Peart, M., Pelin, A., et al. (2018b). Single nucleus sequencing reveals evidence of inter-nucleus recombination in arbuscular mycorrhizal fungi. *elife* 7:e39813. doi: 10.7554/eLife.39813.001

Chen, E. C. H., Morin, E., Beaudet, D., Noel, J., Yildirir, G., Ndikumana, S., et al. (2018a). High intraspecific genome diversity in the model arbuscular mycorrhizal symbiont *Rhizophagus irregularis*. *New Phytol.* 220, 1161–1171. doi: 10.1111/nph.14989

Chen, Y. H., Gols, R., and Benrey, B. (2015). Crop domestication and its impact on naturally selected trophic interactions. *Annu. Rev. Entomol.* 60, 35–58. doi: 10.1146/annurev-ento-010814-020601

Chialva, M., Salvioli di Fossalunga, A., Daghino, S., Ghignone, S., Bagnaresi, P., Chiapello, M., et al. (2018). Native soils with their microbiotas elicit a state of alert in tomato plants. *New Phytol.* 220, 1296–1308. doi: 10.1111/nph.15014

Clapp, J. P., Rodriguez, A., and Dodd, J. C. (2001). Inter- and intra-isolate rRNA large subunit variation in Glomus coronatum spores. *New Phytol.* 149, 539–554. doi: 10.1046/j.1469-8137.2001.00060.x

Corkidi, L., Allen, E. B., Merhaut, D., Allen, M. F., Downer, J., Bohn, J., et al. (2004). Assessing the infectivity of commercial mycorrhizal inoculants in plant nursery conditions. Available at: http://www.anla.org [Accessed October 2, 2018].

Corradi, N., and Brachmann, A. (2017). Fungal mating in the most widespread plant symbionts? *Trends Plant Sci.* 22, 175–183. doi: 10.1016/j.tplants.2016.10.010

Croll, D., Corradi, N., Gamper, H. A., and Sanders, I. R. (2008). Multilocus genotyping of arbuscular mycorrhizal fungi and marker suitability for population genetics. *New Phytol.* 180, 564–568. doi: 10.1111/j.1469-8137.2008.02602.x

Croll, D., Giovannetti, M., Koch, A. M., Sbrana, C., Ehinger, M., Lammers, P. J., et al. (2009). Nonself vegetative fusion and genetic exchange in the arbuscular mycorrhizal fungus *Glomus intraradices*. *New Phytol.* 181, 924–937. doi: 10.1111/j.1469-8137.2008.02726.x

de la Providencia, I. E., de Souza, F. A., Fernandez, F., Delmas, N. S., and Declerck, S. (2005). Arbuscular mycorrhizal fungi reveal distinct patterns of anastomosis formation and hyphal healing mechanisms between different phylogenic groups. *New Phytol.* 165, 261–271. doi: 10.1111/j.1469-8137.2004.01236.x

De la Providencia, I. E., Nadimi, M., Beaudet, D., Morales, G. R., Hijri, M., Rodriguez Morales, G., et al. (2013). Detection of a transient mitochondrial DNA heteroplasmy in the progeny of crossed genetically divergent isolates of arbuscular mycorrhizal fungi. *New Phytol.* 200, 211–221. doi: 10.1111/nph.12372

de Novais, C. B. C. B., Sbrana, C., Júnior, O. J. S., Siqueira, J. O. J. O., Giovannetti, M., Saggin Junior, O. J., et al. (2013). Vegetative compatibility and anastomosis formation within and among individual germlings of tropical isolates of arbuscular mycorrhizal fungi (*Glomeromycota*). *Mycorrhiza* 23, 325–331. doi: 10.1007/s00572-013-0478-y

Dearth, S. P., Castro, H. F., Venice, F., Tague, E. D., Novero, M., Bonfante, P., et al. (2018). Metabolome changes are induced in the arbuscular mycorrhizal fungus Gigaspora margarita by germination and by its bacterial endosymbiont. *Mycorrhiza* 28, 421–433. doi: 10.1007/s00572-018-0838-8

Delaux, P.-M., Varala, K., Edger, P. P., Coruzzi, G. M., Pires, J. C., and Ané, J.-M. (2014). Comparative phylogenomics uncovers the impact of symbiotic associations on host genome evolution. *PLoS Genet.* 10:e1004487. doi: 10.1371/journal.pgen.1004487

Desiro, A., Salvioli, A., Ngonkeu, E. L., Mondo, S. J., Epis, S., Faccio, A., et al. (2014). Detection of a novel intracellular microbiome hosted in arbuscular mycorrhizal fungi. *ISME J.* 8, 257–270. doi: 10.1038/ismej.2013.151

Díaz, G., Azcón-Aguilar, C., and Honrubia, M. (1996). Influence of arbuscular mycorrhizae on heavy metal (Zn and Pb) uptake and growth of *Lygeum spartum* and *Anthyllis cytisoides*. *Plant Soil* 180, 241–249. doi: 10.1007/BF00015307

Douglas, G. L., and Klaenhammer, T. R. (2010). Genomic evolution of domesticated microorganisms. *Annu. Rev. Food Sci. Technol.* 1, 397–414. doi: 10.1146/annurev.food.102308.124134

Egan, P. A., Adler, L. S., Irwin, R. E., Farrell, I. W., Palmer-Young, E. C., and Stevenson, P. C. (2018). Crop domestication alters floral reward chemistry with potential consequences for pollinator health. *Front. Plant Sci.* 9:1357. doi: 10.3389/fpls.2018.01357

Engelmoer, D. J. P., Behm, J. E., and Toby Kiers, E. (2014). Intense competition between arbuscular mycorrhizal mutualists in an in vitro root microbiome negatively affects total fungal abundance. *Mol. Ecol.* 23, 1584–1593. doi: 10.1111/mec.12451

Farmer, M. J., Li, X., Feng, G., Zhao, B., Chatagnier, O., Gianinazzi, S., et al. (2007). Molecular monitoring of field-inoculated AMF to evaluate persistence

in sweet potato crops in China. *Appl. Soil Ecol.* 35, 599–609. doi: 10.1016/j.apsoil.2006.09.012

Fortin, J. A., Bécard, G., Declerck, S., Dalpé, Y., St-Arnaud, M., Coughlan, A. P., et al. (2002). Arbuscular mycorrhiza on root-organ cultures. *Can. J. Bot.* 80, 1–20. doi: 10.1139/b01-139

Gallone, B., Steensels, J., Prahl, T., Soriaga, L., Saels, V., Herrera-Malaver, B., et al. (2016). Domestication and divergence of *Saccharomyces cerevisiae* beer yeasts. *Cell* 166, 1397–1410.e16. doi: 10.1016/j.cell.2016.08.020

Giovannetti, M., Azzolini, D., and Citernesi, A. S. (1999). Anastomosis formation and nuclear and protoplasmic exchange in arbuscular mycorrhizal fungi. *Appl. Environ. Microbiol.* 65, 5571–5575. Available at: http://www.ncbi.nlm.nih.gov/pubmed/10584019 [Accessed April 3, 2018].

Giovannetti, M., Fortuna, P., Citernesi, A. S., Morini, S., and Nuti, M. P. (2001). The occurrence of anastomosis formation and nuclear exchange in intact arbuscular mycorrhizal networks. *New Phytol.* 151, 717–724. doi: 10.1046/j.0028-646x.2001.00216.x

Giovannetti, M., Sbrana, C., Strani, P., Agnolucci, M., Rinaudo, V., and Avio, L. (2003). Genetic diversity of isolates of *Glomus mosseae* from different geographic areas detected by vegetative compatibility testing and biochemical and molecular analysis. *Appl. Environ. Microbiol.* 69, 616–624. doi: 10.1128/AEM.69.1.616-624.2003

Heinemeyer, A., and Fitter, A. H. (2004). Impact of temperature on the arbuscular mycorrhizal (AM) symbiosis: growth responses of the host plant and its AM fungal partner. *J. Exp. Bot.* 55, 525–534. doi: 10.1093/jxb/erh049

Hestrin, R., Hammer, E. C., Mueller, C. W., and Lehmann, J. (2019). Synergies between mycorrhizal fungi and soil microbial communities increase plant nitrogen acquisition. *Commun. Biol.* 2:233. doi: 10.1038/s42003-019-0481-8

Hijri, M., and Sanders, I. R. (2004). The arbuscular mycorrhizal fungus *Glomus intraradices* is haploid and has a small genome size in the lower limit of eukaryotes. *Fungal Genet. Biol.* 41, 253–261. doi: 10.1016/j.fgb.2003.10.011

Hildebrandt, U., Janetta, K., and Bothe, H. (2002). Towards growth of arbuscular mycorrhizal fungi independent of a plant host. *Appl. Environ. Microbiol.* 68, 1919–1924. doi: 10.1128/AEM.68.4.1919-1924.2002

Hull, C. M., Johnson, A. D., and Johnson, A. D. (1999). Identification of a mating type-like locus in the asexual pathogenic yeast *Candida albicans*. *Science* 285, 1271–1275. doi: 10.1126/science.285.5431.1271

Hyten, D. L., Song, Q., Zhu, Y., Choi, I.-Y., Nelson, R. L., Costa, J. M., et al. (2006). Impacts of genetic bottlenecks on soybean genome diversity. Available at: www.pnas.orgcgidoi10.1073pnas.0604379103 [Accessed July 11, 2019].

James, T. Y., Stenlid, J., Olson, Å., and Johannesson, H. (2008). Evolutionary significance of imbalanced nuclear ratios within heterokaryons of the basidiomycete fungus *Heterobasidion parviporum*. *Evolution* 62, 2279–2296. doi: 10.1111/j.1558-5646.2008.00462.x

Jinks, J. L. (1952). Heterokaryosis; a system of adaption in wild fungi. *Proc. R. Soc. Lond. Ser. B Biol. Sci.* 140, 83–99. doi: 10.1098/RSPB.1952.0046

Johnson, N. C. (1993). Can fertilization of soil select less mutualistic mycorrhizae? *Ecol. Appl.* 3, 749–757. doi: 10.2307/1942106

Jung, S. C., Martinez-Medina, A., Lopez-Raez, J. A., and Pozo, M. J. (2012). Mycorrhiza-induced resistance and priming of plant defenses. *J. Chem. Ecol.* 38, 651–664. doi: 10.1007/s10886-012-0134-6

Kameoka, H., Tsutsui, I., Saito, K., Kikuchi, Y., Handa, Y., Ezawa, T., et al. (2019). Stimulation of asymbiotic sporulation in arbuscular mycorrhizal fungi by fatty acids. *Nat. Microbiol.* 4, 1654–1660. doi: 10.1038/s41564-019-0485-7

Koch, A. M., Antunes, P. M., Maherali, H., Hart, M. M., and Klironomos, J. N. (2017). Evolutionary asymmetry in the arbuscular mycorrhizal symbiosis: conservatism in fungal morphology does not predict host plant growth. *New Phytol.* 214, 1330–1337. doi: 10.1111/nph.14465

Kokkoris, V., Hamel, C., and Hart, M. M. (2019a). Mycorrhizal response in crop versus wild plants. *PLoS One* 14:e0221037. doi: 10.1371/journal.pone.0221037

Kokkoris, V., and Hart, M. M. (2019). The role of *in vitro* cultivation on symbiotic trait and function variation in a single species of arbuscular mycorrhizal fungus. *Fungal Biol.* 123, 732–744. doi: 10.1016/j.funbio.2019.06.009

Kokkoris, V., Miles, T., and Hart, M. M. (2019b). The role of *in vitro* cultivation on asymbiotic trait variation in a single species of arbuscular mycorrhizal fungus. *Fungal Biol.* 123, 307–317. doi: 10.1016/j.funbio.2019.01.005

Koskiniemi, S., Sun, S., Berg, O. G., and Andersson, D. I. (2012). Selection-driven gene loss in bacteria. *PLoS Genet.* 8:e1002787. doi: 10.1371/journal.pgen.1002787

Kuhn, G., Hijri, M., and Sanders, I. R. (2001). Evidence for the evolution of multiple genomes in arbuscular mycorrhizal fungi. *Nature* 414, 745–748. doi: 10.1038/414745a

Lin, K., Limpens, E., Zhang, Z., Ivanov, S., Saunders, D. G. O., Mu, D., et al. (2014). Single nucleus genome sequencing reveals high similarity among nuclei of an endomycorrhizal fungus. *PLoS Genet.* 10:e1004078. doi: 10.1371/journal.pgen.1004078

Lippu, J. (1998, 1998). Redistribution of 14C-labelled reserve carbon in *Pinus sylvestris* seedlings during shoot elongation. *Silva Fennica* 32:696. doi: 10.14214/sf.696

López-Uribe, M. M., Appler, R. H., Youngsteadt, E., Dunn, R. R., Frank, S. D., and Tarpy, D. R. (2017). Higher immunocompetence is associated with higher genetic diversity in feral honey bee colonies (*Apis mellifera*). *Conserv. Genet.* 18, 659–666. doi: 10.1007/s10592-017-0942-x

Luginbuehl, L. H., Menard, G. N., Kurup, S., Van Erp, H., Radhakrishnan, G. V., Breakspear, A., et al. (2017). Fatty acids in arbuscular mycorrhizal fungi are synthesized by the host plant. *Science* 356, 1175–1178. doi: 10.1126/science.aan0081

Lumini, E., Bianciotto, V., Jargeat, P., Novero, M., Salvioli, A., Faccio, A., et al. (2007). Presymbiotic growth and sporal morphology are affected in the arbuscular mycorrhizal fungus *Gigaspora margarita* cured of its endobacteria. *Cell. Microbiol.* 9, 1716–1729. doi: 10.1111/j.1462-5822.2007.00907.x

Machida, M., Asai, K., Sano, M., Tanaka, T., Kumagai, T., Terai, G., et al. (2005). Genome sequencing and analysis of *Aspergillus oryzae*. *Nature* 438, 1157–1161. doi: 10.1038/nature04300

Mar Vázquez, M., César, S., Azcón, R., and Barea, J. M. (2000). Interactions between arbuscular mycorrhizal fungi and other microbial inoculants (*Azospirillum*, *Pseudomonas*, *Trichoderma*) and their effects on microbial population and enzyme activities in the rhizosphere of maize plants. *Appl. Soil Ecol.* 15, 261–272. doi: 10.1016/S0929-1393(00)00075-5

Marmann, A., Aly, A., Lin, W., Wang, B., Proksch, P., Marmann, A., et al. (2014). Co-cultivation—a powerful emerging tool for enhancing the chemical diversity of microorganisms. *Mar. Drugs* 12, 1043–1065. doi: 10.3390/md12021043

Marx, D. H. (1981). Variability in ectomycorrhizal development and growth among isolates of *Pisolithus tinctorius* as affected by source, age, and reisolation. *Can. J. For. Res.* 11, 168–174. doi: 10.1139/x81-022

Marx, D. H., and Daniel, W. J. (1976). Maintaining cultures of ectomycorrhizal and plant pathogenic fungi in sterile water cold storage. *Can. J. Microbiol.* 22, 338–341. doi: 10.1139/m76-051

Mateus, I. D., Masclaux, F. G., Aletti, C., Rojas, E. C., Savary, R., Dupuis, C., et al. (2019). Dual RNA-seq reveals large-scale non-conserved genotype×genotype-specific genetic reprograming and molecular crosstalk in the mycorrhizal symbiosis. *ISME J.* 13, 1226–1238. doi: 10.1038/s41396-018-0342-3

Mayo, K., Davis, R. E., and Motta, J. (1986). Stimulation of germination of spores of *Glomus versiforme* by spore-associated bacteria. *Mycologia* 78, 426–431. doi: 10.1080/00275514.1986.12025265

Mehta, B. J., and Cerdá-Olmedo, E. (2001). Intersexual partial diploids of *Phycomyces*. Available at: https://www.genetics.org/content/genetics/158/2/635.full.pdf [Accessed July 11, 2019].

Menge, J. A., Steirle, D., Bagyaraj, D. J., Johnson, E. L. V., and Leonard, R. T. (1978). Phosphorus concentrations in plants responsible for inhibition of mycorrhizal infection. *New Phytol.* 80, 575–578. doi: 10.1111/j.1469-8137.1978.tb01589.x

Meyer, M., Bourras, S., Gervais, J., Labadie, K., Cruaud, C., Balesdent, M.-H., et al. (2017). Impact of biotic and abiotic factors on the expression of fungal effector-encoding genes in axenic growth conditions. *Fungal Genet. Biol.* 99, 1–12. doi: 10.1016/j.fgb.2016.12.008

Moran, N. A., McCutcheon, J. P., and Nakabachi, A. (2008). Genomics and evolution of heritable bacterial symbionts. *Annu. Rev. Genet.* 42, 165–190. doi: 10.1146/annurev.genet.41.110306.130119

Mosse, B., and Hepper, H. (1975). Vesicular-arbuscular mycorrhizal infections in root organ cultures. *Physiol. Plant Pathol.* 5, 215–223. doi: 10.1016/0048-4059(75)90088-0

Naiki, T., and Cook, R. J. (1983). Factors in loss of pathogenicity in *Gaeumannomyces graminis var. tritici*. Available at: https://www.apsnet.org/publications/phytopathology/backissues/Documents/1983Articles/Phyto73n12_1652.PDF [Accessed October 14, 2017].

Naito, M., Desirò, A., González, J. B., Tao, G., Morton, J. B., Bonfante, P., et al. (2017). Candidatus Moeniiplasma glomeromycotorum', an endobacterium of arbuscular mycorrhizal fungi. *Int. J. Syst. Evol. Microbiol.* 67, 1177–1184. doi: 10.1099/ijsem.0.001785

Naumann, M., Schübler, A., and Bonfante, P. (2010). The obligate endobacteria of arbuscular mycorrhizal fungi are ancient heritable components related to the Mollicutes. *ISME J.* 4, 862–871. doi: 10.1038/ismej.2010.21

Nishio, S., Takada, N., Saito, T., Yamamoto, T., and Iketani, H. (2016). Estimation of loss of genetic diversity in modern Japanese cultivars by comparison of diverse genetic resources in Asian pear (*Pyrus* spp.). *BMC Genet.* 17:81. doi: 10.1186/s12863-016-0380-7

Ola, A. R. B., Thomy, D., Lai, D., Brötz-Oesterhelt, H., and Proksch, P. (2013). Inducing secondary metabolite production by the endophytic fungus *Fusarium tricinctum* through coculture with *Bacillus subtilis*. *J. Nat. Prod.* 76, 2094–2099. doi: 10.1021/np400589h

Pan, K., Zhao, N., Yin, Q., Zhang, T., Xu, X., Fang, W., et al. (2014). Induction of a laccase Lcc9 from *Coprinopsis cinerea* by fungal coculture and its application on indigo dye decolorization. *Bioresour. Technol.* 162, 45–52. doi: 10.1016/j.biortech.2014.03.116

Pawlowska, T. E., Douds, D. D., and Charvat, I. (1999). In vitro propagation and life cycle of the arbuscular mycorrhizal fungus *Glomus etunicatum*. *Mycol. Res.* 103, 1549–1556. doi: 10.1017/S0953756299008801

Pawlowska, T. E., and Taylor, J. W. (2004). Organization of genetic variation in individuals of arbuscular mycorrhizal fungi. *Nature* 427, 733–737. doi: 10.1038/nature02290

Pearce, F. (2003). Databases selected: Multiple databases going bananas. Available at: http://courseresources.mit.usf.edu/sgs/ph6934/webpages/CC/module_5/read/going_bananas_pearce.pdf [Accessed July 11, 2019].

Plenchette, C., Declerck, S., Diop, T. A., and Strullu, D. G. (1996). Infectivity of monoaxenic subcultures of the arbuscular mycorrhizal fungus *Glomus versiforme* associated with Ri-T-DNA-transformed carrot root. *Appl. Microbiol. Biotechnol.* 46, 545–548. doi: 10.1007/s002530050858

Ploetz, R. C. (2003). "Yes. We won't have bananas." What realistic threats do diseases pose to banana production? *Pestic. Outlook* 14, 62–64. doi: 10.1039/b303002b

Porcel, R., Aroca, R., and Ruiz-Lozano, J. M. (2012). Salinity stress alleviation using arbuscular mycorrhizal fungi. A review. *Agron. Sustain. Dev.* 32, 181–200. doi: 10.1007/s13593-011-0029-x

Pozo, M. J., and Azcón-Aguilar, C. (2007). Unraveling mycorrhiza-induced resistance. *Curr. Opin. Plant Biol.* 10, 393–398. doi: 10.1016/j.pbi.2007.05.004

Purin, S., and Morton, J. B. (2011). *In situ* analysis of anastomosis in representative genera of arbuscular mycorrhizal fungi. *Mycorrhiza* 21, 505–514. doi: 10.1007/s00572-010-0356-9

Ram, S. G., Thiruvengadam, V., and Vinod, K. K. (2007). Genetic diversity among cultivars, landraces and wild relatives of rice as revealed by microsatellite markers. *J. Appl. Genet.* 48, 337–345. doi: 10.1007/BF03195230

Reif, J. C., Zhang, P., Dreisigacker, S., Warburton, M. L., van Ginkel, M., Hoisington, D., et al. (2005). Wheat genetic diversity trends during domestication and breeding. *Theor. Appl. Genet.* 110, 859–864. doi: 10.1007/s00122-004-1881-8

Roesti, D., Ineichen, K., Braissant, O., Redecker, D., Wiemken, A., and Aragno, M. (2005). Bacteria associated with spores of the arbuscular mycorrhizal fungi *Glomus geosporum* and *Glomus constrictum*. *Appl. Environ. Microbiol.* 71, 6673–6679. doi: 10.1128/AEM.71.11.6673-6679.2005

Ropars, J., Sędzielewska Toro, K., Noel, J., Pelin, A., Charron, P., Farinelli, L., et al. (2016, 2016). Evidence for the sexual origin of heterokaryosis in arbuscular mycorrhizal fungi. *Nat. Microbiol.* 1:16033. doi: 10.1038/nmicrobiol.2016.33

Roper, M., Ellison, C., Taylor, J., and N, G. (2011). Nuclear and genome dynamics in multinucleate ascomycete fungi. *Curr. Biol.* 21, R786–R793. doi: 10.1016/j.cub.2011.06.042

Rosikiewicz, P., Bonvin, J., and Sanders, I. R. (2017). Cost-efficient production of *in vitro Rhizophagus* irregularis. *Mycorrhiza* 27, 477–486. doi: 10.1007/s00572-017-0763-2

Ross, I. K., Loftus, M. G., and Foster, L. M. (1991). Homokaryon-dikaryon phenotypic switching in an arginine requiring mutant of *Coprinus congregatus*. *Mycol. Res.* 95, 776–781. doi: 10.1016/S0953-7562(09)80037-3

Ruiz-Lozano, J. M., and Aroca, R. (2010). "Host response to osmotic stresses: stomatal behaviour and water use efficiency of arbuscular mycorrhizal plants" in *Arbuscular mycorrhizas: Physiology and function* (The Netherlands: Springer), 239–256.

Salvioli, A., Chiapello, M., Fontaine, J., Hadj-Sahraoui, A. L., Grandmougin-Ferjani, A., Lanfranco, L., et al. (2010). Endobacteria affect the metabolic profile of their host *Gigaspora margarita*, an arbuscular mycorrhizal fungus. *Environ. Microbiol.* 12, 2083–2095. doi: 10.1111/j.1462-2920.2010.02246.x

Salvioli, A., Ghignone, S., Novero, M., Navazio, L., Venice, F., Bagnaresi, P., et al. (2016). Symbiosis with an endobacterium increases the fitness of a mycorrhizal fungus, raising its bioenergetic potential. *ISME J.* 10, 130–144. doi: 10.1038/ismej.2015.91

Samils, N., Oliva, J., and Johannesson, H. (2014). Nuclear interactions in a heterokaryon: insight from the model Neurospora tetrasperma. *Proc. R. Soc. B Biol. Sci.* 281, 20140084–20140084. doi: 10.1098/rspb.2014.0084

Sawers, R. J. H., Gutjahr, C., and Paszkowski, U. (2008). Cereal mycorrhiza: an ancient symbiosis in modern agriculture. *Trends Plant Sci.* 13, 93–97. doi: 10.1016/j.tplants.2007.11.006

Sbrana, C., Fortuna, P., and Giovannetti, M. (2011). Plugging into the network: belowground connections between germlings and extraradical mycelium of arbuscular mycorrhizal fungi. *Mycologia* 103, 307–316. doi: 10.3852/10-125

Sbrana, C., Strani, P., Pepe, A., de Novais, C. B., and Giovannetti, M. (2018). Divergence of *Funneliformis mosseae* populations over 20 years of laboratory cultivation, as revealed by vegetative incompatibility and molecular analysis. *Mycorrhiza* 28, 329–341. doi: 10.1007/s00572-018-0830-3

Smith, S. E., and Read, D. J. (2008). *Mycorrhizal symbiosis*. London: Academic Press.

Speakman, J. B. (1982). A simple, reliable method of producing perithecia of *Gaeumannomyces gramnis* var. tritici and its application to isolates of Phialophora spp. *Trans. Br. Mycol. Soc.* 79, 350–353. doi: 10.1016/S0007-1536(82)80129-0

Stockinger, H., Walker, C., and Schuessler, A. (2009). "Glomus intraradices DAOM197198", a model fungus in arbuscular mycorrhiza research, is not Glomus intraradices. *New Phytol.* 183, 1176–1187. doi: 10.1111/j.1469-8137.2009.02874.x

Sugiura, Y., Akiyama, R., Tanaka, S., Yano, K., Kameoka, H., Kawaguchi, M., et al. (2019). Myristate as a carbon and energy source for the asymbiotic growth of the arbuscular mycorrhizal fungus Rhizophagus irregularis. bioRxiv 731489 [Preprint]. doi: 10.1101/731489

Tarbell, T. J., and Koske, R. E. (2007). Evaluation of commercial arbuscular mycorrhizal inocula in a sand/peat medium. *Mycorrhiza* 18, 51–56. doi: 10.1007/s00572-007-0152-3

Tenger-Trolander, A., Lu, W., Noyes, M., and Kronforst, M. R. (2019). Contemporary loss of migration in monarch butterflies. *Proc. Natl. Acad. Sci. USA* 116, 14671–14676. doi: 10.1073/pnas.1904690116

Thomson, B. D., Malajczuk, N., Grove, T. S., and Hardy, G. E. S. (1993). Improving the colonization capacity and effectiveness of ectomycorrhizal fungal cultures by association with a host plant and re-isolation. *Mycol. Res.* 97, 839–844. doi: 10.1016/S0953-7562(09)81159-3

Thomson, B. D., Robson, A. D., and Abbott, L. K. (1986). Effects of phosphorus on the formation of mycorrhizas by *Gigaspora calospora* and *Glomus fasciculatum* in relation to root carbohydrates. *New Phytol.* 103, 751–765. doi: 10.1111/j.1469-8137.1986.tb00850.x

Tisserant, E., Malbreil, M., Kuo, A., Kohler, A., Symeonidi, A., Balestrini, R., et al. (2013). Genome of an arbuscular mycorrhizal fungus provides insight into the oldest plant symbiosis. *Proc. Natl. Acad. Sci. USA* 110, 20117–20122. doi: 10.1073/pnas.1313452110

Torres-Cortes, G., Ghignone, S., Bonfante, P., and Schussler, A. (2015). Mosaic genome of endobacteria in arbuscular mycorrhizal fungi: Transkingdom gene transfer in an ancient mycoplasma-fungus association (Vol 112, pg 7785, 2015). *Proc. Natl. Acad. Sci. USA* 112, E5376–E5376. doi: 10.1073/pnas.1516662112

Vannini, C., Carpentieri, A., Salvioli, A., Novero, M., Marsoni, M., Testa, L., et al. (2016). An interdomain network: the endobacterium of a mycorrhizal fungus promotes antioxidative responses in both fungal and plant hosts. *New Phytol.* 211, 265–275. doi: 10.1111/nph.13895

Wang, G. M., Stribley, D. P., Tinker, P. B., and Walker, C. (1993). Effects of pH on arbuscular mycorrhiza I. field observations on the long-term liming experiments at Rothamsted and Woburn. *New Phytol.* 124, 465–472. doi: 10.1111/j.1469-8137.1993.tb03837.x

Weese, D. J., Heath, K. D., Dentinger, B. T. M., and Lau, J. A. (2015). Long-term nitrogen addition causes the evolution of less-cooperative mutualists. *Evolution* 69, 631–642. doi: 10.1111/evo.12594

Whitehead, S. R., Turcotte, M. M., and Poveda, K. (2017). Domestication impacts on plant–herbivore interactions: a meta-analysis. *Philos. Trans. R. Soc. B Biol. Sci.* 372:20160034. doi: 10.1098/rstb.2016.0034

Willmitzer, L., Sanchez-Serrano, J., Buschfeld, E., and Schell, J. (1982). DNA from *Agrobacterium rhizogenes* in transferred to and expressed in axenic hairy root plant tissues. *MGG Mol. Gen. Genet.* 186, 16–22. doi: 10.1007/BF00422906

Wilson, J. M. (1984). Comparative development of infection by 3 vesicular arbuscular mycorrhizal fungi. *New Phytol.* 97, 413–426. doi: 10.1111/j.1469-8137.1984.tb03607.x

Wyss, P., and Bonfante, P. (1993). Amplification of genomic DNA of arbuscular-mycorrhizal (AM) fungi by PCR using short arbitrary primers. *Mycol. Res.* 97, 1351–1357. doi: 10.1016/S0953-7562(09)80169-X

Zeder, M. A. (2006). Central questions in the domestication of plants and animals. *Evol. Anthropol. Issues News Rev.* 15, 105–117. doi: 10.1002/evan.20101

Conflict of Interest: The authors declare that the research was conducted in the absence of any commercial or financial relationships that could be construed as a potential conflict of interest.

frontiers in Plant Science

ORIGINAL RESEARCH
published: 30 October 2019
doi: 10.3389/fpls.2019.01312

Contrasting Nitrogen Fertilisation Rates Alter Mycorrhizal Contribution to Barley Nutrition in a Field Trial

Tom Thirkell[1,2*†], *Duncan Cameron*[2] *and Angela Hodge*[1]

[1] *Department of Biology, University of York, York, United Kingdom,* [2] *Department of Animal and Plant Sciences, University of Sheffield, Sheffield, United Kingdom*

Controlled environment studies show that arbuscular mycorrhizal fungi (AMF) may contribute to plant nitrogen (N) uptake, but the role of these near-ubiquitous symbionts in crop plant N nutrition under natural field conditions remains largely unknown. In a field trial, we tested the effects of N fertilisation and barley (*Hordeum vulgare* L.) cultivar identity on the contribution of AMF to barley N uptake using ^{15}N tracers added to rhizosphere soil compartments. AMF were shown capable of significantly increasing plant ^{15}N acquisition from root exclusion zones, and this was influenced by nitrogen addition type, N fertiliser application rate and barley cultivar identity. Our data demonstrate a previously overlooked potential route of crop plant N uptake which may be influenced substantially and rapidly in response to shifting agricultural management practices.

Keywords: arbuscular mycorrhiza, nitrogen, barley, field trial, plant ecophysiology

OPEN ACCESS

Edited by:
Paola Bonfante,
University of Turin, Italy

Reviewed by:
Jan Jansa,
Institute of Microbiology (ASCR), Czechia
Erik Verbruggen,
University of Antwerp, Belgium

****Correspondence:***
Tom Thirkell
t.j.thirkell@leeds.ac.uk

†Present address:
Tom Thirkell,
Centre for Plant Sciences, University of Leeds, United Kingdom

Specialty section:
This article was submitted to Plant Microbe Interactions, a section of the journal Frontiers in Plant Science

Received: *20 May 2019*
Accepted: *20 September 2019*
Published: *30 October 2019*

Citation:
Thirkell T, Cameron D and Hodge A (2019) Contrasting Nitrogen Fertilisation Rates Alter Mycorrhizal Contribution to Barley Nutrition in a Field Trial. Front. Plant Sci. 10:1312. doi: 10.3389/fpls.2019.01312

INTRODUCTION

Nitrogen (N) is usually the most limiting mineral nutrient to plant growth (Agren et al., 2012) and maintaining modern agricultural production requires frequent and substantial application of fertiliser to farm soils. In various forms an estimated 50 MT year^{-1} fertiliser N is applied to agricultural land worldwide (Ladha et al., 2016). Assimilation of applied N by crops may be under 50% (Ladha et al., 2005, Masclaux-Daubresse et al., 2010); a significant fraction of this applied N is wasted — lost through processes including volatilisation, microbial immobilisation, runoff, and leaching (Ladha et al., 2016, Cameron et al., 2013). There is economic and ecological pressure on farmers to optimise the N uptake efficiency of crop plants (Hawkesford, 2014) and by reducing the reliance on non-renewable inputs, improve the sustainability of agriculture (Pretty, 2008). This progress will require the integration of biological and ecological processes into agriculture, and better understanding of soil microbial communities and their roles in nutrient cycling (Rillig et al., 2016, Pretty, 2018).

As near-ubiquitous symbionts of cereal crops, arbuscular mycorrhizal fungi (AMF) are prime targets to investigate the role of soil biota in improving agricultural sustainability (Gosling et al., 2006, Thirkell et al., 2017, Rillig et al., 2019). The majority of land plant species engage in symbiosis with these fungi, which may aid plants' mineral nutrient uptake from soils, in exchange for photosynthetic carbon (C) from their plant hosts (Smith and Read, 2008). The influence that AMF mycelia may exert over nutrient dynamics in agricultural systems is not limited to direct effects on plant nutrient acquisition however; the presence of AMF has been shown to reduce mineral fertiliser leaching (Cavagnaro et al., 2015) and to influence greenhouse gas emissions (Storer et al., 2018). While the role of AMF in biogeochemical cycles is undoubtedly complex, of pressing need is

to determine the extent to which plants rely on these symbionts for mineral nutrient acquisition.

It is well established that AMF can contribute to plant N uptake (Ames et al., 1983; Hodge et al., 2001; Leigh et al., 2009; Thirkell et al., 2016), but the extent to which this takes place, and whether it is ecologically or agriculturally relevant is unclear (Smith and Smith, 2011a). This is in part due to relatively little experimental attention. There remains in the literature a focus on the role of AMF in plant phosphorus (P) uptake (Smith and Smith, 2011a; Karasawa et al., 2012; Ezawa and Saito, 2018), and consideration of symbiotic N uptake is often restricted to diazotrophic bacteria while AMF are often overlooked (Garcia et al., 2016).

Improved access to poorly-mobile soil P is, in most instances, the primary benefit of AMF to their plant hosts (Smith and Read, 2008). The relative immobility of inorganic P (Pi) in soil means that plant uptake of Pi from the rhizosphere can outpace Pi diffusion from the surrounding bulk soil and the subsequent P-depletion zones that form around the root are narrow and sharply defined. By engaging in symbiosis with AMF, with a mycelium spreading several centimetres beyond the rhizosphere, the plant effectively increases the volume of soil from which it can acquire nutrients, particularly poorly mobile ions such as Pi (Sanders and Tinker, 1973; Hodge, 2017). Nitrate (NO_3^-) and ammonium (NH_4^+), the predominant forms in which plants and fungi acquire N (Marschner, 2011), are more mobile in soil than orthophosphate (Tinker and Nye, 2000). Despite this, a zone of N-depletion may still form around the root (Brackin et al., 2017), in which case AMF may facilitate improved N capture for their plant hosts. With smaller diameters than plant roots, AMF hyphae may also penetrate soil micropores more effectively than a plant root, and thereby be present when inorganic N forms are released through microbial decomposition processes and effectively scavenge for this released inorganic N (Hodge, 2014).

Results from microcosm studies are conflicting as to the importance of AMF in plant N uptake (Hodge and Storer, 2015). While a number of studies have shown no improvement of N uptake by AM plants versus non-mycorrhizal counterparts (Cui and Caldwell, 1996a; Cui and Caldwell, 1996b; Reynolds et al., 2005; Kahkola et al., 2012), it is possible that AMF make an invisible contribution to nutrient acquisition which cannot easily be identified without the use of isotope tracing techniques. Mycorrhizal downregulation of plant root phosphate transporters has been identified in a number of studies (Smith et al., 2003; Smith et al., 2004). In this situation, AMF may be responsible for the majority of a plant's P acquisition, but root transporter downregulation may result in reduced plant P uptake compared to non-mycorrhizal control plants (Smith et al., 2003; Smith et al., 2004). Whether a similar phenomenon occurs in mycorrhizal root N uptake remains unclear. Isotope tracing data does, however, show that AMF can transfer substantial amount of N to a host plant (Leigh et al., 2009; Thirkell et al., 2016), while the contribution of AMF to field-grown plant N uptake is unknown.

AMF are capable of acquiring N from decomposing organic sources (Leigh et al., 2009; Hodge and Fitter, 2010; Herman et al 2012; Barrett et al., 2014; Thirkell et al., 2016) and even to acquire some organic N directly from the hyphosphere, notably as amino acids (Hawkins et al., 2000; Breuninger et al., 2004; Whiteside et al., 2012a; Whiteside et al., 2012b, Tisserant et al., 2012) and perhaps as dipeptides (Belmondo et al., 2014). As in plants however, the vast majority of N acquired by AMF is thought to be as NO_3^- or NH_4^+ (Govindarajulu et al., 2005; Bucking and Kafle, 2015). Greater N uptake as NO_3^- might be expected as it is usually more abundant than NH_4^+ because of rapid nitrification (Marschner, 2011). However, because N acquired as NO_3^- must be reduced to NH_4^+ before further assimilation, it should be energetically favourable for AMF to acquire N as NH_4^+ (Hodge et al., 2010; Courty et al., 2015). Corroborative data remains equivocal as to AMF "preference" for N types (Johansen et al., 1993; Hawkins and George, 2001). As NO_3^- and NH_4^+ are the most commonly-used forms of fertiliser in Western agriculture, the need to understand mycorrhizal plant acquisition of these N sources is pressing.

Nutrient trade between partners in AM symbioses shows considerable variation in response to biotic factors such as plant and fungal genotype (Smith et al., 2004), in addition to abiotic factors including soil nutrient status (Johnson, 2010; Johnson et al., 2015). Despite substantial experimental data, predictability of the extent to which plants benefit from AMF colonisation remains poor. For example, no universally beneficial fungal isolate has been identified and comparatively few plants are obligate symbionts with AMF.

Despite the widespread distribution of AMF (Smith and Read, 2008; Davison et al., 2015) and the readiness with which they colonise most staple crop plant roots (Smith and Smith, 2011a), little is understood about the function of AMF in the field (Lekberg and Helgason, 2018; Ryan and Graham, 2018). Most published material on the function of AMF is derived from studies conducted under controlled conditions, often comparing AM plants with non-AM controls. While such experiments have provided much valuable data and insight, their findings cannot directly be extrapolated to the field scale, as the occurrence of non-AM cereals in most arable soils is unlikely (Smith and Smith, 2011a). Despite disruptive practices such as tilling and the application of fungicides, there remains a substantial AMF spore bank (and therefore inoculum potential) in agricultural soils (Sosa-Hernandez et al., 2018) and it is very likely that plants in arable field soil will be colonised by AMF (Smith and Smith, 2011a). Further research is needed to begin to understand how AMF might affect crop plant nutrient uptake *in situ*.

Adding ^{15}N isotope tracers to mesh-walled soil compartments in a field trial, we examined the role of AMF in the N acquisition by barley (*Hordeum vulgare* L.) cultivars "Meridian" and "Maris Otter". Isotopic ^{15}N labelling was carried out in plots receiving contrasting N rates to test the impact of N availability on nutrient transfer in the symbiosis. We tested the hypothesis that increased N fertilisation would result in more AMF transfer of N to host plants because AMF, by virtue of their size, would be better able than roots to compete with the soil microbiome for the added N held in physically small microsites. N tracers were added as NH_4^+ or NO_3^- to investigate the relative uptake and transfer of different N sources by AMF.

MATERIALS AND METHODS

Field Trial Design

Data were gathered from a larger field trial, designed and implemented at Sancton, East Riding of Yorkshire (co-ordinates

53°51′10.2″N 0°35′29.1″W), by ADAS (Pendeford, Wolverhampton, UK). The ADAS trial was set up to test how barley yield compares among 6 application rates of ammonium nitrate (NH_4NO_3) fertiliser (Nitram, CF Fertiliser, Ince, Cheshire, UK) ranging from 0–300 kg ha^{-1}. The soil at the trial site comprises a silty rendzina, with a significant proportion of chalk fragments (UKSO, 2016). Soil mineral N, quantified shortly before sowing, was 29.9 kg N ha^{-1}, of which 28 kg was nitrate-N and 1.9 kg ammonium-N. The field site on which the trial was based is a commercial arable farm, with barley (*Hordeum vulgare* L.), oilseed rape (*Brassica napus* L.) and wheat (*Triticum aestivum* L.) grown in a rotation.

The ADAS trial used plots measuring 12 m × 1.5 m, clustered in groups of 6 by N application rate, with each variety represented once per cluster. Each N application rate was applied to 3 replicate clusters, of 6 varieties, meaning 18 clusters in total, with a combined area of 1944 m^2. Experimental clusters of N application rates were separated to each side by buffer zones 6 m wide, and at each end by buffer zones 3 m long (**Figure 1**). Owing to the logistical challenges of sampling the entire trial, the experimental work presented here is gathered from two of the N application rates (60 kg ha^{-1} (N rate 2 in **Figure 1**), and 280 kg ha^{-1} (N rate 5 in **Figure 1**)), and two of the barley cultivars: KWS Meridian (KWS UK Ltd, Thriplow, Hertfordshire, UK), a 6-row feedstock barley; and Maris Otter (Robin Appel, Waltham Chase, Hampshire, UK), a 2-row malting barley, giving 4 treatment groups, with 3 replicate plots per treatment. Meridian and Maris Otter were chosen from the panel of 6 cultivars available in the trial as they represent contrasting ages of barley varieties, developed in the 1960s and 2000s respectively. Further, Maris Otter is a malting barley, characterised by a low grain protein content, while Meridian was developed as a feedstock barley, with a higher grain protein (and therefore N) content. Experimental sampling and isotope labelling were carried out during the post-anthesis, grain filling period — approximate growth stages 70–80 (Zadoks et al., 1974).

Intraradical and Extraradical AMF Quantification

AMF colonisation of both barley varieties was confirmed and then quantified by staining of roots collected from the trial plots. Roots were collected from between 5 and 15 cm below the surface. After clearing in 10% (w/v) KOH for 20 min at 70°C, roots were rinsed in de-ionised water, acidified in 1% (v/v) HCl at 25°C for 10 min and then stained in Trypan Blue at 25°C for 20 min. Roots were then rinsed again in de-ionised water before being left in a 50% (v/v) glycerol solution for 24 h, before being mounted onto microscope slides to allow quantification of root length colonisation (RLC) using the gridline intersect method (McGonigle et al., 1990).

Soil samples were collected from between 5 and 15 cm below the soil surface. As AMF hyphal turnover can be rapid (Staddon et al., 2003), hyphal extraction took place within 6 h of collection to minimise loss due to decomposition. Extraradical hyphal quantity in the plots was determined using an adapted method from Staddon et al. (1999). Briefly, samples of known mass (5–10 g) were suspended in 500 mL of de-ionised water and agitated with a magnetic stirrer plate in order to free the hyphae from soil particles. From this, 200 mL was decanted to a smaller beaker on a magnetic stirrer. Aliquots (10 mL) were removed and vacuum filtered through 0.45 µm nylon mesh (Anachem, Bedfordshire, UK) and hyphal length density (HLD) was quantified using the gridline intersect method (Hodge, 2001).

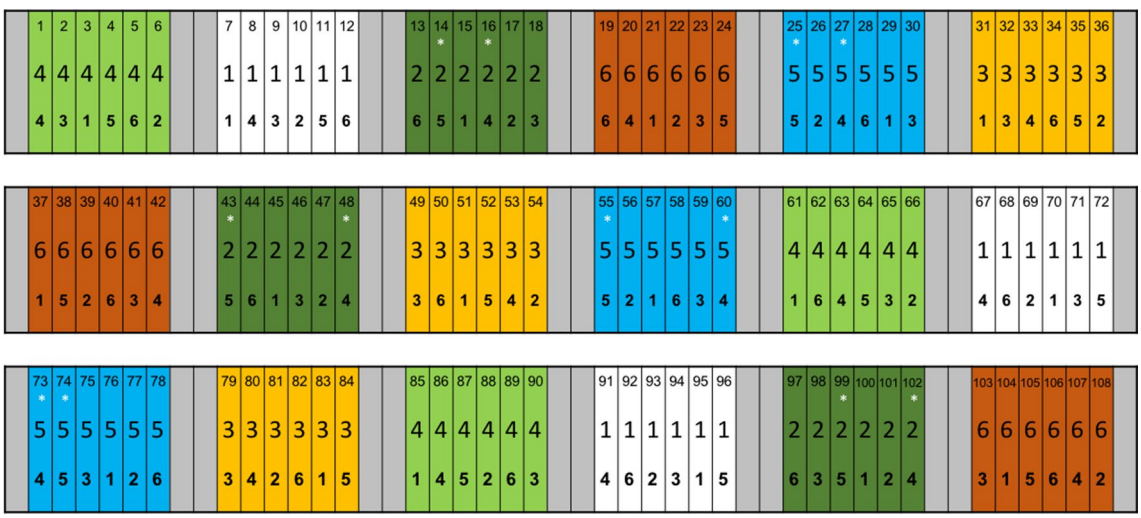

FIGURE 1 | ADAS experiment established at Sancton, East Riding of Yorkshire, UK. Six barley (*Hordeum vulgare* L.) cultivars were planted at the trial site, and received one of 6 N addition rates, ranging from 0 to 300 kg ha^{-1}. Each combination of barley cultivar and N rate was replicated 3 times. Each plot has 3 numbers, denoting: plot identity, N addition rate and barley cultivar, reading top to bottom. Nitrogen addition rate "2" represents 60 kg ha^{-1} and "5" is 280 kg ha^{-1}. Plot colours also represent N addition rate. Meridian barley is denoted by "4" and Maris Otter by "5". Asterisks (*) represent plots from which root samples were taken for analysis of root length colonisation and to which ^{15}N tracer was added. Reproduced with permission from Pete Berry and Kate Storer, ADAS.

^{15}N Stable Isotope Labelling

The AMF contribution to barley N uptake was investigated by adding a solution of ^{15}N (as either $(^{15}NH_4)_2SO_4$ or $K^{15}NO_3$), into mesh-walled cores, into which AMF hyphae could access but plant roots could not, or (as controls for diffusion and mass flow of the added N) cores into which neither AMF hyphae or roots could access. Isotopic ^{15}N was added in the form of Long Ashton nutrient solution (LAS) (Smith et al., 1983), which can be prepared variously to provide ^{15}N as $^{15}NH_4^+$ or $^{15}NO_3^-$ in equimolar concentrations. The LAS was made to the standard protocols except N being 300% the original concentrations. Each core received 5 mL of LAS, containing 0.683 mg ^{15}N. (Long Ashton nutrient solution protocol is included in **Supplementary Information Document 1**).

Hyphal access cores were constructed following an adapted method from Johnson et al. (2001). Lengths of PVC tubing (length 85 mm, internal diameter 13 mm, external diameter 16 mm; internal volume 9.9 cm^3) with 2 windows cut in the sides of the lower $^2/_3$ of the tube so that 50% of the side area was open, were wrapped in a 20 µm nylon mesh (John Stanier and Co., Whitefield, Manchester, UK), fixed with Tensol adhesive cement (Bostik Inc., Wauwatosa, Wisconsin, USA). The open bottom end of each tube was covered with the same size mesh. Control cores, which allowed diffusion and mass flow of solutes but prevent hyphal ingrowth, were covered with 0.45 µm nitrocellulose membrane mesh to prevent root and hyphal ingrowth. Cores were filled with a 1/1 (v/v) mixture of silica sand and TerraGreen® (calcinated attapulgite clay, Oil-Dri, Cambridgeshire, UK), which had been sterilised by autoclaving (121°C for 44 min), providing a uniform substrate into which the ^{15}N solutions could be added.

Each of these cores was then placed inside another, slightly larger core, constructed in the same manner (length 75 mm internal diameter 18 mm, external diameter 21 mm). These cores were also covered in a 20 µm nylon mesh. Such a "core in a core" design allows the placement of zones of defined and uniform size into the soil, to which ^{15}N label solutions could be added. A small (approximately 1 mm) air gap is made between the external mesh wall of one core and the internal mesh wall of the other, which should reduce the rapid diffusion of N from the site of addition, which has been a problem in studies where ^{15}N has been added (Smith and Smith, 2011b). Diffusion and mass flow are unlikely to be prevented entirely, as the pressure of soil on the sides of the core may push the mesh together so that the two layers of mesh make contact. However, the system provides a more stable labelling zone than using a single core, where one mesh layer may be easily damaged (Johnson et al., 2001).

Each of the 12 experimental plots received four cores (1. No AMF Access + $^{15}NH_4^+$; 2. AMF Access + $^{15}NH_4^+$; 3. No AMF Access + $^{15}NO_3^-$; 4. AMF Access + $^{15}NO_3^-$), spaced 3 m apart to avoid contamination of ^{15}N from neighbouring cores (**Figure 2**). Placement of cores took place 8 weeks before label addition to allow hyphal ingrowth from the bulk soil. A piece of tape was placed over the top of cores to minimise contamination. This tape was removed for ^{15}N addition and then replaced.

Sample Collection and Preparation

After 7 days, the nearest plant to each labelling core was cut at ground level and removed, dried at 70°C for 48 h and homogenised in a kitchen blender (Morphy Richards, Mexborough, South Yorkshire, UK) then in a ball mill (MM400 Ball Mill, Retsch GmbH, Haan, Germany). Homogenised shoot samples of known mass (3 mg ± 0.5 mg) were used to quantify ^{15}N and N content, performed by isotope ratio mass spectrometry (IRMS) (PDZ 2020, Sercon Ltd, Crewe, UK).

Statistical Analysis

For all data, statistical analysis was performed using the "R 3.1.0" statistical package, through the "RStudio" integrated development

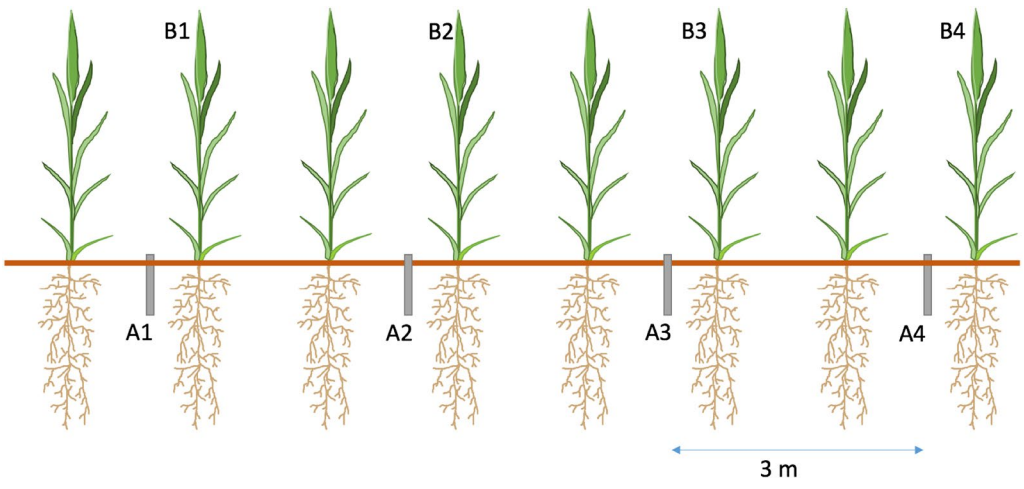

FIGURE 2 | Diagram of ^{15}N addition experiment. PVC cores were inserted adjacent to barley (*Hordeum vulgare* L.) plants, four cores per plot, spaced 3 m apart. Cores were organised as follows A1 – AMF Access + Ammonium (NH_4^+); A2 - No AMF Access + Nitrate (NO_3^-); A3 - AMF Access + NO_3^-; A4 - No AMF Access + NH_4^+ Each core received 0.683 mg ^{15}N added as Long Ashtons nutrient solution. Plant shoots closest to the core (B1-4) were removed, dried and homogenised for N analysis. B1-B4 denote shoot samples taken.

environment (R foundation for Statistical Computing, Vienna, Austria). Data were tested for normality using Shapiro-Wilk and Kolmogorov-Smirnov tests, and Levene's test was used to confirm homogeneity of variance. Where these tests suggested data did not match test assumptions, data were square-root or log-transformed prior to analysis. Data for root length colonisation, hyphal length density, barley N concentration and biomass were tested by two-way ANOVA, using N addition rate and barley variety as explanatory variables. As two additional explanatory variables were added in the trial for ^{15}N uptake (N addition type, ammonium/nitrate; AM treatment, access/no access), and the small number of replicates in the ADAS field trial, it was not possible to test these factors and the N addition rate and barley cultivar at once. As such, data were split into barley cultivar and N application rate for the ^{15}N data and tested by two-way ANOVA. Here, ^{15}N enrichment was the response variable, while N type and AMF access treatment were the explanatory variables.

RESULTS

Shoot acquisition of ^{15}N added to mesh cores was significantly improved by allowing AMF access into cores, but only when added as $^{15}NO_3^-$, and only in the High-N plots of Meridian barley (**Figure 3**). T-tests indicate that only in High-N Meridian plots receiving $^{15}NO_3^-$ were ^{15}N enrichment levels greater in the AM access treatment than in the no access controls ($T_2 = 4.48$, $p = 0.023$) (**Supplementary Information, Figure 1**). A two-way ANOVA showed that in High-N Meridian, there was a significant effect of N source ($F_{1,8} = 12.73$, $p = 0.007$) and AMF access to cores ($F_{1,8} = 27.86$, $p = 0.007$). There was also a significant interaction between N source and AMF access ($F_{1,8} = 14.25$, $p = 0.005$) (**Figure 3**). In High-N Meridian with AMF access, the harvested plants, i.e. those individuals closest to the core to which the isotope label was added, acquired on average 1.62% of the ^{15}N supplied. Other treatment groups saw no greater plant uptake of ^{15}N where AMF could access the isotope label than in no-access controls. Excepting High-N Meridian plots, mean shoot ^{15}N content did not differ among treatments and controls, indicating similar plant acquisition of N following diffusion/mass flow out and into the soil, but minimal fungal-mediated uptake.

All plant roots studied were found to be colonised by AMF, indicating a substantial inoculum potential of the soil at the trial site, although no differences were found between cultivar or N-rate treatments ($p > 0.05$). Mean colonisation was 33.7% (± 3.52% SEM) across all treatment groups (**Figure 4**). Extraradical mycelium (ERM) hyphal densities, measured in the zones to which ^{15}N was added, were not different among treatment groups ($p > 0.05$). Mean ERM hyphal density across all treatments was 2.49 m g^{-1} DW soil (± 0.31 m g^{-1} SEM). In both cultivars, High-N plots supported ~ 60% higher shoot N content than Low-N plots ($F_{1,8} = 74.55$, $p < 0.001$), and shoot N concentration was significantly higher in High-N than Low-N plots ($F_{1,8} = 84.28$, $p < 0.001$). Mean shoot N concentration was 9.30 mg g^{-1} DW in Low-N blocks of Maris Otter, and 14.75 mg g^{-1} DW in the High-N. Meridian showed a very similar trend, as N concentration increased from 9.57 mg g^{-1} DW in Low-N plots to 14.38 mg g^{-1} DW in the High N. Shoot N concentration and content did not differ between the two cultivars tested. Shoot DW did not differ between the varieties or the N addition rates.

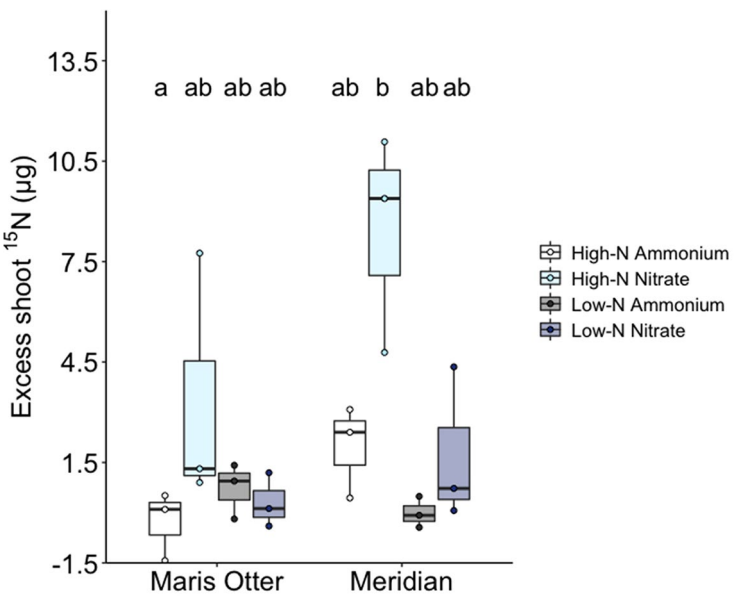

FIGURE 3 | Excess ^{15}N content in Maris Otter and Meridian shoots (calculated by subtracting shoot ^{15}N content in each "Access" unit from the mean of the corresponding values in the "No Access" units). Shoot ^{15}N enrichment was significantly higher than "no access" controls when supplied as nitrate to Meridian barley in High-N plots. Circles represent individual data points, boxplot centre bars represent the median values. High-N + ammonium groups are represented by white bars, High-N + nitrate by light blue bars, Low-N + ammonium by dark grey bars and Low-N + nitrate by dark blue bars. Data shown are means ± SEM, n = 3. Bars sharing the same letter are not significantly different.

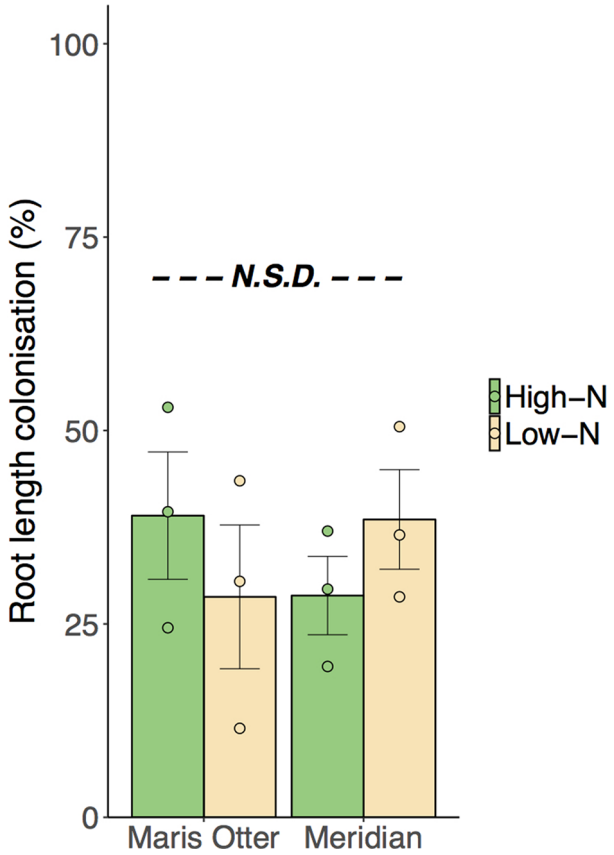

FIGURE 4 | Percentage root length colonisation, as determined by Trypan Blue staining, was not significantly different between treatments. All inspected plants were colonised by arbuscular mycorrhizal fungi (AMF), confirmed by presence of characteristic structures, arbuscules and vesicles. Mean colonisation ranged from 28.5% in Maris Otter in Low N, to 38.0% in Meridian Low-N, but no groups were significantly different. Circles represent individual data points. High-N groups are denoted by green bars, Low-N groups are denoted by yellow bars. "N.S.D." indicates that there were no significant differences among treatment means. Data shown are means ± SEM, n = 3.

DISCUSSION

The enrichment of ^{15}N in barley shoots suggests a role for AMF-facilitated N acquisition by crop plants, a phenomenon not previously observed in a field setting. Moreover, our data suggest this route of N uptake is dependent upon barley cultivar identity, the N form added and the rate at which N has previously been applied to the plots. AMF have been shown to transfer substantial quantities of N to plants in root organ culture experiments (Jin et al., 2005) although caution must be exercised before extrapolating these values to crop plant systems as they are far-removed from realistic mycorrhizal physiology. Whole-plant microcosm studies conducted under greenhouse conditions have given mixed results as to whether AMF may contribute to plant N nutrition (Hodge and Storer, 2015). Our data provide the first suggestion that AMF may have a role in cereal crop N uptake in the field. Our data also suggest that short-term changes in N fertilisation regimes can elicit shifts in AM functioning.

While our data suggest a preference for AMF to transfer N to plants when provided to this system as NO_3^- rather than NH_4^+, previous experimental evidence as to inorganic N source preference by AMF is equivocal (Johansen et al., 1993; Hawkins and George, 2001). Higher uptake of NO_3^- than NH_4^+ is contrary to models which suggest NH_4^+ acquisition should be less energetically expensive (Govindarajulu et al., 2005). Hyphal NH_4^+ uptake may be retarded by problems of charge balancing that are perhaps not encountered when N is acquired as NO_3^-. Simultaneous uptake of NO_3^- and cations such as K^+, Ca^{2+} or Mg^{2+} from the soil may avoid changes in electrochemical potential across exchange surfaces, allowing N acquisition. Meanwhile, NH_4^+ uptake would require proton secretion (or anion uptake), which may shift soil pH making further NH_4^+ uptake more difficult. Nitrate-N comprised over 90% of the available N in the soil before the trial was planted, a trend which is not unusual, as NO_3^- often dominates inorganic N pools in arable soils (Marschner, 2011). These relative abundances of N sources may have led to AMF hyphal physiology being acclimated to nitrate uptake (Garraway and Evans, 1984), meaning suddenly-available NH_4^+ could not be acquired effectively. Although the movement and cycling of nitrate and ammonium are known to be influenced by soil moisture (Homyak et al., 2017), precipitation data for the site (**Supplementary Information, Table 1**) indicates no extraordinary rainfall in the weeks over which the experiment took place, suggesting this was of minor importance here.

While recovery of only 1.6% of the ^{15}N label seems low, total ^{15}N recovery is likely to have been greater than the data suggests. Our data are derived from the aboveground tissue of one plant proximal to the mesh-walled core into which isotopes were added, and it is probable that the roots of numerous plants would have been in close proximity to the core. As such, further ^{15}N is likely to have been acquired by multiple plants. Furthermore, greater ^{15}N uptake into plant shoots may have been recorded if the shoot tissue samples had been taken longer after ^{15}N addition to the mesh-walled cores.

Mesh-walled exclusion cores have been used to quantify AMF-plant nutrient dynamics in a number of studies (Johnson et al., 2001; Field et al., 2012; Field et al., 2016), and are of particular utility where the establishment of truly non-mycorrhizal control plants is not feasible, as in this study. The use of a 0.45 µm nitrocellulose membrane to exclude AMF in-growth to soil compartments is a well-established methodology in the literature (Hodge et al., 2001; Leigh et al., 2009; Thirkell et al., 2016; Storer et al., 2018), although some concerns arise in relation to the effects of such small pore sizes on solute movement, although in the case of studies investigating mycorrhizal P uptake, such effects have been determined to be insignificant (see Zhang et al., 2016; Svenningsen et al., 2018). Our data show increased plant ^{15}N uptake in plots only where N was supplied as nitrate, to Meridian barley, and in plots which had received high rates of N fertiliser (**Figure 3**). Were the movement of N through these systems determined by the porosity of the membranes used in "no access" treatments, we might expect ^{15}N enrichment in all plots which received $^{15}NO_3^-$, which is not the case. Alternative control treatments to disentangle the effects of AMF on plant nutrition might be tested further in future studies to determine the relative merits of each method. Non-mycorrhiza-forming mutants of a

number of cereals have been developed (Paszkowski et al., 2006; Watts-Williams and Cavagnaro, 2015) but to date no mycorrhizal-defective barley mutants are available against which data from hyphal exclusion experiments can be compared. Furthermore, an AMF-colonised plant is morphologically (Gutjahr et al., 2009) and physiologically (Luginbuehl and Oldroyd, 2017) distinct from one which remains uncolonised, and comparisons between AM and mycorrhiza-defective mutants may erroneously conflate these differences and ascribe all contrasts to the lack of mycorrhizas. Combinations of experimental approaches may be employed here to improve the rigour of field experimentation, although the logistics of such trials may prove represent a significant challenge.

Identifying the mechanisms responsible for differential nitrogen transfer from fungus to plant are beyond the scope of this study, but a number of possibilities may be considered. Numerous studies have demonstrated shifts in AMF community composition or structure following N fertilisation, in grassland (Egerton-Warburton and Allen, 2000; Egerton-Warburton et al., 2007; Antoninka et al., 2011; Jiang et al., 2018) and arable systems (Verbruggen et al., 2010; Avio et al., 2013; Liu et al., 2014; Williams et al., 2017). As AMF isolates are known to be functionally different (Avio et al., 2006; Mensah et al., 2015) any N-driven shifts in AMF community have the potential to influence the N cycling in the system (Herman et al., 2012). Future experimental testing of the AMF community composition within cereal roots, combined with isotopic tracer studies may elucidate any link between the structure and function of AMF communities in agronomic systems.

CONCLUSIONS

Our data show that AMF transfer of N to plant hosts is influenced by agricultural management decisions, here the cultivar of barley and the rate at which inorganic N fertiliser is supplied. The extent to which symbiotic soil microbes might enhance total nutrient uptake in the field remains to be tested; despite demonstrating a mechanism by which plants acquire N, our data cannot indicate whether non-AMF plants in the same field conditions might show enhanced nutrition. Further experimental investigation is required for a wider perspective on the influence of these fungi on their crop plant hosts, and therefore their importance in agricultural systems.

DATA AVAILABILITY STATEMENT

The datasets generated for this study are included within the supplementary information of this manuscript.

AUTHOR CONTRIBUTIONS

TT, DC, and AH designed the study. TT carried out experimental work and data analysis and wrote the initial draft of the manuscript. All authors contributed to revisions of the manuscript, and read and approved the final submitted version.

FUNDING

This work was supported by a BBSRC White Rose DTP grant: BB/J014443/1.

ACKNOWLEDGMENTS

We thank Kate Storer and Pete Berry from ADAS for permission to use their field trial, and for discussion about the experiment. The barley trial used here was jointly funded by AHDB and CF Fertilisers. We thank Andrew Manfield, on whose land the trial was sited. We thank Heather Walker for help with the IRMS. This manuscript is an adapted and revised version of a thesis chapter submitted by Tom Thirkell for the degree of Doctor of Philosophy at the University of York, UK, in 2017. Experimental data is presented in the **Supplementary Material.**

SUPPLEMENTARY MATERIAL

The Supplementary Material for this article can be found online at: https://www.frontiersin.org/articles/10.3389/fpls.2019.01312/full#supplementary-material

REFERENCES

Agren, G. I., Wetterstedt, J. A. M., and Billberger, M. F. K. (2012). Nutrient limitation on terrestrial plant growth - modeling the interaction between nitrogen and phosphorus. *New Phytol.* 194, 953–960. doi: 10.1111/j.1469-8137.2012.04116.x

Ames, R. N., Reid, C. P. P., Porter, L. K., and Cambardella, C. (1983). Hyphal uptake and transport of nitrogen from 2 ^{15}N-labeled sources by *Glomus mosseae*, a vesicular arbuscular mycorrhizal fungus. *New Phytol.* 95, 381–396. doi: 10.1111/j.1469-8137.1983.tb03506.x

Antoninka, A., Reich, P. B., and Johnson, N. C. (2011). Seven years of carbon dioxide enrichment, nitrogen fertilization and plant diversity influence arbuscular mycorrhizal fungi in a grassland ecosystem. *New Phytol.* 192, 200–214. doi: 10.1111/j.1469-8137.2011.03776.x

Avio, L., Castaldini, M., Fabiani, A., Bedini, S., Sbrana, C., Turrini, A., et al. (2013). Impact of nitrogen fertilization and soil tillage on arbuscular mycorrhizal fungal communities in a mediterranean agroecosystem. *Soil Biol. Biochem.* 67, 285–294. doi: 10.1016/j.soilbio.2013.09.005

Avio, L., Pellegrino, E., Bonari, E., and Giovannetti, M. (2006). Functional diversity of arbuscular mycorrhizal fungal isolates in relation to extraradical mycelial networks. *New Phytol.* 172, 347–357. doi: 10.1111/j.1469-8137.2006.01839.x

Barrett, G., Campbell, C. D., and Hodge, A. (2014). The direct response of the external mycelium of arbuscular mycorrhizal fungi to temperature and the implications for nutrient transfer. *Soil Biol. Biochem.* 78, 109–117. doi: 10.1016/j.soilbio.2014.07.025

Belmondo, S., Fiorilli, V., Perez-Tienda, J., Ferrol, N., Marmeisse, R., and Lanfranco, L. (2014). A dipeptide transporter from the arbuscular mycorrhizal fungus *Rhizophagus irregularis* is upregulated in the intraradical phase. *Front. Plant Sci.* 5, 1–11. doi: 10.3389/fpls.2014.00436

Brackin, R., Atkinson, B. S., Sturrock, C. J., and Rasmussen, A. (2017). Roots-eye view: Using microdialysis and microct to non-destructively map root nutrient

depletion and accumulation zones. *Plant Cell Environ.* 40, 3135–3142. doi: 10.1111/pce.13072

Breuninger, M., Trujillo, C. G., Serrano, E., Fischer, R., and Requena, N. (2004). Different nitrogen sources modulate activity but not expression of glutamine sythetase in arbuscular mycorrhizal fungi. *Fungal Genet. Biol.* 41 (5), 542–552. doi: 10.1016/j.fgb.2004.01.003

Bucking, H., and Kafle, A. (2015). Role of arbuscular mycorrhizal fungi in the nitrogen uptake of plants: current knowledge and research gaps. *Agronomy-Basel* 5, 587–612. doi: 10.3390/agronomy5040587

Cameron, K. C., Di, H. J., and Moir, J. L. (2013). Nitrogen losses from the soil/plant system: a review. *Ann. Appl. Biol.* 162, 145–173. doi: 10.1111/aab.12014

Cavagnaro, T. R., Bender, S. F., Asghari, H. R., and Van Der Heijden, M. G. A. (2015). The role of arbuscular mycorrhizas in reducing soil nutrient loss. *Trends Plant Sci.* 20, 283–290. doi: 10.1016/j.tplants.2015.03.004

Courty, P. E., Smith, P., Koegel, S., Redecker, D., and Wipf, D. (2015). Inorganic nitrogen uptake and transport in beneficial plant root-microbe interactions. *Critic. Rev. Plant Sci.* 34, 4–16. doi: 10.1080/07352689.2014.897897

Cui, M., and Caldwell, M. M. (1996a). Facilitation of plant phosphate acquisition by arbuscular mycorrhizas from enriched soil patches.1. Roots and hyphae exploiting the same soil volume. *New Phytol.* 133, 453–460. doi: 10.1111/j.1469-8137.1996.tb01912.x

Cui, M. Y., and Caldwell, M. M. (1996b). Facilitation of plant phosphate acquisition by arbuscular mycorrhizas from enriched soil patches.2. Hyphae exploiting root-free soil. *New Phytol.* 133, 461–467. doi: 10.1111/j.1469-8137.1996.tb01913.x

Davison, J., Moora, M., Opik, M., Adholeya, A., Ainsaar, L., Ba, A., et al. (2015). Global assessment of arbuscular mycorrhizal fungus diversity reveals very low endemism. *Science* 349, 970–973. doi: 10.1126/science.aab1161

Egerton-Warburton, L. M., and Allen, E. B. (2000). Shifts in arbuscular mycorrhizal communities along an anthropogenic nitrogen deposition gradient. *Ecol. Appl.* 10, 484–496. doi: 10.1890/1051-0761(2000)010[0484:SIAMCA]2.0.CO;2

Egerton-Warburton, L. M., Johnson, N. C., and Allen, E. B. (2007). Mycorrhizal community dynamics following nitrogen fertilization: a cross-site test in five grasslands. *Ecol. Monogr.* 77, 527–544. doi: 10.1890/06-1772.1

Ezawa, T., and Saito, K. (2018). How do arbuscular mycorrhizal fungi handle phosphate? New insight into fine-tuning of phosphate metabolism. *New Phytol.* 220, 1116–1121. doi: 10.1111/nph.15187

Field, K. J., Cameron, D. D., Leake, J. R., Tille, S., Bidartondo, M. I., and Beerling, D. J. (2012). Contrasting arbuscular mycorrhizal responses of vascular and non-vascular plants to a simulated palaeozoic CO_2 decline. *Nat. Commun.* 3, 1–8. doi: 10.1038/ncomms1831

Field, K. J., Rimington, W. R., Bidartondo, M. I., Allinson, K. E., Beerling, D. J., Cameron, D. D., et al. (2016). Functional analysis of liverworts in dual symbiosis with Glomeromycota and Mucoromycotina fungi under a simulated palaeozoic CO_2 decline. *ISME J.* 10, 1514–1526. doi: 10.1038/ismej.2015.204

Garcia, K., Doidy, J., Zimmermann, S. D., Wipf, D., and Courty, P. E. (2016). Take a trip through the plant and fungal transportome of mycorrhiza. *Trends Plant Sci.* 21, 937–950. doi: 10.1016/j.tplants.2016.07.010

Garraway, M. O., and Evans, R. C. (1984). *Fungal nutrition and physiology*. USA, John Wiley & Sons: New York.

Gosling, P., Hodge, A., Goodlass, G., and Bending, G. D. (2006). Arbuscular mycorrhizal fungi and organic farming. *Agric. Ecosyst. Environ.* 113, 17–35. doi: 10.1016/j.agee.2005.09.009

Govindarajulu, M., Pfeffer, P. E., Jin, H. R., Abubaker, J., Douds, D. D., Allen, J. W., et al. (2005). Nitrogen transfer in the arbuscular mycorrhizal symbiosis. *Nature* 435, 819–823. doi: 10.1038/nature03610

Gutjahr, C., Casieri, L., and Paszkowski, U. (2009). *Glomus intraradices* induces changes in root system architecture of rice independently of common symbiosis signaling. *New Phytol.* 182, 829–837. doi: 10.1111/j.1469-8137.2009.02839.x

Hawkesford, M. J. (2014). Reducing the reliance on nitrogen fertilizer for wheat production. *J. Cereal Sci.* 59, 276–283. doi: 10.1016/j.jcs.2013.12.001

Hawkins, H. J., and George, E. (2001). Reduced N-15-nitrogen transport through arbuscular mycorrhizal hyphae to *Triticum aestivum* L. Supplied with ammonium vs. nitrate nutrition. *Ann. Bot.* 87, 303–311. doi: 10.1006/anbo.2000.1305

Hawkins, H. J., Johansen, A., and George, E. (2000). Uptake and transport of organic and inorganic nitrogen by arbuscular mycorrhizal fungi. *Plant Soil* 226, 275–285. doi: 10.1023/A:1026500810385

Herman, D. J., Firestone, M. K., Nuccio, E., and Hodge, A. (2012). Interactions between an arbuscular mycorrhizal fungus and a soil microbial community mediating litter decomposition. *FEMS Microbiol. Ecol.* 80, 236–247.10. doi: 10.1111/j.1574-6941.2011.01292.x

Hodge, A. (2001). Arbuscular mycorrhizal fungi influence decomposition of, but not plant nutrient capture from, glycine patches in soil. *New Phytol.* 151, 725–734. doi: 10.1046/j.0028-646x.2001.00200.x

Hodge, A. (2014). Interactions between arbuscular mycorrhizal fungi and organic material substrates. *Adv. Appl. Microbiol.* 89, 47–99. doi: 10.1016/B978-0-12-800259-9.00002-0

Hodge, A. (2017). "Accessibility of inorganic and organic nutrients for mycorrhizas," in *Mycorrhizal mediation of soil fertility, structure and carbon storage*. Eds. N. Johnson, C. Gehring, and J. Jansa (Amsterdam, Netherlands: Elsevier), 129–148. doi: 10.1016/B978-0-12-804312-7.00008-5

Hodge, A., Campbell, C. D., and Fitter, A. H. (2001). An arbuscular mycorrhizal fungus accelerates decomposition and acquires nitrogen directly from organic material. *Nature* 413, 297–299. doi: 10.1038/35095041

Hodge, A., and Fitter, A. H. (2010). Substantial nitrogen acquisition by arbuscular mycorrhizal fungi from organic material has implications for N cycling. *Proc. Natl. Acad. Sci. U.S.A.* 107, 13754–13759. doi: 10.1073/pnas.1005874107

Hodge, A., Helgason, T., and Fitter, A. H. (2010). Nutritional ecology of arbuscular mycorrhizal fungi. *Fungal Ecol.* 3, 267–273. doi: 10.1016/j.funeco.2010.02.002

Hodge, A., and Storer, K. (2015). Arbuscular mycorrhiza and nitrogen: implications for individual plants through to ecosystems. *Plant Soil* 386, 1–19. doi: 10.1007/s11104-014-2162-1

Homyak, P. M., Allison, S. D., Huxman, T. E., Goulden, M. L., and Treseder, K. K. (2017). Effects of drought manipulation on soil nitrogen cycling: a meta-analysis. *J. Geophys. Res. Biogeosci.* 122, 3260–3272. doi: 10.1002/2017JG004146

Jiang, S. J., Liu, Y. J., Luo, J. J., Qin, M. S., Johnson, N. C., Opik, M., et al. (2018). Dynamics of arbuscular mycorrhizal fungal community structure and functioning along a nitrogen enrichment gradient in an alpine meadow ecosystem. *New Phytol.* 220, 1222–1235. doi: 10.1111/nph.15112

Jin, H., Pfeffer, P. E., Douds, D. D., Piotrowski, E., Lammers, P. J., and Shachar-Hill, Y. (2005). The uptake, metabolism, transport and transfer of nitrogen in an arbuscular mycorrhizal symbiosis. *New Phytol.* 168, 687–696. doi: 10.1111/j.1469-8137.2005.01536.x

Johansen, A., Jakobsen, I., and Jensen, E. S. (1993). Hyphal transport by a vesicular-arbuscular mycorrhizal fungus of N applied to the soil as ammonium or nitrate. *Biol. Fertil. Soils* 16, 66–70. doi: 10.1007/BF00336518

Johnson, D., Leake, J. R., and Read, D. J. (2001). Novel in-growth core system enables functional studies of grassland mycorrhizal mycelial networks. *New Phytol.* 152, 555–562. doi: 10.1046/j.0028-646X.2001.00273.x

Johnson, N. C. (2010). Resource stoichiometry elucidates the structure and function of arbuscular mycorrhizas across scales. *New Phytol.* 185, 631–647. doi: 10.1111/j.1469-8137.2009.03110.x

Johnson, N. C., Wilson, G. W. T., Wilson, J. A., Miller, R. M., and Bowker, M. A. (2015). Mycorrhizal phenotypes and the law of the minimum. *New Phytol.* 205, 1473–1484. doi: 10.1111/nph.13172

Kahkola, A. K., Nygren, P., Leblanc, H. A., Pennanen, T., and Pietikainen, J. (2012). Leaf and root litter of a legume tree as nitrogen sources for cacaos with different root colonisation by arbuscular mycorrhizae. *Nutr Cycl Agroecosys* 92, 51–65. doi: 10.1007/s10705-011-9471-z

Karasawa, T., Hodge, A., and Fitter, A. H. (2012). Growth, respiration and nutrient acquisition by the arbuscular mycorrhizal fungus glomus mosseae and its host plant *Plantago lanceolata* in cooled soil. *Plant Cell Environ.* 35, 819–828. doi: 10.1111/j.1365-3040.2011.02455.x

Ladha, J. K., Pathak, H., Krupnik, T. J., Six, J., and Van Kessel, C. (2005). Efficiency of fertilizer nitrogen in cereal production: retrospects and prospects. *Adv. Agro.* 87, 85–156. doi: 10.1016/S0065-2113(05)87003-8

Ladha, J. K., Tirol-Padre, A., Reddy, C. K., Cassman, K. G., Verma, S., Powlson, D. S., et al. (2016). Global nitrogen budgets in cereals: a 50-year assessment for maize, rice, and wheat production systems. *Sci. Rep.* 6, 1–9. doi: 10.1038/srep19355

Leigh, J., Hodge, A., and Fitter, A. H. (2009). Arbuscular mycorrhizal fungi can transfer substantial amounts of nitrogen to their host plant from organic material. *New Phytol.* 181, 199–207. doi: 10.1111/j.1469-8137.2008.02630.x

Lekberg, Y., and Helgason, T. (2018). *In situ* mycorrhizal function - knowledge gaps and future directions. *New Phytol.* 220, 957–962. doi: 10.1111/nph.15064

Liu, W., Jiang, S. S., Zhang, Y. L., Yue, S. C., Christie, P., Murray, P. J., et al. (2014). Spatiotemporal changes in arbuscular mycorrhizal fungal communities under different nitrogen inputs over a 5-year period in intensive agricultural ecosystems on the north china plain. *FEMS Microbiol. Ecol.* 90, 436–453. doi: 10.1111/1574-6941.12405

Luginbuehl, L. H., and Oldroyd, G. E. D. (2017). Understanding the arbuscule at the heart of endomycorrhizal symbioses in plants. *Curr. Biol.* 27, R952–R963. doi: 10.1016/j.cub.2017.06.042

Marschner, H. (2011). *Mineral nutrition of higher plants*. Academic Press: London.

Masclaux-Daubresse, C., Daniel-Vedele, F., Dechorgnat, J., Chardon, F., Gaufichon, L., and Suzuki, A. (2010). Nitrogen uptake, assimilation and remobilization in plants: challenges for sustainable and productive agriculture. *Ann. Bot.* 105, 1141–1157. doi: 10.1093/aob/mcq028

McGonigle, T. P., Miller, M. H., Evans, D. G., Fairchild, G. L., and Swan, J. A. (1990). A new method which gives an objective-measure of colonization of roots by vesicular arbuscular mycorrhizal fungi. *New Phytol.* 115, 495–501. doi: 10.1111/j.1469-8137.1990.tb00476.x

Mensah, J. A., Koch, A. M., Antunes, P. M., Kiers, E. T., Hart, M., and Bucking, H. (2015). High functional diversity within species of arbuscular mycorrhizal fungi is associated with differences in phosphate and nitrogen uptake and fungal phosphate metabolism. *Mycorrhiza* 25, 533–546. doi: 10.1007/s00572-015-0631-x

Paszkowski, U., Jakovleva, L., and Boller, T. (2006). Maize mutants affected at distinct stages of the arbuscular mycorrhizal symbiosis. *Plant J.* 47, 165–173. doi: 10.1111/j.1365-313X.2006.02785.x

Pretty, J. (2008). Agricultural sustainability: concepts, principles and evidence. *Philos. Trans. R. Soc. Lond., B, Biol. Sci.* 363, 447–465. doi: 10.1098/rstb.2007.2163

Pretty, J. (2018). Intensification for redesigned and sustainable agricultural systems. *Science* 362, 908–90+. doi: 10.1126/science.aav0294

Reynolds, H. L., Hartley, A. E., Vogelsang, K. M., Bever, J. D., and Schultz, P. A. (2005). Arbuscular mycorrhizal fungi do not enhance nitrogen acquisition and growth of old-field perennials under low nitrogen supply in glasshouse culture. *New Phytol.* 167, 869–880. doi: 10.1111/j.1469-8137.2005.01455.x

Rillig, M. C., Aguilar-Trigueros, C. A., Camenzind, T., Cavagnaro, T. R., Degrune, F., Hohmann, P., et al. (2019). Why farmers should manage the arbuscular mycorrhizal symbiosis. *New Phytol.* 222, 1171–1175. doi: 10.1111/nph.15602

Rillig, M. C., Sosa-Hernandez, M. A., Roy, J., Aguilar-Trigueros, C. A., Valyi, K., and Lehmann, A. (2016). Towards an integrated mycorrhizal technology: harnessing mycorrhiza for sustainable intensification in agriculture. *Front. Plant Sci.* 7, 1–5. doi: 10.3389/fpls.2016.01625

Ryan, M. H., and Graham, J. H. (2018). Little evidence that farmers should consider abundance or diversity of arbuscular mycorrhizal fungi when managing crops. *New Phytol.* 220, 1092–1107. doi: 10.1111/nph.15308

Sanders, F. E., and Tinker, P. B. (1973). Phosphate inflow into mycorrhizal roots. *Pestic. Sci.* 4, 385–395. doi: 10.1002/ps.2780040316

Smith, F. A., and Smith, S. E. (2011a). What is the significance of the arbuscular mycorrhizal colonisation of many economically important crop plants? *Plant Soil* 348, 63–79. doi: 10.1007/s11104-011-0865-0

Smith, G. S., Johnston, C. M., and Cornforth, I. S. (1983). Comparison of nutrient solutions for growth of plants in sand culture. *New Phytol.* 94, 537–548. doi: 10.1111/j.1469-8137.1983.tb04863.x

Smith, S. E., and Read, D. J. (2008). *Mycorrhizal symbiosis*. Academic Press: London.

Smith, S. E., and Smith, F. A. (2011b). Roles of arbuscular mycorrhizas in plant nutrition and growth: new paradigms from cellular to ecosystem scales. *Annu. Rev. Plant Biol.* 62, 227–250. doi: 10.1146/annurev-arplant-042110-103846

Smith, S. E., Smith, F. A., and Jakobsen, I. (2003). Mycorrhizal fungi can dominate phosphate supply to plants irrespective of growth responses. *Plant Physiol.* 133, 16–20. doi: 10.1104/pp.103.024380

Smith, S. E., Smith, F. A., and Jakobsen, I. (2004). Functional diversity in arbuscular mycorrhizal (AM) symbioses: the contribution of the mycorrhizal P uptake pathway is not correlated with mycorrhizal responses in growth or total P uptake. *New Phytol.* 162, 511–524. doi: 10.1111/j.1469-8137.2004.01039.x

Sosa-Hernandez, M. A., Roy, J., Hempel, S., Kautz, T., Kopke, U., Uksa, M., et al. (2018). Subsoil arbuscular mycorrhizal fungal communities in arable soil differ from those in topsoil. *Soil Biol. Biochem.* 117, 83–86. doi: 10.1016/j.soilbio.2017.11.009

Staddon, P. L., Fitter, A. H., and Graves, J. D. (1999). Effect of elevated atmospheric co2 on mycorrhizal colonization, external mycorrhizal hyphal production and phosphorus inflow in *Plantago lanceolata* and *Trifolium repens* in association with the arbuscular mycorrhizal fungus *Glomus mosseae*. *Global Change Biol.* 5, 347–358. doi: 10.1046/j.1365-2486.1999.00230.x

Staddon, P. L., Ramsey, C. B., Ostle, N., Ineson, P., and Fitter, A. H. (2003). Rapid turnover of hyphae of mycorrhizal fungi determined by AMS microanalysis of 14C. *Science* 300 (5622), 1138–1140. doi: 10.1126/science.1084269

Storer, K., Coggan, A., Ineson, P., and Hodge, A. (2018). Arbuscular mycorrhizal fungi reduce nitrous oxide emissions from N_2O hotspots. *New Phytol.* 220, 1285–1295. doi: 10.1111/nph.14931

Svenningsen, N. B., Watts-Williams, S. J., Joner, E. J., Battini, F., Efthymiou, A., Cruz-Paredes, C., et al. (2018). Suppression of the activity of arbuscular mycorrhizal fungi by the soil microbiota. *ISME J.* 12, 1296–1307. doi: 10.1038/s41396-018-0059-3

Thirkell, T. J., Cameron, D. D., and Hodge, A. (2016). Resolving the 'nitrogen paradox' of arbuscular mycorrhizas: fertilization with organic matter brings considerable benefits for plant nutrition and growth. *Plant Cell Environ.* 39, 1683–1690. doi: 10.1111/pce.12667

Thirkell, T. J., Charters, M. D., Elliott, A. J., Sait, S. M., and Field, K. J. (2017). Are mycorrhizal fungi our sustainable saviours? Considerations for achieving food security. *J. Ecol.* 105, 921–929, 2745.12788. doi: 10.1111/1365-2745.12788

Tinker, P. B., and Nye, P. H. (2000). *Solute movement in the rhizosphere*. Oxford University Press: Oxford.

Tisserant, E., Kohler, A., Dozolme-Seddas, P., Balestrini, R., Benabdellah, K., Colard, A., et al. (2012). The transcriptome of the arbuscular mycorrhizal fungus *Glomus intraradices* (DAOM 197198) reveals functional tradeoffs in an obligate symbiont. *New Phytol.* 193, 755–769. doi: 10.1111/j.1469-8137.2011.03948.x

UKSO. 2016. *Soilscapes for England and Wales* [Online]. Available: http://mapapps2.bgs.ac.uk/ukso/home.html [Accessed 20/08 2016].

Verbruggen, E., Roling, W. F. M., Gamper, H. A., Kowalchuk, G. A., Verhoef, H. A., and Van Der Heijden, M. G. A. (2010). Positive effects of organic farming on below-ground mutualists: large-scale comparison of mycorrhizal fungal communities in agricultural soils. *New Phytol.* 186, 968–979. doi: 10.1111/j.1469-8137.2010.03230.x

Watts-Williams, S. J., and Cavagnaro, T. R. (2015). Using mycorrhiza-defective mutant genotypes of non-legume plant species to study the formation and functioning of arbuscular mycorrhiza: a review. *Mycorrhiza* 25, 587–597. doi: 10.1007/s00572-015-0639-2

Whiteside, M. D., Digman, M. A., Gratton, E., and Treseder, K. K. (2012a). Organic nitrogen uptake by arbuscular mycorrhizal fungi in a boreal forest. *Soil Biol. Biochem.* 55, 7–13. doi: 10.1016/j.soilbio.2012.06.001

Whiteside, M. D., Garcia, M. O., and Treseder, K. K. (2012b). Amino acid uptake in arbuscular mycorrhizal plants. *Plos One* 7, 1–4. doi: 10.1371/journal.pone.0047643

Williams, A., Manoharan, L., Rosenstock, N. P., Olsson, P. A., and Hedlund, K. (2017). Long-term agricultural fertilization alters arbuscular mycorrhizal fungal community composition and barley (*Hordeum vulgare*) mycorrhizal carbon and phosphorus exchange. *New Phytol.* 213, 874–885. doi: 10.1111/nph.14196

Zadoks, J. C., Chang, T. T., Konzak, C. F,. (1974). A decimal code for the growth stages of cereals. *Weed Res.* 14 (6), 415–421. doi: 10.1111/j.1365-3180.1974.tb01084.x

Zhang, L., Xu, M. G., Liu, Y., Zhang, F. S., Hodge, A., and Feng, G. (2016). Carbon and phosphorus exchange may enable cooperation between an arbuscular mycorrhizal fungus and a phosphate-solubilizing bacterium. *New Phytol.* 210, 1022–1032. doi: 10.1111/nph.13838

Conflict of Interest: The authors declare that the research was conducted in the absence of any commercial or financial relationships that could be construed as a potential conflict of interest.

frontiers in Plant Science

ORIGINAL RESEARCH
published: 12 December 2019
doi: 10.3389/fpls.2019.01617

Imbalanced Regulation of Fungal Nutrient Transports According to Phosphate Availability in a Symbiocosm Formed by Poplar, Sorghum, and *Rhizophagus irregularis*

OPEN ACCESS

Edited by:
Raffaella Balestrini, Italian National Research Council (IPSP-CNR), Italy

Reviewed by:
Philipp Franken, Friedrich Schiller University Jena, Germany
Cristiana Sbrana, Istituto di Biologia e Biotecnologia Agraria (IBBA), Italy

***Correspondence:**
Pierre-Emmanuel Courty
pierre-emmanuel.courty@inra.fr

†These authors have contributed equally to this work

Specialty section:
This article was submitted to Plant Microbe Interactions, a section of the journal Frontiers in Plant Science

Received: *31 July 2019*
Accepted: *18 November 2019*
Published: *12 December 2019*

Citation:
Calabrese S, Cusant L, Sarazin A, Niehl A, Erban A, Brulé D, Recorbet G, Wipf D, Roux C, Kopka J, Boller T and Courty P-E (2019) Imbalanced Regulation of Fungal Nutrient Transports According to Phosphate Availability in a Symbiocosm Formed by Poplar, Sorghum, and Rhizophagus irregularis. Front. Plant Sci. 10:1617. doi: 10.3389/fpls.2019.01617

Silvia Calabrese[1†], Loic Cusant[2†], Alexis Sarazin[3†], Annette Niehl[1], Alexander Erban[4], Daphnée Brulé[1,5], Ghislaine Recorbet[5], Daniel Wipf[5], Christophe Roux[2], Joachim Kopka[4], Thomas Boller[1] and Pierre-Emmanuel Courty[1,5]*

[1] Department of Environmental Sciences, Botany, Zurich-Basel Plant Science Center, University of Basel, Basel, Switzerland, [2] Laboratoire de Recherche en Sciences Végétales, Université de Toulouse, UPS, CNRS, Castanet-Tolosan, France, [3] Department of Biology at the Swiss Federal Institute of Technology Zurich, Zurich, Switzerland, [4] Max Planck Institute of Molecular Plant Physiology, Potsdam-Golm, Germany, [5] Agroécologie, AgroSup Dijon, CNRS, INRAE, Univ. Bourgogne, Univ. Bourgogne Franche-Comté, Dijon, France

In arbuscular mycorrhizal (AM) symbiosis, key components of nutrient uptake and exchange are specialized transporters that facilitate nutrient transport across membranes. As phosphate is a nutrient and a regulator of nutrient exchanges, we investigated the effect of P availability to extraradical mycelium (ERM) on both plant and fungus transcriptomes and metabolomes in a symbiocosm system. By perturbing nutrient exchanges under the control of P, our objectives were to identify new fungal genes involved in nutrient transports, and to characterize in which extent the fungus differentially modulates its metabolism when interacting with two different plant species. We performed transportome analysis on the ERM and intraradical mycelium of the AM fungus *Rhizophagus irregularis* associated to *Populus trichocarpa* and *Sorghum bicolor* under high and low P availability in ERM, using quantitative RT-PCR and Illumina mRNA-sequencing. We observed that mycorrhizal symbiosis induces expression of specific phosphate and ammonium transporters in both plants. Furthermore, we identified new AM-inducible transporters and showed that a subset of phosphate transporters is regulated independently of symbiotic nutrient exchange. mRNA-Sequencing revealed that the fungal transportome was not similarly regulated in the two host plant species according to P availability. Mirroring this effect, many plant carbohydrate transporters were down-regulated in *P. trichocarpa* mycorrhizal root tissue. Metabolome analysis revealed further that AM root colonization led to a modification of root primary metabolism under low and high P availability and to a decrease of primary metabolite pools in general. Moreover, the down regulation of the sucrose transporters suggests that the plant limits carbohydrate long distance transport

(i.e. from shoot to the mycorrhizal roots). By simultaneous uptake/reuptake of nutrients from the apoplast at the biotrophic interface, plant and fungus are both able to control reciprocal nutrient fluxes.

Keywords: arbuscular mycorrhizal fungi, symbiocosm, extraradical mycelium, intraradical mycelium, phosphorus, ammonium, carbohydrates transporters, lipid metabolism

HIGHLIGHT

Gene expression analysis in arbuscular mycorrhizal symbiosis upon phosphate variations reveals imbalanced fungal gene regulation between perennial/C3 and annual/C4 host, highlights new mycorrhiza-inducible transporters and suggests active fungal carbohydrate uptake.

INTRODUCTION

Phosphorus (P), and nitrogen (N), are among the most essential nutrients for plants. As P is present in many biological compounds and is involved in many key metabolic processes, it can make up to 0.2% of the dry weight of a plant (Schachtman et al., 1998). In living plants, the cellular inorganic phosphate (Pi) concentration ranges between 1 and 10 mM whereas the soil water Pi concentration, is about 10,000-times less (Rausch and Bucher, 2002; Ai et al., 2009; Branscheid et al., 2010): Due to its negative charge and its low mobility, Pi is rapidly sequestered by cations and organic substances in the soil (e.g. clay) and therefore only barely accessible to plants (Poirier and Bucher, 2002; Aung et al., 2006; Chiou et al., 2006; Javot et al., 2007a; Tatry et al., 2009). To prevent mineral nutrient deficiency, and P deficiency in particular, a majority of land plants form symbioses with the so called arbuscular mycorrhizal (AM) fungi. In the AM symbiosis the AM fungus provides macro and micro nutrients to the plants and in return receives carbohydrates from the host plant (Smith and Read, 2008). AM fungi have a broad host range: each fungal species, each genet can colonize several plant individuals, also from different species, connected each other and forming a so called common mycorrhizal network (Walder et al., 2012; Fellbaum et al., 2014). The extraradical mycelium (ERM) of the AM fungi engaged in such a network is able to acquire nutrients that are out of reach or not accessible to the plant partners. For a given plant, this makes the mycorrhizal uptake pathway often more effective than the direct uptake pathway (Wipf et al., 2019). The nutrients taken up by the ERM are transported to the hyphal network inside the host root *via* the intraradical mycelium (IRM), which forms highly branched tree-like structures (arbuscules) inside the root cortical cells. The arbuscules are still surrounded by the plant cell-derived periarbuscular membrane and the inter-membrane interstice, the periarbuscular space. Within this structure, the mineral nutrients acquired by the AM fungus are exported to the periarbuscular space, and taken up by plant nutrient transporters of the periarbuscular membrane (Smith and Smith, 2011).

With respect to Pi, the extent to which plants cover their Pi-demand through the AM fungus ranges from only a small percentage to 100% (Paszkowski, 2006; Javot et al., 2007a). The Pi taken up by the ERM is incorporated into poly-P, transported to the arbuscules, hydrolyzed and translocated to the periarbuscular space (Ezawa et al., 2002; Javot et al., 2007a; Kikuchi et al., 2016). Essential key players in this process are transporters and permeases that facilitate uptake and transport of nutrients across membranes. The expression of transporters is regulated by nutrient availability. In this way, a steady and efficient translocation of nutrients adapted to given environmental conditions can be guaranteed (Smith and Smith, 2011; Courty et al., 2015; Garcia et al., 2016; Wipf et al., 2019).

In AM fungi, only few phosphate transporters (PT) were characterized so far: one in *Funneliformis mosseae* (GmosPT, Benedetto et al., 2005) and *Glomus versiforme* (GvPT, Harrison and Buuren 1995), and seven in *Rhizophagus irregularis* (formerly *Glomus intraradices*, RiPT1-RiPT7; Maldonado-Mendoza et al., 2001; Walder et al., 2016). Expression of the three high affinity transporters, *RiPT1*, *GvPT,* and *GmosPT*, is dependent on external Pi concentrations in the ERM (Harrison and Buuren, 1995; Maldonado-Mendoza et al., 2001; Benedetto et al., 2005). Reduced expression of *GmosPT* in the IRM compared to the ERM suggested a concentration-dependent regulation of PTs in the symbiotic root tissue.

In plants, the family of PTs can be divided into three subfamilies. Subfamily I transporters (Pht1) are membrane bound H^+/P symporters driven by an H^+ gradient. They are a subgroup of the major facilitator superfamily to which most of the PTs known to date belong (Pao et al., 1998). Subfamily II members are located in the plastids and function as antiporters (Poirier and Bucher, 2002; Rausch and Bucher, 2002; Javot et al., 2007b); members of the subfamily III are located in the mitochondrial inner membrane and are predicted to function as H^+/P symporters or as P/OH^- antiporters (Takabatake et al., 1999; Javot et al., 2007b). In mycorrhizal plants, some Pht1 PT are specifically induced during symbiotic interaction. The first mycorrhiza-inducible PT was identified in *Solanum tuberosum* (StPT3) and was localized in arbusculated root sections (Rausch et al., 2001). Then, more mycorrhiza-inducible transporters were identified in several other plants (Harrison et al., 2002; Glassop et al., 2005; Nagy et al., 2005; Loth-Pereda et al., 2011). StPT3 and MtPT4 from *Medicago truncatula* were present in the periarbuscular membrane only. Furthermore, it was demonstrated that MtPT4-deficient plants

Abbreviations: AM, Arbuscular mycorrhiza; AMF, Arbuscular mycorrhizal fungi; AMT, Ammonium transporter; ERM, Extraradical mycelium; IRM, Intraradical mycelium; N, Nitrogen; P, Phosphorus; Pi, inorganic phosphate; PT, Phosphate transporter; GS/GOGAT, glutamine synthetase/glutamine oxoglutarate aminotransferase.

accumulated Pi as poly-P in the arbuscules, which resulted in a premature collapse of the arbuscules and in inefficient symbiosis (Javot et al., 2007a; Breuillin-Sessoms et al., 2015).

For N, it was long assumed that AM symbiosis plays only a minor role in plant nutrition. In the soil, inorganic N is mostly present as nitrate or ammonium, both of which are readily mobile in the soil. Therefore, it was assumed that AM fungi take up N with the same efficiency as plants (Marschner and Dell, 1994; Hodge et al., 2010; Smith and Smith, 2011). But, it was shown that AM fungi can contribute up to 42% of the plant N demand (Frey and Schüepp, 1993; Mäder et al., 2000; Govindarajulu et al., 2005). In addition to the uptake of ammonium and nitrate, it was shown that AM fungi can take up N in the form of organic molecules (*i.e.* small peptides and amino acids) (Bago et al., 1996; Hawkins et al., 2000; Govindarajulu et al., 2005; Jin et al., 2005) and possibly also in the form of more complex organic compounds (Leigh et al., 2009; Hodge et al., 2010). However, in plants as well as in AM fungi, it was shown that ammonium is the preferred N source, as it can be directly incorporated into glutamine by the glutamine synthetase/glutamine oxoglutarate aminotransferase (GS/GOGAT) pathway whereas nitrate needs to be reduced to ammonium before N assimilation in the GS/GOGAT pathway (Villegas et al., 1996; Hawkins et al., 2000; Toussaint et al., 2004). In the ERM of AM fungi, the glutamine is further metabolized into amino acids such as arginine, alanine and asparagine for transport. Studies using ^{15}N showed that arginine was the most common labelled amino acid in the ERM of AM fungi (Govindarajulu et al., 2005). Arginine is then transported from the ERM to the IRM where it is cleaved by arginases in the arbuscules. The released ammonium is transported to the periarbuscular space where it can be taken up by the plant ammonium transporters (AMT). So far, only six transporters have been identified and functionally characterized in Glomeromycotina, three in *R. irregularis* GintAMT1, GintAMT2 and GintAMT3 (López-Pedrosa et al., 2006; Pérez-Tienda et al., 2011; Calabrese et al., 2016), and three in *Geosiphon pyriformis* (GpAmt1, GpAmt2, GpAmt3; Ellerbeck et al., 2013).

In plants, the family of AMT can be divided into two subfamilies: subfamily I and subfamily II (reviewed in Courty et al., 2015). While members of the subfamily I were found to be mostly expressed in roots, members of the subfamily II were preferentially expressed in shoots (Couturier et al., 2007). Several mycorrhiza-inducible AMTs have been identified through gene expression analysis in several plant species (Gomez et al., 2009; Guether et al., 2009), including *PtAMT1.2* in poplar (Selle et al., 2005; Couturier et al., 2007) and *SbAMT3.1* and *SbAMT4* in sorghum (Koegel et al., 2013).

In return for the mineral nutrient, the AM fungi receives photosynthetates from the plants. In absence of gene encoding fatty acid synthase in their genome (Wewer et al., 2014; Tang et al., 2016), AM fungi are dependent to host fatty acids. Although the mechanism of transfer remains unknown, it was demonstrated that palmitic acid is transferred from plant roots to symbiotic mycelium, putatively esterified as mono-acyl-glycerol (Bravo et al., 2017; Jiang et al., 2017; Luginbuehl et al., 2017). Research on sugar transporter (SUT) expression in plants is not as consistent. Mycorrhization caused either increased or decreased expression of SUTs in root and shoots of the host plants (Ge et al., 2008; Boldt et al., 2011; Doidy et al., 2012a). A new class of SUT, the SWEETs, was identified. These transporters are located in the plasma membrane and have been shown to function as bidirectional sugar uniporters (Chen et al., 2010). Due to their involvement in rhizobial symbiosis it is assumed that they may also play a role in other biotrophic plant symbioses such as the AM symbiosis (Gamas et al., 1996; Doidy et al., 2012b).

In the AM fungus *R. irregularis,* four carbohydrate transporters have been identified (Helber et al., 2011). The gene encoding the monosaccharide transporter (MST) *RiMST2* was the most highly expressed transporter in symbiotic tissue, and it could be localized in the arbuscules and in the IRM. Within this line, An et al. (2019) recently showed that the expression of the gene encoding *M. truncatula SWEET1b* transporter is strongly enhanced in arbuscule-containing cells compared to roots and localizes to the peri-arbuscule membrane.

A comprehensive view of symbiosis under environmental and nutritional stress is important in times of climate change and resource shortening, as AM symbiosis is a key component of nutrient uptake and exchange through their transport systems. However, despite accumulating knowledge about transporter expression and metabolic activity in AM symbiosis, we still lack a precise understanding about their regulation and their importance for metabolism. Here, our objectives were to define the effects of P availability on two plants connected through a mycorrhizal network. Therefore, we analyzed the effects of mycorrhization and contrasting P nutrition on the transporter expression and metabolite accumulation in *Populus trichocarpa* (poplar) *and Sorghum bicolor* (sorghum) when colonized by the AM fungus *R. irregularis.* Our main focus was on the regulatory role of the mycorrhization and P nutrition on the expression of the Pht1 PTs in the plants and in the AM fungus. Further we assessed the effect of the applied conditions on AMTs and carbohydrate transporters. In the AM fungus *R. irregularis*, we determined expression of PTs, AMTs, MST, and fatty acid metabolism in the ERM and in the IRM of colonized poplar and sorghum roots. We identified new specific mycorrhiza-inducible PTs and AMTs in poplar and sorghum. Moreover, our data allowed us to gain further insight into symbiotic carbon exchange.

MATERIAL AND METHODS

Experimental Set-Up

Experiments were performed with *P. trichocarpa* cuttings (clone 10174, Orléans, France) and *S. bicolor* (L.) Moench, cv Pant-5. Sorghum seeds were kindly provided by Indian Grassland and Fodder Research Institute (Chaudhary Charan Singh Agriculture University of Hissar, Haryana, India) and Govind Ballabh Pant University of Agriculture and Technology (Pantanagar, Uttaranchal, India). Seeds were surface-sterilized in 2.5% KClO for 10 min, rinsed several times with sterile deionized water and soaked overnight in sterile deionized water. Seeds were germinated in the dark at 25°C for 3 days. Plants were inoculated with 1 ml liquid inoculum of *R. irregularis*, isolate BEG75 (Inoculum Plus, Dijon, France), in 0.01 M citrate buffer

(pH 6) with about 110 spores/ml. The microcosms were set up in tripartite compartments (mycorrhizal treatment) or single compartments (non-mycorrhizal treatments). Compartments were filled with an autoclaved (120°C, 20 min) quartz sand (Alsace, Kaltenhouse, Trafor AG, Basel): zeolite (Symbion, Czech Republic) substrate (1:1, w:w). In the tripartite compartment system poplar cuttings were planted in the left compartment and sorghum seedlings in the right compartment. Both plants were inoculated with *R. irregularis* to create a common mycorrhizal network and to increase poplar root colonization (**Figure S1**). Compartments were separated by two 21 μm meshes and one 3 mm mesh, to allow the AM fungus to grow from one compartment to the other but to avoid plant roots protruding the neighboring compartment. As control, non-inoculated poplar and sorghum plantlets grew in single compartments receiving the Pi containing fertilizer treatments directly to their roots. Plants were fertilized once a week with 10 ml Hoagland solution without P, until all plants showed signs of P depletion, indicated by anthocyan accumulation. From the 22nd week high-P (560 μM) or low-P (28 μM) containing Hoagland solution was applied to the first compartment for 9 weeks, to obtain ERM and to ensure that P was delivered *via* the mycorrhizal uptake pathway. Control plants received fertilizer treatment directly to their root systems.

Harvest

The ERM was harvested by dispersing the substrate with tap water and fishing it from the surface using a 32 μM mesh. These steps were repeated several times. Afterwards the cleaned ERM samples were snap frozen in liquid N and stored at -80°C.

For RNA extractions, two leaves from the top of Poplar plants and two young leaves of Sorghum plants were snap frozen in liquid N and stored at -80°C. The rest of the shoots was harvested and dried in an oven at 55°C for 4 days for total P measurement.

Roots were removed from substrate under tap water and cut into ~1 cm small pieces. Two subsamples of about 100 mg were immediately frozen in liquid N and stored at -80°C. One subsample of about 100 mg was taken for root colonization measurements. The remaining roots were placed in a paper bag and dried at 55°C for 3.5 days for determination of total P and N content.

Colonization Measurements and P Extraction

Roots were immersed in 10% KOH and stored at 4°C overnight. The next day, the roots were rinsed with tap water and immersed in 2% HCl for 1 h at room temperature. Then, the roots were rinsed with tap water, immersed in 0.005% trypan blue (w:v in lactic-acid: glycerol: water, 1:1:1, v:v:v) and stored at 4°C o/n. The next day, the roots were rinsed and immersed in lactic-acid glycerol water (1:1:1, v:v:v) for destaining (Brundrett et al., 1984). Total colonization count was performed using the magnified intersection method (McGonigle et al., 1990). Differences between means of variables were assessed by t-test ($p < 0.05$), using Microsoft Excel 2010.

For determination of P concentration in the plants, dried root and shoot samples of six biological replicates were ground using a ball mill. Up to 500 mg were used for the modified P extraction method by Murphy and Riley (1962).

RNA Extraction

Total RNA was extracted from six biological replicates per plant species and mycelium, respectively. Total RNA was extracted from lyophilized extraradical mycelia, root and leaf samples using the RNeasy Plant Mini Kit (Qiagen, Courtaboeuf, France). RNA extracts were DNase treated with the DNA-free™ Kit, DNase Treatment and Removal Reagents (AMBION® by life technologies). Total RNA was quantified with the Qbit RNA BR Assay kit and purity was estimated using the Nanodrop (ND-1000, Witec, Switzerland).

Reverse Transcription and qRT-PCR

cDNAs from three biological replicates were obtained using the iScript™ cDNA Synthesis Kit (BIO RAD Laboratories, Paolo Alto, CA, United States), using 200 ng of total RNA per reaction, using same RNA extracts as for mRNA sequencing. For quantification a two-step quantitative RT-PCR approach was used. Gene specific primers were designed in Primer 3 (http://frodo.wi.mit.edu/cgi-bin/primer3/primer3_www.cgi) and tested as well in amplify 3.1 (http://engels.genetics.wisc.edu/amplify). Target gene expressions were normalized to the expression of the reference gene ubiquitin in Poplar (Potri.015G013600) and Sorghum (Sb10g026870) and translation elongation factor in *R. irregularis,* respectively. All primers used are listed in **Table S1**. qRT-PCRs were run in a 7500 real-time PCR system (Roche) using the following settings: 95°C for 3 min and then 40 cycles of 95°C for 30 s, 60°C for 1 min and 72°C for 30 s. There were three biological and three technical replicates per treatment. Differences in gene expression between applied conditions were tested by a one-way ANOVA using SPSS Statistics, version 22 (IBM, Chicago, USA).

RNA Sequencing and Data Analysis

Total RNA sequencing was done for three biological replicates per condition. Eighteen libraries were prepared and paired-end Illumina HiSeq mRNA sequencing (2x100bp RNA-Seq) was performed by Beckman Coulter Genomics France (Grenoble, France), which produced around 2 × 80 million reads per library in average. After quality check using FastQC, adaptor sequences were removed using FASTX-Toolkit. Only inserts of at least 30-nt were conserved for further analysis. Reads were mapped with CLC Genomics Workbench 11 (CLC Bio workbench, Qiagen, Aarhus, Denmark) using manufacturer's recommendations on Poplar genome and gene annotation Ptrichocarpa_210_v3.0 (Tuskan et al., 2006), on Sorghum genome and gene annotation Sbicolor_313_v3.1 (McCormick et al., 2018), and on *R. irregularis* gene annotation Rhiir2-1 (Morin et al., 2019). The mapped reads for each transcript were calculated and normalized as RPKM for calculating gene expression (reads per kilobase of transcripts per

million reads mapped—Mortazavi et al., 2008). Intact and broken pairs were both counted as one. The RPKMs of each transcript in different conditions were compared using proportion-based test statistics (Baggerly et al., 2003) implemented in CLC genomic Workbench suite. This beta-binomial test compares the proportions of counts in a group of samples against those of another group of samples. Different weights are given to the samples, depending on their sizes (total counts). The weights are obtained by assuming a Beta distribution on the proportions in a group, and estimating these, along with the proportion of a binomial distribution, by the method of moments. The result is a weighted *t*-type test statistic. We then calculated false discovery rate correction for multiple-hypothesis test (Benjamini and Hochberg, 1995). Only genes showing a difference of 10 reads between compared conditions were considered as significantly expressed. Genes were considered as differentially expressed when meeting the requirements of fold change ≥|2| and false discovery rate ≤ 0.05.The expression was then normalized using RPKM. Raw RNAseq data and global mapping data analyses were deposited at GEO (GSE138316).

Metabolite Profiling and Data Analysis

For extraction of soluble metabolites about 90 mg of deep frozen poplar root and ERM samples (three biological replicates per condition) were pulverized in liquid N. Metabolite profiling was performed as described in (Dethloff et al., 2014) by gas chromatography coupled to electron impact ionization/time-of-flight mass spectrometry (GC-EI/TOF-MS) using an Agilent 6890N24 gas chromatograph (Agilent Technologies, Böblingen, Germany; http://www.agilent.com). Guidelines for manually supervised metabolite identification were the presence of at least 3 specific mass fragments per compound and a retention index deviation < 1.0% (Strehmel et al., 2008). For quantification purposes all mass features were evaluated for best specific, selective and quantitative representation of observed analytes. Laboratory and reagent contaminations were evaluated and removed according to non-sample control experiments. Metabolites were routinely assessed by log2-transformed relative changes expressed as response ratios. Statistical testing, namely two-way analysis of variance (ANOVA) and Wilcoxon–Mann–Whitney testing of significance were performed using relative abundances or log2-transformed ratios. Statistical assessments and data visualizations were performed using the multi-experiment viewer software, MeV (Version 4.9; http://www.tm4.org/mev.html; Saeed et al., 2006) and the Microsoft-Excel 2010 program.

RESULTS

Colonization, and N and P Measurements

AM colonization of roots was between 79 and 87% (poplar) and about 93% (sorghum) (**Table S2**). Non-AM plants were not colonized. The hyphal colonization and the percentage of vesicles were not significantly different between low-P and high-P treatments in sorghum and poplar plants. However, significantly, sorghum roots contained three times more arbuscules in the low-P treatment, indicating that P starvation supported mycorrhization.

P treatment had significant effects on P content in the shoots and roots of poplar and sorghum (**Figure S2**). High-P treatment on ERM increased P content in roots and shoots, except for the roots from non-AM sorghum plants. Under the same P supply conditions, non-AM poplar accumulated more P than AM poplar whereas in AM sorghum, P accumulation was comparable to non-AM plants.

P treatment had significant effects on N content in the shoots of poplar, but marginally on sorghum (**Figure S2**). High-P treatment increased N content in poplar shoots. Under the same P supply conditions, AM poplar accumulated more P than non-AM poplar whereas in AM sorghum, N accumulation was comparable to non-AM plants.

Patterns of Extraradical Mycelium and Intraradical Mycelium Expressomes in the Symbiocosm

Incidence of Phosphate Availability

The symbiotic part of the mycelium in roots (IRM) showed different gene expression patterns according to phosphate concentration and plant host. The total number of differentially expressed genes (DEG) differs around 10 fold between the two plants with 298 genes differentially regulated in *S. bicolor* plants against 3,162 in *P. trichocarpa* in response to phosphate treatment (**Figure 1A**). High phosphate concentration has a fewer incidence on the IRM transcriptome in *S. bicolor* than in *P. trichocarpa* whereas the fungus is connected to both plants, indicating that the allocation of mineral nutrients is more tightly regulated in *P. trichocarpa* than in *S. bicolor*. In both plants, the number of up regulated fungal genes is 10 times the number of down regulated fungal genes in high-P condition compared to low-P. This indicates that the fungus is metabolically more active in high-P condition, consistent with the fact that adding a high-P solution in the common mycorrhizal network compartment enhances the fungal-dependent Pi acquisition pathway. Only two fungal genes were significantly up regulated in both plants in response to high-P treatment and are involved in vesicular cargo. In Sorghum, the few up regulated genes were involved in vesicular trafficking, lipid binding, nitrate reduction and general transport. In *P. trichocarpa*, the genes up regulated by high-P belonged to vesicle metabolism, fatty acid metabolism and transport of N, Pi, sugars, and water. Interestingly, only one gene (a short chain dehydrogenase) was significantly up regulated in both plants and in the ERM in response to high-P treatment.

It is noteworthy that on the one hand, while cultivated in high-P, 3,408 genes were overexpressed in IRM (either in *S. bicolor*, or in *P. trichocarpa* or in both host plants) against 73 in the ERM compartment. On the other hand, while grown in low-P, the number of up regulated genes *in planta* dropped to 294 against 209 in the ERM. These overall expressome patterns suggest that when Pi is abundant in soil, the fungus invests little energy in recruiting the Pi but is highly active in exchanging this nutrient with the plants. On the opposite, when Pi is scarce in the medium, the extra radicle mycelium has to put a lot of energy in recovering the mineral in the soil but has fewer nutrients to exchange with the plants.

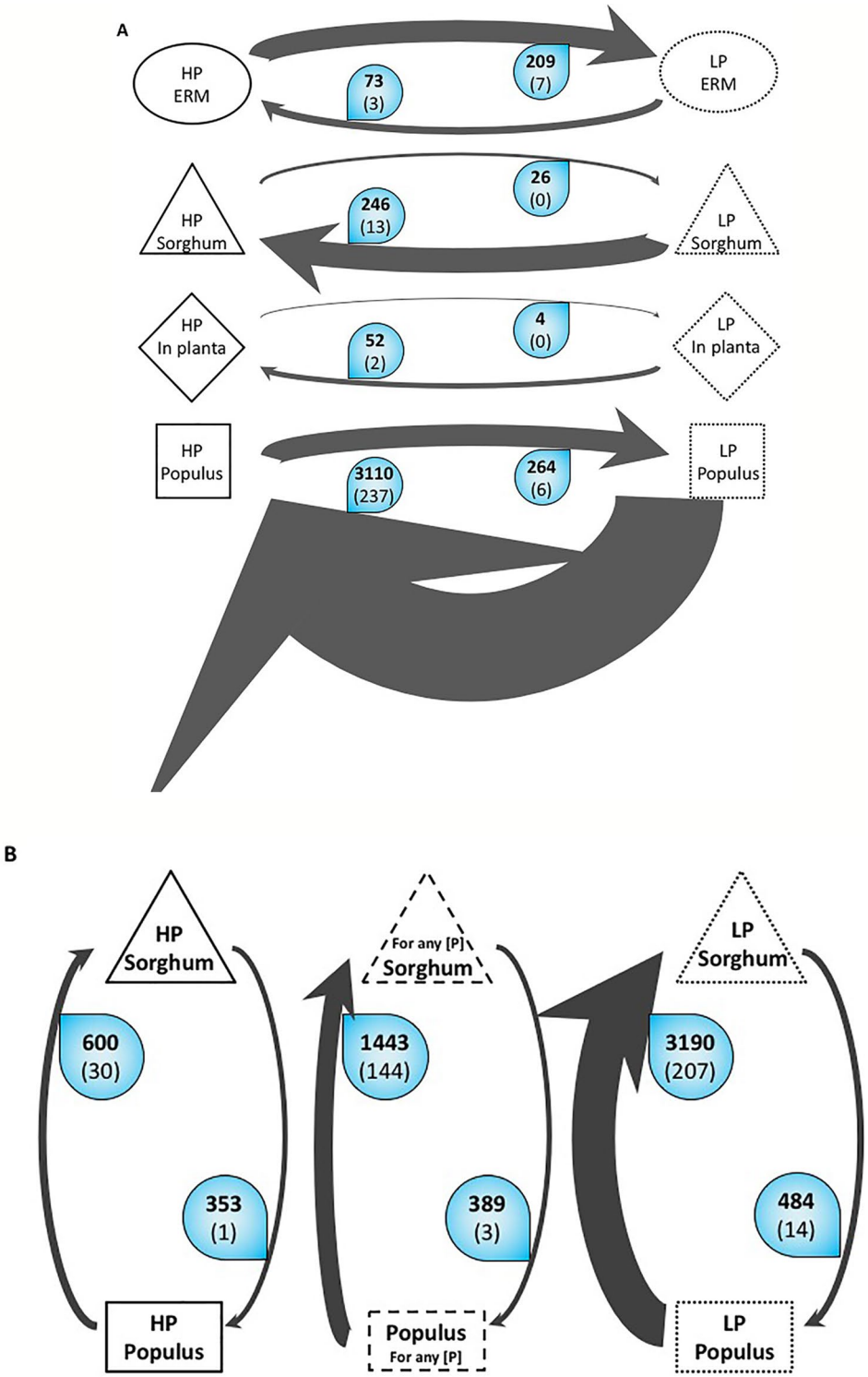

FIGURE 1 | Overall variations of the number of Differentially Expressed Genes (DEG) of *R. irregularis* **(A)** Variations according to P. The arrows represent the number of differentially expressed genes in *R. irregularis*. Black bold numbers represent the number of genes with a fold change ≥2 and a false discovery rate ≤ 0.05. White numbers in brackets represent the number of genes involved in the transportome. The width of the arrow is proportional to the number of up-regulated genes. For example, the top arrow means that in the ERM grown in Low Phosphate, 209 genes are significantly up regulated at least two times compared to the ERM grown in High Phosphate. Among these 209 genes, seven are involved in the transportome. **(B)**. Variations according to host plant. The arrows represent number of differentially expressed genes in *R. irregularis* between the two compared conditions. Black bold numbers represent the number of genes with a fold change ≥2 and a false discovery rate ≤ 0.05. White numbers in brackets represent the number of genes involved in the transportome. The width of the arrow is proportional to the number of up-regulated genes. ERM, extraradical mycelium; HP, high phosphate; LP, low phosphate; *in planta*, intraradical mycelium of both sorghum and poplar.

Incidence of Host Plant

We correlated the difference of DEG in the IRM in the two host plants connected by the same fungus at a given time point to the amount of nutrient resources that the fungus allocates to the two plants. Even though AM fungus has a very broad host range, their expressome differs according to host independently to P concentration (**Figure 1B**). In poplar, only 389 DEG were found among which only three are involved in the transportome (one vesicle transport and two transporters). In *S. bicolor*, a set of 1,443 fungal genes were found up-regulated, indicating active exchanges. A tenth of them (144) is involved in the transportome, representing all metabolisms (fatty acids, N, phosphate, sugars, potassium, general transporters, water, and vesicle transport). This difference indicates that AM symbiosis is more active and more tightly regulated in sorghum than in poplar (**Figure 1B**). The total P concentrations measured in the two mycorrhizal plants is consistent with this observation as more P was accumulated in mycorrhizal sorghum than in mycorrhizal poplar under low P fertilization (**Figure S2**).

In the mesocosm grown in low-P, the fungus does not allocate nutrients equally between the different host plants. The number of genes up regulated in *S. bicolor* is 6.5 times the number of genes overexpressed in *P. trichocarpa* (3,190 and 484 respectively). Not all these genes are supposed to be involved in trophic exchanges but the genes involved in transportome between the two plants showed a similar pattern. In *S. bicolor*, 207 fungal genes were up regulated, corresponding to all the different metabolisms and transporters we investigated (fatty acids, N, phosphate, sugars, transporters, water and vesicle transport, with the exception of potassium). In *P. trichocarpa* however, only 14 genes belonged to our transportome list and were involved in sugar transport, vesicle trafficking, and general transporters. In low-P condition, the AMF seems to favor the exchanges with the Sorghum at the expense of the Poplar. This observation correlates with the total phosphate measured in the two plants (**Figure S2**).

Under high-P, the difference in gene expression is lower than in low-P. We observe only a 2-fold difference between the number of over expressed genes in *S. bicolor* and *P. trichocarpa* (600 and 353 respectively). Moreover, the number of genes involved in transportome is much lower. Only one gene involved in vesicular trafficking is specifically expressed in *P. trichocarpa*. In *S. bicolor*, 30 genes involved in fatty acid metabolism, sugar transport, vesicle transport and general transport were recovered. The high-P makes it easily recoverable by the AM fungus and improves symbiotic exchanges with both plants, thus minimizing the preference for *S. bicolor* over *P. trichocarpa*. This balanced fungal transcriptome is supported by plant P concentration as the measurements in the two plants are very close, with a slight abundance in poplar.

Regulation of Phosphate Transporter Expression

Gene Expression of Plant Pht1 Transporters

Using qRT-PCR, we measured the expression of the twelve Pht1 PT in roots and shoots of AM and non-AM poplar plants grown in high-P and low-P conditions. *PtPT8* and *PtPT10* were induced in AM-roots only, which implies an important role of these two transporters in symbiotic Pi uptake at the periarbuscular space (**Figure S3**).

Low-P treatment and mycorrhization induced expression of *PtPT1.1*, *PtPT1.2*, *PtPT1.4*, *PtPhT1.7*, and *PtPT1.11* in roots (**Figure S3B**). *PtPT1.2*, *PtPT1.4* and *PtPT1.11* were strongly induced in shoots, suggesting that these transporters are involved in intercellular Pi transfer and Pi transport over long distances, respectively (**Figure S3A**). *PtPT1.3* and *PtPT1.6* were neither expressed in roots nor in shoots. mRNA-Seq analysis independently confirmed our results for Pht1 expression (**Figure S4**).

In sorghum, *SbPT1.8* and *SbPT1.10* were induced in AM roots like *PtPT1.8* and *PtPT1.10* (**Figure S5**). *SbPT1.1*, *SbPT1.2*, *SbPT1.4*, *SbPT1.6*, and *SbPT1.7* were significantly induced in the non-AM low-P treatment. It seems that mycorrhization complemented sufficiently the P deficiency by increased Pi transfer to its host plant (**Figure S2**). In comparison to poplar Pht1, sorghum Pht1 was more susceptible to mycorrhization than to Pi concentration.

Gene Expression of Mycorrhizal Phosphate Transporters

In mycorrhizal poplar plants, qRT-PCR analysis of PT in the AM fungus *R. irregularis* in the ERM and IRM revealed expression of *RiPT1*, *RiPT3*, *RiPT5*, and *RiPT7*, with highest expression values for *RiPT1* (**Figure 2A**). *RiPT1* was significantly more expressed in the IRM compared to the ERM in low-P treatment. *RiPT1* expression was significantly higher under low-P treatment in the ERM and the IRM compared to high-P treatment. *RiPT7* tended to be highly expressed in the IRM compared to the ERM and *RiPT3* was lowly expressed in the ERM and induced in high-P treatment in the IRM. In Sorghum, we observed similar expression patterns except for *RiPT3* and *RiPT7*, significantly induced in the IRM than in the ERM (**Figure 2B**).

Regulation of Transporters Involved in Nitrogen Exchange

Gene Expression of Plant Ammonium Transporters

As N is a major component of AM symbiosis, transcript abundances of AMTs in poplar were analyzed (**Figure S6**). The expression of three of them (*PtAMT1.1*, *PtAMT1.2*, and *PtAMT3.1*) was dependent of either mycorrhizal symbiosis of P-treatment or both. We then measured their expression in poplar by qRT-PCR. While *PtAMT1.1* and *PtAMT1.2* were described as induced in poplar upon mycorrhization with the ectomycorrhizal fungi *Paxillus involutus* (Couturier et al., 2007) and *Amanita muscaria* (Selle et al., 2005), no previous expression data were available for *PtAMT3.1*. Interestingly, *PtAMT3.1* clustered next to the three AM-inducible transporters GmAMT3.*1* (Kobae et al., 2010), *SbAMT3.1* (Koegel et al., 2013), and *OsAMT3.1* (Pérez-Tienda et al., 2014) (**Figure S6**). Here, *PtAMT1.1* was induced in the AM low-P treatment and the *PtAMT1.2* and *PtAMT3.1* were induced in the AM treatments (**Figure 3**). In addition, *PtAMT1.2* and *PtAMT3.1* were even higher expressed in the high-P condition, suggesting that both AMTs play a major role in symbiotic N transfer. Higher expression of these transporters under AM high-P condition might point to an increased N transfer when the AM fungus has access to more Pi. In shoots, we

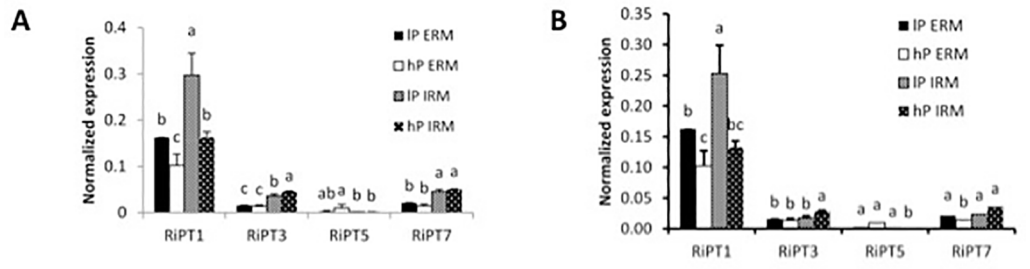

FIGURE 2 | Quantification by qRT-PCR of the transcript abundances of phosphate transporters in *R. irregularis* when associated *with P. trichocarpa* **(A)** *and S. bicolor* **(B)**. Quantification of transcript levels of transporters in the ERM and in the IRM of the host plant under high (hP) and low (lP) availability of P. Values are means of three biological and three technical replicates. Error bars represent the SE. Translational elongation factor was used as a reference transcript. Statistical analysis was performed by analysis of variance for each gene, followed by Tuckey honest significant difference. Lower case letters indicate significant difference(Tukey's t-test; $p < 0.05$).

PtAMT1.1 has a similar expression pattern as in roots. *PtAMT3.1* was only marginally expressed and *PtAMT1.2* was not expressed in leaves (**Figure 3**). mRNA-Seq confirmed our observations for AMT expression levels in the roots of Poplar (**Figure S6**). In a previous transcriptome study (Calabrese et al., 2017), in which AM poplar plants were exposed to N deficiency, *PtAMT4.1*, *PtAMT4.2*, and *PtAMT4.3* were AM-induced. Consistent with this previous study, we observed a specific induction of *PtAMT2.2*, *PtAMT4.1*, *PtAMT4.2*, and *PtAMT4.3* upon mycorrhization even though these transporters were expressed at lower levels compared to *PtAMT1.2* and *PtAMT3.1*.

In Sorghum, *SbAMT3.1* was specifically induced in AM-roots, and *SbAMT1.1* and *SbAMT1.2* were induced in the non-AM low-P treatment (**Figure S7**). However, *SbAMT1.1* and *SbAMT1.2* were nearly twice more expressed in shoots compared to roots.

Gene Expression Ammonium Transporters in *Rhizophagus Irregularis*

Quantitative expression analysis of the three AMTs in the AM fungus revealed that their expression is not significantly different in the ERM between the low-P and high-P treatments. The expression of *GintAMT3* was significantly higher in the IRM compared to the ERM (Calabrese et al., 2017). *GintAMT2* and *GintAMT1* were equally expressed in the ERM and IRM in poplar and sorghum (**Figure 4**). *GintAMT2* was significantly highly expressed in the IRM of sorghum compared to poplar. Specific induction of *GintAMT3* in the IRM might indicate a possible localization of the transporter at the arbuscular side for the transfer of ammonium to the periarbuscular side to enable ammonium uptake for the plant.

Gene Expression of Amino Acid and H+/ Oligopeptide Transporters

In our study, we identified several amino acid transporters and H+/oligopeptide symporters that were either specifically induced or repressed upon mycorrhization (**Table S3**). Here, root colonization highly induced expression of two H^+/ oligopeptide transporters. Potri.005G233500, a homologous gene of *AtPTR1* shown to transport di-/tripeptides with low selectivity in *Arabidopsis thaliana*, was highly induced. AtPTR1 is situated in the plasma membrane of vascular tissue which indicates a role in long-distance transport (Dietrich et al., 2004). *AtPTR3*, a homologue of Potri.002G258900, was induced upon salt stress and was shown to be regulated by methyl jasmonate, salicylic acid and abscisic acid. Further AtPTR3 was induced upon inoculation of the plant with

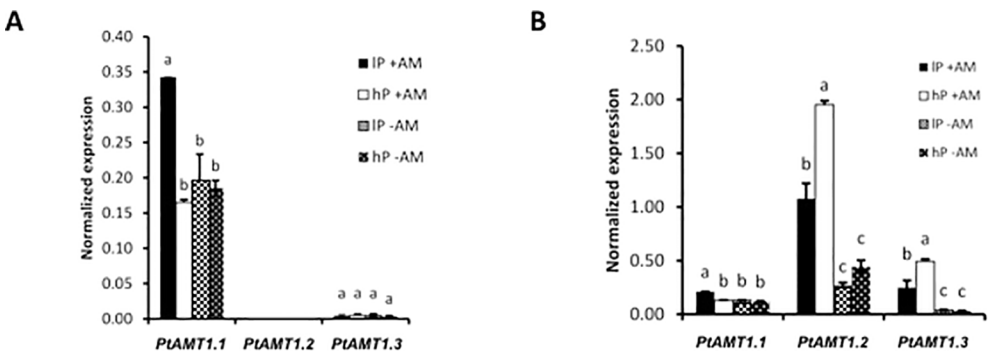

FIGURE 3 | Quantification by qRT-PCR of the transcript abundances of the three ammonium transporters of poplar *PtAMT1.1, PtAMT1.2, and PtAMT3.1* in the shoot **(A)** and root **(B)** of mycorrhized (+AM) and non-mycorrhized (-AM) *P. trichocarpa* under low P (lP) and high P (hP) condition. Values are the means of three biological replicates and three technical replicates, each. Error bars represent the SE. Ubiquitin was used as reference transcript. Statistical analysis was performed by analysis of variance (ANOVA) per gene, followed by Tuckey honest significant difference test (Tuckey HSD; $p < 0.05$). Lower case letters indicate significant difference (Tukey's t-test; $p < 0.05$).

pathogens. A reduced activation of AtPTR3 in *hrpA* mutant indicated that it is a defense related gene protecting the plant against abiotic and biotic stress (Karim et al., 2005; Karim et al., 2006). The differential expression of these transporters upon mycorrhization may suggest a role of the transporters in N uptake but also a role in AM root colonization.

Gene Expression Related to Carbon Exchange

Gene Expression of Sugar Transporters

Quantitative expression analysis using qRT-PCR of five SUT (*SUT1* and *SUT3* to *SUT6*) in poplar revealed that all were expressed (**Figures S8** and **S9**). *SUT1* was only marginally expressed while *SUT4* was strongly expressed in roots and shoots. While *SUT1* and *SUT4* were not differentially expressed upon mycorrhization, surprisingly, *SUT3* was down-regulated upon mycorrhization in roots and shoots of poplar. Interestingly, *SUT6* was down-regulated in shoots by mycorrhization. In sorghum, *SUT1* was also down-regulated (**Figure S10**). In Poplar, we screened our transcriptome data set for other carbohydrate transporters. We found three carbohydrate transporters induced and four repressed upon mycorrhization (**Table S3**). Among them, only the transporter/spinster transmembrane protein Potri.001G286600 presents characteristics for plasma membrane localization. The UDP-galactose transporter related proteins are localized at the lumen of the Golgi cisternae (Norambuena et al., 2002). On the fungal side, the MST *GintMST2* was specifically induced in the IRM of mycorrhizal poplar and sorghum and its expression was not affected by P concentration (**Figure 5**). The induction of *GintMST2* gene expression suggested a role in symbiotic carbohydrate transfer but functional properties still need to be determined. The down-regulation of plant MSTs expression in mycorrhizal conditions whereas the fungal *GintMST2* is still expressed in the IRM indicate that the AM fungus obtains the sugar from the intercellular space without the cooperation of the plant itself, turning the AM root into a sink for sugars.

Expression of Fatty Acid Genes

Expression of different genes involved in fatty acid synthesis and transfer were screened. The expression of these genes is mandatory in order to accommodate the AM fungus and allow the formation of the arbuscules. *Ram2*, *FatM*, and *STR1* were specifically expressed in mycorrhizal Sorghum and *STR2*, *CCaMK*, *RAD1*, *Cyclops*, and *Castor*/*pollux* were upregulated when the plant was in symbiosis (**Table S4**). These genes followed the same pattern of expression in poplar either in low-P or in high-P condition.

On the fungal side, no fatty acid transporter has been identified yet, suggesting another form of acquisition. However, many genes involved in fatty acid metabolism were overexpressed in the different plants. Multiple lipases and lipid recognition proteins are over expressed *in planta* compared to the ERM (**Table S5**). These might play a role both in managing the TAG stock or acquiring fatty acids from the host plant.

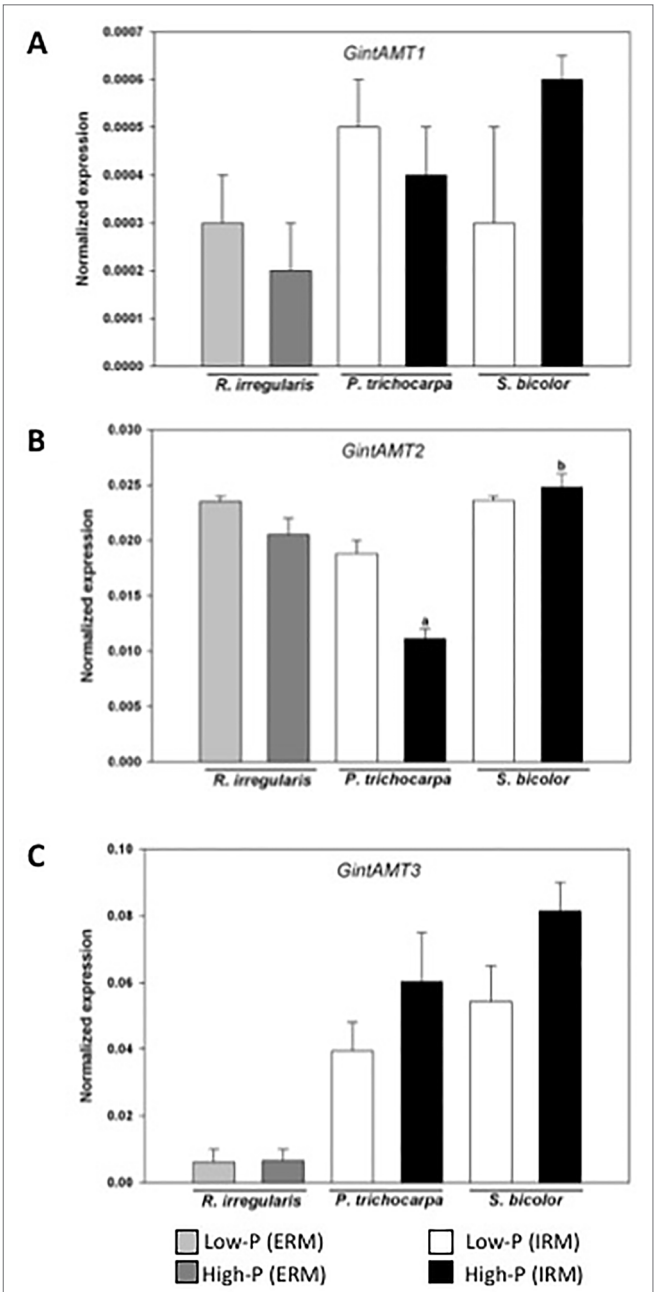

FIGURE 4 | Quantification by qRT-PCR of the transcript abundances of ammonium transporters in *R. irregularis*. Transcript abundances were measured under low-P and high-P availability. Transcript abundances of the three transporters GintAMT1 (A), GintAMT2 (B), and GintAM3 (C) were measured in the extra-radical mycelium (ERM) and in the intraradical mycelium (IRM) when associated to the host plants poplar and sorghum. Values are means of three biological and three technical replicates. Translational elongation factor was used as a reference transcript. Statistical analysis was performed by analysis of variance for each gene, followed by Tuckey honest significant difference test (Tuckey HSD; $p < 0.05$). Lower case letters indicate significant difference(Tukey's t-test; $p < 0.05$).

Three desaturases and one elongase show a slight increase in expression *in planta* compared to *ex planta*. Pi addition had little effect on the ERM but increased the expression of several lipases *in planta*.

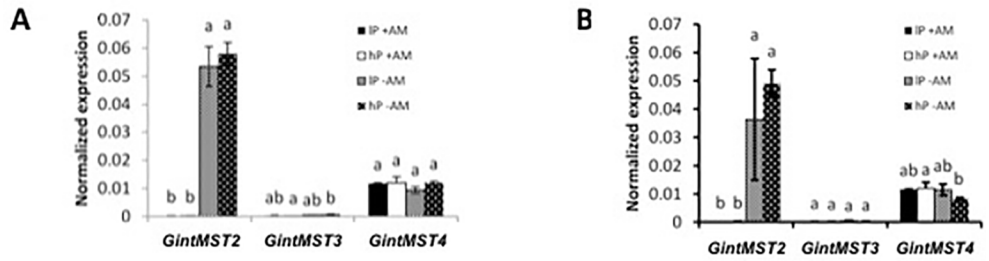

FIGURE 5 | Quantification by qRT-PCR of the transcript abundances of monosaccharide transporters (MST) in *R. irregularis when associated with P. trichocarpa* **(A)** *and S. bicolor* **(B)**. Quantification of transcript levels of transporters in the ERM and in the IRM of the host plant under high (hP) and low (lP) availability of P. Values are means of three biological and three technical replicates. Error bars represent the SE. Translational elongation factor was used as a reference transcript. Statistical analysis was performed by analysis of variance for each gene, followed by Tuckey honest significant difference. Lower case letters indicate significant difference(Tukey's t-test; $p < 0.05$).

Primary Metabolism of Poplar and Sorghum Roots, and the ERM of *R. Irregularis*

To gain further insights into the changes of root primary metabolism caused by the interaction between poplar, sorghum and *R. irregularis* we conducted GC-MS metabolite profiling experiments. Under our experimental conditions, the ERM metabolite profile of *R. irregularis* was not significantly affected by P conditions (**Tables 1** and **S6**). In the ERM, we observed slight but mostly non-significant increases of organic acids, glucose, trehalose, glycine and of amino acids with branched aliphatic side chains, with leucine as the only significant increase in our experiment (**Tables 1** and **S6**).

In contrast, non-AM low-P treatment on poplar roots increased general organic acid and amino acid pools and coincidently decreased pools of glucose-6-phosphate or fructose-6-phosphate (**Tables 2** and **S7**). Analysis of variance indicated significant general accumulation of only few metabolites, *i.e.*, 4-amino-butanoic acid (GABA), isoleucine, phenylalanine, serine, threonic acid, ribonic acid, and arabinonic acid-1,4-lactone independently of the mycorrhizal status (**Tables 2** and **S7**). AM colonization enhanced nutrient acquisition in the low-P treatment (**Tables 2** and **S7**). In addition, mycorrhization modified the root primary metabolism under low-P and high-P and caused a general decrease of the metabolite pools. Thirty-eight out of 79 monitored primary metabolite pools were decreased with only one exception besides few still non-identified metabolites, namely trehalose (**Tables 2** and **S7**). Trehalose is a major storage carbohydrate of AM fungi (Bécard et al., 1991). Mycorrhization not only decreased the main organic acids of the TCA cycle, e.g., malic acid, aconitic acid, 2-oxo-glutaric acid, succinic acid, and fumaric acid, but also many amino acids including aspartic and glutamic acid, as well as phenylalanine, glycine, serine, leucine, isoleucine and valine. In addition, mycorrhization decreased the glucose-6-phosphate, fructose-6-phosphate, *myo*-inositol, and galactinol pools and additional carbohydrates including maltose. For sorghum, the effect of P treatment on AM colonized plants was studied only. Compared to poplar, AM sorghum plants are slightly affected by the low-P treatment; we observed only a slight significant decrease of fructose-6-phosphate, glucose-6-phosphate, and phosphoric acid under low-P treatment (**Table 3**).

TABLE 1 | Relative abundances of metabolites detected in the ERM of *R. irregularis* in response to low (lP) and high P (hP) concentrations.

Class	Name	log2 ratio lP vs hP	p-value
Acids	Aconitic acid, cis-	-0.53	0.275
Acids	Benzoic acid	0.02	0.827
Acids	Benzoic acid, 4-hydroxy-	0.04	0.827
Acids	Citric acid	0.25	0.827
Acids	Fumaric acid	0.36	0.513
Acids	Isocitric acid	0.32	0.513
Acids	Lactic acid	-0.34	0.275
Acids	Malic acid	0.60	0.275
Acids	Pyruvic acid	0.11	0.275
Acids	Quinic acid	-1.88	0.513
Acids	Succinic acid	0.26	0.827
Alcohols	Benzylalcohol	-0.18	0.513
Amino Acids	Aspartic acid	-0.24	0.513
Amino Acids	Glutamic acid	-0.44	0.513
Amino Acids	Glycine	0.80	0.275
Amino Acids	Isoleucine	0.63	0.513
Amino Acids	Leucine	0.19	**0.050**
Amino Acids	Lysine	0.11	0.564
Amino Acids	Ornithine	-1.28	0.127
Amino Acids	Phenylalanine	-0.12	0.827
Amino Acids	Pyroglutamic acid	-0.06	0.513
Amino Acids	Serine	0.19	0.827
Amino Acids	Valine	0.62	0.513
N- Compounds	Ethanolamine	0.15	0.275
N- Compounds	Putrescine	0.14	0.513
N- Compounds	Pyridine, 2-hydroxy-	0.02	0.827
Phenylpropanoids	Caffeic acid, trans-	-0.03	1.000
Phosphates	Phosphoric acid	0.25	0.513
Phosphates	Phosphoric acid monomethyl ester	-0.06	0.827
Polyols	Arabitol	-0.07	0.827
Polyols	Glycerol	-0.24	0.513
Polyols	Inositol, myo-	0.05	0.827
Polyols	Mannitol	-0.92	0.513
Sugar Conjugates	Galactinol	-2.29	0.248
Sugar Conjugates	Salicin	-4.25	1.000
Sugars	Glucose	0.41	0.127
Sugars	Glucose, 1,6-anhydro-, beta-	0.11	0.513
Sugars	Rhamnose	0.16	0.513
Sugars	Ribose	-0.32	0.564
Sugars	Sucrose	-0.06	0.827
Sugars	Trehalose, alpha,alpha'-	0.39	0.127

Data was log transformed and tested by Wilcoxon rank sum test ($p < 0.05$, $n = 3$) in MeV v4.9 (http://www.tm4.org/mev.html). Significant p-values are highlighted in bold.

TABLE 2 | Relative abundances of metabolites detected in poplar roots. Abundances were measured in the mycorrhized (+AM) and non-mycorrhized (-AM) poplar roots under high (hP) and low (lP) P availability.

Class	Name	log2 ratios					2-way ANOVA		
		+AM vs -AM	lP+AM vs hP+AM	lP-AM vs hP -AM	lP+AM vs lP -AM	hP +AM vs hP-AM	Effect of mycorrhization	Effect of p-availability	Effect of interaction
Acids	Aconitic acid, cis-	-1.62	-0.01	-0.17	-1.54	-1.69	**0.006**	0.863	0.934
Acids	Benzoic acid	-0.63	-0.18	0.72	-1.03	-0.13	**0.013**	0.182	**0.034**
Acids	Benzoic acid, 3,4-dihydroxy-	-0.16	-0.09	0.13	-0.27	-0.05	0.750	0.839	0.602
Acids	Benzoic acid, 4-hydroxy-	0.09	-0.10	0.83	-0.32	0.62	0.767	0.426	0.162
Acids	Citric acid	0.46	0.06	0.65	0.20	0.78	0.054	0.125	0.172
Acids	Fumaric acid	-0.87	0.25	0.34	-0.92	-0.82	**0.038**	0.325	0.814
Acids	Glutaric acid, 2-hydroxy-	-1.59	-0.28	0.58	-2.00	-1.14	**0.003**	0.546	0.420
Acids	Glutaric acid, 2-oxo-	-1.70	0.18	1.64	-2.21	-0.75	**0.009**	0.111	0.180
Acids	Glutaric acid, 3-hydroxy-3-methyl-	-0.87	-0.37	0.80	-1.41	-0.24	0.065	0.549	0.199
Acids	Isocitric acid	0.57	0.18	0.86	0.29	0.97	0.054	0.084	0.190
Acids	Lactic acid	-0.74	-0.68	1.36	-1.65	0.39	0.083	0.389	**0.013**
Acids	Malic acid	0.07	-0.21	0.72	-0.35	0.57	0.958	0.412	0.135
Acids	Malic acid, 2-isopropyl-	ND	ND	1.04	ND	ND	ND	ND	ND
Acids	Malic acid, 2-methyl-	ND	ND	0.85	ND	ND	ND	ND	ND
Acids	Pyruvic acid	0.31	0.05	0.29	0.20	0.44	0.147	0.400	0.454
Acids	Quinic acid	-0.15	-0.79	0.92	-0.98	0.72	0.895	0.723	0.092
Acids	Shikimic acid	-2.32	-0.73	0.82	-3.08	-1.53	**0.000**	0.658	**0.008**
Acids	Succinic acid	-0.85	0.04	0.72	-1.14	-0.46	**0.032**	0.212	0.552
Acids	Vanillic acid	-0.29	0.18	0.51	-0.44	-0.10	0.353	0.258	0.631
Alcohols	Benzylalcohol	-0.37	-0.09	0.95	-0.81	0.23	0.479	0.180	0.104
Amino Acids	Aspartic acid	-4.52	0.82	0.59	-4.43	-4.66	**0.000**	0.134	0.845
Amino Acids	Butanoic acid, 4-amino-	-3.03	0.68	0.51	-2.96	-3.13	**0.000**	**0.032**	0.572
Amino Acids	Glutamic acid	-2.87	1.27	-0.85	-1.88	-4.01	**0.001**	0.574	0.090
Amino Acids	Glycine	-0.92	0.44	0.63	-1.01	-0.80	**0.023**	0.112	0.736
Amino Acids	Isoleucine	-1.75	0.51	0.66	-1.81	-1.67	**0.000**	**0.041**	0.873
Amino Acids	Leucine	-1.25	-0.06	0.34	-1.44	-1.04	**0.001**	0.483	0.306
Amino Acids	Phenylalanine	-3.55	0.76	0.65	-3.51	-3.61	**0.000**	**0.048**	0.964
Amino Acids	Pyroglutamic acid	-1.45	0.24	-0.05	-1.31	-1.60	**0.001**	0.532	0.762
Amino Acids	Serine	-1.09	0.45	0.58	-1.14	-1.02	**0.000**	**0.014**	0.765
Amino Acids	Valine	-2.32	-0.09	0.78	-2.71	-1.83	**0.000**	0.224	0.118
Aromatic	Catechol	-1.33	1.43	1.85	-1.43	-1.00	0.245	0.276	0.598
N- Compounds	Ethanolamine	-0.05	-0.16	-0.02	-0.13	0.02	0.927	0.722	0.594
N- Compounds	Phenol, 2-amino-	-1.28	0.26	0.87	-1.53	-0.91	**0.019**	0.242	0.306
N- Compounds	Putrescine	0.19	0.02	0.19	0.11	0.27	0.362	0.499	0.616
N- Compounds	Pyridine, 2-hydroxy-	-0.08	-0.33	0.34	-0.41	0.25	0.803	0.872	0.161
Phenylpropanoids	Caffeic acid, cis-	0.15	0.03	0.91	-0.21	0.66	0.298	0.070	0.075
Phenylpropanoids	Caffeic acid, trans-	-0.05	0.06	1.14	-0.48	0.60	0.666	0.056	0.070
Phenylpropanoids	Cinnamic acid, 4-hydroxy-	ND	ND	0.60	ND	-0.47	ND	ND	ND
Phenylpropanoids	Epicatechin	-0.14	-0.16	0.60	-0.50	0.26	0.668	0.323	0.138
Phenylpropanoids	Ferulic acid, trans-	-0.12	0.10	0.94	-0.47	0.37	0.703	0.066	0.121
Phenylpropanoids	Quinic acid, 3-caffeoyl-, cis-	1.01	0.16	0.07	1.05	0.96	0.102	0.745	0.572
Phenylpropanoids	Quinic acid, 3-caffeoyl-, tran	0.80	0.13	0.42	0.68	0.96	0.155	0.487	0.347
Phosphates	Fructose-6-phosphate	-1.85	-0.51	-0.22	-2.01	-1.73	**0.003**	0.420	0.806
Phosphates	Glucose-6-phosphate	-2.22	-1.10	-0.43	-2.64	-1.97	**0.000**	0.065	0.453

(*Continued*)

TABLE 2 | Continued

Class	Name	log2 ratios					2-way ANOVA		
		+AM vs -AM	IP+AM vs hP+AM	IP-AM vs hP -AM	IP+AM vs IP -AM	hP +AM vs hP-AM	Effect of mycorrhization	Effect of p-availability	Effect of interaction
Phosphates	myo-Inositol-phosphate	ND	ND	-1.11	-1.17	ND	ND	ND	ND
Phosphates	Phosphoric acid	-3.48	0.45	-2.86	-1.22	-4.54	**0.042**	0.634	0.468
Phosphates	Phosphoric acid monomethyl ester	-2.35	-0.39	-0.05	-2.53	-2.20	**0.001**	0.648	0.676
Polyhydroxy Acids	Arabinonic acid-1,4-lactone	-0.18	0.51	1.57	-0.52	0.53	0.914	**0.001**	**0.041**
Polyhydroxy Acids	Galactaric acid	-1.18	-0.25	0.81	-1.66	-0.60	**0.011**	0.455	0.209
Polyhydroxy Acids	Galactonic acid	-1.45	-0.63	0.64	-2.08	-0.81	**0.002**	0.963	0.100
Polyhydroxy Acids	Gluconic acid	-1.14	-0.22	1.22	-1.73	-0.29	**0.018**	0.217	0.139
Polyhydroxy Acids	Glyceric acid	-1.62	-0.28	0.20	-1.87	-1.38	**0.000**	0.900	0.238
Polyhydroxy Acids	Gulonic acid	-0.36	0.04	0.62	-0.61	-0.03	0.425	0.257	0.311
Polyhydroxy Acids	Lyxonic acid-1,4-lactone	-0.11	0.30	0.91	-0.35	0.26	0.772	0.080	0.292
Polyhydroxy Acids	Ribonic acid	-1.15	0.42	0.51	-1.19	-1.10	**0.001**	**0.048**	0.686
Polyhydroxy Acids	Saccharic acid	-1.77	0.01	1.37	-2.30	-0.94	**0.001**	0.065	**0.039**
Polyhydroxy Acids	Threonic acid	-2.04	0.50	1.05	-2.24	-1.69	**0.000**	**0.019**	0.292
Polyols	Arabitol	-1.19	-0.20	0.26	-1.42	-0.97	**0.004**	0.722	0.471
Polyols	Galactitol	-0.16	0.54	-0.46	0.33	-0.67	0.507	0.853	0.143
Polyols	Glycerol	0.17	-0.86	-0.12	-0.27	0.48	0.927	0.307	0.475
Polyols	Inositol, myo-	-2.84	0.98	0.26	-2.56	-3.28	**0.000**	0.123	0.422
Polyols	Mannitol	-0.23	0.26	-0.86	0.39	-0.74	0.896	0.895	0.468
Sugar Conjugates	Galactinol	-2.34	0.70	-0.99	-1.45	-3.14	**0.010**	0.829	0.391
Sugar Conjugates	Salicin	-0.94	0.72	1.58	-1.21	-0.35	0.193	0.137	0.275
Sugar Conjugates	Salicylic acid-glucopyranoside	-2.48	-0.06	-1.13	-1.84	-2.90	**0.038**	0.913	0.998
Sugars	Arabinose	-1.21	-0.18	0.38	-1.48	-0.92	**0.008**	0.776	0.575
Sugars	Fructose	0.65	0.30	> 0.01	0.79	0.49	0.300	0.769	0.986
Sugars	Galactose	0.22	-0.38	0.64	-0.26	0.75	0.984	0.813	0.615
Sugars	Glucose	0.18	0.23	-0.23	0.41	-0.05	0.728	0.791	0.941
Sugars	Glucose, 1,6-anhydro-, beta-	-0.75	-0.13	0.70	-1.13	-0.29	**0.001**	0.076	**0.018**
Sugars	Maltose	-1.35	0.36	0.85	-1.55	-1.05	**0.006**	0.139	0.622
Sugars	Mannose	0.05	-0.68	-0.03	-0.32	0.33	0.800	0.791	0.866
Sugars	Raffinose	-1.59	1.23	-4.14	2.12	-3.25	0.602	0.766	0.173
Sugars	Rhamnose	-1.00	-0.04	0.48	-1.24	-0.72	**0.009**	0.674	0.351
Sugars	Ribose	-1.96	0.13	0.89	-2.28	-1.52	**0.001**	0.258	0.258
Sugars	Sucrose	0.10	-0.02	0.11	0.04	0.17	0.534	0.669	0.658
Sugars	Trehalose, alpha,alpha'-	1.20	-0.49	-0.18	1.03	1.33	**0.046**	0.883	0.841
Sugars	Xylose	-0.50	-0.12	0.94	-0.95	0.10	0.639	0.526	0.363
Sugars	Xylulose	ND	ND	1.14	-2.36	ND	ND	ND	ND

Data was log transformed and tested by y 2-way analysis of variance (ANOVA) ($p < 0.05$, $n = 3$) in MeV v4.9 (http://www.tm4.org/mev.html). Significant p-values are highlighted in bold. Log2 values >1 and <-1 are color-marked (blue and orange, respectively) if $p < 0.05$.

DISCUSSION

In this study, we described the effects of P supply and AM colonization on PTs, AMTs, carbohydrate transporters and lipid genes in poplar and sorghum, and in the ERM and IRM of the AM fungus *R. irregularis*.

Differential Resource Allocation in the Common Mycorrhizal Network

In the symbiocosm, we observed disequilibrium in fungal DEG patterns according to sorghum and poplar symbiotic tissues in response to high-P concentration supplied to ERM. Sorghum is an annual grass with a C4 metabolism, and poplar a perennial tree with a C3 metabolism. The fungal transportome in the fast growing Poaceae is always more important than in poplar in any given P concentration. It has been shown that the fungus is able to adapt its resource allocation to the best symbiont available (Fellbaum et al., 2014; Whiteside et al., 2019). Our data provide same conclusion at the transcriptomic level. However, we have no information about the extent of the ERM developed from roots of each of the two host plants, so differences observed between the two hosts may depend also on a differential ability of the symbiont to form functional ERM. Anyway, we could hypothesize that the perennial poplar plant is less mycorrhiza-dependent than the annual sorghum.

TABLE 3 | Relative abundances of metabolites detected in sorghum roots. Abundances were measured in the mycorrhized (+AM) sorghum roots under high (hP) and low (lP) P availability.

Class	Name	log2 ratios	2-way ANOVA
		IP+AM vs hP+AM	Effect of p-availability
Acids	Aconitic acid, cis-	0.31	**0.04**
Acids	Benzoic acid	0.97	0.51
Acids	Benzoic acid. 3,4-dihydroxy-	0.63	0.22
Acids	Benzoic acid, 4-hydroxy-	0.98	0.51
Acids	Citric acid	1.30	0.51
Acids	Fumaric acid	1.34	0.51
Acids	Glutaric acid, 2-hydroxy-	1.44	**0.04**
Acids	Glutaric acid, 2-oxo-	0.97	0.51
Acids	Glutaric acid, 3-hydroxy-3-methyl-	ND	ND
Acids	Isocitric acid	1.29	0.51
Acids	Lactic acid	2.08	0.13
Acids	Malic acid	1.19	0.83
Acids	Malic acid, 2-isopropyl-	ND	ND
Acids	Malic acid, 2-methyl-	ND	ND
Acids	Pyruvic acid	1.10	0.51
Acids	Quinic acid	1.22	0.83
Acids	Shikimic acid	1.71	0.28
Acids	Succinic acid	2.21	0.51
Acids	Vanillic acid	1.10	0.83
Alcohols	Benzylalcohol	1.18	0.51
Amino Acids	Aspartic acid	1.97	0.51
Amino Acids	Butanoic acid, 4-amino-	2.32	0.28
Amino Acids	Glutamic acid	1.30	0.51
Amino Acids	Glycine	1.03	0.83
Amino Acids	Isoleucine	1.05	0.83
Amino Acids	Leucine	1.13	0.22
Amino Acids	Phenylalanine	1.13	0.83
Amino Acids	Pyroglutamic acid	0.91	0.28
Amino Acids	Serine	1.01	0.51
Amino Acids	Valine	1.14	0.83
Aromatic	Catechol	ND	ND
N- Compounds	Ethanolamine	1.11	0.83
N- Compounds	Phenol, 2-amino-	ND	ND
N- Compounds	Putrescine	1.08	0.83
N- Compounds	Pyridine, 2-hydroxy-	1.15	0.83
Phenylpropanoids	Caffeic acid, cis-	ND	ND
Phenylpropanoids	Caffeic acid, trans-	1.22	0.28
Phenylpropanoids	Cinnamic acid, 4-hydroxy-, trans-	1.19	0.83
Phenylpropanoids	Epicatechin	2.13	0.51
Phenylpropanoids	Ferulic acid, trans-	ND	ND
Phenylpropanoids	Quinic acid, 3-caffeoyl-, cis-	1.48	0.83
Phenylpropanoids	Quinic acid, 3-caffeoyl-, trans-	7.08	0.22
Phosphates	Fructose-6-phosphate	0.63	**0.04**
Phosphates	Glucose-6-phosphate	0.61	**0.04**
Phosphates	myo-Inositol-phosphate	ND	ND
Phosphates	Phosphoric acid	0.69	**0.04**
Phosphates	Phosphoric acid monomethyl ester	0.75	0.28
Polyhydroxy Acids	Arabinonic acid-1,4-lactone	ND	ND
Polyhydroxy Acids	Galactaric acid	0.73	0.28
Polyhydroxy Acids	Galactonic acid	1.06	0.83
Polyhydroxy Acids	Gluconic acid	0.70	0.51
Polyhydroxy Acids	Glyceric acid	1.34	0.22
Polyhydroxy Acids	Gulonic acid	ND	ND
Polyhydroxy Acids	Lyxonic acid-1,4-lactone	1.50	0.83
Polyhydroxy Acids	Ribonic acid	1.12	0.51
Polyhydroxy Acids	Saccharic acid	1.34	0.51
Polyhydroxy Acids	Threonic acid	0.94	0.83
Polyols	Arabitol	0.53	0.28
Polyols	Galactitol	2.07	0.51
Polyols	Glycerol	1.08	0.83
Polyols	Inositol, myo-	1.26	0.83
Polyols	Mannitol	0.71	0.51
Sugar Conjugates	Galactinol	1.67	0.28
Sugar Conjugates	Salicin	1.05	0.51
Sugar Conjugates	Salicylic acid-glucopyranoside	ND	ND
Sugars	Arabinose	1.06	0.51
Sugars	Fructose	0.86	0.83
Sugars	Galactose	1.71	0.51
Sugars	Glucose	1.47	0.83
Sugars	Glucose, 1,6-anhydro-, beta-	1.09	0.51
Sugars	Maltose	2.33	0.22
Sugars	Mannose	ND	ND
Sugars	Raffinose	1.21	0.83
Sugars	Rhamnose	0.54	0.05
Sugars	Ribose	1.48	0,51
Sugars	Sucrose	1.18	0.51
Sugars	Trehalose, alpha,alpha'-	0.93	0.83
Sugars	Xylose	2.44	0.51
Sugars	Xylulose	2.17	1.00

Data was log transformed and tested by Wilcoxon rank sum test ($p < 0.05$, $n = 3$) in MeV v4.9 (http://www.tm4.org/mev.html). Significant p-values are highlighted in bold. Log2 values >1 are color-marked in blue if $p < 0.05$.

Symbiotic Phosphorus Exchange

In our study, we confirmed the expression of *PtPT1.10* in Poplar AM roots only (**Figure S3**) as already reported (Loth-Pereda et al., 2011). In addition, *PtPT1.8* was also expressed in AM roots only. In sorghum roots, AM colonization induced the specific expression of *SbPT1.8*, *SbPT1.10* and partially of *SbPT1.11* (**Figure S5**). The specific induction of *PtPT1.8* and *PtPT1.10* in poplar and of *SbPT1.8*, *SbPT1.10* in sorghum upon mycorrhization strongly suggested that there is a symbiosis-dependent Pi uptake system. In *M. truncatula*, it has been shown that *MtPT4* is specifically expressed in the periarbuscular membrane (Harrison et al., 2002). The specific induction of *PtPT1.8* and *PtPT1.10* in poplar and of *SbPT1.8*, *SbPT1.10* in sorghum suggested that these transporters are localized at the periarbuscular membrane (**Figure 6**).

On the fungal side, the PTs of *R. irregularis* were expressed in the ERM and in the IRM of poplar and sorghum roots. The high affinity transporter *RiPT1* was previously found to be

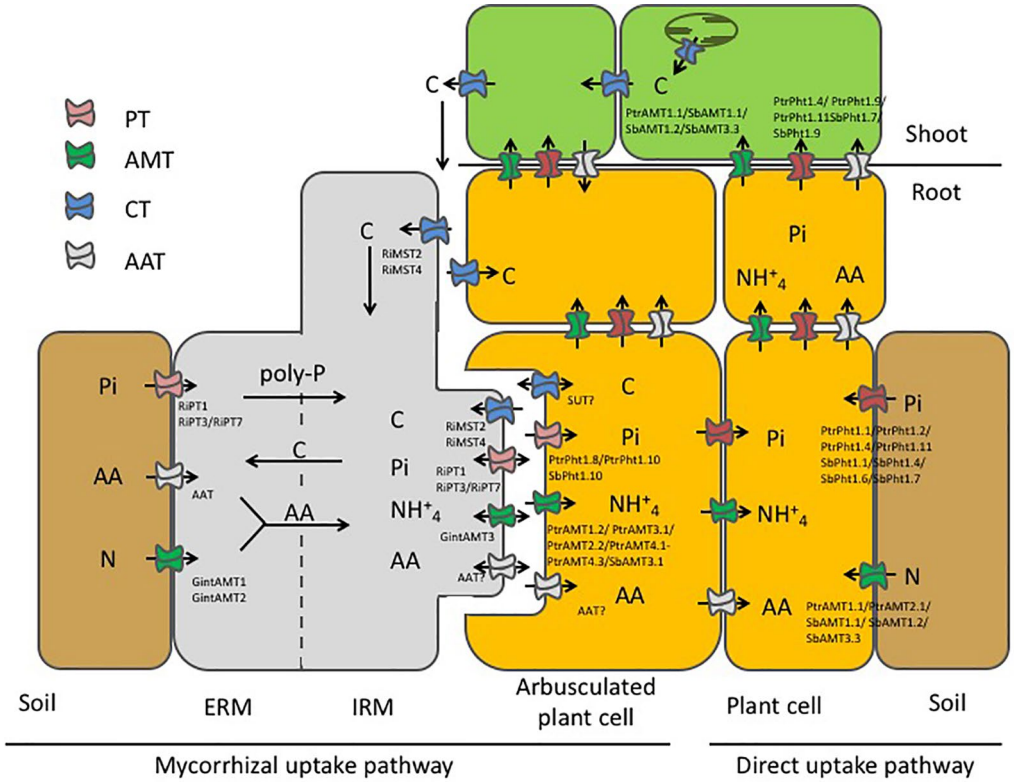

FIGURE 6 | Schematic representation of the mycorrhizal nutrient uptake pathway and the direct nutrient uptake pathway in our model systems poplar and sorghum when colonized by *R. irregularis*. In the direct uptake pathway (right hand side) nutrients, *i.e.* inorganic phosphate (Pi) and nitrogen (N) are taken up from the rhizosphere by phosphate transporters (PT) and ammonium transporters (AMT) and are transported to the shoot. In symbiotic interaction, the AMF partially takes over nutrition of the plant. Nutrients are taken up by specialized transporters in the extraradical mycelium (ERM) and are further transported to the intraradical mycelium (IRM) where they are transferred to the periarbuscular space, to be taken up by plant transporters. N has been suggested to be additionally taken up from the soil in form of amino acids (AA) by predicted amino acid transporters (AAT). In exchange for the transfer of the mineral nutrients the mycorrhizal fungus is rewarded with essential carbohydrates from the plant. As some transporters were specifically induced by mycorrhization a possible localization at the periarbuscular membrane was assumed for the plant transporters. High induction of mycorrhizal transporters in the IRM compared to the extraradical mycelium ERM suggest that these transporters are mainly involved in nutrient exchange at the symbiotic interface. The reality is probably much more complex, with reuptake of nutrients (double-headed arrow) at the biotrophic interface, allowing both partners to, at least partially, control the exchanges.

regulated in the ERM by external Pi concentration (Maldonado-Mendoza et al., 2001) and expressed at the arbuscular side (Fiorilli et al., 2013). Here, *RiPT1* was up-regulated by external low-P concentrations in the ERM but also in the IRM. High expression of *RiPT1* suggests that *RiPT1* is the main transporter for Pi uptake and symbiotic Pi transfer in our conditions. Maldonado-Mendoza et al. (2001) predicted the existence of other PTs operating at high external P concentrations. Indeed, *RiPT3* and *RiPT7* were expressed but not affected by the nutrient conditions in the ERM. It might be that higher Pi concentrations are needed to increase expression of these possible high affinity transporters. Clearly, *RiPT3* and *RiPT7* were induced in the IRM with sorghum, with a similar tendency in poplar, suggesting that they participate also in Pi transfer/exchanges in the symbiosis.

P-Dependent Regulation of Phosphate Transporter Expression

Low-P conditions induced expression of *PtPT1.1*, *PtPT1.2*, *PtPT1.4,* and *PtPT1.11* in poplar roots, showing that expression and regulation of PTs is dependent on Pi availability (**Figure S3**). In the mycorrhizal microcosm, the only Pi source was the AM fungal symbiont, and the absence of a direct Pi source further increased expression of these four transporters. As we still observed a Pi-dependent regulation of transporter expression, our data suggest that these PTs are regulated by external and internal Pi-concentrations and are regulated independently by the mycorrhizal pathway. Increased expression of PTs in low-P condition further suggests that the AM fungus supplies the host plant with more Pi if the fungus itself has increased access to Pi. By regulating these PTs independently poplar ensures a P nutrition uncoupled from the AM symbiont. Symbiosis-independent P-nutrition is necessary for perennial plants as mycorrhizal abundance varies in nature with the seasons (Courty et al., 2008; Dumbrell et al., 2011).

The fact that *PtPT1.2*, *PtPT1.4,* and *PtPT1.11* expression was also induced upon P-limiting conditions in the shoots suggests that they function in Pi uptake at the root-soil interface as well as in intercellular distribution and translocation of Pi from root to shoot. *PtPT1.9* was mainly expressed in the shoot, which suggests that it is mainly responsible for Pi allocation in the shoots.

Sorghum on the other hand turned out to be more mycorrhiza-dependent than poplar. Under mycorrhization PTs were equally low expressed as under a non-mycorrhizal high-P condition, indicating that the AM fungus was able to cover the Pi needs of sorghum. Induction of PT in the shoots in the non-mycorrhizal low-P condition further showed that the plant suffered of P deficiency and therefore probably reallocated Pi from old leaves (source) to young leaves (sink). The stronger dependency of sorghum to the AM fungus was also indicated by Pi-accumulation in mycorrhizal and non-mycorrhizal sorghum (**Figure S2**).

Symbiotic Nitrogen Exchange

As symbiotic N transfer is also an important aspect of AM symbiosis we analyzed the effects of mycorrhization and Pi availability on plant and AM fungal AMT expression (**Figure 6**). P-content has a stronger effect on poplar N contain than mycorrhization. Sorghum N nutrition is not affected by Pi availability. In poplar, mycorrhization induced expression of three AMTs. Our results are supported by previous studies which showed that *PtAMT1.1* and *PtAMT1.2* were mycorrhiza-inducible when poplar was mycorrhiza, suggesting a sensor role l with the ectomycorrhizal fungi *P. involutus* (Couturier et al., 2007) and *A. muscaria* (Selle et al., 2005) (**Figure S6**). In addition, we found that *AMT3.1* is as well a mycorrhiza-inducible transporter in the roots, which is in contrast to the data of Couturier et al. (2007) who detected *PtAMT3.1* solely in senescing leaves. In shoots, the expression of *PtAMT1.1* is mediated by Pi availability under mycorrhizal conditions. Further, increased expression of *PtAMT1.2* and *PtAMT3.1* suggests an increased ammonium transfer when the fungal needs of Pi are accomplished. Analysis of the transcriptome dataset revealed that *PtAMT4.1*, *PtAMT4.2,* and *PtAMT4.3* were also induced upon mycorrhization independently from the P supply of the fungus as it was the case in our previous study where mycorrhizal poplar was set under N stress (Calabrese et al., 2017).

As there is an ongoing debate on whether amino acids as an organic N source can be taken up by AM fungi and transferred from the fungus to the plant (reviewed in Hodge and Storer, 2015) we screened the transcriptome data of poplar and identified several amino acid transporters and H^+/oligopeptide symporters that were either induced or repressed upon mycorrhization (**Table S3**). Specific induction of amino acid transporters and one of the H^+/oligopeptide transporters indicate that amino acids are transferred from the AM fungus to the plant as an alternative N source. However, our metabolome analysis on mycorrhizal and non-mycorrhizal poplar roots showed that mycorrhization reduced the abundance of most metabolites including amino acids in the colonized roots tissue (**Tables 2** and **S7**), suggesting high rates of metabolic turnover by the fungus or the host roots or, alternatively, transport to the shoots. Interestingly, an accumulation of relevant metabolites might be detectable in the shoots as it was demonstrated by Whiteside et al. (2012) for the amino acids phenylalanine, lysine, asparagine, arginine, histidine, cysteine, methionine, and tryptophan with quantum dot analysis.

In the well-established mycorrhizal symbiosis described here, *GintAMT3* was significantly induced in the IRM in both hosts, poplar and sorghum (**Figure 4**), indicating a major participation of this transporter in the exchanges of ammonium at the arbuscule (Calabrese et al., 2017). High *GinAMT2* expression levels independent of Pi-supply and localization in the ERM and IRM indicate that it is a low affinity transporter for ammonium. Moreover, *GinAMT2* displays high sequence similarity to *GintAMT3* which is a low affinity transporter (Calabrese et al., 2017). *GintAMT1* on the other hand, a high affinity transporter, was expressed at low levels in the ERM and IRM independent of the P availability. Together, these findings indicate that GintAMT1 and *GintAMT2* are mainly involved in the uptake of ammonium in the ERM and in the IRM, and that GintAMT3 is mainly involved in the exchanges/competition of/for ammonium at the biotrophic interface between the AMF and its host plant.

In sorghum, only *SbAMT3.1* was induced in mycorrhizal roots (**Figure S7**). In contrast to Koegel et al. (2013) *SbAMT4* was not expressed in our experimental conditions. Induced expression of *SbAMT1.1* and *SbAMT1.2* in the low-P condition suggests that upon sensing of nutrient stress the plant activates a general nutrient uptake program to avoid running short on one or more essential nutrients. In addition our data show that regulation of sorghum AMTs is less mycorrhiza-dependent than nutrient-dependent. Under mycorrhization the plant is supplied with sufficient P and N to keep the P and N level constant within the plant. This scenario may explain the unchanged expression of the SbAMTs. Interestingly, mycorrhization induced expression of *SbAMT1.1* and *SbAMT1.2* in the shoots in low-P and of *SbAMT3.3* in high-P conditions. An increased translocation rate of ammonium from root to shoot upon mycorrhization may be a possible explanation. Moreover, *SbAMT1.1* and *SbAMT1.2* expression levels have a tendency to be also concentration dependent. Strong induction of *SbAMT3.3* in the shoots indicated an increased ammonium flux during high-P and mycorrhizal condition.

Symbiotic Carbon Exchange

In order to shed some light on symbiotic carbon exchange we used qRT-PCR and mRNA-Seq analysis to identify possible transporters that enable carbohydrate transport from the plant to the fungus. Interestingly, quantitative RT-PCR expression analysis and mRNA-Seq analysis revealed downregulation of carbohydrate transporters in poplar (**Figure S8** and **Figure 6**) and sorghum (**Figure S9**), which might indicate that carbohydrates are actively sequestered by the fungus. But we also identified two carbohydrate transporters induced upon mycorrhization (**Table S3**). The UDP-galactose transporters are intracellular transporters situated in the cisternae of the Golgi lumen where UDP-galactose is used for synthesis of non-cellulosic polysaccharides and glycoproteins (Norambuena et al., 2002). Only recently, it was shown that they also transport rhamnose (Rautengarten et al., 2014). In the Golgi-network and the early endosome the newly synthesized proteins are sorted either for the secretion to the plasma membrane, the extracellular matrix or for degradation (Feraru et al., 2012; Brandizzi and Barlowe, 2013; McFarlane et al., 2014). Induced expression of UDP-galactose therefore indicates an increased

transport activity of proteins to colonized cells which goes along with increased plasma membrane synthesis. In *M. truncatula*, it has been shown that arbuscule development goes along with the synthesis of the periarbuscular membrane which is distinct from the plasma membrane (Pumplin and Harrison, 2009). Further it has been shown that AM-induced transporters are specifically directed to the periarbuscular membrane and an involvement of the trans-Golgi for PT has been implicated (Pumplin et al., 2012). The other transporter induced upon mycorrhization is a SUT/spinster transmembrane protein, a member of the major facilitator proteins, which makes it a candidate for being localized at the cell membrane eventually stimulating carbohydrate transport to the AM symbiont.

Interesting is also that a glucose-6-phosphate/phosphate and phosphoenolpyruvate/phosphate antiporter was induced. Glucose-6 phosphate/phosphate antiporters are normally expressed in non-green plastids and serves as carbohydrate importer. In amyloplasts glucose-6 phosphate/phosphate antiporters are located at the site of starch and fatty acids synthesis (Kammerer et al., 1998; Flügge, 2001). Phosphoenolpyruvate/phosphate antiporter mediates the transport of the transport of Phosphoenolpyruvate into the organelles as in amyloplasts, for the synthesis of aromatic amino acids and several secondary compounds. Increased activity of this transporter suggests a decrease of freely available sugars, of storing starch and of aromatic amino acids synthesis. These results shed light the link between carbon, phosphorus, but also N.

In the AM fungi *G. pyriformis* and *R. irregularis* several carbohydrate transporters were identified. For GpMST1 and RiMST2, it was shown that they specifically transport monosaccharides. *RiMST2* was found to be expressed at the arbuscular site and in the intraradical hyphae (Schüßler et al., 2006; Helber et al., 2011). Helber et al. (2011) proposed a model in which the absorbed sugars might derive from cell wall degradation but this is contradictory to previous observations in which carbohydrate transfer varied with the source strength of the host plant (Olsson et al., 2010; Fellbaum et al., 2014; Zhang et al., 2015). We demonstrated that RiMST2 was induced in the IRM of its host plants poplar (**Figure 3**) and sorghum (**Figure 3**) and that its expression level remained unchanged by Pi availability. The metabolome analysis revealed further that mycorrhization significantly decreased the abundance of monosaccharides (i.e. glucose, rhamnose and ribose) in AM poplar roots. In AM fungi it has been shown that hexoses received from the host plants are transformed to glycogen, trehalose. Our observations are consistent with these findings that monosaccharides are taken up mainly by RiMST2 from the apoplast, converted into disaccharides (*i.e.* trehalose) for transport and hydrolyzed in the ERM into monosaccharides, ready for direct usage or for storage. The mycorrhizal-dependent downregulation of carbohydrate transporters and monosaccharide abundance in poplar roots, along with reduced RiMST2 expression at the arbuscular site and in the IRM suggests that the fungus actively sequesters the sugars on its own demand.

Taken together our data suggest that the plant strictly regulates carbohydrate allocation on mycorrhizal roots. With the Sugar transporter/spinster transmembrane protein a possible candidate for symbiotic carbon transfer from the plant to the periarbuscular space is found. The fungus may take up sugars from there by RiMST2.

AMF are fatty acid (FA) auxotrophs as their fatty acids are provided by their host plant (McLean et al., 2017). To date, mechanisms of FA transport are unknown. We observed that fungal lipid metabolism is highly expressed in the IRM. While many lipases, elongases, and desaturases are expressed both in the ERM and IRM, they might play a role in the storage and use of triglycerides in lipid droplets. However, their over-expression *in planta* could be a clue of the recovering process of FA from the plant.

CONCLUSION

Here, we demonstrated that mycorrhization leads to specific induction of a variety of transporters. As P and N are key elements of mycorrhizal symbiosis, we tested the expression of PT and AMT and show that mycorrhization specifically induces expression of a selection of PT and AMTs in poplar and in sorghum. Further, we identified one carbohydrate transporter specifically induced in mycorrhizal root tissue that might be a possible candidate for symbiotic carbon exchange. By contrast, other carbohydrate transporters were down-regulated upon mycorrhization indicating that the plant may not volunteer provision of carbohydrates in exchange for mineral nutrients. We further showed that some nutrient transporters are more strongly expressed in the IRM compared to the ERM, which indicates that they are directly involved in nutrient transfer at the arbuscular membrane or, as in the case of MST, in nutrient uptake into the intraradical hyphae (**Figure 6**). Nevertheless, despite its importance, the release of major nutrients taken up by the ERM into the root apoplasm occurs through widely unknown mechanisms, which must include the differentiation and polarization of the fungal membrane transport functions. Transport processes across the polarized membrane interfaces are of major importance in the functioning of the established mycorrhizal association as the symbiotic relation is based on an apparent 'fair-trade' between fungus and host plant. PTs and AMTs are active transporters and they are able to transport nutrients against the direction of concentration gradients using electrochemical potential differences build up by proton-pumping ATPases. In fact, the reality is probably much more complex, with reuptake of nutrients at the biotrophic interface allowing both partners to, at least partially, control the exchanges (**Figure 6**).

In agriculture, vast amounts of mineral fertilizers are applied to the field to increase crop yield. Indeed, the amount of applied fertilizer might actually exceed the plant needs for mineral nutrients. Collecting data such as ours will help to further deepen our understanding of the plant-AM symbiosis and may lead to development of a more sustainable agriculture with a reduced fertilizer input and improved adaptation to changing environmental conditions.

DATA AVAILABILITY STATEMENT

Raw RNAseq data and global mapping data analyses were deposited at GEO (GSE138316).

AUTHOR CONTRIBUTIONS

SC made the major part of the experiments. AS and LC made in silico analysis. JK and AE performed metabolite analysis. All co-authors participated in writing.

FUNDING

This project was supported by the Swiss National Science Foundation (grants no. PZ00P3_136651 to P-EC and no. 127563 to TB). The authors thank the following Institutions for financial support: the Burgundy Franche Comté Regional Council, the division of Plant Health and Environment of the French National Institute for Agricultural Research (INRA).

ACKNOWLEDGMENTS

We would like to thank De-Roman Yvan for his help in establishing the fungal transportome list. LRSV is part of the TULIP 'Laboratoire d'Excellence' (ANR-10-LABX-41). The authors are grateful to the anonymous reporters for constructive comments on the manuscript.

SUPPLEMENTARY MATERIAL

The Supplementary Material for this article can be found online at: https://www.frontiersin.org/articles/10.3389/fpls.2019.01617/full#supplementary-material

TABLE S1 | Primer used for qRT-PCR in P. trichocarpa, S. bicolor and R. irregularis.

TABLE S2 | Percentage of colonized P. trichocarpa and S. bicolor roots colonized by R. irregularis. Statistical analysis was performed on six biological replicates by T.TEST ($p<0.05$) for each plant species. Significant differences are indicated by lower case letters.

TABLE S3 | Differentially expressed amino acid and carbohydrate transporters in P. trichocarpa. Significant p-values ($p<0.05$) are highlighted in bold.

TABLE S4 | P. trichocarpa and S. bicolor transporters regulated by mycorrhizal symbiosis and P treatment.

TABLE S5 | Name of fungal genes regulated by P treatment and during the interaction with P. trichocarpa and S. bicolor.

TABLE S6 | Relative abundances of metabolites detected in the ERM of R. irregularis. Data was log transformed and tested by Wilcoxon rank sum test ($p<0.05$) in MeV v4.9 (http://www.tm4.org/mev.html). Significant p-values are highlighted in bold.

TABLE S7 | Relative abundances of metabolites detected poplar roots. Abundances were measured in the mycorrhized (+AM) and non-mycorrhized (-AM) poplar roots under high (hP) and low (lP) P availability. Data was log transformed and tested by y 2-way analysis of variance (ANOVA) ($p<0.05$) in MeV v4.9 (http://www.tm4.org/mev.html). Significant p-values are highlighted in bold.

REFERENCES

Ai, P., Sun, S., Zhao, J., Fan, X., Xin, W., Guo, Q., et al. (2009). Two rice phosphate transporters, OsPht1;2 and OsPht1;6, have different functions and kinetic properties in uptake and translocation. *Plant J.* 57, 798–809. doi: 10.1111/j.1365-313X.2008.03726

An, J., Zeng, T., Ji, C., de Graaf, S., Zheng, Z., Xiao, T. T., et al. (2019). A *Medicago truncatula* transporter implicated in arbuscule maintenance during arbuscular mycorrhizal symbiosis. *New Phytol.* 224, 396–408. doi: 10.1111/nph.15975

Aung, K., Lin, S. I., Wu, C. C., Huang, Y. T., Su, C., and Chiou, T. J. (2006). pho2, a phosphate overaccumulator, is caused by a nonsense mutation in a microRNA399 target gene. *Plant Physiol.* 141, 1000–1011. doi: 10.1104/pp.106.078063

Baggerly, K. A., Deng, L., Morris, J. S., and Marcelo Aldaz, C. (2003). Differential expression in SAGE: accounting for normal between-library variation. *Bioinformatics* 19, 1477–1483. doi: 10.1093/bioinformatics/btg173

Bago, B., Vierheilig, H., Piché, Y., and Azcón-Aguilar, C. (1996). Nitrate depletion and pH changes induced by the extraradical mycelium of the arbuscular mycorrhizal fungus *Glomus intraradices* grown in monoxenic culture. *New Phytol.* 133, 273–280. doi: 10.1111/j.1469-8137.1996.tb01894

Bécard, G., Doner, L., Rolin, D., Douds, D., and Pfeffer, P. (1991). Identification and quantification of trehalose in vesicular-arbuscular mycorrhizal fungi by *in vivo* 13C NMR and HPLC analyses. *New Phytol.* 118, 547–552. doi: 10.1111/j.1469-8137.1991.tb00994.x

Benedetto, A., Magurno, F., Bonfante, P., and Lanfranco, L. (2005). Expression profiles of a phosphate transporter gene (GmosPT) from the endomycorrhizal fungus. *Glomus mosseae. Mycorrhiza* 15, 620–627. doi: 10.1007/s00572-005-0006-9

Benjamini, Y., and Hochberg, Y. (1995). Controlling the false discovery rate: a practical and powerful approach to multiple testing. *J. R. Stat. Soc B.* 57, 289–300. doi: 10.1111/j.2517-6161.1995.tb02031

Boldt, K., Pörs, Y., Haupt, B., Bitterlich, M., Kühn, C., Grimm, B., et al. (2011). Photochemical processes, carbon assimilation and RNA accumulation of sucrose transporter genes in tomato arbuscular mycorrhiza. *J. Plant Physiol.* 168, 1256–1263. doi: 10.1016/j.jplph.2011.01.026

Brandizzi, F., and Barlowe, C. (2013). Organization of the ER-Golgi interface for membrane traffic control. *Nat. Rev. Mol. Cell Biol.* 14, 382–392. doi: 10.1038/nrm3588

Branscheid, A., Sieh, D., Pant, B. D., May, P., Devers, E. A., Elkrog, A., et al. (2010). Expression pattern suggests a role of miR399 in the regulation of the cellular response to local Pi increase during arbuscular mycorrhizal symbiosis. *Mol. Plant-Microbe In.* 23, 915–926. doi: 10.1094/MPMI-23-7-0915

Bravo, A., Brands, M., Wewer, V., Dörmann, P., and Harrison, M. J. (2017). Arbuscular mycorrhiza-specific enzymes FatM and RAM2 fine-tune lipid biosynthesis to promote development of arbuscular mycorrhiza. *New Phytol.* 214, 1631–1645. doi: 10.1111/nph.14533

Breuillin-Sessoms, F., Floss, D. S., Gomez, S. K., Pumplin, N., Ding, Y., Levesque-Tremblay, V., et al. (2015). Suppression of arbuscule degeneration in *Medicago truncatula* phosphate transporter4 mutants is dependent on the ammonium transporter 2 family protein AMT2;3. *Plant Cell* 27, 1352–1366. doi: 10.1105/tpc.114.131144

Brundrett, M. C., Piché, Y., and Peterson, R. L. (1984). A new method for observing the morphology of vesicular–arbuscular mycorrhizae. *Can. J. Bot.* 62, 2128–2134. doi: 10.1139/b84-290

Calabrese, S., Pérez-Tienda, J., Ellerbeck, M., Arnould, C., Chatagnier, O., Boller, T., et al. (2016). GintAMT3 – a low-affinity ammonium transporter of the arbuscular mycorrhizal. *Rhizophagus irregularis. Front. Plant Sci.* 7, art 679. doi: 10.3389/fpls.2016.00679

Calabrese, S., Kohler, A., Niehl, Veneault-Fourrey, C., Boller, T., and Courty, P.-E. (2017). Transcriptome analysis of the *Populus trichocarpa–Rhizophagus irregularis* mycorrhizal symbiosis. regulation of plant and fungal transportomes under nitrogen starvation. *Plant Cell Physiol.* 58, 1003–1017. doi: 10.1093/pcp/pcx044

Chen, L. Q., Hou, B. H., Lalonde, S., Takanaga, H., Hartung, M. L., Qu, X. Q., et al. (2010). Sugar transporters for intercellular exchange and nutrition of pathogens. *Nature* 468, 527–532. doi: 10.1038/nature09606

Chiou, T. J., Aung, K., Lin, S. I., Wu, C. C., Chiang, S. F., and Su, C. L. (2006). Regulation of phosphate homeostasis by microRNA in Arabidopsis. *Plant Cell* 18, 412–421. doi: 10.1105/tpc.105.038943

Courty, P. E., Franc, A., Pierrat, J. C., and Garbaye, J. (2008). Temporal changes in the ectomycorrhizal community in two soil horizons of a temperate oak forest. *Appl. Environ. Microb.* 74, 5792–5801. doi: 10.1128/AEM.01592-08

Courty, P. E., Smith, P., Koegel, S., Redecker, D., and Wipf, D. (2015). Inorganic nitrogen uptake and transport in beneficial plant root-microbe interactions. *Crit. Rev. Plant Sci.* 34, 4–16. doi: 10.1080/07352689.2014.897897

Couturier, J., Montanini, B., Martin, F., Brun, A., Blaudez, D., and Chalot, M. (2007). The expanded family of ammonium transporters in the perennial poplar plant. *New Phytol.* 174, 137–150. doi: 10.1111/j.1469-8137.2007.01992

Dethloff, F., Erban, A., Orf, I., Alpers, J., Fehrle, I., Beine-Golovchuk, O., et al. (2014). Profiling methods to identify cold-regulated primary metabolites using gas chromatography coupled to mass spectrometry. *In Plant Cold Acclimation. Springe* 1166, 171–197. doi: 10.1007/978-1-4939-0844-8_14

Dietrich, D., Hammes, U., Thor, K., Suter-Grotemeyer, M., Flückiger, R., Slusarenko, A. J., et al. (2004). AtPTR1, a plasma membrane peptide transporter expressed during seed germination and in vascular tissue of Arabidopsis. *Plant J.* 40, 488–499. doi: 10.1111/j.1365-313X.2004.02224

Doidy, J., Grace, E., Kühn, C., Simon-Plas, F., Casieri, L., and Wipf, D. (2012a). Sugar transporters in plants and in their interactions with fungi. *Trends Plant Sci.* 17, 413–422. doi: 10.1016/j.tplants.2012.03.009

Doidy, J., van Tuinen, D., Lamotte, O., Corneillat, M., Alcaraz, G., and Wipf, D. (2012b). The *Medicago truncatula* sucrose transporter family: characterization and implication of key members in carbon partitioning towards arbuscular mycorrhizal fungi. *Mol. Plant* 5, 1346–1358. doi: 10.1093/mp/sss079

Dumbrell, A. J., Ashton, P. D., Aziz, N., Feng, G., Nelson, M., Dytham, C., et al. (2011). Distinct seasonal assemblages of arbuscular mycorrhizal fungi revealed by massively parallel pyrosequencing. *New Phytol.* 190, 794–804. doi: 10.1111/j.1469-8137.2010.03636

Ellerbeck, M., Schüßler, A., Brucker, D., Dafinger, C., Loos, F., and Brachmann, A. (2013). Characterization of three ammonium transporters of the Glomeromycotan fungus. *Geosiphon pyriformis. Eukaryot. Cell* 12, 1554–1562. doi: 10.1128/EC.00139-13

Ezawa, T., Smith, S., and Smith, F. A. (2002). P metabolism and transport in AM fungi. *Plant Soil* 244, 221–230. doi: 10.1023/A:1020258325010

Fellbaum, C. R., Mensah, J. A., Cloos, A. J., Strahan, G. E., Pfeffer, P. E., Kiers, E. T., et al. (2014). Fungal nutrient allocation in common mycorrhizal networks is regulated by the carbon source strength of individual host plants. *New Phytol.* 203, 646–656. doi: 10.1111/nph.12827

Feraru, E., Feraru, M. I., Asaoka, R., Paciorek, T., De Rycke, R., Tanaka, H., et al. (2012). BEX5/RabA1b regulates trans-Golgi network-to-plasma membrane protein trafficking in Arabidopsis. *Plant Cell* 24, 3074–3086. doi: 10.1105/tpc.112.098152

Fiorilli, V., Lanfranco, L., and Bonfante, P. (2013). The expression of GintPT, the phosphate transporter of *Rhizophagus irregularis*, depends on the symbiotic status and phosphate availability. *Planta* 237, 1267–1277. doi: 10.1007/s00425-013-1842-z

Flügge, U. I. (2001). Plant chloroplasts and other plastids, in *Encycl Life Sci* (London: Macmillan).

Frey, B., and Schüepp, H. (1993). Acquisition of nitrogen by external hyphae of arbuscular mycorrhizal fungi associated with *Zea mays* L. *New Phytol.* 124, 221–230. doi: 10.1111/j.1469-8137.1993.tb03811.x

Gamas, P., de Carvalho Niebel, F., Lescure, N., and Cullimore, J. V. (1996). Use of a subtractive hybridization approach to identify new *Medicago truncatula* genes induced during root nodule development. *Mol. Plant Microbe In.* 9, 233–242. doi: 10.1094/mpmi-9-0233

Garcia, K., Doidy, J., Zimmermann, S., Wipf, D., and Courty, P. E. (2016). Take a trip through the plant and fungal transportome of mycorrhiza. *Trends Plant Sci.* 21, 937–950. doi: 10.1016/j.tplants.2016.07.010

Ge, L., Sun, S., Chen, A., Kapulnik, Y., and Xu, G. (2008). Tomato sugar transporter genes associated with mycorrhiza and phosphate. *Plant Growth Regul.* 55, 115–123. doi: 10.1007/s10725-008-9266-7

Glassop, D., Smith, S., and Smith, F. (2005). Cereal phosphate transporters associated with the mycorrhizal pathway of phosphate uptake into roots. *Planta* 222, 688–698. doi: 10.1007/s00425-005-0015-0

Gomez, S. K., Javot, H., Deewatthanawong, P., Torres-Jerez, I., Tang, Y., Blancaflor, E., et al. (2009). *Medicago truncatula* and *Glomus intraradices* gene expression in cortical cells harboring arbuscules in the arbuscular mycorrhizal symbiosis. *BMC Plant Biol.* 9, 10. doi: 10.1186/1471-2229-9-10

Govindarajulu, M., Pfeffer, P. E., Jin, H., Abubaker, J., Douds, D. D., Allen, J. W., et al. (2005). Nitrogen transfer in the arbuscular mycorrhizal symbiosis. *Nature* 435, 819–823. doi: 10.1038/nature03610

Guether, M., Neuhäuser, B., Balestrini, R., Dynowski, M., Ludewig, U., and Bonfante, P. (2009). A mycorrhizal-specific ammonium transporter from *Lotus japonicus* acquires nitrogen released by arbuscular mycorrhizal fungi. *Plant Physiol.* 150, 73–83. doi: 10.1104/pp.109.136390

Harrison, M. J., and Buuren, M. L. (1995). A phosphate transporter from the mycorrhizal fungus *Glomus versiforme*. *Nature* 378, 626–629. doi: 10.1038/378626a0

Harrison, M. J., Dewbre, G. R., and Liu, J. (2002). A phosphate transporter from *Medicago truncatula* involved in the acquisition of phosphate released by arbuscular mycorrhizal fungi. *Plant Cell* 14, 2413–2429. doi: 10.1105/tpc.004861

Hawkins, H. J., Johansen, A., and George, E. (2000). Uptake and transport of organic and inorganic nitrogen by arbuscular mycorrhizal fungi. *Plant Soil* 226, 275–285. doi: 10.1023/A:1026500810385

Helber, N., Wippel, K., Sauer, N., Schaarschmidt, S., Hause, B., and Requena, N. (2011). A versatile monosaccharide transporter that operates in the arbuscular mycorrhizal fungus *Glomus* sp is crucial for the symbiotic relationship with plants. *Plant Cell* 23, 3812–3823. doi: 10.1105/tpc.111.089813

Hodge, A., and Storer, K. (2015). Arbuscular mycorrhiza and nitrogen: implications for individual plants through to ecosystems. *Plant Soil* 386, 1–19. doi: 10.1016/j.funeco.2010.02.002

Hodge, A., Helgason, T., and Fitter, A. H. (2010). Nutritional ecology of arbuscular mycorrhizal fungi. *Fungal Ecol.* 3, 267–273. doi: 10.1016/j.funeco.2010.02.002

Javot, H., Penmetsa, R. V., Terzaghi, N., Cook, D. R., and Harrison, M. J. (2007a). A *Medicago truncatula* phosphate transporter indispensable for the arbuscular mycorrhizal symbiosis. *P. Natl. Acad. Sci. U.S.A.* 104, 1720–1725. doi: 10.1073/pnas.0608136104

Javot, H., Pumplin, N., and Harrison, M. J. (2007b). Phosphate in the arbuscular mycorrhizal symbiosis: transport properties and regulatory roles. *Plant Cell Env.* 30, 310–322. doi: 10.1111/j.1365-3040.2006.01617

Jiang, Y., Wang, W., Xie, Q., Liu, N., Liu, L., Wang, D., et al. (2017). Plants transfer lipids to sustain colonization by mutualistic mycorrhizal and parasitic fungi. *Science* 356, 1172–1175. doi: 10.1126/science.aam9970

Jin, H., Pfeffer, P. E., Douds, D. D., Piotrowski, E., Lammers, P. J., and Shachar-Hill, Y. (2005). The uptake, metabolism, transport and transfer of nitrogen in an arbuscular mycorrhizal symbiosis. *New Phytol.* 168, 687–696. doi: 10.1111/j.1469-8137.2005.01536

Kammerer, B., Fischer, K., Hilpert, B., Schubert, S., Gutensohn, M., Weber, A., et al. (1998). Molecular characterization of a carbon transporter in plastids from heterotrophic tissues: the glucose 6-phosphate/phosphate antiporter. *Plant Cell* 10, 105–117. doi: 10.1105/tpc.10.1.105

Karim, S., Lundh, D., Holmström, K. O., Mandal, A., and Pirhonen, M. (2005). Structural and functional characterization of AtPTR3, a stress-induced peptide transporter of Arabidopsis. *J. Mol. Model.* 11, 226–236. doi: 10.1007/s00894-005-0257-6

Karim, S., Holmström, K. O., Mandal, A., Dahl, P., Hohmann, S., Brader, G., et al. (2006). AtPTR3, a wound-induced peptide transporter needed for defence against virulent bacterial pathogens in Arabidopsis. *Planta* 225, 1431–1445. doi: 10.1007/s00425-006-0451-5

Keymer, A., Pimprikar, P., Wewer, V., Huber, C., Brands, M., Bucerius, S. L., et al. (2010). Localized expression of arbuscular mycorrhiza-inducible ammonium transporters in soybean. *Plant Cell Physiol.* 51, 1411–1415. doi: 10.1093/pcp/pcq099

Kikuchi, Y., Hijikata, N., Ohtomo, R., Handa, Y., Kawaguchi, M., Saito, K., et al. (2016). Aquaporin-mediated long-distance polyphosphate translocation directed towards the host in arbuscular mycorrhizal symbiosis: application of virus-induced gene silencing. *New Phytol.* 211, 1202–1208. doi: 10.1111/nph.14016

Koegel, S., Ait Lahmidi, N., Arnould, C., Chatagnier, O., Walder, F., Ineichen, K., et al. (2013). The family of ammonium transporters (AMT) in Sorghum bicolor: two AMT members are induced locally, but not systemically in roots colonized by arbuscular mycorrhizal fungi. *New Phytol.* 198, 853–865. doi: 10.1111/nph.12199

López-Pedrosa, A., González-Guerrero, M., Valderas, A., Azcón-Aguilar, C., and Ferrol, N. (2006). GintAMT1 encodes a functional high-affinity ammonium

transporter that is expressed in the extraradical mycelium of *Glomus intraradices*. *Fung. Genet. Biol.* 43, 102–110. doi: 10.1016/j.fgb.2005.10.005

Leigh, J., Hodge, A., and Fitter, A. H. (2009). Arbuscular mycorrhizal fungi can transfer substantial amounts of nitrogen to their host plant from organic material. *New Phytol.* 181, 199–207. doi: 10.1111/j.1469-8137.2008.02630

Loth-Pereda, V., Orsini, E., Courty, P. E., Lota, F., Kohler, A., Diss, L., et al. (2011). Structure and expression profile of the phosphate Pht1 transporter gene family in mycorrhizal *Populus trichocarpa*. *Plant Physiol.* 156, 2141–2154. doi: 10.1104/pp.111.180646

Luginbuehl, L. H., Menard, G. N., Kurup, S., Van Erp, H., Radhakrishnan, G. V., Breakspear, A., et al. (2017). Fatty acids in arbuscular mycorrhizal fungi are synthesized by the host plant. *Science* 356, 1175–1178. doi: 10.1126/science.aan0081

Mäder, P., Vierheilig, H., Streitwolf-Engel, R., Boller, T., Frey, B., Christie, P., et al. (2000). Transport of 15N from a soil compartment separated by a polytetrafluoroethylene membrane to plant roots *via the* hyphae of arbuscular mycorrhizal fungi. *New Phytol.* 146, 155–161. doi: 10.1046/j.1469-8137.2000.00615

Maldonado-Mendoza, I. E., Dewbre, G. R., and Harrison, M. J. (2001). A phosphate transporter gene from the extra-radical mycelium of an arbuscular mycorrhizal fungus *Glomus intraradices* is regulated in response to phosphate in the environment. *Mol. Plant Microbe In.* 14, 1140–1148. doi: 10.1094/MPMI.2001.14.10.1140

Marschner, H., and Dell, B. (1994). Nutrient uptake in mycorrhizal symbiosis. *Plant Soil* 159, 89–102. doi: 10.1007/BF00000098

McCormick, R., Truong, S., Sreedasyam, A., Jenkins, J., Shu, S., Sims, D., et al. (2018). The Sorghum bicolor reference genome: Improved assembly, gene annotations, a transcriptome atlas, and signatures of genome organization. *Plant J.* 93 (2), 338–354.

McFarlane, H. E., Watanabe, Y., Yang, W., Huang, Y., Ohlrogge, J., and Samuels, A. L. (2014). Golgi- and trans-Golgi network-mediated vesicle trafficking is required for wax secretion from epidermal cells. *Plant Physiol.* 164, 1250–1260. doi: 10.1104/pp.113.234583

McGonigle, T. P., Miller, M. H., Evans, D. G., Fairchild, G. L., and Swan, J. A. (1990). A new method which gives an objective measure of colonization of roots by vesicular—arbuscular mycorrhizal fungi. *New Phytol.* 115, 495–501. doi: 10.1111/j.1469-8137.1990.tb00476.x

McLean, A. M., Bravo, A., and Harrison, M. J. (2017). Plant signaling and metabolic pathways enabling arbuscular mycorrhizal symbiosis. *Plant Cell* 29, 2319–2335. doi: org/10.1105/tpc.17.00555

Morin, E., Miyauchi, S., San Clemente, H., Chen, E. C. H., Pelin, A., de la Providencia, I., et al. (2019). Comparative genomics of *Rhizophagus irregularis,* R. cerebriforme, R. *diaphanus* and *Gigaspora rosea* highlights specific genetic features in Glomeromycotina. *New Phytol.* 222, 1584–1598. doi: 10.1111/nph.15687

Mortazavi, A., Williams, B. A., McCue, K., Schaeffer, L., and Wold, B. (2008). Mapping and quantifying mammalian transcriptomes by RNA-Seq. *Nat. Methods* 5, 621–628. doi: org/10.1038/nmeth.1226

Murphy, J., and Riley, J. P. (1962). A modified single solution method for the determination of phosphate in natural waters. *Anal. Chim. Acta* 27, 31–36. doi: 10.1016/S0003-2670(00)88444-5

Nagy, R., Karandashov, V., Chague, V., Kalinkevich, K., Tamasloukht, M. B., Xu, G., et al. (2005). The characterization of novel mycorrhiza-specific phosphate transporters from *Lycopersicon esculentum* and *Solanum tuberosum* uncovers functional redundancy in symbiotic phosphate transport in solanaceous species. *Plant J.* 42, 236–250. doi: 10.1111/j.1365-313X.2005.02364

Norambuena, L., Marchant, L., Berninsone, P., Hirschberg, C. B., Silva, H., and Orellana, A. (2002). Transport of UDP-galactose in plants: identification and functional characterization of AtUTr1, an *Arabidopsis thaliana* UDP-galactose/UDP-glucose transporter. *J. Biol. Chem.* 277, 32923–32929. doi: 10.1074/jbc.M204081200

Olsson, P. A., Rahm, J., and Aliasgharzad, N. (2010). Carbon dynamics in mycorrhizal symbioses is linked to carbon costs and phosphorus benefits. *FEMS Microbiol. Ecol.* 72, 125–131. doi: 10.1111/j.1574-6941.2009.00833

Pao, S. S., Paulsen, I. T., and Saier, M. H. (1998). Major facilitator superfamily. *Microbiol. Mol. Biol. Rev.* 62, 1–34.

Paszkowski, U. (2006). A journey through signaling in arbuscular mycorrhizal symbioses. *New Phytol.* 172, 35–46. doi: 10.1111/j.1469-8137.2006.01840

Pérez-Tienda, J., Testillano, P. S., Balestrini, R., Fiorilli, V., Azcón-Aguilar, C., and Ferrol, N. (2011). GintAMT2, a new member of the ammonium transporter family in the arbuscular mycorrhizal fungus *Glomus intraradices*. *Fung. Genet. Biol.* 48, 1044–1055. doi: 10.1016/j.fgb.2011.08.003

Pérez-Tienda, J., Corrêa, A., Azcón-Aguilar, C., and Ferrol, N. (2014). Transcriptional regulation of host transporters and GS/GOGAT pathway in arbuscular mycorrhizal rice roots. *Plant Physiol. Biochem.* 75, 1–8. doi: 10.1016/j.plaphy.2013.11.029

Poirier, Y., and Bucher, M. (2002). Phosphate transport and homeostasis in Arabidopsis. in *The Arabidopsis Book* eds. C.R. Sommerville, and E.M. Meyerowitz (Rockville, Maryland: American Society of Plant Biologists).

Pumplin, N., and Harrison, M. J. (2009). Live-cell imaging reveals periarbuscular membrane domains and organelle location in *Medicago truncatula* roots during arbuscular mycorrhizal symbiosis. *Plant Physiol.* 151, 809–819. doi: 10.1104/pp.109.141879

Pumplin, N., Zhang, X., Noar, R. D., and Harrison, M. J. (2012). Polar localization of a symbiosis-specific phosphate transporter is mediated by a transient reorientation of secretion. *P. Natl. Acad. Sci. U .S. A.* 109, 665–672. doi: 10.1073/pnas.1110215109

Rausch, C., and Bucher, M. (2002). Molecular mechanisms of phosphate transport in plants. *Planta* 216, 23–37. doi: 10.1007/s00425-002-0921-3

Rausch, C., Daram, P., Brunner, S., Jansa, J., Laloi, M., Leggewie, G., et al. (2001). A phosphate transporter expressed in arbuscule-containing cells in potato. *Nature* 414, 462–470. doi: 10.1038/35106601

Rautengarten, C., Ebert, B., Moreno, I., Temple, H., Herter, T., Link, B., et al. (2014). The Golgi localized bifunctional UDP-rhamnose/UDP-galactose transporter family of Arabidopsis. *P. Natl. Acad. Sci. U.S.A.* 111, 11563–11568. doi: 10.1073/pnas.1406073111

Saeed, A. I., Bhagabati, N. K., Braisted, J. C., Liang, W., Sharov, V., Howe, E. A., et al. (2006). TM4 microarray software suite. *Method. Enzymol.* 411, 134–193. doi: 10.1016/S0076-6879(06)11009-5

Schüßler, A., Martin, H., Cohen, D., Fitz, M., and Wipf, D. (2006). Characterization of a carbohydrate transporter from symbiotic glomeromycotan fungi. *Nature* 444, 933–936. doi: 10.1038/nature05364

Schachtman, D. P., Reid, R. J., and Ayling, S. M. (1998). Phosphorus uptake by plants: from soil to cell. *Plant Physiol.* 116, 447–453. doi: 10.1104/pp.116.2.447

Selle, A., Willmann, M., Grunze, N., Geßler, A., Weiß, M., and Nehls, U. (2005). The high-affinity poplar ammonium importer PttAMT1.2 and its role in ectomycorrhizal symbiosis. *New Phytol.* 168, 697–706. doi: 10.1111/j.1469-8137.2005.01535

Smith, S. E., and Read, D. J. (2008). *Mycorrhizal symbiosis*. 3rd (London: Academic Press).

Smith, S. E., and Smith, F. A. (2011). Roles of arbuscular mycorrhizas in plant nutrition and growth: new paradigms from cellular to ecosystem scales. *Annu. Rev. Plant Biol.* 62, 227–250. doi: 10.1146/annurev-arplant-042110-103846

Strehmel, N., Hummel, J., Erban, A., Strassburg, K., and Kopka, J. (2008). Retention index thresholds for compound matching in GC–MS metabolite profiling. *J. Chromatogr. B* 871, 182–190. doi: 10.1016/j.jchromb.2008.04.042

Takabatake, R., Hata, S., Taniguchi, M., Kouchi, H., Sugiyama, T., and Izui, K. (1999). Isolation and characterization of cDNAs encoding mitochondrial phosphate transporters in soybean, maize, rice, and Arabidopsis. *Plant Mol. Biol.* 40, 479–486. doi: 10.1023/A:1006285009435

Tang, N., San Clemente, H., Roy, S., Becard, G., Zhao, B., and Roux, C. (2016). A survey of the gene repertoire of *Gigaspora rosea* unravels conserved features among glomeromycota for obligate biotrophy. *Front. Microbiol.* 7, 233. doi: 10.3389/fmicb.2016.00233

Tatry, M. V., El Kassis, E., Lambilliotte, R., Corratgé, C., Van Aarle, I., Amenc, L. K., et al. (2009). Two differentially regulated phosphate transporters from the symbiotic fungus *Hebeloma cylindrosporum* and phosphorus acquisition by ectomycorrhizal *Pinus pinaster*. *Plant J.* 57, 1092–1102. doi: 10.1111/j.1365-313X.2008.03749

Toussaint, J. P., St-Arnaud, M., and Charest, C. (2004). Nitrogen transfer and assimilation between the arbuscular mycorrhizal fungus Glomus intraradices Schenck and Smith and Ri T-DNA roots of Daucus carota L. in an in vitro compartmented system. *Can. J. Microbiol.* 50, 251–260. doi: 10.1139/w04-009

Tuskan, G. A., Difazio, S., Jansson, S., Bohlmann, J., Grigoriev, I., Hellsten, U., et al. (2006). The genome of black cottonwood, *Populus trichocarpa* (Torr. and Gray). *Science* 313, 1596–1604. doi: 10.1126/science.1128691

Villegas, J., Williams, R. D., Nantais, L., Archambault, J., and Fortin, J. A. (1996). Effects of N source on pH and nutrient exchange of extramatrical mycelium in a mycorrhizal Ri T-DNA transformed root system. *Mycorrhiza* 6, 247–251. doi: 10.1007/s005720050132

Walder, F., Niemann, H., Natarajan, M., Lehmann, M. F., Boller, T., and Wiemken, A. (2012). Mycorrhizal networks: common goods of plants shared under unequal terms of trade. *Plant Physiol.* 159, 789–797. doi: 10.1104/pp.112.195727

Walder, F., Boller, T., Wiemken, A., and Courty, P. E. (2016). Regulation of plants' phosphate uptake in common mycorrhizal networks: role of intraradical fungal phosphate transporters. *Plant Signal. Behav.* 11, e1131372. doi: 10.1080/15592324.2015.1131372

Wewer, V., Brands, M., and Dörmann, P. (2014). Fatty acid synthesis and lipid metabolism in the obligate biotrophic fungus *Rhizophagus irregularis* during mycorrhization of *Lotus japonicus*. *Plant J.* 79, 398–412. doi: 10.1111/tpj.12566

Whiteside, M. D., Garcia, M. O., and Treseder, K. K. (2012). Amino acid uptake in arbuscular mycorrhizal plants. *PloS One* 7, e47643. doi: 10.1371/journal.pone.0047643

Whiteside, M. D., Werner, G. D. A., Caldas, V. E. A., van't Padje, A., Dupin, S. E., Elbers, B., et al. (2019). Mycorrhizal fungi respond to resource inequality by moving phosphorus from rich to poor patches across networks. *Curr. Biol.* 29, 2043–2050. doi: 10.1016/j.cub.2019.04.061

Wipf, D., Krajinski, F., van Tuinen, D., Recorbet, G., and Courty, P. E. (2019). Trading on the arbuscular mycorrhiza market: from arbuscule to common mycorrhizal networks. *New Phytol.* 223, 1127–1142. doi: 10.1111/nph.15775

Zhang, H., Ziegler, W., Han, X., Trumbore, S., and Hartmann, H. (2015). Plant carbon limitation does not reduce nitrogen transfer from arbuscular mycorrhizal fungi to *Plantago lanceolata*. *Plant Soil* 396369-380, 1–12. doi: 10.1007/s11104-015-2599-x

Conflict of Interest: The authors declare that the research was conducted in the absence of any commercial or financial relationships that could be construed as a potential conflict of interest.

frontiers in Plant Science

ORIGINAL RESEARCH
published: 20 December 2019
doi: 10.3389/fpls.2019.01628

TPLATE Recruitment Reveals Endocytic Dynamics at Sites of Symbiotic Interface Assembly in Arbuscular Mycorrhizal Interactions

*Giulia Russo[1], Gennaro Carotenuto[2], Valentina Fiorilli[2], Veronica Volpe[2], Antonella Faccio[3], Paola Bonfante[2], Mireille Chabaud[4], Marco Chiapello[3], Daniel Van Damme[5,6] and Andrea Genre[2]**

[1] Department of Agricultural, Forest and Food Sciences, University of Torino, Torino, Italy, [2] Department of Life Sciences and Systems Biology, University of Torino, Torino, Italy, [3] Institute for Sustainable Plant Protection, National Research Council, Torino, Italy, [4] LIPM, Université de Toulouse, INRAE, CNRS, Castanet-Tolosan, France, [5] Department of Plant Biotechnology and Bioinformatics, Ghent University, Ghent, Belgium, [6] VIB Department of Plant Systems Biology, Ghent University, Ghent, Belgium

OPEN ACCESS

Edited by:
Didier Reinhardt, Université de Fribourg, Switzerland

Reviewed by:
Sabine Dagmar Zimmermann, Délégation Languedoc Roussillon (CNRS), France
Viktor Zarsky, Charles University, Czechia

***Correspondence:**
Andrea Genre
andrea.genre@unito.it

Specialty section:
This article was submitted to Plant Microbe Interactions, a section of the journal Frontiers in Plant Science

Received: *11 July 2019*
Accepted: *19 November 2019*
Published: *20 December 2019*

Citation:
Russo G, Carotenuto G, Fiorilli V, Volpe V, Faccio A, Bonfante P, Chabaud M, Chiapello M, Van Damme D and Genre A (2019) TPLATE Recruitment Reveals Endocytic Dynamics at Sites of Symbiotic Interface Assembly in Arbuscular Mycorrhizal Interactions. Front. Plant Sci. 10:1628. doi: 10.3389/fpls.2019.01628

Introduction: Arbuscular mycorrhizal (AM) symbiosis between soil fungi and the majority of plants is based on a mutualistic exchange of organic and inorganic nutrients. This takes place inside root cortical cells that harbor an arbuscule: a highly branched intracellular fungal hypha enveloped by an extension of the host cell membrane—the perifungal membrane—which outlines a specialized symbiotic interface compartment. The perifungal membrane develops around each intracellular hypha as the symbiotic fungus proceeds across the root tissues; its biogenesis is the result of an extensive exocytic process and shows a few similarities with cell plate insertion which occurs at the end of somatic cytokinesis.

Materials and Methods: We here analyzed the subcellular localization of a GFP fusion with TPLATE, a subunit of the endocytic TPLATE complex (TPC), a central actor in plant clathrin-mediated endocytosis with a role in cell plate anchoring with the parental plasma membrane.

Results: Our observations demonstrate that *Daucus carota* and *Medicago truncatula* root organ cultures expressing a 35S::*At*TPLATE-GFP construct accumulate strong fluorescent green signal at sites of symbiotic interface construction, along recently formed perifungal membranes and at sites of cell-to-cell hyphal passage between adjacent cortical cells, where the perifungal membrane fuses with the plasmalemma.

Discussion: Our results strongly suggest that TPC-mediated endocytic processes are active during perifungal membrane interface biogenesis—alongside exocytic transport. This novel conclusion, which might be correlated to the accumulation of late endosomes in the vicinity of the developing interface, hints at the involvement of TPC-dependent membrane remodeling during the intracellular accommodation of AM fungi.

Keywords: arbuscular mycorrhizas, *Medicago truncatula*, *Daucus carota*, endocytosis, symbiosis, live cell imaging, confocal laser scanning microscope, transmission electron microscope

INTRODUCTION

Arbuscular mycorrhizal (AM) symbiosis with Glomeromycotina fungi supports life of most land plants, including the majority of crop species, providing their roots with a more efficient access to soil nutrients (Gutjahr and Parniske, 2013). In change, host plants share with their symbiotic fungi up to 20% of photosynthesis-derived carbon, in form of sugars and lipids (Bago et al., 2002; McLean et al., 2017). This nutrient exchange takes place in highly branched hyphae, called arbuscules, that are accommodated inside the living root cells (Gutjahr and Parniske, 2013). This intimate intracellular interaction is achieved through the assembly of a novel host cell compartment, called the symbiotic interface (Gutjahr and Parniske, 2013).

Enveloped by the perifungal membrane, a specialized extension of the host plasmalemma (Pumplin and Harrison, 2009), the symbiotic interface surrounds intracellular hyphae and arbuscules with plant cell wall-related compounds.

Furthermore, live cell investigations have revealed how the symbiotic interface is assembled within the prepenetration apparatus (PPA), a broad cytoplasmic aggregation (Genre et al., 2005; Genre et al., 2008), where the secretory process is focused and coordinated (Genre et al., 2012).

We have recently demonstrated that root colonization by AM fungi is associated with cell cycle reactivation (Carotenuto et al., 2019a; Carotenuto et al., 2019b), suggesting that symbiotic interface biogenesis could evolutionarily and developmentally be related to cell plate assembly (Russo et al., 2019).

Indeed, analogous cellular features have been described for the two processes. Firstly, the composition of the interface materials has been described as largely analogous to that of the cell plate, the non-structured cell wall that divides daughter cells at the end of mitosis (Balestrini and Bonfante, 2005; Balestrini and Bonfante, 2014). Secondly, ultrastructural details of the PPA aggregate present remarkable similarities with the organization of subcellular compartments during cell plate assembly (Genre et al., 2012). This includes the concentration of Golgi stacks and proliferation of trans-Golgi membranes (Genre et al., 2012). In this frame, the occurrence of late endosomes/multivesicular bodies (MVB) in the PPA aggregate has raised the question whether the PPA-driven exocytic activity could be associated with endocytic processes (Genre et al., 2008; Genre et al., 2012). Indeed, the massive exocytic process directed to the cell plate by phragmoplast microtubules during plant cell division (Lee and Liu, 2013; Boruc and Van Damme, 2015) is associated with extensive endocytic recycling of surplus membrane (Backues et al., 2007). In fact, a key actor of the endocytic process—the adaptin-related protein TPLATE, a subunit of the octameric TPLATE adaptor complex (TPC), has been shown to accumulate on both the cell plate membrane and the plasmalemma at the cortical division zone surrounding the cell plate insertion site, where the cell plate will eventually fuse (Van Damme et al., 2006; Van Damme et al., 2011; Gadeyne et al., 2014). *TPLATE* and other endocytic players (Gadeyne et al., 2014) have been shown to be upregulated during early AM development (Russo et al., 2019), and TPLATE-GFP-decorated cell walls have highlighted the occurrence of ectopic cell divisions in the root area that is preparing to accommodate arbuscules (Russo et al., 2019).

The present study, largely based on live cell imaging of *D. carota* and *M. truncatula* ROCs colonized by the AM fungus *Gigaspora gigantea*, suggests PPA-associated endocytic activity at the sites of perifungal membrane assembly. In particular, the endocytic marker accumulates at the growing tips of the perifungal membrane and at sites of perifungal membrane fusion with the peripheral plasmalemma, in striking analogy with the described TPLATE localization during cell plate expansion and fusion. Our results support the involvement of intense endocytic processes, likely related to perifungal membrane modeling and the recycling of membrane surplus at sites of hyphal exit from the host cell.

METHODS

Plant and Fungal Materials

Agrobacterium rhizogenes-transformed root organ cultures (ROCs) expressing the *35S::AtTPLATE-GFP* vector (Van Damme et al., 2004) were obtained from *Medicago truncatula* Jemalong A17 wild-type and *dmi3-1* seedlings (Sagan et al., 1995; kindly provided by M. Chabaud, LIPM, INRA, Toulouse, France), according to Boisson-Dernier et al. (2001). ROCs from *Daucus carota* var Sativus expressing the same vector were obtained according to Bécard and Fortin (1988). For both species, transformed roots with a high level of fluorescence were selected 21 days after transformation, decontaminated and subcultured on M medium (Bécard and Fortin, 1988) at 25°C in the dark for subsequent use as ROCs. ROC generation was repeated in two independent experiments for each species and line, with overlapping results in terms of GFP fluorescence pattern. In each case, a single representative clone was chosen for further studies. Transformation efficiency and expression of *35S::AtTPLATE-GFP* was checked with GFP specific primers on both genomic DNA and cDNA obtained from all the selected lines, as described in Russo et al. (2019).

G. gigantea (isolate HC/FE30, Herbarium Cryptogamicum Fungi, University of Torino, Italy), which is characterized by strong cytoplasmic autofluorescence (Genre et al., 2005), was used to inoculate ROCs *in vitro* for confocal imaging. Spores of *G. gigantea* were collected from pot cultures in sand (with leek and clover, respectively), surface-sterilized, and stored at 4°C according to Bécard and Fortin (1988) until inoculation.

Confocal Microscopy

The targeted AM inoculation technique for studying early stages of the symbiotic association between *Gigaspora* species and transformed root cultures, developed by Chabaud et al. (2002) and adapted for confocal observation by Genre et al. (2005), was applied to both *M. truncatula* and *D. carota* ROCs expressing *35S::AtTPLATE-GFP*. An upright Leica TCS SP2 confocal microscope fitted with a long distance 40X water-immersion objective (HCX Apo 0.80) was used for imaging living ROCs directly in the Petri dishes. The argon laser band of 488 nm was used to excite both GFP and *G. gigantea* autofluorescence. The two

signals were separated using specific emission windows: 500 to 525 nm for GFP and 590 to 630 nm for fungal autofluorescence. The latter channel was then false-colored in red to maximize the contrast in overlapping images.

Confocal images presented in figures are representative of the observations performed on a minimum of 30 infection units from at least 10 independent ROC specimens for each plant species.

Electron Microscopy

Following the identification of GFP-labeled PPAs in the inner cortex through confocal microscopy, five *D. carota* ROC segments were excised and processed for transmission electron microscopy (TEM) according to Genre et al. (2008). After fixation, samples were infiltrated and embedded in a thin layer of Epon-Araldite (Hoch, 1986) resin. Fungal colonization sites within flat-embedded samples were selected under an optical microscope, excised with a razor blade, and mounted on resin stubs prior to ultramicrotomy. Ultrathin (70 nm) sections were cut, counterstained, and observed using a Philips CM10 TEM.

RESULTS

TPLATE-GFP Accumulates in Epidermal PPA

TPLATE localization was studied through the expression of a 35S::*At*TPLATE-GFP fusion protein in *M. truncatula* and *D. carota* ROCs. This construct had previously been used in both species to mark cell divisions in meristematic and differentiated root tissues (Russo et al., 2019). The same GFP fusion was also expressed in ROCs derived from the non-mycorrhizal *dmi3-1* mutant of *M. truncatula* (Sagan et al., 1995; Levy et al., 2004), where the loss of *Does not Make Infection 3* (a nuclear localized calcium-and-calmodulin-dependent kinase) blocks a symbiotic signal transduction pathway and halts fungal colonization to the surface of epidermal cells (Morandi et al., 2005). ROCs were colonized with the autofluorescent AM fungus *G. gigantea* and dozens of infection sites, at different stages of root colonization, were observed for each experimental condition through confocal live cell imaging.

A significant accumulation of TPLATE-GFP was observed in both *M. truncatula* and *D. carota* epidermal root cells in the PPA area (**Figure 1**): prior to root cell penetration the GFP signal was strong between the repositioned nucleus and the hyphopodium contact site, clearly highlighting both developing (**Figures 1A**, **B**) and fully formed PPAs (**Figure 1C**). For comparison, the fluorescence patterns of free DsRED (diffusing in the cytosol and nucleus) and PIP2-GFP (labeling a plasma membrane aquaporin) are presented in **Supplementary Figure 1**. Significantly, no intracellular accumulation of TPLATE-GFP was observed in the contacted epidermal cells of *dmi3-1* mutants (**Figure 1D**).

Due to the acknowledged role of the TPLATE complex (TPC) in endocytosis, our observations in two phylogenetically distant plants suggest that the activation of endocytic processes are part of the AM prepenetration responses in epidermal cells. This conclusion is further supported by the absence of TPLATE accumulation in *dmi3-1* mutants of *M. truncatula*, where PPAs (Genre et al., 2005) and epidermal cell penetration (Levy et al., 2004) are blocked, and *TPLATE*, *AP2A1*, and *Clathrin* are not upregulated upon AM inoculation (Russo et al., 2019).

Perifungal Membrane Dynamics in the Cortex Recruit TPLATE

As we extended our observations to inner root tissues, following the progress of fungal development, we remarked that intense TPLATE accumulation in PPAs was also present in outer cortical cells (**Figure 2**). In detail, by the time the penetrating hypha had reached the inner side of the epidermal cell (**Figure 2A**), an intense TPLATE-GFP labeling could be spotted in the underlying cortical cell, within the developing PPA aggregation opposite the hyphal tip. Comparably intense GFP signals could also be seen in more advanced PPAs in the outer cortex of both *M. truncatula* and *D. carota* (**Figures 2B**, **C**).

The limited translucence of *M. truncatula* ROCs (Genre et al., 2008) restricted our ability to obtain clear images of the inner cell layers. Consequently, cortex colonization was more extensively studied in the thinner and clearer *D. carota* ROCs expressing the same TPLATE-GFP fusion.

A diffuse TPLATE-GFP signal highlighted cortical PPAs of different developmental stages (**Figures 2C**, **D**), from small nucleus-associated aggregates appressed to transverse cell walls (**Figure 2C**) to broad arrow-shaped PPAs (**Figure 2D**), typical of the carrot root cortex (Genre et al., 2008), where intraradical colonization proceeds from cell to cell (*Paris*-type pattern; Dickson, 2004). Intense TPLATE accumulation was also observed around the tips of linear (**Figures 2C**, **D**) and branched hyphae (**Figure 2E**, **F**) in both outer and inner cortical cell layers. Furthermore, a fainter GFP signal extending along the perifungal membrane behind the growing hyphal tip was occasionally visible in both epidermal (**Figure 2A**) and cortical cells (**Figure 2E**).

Lastly, diffuse fluorescence was present around newly formed arbuscules that had not yet fully occupied the lumen of inner cortical cells (**Figure 2G**). By contrast, no relevant GFP accumulation was recorded around fully developed arbuscules (**Figure 2H**).

Overall, our observations of *M. truncatula* and carrot roots indicate that TPLATE-GFP is recruited to the sites of perifungal membrane development in the PPA of both plant species and strongly suggest the involvement of endocytic processes in all cell types engaged in AM colonization, before and during the development of intracellular hyphae, hyphal branches, and arbuscules.

This conclusion appeared in line with previous detection of MVBs in the PPA aggregate (Genre et al., 2008; Genre et al., 2012). Indeed, our new TEM observations of carrot cortical PPAs (**Figure 3**) confirmed the presence of membrane-delimited compartments of different size, containing several intraluminal vesicles, that can be ascribed with confidence to the class of MVBs, or late endosomes. Their presence appears now congruous with our localization of TPLATE-GFP in the PPA,

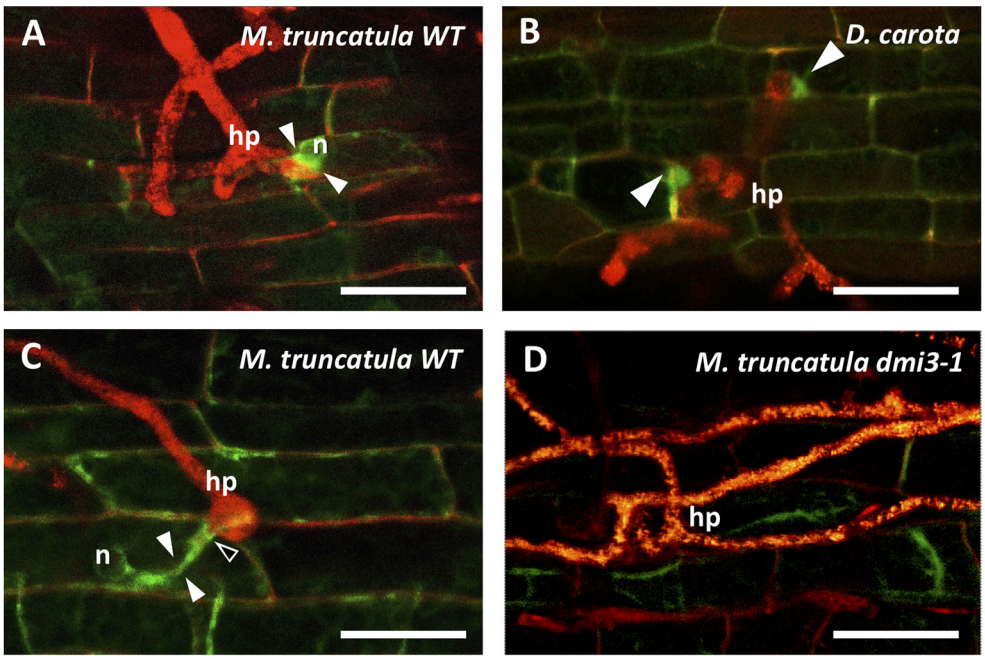

FIGURE 1 | Accumulation of TPLATE-GFP in the prepenetration apparatus of *Medicago truncatula* and *Daucus carota* root epidermal cells. In the presence of a hyphopodium (hp) on the root surface of *M. truncatula* WT ROCs **(A**, **C)** and *D. carota* ROCs **(B)**, intense TPLATE-GFP fluorescence is observed in the PPA area (arrowheads), during the initial nuclear repositioning (n) **(A)**, at two sites of fungal contact within the same hyphopodium **(B)** and during the following extension of the PPA **(C)**. Furthermore, a thin line of intense fluorescence is also visible in C, outlining the point (empty arrowhead) where the penetrating hypha is developing. In contrast, no GFP accumulation is visible on the root surface at the hyphopodium contact site of *M. truncatula dmi3-1* mutants **(D)** that are impaired in PPA formation and fungal colonization. Bars = 50 μm.

hinting to occurrence of endocytic processes during intracellular fungal accommodation.

TPLATE Labeling at Sites of Cell-to-Cell Hyphal Passage in Carrot

Tissue translucency and *Paris*-type colonization allowed a very accurate observation of fungal proliferation and associated cell responses in the outer cortex of carrot. Beside hyphal tip-associated TPLATE-GFP labeling in PPA aggregates (**Figures 4A–C**) a remarkable accumulation of fluorescent signal was also observed along the transverse wall corresponding to the predicted exit site (es) of the hypha from the colonized cell (**Figure 4A**). This transverse wall-associated labeling appeared to persist during and after hyphal cell-to-cell passage (**Figures 4B, C**). This is particularly evident when comparing the panels of **Figures 4B, C**, which frame the same cells as the hyphal tip grows across the transverse wall over an interval of 1 h. Such localized accumulations of membrane-associated TPLATE-GFP are clearly different from the homogeneous distribution of a membrane protein such as the aquaporin *At*PIP2 (**Supplementary Figures 1E, F**).

Such consistent observations hint at a role for TPC-related endocytosis in the fusion between the developing perifungal membrane and the plasmalemma at the cell exit site, a rather unusual event in plant cell dynamics that predictably involves the removal of a consistent membrane surplus.

DISCUSSION

Endocytosis in Host Cell Penetration

Our previous results (Russo et al., 2019) on the upregulation of endocytic markers such as *Clathrin*, *AP2A1*, and *TPLATE* during early AM interactions, had suggested a role for clathrin-mediated endocytosis in AM fungal accommodation. Our current live-cell observations in carrot and wild-type—but not *dmi3-1*—Medicago, showing TPLATE-GFP accumulation in PPAs and along the perifungal membranes, provide more direct evidence of endocytosis in symbiotic processes of membrane remodeling and interface biogenesis for all colonized cells.

This proposed role for endocytosis in AM fungal accommodation complements previous demonstrations of the exocytic origin of the symbiotic interface (Genre et al., 2012; Ivanov et al., 2012). In fact, focused exocytic events in the plant cell are normally associated with endocytic recycling of surplus membrane (Samaj et al., 2004; Ketelaar et al., 2008). Significantly, this is the case for cell plate formation (Dhonukshe et al., 2006; Backues et al., 2007; McMichael and Bednarek, 2013) and the analogous accumulation of TPLATE at sites of perifungal membrane assembly supports the hypothesis that the whole membrane remodeling process set in motion to perform cell division is recruited by AM host cells for fungal accommodation.

Alongside membrane modeling, clathrin-mediated endocytosis is also known to be involved in receptor turnover

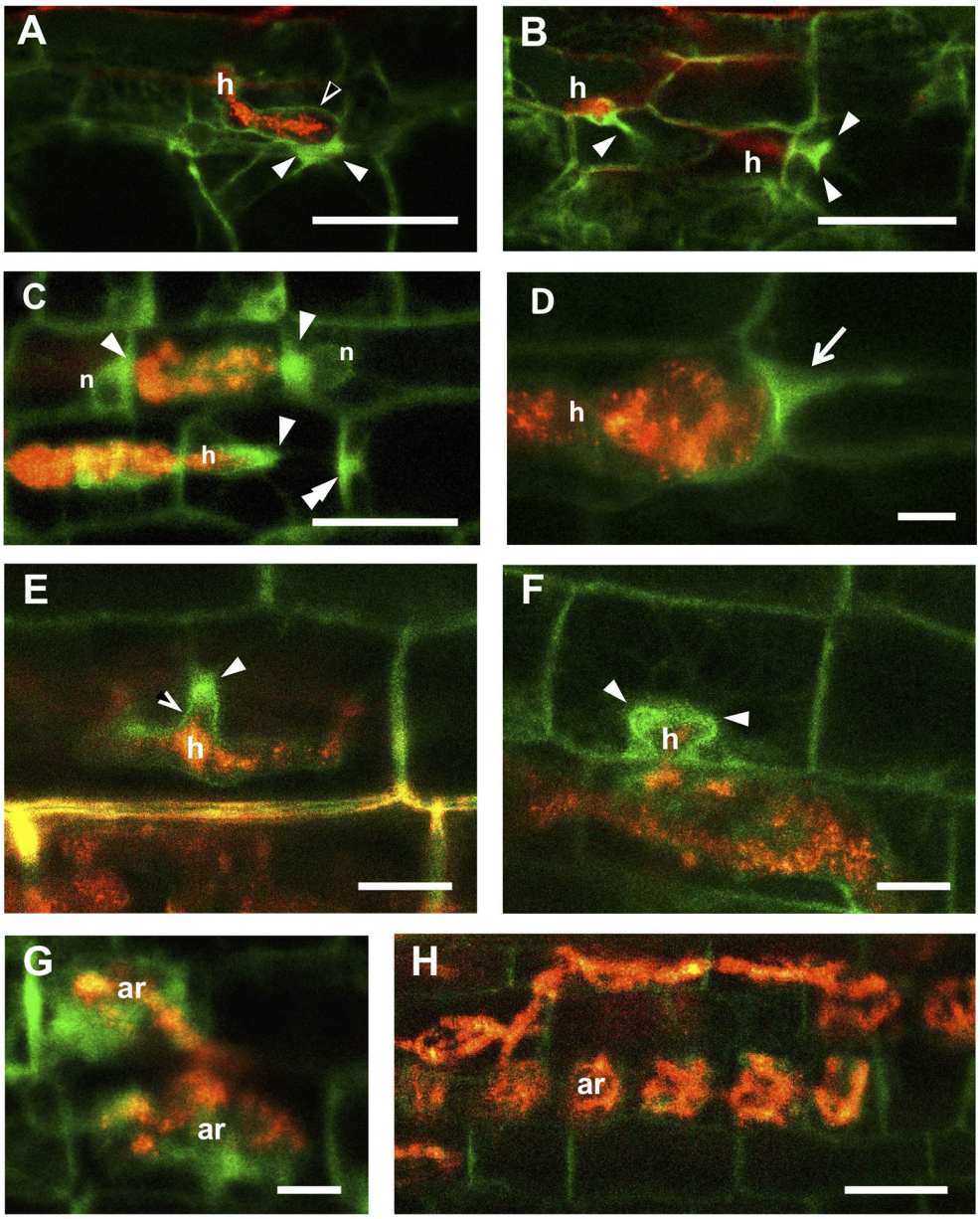

FIGURE 2 | TPLATE-GFP labeling of symbiotic interface in deeper layers of *Medicago truncatula* and *Daucus carota* roots. **(A)** shows an intracellular hypha (h) inside an *M. truncatula* root epidermal cell. The perifungal membrane appears outlined by a faint GFP signal (empty arrowhead), whereas intense fluorescence accumulates in the developing PPA in the underlying outer cortical cell (arrowheads). An analogous situation is presented in **(B)**, where two hyphae (h) are imaged as they pass from cell to cell in the cortex: in both cases an intense fluorescence marks the PPAs (arrowheads). PPAs labeling at different developmental stages are also observed in the cortex of *D. carota* **(C–F)**. Bright GFP signals are visible around the tips and branches of intracellular hyphae (arrowheads); along the cell wall at predicted hyphal exit site (double arrowhead in **C**); and along the perifungal membrane behind the growing hyphal tip (empty arrowhead in **E**). In **(D)** a *Gigaspora gigantea* hypha is on the point of passing from one cell to the next in the same file: the GFP signal marks the typical arrow-shaped PPA (arrow) of *Paris*-type mycorrhizas. **(G)** shows two young arbuscules (ar) surrounded by diffuse GFP fluorescence, suggesting that TPLATE is also involved in arbuscule accommodation, while this intense signal is lost in cortical cells that harbor older arbuscules **(H)**. Bars = 50 μm in **(A–C, H)**; 10 μm in **(D–G)**.

and internalization, with the generation of signaling endosomes (Ben Khaled et al., 2015). In the context of AM interactions, it will be interesting to investigate whether this process plays a role in the perception and translocation of fungal elicitors and effectors within the host cell.

Membrane Remodeling at Host Cell Exit Sites

While PPA-associated membrane proliferation from the site of fungal entry in the cell generates an extension of the plasmalemma (the perifungal membrane), hyphal exit from the cell lumen

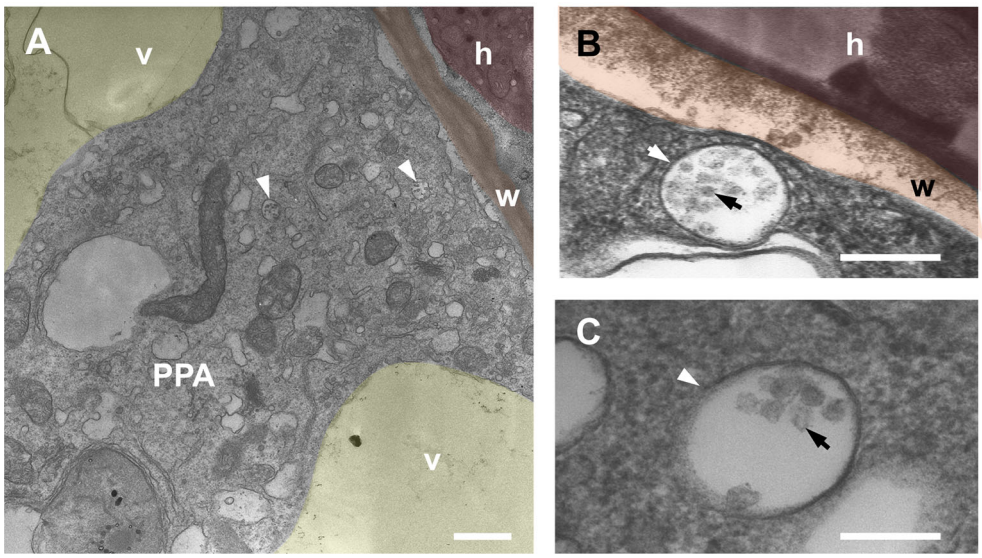

FIGURE 3 | TEM imaging of multivesicular bodies within *Daucus carota* PPA aggregates. Panel **(A)** shows a PPA inside a cortical cell of *D. carota*. The cytoplasmic aggregation splitting the vacuole (v, yellow) is assembled in front of an intraradical hypha (h, red) that is contacting the cell wall (w, orange). Several multivesicular bodies (MVBs) are visible (arrows). High magnification close-ups of single MVBs are presented in panels **(B** and **C)**, highlighting the characteristic presence of an outer endosomal membrane (white arrow) and several intraluminal vesicles (black arrow). Bars = 0.8 μm in A, 0.2 μm in B, 0.1 μm in C; false colors were overlaid to the original TEM images for clarity.

requires a rather different process. As the front of the proliferating perifungal membrane reaches the plasma membrane, fusion must occur between the two in order to generate a complete membrane tunnel surrounding the hypha (**Figures 4D**, **F**). Such a membrane fusion generating a trans-cellular apoplastic compartment is a peculiar event with few analogs in plant cell biology. The closest similarity is with the development of an infection thread carrying rhizobia across legume root tissues, toward a nodule primordium (Gage and Margolin, 2000; Downie, 2014). Nevertheless, 50 million year-old nitrogen-fixing symbioses are believed to have recruited part of the symbiotic responses developed earlier in the course of AM evolution, including intracellular colonization mechanisms (Bonfante and Genre, 2008). A less obvious, but very intriguing analogy is with the fusion of the cell plate membrane with the peripheral plasma membrane at the end of cell division (**Figures 4E**, **G**). In fact, the separation of daughter cells starts with the fusion of finger-like protrusions of the growing cell plate border with the plasmalemma, at the cortical division zone (Samuels et al., 1995). In the light of our current findings, the similarity between such finger-like protrusions and the tip of the perifungal membrane is striking: both membranes at the cell plate border and the cortical division zone are characterized by the active recruitment of TPC members (Van Damme et al., 2011; Gadeyne et al., 2014); our observation of TPLATE-GFP accumulation at fungal exit sites indicates the recruitment of this protein on the two fusing membranes, and is evocative of the co-optation of cell division-related membrane dynamics in symbiotic responses.

Evolutionary-Developmental Implications

Our recent demonstration of cell cycle (Carotenuto et al., 2019a) and cell division reactivation in root cortical cells during AM colonization (Russo et al., 2019), proposed these processes as features of the 400-Myr-old AM symbiosis that were conserved for the origin of symbiotic nitrogen fixation (SNF) between legumes and rhizobia, around 50 Myr ago. While, anyway, cell cycle reactivation has been related to nodule initiation in SNF, the lack of neo-organogenesis in AM left several hypotheses open about the biological role of sparse cell divisions in the AM root cortex.

We speculated that a mechanistic analogy could link the exocytic processes of cell plate and symbiotic interface biogenesis, also based on several analogies in the formation (Lam et al., 2008; Pumplin et al., 2012) and composition in cell wall-related materials (Balestrini and Bonfante, 2014) of the two cell compartments. Our present results substantiate this hypothesis, suggesting that the cell plate deposition machinery, combining exocytic and endocytic processes, has been co-opted in symbiotic interface biogenesis at the origin of AM, and later conserved in SNF interactions.

DATA AVAILABILITY STATEMENT

The datasets generated for this study are available on request to the corresponding author.

AUTHOR CONTRIBUTIONS

GR designed the experiments, developed the transgenic lines, performed confocal microscopy analyses and wrote the text. GC performed transgenic line production, and contributed to the writing. VF, MaC, MiC and VV contributed to transgenic plant

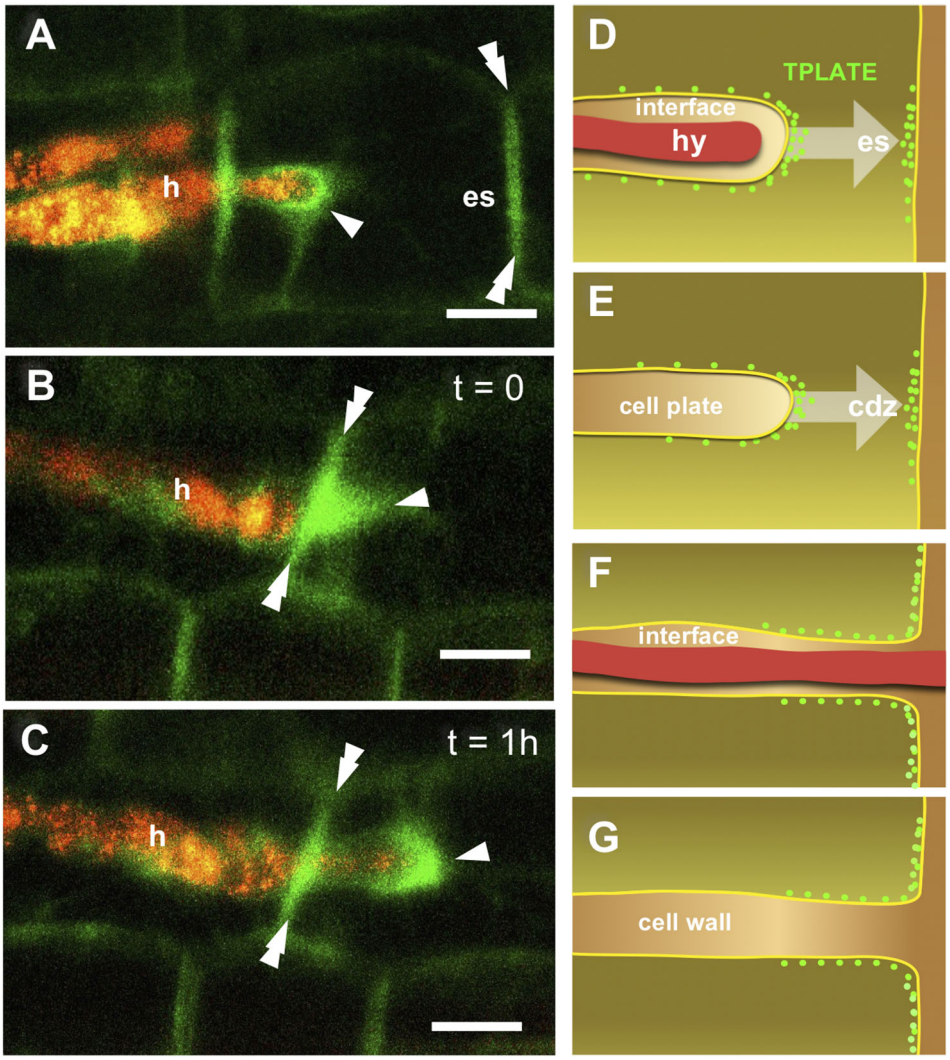

FIGURE 4 | TPLATE-GFP labeling of cell-to-cell hyphal passage in the outer cortex. An intense GFP signal (arrowhead) is visible in **(A)**, around the tip of an intracellular hypha (h). This is associated with the accumulation of TPLATE-GFP along the wall (double arrowheads) that separates the colonized cell from the adjoining uncolonized cell, in the area of the predicted hyphal exit site (es). An elongated PPA (arrowhead) is visible in an uncolonized cell on the right side of panel **(B)**; the hypha growing in the cell on the left has reached the cell wall, where an intense GFP signal has accumulated (double arrowheads). The same site is pictured in **(C)** 1 h later: The hypha has now penetrated the cell on the right; a bright signal surrounds the hyphal tip (arrowheads) and a strong fluorescence is still visible along the cell wall (double arrowhead). Bars = 30 μm. Panels (**D**–**G**) show a schematic view of the analogies between perifungal membrane **(D**, **F)** and cell plate **(E**, **G)** fusion with the peripheral plasma membrane. In both cases, TPLATE accumulation was observed at the front of the developing compartment **(D**, **E)**, and at the exit site (es) or cortical division zone (cdz), respectively. Following membrane fusion **(F**, **G)**, TPLATE diffuses at the junction between the two membranes.

production and text writing. AF and PB performed electron microscopy analyses and contributed to the writing. DD provided the AtTPLATE-GFP vector and contributed to the writing. AG designed the research and experiments and wrote the text.

FUNDING

Financial support for this research was granted by Compagnia di San Paolo (project REPROGRAM – Progetti di Ateneo 2012, Call 01) and UNITO grants Ricerca Locale 2013-2014-2017.

ACKNOWLEDGMENTS

We are grateful to David Barker (LIPM Toulouse) for contributing to produce the root organ culture line expressing PIP2-GFP.

SUPPLEMENTARY MATERIAL

The Supplementary Material for this article can be found online at: https://www.frontiersin.org/articles/10.3389/fpls.2019.01628/full#supplementary-material

REFERENCES

Backues, S. K., Konopka, C. A., McMichael, C. M., and Bednarek, S. Y. (2007). Bridging the divide between cytokinesis and cell expansion. *Curr. Opin. Plant Biol.* 10, 607–615. doi: 10.1016/j.pbi.2007.08.009

Bago, B., Pfeffer, P. E., Zipfel, W., Lammers, P., and Shachar-Hill, Y. (2002). Tracking metabolism and imaging transport in arbuscular mycorrhizal fungi. Metabolism and transport in AM fungi. *Plant Soil* 244, 189–197. doi: 10.1007/978-94-017-1284-2_18

Balestrini, R., and Bonfante, P. (2005). The interface compartment in arbuscular mycorrhizae: a special type of plant cell wall? *Plant Biosyst.* 139, 8–15. doi: 10.1080/11263500500056799

Balestrini, R., and Bonfante, P. (2014). Cell wall remodeling in mycorrhizal symbiosis: a way towards biotrophism. *Front. Plant Sci.* 5, e237. doi: 10.3389/fpls.2014.00237

Bécard, G., and Fortin, J. A. (1988). Early events of vesicular–arbuscular mycorrhiza formation on Ri T-DNA transformed roots. *New Phytol.* 108, 211–218. doi: 10.1111/j.1469-8137.1988.tb03698.x

Ben Khaled, S., Postma, J., and Robatzek, S. (2015). A moving view: subcellular trafficking processes in pattern recognition receptor-triggered plant immunity. *Annu. Rev. Phytopathol.* 53, 379–402. doi: 10.1146/annurev-phyto-080614-120347

Boisson-Dernier, A., Chabaud, M., Garcia, F., Becard, G., Rosenberg, C., and Barker, D. G. (2001). Agrobacterium rhizogenes-transformed roots of Medicago truncatula for the study of nitrogen-fixing and endomycorrhizal symbiotic associations. *Mol. Plant–Microbe Interact.* 14, 695–700. doi: 10.1111/nph.15763

Bonfante, P., and Genre, A. (2008). Plants and arbuscular mycorrhizal fungi: an evolutionary-developmental perspective. *Trends Plant Sci.* 13, 492–498. doi: 10.1016/j.tplants.2008.07.001

Boruc, J., and Van Damme, D. (2015). Endomembrane trafficking overarching cell plate formation. *Curr. Opin. Plant Biol.* 28, 92–98. doi: 10.1094/MPMI.2001.14.6.695

Carotenuto, G., Volpe, V., Russo, G., Politi, M., Sciascia, I., de Almeida-Engler, J., et al. (2019a). Local endoreduplication as a feature of intracellular fungal accommodation in arbuscular mycorrhizas. *New Phytol.* 223, 430–446. doi: 10.1111/nph.15763

Carotenuto, G., Sciascia, I., Oddi, L., Volpe, V., and Genre, A. (2019b). Size matters: three methods for estimating nuclear size in mycorrhizal roots of Medicago truncatula by image analysis. *BMC Plant Biol.* 19, 180. doi: 10.1046/j.1469-8137.2002.00508.x

Chabaud, M., Venard, C., Defaux-Petras, A., Becard, G., and Barker, D. G. (2002). Targeted inoculation of Medicago truncatula in vitro root cultures reveals MtENOD11 expression during early stages of infection by arbuscular mycorrhizal fungi. *New Phytol.* 156, 265–273. doi: 10.1111/j.1469-8137.2004.01095.x

Dhonukshe, P., Baluska, F., Schlicht, M., Hlavacka, A., Samaj, J., Friml, J., et al. (2006). Endocytosis of cell surface material mediates cell plate formation during plant cytokinesis. *Dev. Cell* 10, 137–150. doi: 10.1016/j.cub.2014.01.028

Dickson, S. (2004). The Arum-Paris continuum of mycorrhizal symbioses. *New Phytol.* 163, 187–200. doi: 10.1016/j.cell.2014.01.039

Downie, A. (2014). Legume nodulation. *Curr. Biol.* 24, 184–190. doi: 10.1016/S1369-5274(00)00149-1

Gadeyne, A., Sanchez-Rodrıguez, C., Vanneste, S., Di Rubbo, S., Zauber, H., Vanneste, K., et al. (2014). The TPLATE adaptor complex drives clathrin-mediated endocytosis in plants. *Cell* 156, 691–704. doi: 10.1105/tpc.105.035410

Gage, D. J., and Margolin, W. (2000). Hanging by a thread: invasion of legume plants by rhizobia. *Curr. Opin. Microbiol.* 3, 613–617. doi: 10.1105/tpc.108.059014

Genre, A., Chabaud, M., Timmers, T., Bonfante, P., and Barker, D. G. (2005). Arbuscular mycorrhizal fungi elicit a novel intracellular apparatus in Medicago truncatula root epidermal cells before infection. *Plant Cell* 17, 3489–3499. doi: 10.1093/pcp/pcr170

Genre, A., Chabaud, M., Faccio, A., Barker, D. G., and Bonfante, P. (2008). Prepenetration apparatus assembly precedes and predicts the colonization patterns of arbuscular mycorrhizal fungi within the root cortex of both Medicago truncatula and Daucus carota. *Plant Cell* 20, 1407–1420. doi: 10.1146/annurev-cellbio-101512-122413

Genre, A., Ivanov, S., Fendrych, M., Faccio, A., Zarsky, V., Bisseling, T., et al. (2012). Multiple exocytotic markers accumulate at the sites of perifungal membrane biogenesis in arbuscular mycorrhizas. *Plant Cell Physiol.* 53, 244–255. doi: 10.1007/978-1-4684-5119-1_7

Gutjahr, C., and Parniske, M. (2013). Cell and developmental biology of arbuscular mycorrhiza symbiosis. *Annu. Rev. Cell Dev. Biol.* 29, 593–617. doi: 10.1073/pnas.1200407109

Hoch, H. C. (1986). "Freeze-substitution of fungi," in *Ultrastructure techniques of microorganisms*. Eds. H. C. Aldrich and W. J. Todd (New York: Plenum Press), 183–211. doi: 10.1111/j.1365-2818.2008.02031.x

Ivanov, S., Fedorova, E. E., Limpens, E., De Mita, S., Genre, A., Bonfante, P., et al. (2012). Rhizobium–legume symbiosis shares an exocytotic pathway required for arbuscule formation. *Proc. Natl. Acad. Sci. U. S. A.* 109, 8316–8321. doi: 10.1016/j.pbi.2013.10.008

Ketelaar, T., Galway, M. E., Mulder, B. M., and Emons, A. M. C. (2008). Rates of exocytosis and endocytosis in Arabidopsis root hairs and pollen tubes. *J. Microsc.* 231, 265–273. doi: 10.1126/science.1093038

Lam, S. K., Cai, Y., Hillmer, S., Robinson, D. G., and Jiang, L. (2008). SCAMPs highlight the developing cell plate during cytokinesis in tobacco BY-2 cells. *Plantphysiology* 147, (4), 1637–1645. doi: 10.1104/pp.108.119925

Lee, Y. R., and Liu, B. (2013). The rise and fall of the phragmoplast microtubule array. *Curr. Opin. Plant Biol.* 16, 757–763. doi: 10.1105/tpc.17.00555

Levy, J., Bres, C., Geurts, R., Chalhoub, B., Kulikova, O., Duc, G., et al. (2004). A putative Ca2+ and calmodulin-dependent protein kinase required for bacterial and fungal symbioses. *Science* 303, 1361–1364. doi: 10.1111/nph.12122

McLean, A. M., Bravo, A., and Harrison, M. J. (2017). Plant signaling and metabolic pathways enabling arbuscular mycorrhizal symbiosis. *Plant Cell* 29, 2319–2335. doi: 10.1007/s00572-004-0331-4

McMichael, C. M., and Bednarek, S. Y. (2013). Cytoskeletal and membrane dynamics during higher plant cytokinesis. *New Phytol.* 197, 1039–1057. doi: 10.1104/pp.109.141879

Morandi, D., Prado, E., Sagan, M., and Duc, G. (2005). Characterisation of new symbiotic Medicago truncatula (Gaertn.) mutants, and phenotypic or genotypic complementary information on previously described mutants. *Mycorrhiza* 15, 283–289. doi: 10.1111/nph.15398

Pumplin, N., and Harrison, M. J. (2009). Live-cell imaging reveals periarbuscular membrane domains and organelle location in Medicago truncatula roots during arbuscular mycorrhizal symbiosis. *Plant Physiol.* 151, 809–819. doi: 10.1016/0168-9452(95)04229-N

Pumplin, N., Zhang, X., Noar, R. D., and Harrison, M. J. (2012). Polar localization of a symbiosis-specific phosphate transporter is mediated by a transient reorientation of secretion. *Proc. Natl. Acad. Sci. U.S.A.* 109 (11), E665–E672. doi: 10.1073/pnas.1110215109

Russo, G., Carotenuto, G., Fiorilli, V., Volpe, V., Chiapello, M., Van Damme, D., et al. (2019). Ectopic activation of cortical cell division during the accommodation of arbuscular mycorrhizal fungi. *New Phytol.* 221, 1036–1048. doi: 10.1104/pp.104.040683

Sagan, M., Morandi, D., Tarenghi, E., and Duc, G. (1995). Selection of nodulation and mycorrhizal mutants in the model plant Medicago truncatula (Gaertn.) after cray mutagenesis. *Plant Sci.* 111, 63–71. doi: 10.1083/jcb.130.61345

Samaj, J., Baluska, F., Voigt, B., Schlicht, M., Volkmann, D., and Menzel, D. (2004). Endocytosis, actin cytoskeleton, and signaling. *Plant Physiol.* 135, 1150–1161. doi: 10.1111/j.1365-313X.2004.02222.x

Samuels, A. L., Giddings, TH Jr, and Staehelin, L. A. (1995). Cytokinesis in tobacco BY-2 and root tip cells: a new model of cell plate formation in higher plants. *J. Cell Biol.* 130, 1345–1357. doi: 10.1105/tpc.106.040923

Van Damme, D., Bouget, F.-Y., Van Poucke, K., Inze, D., and Geelen, D. (2004). Molecular dissection of plant cytokinesis and phragmoplast

structure: a survey of GFP-tagged proteins. *Plant J.* 40, 386–398. doi: 10.1073/pnas.1017890108

Van Damme, D., Coutuer, S., De Rycke, R., Bouget, F. Y., Inze, D., and Geelen, D. (2006). Somatic cytokinesis and pollen maturation in arabidopsis depend on TPLATE which has domains similar to coat proteins. *Plant Cell* 18, 3502–3518. doi: 10.1105/tpc.106.040923

Van Damme, D., Gadeyne, A., Vanstraelen, M., Inze, D., Van Montagu, M. C., De Jaeger, G., et al. (2011). Adaptin-like protein TPLATE and clathrin recruitment during plant somatic cytokinesis occurs via two distinct pathways. *Proc. Natl. Acad. Sci. U. S. A.* 108, 615–620. doi: 10.1105/tpc.106.040923

Conflict of Interest: The authors declare that the research was conducted in the absence of any commercial or financial relationships that could be construed as a potential conflict of interest.

frontiers in Plant Science

REVIEW
published: 14 January 2020
doi: 10.3389/fpls.2019.01658

Digging Deeper: In Search of the Mechanisms of Carbon and Nitrogen Exchange in Ectomycorrhizal Symbioses

*Emiko K. Stuart and Krista L. Plett**

Hawkesbury Institute for the Environment, Western Sydney University, Richmond, NSW, Australia

Symbiosis with ectomycorrhizal (ECM) fungi is an advantageous partnership for trees in nutrient-limited environments. Ectomycorrhizal fungi colonize the roots of their hosts and improve their access to nutrients, usually nitrogen (N) and, in exchange, trees deliver a significant portion of their photosynthetic carbon (C) to the fungi. This nutrient exchange affects key soil processes and nutrient cycling, as well as plant health, and is therefore central to forest ecosystem functioning. Due to their ecological importance, there is a need to more accurately understand ECM fungal mediated C and N movement within forest ecosystems such that we can better model and predict their role in soil processes both now and under future climate scenarios. There are a number of hurdles that we must overcome, however, before this is achievable such as understanding how the evolutionary history of ECM fungi and their inter- and intra- species variability affect their function. Further, there is currently no generally accepted universal mechanism that appears to govern the flux of nutrients between fungal and plant partners. Here, we consider the current state of knowledge on N acquisition and transport by ECM fungi and how C and N exchange may be related or affected by environmental conditions such as N availability. We emphasize the role that modern genomic analysis, molecular biology techniques and more comprehensive and standardized experimental designs may have in bringing cohesion to the numerous ecological studies in this area and assist us in better understanding this important symbiosis. These approaches will help to build unified models of nutrient exchange and develop diagnostic tools to study these fungi at various scales and environments.

Keywords: mutualism, symbiosis, nutrition, carbon sequestration, ecosystem modelling, carbon cycle, mycorrhizae

OPEN ACCESS

Edited by:
Raffaella Balestrini, Italian National Research Council (IPSP-CNR), Italy

Reviewed by:
Sabine Dagmar Zimmermann, Délégation Languedoc Roussillon (CNRS), France
Filipa Gillian Cox, University of Manchester, United Kingdom
Uwe Nehls, University of Bremen, Germany

***Correspondence:**
Krista L. Plett
k.plett@westernsydney.edu.au

Specialty section:
This article was submitted to Plant Microbe Interactions, a section of the journal Frontiers in Plant Science

Received: *26 July 2019*
Accepted: *25 November 2019*
Published: *14 January 2020*

Citation:
Stuart EK and Plett KL (2020) Digging Deeper: In Search of the Mechanisms of Carbon and Nitrogen Exchange in Ectomycorrhizal Symbioses. Front. Plant Sci. 10:1658. doi: 10.3389/fpls.2019.01658

INTRODUCTION

Ectomycorrhizal (ECM) fungi are found throughout the world in association with the roots of most forest trees. While ECM fungi are thought to provide their hosts with a range of benefits, including drought (Jones and Smith, 2004; Rapparini and Peñuelas, 2014) and salinity tolerance (Hajiboland et al., 2010), they are primarily categorized as being useful for host nutrient acquisition (Read and Perez-Moreno, 2003; Smith and Read, 2008). These fungi colonize the lateral roots of host trees,

forming interlacing mycelial structures that penetrate between and surround root epidermal cells (**Figures 1A–C**). This unique structure, called the Hartig net, provides a large amount of surface area between the two symbiotic partners and is the site of nutrient exchange. Carbon (C) resources from the host are transferred to the fungus in return for limiting nutrients, which the fungus can either access from beyond the nutrient depletion zone surrounding the host's root system (Smith and Read, 2008) or release from immobilized sources normally inaccessible to the plant.

Ectomycorrhizal fungi are therefore essential contributors to forest ecosystem functioning. By forming a beneficial symbiotic relationship with the roots of 80% to 90% of all temperate and boreal forest trees (Read, 1991; Brundrett, 2004), these fungi drive forest soil processes, such as soil organic matter decomposition, nutrient cycling and C sequestration (Read and Perez-Moreno, 2003; Orwin et al., 2011; Zak et al., 2019). As recently reviewed by Becquer et al. (2019), ECM fungi have the ability to uptake and provide their hosts with a range of macronutrients, including phosphorus, potassium, calcium, magnesium, sulphur, and micronutrients, such as iron, zinc, copper, and manganese. However, they are recognized mostly for their provision of nitrogen (N) because it is the main growth-limiting factor in many forest ecosystems, particularly in the Northern hemisphere (Read et al., 2004; Toljander et al., 2006; Lin et al., 2017). Most of the N in forest soils is in organic form, bound up in soil organic matter or in leaf litter that accumulates on the forest floor (Read, 1991; Bruns et al., 2002). The mineralisation rates of these organic complexes are too slow for sufficient plant N nutrition, however, ECM fungi have some ability to decompose these organic complexes making ECM fungi important players in soil N cycling (Read, 1991; Lindahl et al., 2007; Bödeker et al., 2014; Lindahl and Tunlid, 2015; Shah et al., 2016).

Additionally, ECM fungi are thought to have a role in promoting soil C sequestration (Orwin et al., 2011; Cairney, 2012; Clemmensen et al., 2014). A substantial portion of plant photosynthate is sent belowground to ECM fungal partners (Smith and Read, 2008). While some of this photosynthate is returned to the atmosphere *via* fungal respiration or decay (Talbot et al., 2008), ECM fungi are believed to generally repress soil respiration (Gadgil and Gadgil, 1971; Gadgil and Gadgil, 1975; Averill et al., 2014; Averill and Hawkes, 2016) and thus increase C storage, though this effect may be highly dependent on the fungal species and on soil conditions (Fernandez and Kennedy, 2016; Baskaran et al., 2017).

Owing to their crucial role in soil biogeochemical processes and forest productivity, there is an increasing effort to incorporate mycorrhizal fungi into ecosystem modeling equations (Brzostek et al., 2014; Sulman et al., 2017). This effort is hampered, however, by a lack of knowledge concerning the actual contributions of ECM fungi to all of these soil processes and how soil conditions such as nutrient availability influence outcomes (Deckmyn et al., 2014; Koide et al., 2014). Indeed, while much research on C allocation to ECM fungi and the corresponding transfer of N to host tissues has been conducted, there is no generally accepted mechanism for the control of nutrient flux between the symbiotic partners. Additionally, research into the effects of soil nutrient availability on this exchange give variable and often conflicting results (see *Effect of N Concentrations in Soils*).

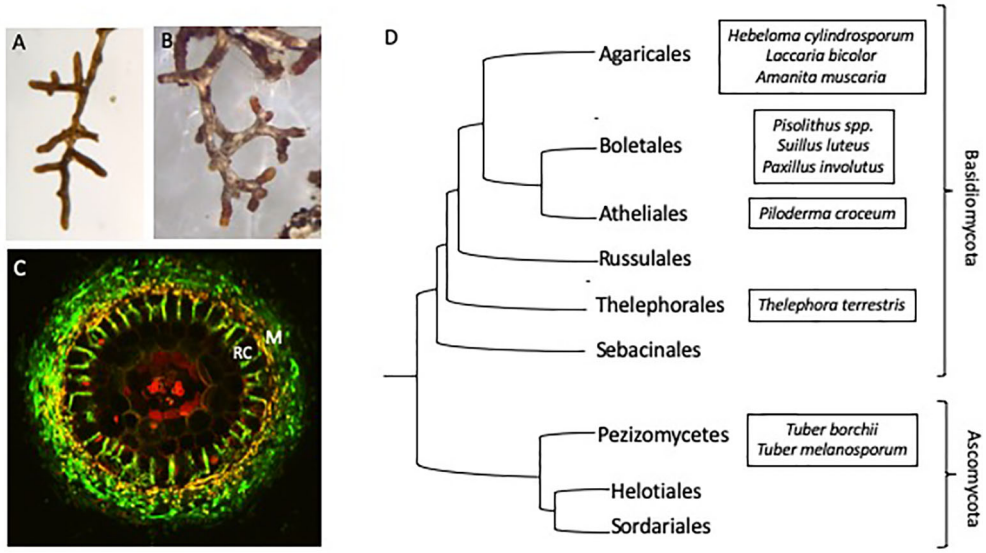

FIGURE 1 | Physiology and phylogeny of ECM fungi **(A)** *Eucalyptus grandis* roots colonized by *Pisolithus microcarpus* and **(B)** *Pinus radiata* colonized roots showing the typical morphology of mycorrhizal root tips. **(C)** Cross section of a mycorrhizal root tip, showing the fungal mantle (M) surrounding the root and ingrowth of fungal hyphae between the root epidermal cells (RC). Fungal hyphae (green) is stained with WGA-FITC. **(D)** Phylogenetic diversity of the major ECM containing orders of fungi with selected model ECM species (adapted from Kohler et al., 2015 and Nagy et al., 2016).

One of the potential contributing factors to the difficulties in generating a unified mechanism for C/N exchange is the complicated evolutionary history of ECM fungi. Ectomycorrhizal fungi are a diverse group of asco- and basidiomycetes, with over 20,000 species that evolved independently from 60 to 80 saprotrophic ancestral lineages (**Figure 1D**; Hibbett et al., 2000; Rinaldi et al., 2008; Tedersoo and Smith, 2013; Martin et al., 2016). Comparatively, within arbuscular mycorrhizal (AM) fungi, approximately 240 species are described, likely descending from a single ancestral lineage (Brundrett, 2002; Lee et al., 2013; Selosse et al., 2015). While all ECM fungi retain in common a unique symbiotic structure and the ability to exchange nutrients with their host, traits such as host and climate range, hyphal growth characteristics and the ability to source soil nutrients vary widely between species (Clemmensen et al., 2014; Pellitier and Zak, 2018). Thus, one simple model of C allocation and N transfer may not suffice for ECM fungi as a whole.

Here in this review we summarize the current state of research concerning the acquisition and transport of soil N by ECM fungi and the C for N trade with their hosts, and consider some of the challenges in the field and opportunities for future research. In particular, we emphasize the role that genome sequencing projects and functional characterization using molecular biology techniques may have in reconciling the collected field data and building mechanisms to model nutrient exchange dynamics.

NUTRIENT UPTAKE AND TRANSPORT

In order to supply plant tissues with N, the ECM fungus must first acquire the nutrient from its environment. Ectomycorrhizal fungi encode a number of transporters for the acquisition of nitrate and ammonium ions from soil, as well as a suite of enzymes and transporters necessary for utilizing organic N sources (Casieri et al., 2013; Nehls and Plassard, 2018; Becquer et al., 2019). Many of these transporters have been well characterized in model ECM species; however, a number of important questions remain unanswered in this area of research. For example, we still need to identify transporters that negotiate the exchange of nutrients at the plant-fungal interface and determine the extent to which fungal transporters are conserved amongst different species of ECM fungi, or how they are regulated under different soil and nutrient conditions. The ability to use N from different organic sources is, for example, particularly variable between species (Courty et al., 2005; Buee et al., 2007; Pena et al., 2013) and even within species (Anderson et al., 1999; Sawyer et al., 2003; Guidot et al., 2005). This knowledge gap presents an excellent opportunity for future studies to refine this area of science.

Inorganic N Import

Ammonium is generally the preferred inorganic N source of ECM fungi, as nitrate is immediately reduced to ammonium after uptake and thus requires more energy to assimilate (Plassard et al., 2000). Ammonium importers AMT1, AMT2 and AMT3 have been functionally characterized in several ECM fungal species, including *Hebeloma cylindrosporum* (Javelle et al., 2001; Javelle et al., 2003), *Tuber borchii* (Montanini et al., 2002) and *Amanita muscaria* (Willmann et al., 2007). Homologues of these genes have also been identified in many other ECM fungal genomes from transcriptomic studies (Lucic et al., 2008; Hortal et al., 2017). AMT1 and AMT2 have been characterized as high affinity ammonium transporters in different fungi, and their expression is most up-regulated in low ammonium conditions (Javelle et al., 2003; Willmann et al., 2007). Nitrate transporters, such as LbNRT2 in *Laccaria bicolor* (Kemppainen et al., 2010) and HcNRT2 in *H. cylindrosporum* (Jargeat et al., 2003), are also present in ECM genomes, allowing for growth on nitrate. Transcriptional regulation of nitrate transporters is usually mirrored by the corresponding regulation of nitrate reductase enzymes, required to assimilate the transported nitrate and reduce it to ammonium (Kemppainen et al., 2009; Kemppainen et al., 2010). The nitrate uptake pathway has been found to be down-regulated by the presence of ammonium, but not by the presence of organic N sources, allowing for the simultaneous uptake of nitrate and organic N (Jargeat et al., 2003; Kemppainen et al., 2010).

Organic N Acquisition and Import

Ectomycorrhizal fungi all evolved from saprotrophic ancestors, and hence retain the ability to decompose organic matter (Kohler et al., 2015; Shah et al., 2016). However, analysis of their genomes displays a strikingly reduced complement of enzymes required for the decomposition of complex organic matter, particularly cell-wall decomposing enzymes (Kohler et al., 2015; Lindahl and Tunlid, 2015). As a result, while most ECM fungi are able to survive on and use organic material, they do so with a reduced capacity as compared to saprotrophs (Shah et al., 2016).

Despite their commonly held ability to decompose organic matter, ECM fungi have different mechanisms and efficiencies of decomposition stemming from their diverse ancestral origins. In fact, there is a high degree of variability in the type and number of genes retained from saprotrophic ancestors amongst investigated ECM fungal species (Kohler et al., 2015) and thus a high variation in decay ability (Pellitier and Zak, 2018). Most ECM fungi appear to use primarily oxidative mechanisms, such as Fenton chemistry, to break down soil organic matter (Rineau et al., 2012; Bödeker et al., 2014; Martin et al., 2016; Shah et al., 2016; Op De Beeck et al., 2018). Fenton chemistry originates from brown-rot saprotrophic ancestors, which use these mechanisms to biodegrade lignified plant cell wall material and obtain nutrition (Eastwood et al., 2011). These mechanisms are considered to be more energetically efficient than the production of secreted class II peroxidases characteristic of white-rot fungi (Eastwood et al., 2011). However, unlike brown-rot saprotrophs, ECM fungi do not appear to use significant amounts of the broken-down organic matter as a C source. Instead, relying on host supplied C, they assimilate primarily N from these organic molecules (Treseder et al., 2006; Lindahl et al., 2007; Le Tacon et al., 2015; Martin et al., 2016; Shah et al., 2016). Meanwhile, several other ECM species from the order Agaricales evolved

from white-rot fungi and a few, including *Cortinarius* species, retained the Class II peroxidases needed for complete organic matter decomposition (Bödeker et al., 2009; Kohler et al., 2015; Lindahl and Tunlid, 2015; Martin et al., 2016).

Ectomycorrhizal fungi also secrete an assortment of peptidases to utilize proteins within the soil (Nehls et al., 2001; Müller et al., 2007; Shah et al., 2013; Rineau et al., 2016) and encode a number of amino acid, oligopeptide, and dipeptide transporters to take up the resulting small peptide products (Nehls et al., 1999; Benjdia et al., 2006; Lucic et al., 2008; Casieri et al., 2013). Expression of these organic N transporters and secretion of peptidase are usually reduced in the presence of ammonium, indicating the fungal preference for uptake of the more easily accessible ammonium from soil (Avolio et al., 2012; Bödeker et al., 2014). Further, the decay of organic matter *via* peptidase secretion to acquire N may be triggered by glucose availability (Rineau et al., 2013); thus, fungi in a mycorrhizal association and receiving sugars from a host plant would be more likely to source organic N from the soil. As in the decay of more complex organic matter, the ability to produce these enzymes and utilize the organic matter varies considerably by ECM species (Courty et al., 2005) and soil conditions (Buee et al., 2007).

Transfer of N to Plant Tissues

Once taken up into the fungal mycelium, N is metabolized, often stored, and eventually transported to other fungal cells (see Nehls and Plassard, 2018 for a review on this subject). Some of this N makes its way to ECM root tips to be passed on to the plant. In order to pass from the fungal cell to the plant cell, N has to transverse two membranes. This necessitates coordination between the expression and activity of fungal exporters and that of the corresponding plant importers. The up-regulation of plant ammonium importer expression in mycorrhizal root tips has led to the theory that ammonium is the principle form of N transferred between the two organisms (Selle et al., 2005; Chalot et al., 2006; Couturier et al., 2007; Chalot and Plassard, 2011; Nehls and Plassard, 2018). Evidence of amino acid transport and the exchange of organic compounds in the apoplastic space also exists, however, with fungal amino acid exporters being up-regulated in mycorrhizal root tips colonized by *L. bicolor* or *Pisolithus microcarpus* (Larsen et al., 2011; Hortal et al., 2017). While most of the research focus is on the regulation of 'classical' N transporters in ECM tissues, aquaporins (Dietz et al., 2011) and voltage-dependent cation channels (Chalot et al., 2006) are also up-regulated in expression in mycorrhizal tissue and have been shown to transport ammonium. Overall, while the transport of N from fungal to plant tissues is certainly an accepted process, neither the form of N transported nor the specific fungal or plant transport mechanisms used are fully known.

Carbon Transfer

While estimates vary, a third or more of tree photosynthate may be directed to ECM associates (Nehls et al., 2010). It is not surprising, therefore, that colonization results in an up-regulation of tree C metabolic and photosynthetic pathways (Nehls et al., 2007; Larsen et al., 2011). These sugars, primarily sucrose, are transported to colonized root tissues and into the apoplastic space between plant and fungal cells using a variety of plant transporters (Hennion et al., 2019). Plants encode a number of sucrose transporters (SUTs), involved in the long-distance transport of sugars in the plant (Doidy et al., 2012). The main sucrose cleavage products, glucose, and fructose, as well as other mono-saccharides, are transported between cellular compartments with mono-saccharide transporters (MSTs) or SWEET transporters (Sugar Will Eventually be Exported Transported; Chen et al., 2010). While most SWEET transporters move monosaccharides, some SWEET transporters, particularly AtSWEET11 and 12, are able to transport sucrose from mesophyll cells (Chen et al., 2012; Doidy et al., 2012). It is not currently known which of the many plant sugar transporters is responsible for the export of sugar to the fungal symbiont.

It is generally understood that plants secrete sucrose into the plant-fungal interface. However, while several monosaccharide importers with increased expression in mycorrhizal root tips have been identified in ECM fungi (Nehls et al., 2007; López et al., 2008), sucrose transporters are notably absent in most ECM fungal genomes (Salzer and Hager, 1991; Martin et al., 2008). These fungi also commonly lack the secreted invertases required to cleave sucrose into usable mono-saccharides (Martin et al., 2008), making sucrose a non-viable source of nutrition. The fungus is thus reliant on the plant, not only for sugars, but additionally for invertases to break down sucrose into a useable form (Salzer and Hager, 1991). Gene expression analyses do indeed reveal the increased expression of plant invertases (Wright et al., 2000; Nehls et al., 2010) at the plant-fungal interface, but interestingly, also the increased expression of a number of plant monosaccharide importers. This may provide the plant with a mechanism to control the loss of sugar resources to the fungus and represent a method for the plant to select for desirable partners by increasing their access to sugar, or conversely, discourage less helpful partners (Nehls et al., 2010). However, this hypothesis remains theoretical as the mechanisms controlling C flux from host to fungus are as yet largely unknown.

Section Summary

While knowledge of the nutrient uptake, transport, and metabolic pathways in ECM fungi is progressing well (Nehls and Plassard, 2018), there are still many missing pieces in the current research models, particularly concerning the regulation of transport at the mycorrhizal interface. This highlights the need for research efforts in the identification and functional characterization of these transporters and of the forms of nutrients exchanged between plant and fungus. Additionally, research into how evolutionary history, genotype, and abiotic factors affect the regulation and activity of these transporters is needed. Improved knowledge about these transporters would allow for better predictions of where nutrients are going belowground, particularly if their regulation is found to correlate to nutrient flux. Such knowledge could lead to the development of a simple diagnostic tool to approximate the rates

of C/N exchange between partners, which is the subject of the next section.

FACTORS CONTROLLING CARBON AND N FLUX

Defining C and N Flux

Having considered the transporters negotiating the exchange of nutrients between ECM fungus and host, we now turn our attention to questions of quantity. What factors determine the amount of nutrition received by each partner in this relationship? Despite its importance, knowledge on what moderates the amount of C and N exchanged, or C/N flux, in ECM symbioses is lacking, particularly in comparison to that of C and P exchange in AM symbioses (Garcia et al., 2015). Many studies on the effects of ECM colonization look at plant growth outcomes, rather than direct nutrient exchange. These studies reveal a variety of growth responses in the plant, ranging from positive to negative (Johnson et al., 1997; Jones and Smith, 2004; Corrêa et al., 2012). While it is often assumed that negative growth responses in plants to ECM fungi occur as a result of excessive C drain compared to the nutritional benefit received, particularly at high N concentrations, C loss has been determined in some studies to be of little or no cost to the plant, so these negative growth results could as easily be due to immobilization of N resources by the ECM fungus (Corrêa et al., 2012). In order to elucidate the causes of these growth outcomes and better understand nutrient cycling and movement in forest environments, a focus on the relative flow rates, or "fluxes," of N and C, and the mechanisms behind their control, is needed. While the measurement of both N and C flux can be challenging, especially in field studies (Hobbie and Hobbie, 2006; Le Tacon et al., 2015), it is important in understanding the mechanisms behind the bidirectional transfer of nutrients that upholds this association.

Several methods, ranging in their accuracy as a proxy for nutrient flux, have been deployed in this area of research. Earlier approaches to understanding this exchange involved measuring absolute C and N amounts in the tissues of plants and fungi and used changing C/N ratios as a proxy for their access to nutrients (Colpaert et al., 1996; Nilsson and Wallander, 2003). Currently, a common method of measuring ECM nutrient flux is the use of isotopic labeling. The addition of either ^{13}C to trees (usually as carbon dioxide; e.g. Högberg et al., 2010) or ^{15}N compounds to soil (e.g. Hasselquist et al., 2016) allows for tracking of the uptake and movement of these nutrients over time. The application of stable ^{15}N is not without disadvantages. It is most suited to shorter-term experiments, and the addition of the usually inorganic label may alter soil chemistry or disturb existing microbial relationships. Additionally, it is very difficult to eliminate the possibility of direct uptake of the label by the tree outside of the mycorrhizal pathway. The use of natural abundances of ^{15}N, possible due to a bias in ECM fungi to preferentially give ^{14}N to the plant (Hobbie and Colpaert, 2003), eliminates some of these issues, but sacrifices sensitivity and thus is best suited to long term studies (Hobbie and Hobbie, 2006; Högberg et al., 2011).

While these techniques are all capable, with varying levels of accuracy and ecological relevance, of quantifying the movement of C and N between plant and fungal partners, the challenge remains to link this data to a mechanism. Future studies could incorporate these physiological techniques to quantify nutrient movement with transcriptomic analyses and other molecular techniques to begin to answer questions concerning the role of each partner in this nutrient trade and causative factors behind nutrient flux (Johnson et al., 2012). Further, an increased effort to harmonize the different methods of measuring C for N exchange would allow for more meaningful comparisons between data sets.

Coupling of C and N Flux

A popular theory behind the regulation of C and P exchange in AM symbioses is the 'reciprocal rewards' concept, whereby plant photosynthate is preferentially transferred to fungal symbionts that provide more nutrients (Kiers et al., 2011; Fellbaum et al., 2012; Fellbaum et al., 2014). This theory has by extension led to the consideration that C allocation to ECM fungi may follow a similar pattern with the amount of C delivered being related to the amount of N sourced by the fungus (Casieri et al., 2013). This theory is attractive in that it provides a mechanism for the stabilization of the mutualism; provision of N to a host is a substantial cost to the ECM fungus, thus if it were not compensated for in some way, individuals providing less host benefit would be expected to flourish at the expense of their more helpful counterparts (Hoeksema and Kummel, 2003; Bever et al., 2009; Moeller and Peay, 2016).

A recent study by Bogar et al. (2019) lent support to this theory. In a *Pinus muriata-Suillus brevipes* symbiosis studied in an artificial soil medium, mycorrhizal root tips that contained higher N concentrations received more plant C. However, this was also true of non-mycorrhizal root tips, suggesting that the plant may simply detect sources of high N and allocate C toward those sources. Similarly, Kaiser et al. (2017) found that for *Fagus sylvatica*-associated fungi, ^{15}N enriched 'hotspots' within the fungal mycelium were also always highly enriched in ^{13}C from the plant, suggesting that reciprocation was occurring. Another study using birch colonized by *Paxillus involutus* demonstrated a reciprocal exchange of C and N under various nutrient conditions (Kytöviita, 2005).

Meanwhile, many other studies have concluded that N and C flux is neither reciprocal nor related (Corrêa et al., 2008; Albarracín et al., 2013; Valtanen et al., 2014; Hasselquist et al., 2016). 2012; Corrêa et al. (2008) found that *Pinus pinaster* trees allocate C to *Pisolithus tinctorius* fungal symbionts whenever it is produced in excess, and continue to allocate that C even when the amount of N provided by the fungus is reduced (Corrêa et al., 2008). Näsholm et al. (2013) found that in N limited boreal forest soils, trees increased C allocation to ECM fungi, but this was not reciprocated with an increase in N transfer. In an *in vitro* system studying the *Eucalyptus grandis-Pisolithus microcarpus* association, Hortal et al. (2017) did not find a correlation between N and C allocation; in fact, *E. grandis* allocated the

most C to the *Pisolithus* isolate that provided the least N. However, when a less beneficial *P. microcarpus* isolate was in competition with a more beneficial isolate, its ability to colonize the root system was reduced, coinciding with an up-regulation of plant defence pathways in only those roots associated with the less beneficial isolate. This indicates that the plant may not necessarily reward symbionts providing better nutritional benefit with proportionally more C, but may sanction less beneficial isolates through restricted root access (Simard et al., 2003; Kemppainen et al., 2009; Hortal et al., 2017).

Together, these studies suggest that while C delivery may under some circumstances be driven by the N content of ECM roots tips, the exchange of nutrients does not always follow a reciprocal exchange. There are, necessarily, other factors determining the transfer of nutrients yet to be discovered. It has been suggested that rather than the N status of a particular root tip, the N status of the tree leaves may be a more important driving factor in C allocation to roots (Nilsson and Wallander, 2003; Corrêa et al., 2008). The particular host and fungal genetic combination and soil abiotic conditions likely plays a role in C/N exchange dynamics as well. Research into the particular mechanisms and signaling events driving C and N trade is needed to better understand how this occurs and to be able to make better predictions of mycorrhizal outcomes in different environments.

Effect of N Concentrations in Soils

The benefit of ECM fungi to tree growth is usually seen most apparently in severely N limited soils (Read et al., 2004; Smith and Read, 2008). For example, a synthesis of global research considering the effect of elevated carbon dioxide concentration on tree growth has shown that growth is limited by N availability, but the addition of ECM fungi can overcome this barrier (Terrer et al., 2016). In opposition to this view, however, is the idea that ECM fungi may not alleviate N limitation in forests, but rather form part of the problem. As ECM fungi themselves require N for their own growth, in N limited conditions they can "hoard" the available N and actually increase the N limitation of the forest soils (Näsholm et al., 2013; Franklin et al., 2014). Compounding the problem, under N limited conditions trees send more C belowground, resulting in more fungal biomass and an increased fungal demand for N (Högberg et al., 2003; Nilsson and Wallander, 2003; Treseder, 2004; Högberg et al., 2010). The balance between ECM fungi as positive growth regulators under limited N or as drivers of that N limitation likely is the result of a complex interaction between tree and fungal genotypes, soil nutrient conditions, and the nutritional needs of each organism (Alberton and Kuyper, 2009).

Studies on the effect of N addition to forest soils on ECM N transfer also show some variable responses. With increasing soil N concentration, some studies demonstrate that ECM fungi begin to mobilize stored N and transfer it to the host tree (Högberg et al., 2011; Näsholm et al., 2013; Hasselquist and Högberg, 2014) while other studies saw an opposite trend (Albarracín et al., 2013). Overall, however, the research overwhelmingly indicates that increased N has a negative impact on ECM communities. N fertilization results in reduced species richness, plant colonization levels, sporocarp production, and mycelial growth in soils, as well as a community shift to more nitrophilic ECM species and saprotrophs (Lilleskov et al., 2002; Nilsson and Wallander, 2003; Parrent et al., 2006; Allen et al., 2010; Pardo et al., 2011; Morrison et al., 2016; Corrales et al., 2017; Averill et al., 2018). Thus, while ECM fungi may, in some circumstances, drive N limitation, that N limitation may be important to their continued persistence and dominance in forest ecosystems. We are, however, left again with no unified theory as to how soil N availability may affect the nutritional benefit received by the host tree from its associated ECM fungi.

Reconciling the Data

Each of the studies on C and N flux referenced above are highly valuable, however, research has still not developed a clear picture of how C and N exchange are related, either to each other, or to the soil N availability. While on the surface, the results of these studies may appear to be in conflict with one another, it is perhaps more useful to consider them as different perspectives on the same question as they consider N for C exchange in a variety of different environmental conditions and using different ECM fungi and host systems. It is possible, given the high degree of genetic variability in each fungal-host combination, that one central mechanism of C for N exchange is not attainable. From this view, more studies are required to complete the picture and determine where the consistencies lie and where we must simply expect variability. Additionally, ECM fungi contribute in many ways to plant health and nutrition beyond N and any one of these factors may also impact nutrient exchange. This highlights the need to complement observational and nutrient tracing studies with an understanding of the molecular mechanisms driving nutrient transfer.

FUTURE RESEARCH DIRECTIONS

ECM fungi affect numerous elements of forest ecosystem functioning and, while progress has been made towards understanding their general contributions to these processes, there remain many unknowns (**Figure 2**). Ecosystem models for nutrient movement incorporating mycorrhizal fungi have seen an increase in predictive power (Brzostek et al., 2014; Sulman et al., 2017; Keller and Phillips, 2019), however, these models are usually limited by assigning a mycorrhizal type as either 'arbuscular' or 'ectomycorrhizal'. It has been suggested that these models could be improved by further dividing ECM fungi into subgroups based on their ecological function (Zak et al., 2019) or taxon-specific traits (Pena and Polle, 2014; Fry et al., 2019). Fungal growth type and foraging strategy may, for example, be simple parameters for ECM fungal classification, as both relate to the C demand of the fungus and its ability to find and source soil nutrients (Agerer, 2001; Clemmensen et al., 2014). Others have suggested that fungal C cost per unit N provided may be useful in characterizing the association (Corrêa et al., 2008; Agren et al., 2019); however, this is a complicated measure that may change dramatically based on external

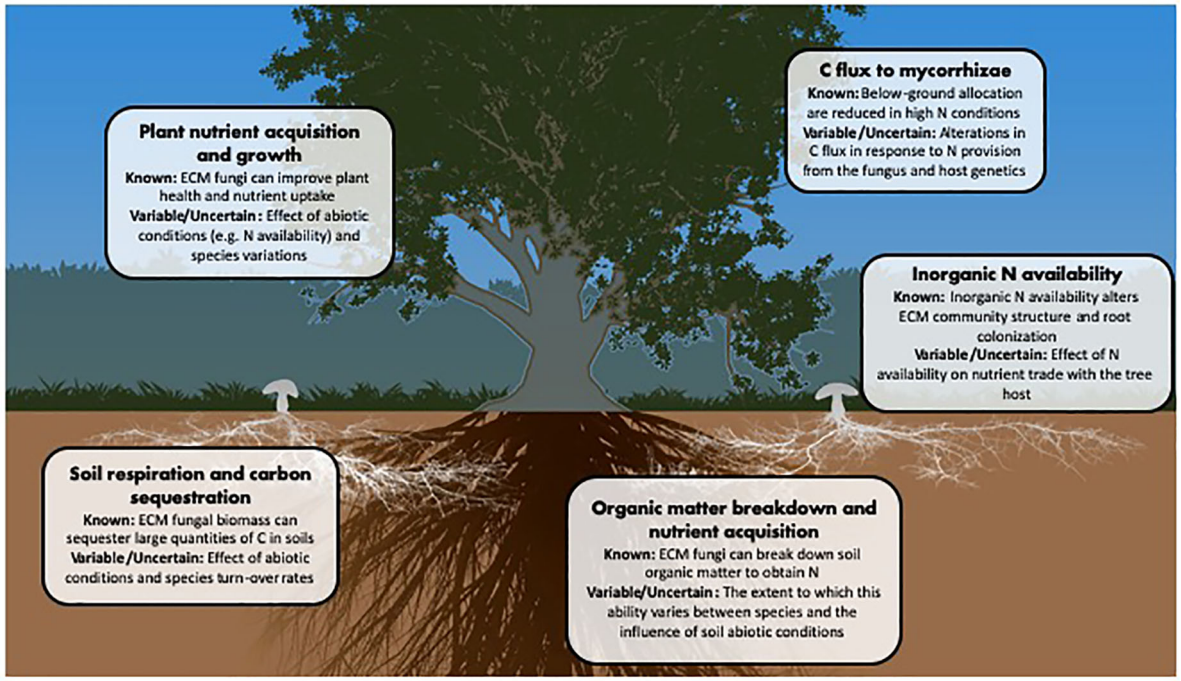

FIGURE 2 | Major ecosystem parameters affected by or affecting ECM fungi.

situations, or even over the lifetime of the mycorrhizal association (Nehls et al., 2016).

The limitation of such an approach is that they are currently relying on a relatively narrow set of model systems—systems that may not best portray the diversity of ECM fungal responses within natural ecosystems (Johnson et al., 2012; Zak et al., 2019). As discussed above, due to the fact that ECM fungal species do not share a single common ancestor, they may in reality have as many differences in function as those traits that they share. Supporting this claim, in a recent comparison of ECM genomes it was found that 7% to 38% of genes induced by symbiosis were species-specific (Kohler et al., 2015) while other studies have found that different species of ECM fungi colonizing the same host under the same conditions elicit different outcomes in terms of both nutrient exchange (Rincón et al., 2007; Alberton and Kuyper, 2009; Jones et al., 2009; Pena and Polle, 2014) and transcriptomic response (Peter et al., 2016). These differential responses can even be found between different fungal isolates of the same species (Plett et al., 2015a; Hazard et al., 2017; Hortal et al., 2017). Likewise, a single ECM fungus can also exhibit unique responses to different hosts (Plett et al., 2015b). Finally, the outcomes of ECM symbioses are affected by many diverse abiotic factors such as N availability, the amount and complexity of organic material in the soil (Plassard et al., 2000), or season (Högberg et al., 2010). Thus, we need to add to the range of studied ECM fungal lineages and abiotic conditions before we can gain a better ability to understand the diverse mechanisms by which ECM fungal communities drive nutrient cycling in forests.

Genomic sequencing and analysis will likely prove extremely important in this last aim, allowing for the assessment of common genetic features between groups of fungi. Linking of common genetic signatures to symbiosis-related outcomes could allow for a more rapid assessment of the likely contribution of an ECM fungus to plant health and nutrient cycling. However, this abundance of genomic information must be accompanied by more detailed molecular studies to elucidate the functions of various genes as many do not have a known function (Martin and Nehls, 2009; Plett et al., 2011). With special relevance to the topics discussed here, there are still large gaps in our knowledge concerning the specific transporters used by both fungi and hosts to transfer nutrients at the plant-fungal interface, particularly in the area of sugar transport. Increased understanding of the transporters involved, and related metabolic proteins, and how their regulation affects nutrient trade between partners would provide more accessible tools to assess efficiency of nutrient trading.

The literature would also suggest that the role of the plant host in determining mycorrhizal outcomes cannot be overlooked. Some manners by which host plants may be able to regulate associations with ECM fungi are by controlling C resources allocated to the ECM symbiont, restricting root colonization by an unhelpful symbiont, or even terminating or sloughing off mycorrhizal root tips with undesirable symbionts (Nehls et al., 2016). These mechanisms need further investigation. Like ECM fungi, host trees have a broad range of genetic diversity. Considering a wide variety of host trees,

therefore, is necessary to determine the specificity of these mechanisms and the role of host genotype in symbiotic outcomes.

Finally, as we unravel the mechanisms underlying ECM symbioses at the molecular scale, we will need to incorporate the effect of biotic complexity at the ecological scale. While the ECM symbiosis is often thought of as an intimate relationship between a plant and a fungus, the natural habitats of ECM associations are, in fact, hugely complex, involving a wide array of interactions between each of the symbiotic partners and neighboring plants and fungi. Thus, findings at the one-on-one interactions level may not be replicated in the larger context (Kennedy, 2010). Therefore, substantial amounts of data will be needed in order to understand how all of these biotic factors affect a given plant-fungal combination in the field. This can be achieved, in part, from increased use of fully factorial experimental designs that incorporate multiple species.

In conclusion, as a whole, ECM fungi have been proposed as key players in nutrient cycling and as essential in equipping trees to survive and adapt to changing abiotic conditions (Lau et al., 2017). However, our ability to exploit or even predict the benefit of these fungi hinges on a greater understanding of their diversity, function, and contribution to nutrient cycles and forest health. Advances in molecular biology and genomic tools grant us the potential to dig deeper and to exploit the wealth of information from ecosystem scale studies and pot experiments and translate this into mechanistic understanding and new tools to better understand this important symbiotic system.

AUTHOR CONTRIBUTIONS

ES and KP envisioned and wrote the manuscript.

ACKNOWLEDGMENTS

The authors wish to acknowledge J. Plett for useful discussions, D. Laugesen for graphic design and the Australian Research Council for funding (DP160102684 and DP190102254).

REFERENCES

Agerer, R. (2001). Exploration types of ectomycorrhizae. *Mycorrhiza* 11, 2. doi: 10.1007/s005720100108

Agren, G., Hyvönen, R., and Baskaran, P. (2019). Ectomycorrhiza, Friend or Foe? *Ecosystems* 22, 1561–1572. doi: 10.1007/s10021-019-00356-y

Albarracín, M. V., Six, J., Houlton, B. Z., and Bledsoe, C. S. (2013). A nitrogen fertilization field study of carbon-13 and nitrogen-15 transfers in ectomycorrhizas of Pinus sabiniana. *Oecologia* 173 (4), 1439–1450. doi: 10.1007/s00442-013-2734-4

Alberton, O., and Kuyper, T. W. (2009). Ectomycorrhizal fungi associated with Pinus sylvestris seedlings respond differently to increased carbon and nitrogen availability: implications for ecosystem responses to global change. *Global Change Biol.* 15, 1. doi: 10.1111/j.1365-2486.2008.01714.x

Allen, M. F., Allen, E. B., Lansing, J. L., Pregitzer, K. S., Hendrick, R. L., Ruess, R. W., et al. (2010). Responses to chronic N fertilization of ectomycorrhizal pinon but not arbuscular mycorrhizal juniper in a pinon-juniper woodland. *J. Arid Environ.* 74, 10. doi: 10.1016/j.jaridenv.2010.05.001

Anderson, I. C., Chambers, S. M., and Cairney, J. W. G. (1999). Intra- and interspecific variation in patterns of organic and inorganic nitrogen utilization by three Australian Pisolithus species. *Mycol. Res.* 103, 2. doi: 10.1017/S0953756299008813

Averill, C., and Hawkes, C. V. (2016). Ectomycorrhizal fungi slow soil carbon cycling. *Ecol. Lett.* 19, 8. doi: 10.1111/ele.12631

Averill, C., Turner, B. L., and Finzi, A. C. (2014). Mycorrhiza-mediated competition between plants and decomposers drives soil carbon storage. *Nature* 505, 7484. doi: 10.1038/nature12901

Averill, C., Dietze, M. C., and Bhatnagar, J. M. (2018). Continental-scale nitrogen pollution is shifting forest mycorrhizal associations and soil carbon stocks. *Global Change Biol.* 24, 10. doi: 10.1111/gcb.14368

Avolio, M., Müller, T., Mpangara, A., Fitz, M., Becker, B., Pauck, A., et al. (2012). Regulation of genes involved in nitrogen utilization on different C/N ratios and nitrogen sources in the model ectomycorrhizal fungus Hebeloma cylindrosporum. *Mycorrhiza* 22, 515. doi: 10.1007/s00572-011-0428-5

Baskaran, P., Hyvönen, R., Berglund, S. L., Clemmensen, K. E., Ågren, G. I., Lindahl, B. D., et al. (2017). Modelling the influence of ectomycorrhizal decomposition on plant nutrition and soil carbon sequestration in boreal forest ecosystems. *New Phytol.* 213, 3. doi: 10.1111/nph.14213

Becquer, A., Guerrero-Galánc, C., Eibensteiner, J. L., Houdinet, G., Bücking, H., Zimmermann, S. D., et al. (2019). "The ectomycorrhizal contribution to tree nutrition," in *Advances in Botanical Research*, vol. 89 . Eds. F. M. Cánovas (Cambridge, MA, USA: Academic Press).

Benjdia, M., Rikirsch, E., Müller, T., Morel, M., Corratgé, C., Zimmermann, S., et al. (2006). Peptide uptake in the ectomycorrhizal fungus Hebeloma cylindrosporum: characterization of two di- and tripeptide transporters (HcPTR2A and B). *New Phytol.* 170, 2. doi: 10.1111/j.1469-8137.2006.01672.x

Bever, J. D., Richardson, S. C., Lawrence, B. M., Holmes, J., and Watson, M. (2009). Preferential allocation to beneficial symbiont with spatial structure maintains mycorrhizal mutualism. *Ecol. Lett.* 12, 1. doi: 10.1111/j.1461-0248.2008.01254.x

Bödeker, I. T., Nygren, C. M., Taylor, A. F., Olson, A., and Lindahl, B. D. (2009). ClassII peroxidase-encoding genes are present in a phylogenetically wide range of ectomycorrhizal fungi. *ISME J.* 3, 12. doi: 10.1038/ismej.2009.77

Bödeker, I. T., Clemmensen, K. E., de Boer, W., Martin, F., Olson, Å., and Lindahl, B. D. (2014). Ectomycorrhizal Cortinarius species participate in enzymatic oxidation of humus in northern forest ecosystems. *New Phytol.* 203, 1. doi: 10.1111/nph.12791

Bogar, L., Peay, K., Kornfeld, A., Huggins, J., Hortal, S., Anderson, I., et al. (2019). Plant-mediated partner discrimination in ectomycorrhizal mutualisms. *Mycorrhiza* 29, 2. doi: 10.1007/s00572-018-00879-7

Brundrett, M. C. (2002). Coevolution of roots and mycorrhizas of land plants. *New Phytol.* 154, 2. doi: 10.1046/j.1469-8137.2002.00397.x

Brundrett, M. C. (2004). Diversity and classification of mycorrhizal associations. *Biol. Rev.* 79, 3. doi: 10.1017/S1464793103006316

Bruns, T. D., Bidartondo, M. I., and Taylor, D. L. (2002). Host specificity in ectomycorrhizal communities: what do the exceptions tell us? *Integr. Comp. Biol.* 42, 2. doi: 10.1093/icb/42.2.352

Brzostek, E. R., Fisher, J. B., and Phillips, R. P. (2014). Modeling the carbon cost of plant nitrogen acquisition: mycorrhizal trade-offs and multipath resistance uptake improve predictions of retranslocation. *J. Geophys. Res. Biogeosci.* 119, 8. doi: 10.1002/2014JG002660

Buee, M., Courty, P. E., Mignot, D., and Garbaye, J. (2007). Soil niche effect on species diversity and catabolic activities in an ectomycorrhizal fungal community. *Soil Biol. Biochem.* 39, 8. doi: 10.1016/j.soilbio.2007.02.016

Cairney, J. W. G. (2012). Extramatrical mycelia of ectomycorrhizal fungi as moderators of carbon dynamics in forest soil. *Soil Biol. Biochem.* 47, 198–208. doi: 10.1016/j.soilbio.2011.12.029

Casieri, L., Lahmidi, N. A., Doidy, J., Veneault-Fourrey, C., Migeon, A., Bonneau, L., et al. (2013). Biotrophic transportome in mutualistic plant fungal interactions. *Mycorrhiza* 23 (8), 597–625. doi: 10.1007/s00572-013-0496-9

Chalot, M., and Plassard, C. (2011). "Ectomycorrhiza and nitrogen provision to the host tree," in *Ecological Aspects of Nitrogen Metabolism in Plants*. Eds. J. C. Polacco and C. D. Todd (Hoboken, NJ, USA: John Wiley & Sons Inc.).

Chalot, M., Blaudez, D., and Brun, A. (2006). Ammonia: a candidate for nitrogen transfer at the mycorrhizal interface. *Trends Plant Sci.* 11, 6. doi: 10.1016/j.tplants.2006.04.005

Chen, L. Q., Hou, B. H., Lalonde, S., Takanaga, H., Hartung, M. L., Qu, X. Q., et al. (2010). Sugar transporters for intercellular exchange and nutrition of pathogens. *Nature* 468, 7323. doi: 10.1038/nature09606

Chen, L. Q., Qu, X. Q., Hou, B. H., Sosso, D., Osorio, S., Fernie, A. R., et al. (2012). Sucrose efflux mediated by SWEET proteins as a key step for phloem transport. *Science* 335, 6065. doi: 10.1126/science.1213351

Clemmensen, K. E., Finlay, R. D., Dahlberg, A., Stenlid, J., Wardle, D. A., and Lindahl, B. D. (2014). Carbon sequestration is related to mycorrhizal fungal community shifts during long-term succession in boreal forests. *New Phytol.* 205, 4. doi: 10.1111/nph.13208

Colpaert, J. V., van Laere, A., and van Assche, J. A. (1996). Carbon and nitrogen allocation in ectomycorrhizal and non-mycorrhizal Pinus sylvestris L. seedlings. *Tree Physiol.* 16, 9. doi: 10.1093/treephys/16.9.787

Corrêa, A., Strasser, R. J., and Martins-Loução, M. A. (2008). Response of plants to ectomycorrhizae in N-limited conditions: which factors determine its variation? *Mycorrhiza* 18, 8. doi: 10.1007/s00572-008-0195-0

Corrêa, A., Gurevitch, J., Martins-Loução, M. A., and Cruz, C. (2012). C allocation to the fungus is not a cost to the plant in ectomycorrhizae. *Oikos* 121, 3. doi: 10.1111/j.1600-0706.2011.19406.x

Corrales, A., Turner, B. L., Tedersoo, L., Anslan, S., and Dalling, J. W. (2017). Nitrogen addition alters ectomycorrhizal fungal communities and soil enzyme activities in a tropical montane forest. *Fungal Ecol.* 27, 14–23. doi: 10.1016/j.funeco.2017.02.004

Courty, P. E., Pritsch, K., Schloter, M., Hartmann, A., and Garbaye, J. (2005). Activity profiling of ectomycorrhiza communities in two forest soils using multiple enzymatic tests. *New Phytol.* 167, 1. doi: 10.1111/j.1469-8137.2005.01401.x

Couturier, J., Montanini, B., Martin, F., Brun, A., Blaudez, D., and Chalot, M. (2007). The expanded family of ammonium transporters in the perennial poplar plant. *New Phytol.* 174, 1. doi: 10.1111/j.1469-8137.2007.01992.x

Deckmyn, G., Meyer, A., Smits, M. M., Ekblad, A., Grebenc, T., and Komarov, A. (2014). Simulating ectomycorrhizal fungi and their role in carbon and nitrogen cycling in forest ecosystems. *Can. J. For. Res.* 44, 6. doi: 10.1139/cjfr-2013-0496

Dietz, S., von Bülow, J., Beitz, E., and Nehls, U. (2011). The aquaporin gene family of the ectomycorrhizal fungus Laccaria bicolor: lessons for symbiotic functions. *New Phytol.* 190, 4. doi: 10.1111/j.1469-8137.2011.03651.x

Doidy, J., Grace, E., Kühn, C., Simon-Plas, F., Casieri, L., and Wipf, D. (2012). Sugar transporters in plants and in their interactions with fungi. *Trends Plant Sci.* 17, 7. doi: 10.1016/j.tplants.2012.03.009

Eastwood, D. C., Floudas, D., Binder, M., Majcherczyk, A., Schneider, P., Aerts, A., et al. (2011). The plant cell wall–decomposing machinery underlies the functional diversity of forest fungi. *Science* 333, 6043. doi: 10.1126/science.1205411

Fellbaum, C. R., Gachomo, E. W., Beesetty, Y., Choudhari, S., Strahan, G. D., Pfeffer, P. E., et al. (2012). Carbon availability triggers fungal nitrogen uptake and transport in arbuscular mycorrhizal symbiosis. *Proc. Natl. Acad. Sci. U. S. A.* 109, 7. doi: 10.1073/pnas.1118650109

Fellbaum, C. R., Mensah, J. A., Cloos, A. J., Strahan, G. E., Pfeffer, P. E., Kiers, E. T., et al. (2014). Fungal nutrient allocation in common mycorrhizal networks is regulated by the carbon source strength of individual host plants. *New Phytol.* 203, 2. doi: 10.1111/nph.12827

Fernandez, C. W., and Kennedy, P. G. (2016). Revisiting the "Gadgil effect": do interguild fungal interactions control carbon cycling in forest soils? *New Phytol.* 209, 4. doi: 10.1111/nph.13648

Franklin, O., Näsholm, T., Högberg, P., and Högberg, M. N. (2014). Forests trapped in nitrogen limitation—an ecological market perspective on ectomycorrhizal symbiosis. *New Phytol.* 203, 2. doi: 10.1111/nph.12840

Fry, E. L., De Long, J. R., Garrido, L. A., Alvarez, N., Carrillo, Y., Castañeda-Gómez, L., et al. (2019). Using plant, microbe, and soil fauna traits to improve the predictive power of biogeochemical models. *Methods Ecol. Evol.* 10, 146–157. doi: 10.1111/2041.21OX.13092

Gadgil, R. L., and Gadgil, P. D. (1971). Mycorrhiza and litter decomposition. *Nature* 233, 133. doi: 10.1038/233133a0

Gadgil, R. L., and Gadgil, P. D. (1975). Suppression of litter decomposition by mycorrhizal roots of Pinus radiata. *N. Z. J. For.* 5, 1.

Garcia, K., Delaux, P. M., Cope, K. R., and Ané, J. M. (2015). Molecular signals required for the establishment and maintenance of ectomycorrhizal symbioses. *New Phytol.* 208, 1. doi: 10.1111/nph.13423

Guidot, A., Verner, M. C., Debaud, J. C., and Marmeisse, R. (2005). Intraspecific variation in use of different organic nitrogen sources by the ectomycorrhizal fungus Hebeloma cylindrosporum. *Mycorrhiza* 15, 3. doi: 10.1007/s00572-004-0318-1

Hajiboland, R., Aliasgharzadeh, N., Laiegh, S. F., and Poschenrieder, C. (2010). Colonization with arbuscular mycorrhizal fungi improves salinity tolerance of tomato (Solanum lycopersicum L.) plants. *Plant Soil* 331, 1. doi: 10.1007/s11104-009-0255-z

Hasselquist, N. J., and Högberg, P. (2014). Dosage and duration effects of nitrogen additions on ectomycorrhizal sporocarp production and functioning: an example from two N-limited boreal forests. *Ecol. Evol.* 4, 15. doi: 10.1002/ece31145

Hasselquist, N. J., Metcalfe, D. B., Marshall, J. D., Lucas, R. W., and Högberg, P. (2016). Seasonality and nitrogen supply modify carbon partitioning in understory vegetation of a boreal coniferous forest. *Ecology* 97, 3. doi: 10.1890/15-0831.1

Hazard, C., Kruitbos, L., Davidson, H., Mbow, F. T., Taylor, A. F. S., and Johnson, D. (2017). Strain identity of the ectomycorrhizal fungus laccaria bicolor is more important than richness in regulating plant and fungal performance under nutrient rich conditions. *Front. Microbiol.* 8, 1874. doi: 10.3389/fmicb.2017.01874

Hennion, N., Durand, M., Vriet, C., Doidy, J., Maurousset, L., Lemoine, R., et al. (2019). Sugars en route to the roots. Transport, metabolism and storage within plant roots and towards microorganisms of the rhizosphere. *Physiol. Plant* 165, 1. doi: 10.1111/ppl.12751

Hibbett, D. S., Gilbert, L. B., and Donoghue, M. J. (2000). Evolutionary instability of ectomycorrhizal symbioses in basidiomycetes. *Nature* 407, 6803. doi: 10.1038/35035065

Hobbie, E. A., and Colpaert, J. V. (2003). Nitrogen availability and colonization by mycorrhizal fungi correlate with nitrogen isotope patterns in plants. *New Phytol.* 157, 1. doi: 10.1046/j.1469-8137.2003.00657.x

Hobbie, J. E., and Hobbie, E. A. (2006). 15N in symbiotic fungi and plants estimates nitrogen and carbon flux rates in arctic tundra. *Ecology* 87, 4. doi: 10.1890/0012-9658(2006)87[816:NISFAP]2.0.CO;2

Hoeksema, J. D., and Kummel, M. (2003). Ecological persistence of the plant-mycorrhizal mutualism: a hypothesis from species coexistence theory. *Am. Nat.* 162, S4. doi: 10.1086/378644

Högberg, M. N., Bååth, E., Nordgren, A., Arnebrant, K., and Högberg, P. (2003). Contrasting effects of nitrogen availability on plant carbon supply to mycorrhizal fungi and saprotrophs—a hypothesis based on field observations in boreal forest. *New Phytol.* 160, 1. doi: 10.1046/j.1469-8137.2003.00867.x

Högberg, M. N., Briones, M. J., Keel, S. G., Metcalfe, D. B., Campbell, C., Midwood, A. J., et al. (2010). Quantification of effects of season and nitrogen supply on tree below-ground carbon transfer to ectomycorrhizal fungi and other soil organisms in a boreal pine forest. *New Phytol.* 187, 2. doi: 10.1111/j.1469-8137.2010.03274.x

Högberg, P., Johannisson, C., Yarwood, S., Callesen, I., Näsholm, T., Myrold, D. D., et al. (2011). Recovery of ectomycorrhiza after 'nitrogen saturation' of a conifer forest. *New Phytol.* 189, 2. doi: 10.1111/j.1469-8137.2010.03485.x

Hortal, S., Plett, K. L., Plett, J. M., Cresswell, T., Johansen, M., Pendall, E., et al. (2017). Role of plant-fungal nutrient trading and host control in determining the competitive success of ectomycorrhizal fungi. *ISME J.* 11, 12. doi: 10.1038/ismej.2017.116

Jargeat, P., Rekangalt, D., Verner, M. C., Gay, G., Debaud, J. C., Marmeisse, R., et al. (2003). Characterisation and expression analysis of a nitrate transporter and nitrite reductase genes, two members of a gene cluster for nitrate assimilation from the symbiotic basidiomycete Hebeloma cylindrosporum. *Curr. Genet.* 43, 3. doi: 10.1007/s00294-003-0387-2

Javelle, A., Rodríguez-Pastrana, B. R., Jacob, C., Botton, B., Brun, A., Andre, B., et al. (2001). Molecular characterization of two ammonium transporters from the ectomycorrhizal fungus Hebeloma cylindrosporum. *FEBS Lett.* 505, 3. doi: 10.1016/S0014-5793(01)02802-2

Javelle, A., Morel, M., Rodríguez-Pastrana, B. R., Botton, B., Brun, A., Andre, B., et al. (2003). Molecular characterization, function and regulation of

ammonium transporters (Amt) and ammonium-metabolizing enzymes (GS, NADP-GDH) in the ectomycorrhizal fungus Hebeloma cylindrosporum. *Mol. Microbiol.* 47, 2. doi: 10.1046/j.1365-2958.2003.03303.x

Johnson, N. C., Graham, J. H., and Smith, F. A. (1997). Functioning of mycorrhizal associations along the mutualism–parasitism continuum. *New Phytol.* 135, 4. doi: 10.1046/j.1469-8137.1997.00729.x

Johnson, D., Martin, F., Cairney, J. W., and Anderson, I. C. (2012). The importance of individuals: intraspecific diversity of mycorrhizal plants and fungi in ecosystems. *New Phytol.* 194, 3. doi: 10.1111/j.1469-8137.2012.04087.x

Jones, M. D., and Smith, S. E. (2004). Exploring functional definitions of mycorrhizas: are mycorrhizas always mutualisms? *Can. J. Bot.* 82, 8. doi: 10.1139/b04-110

Jones, M. D., Grenon, F., Peat, H., Fitzgerald, M., Holt, L., Philip, L. J., et al. (2009). Differences in 15N uptake amongst spruce seedlings colonized by three pioneer ectomycorrhizal fungi in the field. *Fungal Ecol.* 2, 3. doi: 10.1016/j.funeco.2009.02.002

Kaiser, C., Mayerhofer, W., Dietrich, M., Gorka, S., Schintlmeister, A., Reipert, S., et al. (2017). 'Reciprocal trade of Carbon and Nitrogen at the root-fungus interface in ectomycorrhizal beech plants', *EGU General Assembly 2017 Vienna,* Volume: Geophysical Research Abstracts Vol. 19, EGU2017-15133, 2017.

Keller, A. B., and Phillips, R. P. (2019). Leaf litter decay rates differ between mycorrhizal groups in temperate, but not tropical, forests. *New Phytol.* 222, 556–564. doi: 10.1111/nph.15524

Kemppainen, M. J., Dupessis, S., Martin, F. M., and Pardo, A. G. (2009). RNA silencing in the model mycorrhizal fungus Laccaria bicolor: Gene knock-down of nitrate reductase results in inhibition of symbiosis with Populus. *Environ. Microbiol.* 11, 7. doi: 10.1111/j.1462-2920.2009.01912.x

Kemppainen, M. J., Alvarez Crespo, M. C., and Pardo, A. G. (2010). fHANT-AC genes of the ectomycorrhizal fungus Laccaria bicolor are not repressed by l-glutamine allowing simultaneous utilization of nitrate and organic nitrogen sources. *Environ. Microbiol. Rep.* 2, 4. doi: 10.1111/j.1758-2229.2009.00111.x

Kennedy, P. (2010). Ectomycorrhizal fungi and interspecific competition: species interactions, community structure, coexistence mechanisms, and future research directions. *New Phytol.* 187, 895. doi: 10.1111//j.1469-8137.2010.03399.x

Kiers, E. T., Duhamel, M., Beesetty, Y., Mensah, J. A., Franken, O., Verbruggen, E., et al. (2011). Reciprocal rewards stabilize cooperation in the mycorrhizal symbiosis. *Science* 333, 880. doi: 10.1126/science.1208473

Kohler, A., Kuo, A., Nagy, L. G., Morin, E., Barry, K. W., Buscot, F., et al. (2015). Convergent losses of decay mechanisms and rapid turnover of symbiosis genes in mycorrhizal mutualists. *Nat. Genet.* 47, 4. doi: 10.1038/ng3223

Koide, R. T., Fernandez, C. W., and Malcolm, G. (2014). Determining place and process: functional traits of ectomycorrhizal fungi that affect both community structure and ecosystem function. *New Phytol.* 201, 2. doi: 10.1111/nph.12538

Kytöviita, M. M. (2005). Role of nutrient level and defoliation on symbiotic function: experimental evidence by tracing 14C/15N exchange in mycorrhizal birch seedlings. *Mycorrhiza* 15, 1. doi: 10.1007/s00572-004-0337-y

Larsen, P. E., Sreedasyam, A., Trivedi, G., Podila, G. K., Cseke, L. J., and Collart, F. R. (2011). Using next generation transcriptome sequencing to predict an ectomycorrhizal metabolome. *BMC Syst. Biol.* 5, 70. doi: 10.1186/1752-0509-5-70

Lau, J. A., Lennon, J. T., and Heath, K. D. (2017). Microbes rescue plants from climate change. *Proc. Natl. Acad. Sci. U. S. A.* 114, 42. doi: 10.1073/pnas.1715417114

Le Tacon, F., Zeller, B., Plain, C., Hossann, C., Bréchet, C., Martin, F., et al. (2015). Study of nitrogen and carbon transfer from soil organic matter to Tuber melanosporum mycorrhizas and ascocarps using 15N and 13C soil labelling and whole-genome oligoarrays. *Plant Soil* 395, 1–2. doi: 10.1007/s11104-015-2557-7

Lee, E. H., Eo, J. K., Ka, K. H., and Eom, A. H. (2013). Diversity of arbuscular mycorrhizal fungi and their roles in ecosystems. *Mycobiology* 41, 3. doi: 10.5941/MYCO.2013.41.3.121

Lilleskov, E. A., Fahey, T. J., Horton, T. R., and Lovett, G. M. (2002). Belowground ectomycorrhizal fungal community change over a nitrogen deposition gradient in Alaska. *Ecology* 83, 1. doi: 10.1046/j.1469-8137.2002.00367.x

Lin, G., McCormack, M. L., Ma, C., and Guo, D. (2017). Similar below-ground carbon cycling dynamics but contrasting modes of nitrogen cycling between arbuscular mycorrhizal and ectomycorrhizal forests. *New Phytol.* 213, 3. doi: 10.1111/nph.14206

Lindahl, B. D., and Tunlid, A. (2015). Ectomycorrhizal fungi—potential organic matter decomposers, yet not saprotrophs. *New Phytol.* 205, 4. doi: 10.1111/nph.13201

Lindahl, B. D., Ihrmark, K., Boberg, J., Trumbore, S. E., Högberg, P., Stenlid, J., et al. (2007). Spatial separation of litter decomposition and mycorrhizal nitrogen uptake in a boreal forest. *New Phytol.* 173, 3. doi: 10.1111/j.1469-8137.2006.01936.x

López, M. F., Dietz, S., Grunze, N., Bloschies, J., Weiß, M., and Nehls, U. (2008). The sugar porter gene family of Laccaria bicolor: function in ectomycorrhizal symbiosis and soil-growing hyphae. *New Phytol.* 180, 2. doi: 10.1111/j.1469-8137.2008.02539.x

Lucic, E., Fourrey, C., Kohler, A., Martin, F., Chalot, M., and Brun-Jacob, A. (2008). A gene repertoire for nitrogen transporters in Laccaria bicolor. *New Phytol.* 180, 2. doi: 10.1111/j.1469-8137.2008.02580.x

Martin, F., and Nehls, U. (2009). Harnessing ectomycorrhizal genomics for ecological insights. *Curr. Opin. Plant Biol.* 12, 4. doi: 10.1016/j.pbi.2009.05.007

Martin, F., Aerts, A., Ahrén, D., Brun, A., Danchin, E. G., Duchaussoy, F., et al. (2008). The genome of Laccaria bicolor provides insights into mycorrhizal symbiosis. *Nature* 452, 7183. doi: 10.1038/nature06556

Martin, F., Kohler, A., Murat, C., Veneault-Fourrey, C., and Hibbett, D. S. (2016). Unearthing the roots of ectomycorrhizal symbioses. *Nat. Rev. Microbiol.* 14, 12. doi: 10.1038/nrmicro.2016.149

Moeller, H. V., and Peay, K. G. (2016). Competition-function tradeoffs in ectomycorrhizal fungi. *PeerJ* 4, e2270. doi: 10.7717/peerj2270

Montanini, B., Moretto, N., Soragni, E., Percudani, R., and Ottonello, S. (2002). A high-affinity ammonium transporter from the mycorrhizal ascomycete Tuber borchii. *Fungal Genet. Biol.* 36, 1. doi: 10.1016/S1087-1845(02)00001-4

Morrison, E. W., Frey, S. D., Sadowsky, J. J., van Diepen, L. T. A., Thomas, W. K., and Pringle, A. (2016). Chronic nitrogen additions fundamentally restructure the soil fungal community in a temperate forest. *Fungal Ecol.* 23, 1. doi: 10.1016/j.funeco.2016.05.011

Müller, T., Avolio, M., Olivi, M., Benjdia, M., Rikirsch, E., Kasaras, A., et al. (2007). Nitrogen transport in the ectomycorrhiza association: the Hebeloma cylindrosporum-Pinus pinaster model. *Phytochemistry* 68, 1. doi: 10.1016/j.phytochem.2006.09.021

Näsholm, T., Högberg, P., Franklin, O., Metcalfe, D., Keel, S. G., Campbell, C., et al. (2013). Are ectomycorrhizal fungi alleviating or aggravating nitrogen limitation of tree growth in boreal forests? *New Phytol.* 198, 1. doi: 10.1111/nph.12139

Nagy, L. G., Riley, R., Bergmann, P. J., Krizsan, K., Martin, F. M., Grigoriev, I. V., et al. (2016). Genetic bases of fungal white rot wood decay predicted by phylogenomic analysis of correlated gene-phenotype evolution. *Mol. Biol. Evol.* 34, 1. doi: 10.1093/molbev/msw238

Nehls, U., and Plassard, C. (2018). Nitrogen and phosphate metabolism in ectomycorrhizas. *New Phytol.* 220, 4. doi: 10.1111/nph.15257

Nehls, U., Kleber, R., Wiese, J., and Hampp, R. (1999). Isolation and characterization of a general amino acid permease from the ectomycorrhizal fungus Amanita muscaria. *New Phytol.* 144, 2. doi: 10.1046/j.1469-8137.1999.00513.x

Nehls, U., Mikolajewski, S., Magel, E., and Hampp, R. (2001). Carbohydrate metabolism in ectomycorrhizas: gene expression, monosaccharide transport and metabolic control. *New Phytol.* 150, 3. doi: 10.1046/j.1469-8137.2001.00141.x

Nehls, U., Grunze, N., Willmann, M., Reich, M., and Küster, H. (2007). Sugar for my honey: carbohydrate partitioning in ectomycorrhizal symbiosis. *Phytochemistry* 68, 1. doi: 10.1016/j.phytochem.2006.09.024

Nehls, U., Göhringer, F., Wittulsky, S., and Dietz, S. (2010). Fungal carbohydrate support in the ectomycorrhizal symbiosis: a review. *Plant Biol.* 12, 2. doi: 10.1111/j.1438-8677.2009.00312.x

Nehls, U., Das, A., and Neb, D. (2016). "Carbohydrate metabolism in ectomycorrhizal symbiosis," in *Molecular Mycorrhizal Symbiosis*. Eds. F. M. Martin (Hoboken, NJ, USA: John Wiley & Sons Inc.).

Nilsson, L. O., and Wallander, H. (2003). Production of external mycelium by ectomycorrhizal fungi in a Norway spruce forest was reduced in response to nitrogen fertilization. *New Phytol.* 158, 2. doi: 10.1046/j.1469-8137.2003.00728.x

Op De Beeck, M., Troein, C., Peterson, C., Persson, P., and Tunlid, A. (2018). Fenton reaction facilitates organic nitrogen acquisition by an ectomycorrhizal fungus. *New Phytol.* 218, 1. doi: 10.1111/nph.14971

Orwin, K. H., Kirschbaum, M. U., St John, M. G., and Dickie, I. A. (2011). Organic nutrient uptake by mycorrhizal fungi enhances ecosystem carbon storage: a model-based assessment. *Ecol. Lett.* 14, 5. doi: 10.1111/j.1461-0248.2011.01611.x

Pardo, L. H., Fenn, M. E., Goodale, C. L., Geiser, L. H., Driscoll, C. T., Allen, E. B., et al. (2011). Effects of nitrogen deposition and empirical nitrogen critical loads for ecoregions of the United States. *Ecol. Appl.* 21, 8. doi: 10.1890/10-2341.1

Parrent, J. L., Morris, W. F., and Vilgalys, R. (2006). CO2-enrichment and nutrient availability alter ectomycorrhizal fungal communities. *Ecology* 87, 9. doi: 10.1890/0012-9658(2006)87[2278:CANAAE]2.0.CO;2

Pellitier, P. T., and Zak, D. R. (2018). Ectomycorrhizal fungi and the enzymatic liberation of nitrogen from soil organic matter: why evolutionary history matters. *New Phytol.* 217, 1. doi: 10.1111/nph.14598

Pena, R., and Polle, A. (2014). Attributing functions to ectomycorrhizal fungal identities in assemblages for nitrogen acquisition under stress. *ISME J.* 8, 2. doi: 10.1038/ismej.2013.158

Pena, R., Tejedor, J., Zeller, B., Dannenmann, M., and Polle, A. (2013). Interspecific temporal and spatial differences in the acquisition of litter-derived nitrogen by ectomycorrhizal fungal assemblages. *New Phytol.* 199, 2. doi: 10.1111/nph.12272

Peter, M., Kohler, A., Ohm, R. A., Kuo, A., Krützmann, J., Morin, E., et al. (2016). Ectomycorrhizal ecology is imprinted in the genome of the dominant symbiotic fungus Cenococcum geophilum. *Nat. Commun.* 7, 12662. doi: 10.1038/ncomms12662

Plassard, C., Bonafos, B., and Touraine, B. (2000). Differential effects of mineral and organic N sources, and of ectomycorrhizal infection by Hebeloma cylindrosporum, on growth and N utilization in Pinus pinaster. *Plant Cell Environ.* 23, 11. doi: 10.1046/j.1365-3040.2000.00630.x

Plett, J. M., Montanini, B., Kohler, A., Ottonello, S., and Martin, F. (2011). Tapping genomics to unravel ectomycorrhizal symbiosis. *Methods Mol. Biol.* 722, 249–281. doi: 10.1007/978-1-61779-040-9_19

Plett, J. M., Kohler, A., Khachane, A., Keniry, K., Plett, K. L., Martin, F., et al. (2015a). The effect of elevated carbon dioxide on the interaction between Eucalyptus grandis and diverse isolates of Pisolithus sp. is associated with a complex shift in the root transcriptome. *New Phytol.* 206, 4. doi: 10.1111/nph.13103

Plett, J. M., Tisserant, E., Brun, A., Morin, E., Grigoriev, I. V., Kuo, A., et al. (2015b). The Mutualist Laccaria bicolor expresses a core gene regulon during the colonization of diverse host plants and a variable regulon to counteract host-specific defenses. *Mol. Plant Microbe Interact.* 28, 3. doi: 10.1094/MPMI-05-14-0129-FI

Rapparini, F., and Peñuelas, J. (2014). "Mycorrhizal fungi to alleviate drought stress on plant growth," in *Use of Microbes for the Alleviation of Soil Stresses*. Eds. M. Miransari (New York, NY, USA: Springer), 21–42.

Read, D. J., and Perez-Moreno, J. (2003). Mycorrhizas and nutrient cycling in ecosystems—a journey towards relevance? *New Phytol.* 157, 3. doi: 10.1046/j.1469-8137.2003.00704.x

Read, D. J., Leake, J. R., and Perez-Moreno, J. (2004). Mycorrhizal fungi as drivers of ecosystem processes in heathland and boreal forest biomes. *Can. J. Bot.* 82, 8. doi: 10.1139/b04-123

Read, D. J. (1991). Mycorrhizas in ecosystems. *Experientia* 47, 4. doi: 10.1007/bf01972080

Rinaldi, A. C., Comandini, O., and Kuyper, T. W. (2008). Ectomycorrhizal fungal diversity: Separating the wheat from the chaff. *Fungal Divers.* 33, 1–45.

Rincón, A., de Felipe, M. R., and Fernández-Pascual, M. (2007). Inoculation of Pinus halepensis Mill. with selected ectomycorrhizal fungi improves seedling establishment 2 years after planting in a degraded gypsum soil. *Mycorrhiza* 18, 1. doi: 10.1007/s00572-007-0149-y

Rineau, F., Roth, D., Shah, F., Smits, M., Johansson, T., Canbäck, B., et al. (2012). The ectomycorrhizal fungus Paxillus involutus converts organic matter in plant litter using a trimmed brown-rot mechanism involving Fenton chemistry. *Environ. Microbiol.* 14, 6. doi: 10.1111/j.1462-2920.2012.02736.x

Rineau, F., Shah, F., Smits, M., Persson, P., Johansson, T., Carleer, R., et al. (2013). Carbon availability triggers the decomposition of plant litter and assimilation of nitrogen by an ectomycorrhizal fungus. *ISME J.* 7, 10. doi: 10.1038/ismej.2013.91

Rineau, F., Stas, J., Nguyen, N. H., Kuyper, T. W., Carleer, R., Vangronsveld, J., et al. (2016). Ectomycorrhizal fungal protein degradation ability predicted by soil organic nitrogen availability. *J. Appl. Environ. Microbiol.* 82, 5. doi: 10.1128/AEM.03191-15

Salzer, P., and Hager, A. (1991). Sucrose utilization of the ectomycorrhizal fungi amanita muscaria and Hebeloma crustuliniforme depends on the cell wall-bound invertase activity of their host picea abies. *Bot. Acta* 104, 6. doi: 10.1111/j.1438-8677.1991.tb00256.x

Sawyer, N. A., Chambers, S. M., and Cairney, J. W. G. (2003). Variation in nitrogen source utilisation by nine Amanita muscaria genotypes from Australian Pinus radiata plantations. *Mycorrhiza* 13, 4. doi: 10.1007/s00572-003-0229-6

Selle, A., Willmann, M., Grunze, N., Geßler, A., Weiß, M., and Nehls, U. (2005). The high-affinity poplar ammonium importer PttAMT1.2 and its role in ectomycorrhizal symbiosis. *New Phytol.* 168, 3. doi: 10.1111/j.1469-8137.2005.01535.x

Selosse, M. A., Strullu-Derrien, C., Martin, F. M., Kamoun, S., and Kenrick, P. (2015). Plants, fungi and oomycetes: a 400-million year affair that shapes the biosphere. *New Phytol.* 206, 2. doi: 10.1111/nph.13371

Shah, F., Rineau, F., Canback, B., Johansson, T., and Tunlid, A. (2013). The molecular components of the extracellular protein-degradation pathways of the ectomycorrhizal fungus Paxillus involutus. *New Phytol.* 200, 3. doi: 10.1111/nph.12425

Shah, F., Nicolás, C., Bentzer, J., Ellström, M., Smits, M., Rineau, F., et al. (2016). Ectomycorrhizal fungi decompose soil organic matter using oxidative mechanisms adapted from saprotrophic ancestors. *New Phytol.* 209, 4. doi: 10.1111/nph.13722

Simard, S. W., Jones, M. D., and Durall, D. M. (2003). "Carbon and Nutrient Fluxes Within and Between Mycorrhizal Plants," in *Mycorrhizal Ecology*. Eds. M. G. A. van der Heijden and I. R. Sanders (New York, NY, USA: Springer).

Smith, S. E., and Read, D. J. (2008). *Mycorrhizal Symbiosis. 3rd ed. (Cambridge, MA, USA: Academic Press).*

Sulman, B. N., Brzostek, E. R., Medici, C., Shevliakova, E., Menge, D. N. L., and Phillips, R. P. (2017). Feedbacks between plant N demand and rhizosphere priming depend on type of mycorrhizal association. *Ecol. Lett.* 20, 1043–1053. doi: 10.1111/ele.12802

Talbot, J. M., Allison, S. D., and Treseder, K. K. (2008). Decomposers in disguise: mycorrhizal fungi as regulators of soil C dynamics in ecosystems under global change. *Funct. Ecol.* 22, 6. doi: 10.1111/j.1365-2435.2008.01402.x

Tedersoo, L., and Smith, M. E. (2013). Lineages of ectomycorrhizal fungi revisited: Foraging strategies and novel lineages revealed by sequences from belowground. *Fungal Biol. Rev.* 27, 3–4. doi: 10.1016/j.fbr.2013.09.001

Terrer, C., Vicca, S., Hungate, B. A., Phillips, R. P., and Prentice, C. (2016). Mycorrhizal association as a primary control of the CO2 fertilization effect. *Science* 353, 6294. doi: 10.1126/science.aaf4610

Toljander, J. F., Eberhardt, U., Toljander, Y. K., Paul, L. R., and Taylor, A. F. S. (2006). Species composition of an ectomycorrhizal fungal community along a local nutrient gradient in a boreal forest. *New Phytol.* 170, 4. doi: 10.1111/j.1469-8137.2006.01718.x

Treseder, K. K., Torn, M. S., and Masiello, C. A. (2006). An ecosystem-scale radiocarbon tracer to test use of litter carbon by ectomycorrhizal fungi. *Soil Biol. Biochem.* 38, 5. doi: 10.1016/j.soilbio.2005.09.006

Treseder, K. K. (2004). A meta-analysis of mycorrhizal responses to nitrogen, phosphorus, and atmospheric CO2 in field studies. *New Phytol.* 164, 2. doi: 10.1111/j.1469-8137.2004.01159.x

Valtanen, K., Eissfeller, V., Beyer, F., Hertel, D., Scheu, S., and Polle, A. (2014). Carbon and nitrogen fluxes between beech and their ectomycorrhizal assemblage. *Mycorrhiza* 24, 8. doi: 10.1007/s00572-014-0581-8

Willmann, A., Weiß, M., and Nehls, U. (2007). Ectomycorrhiza-mediated repression of the high-affinity ammonium importer gene AmAMT2 in Amanita muscaria. *Curr. Genet.* 51, 71. doi: 10.1007/s00294-006-0106-x

Wright, D. P., Scholes, J. D., Read, D. J., and Rolfe, S. A. (2000). Changes in carbon allocation and expression of carbon transporter genes in Betula pendula Roth. colonized by the ectomycorrhizal fungus Paxillus involutus (Batsch) Fr. *Plant Cell. Environ.* 23, 1. doi: 10.1046/j.1365-3040.2000.00518.x

Zak, D. R., Pellitier, P. T., Argiroff, W. A., Castillo, B., James, T. Y., Nave, L. E., et al. (2019). Exploring the role of ectomycorrhizal fungi in soil carbon dynamics. *New Phytol.* 223, 1. doi: 10.1111/nph.15679

Conflict of Interest: The authors declare that the research was conducted in the absence of any commercial or financial relationships that could be construed as a potential conflict of interest.

frontiers in Plant Science

ORIGINAL RESEARCH
published: 16 January 2020
doi: 10.3389/fpls.2019.01678

MLO Differentially Regulates Barley Root Colonization by Beneficial Endophytic and Mycorrhizal Fungi

Magdalena Hilbert[1†], *Mara Novero*[2†], *Hanna Rovenich*[3†], *Stéphane Mari*[4], *Carolin Grimm*[1], *Paola Bonfante*[2] *and Alga Zuccaro*[1,3*]

[1] Department of Organismic Interactions, Max Planck Institute of Terrestrial Microbiology, Marburg, Germany, [2] Department of Life Sciences and Systems Biology, University of Turin, Turin, Italy, [3] Botanical Institute, Cluster of Excellence on Plant Sciences (CEPLAS), University of Cologne, Cologne, Germany, [4] BPMP, Univ Montpellier, CNRS, INRAE, Montpellier SupAgro, Montpellier, France

OPEN ACCESS

Edited by:
Pierre-Emmanuel Courty,
INRA Centre Dijon Bourgogne Franche-Comté, France

Reviewed by:
Ralph Panstruga,
RWTH Aachen University, Germany
Hannah Kuhn,
RWTH Aachen University, Germany
Brigitte Mauch-Mani,
Université de Neuchâtel, Switzerland

***Correspondence:**
Alga Zuccaro
azuccaro@uni-koeln.de

[†]These authors have contributed equally to this work

Specialty section:
This article was submitted to Plant Microbe Interactions, a section of the journal Frontiers in Plant Science

Received: 09 August 2019
Accepted: 28 November 2019
Published: 16 January 2020

Citation:
Hilbert M, Novero M, Rovenich H, Mari S, Grimm C, Bonfante P and Zuccaro A (2020) MLO Differentially Regulates Barley Root Colonization by Beneficial Endophytic and Mycorrhizal Fungi. Front. Plant Sci. 10:1678. doi: 10.3389/fpls.2019.01678

Loss-of-function alleles of *MLO* (*Mildew Resistance Locus O*) confer broad-spectrum resistance to foliar infections by powdery mildew pathogens. Like pathogens, microbes that establish mutually beneficial relationships with their plant hosts, trigger the induction of some defense responses. Initially, barley colonization by the root endophyte *Serendipita indica* (syn. *Piriformospora indica*) is associated with enhanced defense gene expression and the formation of papillae at sites of hyphal penetration attempts. This phenotype is reminiscent of *mlo*-conditioned immunity in barley leaf tissue and raises the question whether *MLO* plays a regulatory role in the establishment of beneficial interactions. Here we show that *S. indica* colonization was significantly reduced in plants carrying *mlo* mutations compared to wild type controls. The reduction in fungal biomass was associated with the enhanced formation of papillae. Moreover, epidermal cells of *S. indica*-treated *mlo* plants displayed an early accumulation of iron in the epidermal layer suggesting increased basal defense activation in the barley mutant background. Correspondingly, the induction of host cell death during later colonization stages was impaired in *mlo* colonized plants, highlighting the importance of the early biotrophic growth phase for *S. indica* root colonization. In contrast, the arbuscular mycorrhizal fungus *Funneliformis mosseae* displayed a similar colonization morphology on mutant and wild type plants. However, the frequency of mycorrhization and number of arbuscules was higher in *mlo*-5 mutants. These findings suggest that *MLO* differentially regulates root colonization by endophytic and AM fungi.

Keywords: biotrophy, cell death, fungal-root interactions, mutualism, cell wall appositions, Perls/DAB, VPE activity, susceptibility gene

INTRODUCTION

Plants establish diverse beneficial interactions with fungi from different taxa. Root endophytes belonging to the order Sebacinales establish long-lasting beneficial relationships with a broad range of plant species (Weiss et al., 2016). Root colonization by members of this order results in enhanced growth (Varma et al., 1999; Waller et al., 2005; Serfling et al., 2007; Ghimire et al., 2009; Franken,

2012), improved tolerance to abiotic stress (Waller et al., 2005; Baltruschat et al., 2008; Sherameti et al., 2008; Ghimire and Craven, 2011), as well as increased resistance to pathogens (Stein et al., 2008; Waller et al., 2008; Lahrmann et al., 2015; Sarkar et al., 2019). In some cases nutrient status has been reported to play a role in the interaction of the model sebacinoid fungus *Serendipita indica* with some plant species (Shahollari et al., 2005; Sherameti et al., 2005; Nautiyal et al., 2010; Yadav et al., 2010; Kumar et al., 2012). However, *S. indica* colonization of *Nicotiana attenuata* and barley had no effect on host phosphorus (P) and nitrogen (N) content (Barazani et al., 2005; Achatz et al., 2010), suggesting that nutrient exchange is not central to the beneficial effects conferred by sebacinoid fungi. *S. indica* colonizes the rhizodermis and outer root cortex (Deshmukh et al., 2006; Jacobs et al., 2011; Weiss et al., 2016). Following an initial biotrophic growth phase, during which the fungal hyphae remain surrounded by a plant-derived membrane, *S. indica* transitions to cell death-associated colonization that does not result in host disease (Deshmukh et al., 2006; Jacobs et al., 2011; Zuccaro et al., 2011; Lahrmann and Zuccaro, 2012; Qiang et al., 2012; Lahrmann et al., 2013).

Like sebacinoid fungi, arbuscular mycorrhizae (AM) establish beneficial interactions with many plant species (Bonfante and Genre, 2010). AM are obligate biotrophs that rely on their plant hosts as carbon sources in exchange for soil nutrients including P and N (Parniske, 2008). Additionally, AM colonization results in increased plant biomass and confers enhanced resistance to stress and pathogen infection (Khaosaad et al., 2007; Liu J et al., 2007; Pozo and Azcon-Aguilar, 2007). Following the mutual recognition between plant and microbe, AM form specialized hyphae, called hyphopodia, that adhere to the root epidermal surface where penetration hyphae emerge. In the inner root cortex, intracellular hyphae then establish so-called arbuscules, which represent the active interface for nutrient exchange (Genre et al., 2008).

The successful establishment of AM symbioses is genetically controlled by the ancestral common symbiosis pathway (CSP). In legumes, this pathway is required for the establishment of AM as well as root nodule symbiosis with rhizobacteria (Kistner et al., 2005; Gutjahr, 2014; Svistoonoff et al., 2014). In contrast, *S. indica* colonization and development is independent of *Lotus japonicus* and *Arabidopsis thaliana* CSP genes, suggesting that independent host pathways control AM symbiosis and endophytism (Banhara et al., 2015). However, in both cases transient and weak activation of defense responses have been reported during the early phases of colonization that are effectively suppressed by the fungi as the symbioses progress (Harrison, 2005; Schäfer et al., 2009; Camehl et al., 2011; Jacobs et al., 2011). These early defense responses include the formation of papillae at sites of hyphal penetration attempts of *S. indica* on barley (Lahrmann and Zuccaro, 2012). Papillae are dome-shaped cell wall appositions that play a vital role in resistance to plant pathogens (Hückelhoven, 2005; Hückelhoven, 2007; Albersheim et al., 2011; Hückelhoven, 2014). They generally consist of layers of callose, cellulose, arabinoxylan and phenolyic compounds (Chowdhury et al., 2014; Hückelhoven, 2014). Additionally, papillae contain reactive oxygen species (hydrogen peroxide H_2O_2) and in barley their formation appears to be dependent on iron (Fe^{3+}) accumulation in the apoplast (Thordal-Christensen et al., 1997; Hückelhoven et al., 1999; Liu G et al., 2007). Depending on their size, composition and the degree of cross-linking of their constituent parts, papillae can be more or less efficient in halting penetration (Aist and Israel, 1977; Israel et al., 1980; von Röpenack et al., 1998; Asaad et al., 2004; Chowdhury et al., 2014; Hückelhoven, 2014).

In barley, natural as well as chemically induced mutant lines carrying recessive *mlo* (MILDEW RESISTANCE LOCUS O) alleles display broad-spectrum resistance to the obligate biotrophic pathogen *Blumeria graminis* f. sp. *hordei* (*Bgh*), causal agent of the foliar powdery mildew disease (Büschges et al., 1997), and have been successfully employed in agriculture since the late 1970s (Jørgensen, 1992; Lyngkjær et al., 2000; Kusch and Panstruga, 2017). Especially barley spring varieties that are now largely grown in central Europe are resistant to *Bgh* following the introgression of *mlo* alleles (Jørgensen, 1992; McGrann et al., 2014; Kusch and Panstruga, 2017). Compared to wild type susceptible cultivars, these lines display faster formation of larger papillae upon pathogen attack (Jørgensen, 1992; Lyngkjær et al., 2000; Chowdhury et al., 2014). Similar mutations in orthologous genes of wheat, tomato, pea, *A. thaliana*, and many other plant species have since confirmed the importance of *mlo* for resistance to various species of powdery mildew (Elliott et al., 2002; Consonni et al., 2006; Bai et al., 2008; Humphry et al., 2011; Wang et al., 2014; Kusch and Panstruga, 2017). In contrast, some hemibiotrophic and necrotrophic pathogens show enhanced infection on *mlo* mutant plants possibly profiting from the spontaneous induction of leaf cell death (Jarosch et al., 1999; Kumar et al., 2001; McGrann et al., 2014). The contribution of *MLO* to host resistance against root-colonizing microbes is less well understood. Recent evidence suggests that the *mlo* genetic background does not affect barley root infection by the oomycete pathogen *Phytophthora palmivora* (Le Fevre et al., 2016). Similarly, *MLO* does not seem to play a role in the establishment of the beneficial relationships between pea and the rhizobacterium *Rhizobium leguminosarum* bv. *viciae* or the AM fungus *Rhizophagus irregularis* (syn. *Glomus intraradices*) (Humphry et al., 2011). However, transcriptional analyses showed an upregulation of the *Lotus japonicus MLO1-like* (chr1.CM0150.1) gene in cortical cells containing arbuscules of *Gigaspora margarita* (Guether et al., 2009) suggesting that *MLO* may play a regulatory role in AM colonization.

In this study, we used the endophyte *S. indica* and the AM fungus *F. mosseae*, both of which have intracellular lifestyles, to investigate the role of *MLO* in barley root symbioses. Comparative colonization analyses showed differential regulation by *MLO* during endophytism and mycorrhization. The decreased colonization by *S. indica* coincided with enhanced defense responses and papillae formation, highlighting the importance of the biotrophic growth phase for the establishment of the long-term beneficial relationship between *S. indica* and its plant hosts.

MATERIALS AND METHODS

Plant Material and *S. indica* Growth Conditions

Seeds of *mlo*-3, -4, and -5 mutant lines backcrossed to barley cv. Ingrid (Peterhänsel et al., 1997; Jarosch et al., 2003) were kindly provided by Ralph Panstruga. Wild type (WT) barley (*Hordeum vulgare* L. cv. Ingrid) and mutant seeds were surface-sterilized by washing in 70% ethanol for 1–5 min, rinsing in sterile distilled water and soaking in 4%–12% sodium hypochlorite for 1–1.5 h. Seeds were then thoroughly washed in sterile distilled water, placed onto sterile wet filter paper and kept in the dark at room temperature for 3–5 days to allow germination. *S. indica* Sav. Verma, Aj. Varma, Rexer, G. Kost & P. Franken (DSM11827, Deutsche Sammlung von Mikroorganismen und Zellkulturen, Braunschweig, Germany) was grown in liquid complex medium (CM) (Pham et al., 2004) at 130 rpm or on CM medium supplemented with 1.5% agar at 28°C.

Barley Inoculation With *S. indica*

Three-day-old seedlings were placed into sterile jars containing 1/10 plant nutrition medium (PNM) (Basiewicz et al., 2012). For inoculation, *S. indica* chlamydospores were collected from CM agar plates in 0.1% Tween20-water, filtered through Miracloth and pelleted by centrifugation at 3,500 *g* for 5 min. Spores were washed two more times in 0.1% Tween20-water and then re-suspended to a final concentration of $5x10^5$ spores/ml. Mock treatment consisted of 0.1% Tween20-water only. Three milliliters of spore suspension was added onto roots of barley seedlings. Jars were transferred to a growth chamber with a 16 h/8 h day/night (light intensity of 108 µmol/m^2/s) cycle at 22°C/18°C and 60% humidity. All experiments were prepared with three to four biological replicates consisting of pooled material from 4 plants/jar, and two to three independent replicate experiments.

Quantification of *S. indica* Colonization

Mock-treated and *S. indica*-colonized roots were harvested at 3, 5, 7, and 10 days post inoculation. Roots were washed in water and sections of the first 3 cm below the seed were cut and frozen in liquid nitrogen. Genomic DNA from 200 mg of freshly ground material was isolated according to (Doyle and Doyle, 1987). To remove contaminating RNA, samples were treated with 1 µL 10 mg/mL RNaseA (Thermo Fisher Scientific, Schwerte, Germany) and incubated at 37°C for 20 min. Quantitative PCR was performed with 10 ng gDNA template and primers targeting the *S. indica TEF* (*SiTEF*) the barley ubiquitin (*HvUBI*) genes (see **Supplementary Table 1**) in 10 µl SYBR green Supermix (BioRad, Munich, Germany) using the following amplification protocol: initial denaturation for 16 min at 95°C, followed by 40 cycles of 15 s at 95°C, 20 s at 59°C, and 30s at 72°C, and a melt curve analysis. The relative amount of fungal *vs.* plant gDNA was calculated according to the $2^{-\Delta Ct}$ method (Schmittgen and Livak, 2008).

Vacuolar Processing Enzyme (VPE) Activity Assay

Mock-treated and *S. indica*-colonized roots of WT and mutant plants were harvested at 10 dpi. Vacuolar processing enzyme (VPE) activity was measured as described previously (Lahrmann et al., 2013). Briefly, roots were washed in water and sections of the first 4 cm below the seed were cut and frozen in liquid nitrogen. Extracts were prepared from 100 mg freshly ground root material ground in liquid nitrogen with 1 ml extraction buffer [10 mM sodium acetate pH 5.5, 100 mM NaCl, 1 mM EDTA, 2mM dithiothreitol (DTT) and 1mM phenylmethylsulfonyl fluoride (PMSF)]. Plant debris was pelleted by centrifugation at max speed and 4°C for 10 min. To measure VPE activity, 100 µM of the fluorescent VPE-specific substrate Ac-ESEN-MCA (Peptide Institute Inc., Osaka, Japan) was added to 100 µl of root extract supernatants aliquoted into a 96-well plate. Fluorescence intensities were measured in a TECAN Infinite microplate reader (TECAN, Männerdorf, Switzerland) with 360 and 465 nm excitation and emission wavelengths, respectively, at 10 min intervals for 1 h. Buffer with and without substrate was used as control.

Staining and Microscopy of *S. indica*-Inoculated Barley Root Sections

Confocal pictures were taken using a TCS-SP5 confocal microscope (Leica, Bensheim, Germany). Colonized root tissue of WT and mutant plants was collected at indicated time points, boiled for 2 min in 10% potassium hydroxide, washed three times in deionized water, and three additional times in 1x PBS (pH 7.4) for 30 min. Roots were stained by infiltrating colorants four times for 4 min at 260 mbar with 1 min atmospheric pressure breaks. To visualize fungal structures, roots were infiltrated with 10 µg/mL fluorescent Wheat Germ Agglutinin (WGA) AF488 (Invitrogen, Thermo Fisher Scientific, Schwerte, Germany) in 1x PBS. Papillae were visualized following infiltration of 10 µg/mL fluorescent concanavalin A (ConA) AF633 (Invitrogen, Thermo Fisher Scientific, Schwerte, Germany) in 1x PBS. For iron staining, samples were fixed, embedded in resin, sectioned and then stained with the Perls/DAB procedure, as described previously (Roschzttardtz et al., 2009). This method is a sensitive histological test for iron accumulation in plants (Roschzttardtz et al., 2013).

Barley Inoculation With the Mycorrhizal Fungus *F. mosseae*

Following germination on wet filter paper, seedlings were kept 3 days in continuous light (light intensity of 80 µmol/m^2/s). For each experiment, four seedlings of barley WT and *mlo*-5 were placed into separate pots filled with a 7:3 mix of sterile quartz sand/granular *F. mosseae* inoculum (v/v). The *F. mosseae* inoculum was composed of newly formed spores and Sorghum root pieces already colonized by *F. mosseae*. The inoculum was purchased from MycAgro Lab (Dijon, France) and contained a minimum of 10 active propagules/g. Plants were transferred to a growth chamber with a 14 h/10 h day/night cycle at 23°C/21°C. After 2 months of cultivation, one half of the root apparatus was sampled from each plant and stained with Cotton Blue (0.1% in lactic acid) to evaluate the intraradical colonization. The other half was treated with WGA conjugated with the fluorescent probe fluorescein isothiocyanate (FITC) to analyze fungal

penetration in the root epidermal cells by confocal microscopy. The experiment was performed twice.

Quantification of the AM Colonization

For each plant at least 1 m of root tissue was observed under an optical microscope to evaluate the degree of mycorrhizal colonization (Trouvelot et al., 1986). Four parameters were considered: F% (frequency of mycorrhization) reporting the percentage of segments showing internal colonization, M% (intensity of mycorrhization in the root cortex) indicating the average percentage of colonized root segments, a% (percentage of arbuscules in the infected areas) quantifying the average presence of arbuscules within the infected areas, A% (percentage of arbuscules in the entire root apparatus) quantifying the presence of arbuscules in the whole root system.

Details of the AM Penetration

To analyze the fungal penetration through the root epidermis, fifty 0.5 cm root segments were fixed in 4% paraformaldehyde in 0.05 M phosphate buffer pH 7.2, for 4 h at room temperature. Fixed segments were embedded in 8% agarose (Agarose type II-A, Sigma-Aldrich, Taufkirchen, Germany) and cut into 50 μm sections with a vibratome. The sections were incubated for 5 min in 1:30 commercial bleach/phosphate buffer (v/v), carefully rinsed with buffer and incubated for 2 h at room temperature in 1 mg/ml WGA-FITC. Sections were then observed with a Leica TCS SP2 confocal microscope equipped with an Ar/HeNe laser with 543 nm excitation and 580–650 nm emission wavelengths.

Statistical Analyses

Statistically significant effects of plant genotypes on VPE activity in colonized and mock-treated root tissue were determined with ANOVA using R (v3.3.2). Significant differences between treatments were determined with Tukey's *post hoc* test from the Stats package (Miller, 1981; Yandell, 1997). Letters displaying similarities and differences were extracted using the multcompView package (v0.1-7) (Donoghue, 2004; Piepho, 2004). Statistically significant effects of plant genotypes on fungal colonization and activation of defense responses (papillae size and number) were determined using the Welch Two Sample *t* test from the Stats package in R. Asterisks indicate these differences.

RESULTS AND DISCUSSION

MLO Loss-Of-Function Mutations Result in Reduced Barley Root Colonization by *S. indica*

Removal of host genes that are required by invading pathogens for plant colonization, termed susceptibility genes, has been shown to provide disease resistance (van Schie and Takken, 2014). Several natural and mutagen-induced changes in the barley *MLO* locus confer broad-spectrum resistance to the powdery mildew pathogen *Blumeria graminis* f. sp. *hordei* (Jørgensen, 1992; Büschges et al., 1997; Lyngkjær et al., 2000; Kusch and Panstruga, 2017). Similarly, TALEN- and CRISPR-Cas9-introduced targeted mutations in three *MLO* homeoalleles of bread wheat showed their requirement for resistance to wheat powdery mildew (Wang et al., 2014). However, the recessive loss-of-function *mlo* alleles in barley resulted in increased susceptibility to some other fungal pathogens (Jarosch et al., 1999; McGrann et al., 2014). To investigate the role of *MLO* in the establishment of the long-term beneficial relationship between barley and the root endophyte *Serendipita indica*, we used the *mlo*-5 allele backcrossed (BC) into barley cv. Ingrid (hereafter referred to as *mlo*-5), which carries a point mutation in the start codon and is a predicted null allele (Büschges et al., 1997). Mutant and WT plants were inoculated with *S. indica* spores suspended in Tween20-water or Tween20-water alone as mock treatment. To assess the effect of the *mlo*-5 mutation on *S. indica* colonization, we quantified the relative abundance of *S. indica* gDNA as a proxy for fungal biomass in roots of WT barley cv. Ingrid and *mlo*-5 plants by quantitative PCR at 3, 5, and 7 days post inoculation (dpi), representing early and late biotrophic interaction stages and the initial cell death-associated phase, respectively. We observed a significant reduction in fungal biomass in mutant compared to control plants from early through late colonization stages (**Figure 1A**). To confirm this phenotype, we also quantified *S. indica* biomass in roots of colonized *mlo*-3 and *mlo*-4 mutant lines, which display frame shift mutations in exon 11 and 4, respectively, and likewise are predicted null alleles. Similar to *mlo*-5, *mlo*-3 and -4 were less colonized by *S. indica* compared to WT control plants (**Supplementary Figure 1**), suggesting that *MLO* is required for barley root colonization by *S. indica*. This is in contrast to earlier findings where *mlo* triple mutants of *A. thaliana* displayed similar levels of *S. indica* colonization as wild type plants (Acevedo-Garcia et al., 2017). In *A. thaliana* there are 15 members of the MLO family. It could be that in *A. thaliana* roots other MLO members play a role in fungal accommodation than the three mutated genes. Alternatively, it has previously been shown that *S. indica* displays different colonization strategies on barley and *A. thaliana* host plants (Lahrmann et al., 2013). It is, therefore, conceivable that MLO-controlled defense does not play an important role in *S. indica* accommodation in *A. thaliana* roots.

S. indica-Colonized *mlo*-5 Mutant Plants Display Enhanced Papilla Formation During Biotrophic Growth

Enhanced barley resistance to powdery mildew in *mlo* mutants has been associated with enhanced cell wall apposition, or papillae, formation (Skou et al., 1984; Bayles et al., 1990; Wolter et al., 1993). Due to the reduction in *S. indica* colonization in *mlo* plants, we compared papillae formation in inoculated *mlo*-5 mutant and WT roots. To visualize fungal structures and papillae, colonized root tissue was stained with the chitin-specific wheat germ agglutinin (WGA-AF488) and α-mannopyranosyl-/α-glucopyanosyl- specific concanavalin A (ConA-AF633) for confocal microscopy, respectively. While both barley genotypes responded with papillae formation to *S. indica* hyphal penetration attempts, these cell wall appositions were significantly bigger in *mlo*-5 plants compared to the controls (**Figures 1B**, **C**). The number of papillae increased

over time both in WT and *mlo*-5 plants but was significantly higher at 5 dpi in mutant plants (**Figure 1D**). These phenotypes are reminiscent of *mlo*-mediated resistance to *Bgh* in leaves, where the fungus is arrested at the prehaustorial stage when papillae formation occurs in epidermal cells (Skou et al., 1984), highlighting an interesting parallel between *mlo*-dependent leaf and root responses to fungal colonization.

At early stages of WT barley root colonization by *S. indica*, transient papillae development has previously been observed at penetration sites and coincides with the activation of weak barley defense responses at the transcriptional level during the fungus' biotrophic growth phase (Schäfer et al., 2009; Zuccaro et al., 2011; Lahrmann and Zuccaro, 2012). However, most of the papillae formed during the biotrophic colonization of the rhizodermis do not prevent *S. indica* hyphal penetration and disappear once the fungus reaches the root cortex (Zuccaro et al., 2011; Lahrmann and Zuccaro, 2012). The role of papillae in resistance against host cell penetration has been discussed for decades (Zeyen et al., 2002). Recent evidence suggests that so-called effective papillae [cell wall appositions that are formed in response to a local colonization attempt and that cannot be penetrated; (Hückelhoven, 2014)] contain higher quantities of callose, arabinoxylan and cellulose than ineffective papillae in barley (Chowdhury et al., 2014). Noncovalent bonds between arabinoxylan and cellulose have been proposed to maintain the barley cell wall, potentially forming a network of highly cross-linked polysaccharides (McNeil et al., 1975; Chowdhury et al., 2014). Phenolic compounds present in papillae could further enhance the degree of cross-linking giving rise to a tight structure resistant to mechanical penetration. The resistance to mechanical force, however, is unlikely to play a role in the interaction between *S. indica* and barley, since *S. indica* does not form appressorium-like structures. The genome of *S. indica*, like the genome of its orchid mycorrhizal relative *S. vermifera*, harbors a large number of genes encoding hydrolytic enzymes comparable to genomes of hemibiotrophic and necrotrophic pathogens, as well as several white rot saprotrophs (Lahrmann et al., 2013; Lahrmann et al., 2015). The up-regulation of genes encoding putative cell wall degrading enzymes during the pre-penetration stage (Zuccaro et al., 2011) suggests that *S. indica* uses hydrolytic enzymes for host cell penetration. The phenotypic alteration of papillae formed in *mlo*-5 plant roots suggests a change in composition similar to that proposed for papillae in leaves of resistant *mlo* barley plants. Considering that *S. indica* colonization is efficiently arrested in *mlo*-5 mutant plants, we hypothesize that the arsenal of hydrolytic enzymes and effector proteins produced by *S. indica* is not sufficient to overcome altered defenses in *mlo*-5 plants. Additionally, accumulation of toxic compounds at the penetration site in the *mlo*-5 background could decrease the capability of *S. indica* to penetrate the host cell.

The early arrest of *S. indica* colonization in plants carrying the *mlo*-5 allele indicates that the biotrophic phase plays an important role for the establishment of the beneficial barley-endophyte interaction. To test whether a reduction in biotrophic colonization would have an effect on fungal development, we assessed the induction of host root cell death, which is a hallmark of the *S. indica*-plant interaction during later colonization stages, using a well-established vacuolar processing enzyme (VPE) activity assay (Deshmukh et al., 2006; Qiang et al., 2012; Lahrmann et al., 2013). At 10 dpi, root sections of colonized WT and *mlo*-5 plants were collected for total protein extraction. Protein extracts were then incubated with the fluorescent VPE-specific substrate Ac-ESEN-MCA to measure VPE-mediated proteolytic cleavage of MCA. We observed a significant reduction in VPE activity in *S. indica*-treated *mlo*-5 plants compared to WT controls (**Figure 1E**) suggesting a decrease in host cell death. This finding is in agreement with lower colonization levels in *mlo* mutant plants (**Figure 1A**, **Supplementary Figure 1**), Thus, the recessive *mlo* allele effect on the early biotrophic fungal growth also affects the cell death phase.

Reduced *S. indica* Colonization Correlates With an Early Accumulation of Iron At the Epidermal Layer of *mlo*-5 Mutant Plants

The production of reactive oxygen species (ROS) represents a key factor in pathogen resistance, and has been reported to play a role in a number of beneficial associations (Enkerli et al., 1997; Hückelhoven et al., 1999; Fenster and Hause, 2005; Zuccaro et al., 2011; Lahrmann and Zuccaro, 2012). In addition to their direct antimicrobial effects, ROS have been implicated in the fortification of papillae and are emerging as signaling components during plant immunity (Thordal-Christensen et al., 1997; Torres et al., 2006; Baxter et al., 2014).

In cereals, the extracellular production of H_2O_2 and the resulting oxidative burst in response to biotic stress are dependent on the accumulation of iron (Liu G et al., 2007). To visualize iron accumulation, root tissue of infected and mock-treated plants was stained with Perls/DAB. Consistent with our observations on papillae formation in *mlo-5* mutant plants, iron accumulation was apparent at 5 dpi in *S. indica*-colonized mutant plants (**Figure 2A**), whereas iron depositions started to appear at 6 dpi in WT plants (**Figure 2B**). Iron accumulated at the cell periphery throughout the rhizodermal cell layer, suggesting a systemic reaction of this layer. In leaves it was shown that accumulation of Fe^{3+} occurs specifically around the cell wall appositions just below the site of *Bgh* penetration attempts, where it facilitates H_2O_2 production (Greenshields et al., 2007; Liu G et al., 2007), suggesting that the mechanisms underlying iron accumulation and its role in ROS generation may be different in the rhizodermal cell layer. Together, these findings indicate that defense responses are enhanced and occur earlier in the *mlo*-5 mutant resulting in reduced *S. indica* colonization.

Mlo Loss-Of-Function Mutations Result in Enhanced Mycorrhization

Like *S. indica*, *F. mosseae* has an intracellular lifestyle. Transcriptome studies comparing mycorrhizal to non-mycorrhizal conditions in *Lotus japonicus* suggested that *MLO* might play a regulatory role in AM colonization (Guether et al.,

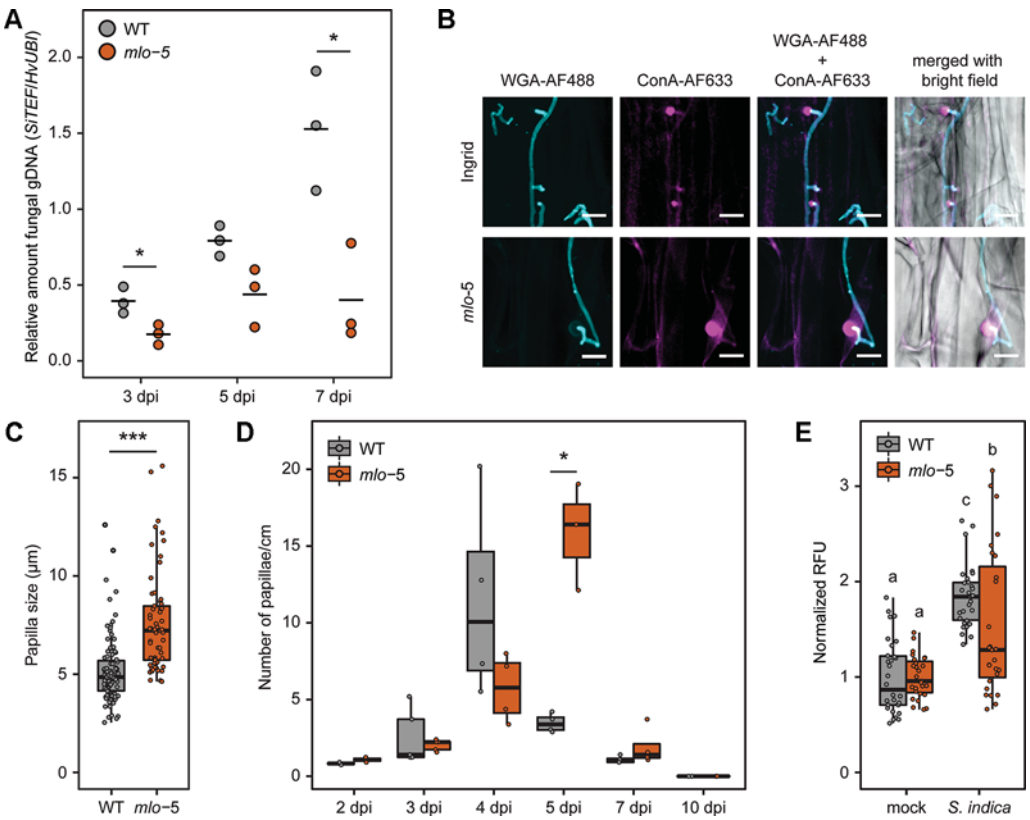

FIGURE 1 | Reduced *S. indica* colonization of barley *mlo*-5 coincides with enhanced root defense. Three-day-old barley seedlings were inoculated with a *S. indica* chlamydospore suspension at a final concentration of $5x10^5$ spores/ml in Tween20-water or Tween20-water alone as mock treatment. **(A)** At 3, 5, and 7 days post inoculation (dpi) seedlings were removed from jars and gDNA was extracted from inoculated root sections as described in the *Materials and Methods*. Fungal colonization in each biological replicate was confirmed by quantitative PCR (n = 3). Statistically significant differences in the relative abundance of fungal gDNA during colonization of wild type (WT) and mutant *mlo*-5 plants were determined with Welch two sample t tests (*p < 0.5). **(B)** Roots of inoculated WT and *mlo*-5 plants were collected and stained with 10 µg/ml Wheat Germ Agglutinin (WGA-AF488, cyan) and 10 µg/ml concanavalin A (ConA-AF633, magenta) for visualization of fungal structures and papillae, respectively. Confocal microscopy shows extraradical growth of *S. indica* and hyphal penetration attempts of WT and *mlo*-5 root tissue. At these sites, the barley host responds with papillae formation. **(C)** Sizes of papillae formed in colonized WT (n=95) and *mlo*-5 (n = 61) roots were determined based on confocal microscopy pictures taken at 3, 4, 5 and 7 dpi. The statistically significant difference in papilla size between wild type (WT) and mutant *mlo*-5 plants throughout colonization was determined with the Welch two sample t test (***p < 0.001). **(D)** The number of papillae formed in colonized WT and *mlo*-5 roots was quantified based on confocal microscopy pictures taken at 2, 3, 4, 5, 7, and 10 dpi (n = 2-4). Statistically significant differences in papilla quantity between barley genotypes were determined with Welch two sample t tests (*p < 0.5). **(E)** Mock-treated and *S. indica*-colonized roots of WT and mutant plants were harvested at 10 dpi. Root cell death was quantified by measuring vacuolar processing enzyme (VPE) activity-dependent fluorescence (Qiang et al., 2012). Letters represent statistically significant differences in VPE activity according to two-way ANOVA (F(1,110) = 7.077, p < 0.01) and Tukey's *post hoc* test.

2009). To test this hypothesis, WT and *mlo*-5 barley plants were inoculated with *F. mosseae* and the rate of AM colonization was determined after 2 months of co-cultivation. Microscopically, we did not observe evident differences in the mycorrhizal phenotype. The extraradical mycelia developed in both plant genotypes (**Figure 3A**, upper panel) and the hyphopodia (**Figure 3A**, middle panel) consisted of similarly swollen hyphae at places where hyphae were in direct contact with the plant epidermal cell. Moreover, arbuscules were produced in cortical cells with a typical branched appearance in colonized WT and *mlo*-5 mutant plants (**Figure 3A**, lower panel). These findings indicate that *MLO* is not essential for the establishment of AM symbiosis and cannot be listed as one of the genes of the AM symbiosis signaling module that are required for the perception of AM-derived signaling molecules (Vigneron et al., 2018). To analyze the first step of the colonization (i.e. the penetration of the epidermal cells) in greater detail, we stained vibratome sections of colonized *mlo*-5 root tissue with WGA-FITC. Confocal microscopy of stained sections revealed that *F. mosseae* follows an intracellular penetration mechanism in the mutant background (**Supplementary Figure 2**), as has been described for *G. margarita* on *Medicago truncatula* roots (Genre et al., 2005; Genre et al., 2008). Similar to *G. margarita*, *F. mosseae* hyphae proliferating from the hyphopodium directly cross the wall of the epidermal cells to which the hyphopodium is adhering (**Supplementary Figure 2**).

We then assessed the success of *F. mosseae* colonization by quantifying the frequency of mycorrhization (F%), the intensity

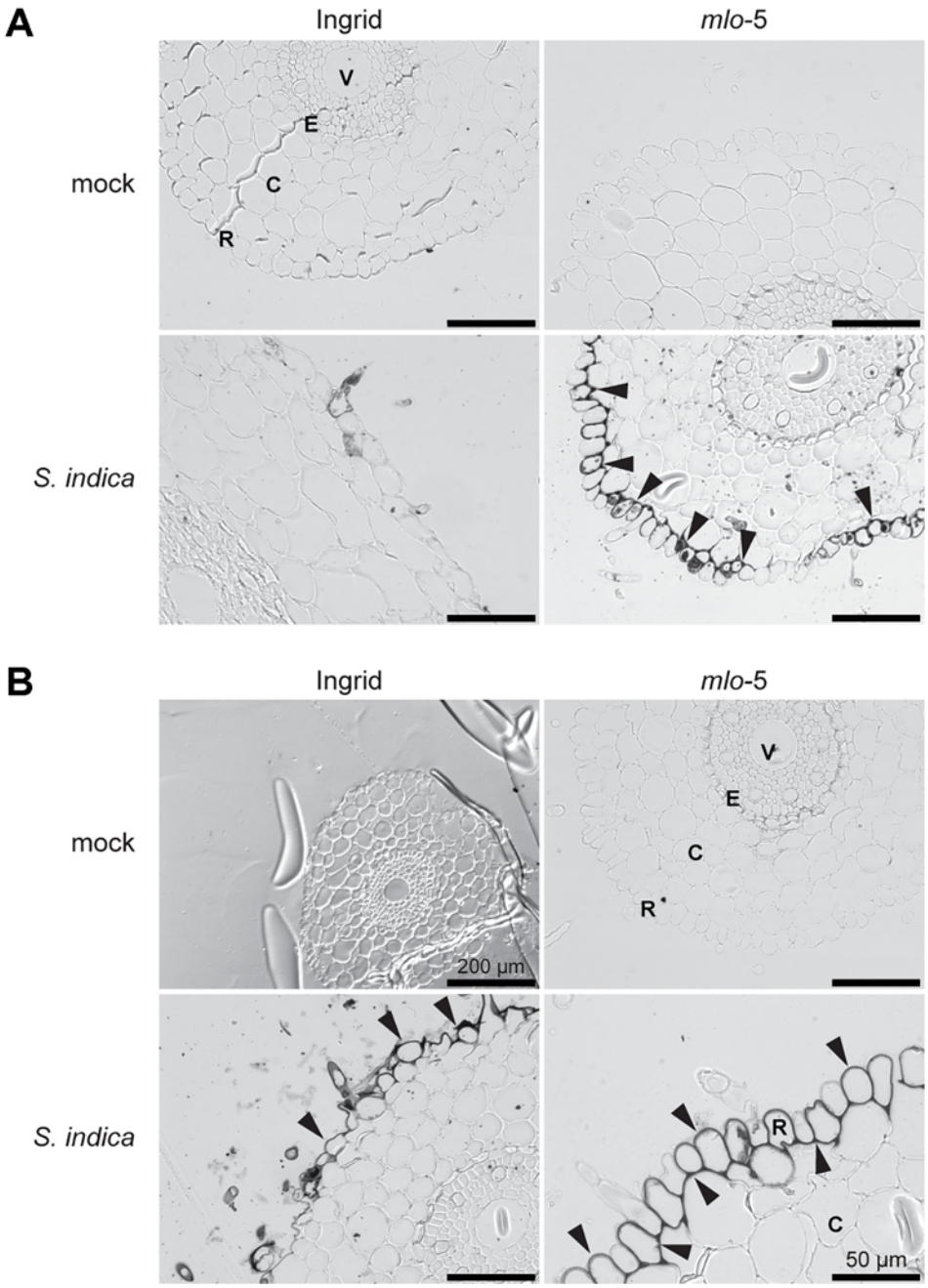

FIGURE 2 | Early accumulation of iron in the epidermal cells of the Ingrid *mlo*-5 mutant upon *S. indica* colonization. Light microscopic pictures show root sections stained with Perls/DAB at 5 **(A)** and 6 dpi **(B)**. Black precipitates, indicative of iron accumulation, appear around root epidermal cells in *mlo*-5 at 5 dpi, whereas iron accumulation in WT plants is only visible after 6 days of *S. indica* colonization (black arrowheads). Size bar = 100 µm unless otherwise indicated. R, rhizodermis; C, cortex; E, endodermis; V, vasculature.

of mycorrhization in the root cortex (M%), the percentage of arbuscules in infected areas (a%), and the presence of arbuscules in the entire root system (A%). In our experiments, F%, a%, and A% were higher in *mlo*-5 mutants compared to WT control plants, while the intensity of mycorrhization did not seem to be affected by the plant phenotype (**Figure 3B**). This is in contrast to the results presented by Ruiz-Lozano and colleagues (1999) who described a negative effect of the *mlo*-5 mutation on *F. mosseae* colonization at 6 weeks. This discrepancy is likely due to differences in inoculum efficiency and the large difference in root material analyzed here (1 m/plant) compared to the earlier study (30 cm/3 plants), or in the time points analyzed. We cannot exclude that colonization of the *mlo-5* mutant plants would be negatively affected at earlier stages, but our data indicate that the

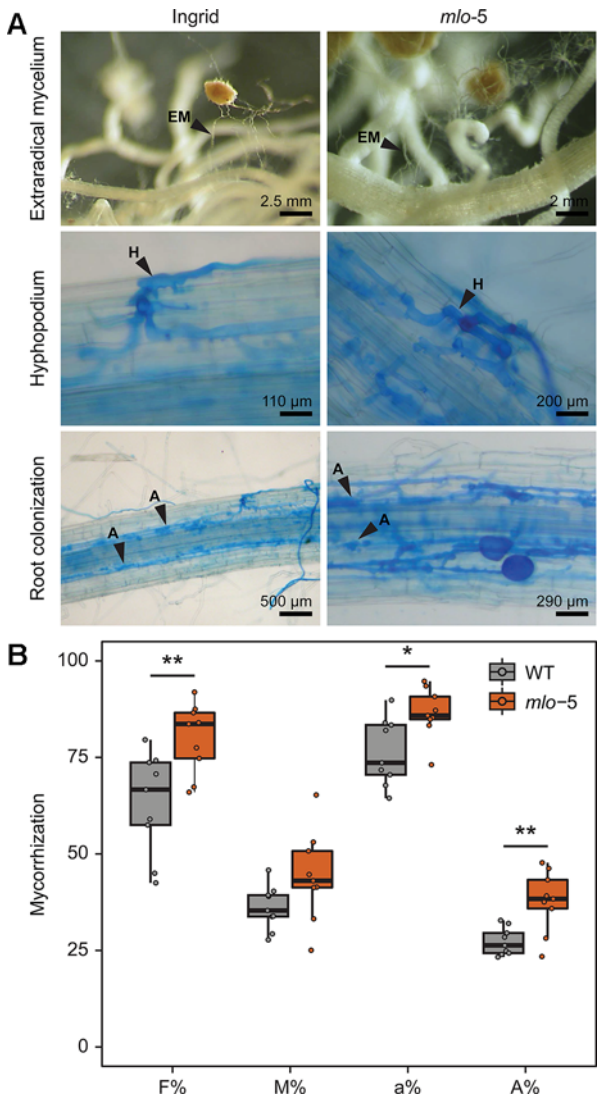

FIGURE 3 | The barley *mlo*-5 allele promotes mycorrhization. Three-day-old seedlings were inoculated with *F. mosseae* inoculum with ≥10 active propagules/g mixed into the soil. After 2 months of cultivation, intraradical colonization was assessed by light microscopy of Cotton blue-stained root tissue in WT and *mlo*-5 plants **(A)**. Black arrowheads indicate extraradical mycelia (EM; upper panel), hyphopodia (H; middle panel), and arbuscules (A; lower panel). **(B)** Mycorrhization was quantified using root tissue stained with fluorescein isothiocyanate-conjugated Wheat Germ Agglutinin (WGA-FITC) following confocal microscopy ($n = 2$). F% reports the percentage of segments showing internal colonization, M% indicates the average percent colonization of root segments, a% quantifies the average presence of arbuscules within the infected areas, A% quantifies the presence of arbuscules in the whole root system. Statistically significant differences in mycorrhization between barley genotypes were determined with Welch two sample *t* tests (*$p < 0.5$, **$p < 0.01$).

absence of this gene is not negatively affecting the symbiosis in the long run. Our observations suggest that *MLO* may be required for optimal AM colonization levels and could be grouped with other so-called downstream genes, which are involved in the re-organization of the plant host cell and facilitate nutrient exchange (Vigneron et al., 2018). While mutations in many of these downstream genes lead to a decrease in colonization success (Wang et al., 2019), the *mlo*-5 allele enhances host susceptibility. *MLO* genes encode plant-specific proteins with seven membrane-spanning domains (Büschges et al., 1997; Devoto et al., 1999; Elliott et al., 2005; Kusch et al., 2016). Despite considerable effort, our knowledge on the biochemical functions of this group of proteins remains limited. However, it has been demonstrated that *mlo*-mediated resistance against *Bgh* relies on actin cytoskeleton function in epidermal cells (Miklis et al., 2007). Similarly, the cytoskeleton is likely involved in the biogenesis of the perifungal membrane, which is an extension of the host plasmalemma surrounding the growing AM intracellular hyphae (Genre and Bonfante, 2002; Genre et al., 2012). Thus, *MLO* may exert control over the number of produced arbuscules through the regulation of cytoskeletal assembly.

CONCLUSIONS

In this study, we show that *MLO* differentially regulates the establishment of beneficial symbioses with the endophyte *S. indica* and the AM fungus *F. mosseae* in barley. During WT colonization by *S. indica* and *F. mosseae*, non-specific defense responses are largely repressed. In contrast, inoculation of *mlo*-5 mutant plants with *S. indica* results in an early activation of strong defense responses, such as accumulation of iron and papillae formation, limiting *S. indica* colonization at the epidermal layer during biotrophic growth and at the onset of the cell death-associated phase, while *F. mosseae* mycorrhization is enhanced in cortex cells at a late colonization stage. Based on these findings, we conclude that the regulatory role of *MLO* may be cell type specific. This hypothesis is in accordance with the recent finding that the *mlo*-5 mutation diminishes *P. palmivora* infection only in young leaf tissue (Le Fevre et al., 2016). Moreover, there seems to be a difference in *mlo* contribution to resistance between monocot and dicot plant species since *mlo* barley and *A. thaliana* mutants display contrasting phenotypes during the interaction with *S. indica*. One explanation could be the prominent role of iron (Fe^{3+})-mediated oxidative (H_2O_2) cross-linking of cell wall appositions in barley and other cereals, which does not occur during the *A. thaliana*-*S. indica* interaction (Greenshields et al., 2007; Liu G et al., 2007; Lahrmann et al., 2013). Additionally, the results presented here corroborate the pleiotropic effects of *mlo* in various plant-microbe interactions. Other genes have been shown to display variable regulative roles depending on the colonization strategy of the microbe. For example, in *M. truncatula* the gene *Nod Factor Perception* (*MtNFP*) is essential for the establishment of N-fixing symbiosis, and, as a consequence *Mtnfp* mutants cannot establish the beneficial interaction (Rey et al., 2013). However, *Mtnfp* mutant lines are more susceptible to pathogens including *Aphanomyces euteiches* and *Colletotrichum trifolii*, indicating that the regulation of plant-microbe symbioses is often dependent on the interacting microbe.

DATA AVAILABILITY STATEMENT

All datasets generated for this study are included in the article/ **Supplementary Material**.

AUTHOR CONTRIBUTIONS

MH, MN, PB, and AZ conceived and designed experiments. MH, MN, SM, and CG carried out experiments and analyzed the data. MN, HR, PB, and AZ wrote the manuscript.

FUNDING

AZ acknowledges support from the Max-Planck-Gesellschaft and the Cluster of Excellence on Plant Sciences (CEPLAS) under Germany's Excellence Strategy—EXC 2048/1—Project ID: 390686111. Research in Torino was supported by the project 60% (local project of University of Torino) to PB.

ACKNOWLEDGMENTS

The authors thank Ralph Panstruga for kindly providing seeds of BC Ingrid *mlo* allele genotypes.

SUPPLEMENTARY MATERIAL

The Supplementary Material for this article can be found online at: https://www.frontiersin.org/articles/10.3389/fpls.2019.01678/full#supplementary-material

REFERENCES

Acevedo-Garcia, J., Gruner, K., Reinstädler, A., Kemen, A., Kemen, E., Cao, L., et al. (2017). The powdery mildew-resistant Arabidopsis mlo2 mlo6 mlo12 triple mutant displays altered infection phenotypes with diverse types of phytopathogens. *Sci. Rep.* 7, 9319. doi: 10.1038/s41598-017-07188-7

Achatz, B., Kogel, K.-H., Franken, P., and Waller, F. (2010). Piriformospora indica mycorrhization increases grain yield by accelerating early development of barley plants. *Plant Signal Behav.* 5, 1685–, 1687. doi: 10.4161/psb.5.12.14112

Aist, J. R., and Israel, H. W. (1977). Papilla formation - timing and significance during penetration of barley coleoptiles by Erysiphe graminis hordei. *Physiol. Plant Pathol.* 67, 455–461. doi: 10.1016/0048-4059(77)90003-0

Albersheim, P., Darvill, A. G., Roberts, K. A., Sederoff, R., and Staehlin, A. (2011). *Cell walls and plant-microbe interactions* (New York, NY, USA: Garland Science, Taylor & Francis).

Asaad, N., den Otter, M. J., and Engberts, J. B. (2004). Aqueous solutions that model the cytosol: studies on polarity, chemical reactivity and enzyme kinetics. *Org. Biomol. Chem.* 2, 1404–1412. doi: 10.1039/b402886d

Büschges, R., Hollricher, K., Panstruga, R., Simons, G., Wolter, M., Frijters, A., et al. (1997). The barley Mlo gene: a novel control element of plant pathogen resistance. *Cell.* 88, 695–705. doi: 10.1016/s0092-8674(00)81912-1

Bai, Y., Pavan, S., Zheng, Z., Zappel, N. F., Reinstadler, A., Lotti, C., et al. (2008). Naturally occurring broad-spectrum powdery mildew resistance in a Central American tomato accession is caused by loss of mlo function. *Mol. Plant Microbe Interact.* 21, 30–39. doi: 10.1094/MPMI-21-1-0030

Baltruschat, H., Fodor, J., Harrach, B. D., Niemczyk, E., Barna, B., Gullner, G., et al. (2008). Salt tolerance of barley induced by the root endophyte Piriformospora indica is associated with a strong increase in antioxidants. *New Phytol.* 180, 501–510. doi: 10.1111/j.1469-8137.2008.02583.x

Banhara, A., Ding, Y., Kuhner, R., Zuccaro, A., and Parniske, M. (2015). Colonization of root cells and plant growth promotion by Piriformospora indica occurs independently of plant common symbiosis genes. *Front. Plant Sci.* 6, 667. doi: 10.3389/fpls.2015.00667

Barazani, O., Benderoth, M., Groten, K., Kuhlemeier, C., and Baldwin, I. T. (2005). Piriformospora indica and Sebacina vermifera increase growth performance at the expense of herbivore resistance in Nicotiana attenuata. *Oecologia.* 146, 234–243. doi: 10.1007/s00442-005-0193-2

Basiewicz, M., Weiss, M., Kogel, K.-H., Langen, G., Zorn, H., and Zuccaro, A. (2012). Molecular and phenotypic characterization of Sebacina vermifera strains associated with orchids, and the description of Piriformospora williamsii sp. nov. *Fungal Biol.* 116, 204–213. doi: 10.1016/j.funbio.2011.11.003

Baxter, A., Mittler, R., and Suzuki, N. (2014). ROS as key players in plant stress signalling. *J. Exp. Bot.* 65, 1229–1240. doi: 10.1093/jxb/ert375

Bayles, C. J., Ghemawat, M. S., and Aist, J. R. (1990). Inhibition by 2-deoxy-D-glucose of callose formation, papilla deposition, and resistance to powdery mildew in an ml-o barley mutant. *Physiol. Mol. Plant Pathol.* 36, 63–72. doi: 10.1016/0885-5765(90)90092-C

Bonfante, P., and Genre, A. (2010). Mechanisms underlying beneficial plant-fungus interactions in mycorrhizal symbiosis. *Nat. Commun.* 1, 48. doi: 10.1038/ncomms1046

Camehl, I., Drzewiecki, C., Vadassery, J., Shahollari, B., Sherameti, I., Forzani, C., et al. (2011). The OXI1 kinase pathway mediates Piriformospora indica-induced growth promotion in Arabidopsis. *PloS Pathog.* 7, e1002051. doi: 10.1371/journal.ppat.1002051

Chowdhury, J., Henderson, M., Schweizer, P., Burton, R. A., Fincher, G. B., and Little, A. (2014). Differential accumulation of callose, arabinoxylan and cellulose in nonpenetrated versus penetrated papillae on leaves of barley infected with Blumeria graminis f. sp. hordei. *New Phytol.* 204, 650–660. doi: 10.1111/nph.12974

Consonni, C., Humphry, M. E., Hartmann, H. A., Livaja, M., Durner, J., Westphal, L., et al. (2006). Conserved requirement for a plant host cell protein in powdery mildew pathogenesis. *Nat. Genet.* 38, 716–720. doi: 10.1038/ng1806

Deshmukh, S., Hückelhoven, R., Schäfer, P., Imani, J., Sharma, M., Weiss, M., et al. (2006). The root endophytic fungus Piriformospora indica requires host cell death for proliferation during mutualistic symbiosis with barley. *Proc. Natl. Acad. Sci. U.S.A.* 103, 18450–18457. doi: 10.1073/pnas.0605697103

Devoto, A., Piffanelli, P., Nilsson, I., Wallin, E., Panstruga, R., von Heijne, G., et al. (1999). Topology, subcellular localization, and sequence diversity of the Mlo family in plants. *J. Biol. Chem.* 274, 34993–35004. doi: 10.1074/jbc.274.49.34993

Donoghue, J. R. (2004). "Implementing Schaffer's multiple comparison procedure for a large number of groups," *Recent Developments in multiple comparison procedures*. (OH, USA: Institute of Mathematical Statistics), 1–23. doi: 10.1214/lnms/1196285622

Doyle, J. J., and Doyle, J. L. (1987). A rapid DNA isolation procedure for small quantities of fresh leaf tissue. *Phytochem. Bull.* 19, 11–15.

Elliott, C., Zhou, F., Spielmeyer, W., Panstruga, R., and Schulze-Lefert, P. (2002). Functional conservation of wheat and rice Mlo orthologs in defense modulation to the powdery mildew fungus. *Mol. Plant Microbe Interact.* 15, 1069–1077. doi: 10.1094/MPMI.2002.15.101069

Elliott, C., Muller, J., Miklis, M., Bhat, R. A., Schulze-Lefert, P., and Panstruga, R. (2005). Conserved extracellular cysteine residues and cytoplasmic loop-loop interplay are required for functionality of the heptahelical MLO protein. *Biochem. J.* 385, 243–254. doi: 10.1042/BJ20040993

Enkerli, J., Bhatt, G., and Covert, S. F. (1997). Nht1, a transposable element cloned from a dispensable chromosome in Nectria haematococca. *Mol. Plant Microbe Interact.* 10, 742–749. doi: 10.1094/MPMI.1997.10.6.742

Fenster, T., and Hause, G. (2005). Accumulation of reactive oxygen species in arbuscular mycorrhizal roots. *Mycorrhiza.* 15, 3743–3779. doi: 10.1007/s00572-005-0363-4

Franken, P. (2012). The plant strengthening root endophyte Piriformospora indica: potential application and the biology behind. *Appl. Microbiol. Biotechnol.* 96, 1455–1464. doi: 10.1007/s00253-012-4506-1

Genre, A., and Bonfante, P. (2002). Epidermal cells of a symbiosis-defective mutant of Lotus japonicus show altered cytoskeleton organisation in the presence of a mycorrhizal fungus. *Protoplasma.* 219, 43–50. doi: 10.1007/s007090200004

Genre, A., Chabaud, M., Timmers, T., Bonfante, P., and Barker, D. G. (2005). Arbuscular mycorrhizal fungi elicit a novel intracellular apparatus in Medicago truncatula root epidermal cells before infection. *Plant Cell.* 17, 3489–3499. doi: 10.1105/tpc.105.035410

Genre, A., Chabaud, M., Faccio, A., Barker, D. G., and Bonfante, P. (2008). Prepenetration apparatus assembly precedes and predicts the colonization patterns of arbuscular mycorrhizal fungi within the root cortex of both Medicago truncatula and Daucus carota. *Plant Cell.* 20, 1407–1420. doi: 10.1105/tpc.108.059014

Genre, A., Ivanov, S., Fendrych, M., Faccio, A., Zarsky, V., Bisseling, T., et al. (2012). Multiple exocytotic markers accumulate at the sites of perifungal membrane biogenesis in arbuscular mycorrhizas. *Plant Cell Physiol.* 53, 244–255. doi: 10.1093/pcp/pcr170

Ghimire, S. R., and Craven, K. D. (2011). Enhancement of switchgrass (Panicum virgatum L.) biomass production under drought conditions by the ectomycorrhizal fungus Sebacina vermifera. *Appl. Environ. Microbiol.* 77, 7063–7067. doi: 10.1128/AEM.05225-11

Ghimire, S. R., Charlton, N. D., and Craven, K. D. (2009). The mycorrhizal fungus, Sebacina vermifera, enhances seed germination and biomass production in swtichgrass (Panicum virgatum L.). *Bioenergy Res.* 2, 51–58. doi: 10.1007/s12155-009-9033-2

Greenshields, D. L., Liu, G., and Wei, Y. (2007). Roles of iron in plant defence and fungal virulence. *Plant Signal Behav.* 2, 300–302. doi: 10.4161/psb.2.44042

Guether, M., Balestrini, R., Hannah, M., He, J., Udvardi, M. K., and Bonfante, P. (2009). Genome-wide reprogramming of regulatory networks, transport, cell wall and membrane biogenesis during arbuscular mycorrhizal symbiosis in Lotus japonicus. *New Phytol.* 182, 200–212. doi: 10.1111/j.1469-8137.2008.02725.x

Gutjahr, C. (2014). Phytohormone signaling in arbuscular mycorhiza development. *Curr. Opin. Plant Biol.* 20, 26–34. doi: 10.1016/j.pbi.2014.04.003

Hückelhoven, R., Fodor, J., Preis, C., and Kogel, K.-H. (1999). Hypersensitive cell death and papilla formation in barley attacked by the powdery mildew fungus are associated with hydrogen peroxide but not with salicylic acid accumulation. *Plant Physiol.* 119, 1251–1260. doi: 10.1104/pp.119.41251

Hückelhoven, R. (2005). Powdery mildew susceptibility and biotrophic infection strategies. *FEMS Microbiol. Lett.* 245, 9–17. doi: 10.1016/j.femsle.2005.03.001

Hückelhoven, R. (2007). Cell wall-associated mechanisms of disease resistance and susceptibility. *Annu. Rev. Phytopathol.* 45, 101–127. doi: 10.1146/annurev.phyto.45.062806.094325

Hückelhoven, R. (2014). The effective papilla hypothesis. *New Phytol.* 204, 438–440. doi: 10.1111/nph.13026

Harrison, M. J. (2005). Signaling in the arbuscular mycorrhizal symbiosis. *Annu. Rev. Microbiol.* 59, 19–42. doi: 10.1146/annurev.micro.58.030603.123749

Humphry, M., Reinstadler, A., Ivanov, S., Bisseling, T., and Panstruga, R. (2011). Durable broad-spectrum powdery mildew resistance in pea er1 plants is conferred by natural loss-of-function mutations in PsMLO1. *Mol. Plant Pathol.* 12, 866–878. doi: 10.1111/j.1364-3703.2011.00718.x

Israel, H. W., Wilson, R. G., Aist, J. R., and Kunoh, H. (1980). Cell wall appositions and plant disease resistance: acoustic microscopy of papillae that block fungal ingress. *Proc. Natl. Acad. Sci. U.S.A.* 77, 2046–2049. doi: 10.1073/pnas.77.42046

Jørgensen, I. H. (1992). Discovery, characterization and exploitation of Mlo powdery mildew resistance in barley. *Euphytica.* 63, 141–152. doi: 10.1007/BF00023919

Jacobs, S., Zechmann, B., Molitor, A., Trujillo, M., Petutschnig, E., Lipka, V., et al. (2011). Broad-spectrum suppression of innate immunity is required for colonization of Arabidopsis roots by the fungus Piriformospora indica. *Plant Physiol.* 156, 726–740. doi: 10.1104/pp.111.176446

Jarosch, B., Kogel, K.-H., and Schaffrath, U. (1999). The ambivalence of the barley Mlo locus: Mutations conferring resistance against powdery mildew (Blumeria graminis f. sp. hordei) enhance susceptibility to the rice blast fungus Magnaporthe grisea. *Mol. Plant Microbe Interact.* 12, 508–514. doi: 10.1094/MPMI.1999.12.6.508

Jarosch, B., Jansen, M., and Schaffrath, U. (2003). Acquired resistance functions in mlo barley, which is hypersusceptible to Magnaporthe grisea. *Mol. Plant Microbe Interact.* 16, 107–114. doi: 10.1094/MPMI.2003.16.2.107

Khaosaad, T., García-Garrido, J. M., Steinkellner, S., and Vierheilig, H. (2007). Take-all disease is systemically reduced in roots of mycorrhizal barley plants. *Soil Biol. Biochem.* 39, 727–734. doi: 10.1016/j.soilbio.2006.09.014

Kistner, C., Winzer, T., Pitzschke, A., Mulder, L., Sato, S., Kaneko, T., et al. (2005). Seven Lotus japonicus genes required for transcriptional reprogramming of the root during fungal and bacterial symbiosis. *Plant Cell.* 17, 2217–2229. doi: 10.1105/tpc.105.032714

Kumar, J., Hückelhoven, R., Beckhove, U., Nagarajan, S., and Kogel, K.-H. (2001). A compromised Mlo pathway affects the response of barley to the necrotrophic fungus Bipolaris sorokiniana (teleomorph: Cochliobolus sativus) and its toxins. *Phytopathol.* 91, 127–133. doi: 10.1094/PHYTO.2001.91.2.127

Kumar, V., Sarma, M. V. R. K., Saharan, K., Srivastava, R., Kumar, L., Sahai, V., et al. (2012). Effect of formulated root endophytic fungus Piriformospora indica and plant growth promoting rhizobacteria fluorescent pseudomonads R62 and R81 on Vigno mungo. *World J. Microbiol. Biotechnol.* 28, 595–603. doi: 10.1007/s11274-011-0852-x

Kusch, S., and Panstruga, R. (2017). mlo-based resistance: an apparently universal "weapon" to defeat powdery mildew disease. *Mol. Plant Microbe Interact.* 30, 179–189. doi: 10.1094/MPMI-12-16-0255-CR

Kusch, S., Pesch, L., and Panstruga, R. (2016). Comprehensive phylogenetic analysis sheds light on the diversity and origin of the MLO family of integral membrane proteins. *Genome Biol. Evol.* 8, 878–895. doi: 10.1093/gbe/evw036

Lahrmann, U., and Zuccaro, A. (2012). Opprimo ergo sum–evasion and suppression in the root endophytic fungus Piriformospora indica. *Mol. Plant Microbe Interact.* 25, 727–737. doi: 10.1094/MPMI-11-11-0291

Lahrmann, U., Ding, Y., Banhara, A., Rath, M., Hajirezaei, M. R., Dohlemann, S., et al. (2013). Host-related metabolic cues affect colonization strategies of a root endophyte. *Proc. Natl. Acad. Sci. U.S.A.* 110, 13965–13970. doi: 10.1073/pnas.1301653110

Lahrmann, U., Strehmel, N., Langen, G., Frerigmann, H., Leson, L., Ding, Y., et al. (2015). Mutualistic root endophytism is not associated with the reduction of saprotrophic traits and requires a noncompromised plant innate immunity. *New Phytol.* 207, 841–857. doi: 10.1111/nph.13411

Le Fevre, R., O'Boyle, B., Moscou, M. J., and Schornack, S. (2016). Colonization of barley by the broad-host hemibiotrophic pathogen Phytophthora palmivora uncovers a leaf development-dependent involvement of Mlo. *Mol. Plant Microbe Interact.* 29, 385–395. doi: 10.1094/MPMI-12-15-0276-R

Liu, G., Greenshields, D. L., Sammynaiken, R., Hirji, R. N., Selvaraj, G., and Wei, Y. (2007). Targeted alterations in iron homeostasis underlie plant defense responses. *J. Cell Sci.* 120, 596–605. doi: 10.1242/jcs.001362

Liu, J., Maldonado-Mendoza, I., Lopez-Meyer, M., Cheung, F., Town, C. D., and Harrison, M. J. (2007). Arbuscular mycorrhizal symbiosis is accompanied by local and systemic alterations in gene expression and an increase in disease resistance in the shoots. *Plant J.* 50, 529–544. doi: 10.1111/j.1365-313X.2007.03069.x

Lyngkjær, M., Newton, A., Atzema, J., and Baker, S. (2000). The barley mlo-gene: an important powdery mildew resistance source. *Agronomie.* 20, 745–756. doi: 10.1051/agro:2000173

McGrann, G. R., Stavrinides, A., Russell, J., Corbitt, M. M., Booth, A., Chartrain, L., et al. (2014). A trade off between mlo resistance to powdery mildew and increased susceptibility of barley to a newly important disease, Ramularia leaf spot. *J. Exp. Bot.* 65, 1025–1037. doi: 10.1093/jxb/ert452

McNeil, M., Albersheim, P., Taiz, L., and Jones, R. L. (1975). The structure of plant cell walls: VII. *Barley Aleurone Cells Plant Physiol.* 55, 64–68. doi: 10.1104/pp.55.1.64

Miklis, M., Consonni, C., Bhat, R. A., Lipka, V., Schulze-Lefert, P., and Panstruga, R. (2007). Barley MLO modulates actin-dependent and actin-independent antifungal defense pathways at the cell periphery. *Plant Physiol.* 144, 1132–1143. doi: 10.1104/pp.107.098897

Miller, R. G. (1981). Simultaneous statistical inference. (New York, NY: Springer), doi: 10.1007/978-1-4613-8122-8

Nautiyal, C. S., Chauhan, P. S., DasGupta, S. M., Seem, K., Varma, A., and Staddon, W. J. (2010). Tripartite interactions among Paenibacillus lentimorbus NRRL B-30488, Piriformospora indica DSM 11827, and Cicer arietinum L. *World J. Microbiol. Biotechnol.* 26, 1393–1399. doi: 10.1007/s11274-010-0312-z

Parniske, M. (2008). Arbuscular mycorrhiza: the mother of plant root endosymbioses. *Nat. Rev. Microbiol.* 6, 763–775. doi: 10.1038/nrmicro1987

Peterhänsel, C., Freialdenhoven, A., Kurth, J., Kolsch, R., and Schulze-Lefert, P. (1997). Interaction analyses of genes required for resistance responses to powdery mildew in barley reveal distinct pathways leading to leaf cell death. *Plant Cell.* 9, 1397–1409. doi: 10.1105/tpc.9.81397

Pham, G. H., Singh, A., Malla, R., Kumari, R., Prasad, R., Sachdev, M., et al. (2004). "Interaction of P. indica with other microorganisms and plants," in *Plant*

Surface Microbiology. Eds. A. Varma, L. Abbott, D. Werner and R. Hampp (Heidelberg, Germany: Springer), 237–265.

Piepho, H.-P. (2004). An algorithm for letter-based representation of all-pairwise comparisons. *J. Comp. Graph. Stat.* 13, 456–466. doi: 10.1198/1061860043515

Pozo, M. J., and Azcon-Aguilar, C. (2007). Unraveling mycorrhiza-induced resistance. *Curr. Opin. Plant Biol.* 10, 393–398. doi: 10.1016/j.pbi.2007.05.004

Qiang, X., Zechmann, B., Reitz, M. U., Kogel, K.-H., and Schäfer, P. (2012). The mutualistic fungus Piriformospora indica colonizes Arabidopsis roots by inducing an endoplasmic reticulum stress-triggered caspase-dependent cell death. *Plant Cell.* 24, 794–809. doi: 10.1105/tpc.111.093260

Rey, T., Nars, A., Bonhomme, M., Bottin, A., Huguet, S., Balzergue, S., et al. (2013). NFP, a LysM protein controlling Nod factor perception, also intervenes in Medicago truncatula resistance to pathogens. *New Phytol.* 198, 875–886. doi: 10.1111/nph.12198

Roschzttardtz, H., Conejero, G., Curie, C., and Mari, S. (2009). Identification of the endodermal vacuole as the iron storage compartment in the Arabidopsis embryo. *Plant Physiol.* 151, 1329–1338. doi: 10.1104/pp.109.144444

Roschzttardtz, H., Conejero, G., Divol, F., Alcon, C., Verdeil, J. L., Curie, C., et al. (2013). New insights into Fe localization in plant tissues. *Front. Plant Sci.* 4, 350. doi: 10.3389/fpls.2013.00350

Ruiz-Lozano, J. M., Gianinazzi, S., and Gianinazzi-Pearson, V. (1999). Genes involved in resistance to powdery mildew in barley differentially modulate root colonization by the mycorrhizal fungus Glomus mosseae. *Mycorrhiza* 9, 237–240. doi: 10.1007/s005720050273

Sarkar, D., Rovenich, H., Jeena, G., Nizam, S., Tissier, A., Balcke, G. U., et al. (2019). The inconspicuous gatekeeper: endophytic *Serendipita vermifera* acts as extended plant protection barrier in the rhizosphere. *New Phytol.* 224, 886–901. doi: 10.1111/nph.15904

Schäfer, P., Pfiffi, S., Voll, L. M., Zajic, D., Chandler, P. M., Waller, F., et al. (2009). Manipulation of plant innate immunity and gibberellin as factor of compatibility in the mutualistic association of barley roots with Piriformospora indica. *Plant J.* 59, 461–474. doi: 10.1111/j.1365-313X.2009.03887.x

Schmittgen, T. D., and Livak, K. J. (2008). Analyzing real-time PCR data by the comparative C(T) method. *Nat. Protoc.* 3, 1101–1108. doi: 10.1038/nprot.2008.73

Serfling, A., Wirsel, S. G., Lind, V., and Deising, H. B. (2007). Performance of the biocontrol fungus Piriformospora indica on wheat under greenhouse and field conditions. *Phytopathol* 97, 523–531. doi: 10.1094/PHYTO-97-4-0523

Shahollari, B., Varma, A., and Oelmuller, R. (2005). Expression of a receptor kinase in Arabidopsis roots is stimulated by the basidiomycete Piriformospora indica and the protein accumulates in Triton X-100 insoluble plasma membrane microdomains. *J. Plant Physiol.* 162, 945–958. 10.1016/j.jplph.2004.08.012

Sherameti, I., Shahollari, B., Venus, Y., Altschmied, L., Varma, A., and Oelmuller, R. (2005). The endophytic fungus Piriformospora indica stimulates the expression of nitrate reductase and the starch-degrading enzyme glucan-water dikinase in tobacco and Arabidopsis roots through a homeodomain transcription factor that binds to a conserved motif in their promoters. *J. Biol. Chem.* 280, 26241–26247. doi: 10.1074/jbc.M500447200

Sherameti, I., Tripathi, S., Varma, A., and Oelmuller, R. (2008). The root-colonizing endophyte Pirifomospora indica confers drought tolerance in Arabidopsis by stimulating the expression of drought stress-related genes in leaves. *Mol. Plant Microbe Interact.* 21, 799–807. doi: 10.1094/MPMI-21-6-0799

Skou, J. P., Jørgensen, J. H., and Lilholt, U. (1984). Comparative studies on callose formation in powdery mildew compatible and incompatible barley. *J. Phytopathol.* 109, 147–168. doi: 10.1111/j.1439-0434.1984.tb00702.x

Stein, E., Molitor, A., Kogel, K.-H., and Waller, F. (2008). Systemic resistance in Arabidopsis conferred by the mycorrhizal fungus Piriformospora indica requires jasmonic acid signaling and the cytoplasmic function of NPR1. *Plant Cell Physiol.* 49, 1747–1751. doi: 10.1093/pcp/pcn147

Svistoonoff, S., Hocher, V., and Gherbi, H. (2014). Actinorhizal root nodule symbioses: what is signalling telling on the origins of nodulation? *Curr. Opin. Plant Biol.* 20, 11–18. doi: 10.1016/j.pbi.2014.03.001

Thordal-Christensen, H., Zhang, Z., Yangdou, W., and Collinge, D. B. (1997). Subcellular localization of H2O2 in plants. H2O2 accumulation in papillae and hypersensitive response during barley-powdery mildew infection. *Plant J.* 11, 1187–1194. doi: 10.1046/j.1365-313X.1997.11061187.x

Torres, M. A., Jones, J. D., and Dangl, J. L. (2006). Reactive oxygen species signaling in response to pathogens. *Plant Physiol.* 141, 373–378. doi: 10.1104/pp.106.079467

Trouvelot, A., Kough, J., and Gianinazzi-Pearson, V. (1986). "Measuring the rate of VA mycorrhization of root systems. Research methods for estimating having a functional significance," in *Proceedings of the 1st European symposium on mycorrhizae: Physiological and genetical aspects of mycorrhizae*. Eds. V. Gianinazzi-Pearson and S. Gianinazzi (Dijon, Paris: INRA), 217–222.

van Schie, C. C., and Takken, F. L. (2014). Susceptibility genes 101: how to be a good host. *Annu. Rev. Phytopathol.* 52, 551–581. doi: 10.1146/annurev-phyto-102313-045854

Varma, A., Savita, V., Sudha,, Sahay, N., Butehorn, B., and Franken, P. (1999). Piriformospora indica, a cultivable plant-growth-promoting root endophyte. *Appl. Environ. Microbiol.* 65, 2741–, 2744.

Vigneron, N., Radhakrishnan, G. V., and Delaux, P. M. (2018). What have we learnt from studying the evolution of the arbuscular mycorrhizal symbiosis? *Curr. Opin. Plant Biol.* 44, 49–56. doi: 10.1016/j.pbi.2018.02.004

von Röpenack, E., Parr, A., and Schulze-Lefert, P. (1998). Structural analyses and dynamics of soluble and cell wall-bound phenolics in a broad spectrum resistance to the powdery mildew fungus in barley. *J. Biol. Chem.* 273, 9013–9022. doi: 10.1074/jbc.273.159013

Waller, F., Achatz, B., Baltruschat, H., Fodor, J., Becker, K., Fischer, M., et al. (2005). The endophytic fungus Piriformospora indica reprograms barley to salt-stress tolerance, disease resistance, and higher yield. *Proc. Natl. Acad. Sci. U.S.A.* 102, 13386–13391. doi: 10.1073/pnas.0504423102

Waller, F., Mukherjee, K., Deshmukh, S. D., Achatz, B., Sharma, M., Schäfer, P., et al. (2008). Systemic and local modulation of plant responses by Piriformospora indica and related Sebacinales species. *J. Plant Physiol.* 165, 60–70. doi: 10.1016/j.jplph.2007.05.017

Wang, Y., Cheng, X., Shan, Q., Zhang, Y., Liu, J., Gao, C., et al. (2014). Simultaneous editing of three homoeoalleles in hexaploid bread wheat confers heritable resistance to powdery mildew. *Nat. Biotechnol.* 32, 947–951. doi: 10.1038/nbt2969

Wang, J. Y., Haider, I., Jamil, M., Fiorilli, V., Saito, Y., Mi, J., et al. (2019). The apocarotenoid metabolite zaxinone regulates growth and strigolactone biosynthesis in rice. *Nat. Commun.* 10, 810. doi: 10.1038/s41467-019-08461-1

Weiss, M., Waller, F., Zuccaro, A., and Selosse, M. A. (2016). Sebacinales - one thousand and one interactions with land plants. *New Phytol.* 211, 20–40. doi: 10.1111/nph.13977

Wolter, M., Hollricher, K., Salamini, F., and Schulze-Lefert, P. (1993). The mlo resistance alleles to powdery mildew infection in barley trigger a developmentally controlled defence mimic phenotype. *Mol. Gen. Genet.* 239, 122–128. doi: 10.1007/bf00281610

Yadav, V., Kumar, M., Deep, D. K., Kumar, H., Sharma, R., Tripathi, T., et al. (2010). A phosphate transporter from the root endophytic fungus Piriformospora indica plays a role in phosphate transport to the host plant. *J. Biol. Chem.* 285, 26532–26544. doi: 10.1074/jbc.M110.111021

Yandell, B. S. (1997). Practical data analysis for designed experiments. (New York, NY: Chapman and Hall/CRC). doi: 10.1201/97802037425

Zeyen, R. J., Carver, T. L. W., and Lyngkjær, M. F. (2002). "Epidermal cell papillae," in *The powdery mildews: a comprehensive treatise*. Eds. R. R. Bélanger, W. R. Bushnell, A. J. Dik and T. L. W. Carver (St Paul, MN, USA: APS Press), 107–125.

Zuccaro, A., Lahrmann, U., Guldener, U., Langen, G., Pfiffi, S., Biedenkopf, D., et al. (2011). Endophytic life strategies decoded by genome and transcriptome analyses of the mutualistic root symbiont Piriformospora indica. *PloS Pathog.* 7, e1002290. doi: 10.1371/journal.ppat.1002290

Conflict of Interest: The authors declare that the research was conducted in the absence of any commercial or financial relationships that could be construed as a potential conflict of interest.

The reviewer [RP] declared providing the plant material for this research and confirms the absence of any other collaboration with the authors to the handling editor.

frontiers in Plant Science

METHODS
published: 26 February 2020
doi: 10.3389/fpls.2020.00063

A Flexible, Low-Cost Hydroponic Co-Cultivation System for Studying Arbuscular Mycorrhiza Symbiosis

Debatosh Das[1,2†‡], *Salar Torabi*[1,2‡], *Philipp Chapman*[2] *and Caroline Gutjahr*[1,2*]

[1] Faculty of Biology, Genetics, LMU Munich, Martinsried, Germany, [2] Plant Genetics, TUM School of Life Sciences Weihenstephan, Technical University of Munich (TUM), Freising, Germany

OPEN ACCESS

Edited by:
Andrea Genre, University of Turin, Italy

Reviewed by:
Didier Reinhardt, Université de Fribourg, Switzerland
Katsuharu Saito, Shinshu University, Japan

***Correspondence:**
Caroline Gutjahr
caroline.gutjahr@tum.de

†Present address:
Debatosh Das, Shenzhen Research Institute, The Chinese University of Hong Kong, Hong Kong, Hong Kong

‡*These authors have contributed equally to this work*

Specialty section:
This article was submitted to Plant Microbe Interactions, a section of the journal Frontiers in Plant Science

Received: *25 July 2019*
Accepted: *16 January 2020*
Published: *26 February 2020*

Citation:
Das D, Torabi S, Chapman P and Gutjahr C (2020) A Flexible, Low-Cost Hydroponic Co-Cultivation System for Studying Arbuscular Mycorrhiza Symbiosis. Front. Plant Sci. 11:63. doi: 10.3389/fpls.2020.00063

Arbuscular mycorrhiza (AM) is a widespread symbiosis between plant roots and fungi of the *Glomeromycotina*, which improves nutrient uptake by plants. The molecular mechanisms underlying development and function of the symbiosis are subject to increasing research activity. Since AM occurs in the soil, most studies targeting a molecular understanding of AM development and function, use solid substrates for co-cultivating plants and AM fungi. However, for some experiments very clean roots, highly controlled nutrient conditions or applications of defined concentrations of signaling molecules (such as hormones) or other small chemicals (such as synthetic inhibitors or signaling agonists) are needed. To this end, hydroponics has been widely used in research on mechanisms of plant nutrition and some hydroponic systems were developed for AM fungal spore amplification. Here, we present a hydroponics set-up, which can be successfully utilized for experimental root colonization assays. We established a "tip-wick" system based on pipette tips and rock wool wicks for co-cultivation of AM fungi with small model plants such as *Lotus japonicus*. A larger "Falcon-wick" system using Falcon tubes and rockwool wicks was developed for larger model plants such as rice. The hydroponic system can also be employed for growing *L. japonicus* hairy roots after transformation by *Agrobacterium rhizogenes*, thus circumventing the laborious cultivation on agar medium-containing Petri dishes during hairy root development. The tip-wick and Falcon-wick systems are easy to use and can be built with low cost, conventional and reusable lab plastic ware and a simple aquarium pump.

Keywords: hydroponics, hairy root transformation, rice, *Lotus japonicus*, arbuscular mycorrhiza

INTRODUCTION

The roots of most land plant species including prominent economic crops are colonized by beneficial soil fungi of the *Glomeromycotina* to form a symbiotic association called arbuscular mycorrhiza (AM) (Smith and Read, 2008). AM fungi (AMF) are obligate biotrophs and depend on sugar and fatty acid supply by the plant host, while plants benefit from improved mineral nutrition, especially with phosphate, better water retention and biotic, as well as abiotic stress tolerance (Smith and Smith, 2011; Roth and Paszkowski, 2017; Keymer and Gutjahr, 2018; Chen et al., 2018). Fossil evidence suggests that AM has evolved since plants conquered land more than 400 Mio years ago

(Remy et al., 1994), suggesting highly adapted genetic and metabolic pathways underlying regulation and function of this symbiosis (Delaux et al., 2015).

Root colonization by AM fungi comprises different steps that can be separated by plant mutants (Gutjahr and Parniske, 2013; MacLean et al., 2017; Choi et al., 2018). After an exchange of molecular signals between the root and the germinating fungal spore (Nadal and Paszkowski, 2013) the tips of growing hyphae attach to the root epidermis by so called hyphopodia. Then the hyphae penetrate the root epidermis and colonize the cortex. Fungal intraradical hyphae spread longitudinally in the root and form specialized highly branched tree-shaped structures, the arbuscules, inside cortical cells (Gutjahr and Parniske, 2013; MacLean et al., 2017; Choi et al., 2018). These arbuscules are surrounded by a plant derived peri-arbuscular membrane and the pair of arbuscule and arbuscule-containing cortex cell is thought to represent the main entity for nutrient exchange between fungus and plant (Luginbuehl and Oldroyd, 2017; Keymer and Gutjahr, 2018). At later stages of the symbiosis, some AM fungi (of the Glomeraceae family) also form vesicles, which are filled with lipids and nuclei and increased vesicle formation is often associated with a decline in the number of intact arbuscules (Kobae et al., 2016).

Although several plant genes required for arbuscular mycorrhiza development and function have been identified (Gutjahr and Parniske, 2013; MacLean et al., 2017; Choi et al., 2018), the interplay of their protein products and the molecular mechanisms regulating root colonization and symbiotic processes are poorly understood and are subject of active investigation.

Since field soil is difficult to wash off from roots and since it may contain numerous microorganisms, which influence the plant and each other, most studies aiming at a molecular understanding of AM development and function use inocula of single fungal isolates and make use of specialized substrates such as quartz sand, a mix of sand and vermiculite, sand and loam or sand and calcined clay. These substrates are more loosely attached to the roots and can be more easily washed off than field soil, although it can be still cumbersome to obtain very clean roots. Solid substrates can have a major disadvantage if the impact of chemical compounds such as hormones, inhibitors, signaling agonist or nutrients on AM development and function is to be examined, because chemicals and nutrients can be adsorbed to the surface of substrate particles or washed out, making it difficult to estimate the exact concentration, to which the roots are exposed. Hydroponic systems can be a solution to this problem. In hydroponics, roots are grown in liquid media, in which nutrient and chemical concentrations can be easily controlled. Furthermore, hydroponic culture provides very clean root material and in addition it represents a practical setup for collecting root exudates.

Hydroponic systems have been previously developed for AM symbiosis and most have been used for commercial inoculum production (reviewed in Ijdo et al., 2011). Several of these hydroponic setups involve growing plants in a solid-substrate for pre-colonization of roots by AMF and transfer to a hydroponics system after several weeks of co-culture (Hawkins and George, 1997; Lee and George, 2005; Utkhede, 2006). Such setups are labor intensive because an extra transfer step is required. Furthermore, they are not suitable for controlled time-course experiments (for example for harvesting colonized roots or root exudates at multiple time points after inoculation) because the growth conditions drastically change during the course of the experiment.

With the interest in studying the molecular mechanisms of AM development and function, we established a hydroponic culture system, in which plants are inoculated with fungal spores directly in the system. The system is easy to set up and requires only simple and general lab plasticware, available in molecular biology laboratories, and simple aquarium supplies. All plastic materials can be reused multiple times. For small plants such as the model legume *Lotus japonicus* we use 1 ml pipette tips and a rockwool wick (called "tip-wick") as a stable support for fungal inoculation and for guiding the inoculated roots into an aerated nutrient solution. For larger plants such as rice we use 50 ml Falcon tubes in the "Falcon-wick" setup. We show that in this system, roots are readily colonized by an AM fungus and express AM marker genes in a similar manner to roots colonized in pot cultures. Moreover, we demonstrate the suitability of the hydroponic system to study the impact of small molecules on root colonization and also to grow *L. japonicus* transgenic hairy roots after *Agrobacterium rhizogenes* transformation, requiring less work input than the classical protocol of growing hairy roots on Petri dishes.

MATERIALS AND METHODS

Set-Up of the Hydroponic Systems

For the basic tip-wick hydroponic setup, for small plants such as *L. japonicus*, the following components are needed: a tip-box for 200 µl pipette tips (TipOne® Pipette Tip System, StarLab, Germany), tip-rack for 1 ml pipette tips (TipOne® Pipette Tip System, StarLab, Germany), rockwool (Grodan, ROCKWOOL B.V., the Netherlands), which is wetted overnight in autoclaved water, 1 ml pipette-tips (e.g., TipOne® Pipette Tip System, StarLab, Germany), aluminum foil, and *L. japonicus* seedlings (**Figure 1**). All components can be re-used multiple times but should be washed, followed by steam autoclaving or sterilization with bleach and 70% ethanol before re-use. Only the rockwool, has to be used fresh each time.

To assemble the tip-wick system, the rack is first covered with aluminum foil to prevent light exposure of the roots and the medium, and to prevent growth of algae. Then, a bottom rockwool layer is inserted into the cut 1 ml pipette tips, such that half of it hangs to the outside and can act as a wick delivering liquid media to the plant. The tip-wick combinations are then placed into the holes of the 1 ml tip rack by pinching them through the aluminum foil layer. Five hundred spores per tip are then placed on top of each rockwool wick in a 100 µl volume of distilled water or nutrient solution. Then the seedlings are transplanted into the tips (one per pipette tip) by enclosing them into a coat of rockwool (rockwool top layer) and inserting them together with the rock wool into the empty upper half of the tip. We advise users to gently fit the rockwool layers into the

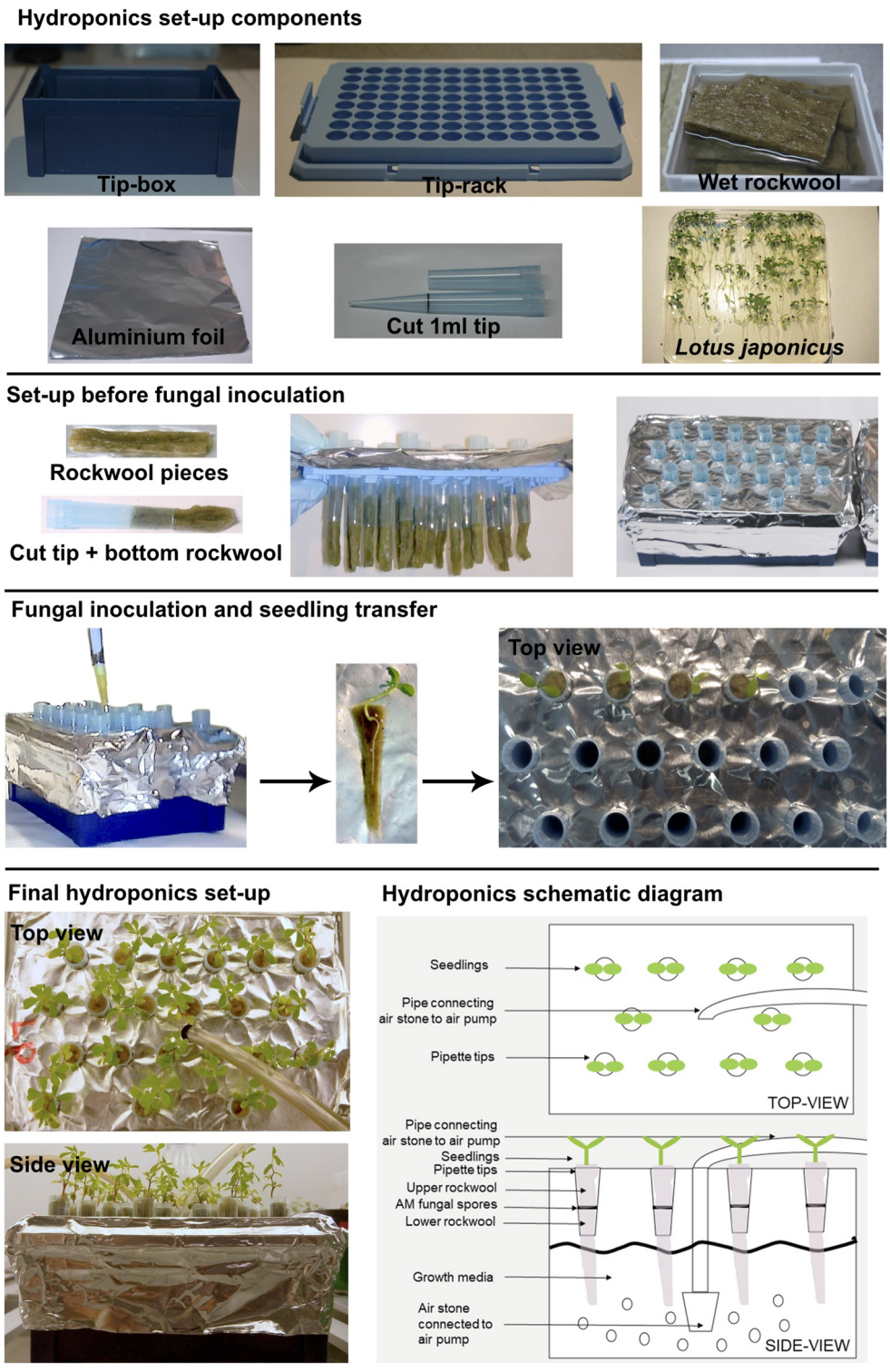

FIGURE 1 | Tip-wick hydroponics. Basic set-up for *Lotus japonicus*.

tip without twisting or turning it. Twisting and turning would make it excessively tight-fitted to the tip and may create anoxic conditions for the growing roots. We also advise users to put less than 15 *L. japonicus* seedlings per 200 µl tip box, as with higher densities the root systems entangle with each other as the roots grow bigger. The aeration tube is inserted in the middle of the tip-rack (**Figure 1**).

The Falcon-wick hydroponic system for bigger plants such as rice (**Figure 5**) is set up in a black 3-liter bucket with plastic lid (JET 30, JOKEY, USA). Six holes with diameter equal to the outer diameter of 50 ml Falcon tubes are drilled at equal distances in a circle into the lid. For planting and support of fungal spores cut Falcon tubes are stuffed with top and bottom rockwool layers: the fungal spores are pipetted onto the bottom layer and then the top layer gently enclosing a rice plant is inserted into the tube. Subsequently, the tubes are inserted into the holes of the bucket lid. The aeration tube is installed through a hole drilled into the side of the bucket above the water level (**Figure 5**). For aeration of both the tip-wick and the Falcon-wick system, a commercial membrane aquarium pump (for example Sera Air 550 R Plus, Germany) is connected with a tube (4/6 mm inner/outer diameter) to a cylindrically shaped air stone (20x30 mm) for the tip-wick and to a round air stone (80 x 15 mm) for the Falcon-wick system and is inserted into the tip-box or bucket as described above.

The hairy root hydroponics is built in a similar manner to the tip-wick system but with a modified lid and plant support. For the lid, a flat 200 µl tip-rack (epTIPS, Eppendorf, USA) is used (**Figure 4**), from which the two side-clips are removed such that it fits deeper into the container and lines up almost precisely with the height of the box. This is needed to ensure sufficient floating of the plants in liquid medium. Cuttings of the seedlings are surrounded by a small piece of pre-wetted rockwool, a cylinder-shaped piece of sponge or a cigarette filter (Filter Tips extra small, Swan, UK) with a recess, and placed into a hole of the inlay. Directly after placing the seedlings into the tip box, they are covered with the lid of the tip box to avoid drying. If the planting was done directly after transformation, the box is placed for 2 days in darkness. After these two days, the plants are placed into a 16/8 h day/night cycle; the lid of the tip box is removed and the box is placed into a growth tray and covered with the transparent lid of the tray to avoid drying of the shoots. After one to 2 weeks, when the seedlings start to develop roots and are adapted to the environment, the lid can be removed gradually or can remain throughout the experiment if the plants are sensitive. In this case, the lid is placed slightly shifted on the tray to allow some ventilation. After the co-cultivation step of 5 days in hydroponics or on Petri dishes, the nutrient solution is changed to a cefotaxime (330 µg/ml) containing solution and aerated with an air stone connected to an aquarium pump. The nutrient solution with cefotaxime is exchanged weekly. After 2 to 3 weeks the plants are screened for successful transformation and can be used for inoculation in pots with AMF or for other types of experiments. A starvation step before inoculation is not necessary because the phosphate concentration in half-Hoagland nutrient solution can be set to AM compatible levels. Moreover, since the plants are already adapted to the environment in the climate chamber, they do not need to be covered and are less stressed in comparison to the classical protocol where they are planted directly from the closed Petri dish to the open pots.

Plant Material and Growth Conditions

Seeds of *L. japonicus* ecotype Gifu B-129 and *Oryza sativa* ssp. *japonica* cv. Nipponbare were sterilized using a solution of 0.1% sodium dodecyl sulfate (SDS) and 5% Bleach and germinated on a 1% water-agar plate for 1–2 weeks before the plants were transplanted to the hydroponics set-up with 500 spores of *Rhizophagus irregularis* (strain DAOM 197198) (Agronutrition, Toulouse, France) or to pots filled with washed and autoclaved quartz-sand and inoculated with 500 spores of *R. irregularis* as described (Pimprikar et al., 2016). Plants were grown in a 16/8 h long day photoperiod with 24/22°C temperature cycles and 60% air humidity. The light intensity was 180 µM/m^2*s (Sylvania LUXLINE PLUS, T5, 39W, light color 830) for most experiments and 150 µM/m^2*s (Polyklima LEDs true daylight dual, with red channel at position 6 and blue channel at position 1) for the experiment shown in **Figure S1**. Half-Hoagland solution with 2.5 µM phosphate was used as growth medium for both tip-wick and Falcon-wick hydroponics with *L. japonicus* and rice, respectively and for *L. japonicus* pot experiments. For hairy root hydroponics Half-Hoagland solution with 25 µM phosphate was used (Hoagland and Arnon, 1950).

Gibberellin and Phosphate Treatment

GA_3 (Sigma-Aldrich, USA) was used to prepare a 50 mM stock solution in absolute ethanol. GA_3 was added directly to the growth media to a final concentration of 1 µM and the control was supplemented with equal amounts of solvent (0.002% ethanol, v/v). For testing the effect of different phosphate concentrations the Half-Hoagland solution was supplemented with 2.5 or 2,500 µM potassium phosphate. The concentration of potassium in the low phosphate medium was adjusted to 2,500 µM using potassium chloride.

Quantification of Root Colonization by *Rhizophagus irregularis*

Roots were harvested from hydroponics and stained with ink and vinegar (Vierheilig et al., 1998). Ink-stained roots were cut into 1 cm pieces and observed under a microscope at 200X magnification to score fungal structures using the magnified gridline-intersect method (McGonigle et al., 1990). Percent colonization is presented as: (number of intersections with fungal structures X 100)/total number of intersections.

Quantification of Transcript Accumulation

Harvested roots were snap frozen in liquid nitrogen and ground in liquid nitrogen. RNA was isolated from the tissue powder using the Spectrum™ Plant Total RNA Kit according to manufacturer's instructions (Sigma-Aldrich, USA). Subsequently, the RNA was treated with DNAse I-Amplification Grade (Sigma-Aldrich, USA), followed by verification of sufficient removal of genomic DNA contamination by PCR using primers exclusively targeting genomic DNA. The quality of extracted RNA was checked by running aliquots of each sample on an agarose gel and quantified using a

NanoDrop™ ND-1000 Spectrophotometer. One microgram of RNA for each sample was used for cDNA synthesis with SuperScript® III First-Strand Synthesis System (ThermoScientific). Primers for *L. japonicus SbtM1, BCP1, PT4,* and *UBIQUITIN* and rice *PT11*, *ARK* (*AM14*), and *CYCLOPHILLIN2* were previously described (Gutjahr et al., 2008; Pimprikar et al., 2016). Quantitative real-time RT-PCR was carried out using mi-real-time EvaGreen® Master Mix (Metabion, Martinsried, Germany), on a QuantStudio 3 Real-Time PCR system (Applied Biosystems, USA). Data were extracted using QuantStudio 3 Real-Time PCR Data Analysis Software and analyzed for normalized expression following the $2^{-\Delta\Delta CT}$ method (Livak and Schmittgen, 2001). The housekeeping genes *L. japonicus UBIQUITIN* and rice *CYCLOPHILLIN2* were used for normalization of gene expression values in the respective species.

Fresh Weight Quantification

Fresh weight of *L. japonicus* roots and rice roots and shoots were measured at 4 wpi and 7 wpi, respectively by weighing on an analytical balance.

Hairy Root Transformation

Hairy root transformation was conducted according to Okamoto et al. (2013). In short, hypocotyls of *L. japonicus* seedlings were dipped in *A. rhizogenes* AR1193 culture transformed with a plasmid carrying an mCherry marker driven by a *UBIQUITIN* promoter (called EV in Pimprikar et al., 2016). Before transformation, the seedlings were germinated for 3–4 days in darkness and for 2–3 days in 16/8 h light/dark cycles on 0.8% water agar plates. For infection, the seedlings were cut in the middle of the hypocotyl on a filter paper with *A. rhizogenes* suspension (containing the DNA construct). After transformation, the seedlings and bacteria were co-cultivated for 2 days in darkness and 3 days in 16/8 h light/dark cycles on Petri dishes containing Gamborg's B5 medium (Duchefa) without sucrose, to avoid overgrowth of the agrobacteria. Then they were transferred to Petri dishes containing Gamborg's B5 medium (Duchefa), 300 μg/ml cefotaxime, and 1% sucrose to inhibit bacterial growth and to develop hairy roots. For regeneration of hairy roots in hydroponics, the seedlings were transferred directly after the transformation or after the co-cultivation step to the hydroponic system containing half Hoagland solution without sucrose. After the co-cultivation step the growth media was supplemented with 300 μg/ml cefotaxime to inhibit bacterial growth. After 2–3 weeks, the root systems were screened for successfully transformed roots using the mCherry fluorescent transformation marker as described before (Pimprikar et al., 2016). The transformation efficiency was determined by calculating the percentage of plants with transformed roots among the total number of *A. rhizogenes* AR1193 infected plants.

Statistical Analysis and Data Display

Graphs were plotted and statistical tests were performed using Prism 6 software (GraphPad, USA).

RESULTS AND DISCUSSION

Tip-Wick Hydroponic Culture Is Suitable to Study Arbuscular Mycorrhiza Development

To understand whether arbuscular mycorrhiza can be studied using a simple hydroponic culture setup we established the tip-wick hydroponics with *L. japonicus* and the AM fungus *R. irregularis* as described in *Materials and Methods*. We compared root growth and colonization by *R. irregularis* between plants grown in hydroponics and in commonly used pots with sand as growth substrate. Due to evaporation, the tip-wick system required around 200 ml of nutrient solution per week for 12–15 plants, while pots were supplemented with 30 ml of media three times per week for 6–9 plants per pot. No significant difference in total root colonization was observed between plants grown in tip-wick hydroponics or sand pots (**Figure 2A**). However, the plants grown in hydroponics had on average a 20% larger root biomass (**Figure 2B**).

Based on the set up of the tip-wick hydroponic system, AM is assumed to develop first in the rockwool layer inside the tip and the fungus should then grow toward the part of the roots, which float free in the nutrient solution. The speed, with which the whole root length is colonized may depend on the oxygen conditions inside the solution and therefore, possibly on the position of a plant relative to the air stone. To examine this, we recorded the spatiotemporal development of AM inside *L. japonicus* roots grown at two different distances to the air stone in the hydroponic setup (**Figure S1A**). To this end we shifted the air stone to the side and harvested the root from positions close to and far from the air stone at 5, 6, and 7 weeks post-inoculation (wpi). Furthermore, we separated the part of the root system growing inside the tip rockwool (tip-roots) from the roots growing outside of the tip and the rockwool (free-roots) (**Figure S1A**). As expected, the colonization inside the tip proceeded faster and reached a plateau at 6 wpi, whereas the colonization in the free roots lagged behind (**Figure S1B**). However, apart from hyphae travelling inside the root, the free roots could also be colonized from the outside from extraradical mycelium in the liquid, as we detected several successful hyphopodia on free roots (**Figure S1C**). The position relative to the air stone also had an effect on colonization, with roots close to the airstone being slightly more strongly colonized than those far from the airstone. However, inside the tip this effect was only significant for arbuscules at 5 wpi and for vesicles at 7 wpi. The strongest effect of the vicinity to the air stone was observed in the free roots at 7 wpi, since between 5 and 7 wpi colonization hardly increased in this part of the root systems (**Figure S1B**). This shows the importance of aeration for efficient colonization of especially the roots growing outside of the rockwool. Thus, the distance to the air stone should be considered when setting up AM experiments in hydroponics. If root length colonization is to be precisely compared across several containers, roots at same positions relative to the air stone should be directly compared. However, for treatments with strong effects, the impact of vicinity to the airstone does not appear to be critical (see **Figure 3**).

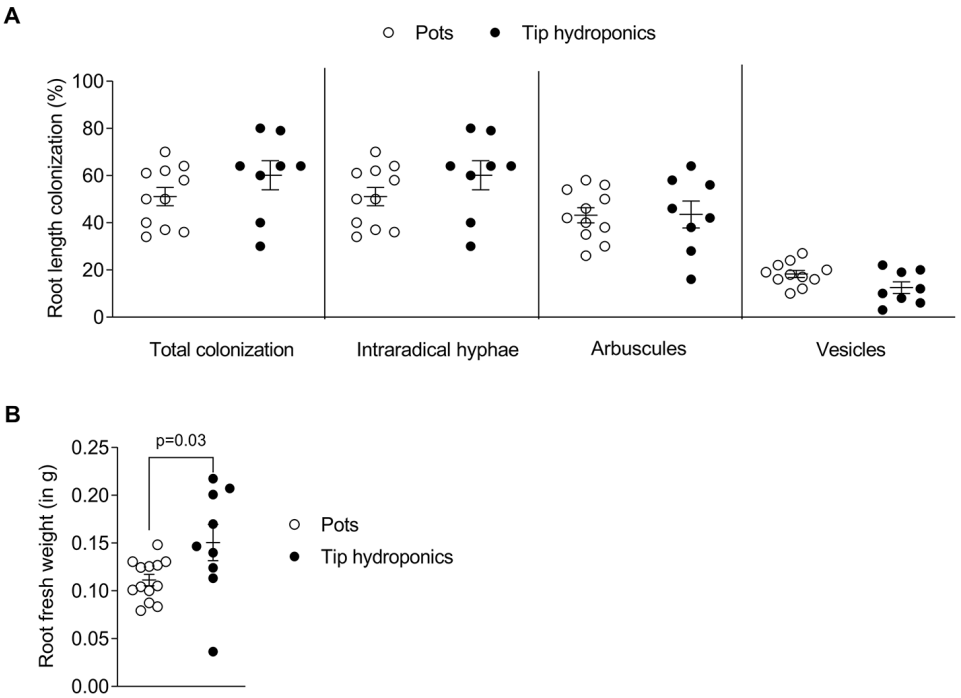

FIGURE 2 | Root length colonization after growth in sand-filled pots *vs*. tip-wick hydroponics. Comparison of **(A)** percent colonization of *Lotus japonicus* roots with *Rhizophagus irregularis* and **(B)** *L. japonicus* root fresh weight in sand-filled pot *vs*. tip-wick hydroponics at 4 weeks post-inoculation (wpi). Mann-Whitney tests were used for statistical comparison (n = 8–15 separate plants from one tip-box or two independent pots).

Gibberellin Treatment Suppresses Root Colonization in Hydroponic Culture

Gibberellins (GAs) are important plant hormones and well-known regulators of plant growth (Tanimoto, 2005). GA also plays a role in AM symbiosis (Floss et al., 2013) and application of active GA (GA_3) inhibits root colonization by AM fungi in pot grown *L. japonicus*, *Medicago truncatula*, pea, and rice (Floss et al., 2013; Takeda et al., 2015; Pimprikar et al., 2016; Yu et al., 2014; El Ghachtouli et al., 1996). To examine whether tip-wick hydroponics can be used for studying the impact of exogenously applied chemicals on AM symbiosis, we ran a proof of concept experiment and treated *L. japonicus* seedlings in this system with 1 μM GA_3 or solvent as a control (without considering the position of plants relative to the air stone). As expected, GA_3 stimulated the growth of *L. japonicus* and we observed a larger root systems and elongated shoots (**Figure 3A**). Simultaneously GA_3 strongly inhibited root colonization by *R. irregularis* (**Figures 3B, C**). The inhibition of root colonization by GA_3 was also reflected at the transcriptional level as previously described (Pimprikar et al., 2016): transcripts of the well-established AM marker genes *SbtM1*, *PT4*, and *BCP1* accumulated to high levels in colonized hydroponically growth roots, but were not activated in GA_3-treated roots in spite of inoculation with *R. irregularis* (**Figure 3D**). High phosphate supply is known to trigger the plant to suppress AM development (Breuillin et al., 2010; Balzergue et al., 2011). We examined whether this was also possible in hydroponics. Indeed, 2500 μM phosphate in the liquid medium lead to a suppression of root length colonization by approximately 40% as compared to 2.5 μM phosphate in the medium (**Figure S2**). Thus, we demonstrate that tip-wick hydroponics can be successfully used for pharmacological or nutrient assays targeted to understand the molecular functioning of AM symbiosis.

Growth of *Lotus japonicus* Hairy Roots in Hydroponic Culture

In *L. japonicus* the generation of stable transgenic lines takes about 1 year. Therefore, hairy root transformation is a commonly used technique in root symbiosis research on model legumes to generate transgenic roots for experimental use (e.g., to study promoter activity with reporter constructs, or to express tagged proteins) in a shorter period of time (Boisson-Dernièr et al., 2001). After dipping seedling hypocotyls into *A. rhizogenes* solution it takes 2 weeks until hairy roots of 2–5 cm develop (Okamoto et al., 2013). Depending on the purpose of the experiment or the plant genotype, the time to grow hairy roots with a usable size can take even longer. Hairy root cultures of *L. japonicus* require intense care because the plants need to be frequently moved to fresh medium with antibiotics to avoid regrowth of agrobacteria. Before inoculation with AM fungi, all transformed plants need to have a well-developed root system

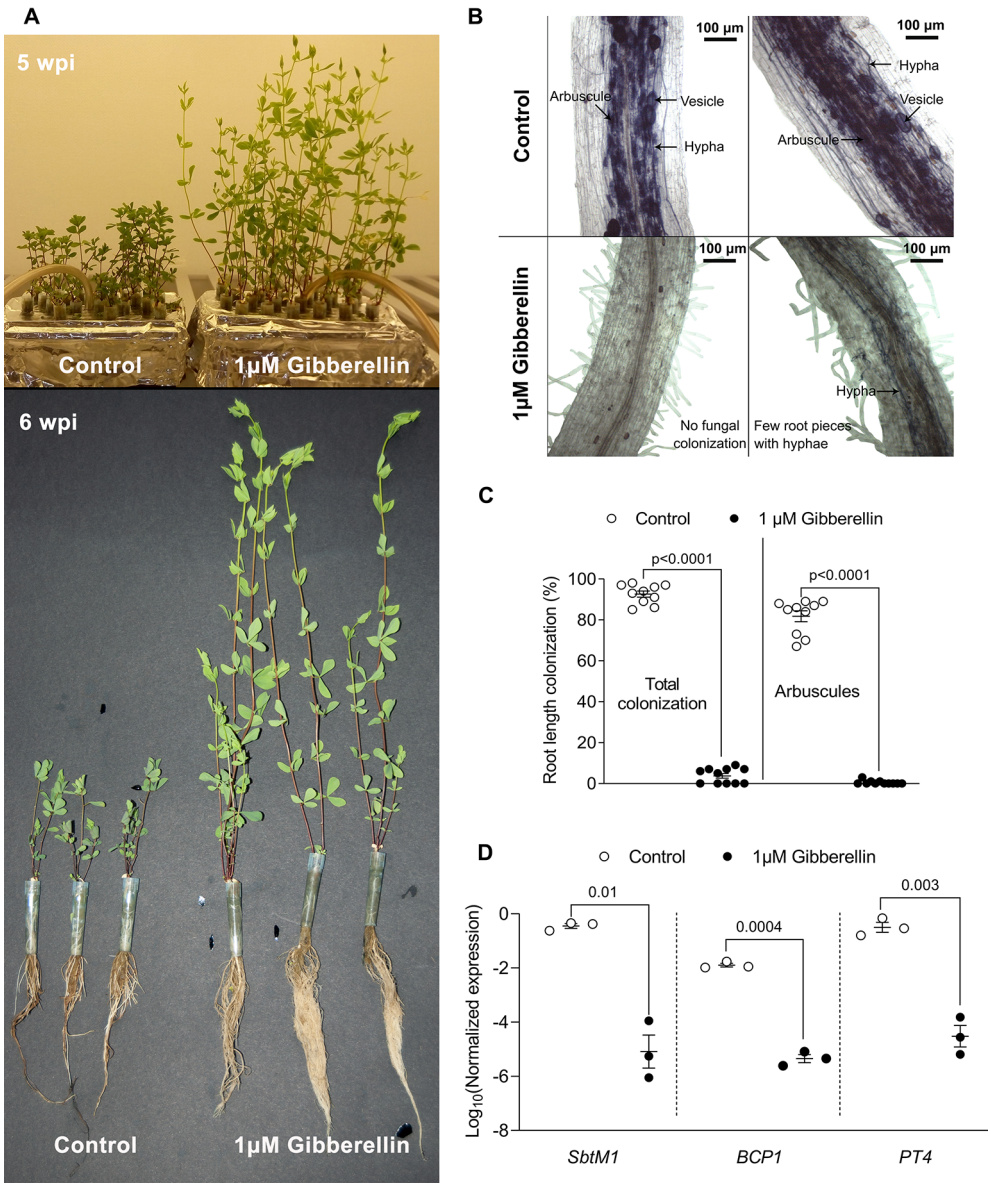

FIGURE 3 | Pharmacological assay in tip-wick hydroponics. **(A)** Effect of 1 µM gibberellin treatment on *Lotus japonicus* growth in tip-wick hydroponics; **(B)** 1 µM gibberellin suppresses root colonization by *Rhizophagus irregularis*. The fungus inside the roots was stained with acid ink. **(C)** Effect of 1 µM gibberellin on percent root length colonization by *R. irregularis* (statistical analysis: Mann-Whitney test, n = 10 separate plants in one tip-box). **(D)** Effect of 1 µM gibberellin on AM marker gene expression (statistics: t-test with Welch's correction, n = 3 consisting of a pool of two root systems each, with the six plants grown in one tip-box). For all analyses, plants were harvested at 6 wpi.

and additionally, the plants need to be starved on low phosphate containing medium for two more weeks before planting them into the pot together with the AM fungus. This means that even with optimal hairy root development, the tissue culture time after transformation can take 4 weeks and more and the plants need to be shifted up to four times to new Petri dishes, which consumes time, plastic ware, and chemicals. We found that, if tissue culture grade sterility of the generated hairy roots is not necessary, the tissue culture steps after transformation can be avoided by growing the hairy roots in hydroponic culture (**Figure 4**).

Directly after transformation, the seedlings can be transferred to the hydroponic system for growth of hairy roots without a decrease in transformation efficiency and with a minimal impact on the survival rate, as compared to a later transfer during root regeneration (**Table 1**). This has the advantage that the transformation does not require tissue culture conditions

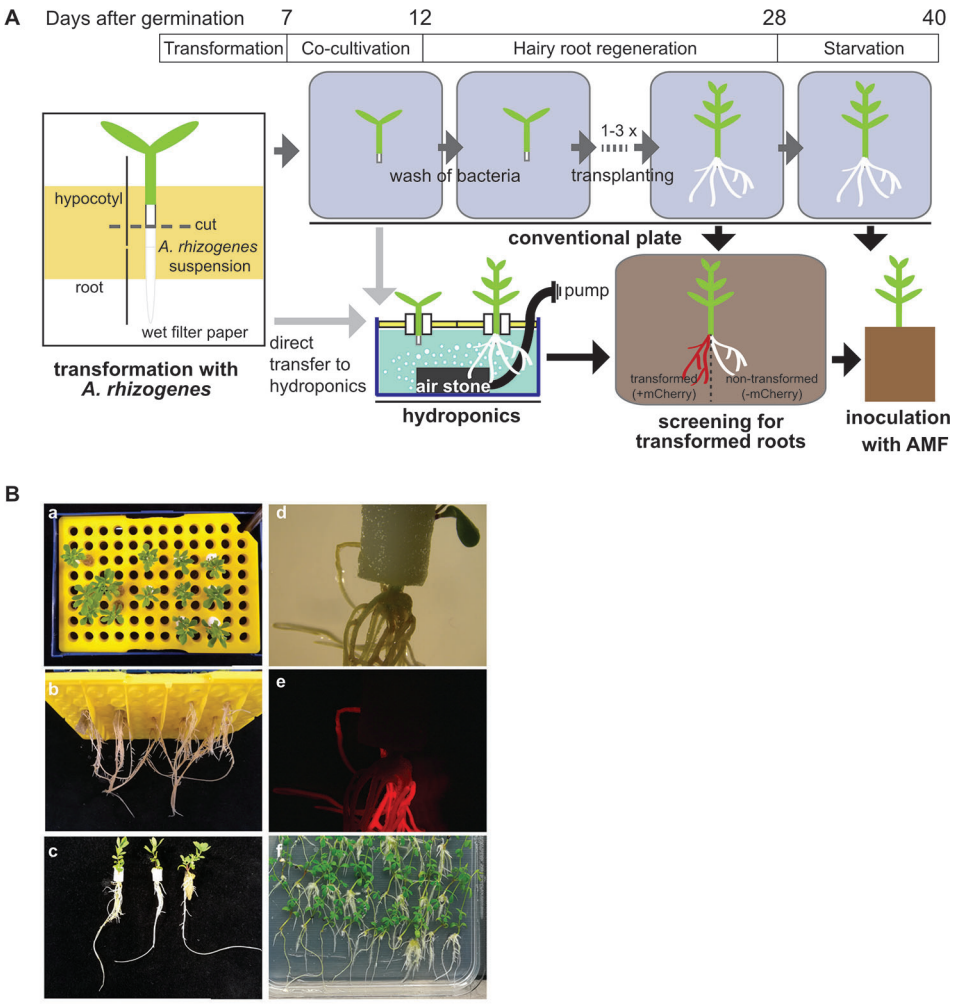

FIGURE 4 | Generation of hairy roots in tip hydroponics. **(A)** Schematic representation of hairy root growth using tip-wick hydroponics. **(B)** Images of mCherry transformed hairy roots of *Lotus japonicus* at 4 weeks post-transformation: (a–c) top, bottom and side view of seedlings grown in hydroponics. Scale bar: 20 mm; (d, e) bright field and fluorescence image of hairy roots generated in hydroponics expressing mCherry as a transformation marker, scale bar: 5 mm; 6. (f) Hairy roots of the same transformation experiment cultivated in square Petri dishes.

TABLE 1 | *Lotus japonicus* hairy root transformation efficiency and plant survival after growth in hydroponic culture.

Transformation	Transfer to hydroponics after	Plant survival in hydroponics [%]	Transformation efficiency after growth in hydroponics [%]	Transformation efficiency after growth on Petri dishes [%]
1	Dipping	70	80	75
2	Dipping	75	60	45
3	Co-cultivation	80	50	55
4	Co-cultivation	85	100	60

Out of four independent transformations with 50 seedlings each, 20 seedlings per experiment were transferred to hydroponics directly after dipping into Agrobacterium rhizogenes *solution and 20 seedlings after the 5 days of co-cultivation with* A. rhizogenes. *Transformation efficiency and plant survival were compared to the classical hairy root transformation method with root regeneration on Petri dishes.*

(clean bench) but can be performed on a clean laboratory bench. However, if many lines are transformed and the work-intensive transformation process shall be split from the transfer to the hydroponic culture among different days, we recommend to perform the transformation and the co-cultivation step under tissue culture conditions using Petri dishes at the clean bench and to transfer to hydroponics the 5 days of co-culture with *A. rhizogenes*.

Falcon-Wick Hydroponics for Colonization of Rice Roots by Arbuscular Mycorrhiza Fungi

We also developed a Falcon-wick hydroponics system for larger AM model plants. We choose the important crop and model plant rice, because it currently represents the prime monocots model for studying molecular mechanisms of mycorrhizal colonization (Nakagawa and Imaizumi-Anraku, 2015). We grew rice in a bigger hydroponics system using Falcon tubes instead of pipette tips as a support (Falcon-wick system, **Figure 5**).

Rice was grown with and without aeration in hydroponics to test, if aeration promotes AM colonization, as it has been observed that rice displays a low AM colonization level in submerged paddy fields (Solaiman and Hirata, 1995; Vallino et al., 2014). In both conditions, roots and shoots grew a similar biomass (**Figure S3**). *R. irregularis* colonized the roots under both conditions without being morphologically affected (**Figure 6A**). Root length colonization under aerated conditions reached about 40% at 7 wpi, similar to colonization levels observed in sand culture in ConeTainers® (Gutjahr et al., 2008). Under non-aerated conditions, root length colonization was lower and reached about 20% (**Figures 6B, C**). We also examined whether the AM-marker genes *PT11* and *ARK* (Gutjahr et al., 2008; Yang et al., 2012; Roth et al., 2018) are normally expressed in hydroponics. Their transcripts accumulated to high levels in colonized roots as compared to non-colonized roots and their transcript accumulation was slightly affected by aeration (**Figure 6C**). Thus, colonization of rice roots appears to function normally at a molecular level in hydroponics. However, for efficient root colonization of rice in the Falcon-wick system aeration is recommended.

CONCLUSION

Here we show that the tip-wick and Falcon-wick hydroponics are practical and easy-to-use setups to study AM, especially when experiments require precise application of chemical compounds or nutrients or very clean root material. Another advantage of hydroponics is that the root growth can be visually monitored in a non-destructive manner, as compared to pot-based growth, because the roots can be repeatedly taken out of the solution and observed. Thus, if required, root growth can be measured repeatedly, which is not possible in pot culture with solid substrates.

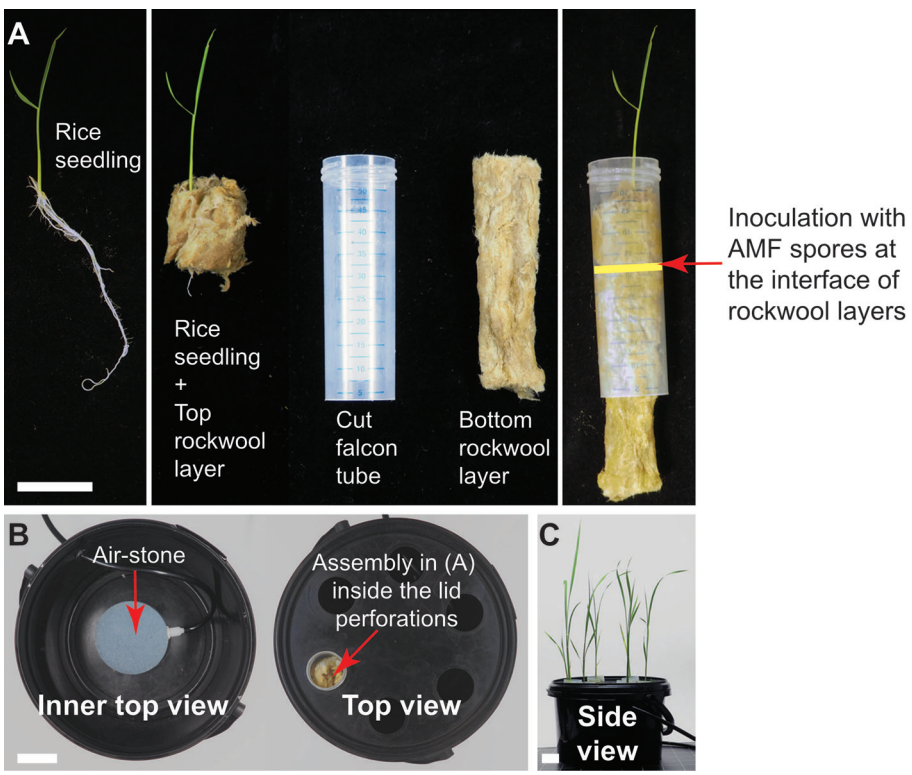

FIGURE 5 | Falcon-wick hydroponics for arbuscular mycorrhiza (AM) of bigger plants such as rice. **(A)** Twelve-day old rice seedling prepared for inoculation with AM fungi (AMF) in hydroponics. Arrow indicates the interface of the two rockwool layers where the AMF spores are placed. **(B)** Top view of the hydroponics set-up in the black bucket. **(C)** Rice growing in hydroponics at 3 wpi. All scale bars: 3 cm.

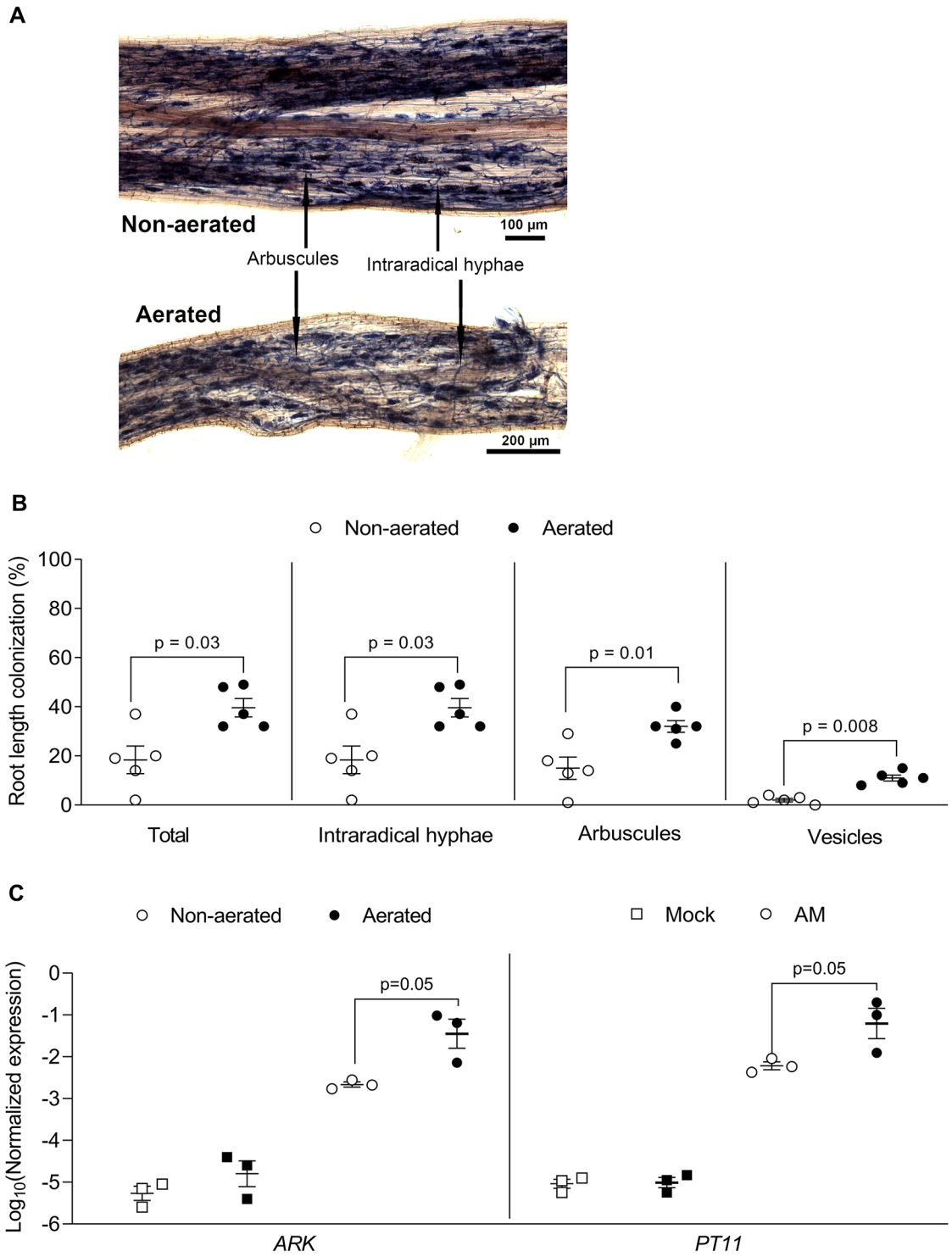

FIGURE 6 | Rice root colonization with *Rhizophagus irregularis* in falcon-wick hydroponics. Rice plants were inoculated with *R. irregularis* and grown in hydroponics for 7 weeks before harvest and analysis. **(A)** Representative images of rice roots colonized with *R. irregularis* and grown in non-aerated and aerated hydroponics. **(B)** Percent root length colonization for different arbuscular mycorrhiza fungi (AMF) structures in rice roots grown in non-aerated and aerated hydroponics (statistics: Mann-Whitney test, n = 5 separate plants grown in one bucket). **(C)** Effect of aeration on AM marker gene expression as determined by quantitative PCR (qPCR). The expression value was of *ARK* and *PT11* was normalized to the expression value of the constitutively expressed gene *CYCLOPHILLIN2* (statistics: Mann-Whitney test, n = 3 independent root systems per treatment).

DATA AVAILABILITY STATEMENT

All datasets generated for this study are included in the article/ **Supplementary Material**.

AUTHOR CONTRIBUTIONS

DD, ST, and CG designed experiments and wrote the manuscript. DD performed all experiments displayed in the manuscript except hairy root transformation, **Figure 6C** and **Figure S1**. ST had the first idea of setting up hydroponics for AM, established both hydroponics systems for AM, for hairy root transformation and performed hairy root transformation as well as experiments for **Figure 6C**. PC performed the experiment for **Figure S1** with help from ST. DD and ST analyzed data with inputs from CG. CG acquired funding.

ACKNOWLEDGMENTS

We thank Antonia Babl for excellent assistance and Dr. Elaine Yeung, Utrecht University for a kind donation of rice seeds. The study was supported by the Emmy Noether program (GU1423/ 1-1) of the Deutsche Forschungsgemeinschaft (DFG) and a grant of Valent BioSciences LLC to CG. The funders had no role or influence in the design of the work. Publication of this work was supported by the German Research Foundation (DFG) and the Technical University of Munich (TUM) in the framework of the Open Access Publishing Program.

SUPPLEMENTARY MATERIAL

The Supplementary Material for this article can be found online at: https://www.frontiersin.org/articles/10.3389/fpls.2020.00063/full#supplementary-material

FIGURE S1 | Spatiotemporal AM colonization in tip-wick hydroponics. (**A**) Experimental set-up to examine the effect of distance to the air stone (c, close; f, far) and position in the root (tip or free) on AM colonization in *L. japonicus* seedlings. (**B**) *L. japonicus* root length colonization by *R. irregularis* at 5, 6, and 7 wpi inside the tip or in free-floating roots, close (open circles) or far (black circles) from the air stone (statistics: Mann-Whitney test, n = 3 separate plants from the three independent tip-boxes). (**C**) Free-floating root length (left) and number of hyphopodia in free-floating root length (right) indicating that the fungus can re-colonize the root from the outside below the rock wool (n = 3 separate plants from three independent tip-boxes). Indications of centimeters on the y-axis refer to root segments below the rock wool. Less than three open or closed circles indicate that not all root systems were long enough to contribute a segment in the indicated category.

FIGURE S2 | High phosphate mediated inhibition of root colonization in tip-wick hydroponics. Effect of 2.5 μM and 2500 μM phosphate on percent root length colonization in *L. japonicus* by *R. irregularis* at 6 wpi (statistical analysis: Mann-Whitney test, n = 9 separate plants from one tip-box).

FIGURE S3 | Rice growth in co-culture with *R. irregularis* in Falcon-wick hydroponics. (**A**) Rice plants grown in non-aerated (left) or aerated (right) hydroponics. (**B**) Root and shoot fresh weights for rice plants grown in non-aerated and aerated hydroponics (statistics: Mann-Whitney test, n = 5 separate plants from one bucket).

REFERENCES

Balzergue, C., Puech-Pages, V., Bécard, G., and Rochange, S. F. (2011). The regulation of arbuscular mycorrhizal symbiosis by phosphate in pea involves early and systemic signalling events. *J. Exp. Bot.* 62, 1049–1060. doi: 10.1093/jxb/erq335

Boisson-Dernièr, A., Chabaud, M., Garcia, F., Bécard, G., Rosenberg, C., and Barker, D. (2001). *Agrobacterium rhizogenes*-transformed roots of *Medicago truncatula* for the study of nitrogen-fixing and endomycorrhizal symbiotic associations. *Mol. Plant-Microbe Interact.* 14, 695–700. doi: 10.1094/MPMI.2001.14.6.695

Breuillin, F., Schramm, J., Hajirezaei, M., Ahkami, A., Favre, P., Druege, U., et al. (2010). Phosphate systemically inhibits arbuscular mycorrhiza development in *Petunia hybrida* and represses genes involved in mycorrhizal functioning. *Plant J.* 64, 1002–1017. doi: 10.1111/j.1365-313X.2010.04385.x

Breuillin-Sessoms, F., Floss, D. S., Gomez, S. K., Pumplin, N., Ding, Y., Levesque-Tremblay, V., et al. (2015). Suppression of arbuscule degeneration in *Medicago truncatula phosphate transporter4* mutants is dependent on the ammonium transporter 2 family protein AMT2; 3. *Plant Cell* 27, 1352–1366. doi: 10.1105/tpc.114.131144

Carbonnel, S., and Gutjahr, C. (2014). Control of arbuscular mycorrhiza development by nutrient signals. *Front. In Plant Sci.* 5, 462. doi: 10.3389/fpls.2014.00462

Chen, M., Arato, M., Borghi, L., Nouri, E., and Reinhardt, D. (2018). Beneficial services of arbuscular mycorrhizal fungi. – From ecology to application. *Front. Plant Sci.* 9. doi: 10.3389/fpls.2018.01270

Choi, J., Summers, W., and Paszkowski, U. (2018). Mechanisms underlying establishment of arbuscular mycorrhizal symbioses. *Annu. Rev. Phytopathol.* 56, 135–160. doi: 10.1146/annurev-phyto-080516-035521

Delaux, P. M., Radhakrishnan, G. V., Jayaraman, D., Cheema, J., Malbreil, M., Volkening, J. D., et al. (2015). Algal ancestor of land plants was preadapted for symbiosis. *Proc. Natl. Acad. Sci.* 112, 13390–13395. doi: 10.1073/pnas.1515426112

Diaz, C. L., Gronlund, M., Schlamann, H. L. M., and Spaink, H. P. (2005). "Induction of hairy roots for symbiotic gene expression studies," in *Lotus japonicus handbook*. Eds. A. J. Marquez, J. Stougaard, M. Udvardi, M. Parniske, H. P. Spaink, G. Saalbach, J. Webb and M. Chiurazzi (The Netherlands: Springer), 261–277. doi: 10.1007/1-4020-3735-X

El Ghachtouli, N., Martin-Tanguy, J., Paynot, M., and Gianinazzi, S. (1996). First-report of the inhibition of arbuscular mycorrhizal infection of Pisum sativum by specific and irreversible inhibition of polyamine biosynthesis or by gibberellic acid treatment. *FEBS Lett.* 385 (3), 189–192. doi: 10.1016/0014-5793(96)00379-1

Floss, D. S., Levy, J. G., Lévesque-Tremblay, V., Pumplin, N., and Harrison, M. J. (2013). DELLA proteins regulate arbuscule formation in arbuscular mycorrhizal symbiosis. *Proc. Natl. Acad. Sci. U. S. A.* 110, E5025–E5034. doi: 10.1073/pnas.1308973110

Gutjahr, C., and Parniske, M. (2013). Cell and developmental biology of arbuscular mycorrhiza symbiosis. *Annu. Rev. Cell Dev. Biol.* 29, 593–617. doi: 10.1146/annurev-cellbio-101512-122413

Gutjahr, C., Banba, M., Croset, V., An, K., Miyao, A., An, G., et al. (2008). Arbusuclar mycorrhiza-specific signalling in rice transcends the common symbiosis pathway. *Plant Cell* 20, 2989–3005. doi: 10.1105/tpc.108.062414

Hawkins, H. J., and George, E. (1997). Hydroponic culture of the mycorrhizal fungus *Glomus mosseae* with *Linum usitatissimum* L., *Sorghum bicolor* L. and *Triticum aestivum* L. *Plant Soil* 196, 143–149. doi: 10.1023/A:1004271417469

Hoagland, and Arnon. (1950). The water-culture method for growing plants without soil. (Berkeley, CA: University of California, College of Agriculture, Agricultural Experiment Station)

Ijdo, M., Cranenbrouck, S., and Declerck, S. (2011). Methods for large-scale production of AM fungi: past, present, and future. *Mycorrhiza* 21, 1–16. doi: 10.1007/s00572-010-0337-z

Keymer, A., and Gutjahr, C. (2018). Cross-kingdom lipid transfer in arbuscular mycorrhiza symbiosis and beyond. *Curr. Opin. Plant Biol.* 44, 137–144. doi: 10.1016/j.pbi.2018.04.005

Kobae, Y., Ohmori, Y., Saito, C., Yano, K., Ohtomo, R., and Fujiwara, T. (2016). Phosphate treatment strongly inhibits new arbuscule development but not the maintenance of arbuscule in mycorrhizal rice roots. *Plant Physiol.* 171, 566–579. doi: 10.1104/pp.16.00127

Lee, Y. J., and George, E. (2005). Development of a nutrient film technique culture system for arbuscular mycorrhizal plants. *HortScience* 40 (2), 378–380. doi: 10.21273/HORTSCI.40.2.378

Livak, K. J., and Schmittgen, T. D. (2001). Analysis of relative gene expression data using real-time quantitative PCR and the $2^{-\Delta\Delta CT}$ method. *Methods* 25, 402–408. doi: 10.1006/meth.2001.1262

Luginbuehl, L. H., and Oldroyd, G. E. (2017). Understanding the arbuscule at the heart of endomycorrhizal symbioses in plants. *Curr. Biol.* 27, R952–R963. doi: 10.1016/j.cub.2017.06.042

MacLean, A. M., Bravo, A., and Harrison, M. J. (2017). Plant signaling and metabolic pathways enabling arbuscular mycorrhizal symbiosis. *Plant Cell* 29, 2319–2335. doi: 10.1105/tpc.17.00555

McGonigle, T., Miller, M., Evans, D., Fairchild, G., and Swan, J. (1990). A new method which gives an objective measure of colonization of roots by vesicular-arbuscular mycorrhizal fungi. *New Phytol.* 115, 495–501

Nadal, M., and Paszkowski, U. (2013). Polyphony in the rhizosphere: presymbiotic communication in arbuscular mycorrhizal symbiosis. *Curr. Opin. In Plant Biol.* 16, 473–479. doi: 10.1016/j.pbi.2013.06.005

Nakagawa, T., and Imaizumi-Anraku, H. (2015). Rice arbuscular mycorrhiza as a tool to study the molecular mechanisms of fungal symbiosis and a potential target to increase productivity. *Rice* 8, 32. doi: 10.1186/s12284-015-0067-0

Okamoto, S., Yoro, E., Suzaki, T., and Kawaguchi, M. (2013). Hairy root transformation in. *Lotus japonicus. BioProtocol* 3 (12), e795. doi: 10.21769/BioProtoc.795

Pimprikar, P., Carbonnel, S., Paries, M., Katzer, K., Klingl, V., et al. (2016). A CCaMK-CYCLOPS-DELLA complex activates transcription of *RAM1* to regulate arbuscule branching. *Curr. Biol.* 26, 987–998. doi: 10.1016/j.cub.2016.01.069

Remy, W., Taylor, T. N., Hass, H., and Kerp, H. (1994). Four hundred-million year-old vesicular arbuscular mycorrhizae. *Proc. Natl. Acad. Sci. U. S. A.* 91, 11841–11843. doi: 10.1073/pnas.91.25.11841

Roth, R., and Paszkowski, U. (2017). Plant carbon nourishment of arbuscular mycorrhizal fungi. *Curr. Opin. Plant Biol.* 39, 50–56. doi: 10.1016/j.pbi.2017.05.008

Roth, R., Chiappello, M., Montero, H., Gehring, P., Grossmann, J., O'Holleran, K., et al. (2018). A serine-threonine receptor-like kinase regulates arbuscular mycorrhiza symbiosis at the peri-arbuscular membrane. *Nat. Commun.* 9, 4677. doi: 10.1038/s41467-018-06865-z

Smith, S. E., and Read, D. J. (2008). *Mycorrhizal symbiosis* (London: Academic: Academic press). doi: 10.1016/B978-0-12-370526-6.X5001-6

Smith, S. E., and Smith, F. A. (2011). Roles of arbuscular mycorrhizas in plant nutrition and growth: new paradigms from cellular to ecosystem scales. *Annu. Rev. Plant Biol.* 62, 227–250. doi: 10.1146/annurev-arplant-042110-103846

Solaiman, M. Z., and Hirata, H. (1995). Effects of indigenous arbuscular mycorrhizal fungi in paddy fields on rice growth and N, P, K nutrition under different water regimes. *Soil Sci. Plant Nutr.* 41, 505–514. doi: 10.1080/00380768.1995.10419612

Takeda, N., Handa, Y., Tsuzuki, S., Kojima, M., Sakakibara, H., and Kawaguchi, M. (2015). Gibberellins interfere with symbiosis signalling and gene expression and alter colonization by arbuscular mycorrhizal fungi in *Lotus japonicus*. *Plant Physiol.* 167, 545–557. doi: 10.1104/pp.114.247700

Tanimoto, E. (2005). Regulation of root growth by plant hormones—roles for auxin and gibberellin. *Crit. Rev. Plant Sci.* 24, 249–265. doi: 10.1080/07352680500196108

Utkhede, R. (2006). Increased growth and yield of hydroponically grown greenhouse tomato plants inoculated with arbuscular mycorrhizal fungi and *Fusarium oxysporum* f. sp. radicis-lycopersici. *Biocontrol* 51, 393–400. doi: 10.1007/s10526-005-4243-9

Vallino, M., Fiorilli, V., and Bonfante, P. (2014). Rice flooding negatively impacts root branching and arbuscular mycorrhizal colonization, but not fungal viability. *Plant Cell Environ.* 37, 557–572. doi: 10.1111/pce.12177

Vierheilig, H., Coughlan, A. P., Wyss, U., and Pich, Y. (1998). Ink and vinegar, a simple staining technique for arbuscular-mycorrhizal fungi. *Appl. Environ. Microbiol.* 64, 5004–5007

Yang, S. Y., Gronlund, M., Jakobsen, I., Grotemeyer, M. S., Rentsch, D., Miyao, A., et al. (2012). Non-redundant regulation of rice arbuscular mycorrhiza by two members of the phosphate transporter 1 gene family. *Plant Cell* 24, 4236–4251. doi: 10.1105/tpc.112.104901

Yu, N., Luo, D., Zhang, X., Liu, J., Wang, W., Jin, Y., et al (2014). A DELLA protein complex controls the arbuscular mycorrhizal symbiosis in plants. *Cell Res.* 24, 130–133.

Conflict of Interest: The authors declare that the research was conducted in the absence of any commercial or financial relationships that could be construed as a potential conflict of interest.

frontiers in Plant Science

ORIGINAL RESEARCH
published: 03 April 2020
doi: 10.3389/fpls.2020.00354

SNARE Complexity in Arbuscular Mycorrhizal Symbiosis

*Rik Huisman, Jan Hontelez, Ton Bisseling and Erik Limpens**

Department of Plant Sciences, Laboratory of Molecular Biology, Wageningen University & Research, Wageningen, Netherlands

How cells control the proper delivery of vesicles and their associated cargo to specific plasma membrane (PM) domains upon internal or external cues is a major question in plant cell biology. A widely held hypothesis is that expansion of plant exocytotic machinery components, such as SNARE proteins, has led to a diversification of exocytotic membrane trafficking pathways to function in specific biological processes. A key biological process that involves the creation of a specialized PM domain is the formation of a host–microbe interface (the peri-arbuscular membrane) in the symbiosis with arbuscular mycorrhizal fungi. We have previously shown that the ability to intracellularly host AM fungi correlates with the evolutionary expansion of both v- (VAMP721d/e) and t-SNARE (SYP132α) proteins, that are essential for arbuscule formation in *Medicago truncatula*. Here we studied to what extent the symbiotic SNAREs are different from their non-symbiotic family members and whether symbiotic SNAREs define a distinct symbiotic membrane trafficking pathway. We show that all tested SYP1 family proteins, and most of the non-symbiotic VAMP72 members, are able to complement the defect in arbuscule formation upon knock-down/-out of their symbiotic counterparts when expressed at sufficient levels. This functional redundancy is in line with the ability of all tested v- and t-SNARE combinations to form SNARE complexes. Interestingly, the symbiotic t-SNARE SYP132α appeared to occur less in complex with v-SNAREs compared to the non-symbiotic syntaxins in arbuscule-containing cells. This correlated with a preferential localization of SYP132α to functional branches of partially collapsing arbuscules, while non-symbiotic syntaxins accumulate at the degrading parts. Overexpression of VAMP721e caused a shift in SYP132α localization toward the degrading parts, suggesting an influence on its endocytic turn-over. These data indicate that the symbiotic SNAREs do not selectively interact to define a symbiotic vesicle trafficking pathway, but that symbiotic SNARE complexes are more rapidly disassembled resulting in a preferential localization of SYP132α at functional arbuscule branches.

Keywords: SNARE, arbuscular mycorrhiza, syntaxin, exocytosis, VAMP, *Medicago*, membrane, symbiosis

OPEN ACCESS

Edited by:
Brigitte Mauch-Mani, Université de Neuchâtel, Switzerland

Reviewed by:
Rucha Karnik, University of Glasgow, United Kingdom
Benoit Lefebvre, Institut National de la Recherche Agronomique de Toulouse, France

****Correspondence:***
Erik Limpens
erik.limpens@wur.nl

Specialty section:
This article was submitted to Plant Microbe Interactions, a section of the journal Frontiers in Plant Science

Received: *19 July 2019*
Accepted: *10 March 2020*
Published: *03 April 2020*

Citation:
Huisman R, Hontelez J, Bisseling T and Limpens E (2020) SNARE Complexity in Arbuscular Mycorrhizal Symbiosis. Front. Plant Sci. 11:354. doi: 10.3389/fpls.2020.00354

INTRODUCTION

The growth and maintenance of eukaryotic cells requires the continuous delivery of vesicles to the plasma membrane (PM); exocytosis. The fusion of vesicles with their target membrane is driven by the interaction of vesicle SNAREs (v-SNAREs or R SNAREs) on the vesicle with a complex of target membrane SNAREs (t-SNAREs) on the target membrane. A t-SNARE complex consists of a Qa, Qb,

and Qc SNARE that each contribute a single SNARE domain, or a Qa and Qb+Qc SNARE, of which the latter contributes two SNARE domains to the complex (Sanderfoot, 2007). In plants, the number of SNAREs involved in exocytosis has expanded to be encoded by families of at least partially redundant proteins (Sanderfoot, 2007). This suggests that expansion of SNARE proteins allowed the adaptation of exocytosis to these different biological processes. Furthermore, the expansion of the number of secretory SNAREs in plants has been suggested to allow the presence of multiple exocytosis pathways in one cell (Sanderfoot, 2007; Łangowski et al., 2016; Kanazawa and Ueda, 2017). We define an exocytosis pathway as the traffic and fusion of a distinct population of vesicles and associated cargo to the PM or subdomain. An example of the use of different exocytosis pathways to create specialized membrane domains can be found in animal cells: in mammalian polarized epithelial cells two PM domains with a distinct protein composition are present; an apical domain and a basolateral domain (Mostov et al., 2003). Trafficking of proteins to these domains is mediated by distinct populations of vesicles, which depend on distinct v-SNAREs (Martinez-Arca et al., 2003) and different t-SNAREs that are present at the two domains (Kreitzer et al., 2003). Whether SNAREs mark distinct exocytotic trafficking pathways in plants as well is currently unknown, although differential effects of syntaxins on secretion have been reported (Kalde et al., 2007; Leucci et al., 2007; Rehman et al., 2008; Waghmare et al., 2018).

A key example of a biological process that depends on specific SNARE proteins is the formation of the peri-arbuscular membrane (PAM) during the endosymbiotic interaction of plants with arbuscular mycorrhizal (AM) fungi (Harrison and Ivanov, 2017). AM fungi colonize the roots of almost all land plants, where they form highly branched hyphal structures in cortical cells, called arbuscules, that are surrounded by the specialized PAM, which creates a symbiotic interface where exchange of nutrients takes place (Gutjahr and Parniske, 2013). Upon entering a cortical cell, first a trunk domain is established, after which the fungus undergoes repeated dichotomous branching by which gradually finer branches appear. These fine branches are characterized by the absence of a structured cell wall and contain specific plant proteins, such as symbiotic phosphate and lipid transporters to control the exchange of nutrients, that distinguish it from the PM which is continuous to the PAM. As such the PAM represents a specialized PM subdomain that involves the polar targeting of membrane vesicles (Pumplin and Harrison, 2009).

It has previously shown that the formation of arbuscules in *Medicago truncatula* (Medicago) depends on the two v-SNAREs MtVAMP721d and MtVAMP721e, and on the Qa-type t-SNARE (syntaxin) isoform MtSYP132α (named MtSYP132A by Pan et al., 2016) which results from alternative splicing (Ivanov et al., 2012; Huisman et al., 2016; Pan et al., 2016). Silencing of MtVAMP721d/e by RNAi results in a phenotype where the formation of arbuscular branches is almost completely blocked (Ivanov et al., 2012). RNAi of MtSYP132α results in small arbuscules that collapse prematurely. The silencing of VAMP721d/e or SYP132α does not affect root development under the tested conditions, suggesting that they are dedicated to symbiosis. For simplicity, we will refer to these SNAREs as 'symbiotic' SNAREs while we will call other SNAREs 'non-symbiotic,' even though the latter ones may be involved in symbiosis as well. These symbiotic SNARE proteins are highly conserved in dicot plants that host AM fungi and are absent in non-host lineages, which is another strong indication that they are dedicated to symbiosis (Ivanov et al., 2012; Huisman et al., 2016; Pan et al., 2016). Since the formation of the PAM depends on both a specialized v- and t-SNARE, it is a particularly interesting model to study whether different SNAREs mark distinct exocytosis pathways in plant cells.

Therefore, we questioned what the difference is between symbiotic SNAREs and their non-symbiotic paralogs, to find out whether they can define a specialized symbiotic exocytosis pathway. We examined the potential functional redundancy between symbiotic SNARES and their closest non-symbiotic paralogs, as well as family members that are expressed in the same cell. Furthermore, we compared the spatiotemporal localization and SNARE-interactions of symbiotic and non-symbiotic SNAREs in arbuscule containing cells. Overall, our data indicate that the symbiotic SNAREs do not selectively interact to define a symbiotic vesicle trafficking pathway, but that symbiotic SNARE complexes are more rapidly disassembled. This results in a preferential localization of SYP132 at functional arbuscule branches, which may be instrumental to form an optimal functioning arbuscule.

RESULTS

The Qa- and R-SNARE Repertoire of Arbuscule-Containing Cells

To guide functional comparisons we first investigated the phylogenetic relationship of exocytosis-related SNAREs and determined their expression levels in arbuscule-containing cells in the model plant Medicago (*Medicago truncatula*). We focused on Qa t-SNAREs called syntaxins (SYP1 class) and the VAMP72 class R-SNAREs, as they form the core members of exocytosis-related SNARE complexes. We divided the individual SNARE genes into orthogroups among a wide range of plant species (**Figure 1A** and **Supplementary Figures S1, S2**). This classification allowed comparison of our data with studies on SNARE interactions in other plant species (**Supplementary Table S1**). Furthermore, comparing SNARE genes from separate orthogroups is most likely to reveal functional specialization, since we expect that there will be a strong selective pressure to maintain functionally different paralogs during evolution, resulting in conserved orthogroups.

The vast expansion of the number of syntaxins occurs at the base of the angiosperms: whereas we found only two conserved orthogroups in the gymnosperms, this number increases to six orthogroups in angiosperms, including the SYP13II orthogroup that we linked to symbiosis earlier (Huisman et al., 2016). As shown before, during evolution this orthogroup is strictly linked to the ability of plant species to interact with AM fungi (Bravo et al., 2016; Huisman et al., 2016). It is conserved in all analyzed AM host plant species (16/16), and lost in all (6/6) analyzed plant

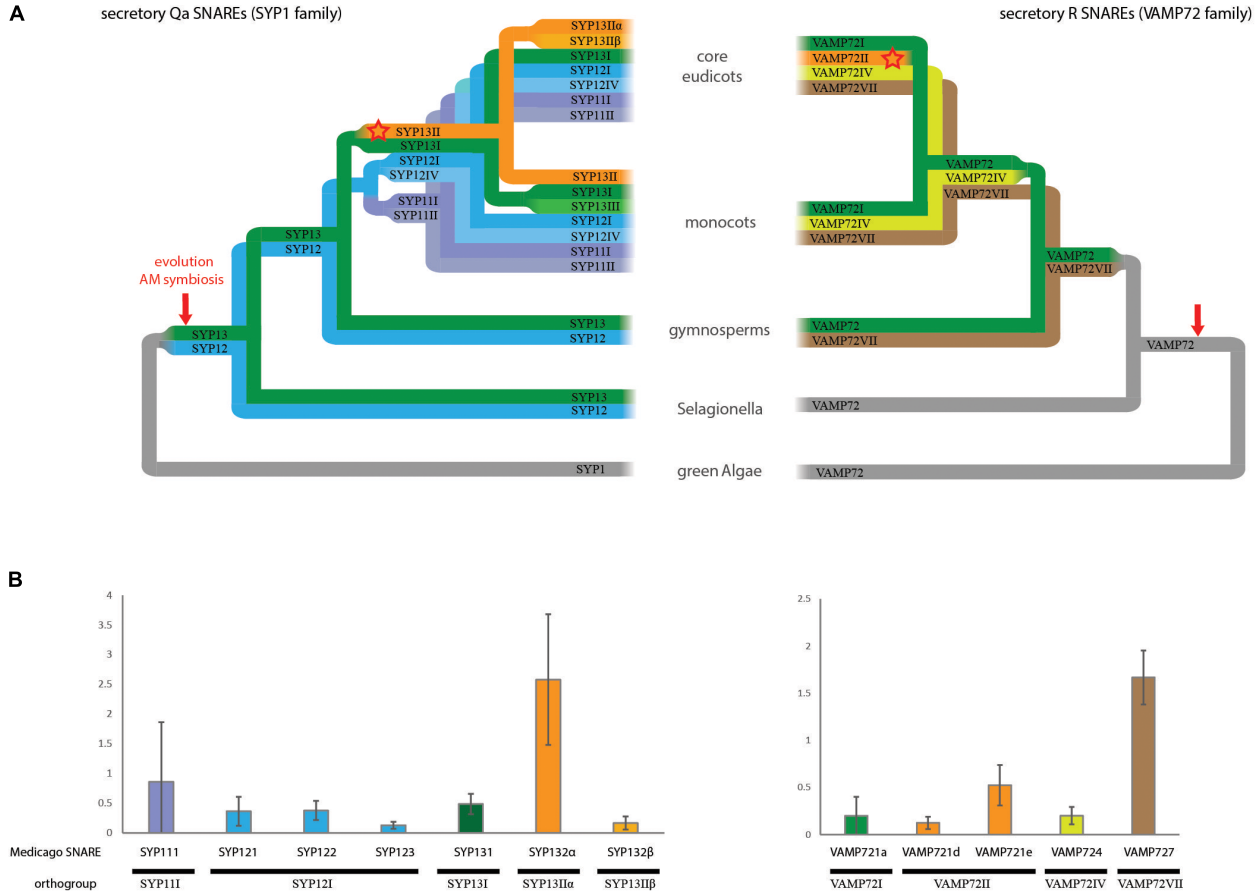

FIGURE 1 | The SNARE repertoire of arbuscule containing cells. **(A)** Schematic phylogenetic trees showing the evolution of the exocytosis related SNARE families SYP1 and VAMP72. The trees are showing orthogroups instead of individual genes, indicated by the use of roman numbers. Orthogroups were named following Sanderfoot (2007). Both schematic trees are based on the actual phylogenetic trees shown in **Supplementary Figures S1, S2**. **(B)** Digital droplet PCR on cDNA from arbuscule containing cells. Only SYP1 and VAMP72 genes that are expressed in arbuscule-containing cells are shown. The copy in each cDNA was normalized against the average expression of all tested genes. Error bars represent standard deviation of three biological replicates.

species that (independently) lost the ability to interact with AM fungi. In the dicot lineage, SYP13II is spliced into two different transcripts encoding the SYP13IIα and SYP13Iiβ proteins.

Within the VAMP72 family, four orthogroups can be found. Most individual VAMP genes of both Arabidopsis and Medicago are the result of independent and recent expansions within the VAMP72I orthogroup. The symbiotic MtVAMP721d and MtVAMP721e genes form a clear group together with other VAMP genes from dicots embedded within the VAMP72I orthogroup. We named this group VAMP72II. VAMP72II does not contain monocot genes, nor genes from *Aquilegia coerulea*, the most basal sequenced eudicot. Thus, the symbiotic VAMPs likely evolved at the base of the dicot lineage, after the split of *A. coerulea*, coinciding with the evolution of alternative splicing of SYP132. The conservation of VAMP72II is largely, but not strictly correlated to the ability of plants to host AM fungi. In particular, it is conserved in 1 out of 5 of the analyzed dicot AM non-host plants (*Striga hermonthica*), while it is lost in 2 out of 10 analyzed dicot AM host plants (*Manihot esculenta* and *Carica papaya*).

To get an accurate overview of the relative expression of symbiotic SNAREs and their orthologs in arbuscule-containing cells, we isolated RNA from these cells using laser microdissection. We used digital droplet PCR (ddPCR) to measure the absolute levels of transcripts of the different SNAREs that showed expression in this cell-type based on qPCR analysis (Huisman et al., 2016). ddPCR allows a more reliable quantitative measurement of expression levels compared to our qPCR approached used earlier (Huisman et al., 2016), as it is not affected by differences in primer efficiencies (Hindson et al., 2013). This analysis confirmed that multiple SNAREs are expressed in arbuscule-containing cells, and showed that MtSYP132α is clearly the dominant syntaxin (**Figure 1B**). Among the VAMPs, *MtVAMP727* is the most highly abundant transcript in arbuscule-containing cells, followed by the symbiotic *MtVAMP721e*.

Based on phylogeny and expression in arbuscule-containing cells we selected SNAREs for functional comparison. We selected the highest expressed symbiotic VAMP MtVAMP721e, along with the expressed genes of all other orthogroups; MtVAMP721a, MtVAMP724, and MtVAMP727. We selected both spliceforms

of the symbiotic SYP13II; MtSYP132α and MtSYP132β, and their closest non-symbiotic paralog SYP131, all of which are expressed in arbuscule-containing cells. Further, we selected the more distantly related MtSYP121, which is also expressed in arbuscule-containing cells (**Figure 1B**).

Most Exocytosis Related SNAREs Locate to the Peri-Arbuscular Membrane

We first investigated whether the different SNARE proteins can localize to the PAM. Therefore, we expressed the different SNAREs fused to GFP from the Medicago PT4 promoter, which is exclusively active in arbuscule-containing cells, and determined their localization by confocal microscopy. All syntaxins localized to the PAM (**Figures 2A–D**), as shown earlier for SYP132α, SYP132β, and SYP121 when expressed from their native promoter (Huisman et al., 2016). Even though v-SNAREs function on vesicles, overexpression typically results in their accumulation on the target membrane (Kwaaitaal et al., 2010; Ivanov et al., 2012). MtVAMP721a, MtVAMP721e, and MtVAMP724 accumulated on the PAM (**Figures 2E–G**). In contrast MtVAMP727 accumulated in punctuate intracellular compartments, as well as on membranes enclosing multiple arbuscular branches and the tonoplast (**Figure 2H**).

Interaction Between v- and t-SNAREs

Next, we tested whether there is specificity in SNARE-SNARE interactions at the PAM, by using a co-immunoprecipitation (co-IP) approach. Therefore, we expressed combinations of GFP-labeled syntaxins and triple HA-tag labeled VAMPs from the PT4 promoter in mycorrhized Medicago roots. As a negative control we tested the interaction with the PAM-localized GFP-tagged MtPT1 (Pumplin et al., 2012). The GFP-tagged proteins were immunoprecipitated from root extracts, and the co-IP of the VAMPs was determined by western blot using an antibody against the HA-tag (**Figure 3**). The experiment was performed twice with similar results (**Supplementary Figure S3**). We noticed that a small amount of HA-labeled VAMPs co-purified with negative control PT1, likely reflecting a weak background of non-solubilized proteins. For all combinations of syntaxins and VAMPs, the anti-GFP blot revealed two bands of around 63 and 25 kDa, representing the SYP-GFP fusion protein and free GFP respectively. On the anti-HA blot, one clear band around 30 kDa was visible for all input fractions corresponding to the 3HA-VAMP fusion proteins. For all combinations, a band was also visible in the IP lane representing the 3HA-VAMP fusion proteins that co-purified with the GFP labeled SYPs. We quantified the fraction of HA-labeled VAMPs from the input samples that was retrieved in the IP samples as a proxy for the amount of interaction between VAMPs and syntaxins. In general, the individual SNAREs showed different co-IP levels: SYP121 and SYP131 appeared to interact stronger than both spliceforms of SYP132, as indicated by the relative signals after co-IP compared to the input fractions in two independent replicate experiments. VAMP724 interacted less than the other VAMPs. Most striking, in case of SYP132α the co-IP of all VAMPs was extremely weak with

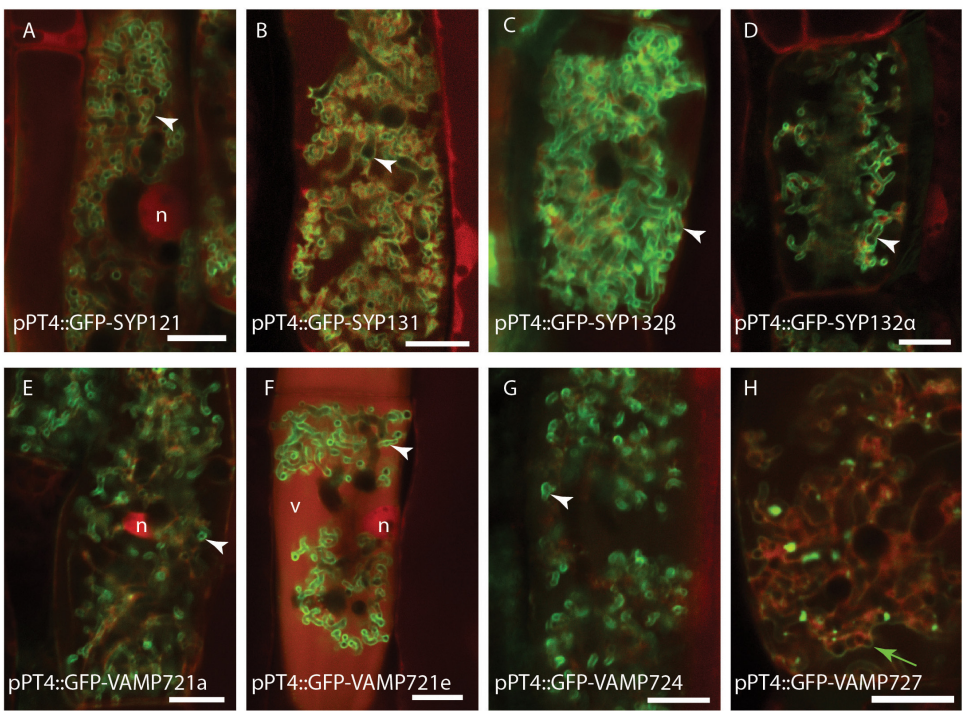

FIGURE 2 | Intracellular localization of syntaxins **(A–D)** and VAMPs **(E–H)** in arbuscule containing cells. Different SNAREs fused to GFP were expressed from the arbuscule specific Medicago PT4 promoter, combined with dsRed that marks the cytoplasm and nucleus (n), as well as occasional accumulation in the vacuoles (v). white arrowheads indicate the PAM, a green arrow indicates the tonoplast. Scalebars are 10 μm.

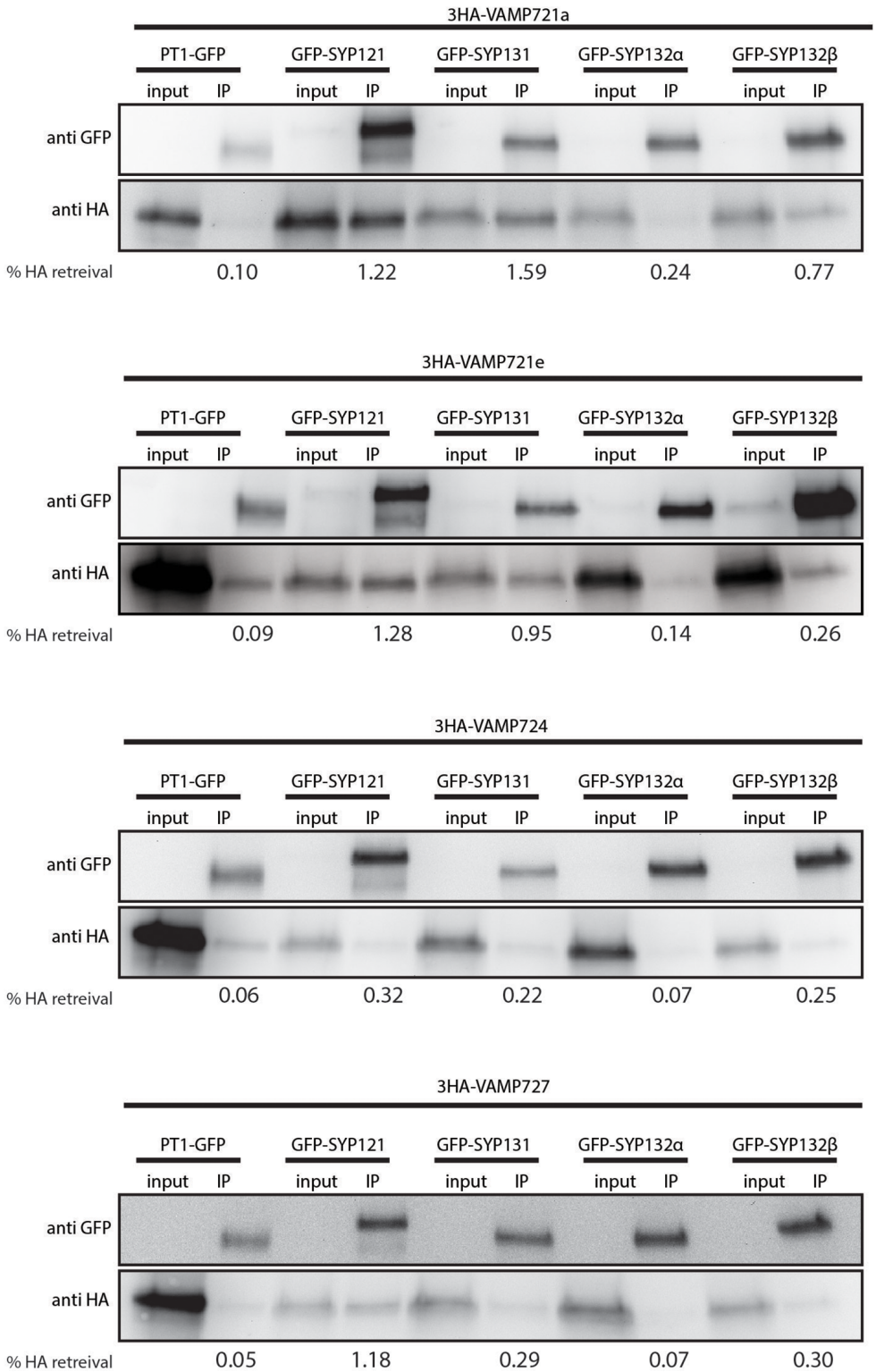

FIGURE 3 | Co-immunoprecipitation analysis of SNARE interactions. Western blot showing GFP-labeled syntaxins or negative control PT1, and 3HA-labeled VAMPs in extracts of mycorrhized Medicago roots before (input) and after immunoprecipitation (IP) using anti-GFP coated beads. The fraction (% HA retrieval) of HA-labeled VAMPs that co-purified with the GFP-labeled bait proteins was quantified as the intensity of the bands in the IP lane, divided by the intensity of the corresponding band in the input lane, and corrected for the volume difference of the two fractions.

signals barely detectable, similar to that observed for the non-interacting control protein MtPT1. To further confirm the ability of SYP132α to interact with VAMPs we used a BiFC approach in *Nicotiana benthamiana* leaves. This showed that SYP132α was able to interact with all tested VAMPs; VAMP721a, VAMP721d, and VAMP721e (**Supplementary Figure S4**). Thus, we consider it most likely that SYP132α can interact with all VAMPs. The lower levels of VAMPs that co-purify with SYP132α may indicate that these complexes are more rapidly disassembled.

Symbiotic SNAREs Are Largely Redundant With Their Non-symbiotic Paralogs

Previously, we already showed that SYP132β can restore arbuscule formation upon knock-down of SYP132α when expressed at sufficient levels (Huisman et al., 2016). To determine whether this also holds for the other non-symbiotic syntaxins we used a similar RNAi complementation approach. Therefore, we combined in one binary vector the RNAi constructs targeting SYP132α or VAMP721d/e (Ivanov et al., 2012; Huisman et al., 2016), and expression cassettes expressing the non-symbiotic SNAREs from the promoter of their symbiotic family member. As positive controls, we expressed VAMP721e lacking its native 3′-UTR or codon-scrambled SYP132α, both of which escape silencing by the RNAi constructs. We used *Agrobacterium rhizogenes* mediated transformation to generate transgenic roots expressing these constructs. 6 weeks after inoculation with AM fungi, roots were harvested and successful RNAi was confirmed in each individual root by qRT-PCR (**Supplementary Figure S5**). Next, we quantified the arbuscule development and level of colonization in the silenced roots and determined the arbuscule phenotype by confocal microscopy after staining with WGA-Alexa488 (**Figures 4A–K** and **Supplementary Figure S6**). Knockdown of *SYP132α* resulted in a severe reduction of mature arbuscules, as most arbuscules were stunted or collapsed. Expression of all of the tested syntaxins was sufficient to restore the arbuscule morphology of SYP132α knockdown to that of non-silenced control roots (**Figures 4A–F**), although complementation with SYP121 resulted in a slightly lower amount of arbuscules that fill the whole cell (**Supplementary Figure S6A**). In a similar way we tested the functional redundancy of VAMP members. The phenotype of VAMP721d/e RNAi is slightly stronger than SYP132α RNAi, as arbuscule formation does not proceed beyond the formation of the arbuscular trunk (Ivanov et al., 2012; **Supplementary Figure S6B**). After expression of VAMP721a, VAMP721e or VAMP724, the arbuscule phenotype was fully restored, showing many mature arbuscules (**Figures 4A,G–J**). In contrast, the arbuscule morphology was not restored after expression of VAMP727 (**Figure 4K**). The levels of mature arbuscules after complementation with VAMP721a or VAMP724 were slightly lower than the empty vector control, but not significantly different from the positive control; complementation with VAMP721e itself (**Supplementary Figure S6B**). It should be noted that the amount of biological replicates was relatively low which could mask subtle phenotypes. Nevertheless, these data show that most non-symbiotic SNAREs can functionally replace their symbiotic counterparts with respect to arbuscule morphology.

Generation of *syp132α-1*, a Constitutively SYP132β-Splicing Mutant

To rule out more subtle effects on arbuscule morphology that could go unnoticed in *A. rhizogenes* transformed roots, we generated a stable CRISPR line in which SYP132 is constitutively spliced into the SYP132β form. This line, named *syp132α-1*, contains a 532 bp deletion, which includes the entire α-specific exon as well as 34 bp of the last intron (**Figure 5C**). Since the deletion in this mutant includes the splice acceptor site in front of the *SYP132α*-specific last exon, we used digital droplet PCR on laser dissected arbuscule-containing cells to test whether a compensatory raise in the β-splice form occurs in arbuscule-containing cells. As shown in **Figure 5D**, the lack of *SYP132α* in the *SYP132α-1* mutant is indeed compensated by an equivalent increase of *SYP132β* levels. In this line we did not observe the premature degradation of arbuscules or impaired symbiosome development phenotype previously observed upon silencing of the *SYP132α* isoform. Instead, the formation of arbuscules as well as symbiosomes appeared similar to wild-type (**Figures 5A,B** and **Supplementary Figure S7**), in line with the RNAi complementations.

This mutant now allowed us to study in more detail whether arbuscule morphology and lifetime were affected when the symbiotic SYP132α is replaced by its non-symbiotic isoform at native levels. We found that the level of colonization (M%) and arbuscule abundance (A%) in *syp132α-1* was identical to wild-type R108 plants (**Figure 6A**). This is further confirmed by the similar expression level of the arbuscule-specific marker PT4 in *syp132α-1* compared to wild-type (**Figure 6B**). Next, we quantified arbuscule size distribution in the *syp132α-1* mutant and wild-type, by measuring the arbuscule size in images of 1000 arbuscules per root of wild-type and mutant plants ($n = 4$). However, no differences in arbuscule size distribution were observed (**Figure 6C**). From the same images we quantified the fraction of collapsed arbuscules, which was not significantly different. To get more direct data on the lifetime of arbuscules, we developed a construct that expresses the fluorescent timer reporter protein dsRed-E5 fused to a nuclear localization tag from the PT4 promoter. DsRed-E5 slowly maturates from green to red fluorescence with a half-time of approximately 10 h (Mirabella et al., 2004). Since the PT4 promoter is switched on at the start of the formation of the PAM (Pumplin et al., 2012), the ratio of red/green fluorescence can be used as a proxy for arbuscule age. We expressed the pPT4::Timer-NLS construct in mycorrhized Medicago roots and determined the red/green ratio of the nucleus of approximately 100 arbuscular cells per root ($n = 4$). We observed a clear correlation between the color of the nucleus and the phenotype of the arbuscule: arbuscules with young (turgoid) branches that did not yet completely fill the cell displayed a low nuclear red/green ratio, while collapsed arbuscules displayed a high nuclear red/green ratio. Mature arbuscules displayed intermediate red/green ratio's (**Figure 6D**). This confirmed the

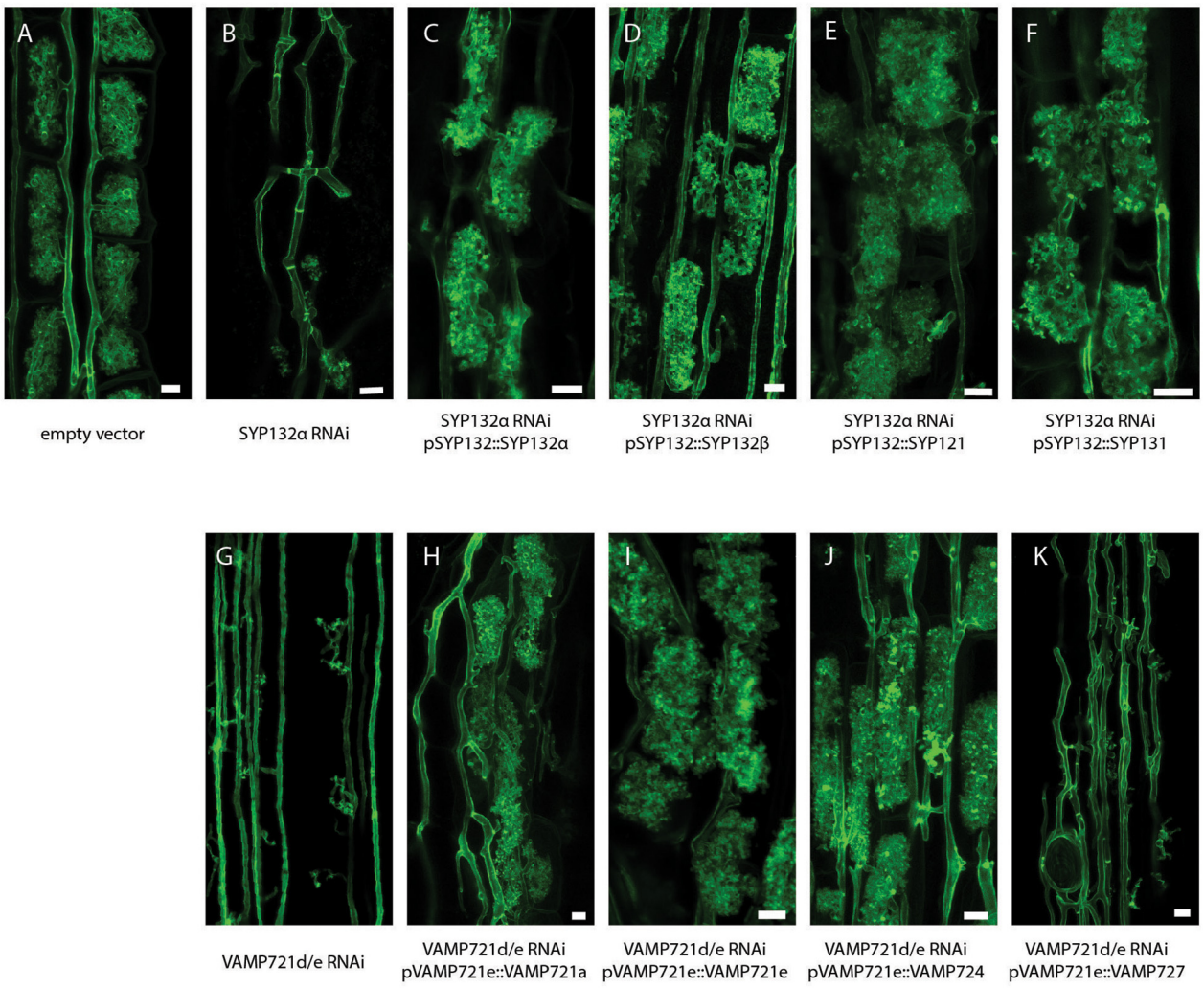

FIGURE 4 | RNAi complementation analysis. Projection of confocal image stacks showing AM fungi in Medicago roots, stained with wheat germ agglutinin conjugated to alexa488 n = 3–4 biological replicates. **(A)** Empty vector control, **(B)** RNAi of SYP132α, **(C–F)** complementation of SYP132 RNAi with other syntaxins, **(G)** RNAi of VAMP721d and -e, and **(H–K)** complementation of VAMP721d/e RNAi with other VAMPs.

suitability of the construct to measure arbuscule age. The age distribution of arbuscule-containing cells in *syp132α-1* plants was not significantly different from the age distribution in wild-type plants (**Figure 6E**). These detailed analyses unequivocally show that SYP132β can functionally replace SYP132α to restore normal arbuscule morphology at native levels.

SYP132α Turnover Is Affected by VAMP721e Expression

Upon examining the co-expression of the different syntaxins and VAMPs used in the co-IP experiment, we noticed a different behavior of SYP132α compared to the non-symbiotic syntaxins upon co-expression with VAMP721e. Previously, we observed a difference in localization between the two SYP132 isoforms when arbuscules start to collapse, with SYP132α being more confined to the non-degrading ("functional") arbuscule branches and SYP132β accumulating on degrading parts (Huisman et al., 2016). However, upon co-expression of SYP132α with VAMP721e both from the PT4 promoter, SYP132α localized mostly to the collapsed part of degrading arbuscules, resembling the behavior of SYP132β (**Figure 7A** and **Supplementary Figure S8**). This localization was observed in 13 out of 13 partially collapsing arbuscules, whereas without overexpression of VAMP721e, SYP132α preferentially localized to the functional branches in 28 out of 29 partially collapsing arbuscules (**Figure 7B** and **Supplementary Figure S8**). This indicates that overexpression of VAMP721e causes the accumulation of SYP132α on collapsing arbuscule domains. It suggests that VAMP721e levels affect the localization of SYP132α. This can be achieved in different ways; either by redirecting the newly synthesized proteins to the degrading arbuscule branches, or by increasing the turnover of SYP132α at the functional branches.

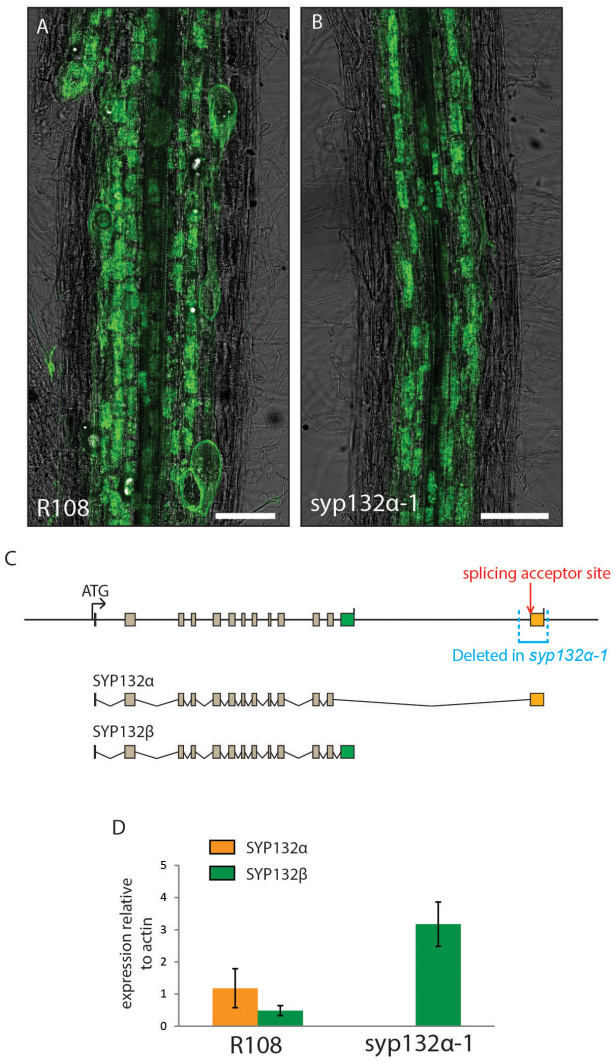

FIGURE 5 | (A,B) Mycorrhized wild-type **(A)** and *syp132α-1* roots stained with WGA-Alexa488. Scale bars are 100 μm. **(C)** Schematic representation of the SYP132 exons in the genome of Medicago, the different spliced transcripts, and the region deleted in the *syp132α-1* mutant. **(D)** Digital droplet PCR measurements of the transcript levels of SYP132α and β in the arbuscule-containing cells of wild-type plants and *syp132α-1* plants. Error bars represent standard deviation of 4 (R108) or 3 (*syp132α-1*) biological replicates.

DISCUSSION

The expansion and evolutionary conservation of symbiotic v- and t-SNAREs in AM (eudicot) host plants suggested that these SNAREs may have specialized to mark a distinct exocytosis pathway to form a symbiotic host–microbe interface. Here we show that the essential role of the symbiotic SNAREs in interface formation, MtVAMP721d/e and MtSYP132α, can be largely explained by their dominant expression levels in arbuscule forming cells. We compared the interaction of a wide range of exocytosis related v- and t-SNAREs in a single cell-type. All tested v- and t-SNAREs that are expressed in arbuscule-containing cells were shown to be able to form complexes at the PAM. This, together with the ability of the majority of non-symbiotic SNARE paralogs to restore the arbuscule morphology defect upon loss of symbiotic SNAREs, shows that the symbiotic SNAREs do not mark a distinct exocytosis pathway that distinguishes traffic to the PAM from traffic to the PM. This is in line with the suggestion by Pumplin et al. (2012) that targeting to the PAM involves a transient reorientation of general secretion. Instead, our data suggest that the symbiotic SNARE complexes are more rapidly disassembled, most likely to confine SYP132α to functional branches.

The use of different SNAREs in specific biological processes most often relates to differences in the spatiotemporal expression and dynamics of these SNAREs (Kanazawa and Ueda, 2017; Slane et al., 2017; **Supplementary Table S1**). In Arabidopsis, different secretory t-SNAREs are expressed in different plant tissues (Enami et al., 2009), show specific subcellular localization patterns (Lauber et al., 1997; Collins et al., 2003; Ângelo Silva et al., 2010; Ichikawa et al., 2014), turnover (Reichardt et al., 2011) or dynamics (Nielsen and Thordal-Christensen, 2012). The only clear example of a plant SNARE that evolved to define a new trafficking pathway is VAMP727, which acquired the ability to interact with vacuolar t-SNAREs and marks vesicles with a distinguishable cargo (Ebine et al., 2011). The low levels of MtVAMP727 on the PAM suggest that most MtVAMP727-labeled vesicles are targeted to other compartments like endosomes and the vacuole. This explains the inability of MtVAMP727 to complement the arbuscule defect in VAMP721d/e RNAi roots, despite the observation that it is the most highly expressed v-SNARE in arbuscule-containing cells.

A striking observation from our co-IP analyses was the lower level of v-SNAREs in complexes with SYP132α in arbuscule-containing cells, compared to the non-symbiotic syntaxins. This might reflect a stricter regulation of SYP132α complexes by accessory factors. SNARE complexes occur in two different states; a *trans*-SNARE complex between the v-SNARE on the vesicle and the t-SNAREs on the target membrane, and a *cis*-SNARE complex where both v- and t-SNAREs are present on the same membrane until they are disassembled by the ATPase NSF and SNAPs (Südhof and Rothman, 2009). It was recently shown that, also before vesicle fusion, SNAREs involved in cytokinesis are transported to their site of action as *cis*-SNARE complexes, which may apply to other secretory SNAREs as well (Karnahl et al., 2017). The actual vesicle fusion event involving *trans*-SNARE complexes is short-lived compared to the lifetime of *cis*-SNARE complexes. Therefore, it is likely that the complexes that are detected in our co-IP study – or any of the previous studies on SNARE interactions in plants – are in fact mostly representing *cis*-SNARE complexes. This may be further exaggerated by the strong expression from the PT4 promoter. In this scenario, the amount of VAMPs that co-purify with syntaxins is not a measure for the amount of vesicle fusion events driven by this particular complex, but merely represents the speed of *cis*-complex formation and dissociation. This implies that SYP132α containing SNARE complexes are more rapidly disassembled, possibly to recycle the syntaxin for subsequent fusion reactions

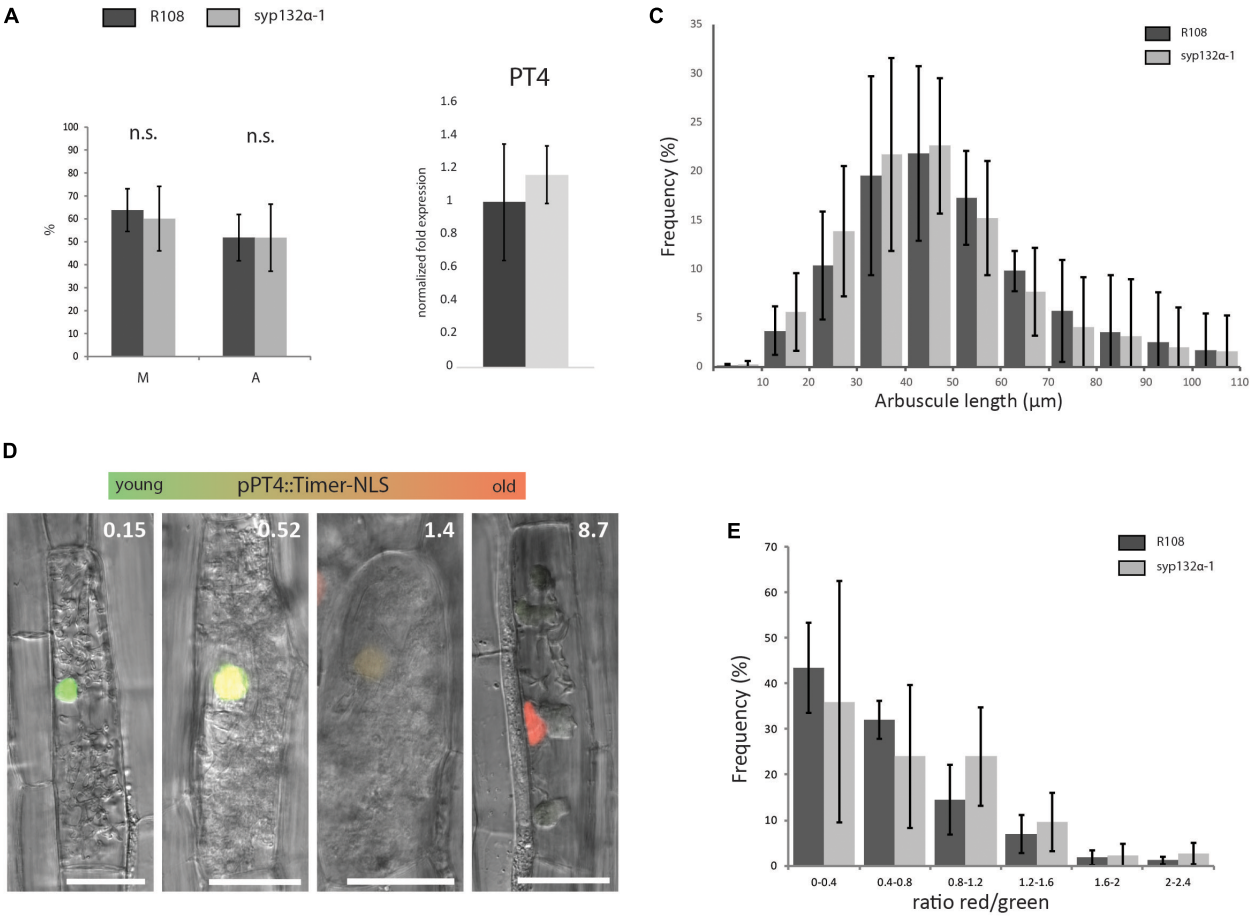

FIGURE 6 | (A) Colonization (M%) and arbuscule abundance (A%) in wild-type and *syp132α-1* roots, 6 weeks after inoculation with *R. irregularis*. Parameters are scored according to Trouvelot et al. (1986). Error bars represent the standard deviation of five biological replicates. **(B)** qRT-PCR on cDNA isolated from mycorrhized roots of wild-type and *syp132α-1* showing the expression of marker gene PT4. Error bars represent the standard deviation of three biological replicates. **(C)** Arbuscule length distribution measured in wild-type and *syp132α-1* roots infected with *R. irregularis.* Around 1000 arbuscules per root were measured. Error bars represent standard deviation of four different roots. **(D)** Confocal laser scanning microscopy images overlaid with DIC images showing expression of nuclear localized dsRed-E5 (Timer) driven by the PT4 promoter in arbuscular cells of wild-type plants. The numbers in the upper-right corner indicate the ratio between red and green fluorescence. **(E)** Age distribution of arbuscules in wild-type and *syp132α-1* roots. The age of ∼100 arbuscules was measured per root. Collapsed arbuscules were not measured. Error bars represent standard deviation of four individual roots. **(A–C,E)** No significant differences between wild-type and syp132α-1 were found (Student's *t*-test $p \leq 0.05$).

at the functional PAM branches or to facilitate the interaction with other proteins.

The lower amount of detected SYP132α containing SNARE complexes correlated with a different localization with respect to degrading arbuscule branches in comparison to the non-symbiotic syntaxins (Huisman et al., 2016). We speculate that the accumulation of SYP132 at the collapsing parts may be related to the structural resemblance of the collapsing arbuscule to the encasement of haustoria from filamentous pathogens, which occurs as result of a defense response toward these pathogens. During the encasement of haustoria multivesicular bodies (MVBs) are redirected toward the haustorial encasement. This results in the inclusion of the inner vesicles of MVB within the deposited cell-wall material as exosomes (Assaad et al., 2004; An et al., 2006; Micali et al., 2011). Following this route, endocytosed membrane proteins including the recycling t-SNARE SYP121 have been shown to accumulate in the encasement (Nielsen et al., 2012). From transmission electron microscopy images, it was shown that collapsed arbuscule branches are encased by depositions of cell-wall like material, with many paramural bodies (Cox and Sanders, 1974). In two recent detailed ultrastructural analyses of the arbuscule interface it was shown that extracellular vesicles and fusion of MVB's also occurs at developing arbuscules, suggesting a tightly regulated process (Ivanov et al., 2019; Roth et al., 2019). Therefore, similar to the accumulation of SYP121 in the encasement of haustoria, we hypothesize that the accumulation of SYPs on collapsing arbuscules may represent a retargeting of MVB's containing endocytosed syntaxins to the PAM "encasement". It would therefore be interesting to test whether a similar differential behavior of SYP132α is also observed upon papilla formation or haustorial encasements of pathogenic microbes.

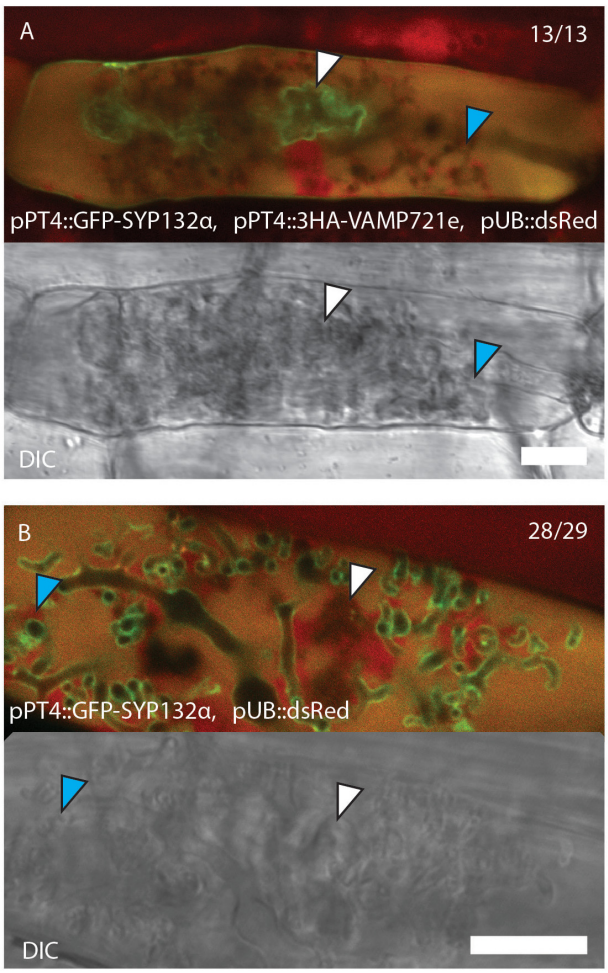

FIGURE 7 | Confocal laser scanning microscopy images and accompanying bright-field images showing the localization of SYP132α fused to GFP with **(A)** and without **(B)** co-expression of triple HA-tag labeled VAMP721e, both driven by the PT4 promoter. Collapsed branches are marked by white arrowheads, functional branches are marked by blue arrowheads. The red signal shows autofluorescence of collapsed arbuscules and the nuclei and cytoplasm that are labeled with dsRed driven by the Arabidopsis ubiquitin 3 promoter. Scale bars are 10 μm.

Over-expression of VAMP721e together with SYP132α caused a shift in the accumulation of SYP132α toward the degrading parts of the arbuscule. Since non-symbiotic syntaxins appear to make more stable complexes with VAMP721e compared to SYP132α, it suggests that a faster dissociation of *cis*-SNARE complexes prevents the redirection of SYP132α to the degrading parts, ensuring a preferential localization at the functional arbuscule domains (Huisman et al., 2016). This supports a so-far understudied role for PM-SNARE complex formation in the regulation of endocytic traffic in plants. Interestingly, it has recently been shown that AtSYP132 (the ortholog of MtSYP131) affects the endocytic traffic of an H+-ATPase, with which it interacts (Xia et al., 2019). Induced expression of AtSYP132 reduced the amount of H+-ATPase proteins at the PM thereby affecting the acidification of the cell wall. This suggests a role for syntaxins in the selective turn-over of proteins at the PM. It is therefore tempting to speculate that MtSYP132α may control the endocytic turnover of specific proteins at the PAM to control arbuscule function, rather than morphology.

A speculative specialization of SYP132α, that can be independent from its role in vesicle fusion, may involve an interaction with PAM localized transporters. Such interaction could affect the functional efficiency of nutrient exchange, without affecting arbuscule morphology *per se*. Similarly, the t-SNARE AtSYP121 was shown to interact with K^+-channels KC1 and KAT1. As a result of this interaction, K^+ uptake is reduced in *Atsyp121* mutants (Grefen et al., 2010). Also in animal systems, syntaxins have been shown to interact with and directly regulate a range of ion channels or transporters (Michaelevski et al., 2003; Chao et al., 2011). Intriguingly, although syntaxins interact with the same v-SNAREs, it has been reported that they can mediate the secretion of distinct cargoes (Kalde et al., 2007; Leucci et al., 2007; Rehman et al., 2008; Waghmare et al., 2018). How different syntaxins control the delivery of different cargo, despite a lack in specificity for different v-SNAREs, will be an interesting future avenue to study how the exocytosis-machinery may be specialized for different biological functions.

MATERIALS AND METHODS

Phylogenetic Analysis of SNAREs

The protein sequences of all SYP1 and VAMP72 family members were retrieved from the Phytozome database[1] for the AM host species; *Aquilegia coerulea, Brachypodium distachyon, Citrus clementina, Carica papaya, Cucumis sativus, Fragaria vesca, Ginkgo biloba, Musa acuminate, Manihot esculenta, Medicago truncatula, Oryza sativa, Phoenix dactylifera, Prunus persica, Populus trichocarpa, Setaria italic, Solanum lycopersicum, Selagionella moelendorfii, Theobroma cacao* and *Vitis vinifera,* and the AM non-host species; *Arabidopsis thaliana, Beta vulgaris, Dianthus caryophyllus, Marchantia polymorpha, Nelumbo nucifera, Physcomitrella patens, Pinus taeda, Striga hermonthica, Spirodela polyrhiza,* and *Utricularia gibba* (**Supplementary Datasheets S1, S2**). To ensure the recovery of all family members, missing species in each orthogroup were confirmed by repeated homology searches using orthologs from that group as an input. The species were choses to include a large and diverse range of AM hosts and non-hosts. The Protein sequences were aligned in Mega5 using the ClustalW algorithm. Subsequently, trees were constructed using the neighbor-joining method with 100 bootstrap iterations.

Plant Growth, Transient Transformation, and Inoculation

For transformation, *A. rhizogenes* MSU440 was used according to Limpens et al. (2004). For nodulation assays, plants were transferred to perlite saturated with Färhaeus medium without $Ca(NO_3)_2$ and grown at 21°C at a 16/8 h light/dark regime. After 3 days, plants were inoculated with Sinorhizobium melilotii 2011

[1]http://www.phytozome.net

and grown for 4 weeks. For mycorrhization assays, plants were transferred to pots containing a 5:3 (v/v) ratio mix of expanded clay and sand, saturated with modified Hoagland medium (5 mM $MgSO_4$, 2.5 mM $Ca(NO_3)_2$, 2.5 mM KNO_3, 2 mM NH_4NO_3, 500 μM MES, 50 μM NaFeEDTA, 20 μM KH_2PO_4, 12.5 μM HCl, 10 μM H_3BO_3, 2 μM $MnCl_2$, 1 μM $ZnSO_4$, 0.5 μM $CuSO_4$, 0.2 μM Na_2MoO_4, 0.2 μM $CoCl_2$, pH 6.1). Plants were inoculated with dried Rhizophagus irregularis infected maize roots obtained from Plant Health Cure[2]. Plants were grown for 4 weeks at 21°C at a 16/8 h light/dark regime.

Laser Capture Microdissection and ddPCR

Roots of mycorrhized Medicago plants and uninfected control plants were harvested and fixed in Farmer's fixative (75% ethanol, 25% acetic acid) substituted with 0.01% Chlorazol Black E to stain AM fungi, and vacuum infiltrated for 30 min on ice. Then, the roots were incubated in Farmer's fixative for 16 h at 4°C on a spinning wheel. After fixation, the roots were dehydrated in an ethanol dehydration series (80, 85, 90, 95% 30 min each followed by 100%, overnight) Steedman wax was prepared by mixing 90% polyethylene glucol400 distearate and 10% 1-hexadecanol at 65°C. Steedman wax was infiltrated by incubating the roots in 50% Steedman wax and 50% ethanol for 2 h at 38°C, followed by three incubations in 100% Steedman wax for 2 h at 38°C. Finally, the samples were transferred to room temperature to allow the wax to solidify. Solidified blocks of Steedman wax were cut into 20 μm thick sections using a microtome, and transferred to PEN-membrane slides (Leica). Three replicates of Arbuscule containing cells and uninfected cortical cells were collected using a Leica LMD7000 laser capture microdissection microscope. RNA was isolated using a RNeasy micro kit (Qiagen). cDNA was synthesized using the iScript cDNA synthesis kit (Bio-Rad). in a total volume of 20 μl. 1 μl cDNA was then used per ddPCR reaction. For this, a ddPCR mastermix containing evaGreen as a probe was used (BioRad), as well gene specific primers (1–24, **Supplementary Table S2**). Then the PCR mix was suspended in oil using the QX200 Droplet Generator (Biorad). The PCR was carried out following manufacturer's instructions. Subsequently, the absolute number of positive droplets was counted using a QX200 Droplet Reader.

Whole Root RNA Isolation, cDNA Synthesis, qRT-PCR

RNA was isolated from plant tissue using the EZNA Plant RNA mini kit (omega). cDNA was synthesized from 1 μg of RNA using the iScript cDNA synthesis kit (BioRad). Equal amounts of cDNA were used for qPCR using SYBR green supermix (Bio-Rad) in a Bio-Rad CFX connect real-time system qPCR machine. Gene expression levels were determined using gene specific primers listed in **Supplementary Table S2**. The gene expression was normalized using Actin2 and Ubiquitin10 as reference genes. To confirm RNA silencing levels, five biological replicates were checked. Only plants in which silencing resulted in trancript levels below 20% of the empty vector control were considered in subsequent phenotypic analysis. These were 3–4 biological replicates per construct.

Plasmid Construction

All expression cassettes were created using multisite gateway technology (Invitrogen) in the pKGW-RR-MGW destination vector. For all reactions a pENTR2-3 carrying a 35S terminator was used (Ovchinnikova et al., 2011).

The SYP132α RNAi construct, the empty RNAi control vector, a pENTR4-1 vector carrying a PT4 promoter, a pENTR4-1 carrying a PT4 promoter fused to GFP, The pENTR1-2 vectors containing the coding sequences of SYP121, SYP122, SYP132α, and SYP132β and a pENTR4-1 carrying the SYP132 promoter are described in Huisman et al. (2016).

The VAMP721d/e RNAi vector, the pENTR1-2 vectors containing the coding sequences of VAMP721a, VAMP721d and VAMP721e, and the pENTR4-1 carrying the VAMP721e promoter are described in Ivanov et al. (2012).

To obtain a pENTR4-1 containing a triple HA-tag driven by the PT4 promoter, A triple HA tag flanked by AscI and Acc65I restriction sites was *de novo* synthesized (Integrated DNA technologies). Using AscI-Acc65I restriction-ligation, The GFP in the pENTR4-1 pPT4::GFP was swapped for the triple HA-tag. A pENTR1-2 carrying a Timer-NLS construct was generated by amplifying the timer-NLS cds from a vector described in Mirabella et al. (2004), using primers 53 and 54 (**Supplementary Table S2**) adding a cacc sequences in the forward primer. The PCR fragment was then cloned into a pENTR/D-TOPO entry vector using TOPO cloning (Invitrogen). A pENTR4-1 carrying the fluorescent timer driven by the PT4 promoter was constructed by amplifying the timer cds using primers 55 and 56 (**Supplementary Table S2**), while adding AscI-KpnI restriction sites. By AscI-KpnI restriction digestion, the GFP of the pENTR4-1 pPT4-GFP was swapped for Timer. pENTR2-3 vectors containing nGFP or cGFP were obtained from VIB Ghent. For n-terminal split GFP fusions, nGFP and cGFP were amplified from these vectors using primers 41–44 listed in **Supplementary Table S2**. Primers were designed to remove stop codons, and to add a start codon and AscI/Acc65I restriction sites. Subsequently, both fragments were cloned into a pENTR4-1 vector containing a 35S promoter using AscI-Acc65I restriction/ligation. pENTR1-2 vectors containing the coding sequence of SYP131, VAMP724 and VAMP727 were constructed by amplifying the respective genes from Medicago A17 cDNA using primers 29–34, adding a cacc sequence adapter at the 5′ end. The PCR fragment was then cloned into a pENTR/D-TOPO entry vector using TOPO cloning (Invitrogen). To combine GFP fusion cassettes with 3HA fusion cassettes, the GFP fusion constructs were amplified using primers 35 and 36 (**Supplementary Table S2**), adding SpeI and SwaI restriction sites. The HA fusion constructs were amplified using primers 37 and 38 (**Supplementary Table S2**), adding SwaI and ApaI restriction sites. Using three-point restriction/ligation, the two constructs were inserted into a pKGW-MGW binary vector. To combine SNARE expression cassettes with RNAi constructs for RNAi complementation, the SNARE expression cassette was amplified using primers 39 and 40 (**Supplementary Table S2**),

[2]http://www.phc.eu

adding ApaI and Eco81I restriction sites. Using ApaI-Eco81I restriction/ligation, the cassetes were inserted into the SYP132α and VAMP721d/e RNAi vectors.

To make a CRISPR-Cas9 construct for SYP132α we made use of the pCAMBIA1302-Cas9 vector described by Jiang et al. (2013). A 20 bp region (GCAACTGATCATGTGAAGTC) targeting the last exon of SYP132α was chosen as sgRNA target sequence. Overlap PCR was performed to introduce the selected 20 bp target sequence into the U6-sgRNA cassette from pCAMBIA1302-Cas9, flanked by SalI and KpnI restriction sites, using the primers 45–48 (**Supplementary Table S2**). The resulting SYP132α-sgRNA fragment was introduced into the pCAMBIA-CAS9 vector via SalI-KpnI restriction-ligation. pCAMBIA-CAS9 additionally contains the CAS9 gene under the control of the CaMV35 promoter and a hygromycin resistance gene for selection in the plant.

Microscopy and Quantification

For confocal imaging, a Leica SP8 confocal microscope was used. An excitation wavelength of 488 nm was used for GFP and WGA-alexa 488. An excitation wavelength of 543 nm was used for dsRed. Appropriate emission range settings were used to separate the fluorophores used in each experiment. For quantification of fluorescence levels, ImageJ software was used. The average arbuscule size was determined from 1000 arbuscules in each of the four roots per genotype.

Mycorrhizal Staining and Quantification of Colonization Levels

For quantification of colonization levels, roots were incubated in 10% (w/v) KOH at 98°C for 10 min. Then roots were washed three times with 5% acetic acid. After washing, the roots were stained in 5% ink in 5% acetic acid, for 2 min at 98°C. after staining the roots were destained in 5% acetic acid, refreshing the destaining solution several times. For staining with WGA alexafluor 488, roots were incubated in 10% (w/v) KOH at 60°C for 3 h. Then, roots were washed three times in PBS (150 mM NaCl, 10 mM Na_2HPO_4, 1.8 mM KH_2PO_4, pH 7.4), and incubated in 0.2 μg/mL WGA-Alexafluor 488 (Molecular Probes) in PBS at room temperature for 16 h. For quantification of colonization levels, roots were cut into 1 cm fragments, and the colonization and arbuscule abundance was scored and calculated according to Trouvelot et al. (1986).

Co-immunoprecipitation

The roots of mycorrhized plants (5 weeks post-inoculation) expressing different combinations of GFP-labeled syntaxins and 3HA-labeled VAMPs were harvested, and residual sand was washed away. The roots were flash-frozen in liquid nitrogen, and ground using a mortar and pestle. One gram of plant material was added to 6 ml of RIPA buffer [10 mM Tris/HCl pH 7.5, 150 mM NaCl, 0.1% SDS, 1% Triton X-100, 1% sodium deoxycholate, 0.5 mM EDTA, 1 mM PMSF (from a 100x stock in isopropanol), 20 μM MG132, 1x protease inhibitor mix (Roche cOmplete, EDTA free)], and ground in a potter tube. After 20 min incubation on ice, the extracts were centrifuged twice at 9000 *g* after which the supernatant was transferred to a new tube each time. The input fraction was harvested at this point, and mixed in a 1:1 ratio with 4x SDS-sample buffer (200 mM Tris HCl 6.8, 8% SDS, 40% glycerol, 4% β-mercaptoethanol, 50 mM EDTA, 0.08% bromophenol blue). Then 30 μl of anti-GFP coated agarose beads (Chromotek), equilibrated in washing buffer [50 mM Tris HCl 8.0, 150 mM NaCl, 0.1% Triton X-100, 1x protease inhibitor mix (Roche cOmplete, EDTA free)] were added to the protein extracts. The samples were incubated for 1 h at 4°C on a spinning wheel. Then, the beads were harvested by centrifugation at 2000 *g* for 2 min, and washed three times with 1 ml of washing buffer. The washing buffer was removed, and 100 μl 2x SDS-sample buffer was added, after which the samples were incubated for 10 min at 98°C. After centrifugation for 2 min at 2700 *g*, the supernatant was transferred to a new tube and stored at −20°C until gel electrophoresis.

Western Blotting

Proteins were separated on a precast 4–12% poly acrylamide gradient mini-gel (Bio-Rad) at 300 V. Then the proteins were transferred to a PVDF membrane using the BioRad Trans-Blot turbo system. The blot was blocked for 1 h with 3% BSA in TBST (50 mM Tris HCl 7.4, 150 mM NaCl, 0.3% Tween 20) while shaking and washed three times with TBST. Antibodies against GFP (Miltenyi Biotec) or HA (Pierce scientific) conjugated to horse radish peroxidase diluted 5000x in TBST with 1% BSA were added, and incubated for 1 h while shaking. Then, the blot was washed three times with TBST, and one time with TBS (50 mM Tris HCl 7.4, 150 mM NaCl). Finally, 1 ml of supersignal west femto ECL substrate (Thermo scientific) was added to the blot, and luminescence was measured for 5 min, using a G:box detection system (Syngene).

Stable Transformation of *Medicago truncatula*

The binary plasmid carrying SYP132α-sgRNA/35S::CAS9 construct the was introduce into *Agrobacterium tumefaciens* AGL1 via electroporation. Stable transformation of *Medicago truncatula* R108 cotyledon and young leaf explants was done according to Chabaud et al. (2003). Transformants were selected using 10 mg/L hygromycin B. DNA was extracted from the transformed lines using the standard CTAB miniprep method. The resulting lines were genotyped, and resulting PCR amplicons sequenced, using the primers 49 and 50 (**Supplementary Table S2**). The presence of the Cas9 gene in the obtained lines was checked by PCR using primers 51 and 52 (**Supplementary Table S2**).

Agrobacterium Infiltration of *Nicotiana benthamiana*

Agrobacterium tumefaciens C58 expressing split-GFP constructs were grown in liquid LB with appropriate antibiotics for 2 days at 28°C. The bacteria were collected by centrifugation, resuspended in MMi medium [10 g/l sucrose, 5 g/l MS basal salts (Duchefa), 2 g/l MES, 200 μM acetosyringone, pH 5.6] to an OD_{600} of 0.1 and incubated for 1 h at room temperature.

Different combinations of split-GFP constructs were made by mixing the appropriate bacterial suspensions in a 1:1 ratio. The suspensions were then injected into the leaves of *Nicotiana benthamiana* plants which were then grown in a greenhouse at 21°C. Three days post-infiltration, the infiltrated parts were analyzed by confocal microscopy.

DATA AVAILABILITY STATEMENT

All datasets generated for this study are included in the article/**Supplementary Material**.

AUTHOR CONTRIBUTIONS

RH, JH, and EL performed experiments and data analyses. RH and EL conceived experiments. RH, TB, and EL wrote the manuscript.

FUNDING

RH, TB, and EL were supported by the European Research Council (ERC-2011-AdG294790).

ACKNOWLEDGMENTS

We would like to thank Guido Hooiveld for assistance with the digital droplet PCR. Contents of this manuscript have appeared in RH Ph.D. thesis (Huisman, 2018).

SUPPLEMENTARY MATERIAL

The Supplementary Material for this article can be found online at: https://www.frontiersin.org/articles/10.3389/fpls.2020.00354/full#supplementary-material

REFERENCES

An, Q., Hückelhoven, R., Kogel, K. H., and van Bel, A. J. E. (2006). Multivesicular bodies participate in a cell wall-associated defence response in barley leaves attacked by the pathogenic powdery mildew fungus. *Cell. Microbiol.* 8, 1009–1019. doi: 10.1111/j.1462-5822.2006.00683.x

Ângelo Silva, P., Ul-Rehman, R., Rato, C., Di Sansebastiano, G.-P., and Malhó, R. (2010). Asymmetric localization of *Arabidopsis* SYP124 syntaxin at the pollen tube apical and sub-apical zones is involved in tip growth. *BMC Plant Biol.* 10:179. doi: 10.1186/1471-2229-10-179

Assaad, F. F., Qiu, J. L., Youngs, H., Ehrhardt, D., Zimmerli, L., Kalde, M., et al. (2004). The PEN1 syntaxin defines a novel cellular compartment upon fungal attack and is required for the timely assembly of papillae. *Mol. Biol. Cell* 15, 5118–5129. doi: 10.1091/mbc.e04-02-0140

Bravo, A., York, T., Pumplin, N., Mueller, L. A., and Harrison, M. J. (2016). Genes conserved for arbuscular mycorrhizal symbiosis identified through phylogenomics. *Nat. Plants* 2:15208. doi: 10.1038/nplants.2015.208

Chabaud, M., De Carvalho-Niebel, F., and Barker, D. G. (2003). Efficient transformation of Medicago truncatula cv. Jemalong using the hypervirulent *Agrobacterium tumefaciens* strain AGL1. *Plant Cell Rep.* 22, 46–51. doi: 10.1007/s00299-003-0649-y

Chao, C. C. T., Mihic, A., Tsushima, R. G., and Gaisano, H. Y. (2011). SNARE protein regulation of cardiac potassium channels and atrial natriuretic factor secretion. *J. Mol. Cell. Cardiol.* 50, 401–407. doi: 10.1016/j.yjmcc.2010.11.018

Collins, N. C., Thordal-Christensen, H., Lipka, V., Bau, S., Kombrink, E., Qiu, J.-L. L., et al. (2003). SNARE-protein-mediated disease resistance at the plant cell wall. *Nature* 425, 973–977. doi: 10.1038/nature02076

Cox, G., and Sanders, F. (1974). Ultrastructure of the host—fungus interface in a vesicular—arbuscular mycorrhiza. *New Phytol.* 73, 901–912. doi: 10.1111/j.1469-8137.1974.tb01319.x

Ebine, K., Fujimoto, M., Okatani, Y., Nishiyama, T., Goh, T., Ito, E., et al. (2011). A membrane trafficking pathway regulated by the plant-specific RAB GTPase ARA6. *Nat. Cell Biol.* 13, 853–859. doi: 10.1038/ncb2270

Enami, K., Ichikawa, M., Uemura, T., Kutsuna, N., Hasezawa, S., Nakagawa, T., et al. (2009). Differential expression control and polarized distribution of plasma membrane-resident SYP1 SNAREs in *Arabidopsis thaliana*. *Plant Cell Physiol.* 50, 280–289. doi: 10.1093/pcp/pcn197

Grefen, C., Chen, Z., Honsbein, A., Donald, N., Hills, A., and Blatt, M. R. (2010). A novel motif essential for SNARE interaction with the K^+ channel KC1 and channel gating in *Arabidopsis*. *Plant Cell* 22, 3076–3092. doi: 10.1105/tpc.110.077768

Gutjahr, C., and Parniske, M. (2013). Cell and developmental biology of arbuscular mycorrhiza symbiosis. *Ann. Rev. Cell Dev. Biol.* 29, 593–617. doi: 10.1146/annurev-cellbio-101512-122413

Harrison, M. J., and Ivanov, S. (2017). Exocytosis for endosymbiosis: membrane trafficking pathways for development of symbiotic membrane compartments. *Curr. Opin. Plant Biol.* 38, 101–108. doi: 10.1016/j.pbi.2017.04.019

Hindson, C. M., Chevillet, J. R., Briggs, H. A., Gallichotte, E. N., Ruf, I. K., Hindson, B. J., et al. (2013). Absolute quantification by droplet digital PCR versus analog real-time PCR. *Nat. Methods* 10, 1003–1005. doi: 10.1038/nmeth.2633

Huisman, R. (2018). *Formation of a Symbiotic Host-Microbe Interface: The Role of SNARE-Mediated Regulation of Exocytosis*. Ph.D. thesis, Wageningen University, Wageningen.

Huisman, R., Hontelez, J., Mysore, K. S., Wen, J., Bisseling, T., and Limpens, E. (2016). A symbiosis-dedicated SYNTAXIN OF PLANTS 13II isoform controls the formation of a stable host-microbe interface in symbiosis. *New Phytol.* 211, 1338–1351. doi: 10.1111/nph.13973

Ichikawa, M., Hirano, T., Enami, K., Fuselier, T., Kato, N., Kwon, C., et al. (2014). Syntaxin of plant proteins SYP123 and SYP132 mediate root hair tip growth in *Arabidopsis thaliana*. *Plant. Cell Physiol.* 55, 790–800. doi: 10.1093/pcp/pcu048

Ivanov, S., Austin, J., Berg, R. H., and Harrison, M. J. (2019). Extensive membrane systems at the host-arbuscular mycorrhizal fungus interface. *Nat. Plants* 5, 194–203. doi: 10.1038/s41477-019-0364-5

Ivanov, S., Fedorova, E. E., Limpens, E., De Mita, S., Genre, A., Bonfante, P., et al. (2012). Rhizobium-legume symbiosis shares an exocytotic pathway required for arbuscule formation. *Proc. Natl. Acad. Sci. U.S.A.* 109, 8316–8321. doi: 10.1073/pnas.1200407109

Jiang, W., Zhou, H., Bi, H., Fromm, M., Yang, B., and Weeks, D. P. (2013). Demonstration of CRISPR/Cas9/sgRNA-mediated targeted gene modification in *Arabidopsis*, tobacco, sorghum and rice. *Nucleic Acids Res.* 41:E188. doi: 10.1093/nar/gkt780

Kalde, M., Nühse, T. S., Findlay, K., and Peck, S. C. (2007). The syntaxin SYP132 contributes to plant resistance against bacteria and secretion of pathogenesis-related protein 1. *Proc. Natl. Acad. Sci. U.S.A.* 104, 11850–11855. doi: 10.1073/pnas.0701083104

Kanazawa, T., and Ueda, T. (2017). Exocytic trafficking pathways in plants: why and how they are redirected. *New Phytol.* 215, 952–957. doi: 10.1111/nph.14613

Karnahl, M., Park, M., Mayer, U., Hiller, U., and Jürgens, G. (2017). ER assembly of SNARE complexes mediating formation of partitioning membrane in Arabidopsis cytokinesis. *eLife* 6:e23327. doi: 10.7554/eLife.25327

Kreitzer, G., Schmoranzer, J., Low, S. H., Li, X., Gan, Y., Weimbs, T., et al. (2003). Three-dimensional analysis of post-Golgi carrier exocytosis in epithelial cells. *Nat. Cell Biol.* 5, 126–136. doi: 10.1038/ncb917

Kwaaitaal, M., Keinath, N. F., Pajonk, S., Biskup, C., and Panstruga, R. (2010). Combined bimolecular fluorescence complementation and Forster resonance energy transfer reveals ternary SNARE complex formation in living plant cells. *Plant Physiol.* 152, 1135–1147. doi: 10.1104/pp.109.151142

Łangowski, Ł., Wabnik, K., Li, H., Vanneste, S., Naramoto, S., Tanaka, H., et al. (2016). Cellular mechanisms for cargo delivery and polarity maintenance at different polar domains in plant cells. *Cell Discov.* 2:16018. doi: 10.1038/celldisc.2016.18

Lauber, M. H., Waizenegger, I., Steinmann, T., Schwarz, H., Mayer, U., Hwang, I., et al. (1997). The *Arabidopsis* KNOLLE protein is a cytokinesis-specific syntaxin. *J. Cell Biol.* 139, 1485–1493. doi: 10.1083/jcb.139.6.1485

Leucci, M. R., Di Sansebastiano, G.-P., Gigante, M., Dalessandro, G., and Piro, G. (2007). Secretion marker proteins and cell-wall polysaccharides move through different secretory pathways. *Planta* 225, 1001–1017. doi: 10.1007/s00425-006-0407-9

Limpens, E., Ramos, J., Franken, C., Raz, V., Compaan, B., Franssen, H., et al. (2004). RNA interference in *Agrobacterium rhizogenes*-transformed roots of *Arabidopsis* and *Medicago truncatula*. *J. Exp. Bot.* 55, 983–992. doi: 10.1093/jxb/erh122

Martinez-Arca, S., Rudge, R., Vacca, M., Raposo, G., Camonis, J., Proux-Gillardeaux, V., et al. (2003). A dual mechanism controlling the localization and function of exocytic v-SNAREs. *Pro. Natl. Acad. Sci. U.S.A.* 100, 9011–9016. doi: 10.1073/pnas.1431910100

Micali, C. O., Neumann, U., Grunewald, D., Panstruga, R., and O'Connell, R. (2011). Biogenesis of a specialized plant-fungal interface during host cell internalization of *Golovinomyces orontii* haustoria. *Cell. Microbiol.* 13, 210–226. doi: 10.1111/j.1462-5822.2010.01530.x

Michaelevski, I., Chikvashvili, D., Tsuk, S., Singer-Lahat, D., Kang, Y., Linial, M., et al. (2003). Direct interaction of target SNAREs with the Kv2.1 channel: modal regulation of channel activation and inactivation gating. *J. Biol. Chem.* 278, 34320–34330. doi: 10.1074/jbc.m304943200

Mirabella, R., Franken, C., Krogt, G. N. M., Bisseling, T., and Geurts, R. (2004). Use of the fluorescent timer DsRED-E5 as reporter to monitor dynamics of gene activity in plants. *Plant Physiol.* 135, 1879–1887. doi: 10.1104/pp.103.038539

Mostov, K., Su, T., and Ter Beest, M. (2003). Polarized epithelial membrane traffic: conservation and plasticity. *Nat. Cell Biol.* 5, 287–293. doi: 10.1038/ncb0403-287

Nielsen, M. E., Feechan, A., Böhlenius, H., Ueda, T., and Thordal-Christensen, H. (2012). *Arabidopsis* ARF-GTP exchange factor, GNOM, mediates transport required for innate immunity and focal accumulation of syntaxin PEN1. *Proc. Natl. Acad. Sci. U.S.A.* 109, 11443–11448. doi: 10.1073/pnas.1117596109

Nielsen, M. E., and Thordal-Christensen, H. (2012). Recycling of *Arabidopsis plasma* membrane PEN1 syntaxin. *Plant Signal. Behav.* 7, 1541–1543. doi: 10.4161/psb.22304

Ovchinnikova, E., Journet, E.-P., Chabaud, M., Cosson, V., Ratet, P., Duc, G., et al. (2011). IPD3 controls the formation of nitrogen-fixing symbiosomes in pea and *Medicago* Spp. *Mol. Plant Microbe Interact.* 24, 1333–1344. doi: 10.1094/MPMI-01-11-0013

Pan, H., Oztas, O., Zhang, X., Wu, X., Stonoha, C., Wang, E., et al. (2016). A symbiotic SNARE protein generated by alternative termination of transcription. *Nat. Plants* 2:15197. doi: 10.1038/nplants.2015.197

Pumplin, N., and Harrison, M. J. (2009). Live-cell imaging reveals periarbuscular membrane domains and organelle location in *Medicago truncatula* roots during arbuscular mycorrhizal symbiosis. *Plant Physiol.* 151, 809–819. doi: 10.1104/pp.109.141879

Pumplin, N., Zhang, X., Noar, R. D., and Harrison, M. J. (2012). Polar localization of a symbiosis-specific phosphate transporter is mediated by a transient reorientation of secretion. *Proc. Natl. Acad. Sci. U.S.A.* 109, E665–E672. doi: 10.1073/pnas.1110215109

Rehman, R. U., Stigliano, E., Lycett, G. W., Sticher, L., Sbano, F., Faraco, M., et al. (2008). Tomato Rab11a characterization evidenced a difference between SYP121-dependent and SYP122-dependent exocytosis. *Plant Cell Physiol.* 49, 751–766. doi: 10.1093/pcp/pcn051

Reichardt, I., Slane, D., El Kasmi, F., Knöll, C., Fuchs, R., Mayer, U., et al. (2011). Mechanisms of functional specificity among plasma-membrane syntaxins in *Arabidopsis*. *Traffic* 12, 1269–1280. doi: 10.1111/j.1600-0854.2011.01222.x

Roth, R., Hillmer, S., Funaya, C., Chiapello, M., Schumacher, K., Lo Presti, L., et al. (2019). Arbuscular cell invasion coincides with extracellular vesicles and membrane tubules. *Nat. Plants* 5, 204–211. doi: 10.1038/s41477-019-0365-4

Sanderfoot, A. (2007). Increases in the number of SNARE genes parallels the rise of multicellularity among the green plants. *Plant Physiol.* 144, 6–17. doi: 10.1104/pp.106.092973

Slane, D., Reichardt, I., El Kasmi, F., Bayer, M., and Jürgens, G. (2017). Evolutionarily diverse SYP1 Qa-SNAREs jointly sustain pollen tube growth in Arabidopsis. *Plant J.* 92, 375–385. doi: 10.1111/tpj.13659

Südhof, T. C., and Rothman, J. E. (2009). Membrane fusion: grappling with SNARE and SM proteins. *Science* 323, 474–477. doi: 10.1126/science.1161748

Trouvelot, A., Kough, J. L., and Gianinazzi-Pearson, V. (1986). "Mesure du taux de mycorhization VA d'un système radiculaire. Recherche de méthodes d'estimation ayant une signification fonctionnelle," in *Physiological and Genetical Aspects of Mycorrhizae*, eds V. Gianinazzi-Pearson and S. Gianinazzi (Paris: INRA Press), 217–220.

Waghmare, S., Lileikyte, E., Karnik, R., Goodman, J. K., Blatt, M. R., and Jones, A. M. E. (2018). SNAREs SYP121 and SYP122 mediate the secretion of distinct cargo subsets. *Plant Physiol.* 178, 1679–1688. doi: 10.1104/pp.18.00832

Xia, L., Marquès-Bueno, M. M., Bruce, C. G., and Karnik, R. (2019). Unusual roles of secretory snare syp132 in plasma membrane H^+-ATPase traffic and vegetative plant growth. *Plant Physiol.* 180, 837–858. doi: 10.1104/pp.19.00266

Conflict of Interest: The authors declare that the research was conducted in the absence of any commercial or financial relationships that could be construed as a potential conflict of interest.

frontiers in Plant Science

ORIGINAL RESEARCH
published: 07 July 2020
doi: 10.3389/fpls.2020.00912

More Filtering on SNP Calling Does Not Remove Evidence of Inter-Nucleus Recombination in Dikaryotic Arbuscular Mycorrhizal Fungi

Eric C. H. Chen[1†], Stephanie Mathieu[1], Anne Hoffrichter[2], Jeanne Ropars[3], Steven Dreissig[4], Jörg Fuchs[4], Andreas Brachmann[2] and Nicolas Corradi[1]*

[1] Department of Biology, University of Ottawa, Ottawa, ON, Canada, [2] Genetics, Biocenter, LMU Munich, Martinsried, Germany, [3] Ecologie Systématique Evolution, CNRS, AgroParisTech, Université, Paris-Saclay, Paris, France, [4] Leibniz Institute of Plant Genetics and Crop Plant Research, Gatersleben, Germany

OPEN ACCESS

Edited by:
Andrea Genre,
University of Turin, Italy

Reviewed by:
Erik Limpens,
Wageningen University & Research, Netherlands
Yuuki Kobayashi,
The Graduate University for Advanced Studies (Sokendai), Japan

***Correspondence:**
Nicolas Corradi
ncorradi@uottawa.ca

†Present address:
Eric C. H. Chen,
Department of Biological Sciences, Graduate School of Science, The University of Tokyo, Tokyo, Japan

Specialty section:
This article was submitted to Plant Microbe Interactions, a section of the journal Frontiers in Plant Science

Received: 17 March 2020
Accepted: 04 June 2020
Published: 07 July 2020

Citation:
Chen ECH, Mathieu S, Hoffrichter A, Ropars J, Dreissig S, Fuchs J, Brachmann A and Corradi N (2020) More Filtering on SNP Calling Does Not Remove Evidence of Inter-Nucleus Recombination in Dikaryotic Arbuscular Mycorrhizal Fungi. Front. Plant Sci. 11:912. doi: 10.3389/fpls.2020.00912

Evidence for the existence of dikaryote-like strains, low nuclear sequence diversity and inter-nuclear recombination in arbuscular mycorrhizal fungi has been recently reported based on single nucleus sequencing data. Here, we aimed to support evidence of inter-nuclear recombination using an approach that filters SNP calls more conservatively, keeping only positions that are exclusively single copy and homozygous, and with at least five reads supporting a given SNP. This methodology recovers hundreds of putative inter-nucleus recombination events across publicly available sequence data from individual nuclei. Challenges related to the acquisition and analysis of sequence data from individual nuclei are highlighted and discussed, and ways to address these issues in future studies are presented.

Keywords: recombination and evolution, single nucleus sequencing, parasexuality, dikaryosis, arbuscular mycorrhizal fungi

INTRODUCTION

Genome-based analyses have uncovered a large number of signatures of sexual reproduction in the arbuscular mycorrhizal fungi (AMF), challenging the notion that these organisms are ancient asexuals (Halary et al., 2011, 2013; Tisserant et al., 2013; Riley et al., 2014; Corradi and Brachmann, 2016; Ropars et al., 2016; Chen et al., 2018a). Notably, genome analyses showed that model AMF in the genus *Rhizophagus* can be either homokaryotic, carrying thousands of nuclei with a similar genotype, or dikaryotic, whereby nuclei from two parental genotypes are continuously present in the cytoplasm.

Furthermore, the nuclei of dikaryotic AMF isolates each carry one of two divergent regions that resemble the mating-type (MAT) loci of sexual fungi – i.e., putative idiomorphs. The MAT-locus is a genomic region that governs sexual identity in fungi (Fraser and Heitman, 2003; Heitman et al., 2013). In dikaryotic sexual fungi, co-existing nuclei are expected to recombine either through sex

(Lee et al., 2010; Heitman, 2015) or somatic events (Xu et al., 1996; Clark and Anderson, 2004; Anderson and Kohn, 2007; also see review from Yildirir et al., 2020). To confirm the existence of low nuclear diversity and dikaryotic stages in AMF, as well as to test whether recombination occurs among co-existing nuclei, a recent study sequenced 86 single nuclei from seven AMF isolates (Chen et al., 2018b). This study supported the hypothesis that two genotypes co-exist in some AMF isolates, and confirmed that overall nuclear genetic diversity is low in these organisms. Remarkably, it also showed evidence that rare inter-nucleus recombination events can be found in dikaryotic AMF strains (Chen et al., 2018b).

The discovery of inter-nuclear recombination in AMF was, however, challenged. Specifically, it was suggested that recombination events in AMF drop significantly once heterozygous, duplicated regions covering SNPs and sites supported by less than five reads are removed from available datasets from single nuclei (Auxier and Bazzicalupo, 2019). Here, we show that the removal of duplicates, heterozygous positions and sites supported by less than five reads still retrieves significant inter-nuclear recombination within available datasets (Chen et al., 2018b). Lastly, we find little support that recombinant sites identified along low coverage regions (Chen et al., 2018b) are artifactual.

RESULTS

Hundreds of Cases Involving Inter-Nucleus Recombination Are Retrieved Using Stringent Filtering in Dikaryotic Isolates of *Rhizophagus Irregularis*

Reports of rare inter-nucleus recombination in AMF (Chen et al., 2018b) were based on the analysis of downstream and upstream regions surrounding SNPs, and present in either one or two copies in AMF dikaryotic genome assemblies. Heterozygous sites were also removed in that study, with the exception of genotypes carrying heterozygosity that were identical to those found in homozygous nuclei. Finally, the abovementioned study also analyzed all sites with a coverage of 2 or higher.

Here, we implement a more conservative approach for analyzing the same single nucleus genome datasets, which are always noisy. Because conservative methods can be applied to study larger datasets, we implemented it to a larger dataset – i.e., 1000 contiguous, as opposed to 100 analyzed in Chen et al. (2018b) - to gather a better view of recombination events in AMF dikaryons. The method focuses on sites with a coverage >5, and removes duplicates and nuclei with heterozygous positions. This method allowed us to search for putative inter-nuclear recombination events along 37 to 50% of the three dikaryotic reference genomes SL1, A4, and A5 (Note that the average assembly coverage for single nuclei Illumina read varies from 11% for SL1 to 58% for A5).

We mapped reads from single nuclei against their corresponding dikaryotic reference genomes (e.g., single nuclei reads from SL1 against SL1 reference genome, etc.) and scored SNPs using Freebayes with following parameters: -p 1 -m 30 -K -q 20 -C 2. We consider as evidence of inter-nucleus recombination cases where: (1) one or two contiguous SNPs match the haplotype carried by nuclei with the opposite MAT locus (a genomic regions putatively involved in sex determination in AMF); and (2) at least three contiguous SNPs match the haplotype carried by nuclei with the opposite MAT locus.

For scenario #1, which was not analyzed by a recent comment on Chen et al., 2018b, we detected a total of 913 cases (SL1:115; A5:193; A4:605). These mutational events are unlikely to represent sequencing errors or somatic mutations, as they always produce the opposite co-existing genotype (as opposed to random, nucleus-specific substitutions). These sites were recovered along single copy, homozygous sites with at least five reads supporting the given SNP position.

For the scenario #2, where variation along individual single nuclei spans more than three contiguous SNPs, our analysis recovered 195 recombinant blocks (SL1: 36; A5: 30; A4: 129; **Supplementary Tables S1, S2**). Of these, 3, 2, and 7 blocks are, respectively found in the first 100 scaffolds. Remarkably, these recombinant blocks include up to 17 contiguous SNPs, and between 172 (in the isolate A5) to 635 (in the isolate A4) SNPs in total. Blocks can encompass up to 7 kb of individual nuclear genomes (**Supplementary Tables S1, S2**).

This re-analysis of the original dataset published in Chen et al. (2018b) shows that using more stringent filters, i.e., single copy and homozygous sites with at least five reads supporting a SNP, does not remove evidence of inter-nuclear recombination. It also confirms that putative inter-nuclear recombination is indeed a rare event in AMF dikaryons, as was originally reported by Chen et al. (2018b) Note that the report of inter-nuclear recombination by Chen et al. (2018b) was based on observed patterns, as opposed to "bin counting." Furthermore, the higher recombination rates originally observed by Chen et al. (2018b) in the isolate SL1 was primarily based on a more continuous genome assembly obtained using ALLPATHS-LG (Butler et al., 2008). This assembly is not analyzed here to ensure for direct comparisons of recombination events between AMF dikaryotic isolates – i.e., all assemblies analyzed here were obtained using SPades (Bankevich et al., 2012).

Recombination in Low Coverage and High-Coverage Sites

Wide read coverage variability is a hallmark of all single nuclei sequencing studies, as this method relies on DNA amplification procedures such as multiple amplification displacement (MDA) to improve yield. As a result of this variability, low coverage calls - i.e., positions supported by less than five reads - represent 35 to 54% of available single nucleus data from dikaryotic isolates. Evidently, a very significant amount of sequence data from AMF single nuclei is located in regions with low coverage.

The application of best practices in genome analysis – e.g., the removal of low coverage positions – are key steps to improve SNP validation in uniformly covered genome references. However, such practices also automatically eradicate a significant amount of data from single nucleus sequencing projects. This begs the question; are low coverage SNP calls identified along single nucleus data mostly untrustworthy and random? Our data suggests that they are not.

This view is supported by data available for the two dikaryotic isolates A4 and A5. Specifically, the genotypes of single nuclei isolated from these two isolates were mainly produced from positions with low read depth (Auxier and Bazzicalupo, 2019). However, despite the overabundance of low coverage sites, the 150 base pairs paired-end Illumina reads from single nuclei still did their job well, mapping with high fidelity to their genome assemblies to generate a clear dikaryotic patterns for these isolates (see Figure 2a,b in Chen et al., 2018b). In both cases, each genotype is linked with a specific MAT-locus (Chen et al., 2018b); a dichotomy that should not emerge if the abundant low coverage sites produced mostly false SNP calls in dikaryotic isolates.

Consistent with this, we found that low coverage reads in 5 homokaryotic isolates (isolates A1, C2, B3 belonging to *Rhizophagus irregularis* species, *Rhizophagus diaphanus* - MUCL-43196, and *R. cerebriforme* - DAOM227022) produce high quality reference genotypes >99.985% of the time, regardless of size and fragmentation of the assembly (**Figure 1**). Note that the high accuracy of these calls is virtually identical to those made with much larger coverage - i.e., from 5 to 100 (99.987%).

To further analyze low coverage calls in dikaryotic strains, we investigated if those could validate a dikaryotic genotype found years earlier using PCR and Sanger sequencing (Ropars et al., 2016). These genotypes were originally identified from the A5 scaffolds 2, 17, 37, and 641 (see columns representing individual nuclei from A5 in Figure 3 of Ropars et al., 2016). Remarkably, by implementing the same read mapping method used by Chen et al. (2018b), the exact genotypes originally found by Ropars et al. (2016) are fully recovered using the paired-end nucleus Illumina reads from A5. In all cases, the genotypes are linked with their respective MAT-locus and, notably, all positions (16/16) with a read depth ranging from 1 to 4 produce the expected genotype (**Supplementary Table S3**), further supporting the notion that the 150 paired-end reads can distinguish nucleus-specific homologous single copy regions.

We also aimed to determine if positions supported by two to four reads would result in a dramatic increase in recombination events. Again, this would be expected if these SNP calls were mainly spurious. To do this, we sought evidence of inter-nucleus recombination along single copy, homozygous regions with minimum two reads supporting a SNP position. This analysis retrieved, respectively, 73, 168, and 31 recombinant blocks in SL1, A4 and A5, ranging from a minimum of 3 to a maximum of 21 contiguous SNPs (**Supplementary Tables S4, S5**). Overall, the number of recombinant blocks supported by less than five reads varies, but does nevertheless remains within the same range – e.g., the number of blocks increases by 3% for A5 and 23% for A4). The larger block number increase seen in SL1 (36 to 73) simply reflects the low nucleus-specific coverage of this isolate, which results from a genome reference that has more than twice the number of contigs compared to other dikaryotic isolates, despite being generated with longer mate-pair libraries and higher coverage. In our view, the unique high genome fragmentation of SL1 indicates the higher genetic complexity of this isolate – e.g., higher recombination rates? (**Supplementary Table S1**).

The putative recombination events found along regions supported by less than 5 reads (**Supplementary Tables S4, S5**) include cases where single nuclei swap genotypes back and forth along up to 60 Kb (**Figures 2**, **3**); something that is difficult to explain based on low coverage alone. Lastly, we find that many recombinant sites are also found in single copy regions with read coverage much higher than five (see a few examples in **Supplementary Table S6)**. As such, evidence of inter-nucleus recombination in available single nucleus sequence datasets is also supported by very high coverage data along single copy regions.

Overall, the wide coverage of heterogeneity characteristic of individual nuclei sequencing clearly makes the application of best practices in genome analysis difficult – e.g., >50% of the data could be removed solely based on coverage threshold of five alone, despite evidence that most of these sites of high quality. Therefore, even though such practice should always be applied to study data from individual nuclei to support their genotyping, low coverage data should not be completely dismissed *a priori* and may be best analyzed on a case-by-case basis for quality.

Confirming That Nucleus 07 (SL1) Carries the MAT-5 Locus Would Be Compelling Evidence Against Recombination in This Nucleus

Using PCR and sequencing, Chen et al. (2018b) found that Nucleus 07 of SL1 (SL1_07) carries the MAT-locus 1, even though its nuclear genotype often resembles that of co-existing MAT-5 nuclei. It was noted that Illumina reads covering the MAT-locus 1 are not present in the in SL1_07 single nucleus data, and it was thus suggested that this specific sample may have been mixed-up (Auxier and Bazzicalupo, 2019).

Interestingly, we also note that: (1) Illumina reads that map the MAT-locus 5 are also absent from the SL1_07 data, even though their presence would provide compelling evidence against recombination in this nucleus and support of sample mix-up; (2) Other nuclei have no evidence of read mapping along the MAT-locus and all still had their MAT-locus identity properly confirmed by PCR/Sanger like SL1_07; (3) SL1_07 carries substantial evidence of recombination beyond the MAT-locus, particularly in the ALLPaths-LG assembly [see Supplementary file 7 in Chen et al. (2018b)].

Clearly, the absence of sequencing reads covering the MAT-locus provides no evidence against the presence of recombination in the nucleus SL1_07.

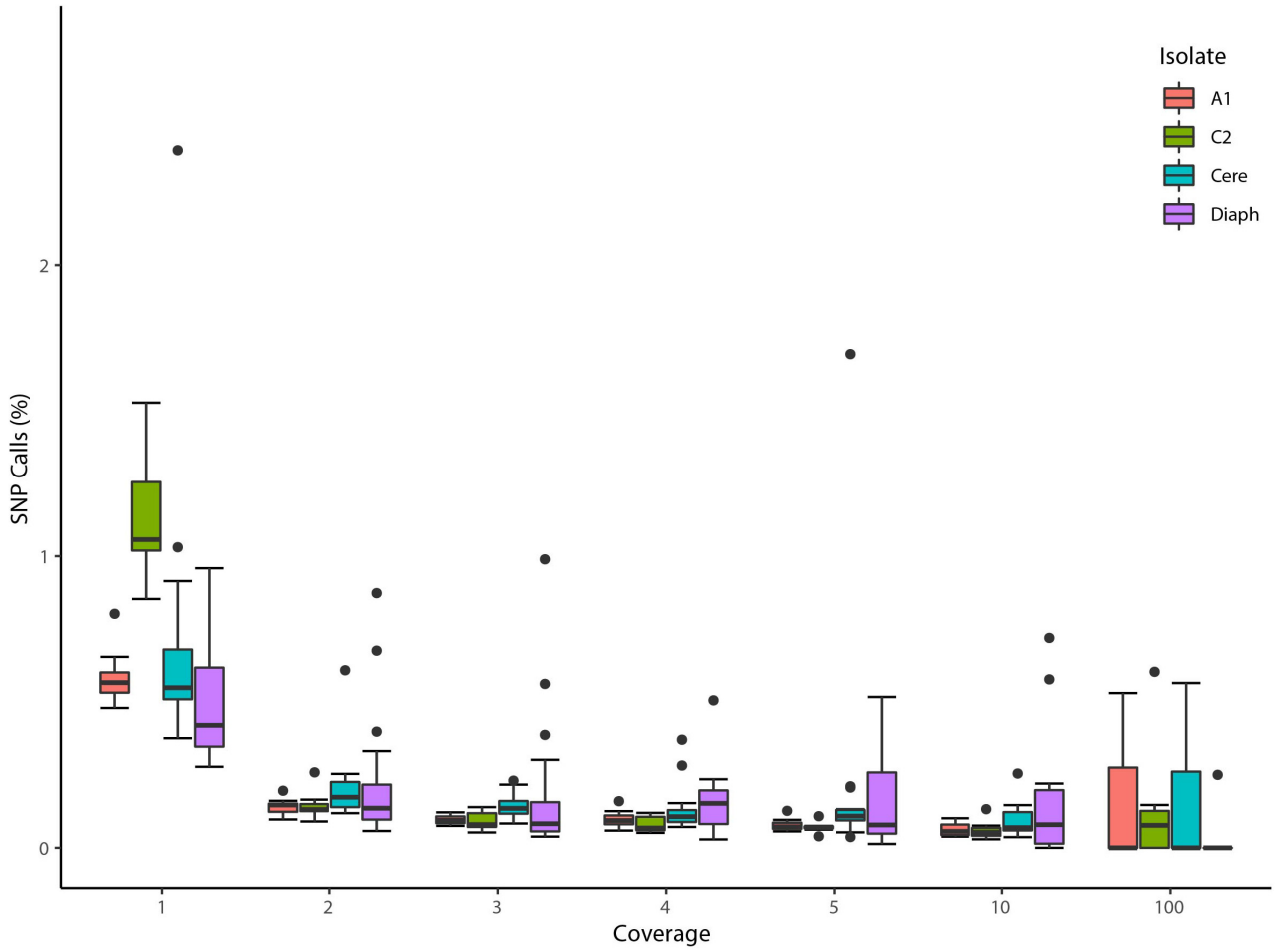

FIGURE 1 | Validation of low coverage depth SNP calls based on single nuclei Illumina reads from four homokaryotic strains. The boxplot represents the percentage of SNPs found to be in disagreement with reference assemblies in two *R. irregularis* isolates (A1 and C2), *R. cerebriforme* (Cere), and *R. diaphanous* (Diaph) organized by the number of reads supporting a given SNP. Boxes represent 25–75% percentile and whiskers represent the largest and smallest value within 1.5 interquartile range above 75th or below 25th percentile. One outlier from *R. diaphanus* is not shown (SN17, coverage 100: 1 mismatch out of 36 positions).

CONCLUSION

The aim of Chen et al. (2018b) was not to make an inventory of inter-nucleus recombination events in AMF but rather to:

(a) Validate the existence of a unique dikaryotic condition in some AMF isolates, whereby several thousands of nuclei that are copies of two parental genotypes co-exist in one large cell following plasmogamy between compatible homokaryons.
(b) Identify the degree of nuclear diversity within the AMF mycelium, which is found to be always low in the genus *Rhizophagus*.
(c) Detect evidence of inter-nucleus recombination in three dikaryotic isolates.

A recent comment on the single nucleus analyses recently published focused exclusively on point (c). Yet, by re-analyzing the same single nucleus data with more stringent filters (single copy and homozygous sites with more than five reads supporting a SNP), we still find that dikaryotic isolates carry significant evidence of inter-nucleus genetic exchange.

At a minimum, these findings confirm what is already known – i.e., co-existing nuclei in conventional dikaryotic cells (2 nuclei/cell) show footprints of recombination similar to those observed here (Clark and Anderson, 2004; Anderson and Kohn, 2007; Yildirir et al., 2020). As such, to suggest that AMF do not undergo similar processes, one must assume that millions of nuclei from two parental genotypes can co-exist in the same cytoplasm for decades without undergoing genetic interactions.

Despite present findings, it is fitting to end on a cautionary note regarding the use of read mapping to genotype individual nuclei. Specifically, even though the present work validates previous findings (identification of dikaryotic genotypes, low diversity) and the methodology we used is appropriate to test inter-nuclear recombination, the work of Chen et al. (2018b)

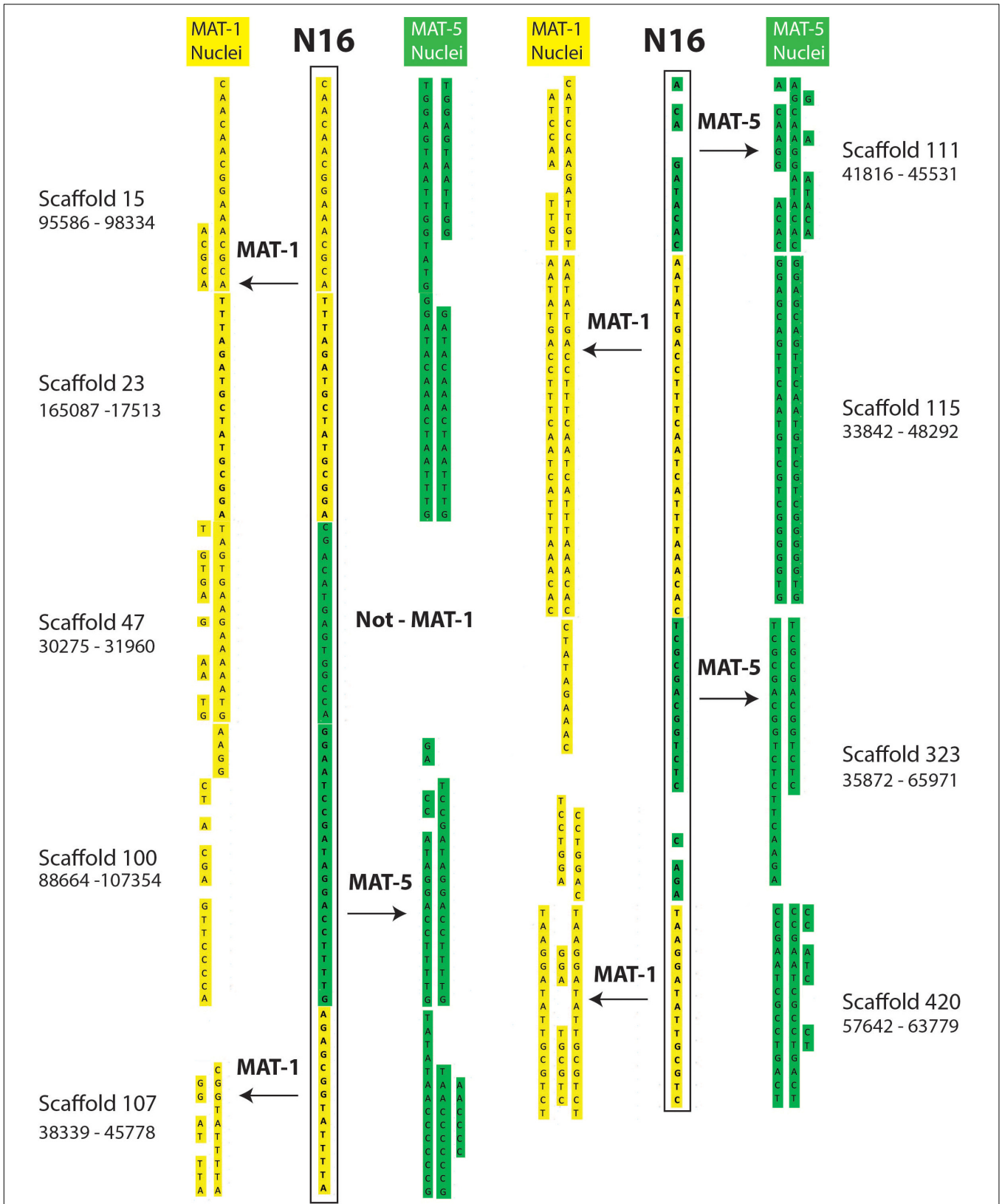

FIGURE 2 | Examples of inter-nucleus recombination in a nucleus of the dikaryotic isolate SL1. The regions are found along homozygous regions present only once in the reference genome of SL1. The nucleus 16 of SL1 carries a genotype that is overwhelmingly similar to nuclei carrying the MAT-1 locus (yellow). In several instances, however, the SN16 is found to switch alleles to carry the other co-existing genotype (green) over several kilobases.

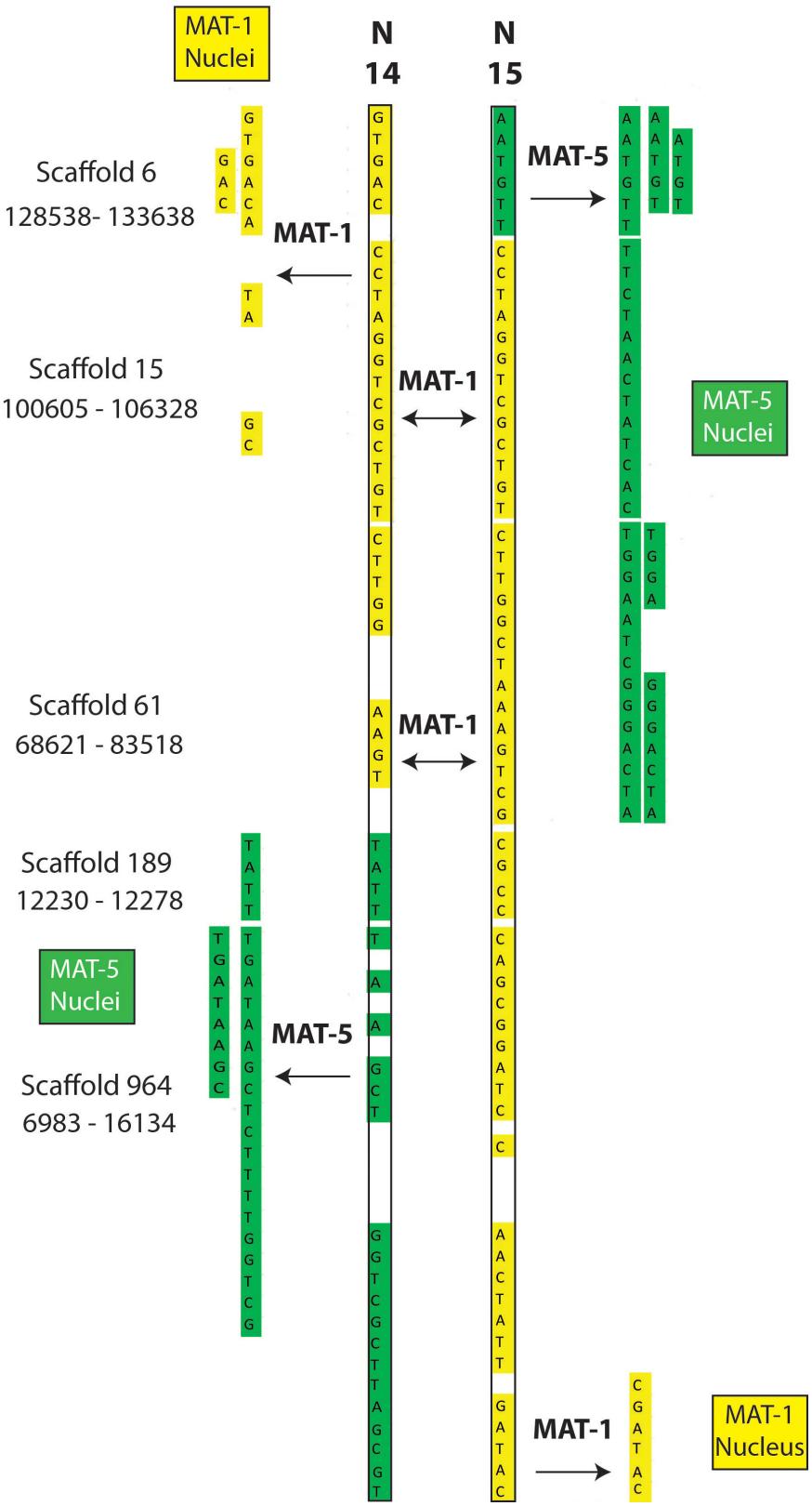

FIGURE 3 | Examples of recombination involving two nuclei (SN14 and SN15) of the dikaryotic isolate SL1. The regions are found along homozygous regions present only once in the reference genome of SL1. The nuclei N14 and 15 from SL1 carry the MAT-1 locus (validated by PCR) and, accordingly, their sequenced genotypes are almost identical. In some cases, however, each nucleus swaps genotype with the opposite MAT locus (i.e., genotype becomes green).

also relies on sequence data that can vary dramatically in terms of coverage and quality [as a result, for example, of multiple displacements during genome amplification, PCR bias during Illumina sequencing, or rare DNA cross-contamination (Dreissig et al., 2015, 2017)]. It also relies on a reference genome and predetermined mapping thresholds that can all independently affect the analysis output.

Thus, like for any biological finding, it will be important for future studies to validate the presence of inter-nucleus recombination using alternative methods. To this end, plans are underway to sequence individual AMF nuclei using long-read sequencing technologies, and perform single nuclei genotyping using complete, phased genome references for all dikaryotic AMF isolates. Long-read sequencing will be important to reveal the exact origin of the heterozygous sites in single nuclei datasets – i.e., whether some of these represent miss-mapped reads, sequence errors, aneuploidy or contaminants - as these are often found along recombination tracts (see paper and Auxier and Bazzicalupo, 2019). Lastly, producing a recombining progeny by crossing compatible homokaryotic AMF isolates will be key to conclusively demonstrate how/when sexual reproduction (meiosis) occurs in AMF.

MATERIALS AND METHODS

Obtaining Genotype Files

For filtering and generating genotype files in **Supplementary Tables S2, S5**, the original method described in Chen et al. (2018b) was used with three modifications. First, the number of BLAST hits allowed is reduced to just one (from two) so that no duplicated region is taken into account. The second modification relates to the treatment of heterozygosity. Sites for individual nuclei that did not pass the 10-to-1 alternate to reference allele test based on Freebayes (Garrison and Marth, 2012). SNP caller (hence forth referred to as "10-to-1") are now removed, even in cases where their genotype is confirmed by homozygous nuclei, which was the approach originally used in Chen et al. (2018b). The final modification is extending the number of scaffolds surveyed to first 1000 scaffolds (from 100).

Homokaryon Low-Coverage Read Analysis

To assess the fidelity of low coverage calls (**Figure 1**), homokaryon isolate A1, C2, *R. cerebriforme*, and *R. diaphanus*, are used. From the mapped BAM file of each single nucleus sequencing, we extracted positions from the first 10 scaffolds whose position have coverage of 1, 2, 3, 4, 5, 10, and 100. For each nucleus, positions with indel calls are filtered out. The 10-to-1 is also used on heterozygous positions. Finally, the percentage of homozygous mismatches are then calculated and collected across nuclei of each isolate before plotting in R via ggplot2, reshape2, grid, and grid_extra.

The difference in the number of recombined blocks identified in our study and a recent challenge may be a consequence of the treatment of heterozygous sites. Specifically, in the recent challenge to Chen et al. (2018b), it appears (based on their script) that the presence of heterozygosity in one nucleus (something that can be created by a single miss-mapped read) immediately results in complete removal of all homologous sites from all other co-exiting nuclei, regardless of whether these sites are homozygous and with high coverage. This approach drastically reduces opportunities to compare *bona-fide* genotypes/blocks.

In contrast to this, in our methodology the heterozygous nuclei – i.e., potential artifactual recombinants - are completely removed and not analyzed, but the co-existing nuclei with homologous homozygous and high coverage positions are kept for downstream analyses.

Genotype Identity

The goal of color labels is to make it easier the observation of recombination footprints between nuclei. It is not to produce complete haplotypes. We assign genotype color first based on parsimony using nuclei with PCR validated mating type: the mating type with more nuclei showing a particular genotype gets a color assigned. If it is a tie, or there is no PCR-proven mating type, then color that does not suggest new recombination is assigned (no change of color down the column). If that fails, first genotype in that row to be *MAT*-A. The exception is SL1's nucleus SN07 where in tied situations the color corresponding to *MAT*-5 is assigned, which is consistent with its genotype clustering with other *MAT*-5 nuclei (Chen et al., 2018b).

To score recombination events in scenario #1, a site is flagged as "recombining" if it starts to share one of two consecutive SNP with nuclei of the other MAT-locus along the same scaffold. For scenario #2, the same process is used, but a minimum of 3 consecutive SNP must be present.

For both scenarios, we count the number of events in each nucleus. For example, if 2 nuclei show recombination at the same location, the total number of events identified would be 2. Finally, in SL1's SN07, we sometimes manually correct the coloring to highlight instances where it did not have recombination. This is purely for clarity only and does not affect the counting of recombination events.

Obtaining Read Support of Each Position

To generate the read support for **Figure 1** and **Supplementary Tables S1–S6**, we opt to use bam-readcount[1] (version 0.8.0). We used the original bam files from Chen et al. (2018b). and queries for positions of interest. In the reanalysis of genotypes from Ropars et al., 2016, we used BLAST to identify the location of PCR products.

DATA AVAILABILITY STATEMENT

Publicly available datasets were analyzed in this study. This data can be found here: ID LLXH00000000, LLXI00000000, LLXJ00000000, LLXK00000000, LLXL00000000, and PRJNA477348.

[1]https://github.com/genome/bam-readcount

AUTHOR CONTRIBUTIONS

EC: hypothesis, formal analysis, validation, investigation, visualization, methodology, and writing–review and editing. SM: validation, investigation, and visualization. AH: formal analysis, validation, investigation, visualization, methodology, and writing–review and editing. JR: review and editing, and hypothesis. JF, SD, and AB: review and editing. NC: writing, hypothesis, and visualization. All authors contributed to the article and approved the submitted version.

FUNDING

Our research is kindly funded by the Discovery program of the Natural Sciences and Engineering Research Council (RGPIN-2020-05643) and a Discovery Accelerator Supplements Program (RGPAS-2020-00033). NC is a University of Ottawa Research Chair in Microbial Genomics. This manuscript has been released as a pre-print at *bioRxiv*, Chen et al. (2020).

SUPPLEMENTARY MATERIAL

The Supplementary Material for this article can be found online at: https://www.frontiersin.org/articles/10.3389/fpls.2020.00912/full#supplementary-material

TABLE S1 | Genotype file with minimum coverage of 5, with heterozygous sites as defined in Chen et al. (2018b) and Auxier and Bazzicalupo (2019) removed, and single-copy regions. Yellow and Green colors highlight the two co-existing genotypes. Nuclei highlighted in yellow and green had their MAT locus validated by PCR. Nuclei with cells highlighted in light green carry a genotype that is mostly associated with green nuclei validated by PCR, while those with cells highlighted in orange carry a genotype that is mostly associated with yellow nuclei validated by PCR.

TABLE S2 | Recombination blocks (Scenario #2) obtained from genotype file with at least five reads supporting a SNP in the first 1000 contiguous. Based on **Supplementary Table S1**.

TABLE S3 | Confirmation of genotypes found by Ropars et al., 2016 Nature Microbiology using PCR and Sanger sequencing. F (A) = = Reads supporting genotype (reads against genotype). Read depth is shown on the left columns for each position. Numbers in bold represent valid genotypes with very low read depth, i.e., 1 to 5.

TABLE S4 | Recombination blocks (Scenario #2) obtained from genotype file with at least two reads supporting a SNP in the first 1000 contiguous. Based on **Supplementary Table S5**.

TABLE S5 | Genotype file with minimum coverage of 2, with heterozygous sites as defined in Chen et al. (2018b) and Auxier and Bazzicalupo (2019) removed, and based on regions found only once in the reference genome. Yellow and Green colors highlight the two co-existing genotypes. Nuclei highlighted in yellow and green in had their mating-type locus validated by PCR. Nuclei with cells highlighted in light green carry a genotype that is mostly associated with green nuclei validated by PCR, while those with cells highlighted in orange carry a genotype that is mostly associated with yellow nuclei validated by PCR.

TABLE S6 | Examples of recombination with high coverage. Nuclei ID are colored for identification purposes. Yellow and dark green *MAT*-locus that is PCR verified. Yellow and Green colors highlight the two co-existing genotypes. Nuclei highlighted in yellow and green in had their mating-type locus validated by PCR. Nuclei with cells highlighted in light green carry a genotype that is mostly associated with green nuclei validated by PCR, while those with cells highlighted in orange carry a genotype that is mostly associated with yellow nuclei validated by PCR.

REFERENCES

Anderson, J. B., and Kohn, L. M. (2007). "Dikaryons, diploids, and evolution," in *Sex in Fungi*. eds J. Heitman, J. Kronstad, J. Taylor, and L. Casselton (Washington, DC: ASM Press), 333–348. doi: 10.1128/9781555815837.ch20

Auxier, B., and Bazzicalupo, A. (2019). Comment on "single nucleus sequencing reveals evidence of inter-nucleus recombination in arbuscular mycorrhizal fungi". *eLife* 8, 1–9. doi: 10.7554/eLife.47301

Bankevich, A., Nurk, S., Antipov, D., Gurevich, A. A., Dvorkin, M., Kulikov, A. S., et al. (2012). SPAdes: a new genome assembly algorithm and its applications to single-cell sequencing. *J. Comput. Biol.* 19, 455–477. doi: 10.1089/cmb.2012.0021

Butler, J., MacCallum, I., Kleber, M., Shlyakhter, I. A., Belmonte, M. K., Lander, E. S., et al. (2008). ALLPATHS: de novo assembly of whole-genome shotgun microreads. *Genome Res.* 18, 810–820. doi: 10.1101/gr.7337908

Chen, E. C. H., Mathieu, S., Hoffrichter, A., Ropars, J., and Dreissig, S. (2020). More filtering on SNP calling does not remove evidence of inter- nucleus recombination in dikaryotic arbuscular mycorrhizal fungi. *bioRxiv [Preprint]* doi: 10.1101/2020.01.15.906412

Chen, E. C. H., Morin, E., Beaudet, D., Noel, J., Yildirir, G., Ndikumana, S., et al. (2018a). High intraspecific genome diversity in the model arbuscular mycorrhizal symbiont *Rhizophagus irregularis*. *New Phytol.* 220, 1161–1171. doi: 10.1111/nph.14989

Chen, E. C., Mathieu, S., Hoffrichter, A., Sedzielewska-Toro, K., Peart, M., Pelin, A., et al. (2018b). Single nucleus sequencing reveals evidence of inter-nucleus recombination in arbuscular mycorrhizal fungi. *eLife* 7, 1–17. doi: 10.7554/elife.39813

Clark, T. A., and Anderson, J. B. (2004). Dikaryons of the basidiomycete fungus *Schizophyllum* commune: evolution in long-term culture. *Genetics* 167, 1663–1675. doi: 10.1534/genetics.104.027235

Corradi, N., and Brachmann, A. (2016). Fungal mating in the most widespread plant symbionts? *Trends Plant Sci.* 22, 175–183. doi: 10.1016/j.tplants.2016.10.010

Dreissig, S., Fuchs, J., Cápal, P., Kettles, N., Byrne, E., and Houben, A. (2015). Measuring meiotic crossovers via multi-locus genotyping of single pollen grains in barley. *PLoS One* 10:e0137677. doi: 10.1371/journal.pone.0137677

Dreissig, S., Fuchs, J., Himmelbach, A., Mascher, M., and Houben, A. (2017). Sequencing of single pollen nuclei reveals meiotic recombination events at megabase resolution and circumvents segregation distortion caused by postmeiotic processes. *Front. Plant Sci.* 8:1620. doi: 10.3389/fpls.2017.008072901620

Fraser, J. A., and Heitman, J. (2003). Fungal mating-type loci. *Curr. Biol.* 13, R792–R795. doi: 10.1016/j.cub.2003.09.046

Garrison, E., and Marth, G. (2012). Haplotype-based variant detection from short-read sequencing. *arXiv [Preprint]* Available online at: http://arxiv.org/abs/1207.3907v2 (accessed May 15, 2020).

Halary, S., Daubois, L., Terrat, Y., Ellenberger, S., Wöstemeyer, J., and Hijri, M. (2013). Mating type gene homologues and putative sex pheromone-sensing pathway in arbuscular mycorrhizal fungi, a presumably asexual plant root symbiont. *PLoS One* 8:e80729. doi: 10.1371/journal.pone.0080729

Halary, S., Malik, S.-B., Lildhar, L., Slamovits, C. H., Hijri, M., and Corradi, N. (2011). Conserved meiotic machinery in Glomus spp., a putatively ancient asexual fungal lineage. *Genome Biol. Evol.* 3, 950–958. doi: 10.1093/gbe/evr089

Heitman, J. (2015). Evolution of sexual reproduction: a view from the fungal kingdom supports an evolutionary epoch with sex before sexes. *Fungal Biol. Rev.* 29, 108–117. doi: 10.1016/j.fbr.2015.08.002

Heitman, J., Sun, S., and James, T. Y. (2013). Evolution of fungal sexual reproduction. *Mycologia* 105, 1–27. doi: 10.2307/24637440

Lee, S. C., Ni, M., Li, W. J., Shertz, C., and Heitman, J. (2010). The evolution of sex: a perspective from the fungal kingdom. *Microbiol. Mol. Biol. Rev.* 74, 298–340. doi: 10.1128/Mmbr.00005-10

Riley, R., Charron, P., Idnurm, A., Farinelli, L., Dalpé, Y., Martin, F., et al. (2014). Extreme diversification of the mating type–high-mobility group (MATA-HMG) gene family in a plant-associated arbuscular mycorrhizal fungus. *New Phytol.* 201, 254–268. doi: 10.1111/nph.12462

Ropars, J., Toro, K. S., Noel, J., Pelin, A., Charron, P., Farinelli, L., et al. (2016). Evidence for the sexual origin of heterokaryosis in arbuscular mycorrhizal fungi. *Nat. Microbiol.* 1:16033.

Tisserant, E., Malbreil, M., Kuo, A., Kohler, A., Symeonidi, A., Balestrini, R., et al. (2013). Genome of an arbuscular mycorrhizal fungus provides insight into the oldest plant symbiosis. *Proc. Natl. Acad. Sci. U. S. A* 110, 20117–20122. doi: 10.1073/pnas.1313452110

Xu, J., Horgen, P. A., and Anderson, J. B. (1996). Somatic recombination in the cultivated mushroom *Agaricus bisporus*. *Mycol. Res.* 100, 188–192. doi: 10.1016/S0953-7562(96)80119-80115

Yildirir, G., Malar, C. M., Kokkoris, V., and Corradi, N. (2020). Parasexual and sexual reproduction in arbuscular mycorrhizal fungi: room for both. *Trends Microbiol.* 28, 518–520. doi: 10.1016/j.tim.2020.03.013

Conflict of Interest: The authors declare that the research was conducted in the absence of any commercial or financial relationships that could be construed as a potential conflict of interest.

Advantages of publishing in Frontiers

OPEN ACCESS
Articles are free to read for greatest visibility and readership

FAST PUBLICATION
Around 90 days from submission to decision

HIGH QUALITY PEER-REVIEW
Rigorous, collaborative, and constructive peer-review

TRANSPARENT PEER-REVIEW
Editors and reviewers acknowledged by name on published articles

Frontiers
Avenue du Tribunal-Fédéral 34
1005 Lausanne | Switzerland

Visit us: www.frontiersin.org
Contact us: frontiersin.org/about/contact

REPRODUCIBILITY OF RESEARCH
Support open data and methods to enhance research reproducibility

DIGITAL PUBLISHING
Articles designed for optimal readership across devices

FOLLOW US
@frontiersin

IMPACT METRICS
Advanced article metrics track visibility across digital media

EXTENSIVE PROMOTION
Marketing and promotion of impactful research

LOOP RESEARCH NETWORK
Our network increases your article's readership